LEABHARLANN CHOLÁISTE NA TRÍONÓIDE, BAILE ÁTHA CLIATH | TRINITY COLLEGE LIBRARY DUBLIN
Ollscoil Átha Cliath | The University of Dublin

Terms and Conditions of Use of Digitised Theses from Trinity College Library Dublin

Copyright statement

All material supplied by Trinity College Library is protected by copyright (under the Copyright and Related Rights Act, 2000 as amended) and other relevant Intellectual Property Rights. By accessing and using a Digitised Thesis from Trinity College Library you acknowledge that all Intellectual Property Rights in any Works supplied are the sole and exclusive property of the copyright and/or other IPR holder. Specific copyright holders may not be explicitly identified. Use of materials from other sources within a thesis should not be construed as a claim over them.

A non-exclusive, non-transferable licence is hereby granted to those using or reproducing, in whole or in part, the material for valid purposes, providing the copyright owners are acknowledged using the normal conventions. Where specific permission to use material is required, this is identified and such permission must be sought from the copyright holder or agency cited.

Liability statement

By using a Digitised Thesis, I accept that Trinity College Dublin bears no legal responsibility for the accuracy, legality or comprehensiveness of materials contained within the thesis, and that Trinity College Dublin accepts no liability for indirect, consequential, or incidental, damages or losses arising from use of the thesis for whatever reason. Information located in a thesis may be subject to specific use constraints, details of which may not be explicitly described. It is the responsibility of potential and actual users to be aware of such constraints and to abide by them. By making use of material from a digitised thesis, you accept these copyright and disclaimer provisions. Where it is brought to the attention of Trinity College Library that there may be a breach of copyright or other restraint, it is the policy to withdraw or take down access to a thesis while the issue is being resolved.

Access Agreement

By using a Digitised Thesis from Trinity College Library you are bound by the following Terms & Conditions. Please read them carefully.

I have read and I understand the following statement: All material supplied via a Digitised Thesis from Trinity College Library is protected by copyright and other intellectual property rights, and duplication or sale of all or part of any of a thesis is not permitted, except that material may be duplicated by you for your research use or for educational purposes in electronic or print form providing the copyright owners are acknowledged using the normal conventions. You must obtain permission for any other use. Electronic or print copies may not be offered, whether for sale or otherwise to anyone. This copy has been supplied on the understanding that it is copyright material and that no quotation from the thesis may be published without proper acknowledgement.

Synthesis and Studies of Cyclen Based Lanthanide Complexes for the Detection of Ions and Molecules and the Hydrolysis of Phosphodiesters

By Andrew Harte,
January 2005

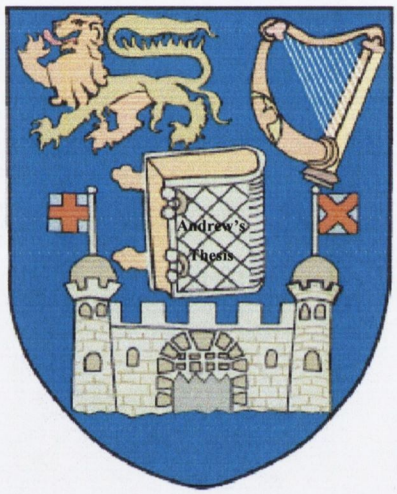

University of Dublin Trinity College

Based on research carried out under the direction of
Prof. Thorfinnur Gunnlaugsson

A thesis submitted to the Department of Chemistry, University of Dublin, Trinity College for the degree of Doctor of Philosophy.

Synthesis and Studies of Cyclen Based Lanthanide Complexes for the Detection of Ions and Molecules and the Hydrolysis of Phosphodiesters

By Andrew Harte,
January 2005

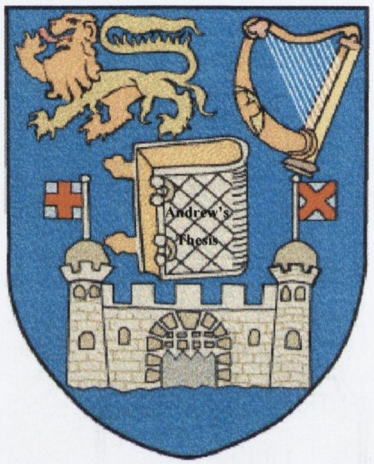

University of Dublin Trinity College

Based on research carried out under the direction of
Prof. Thorfinnur Gunnlaugsson

A thesis submitted to the Department of Chemistry, University of Dublin, Trinity College for the degree of Doctor of Philosophy.

TRINITY COLLEGE
10 JUL 2006
LIBRARY DUBLIN
THESIS
7938

Declaration

This thesis is submitted for the degree of Doctor of Philosophy to the University of Dublin, Trinity College and has not been submitted for any degree or examination to this or any other University. Other than where acknowledged, all work described herein is original and carried out by the author.

Andrew Harte

Andrew Harte

DECLARATION

This thesis has not been submitted as an exercise for a degree at any other university. Except where stated, the work described therein was carried out by me alone.

I give permission for the Library to lend or copy this thesis upon request.

Signed: Andrew Harte

Acknowledgements

I want to say Thank You to all the people who have helped and encouraged me throughout my time at Trinity. Thanks to all the members of the Gunnlaugsson group, who are less like colleagues and more like family. Ann Marie, Aoife, Caroline, Celine, Cidalia, Claire, Danny, Debbie, Emma, Eoin, Flo, Fred, Gary, Jilly, Joe, Julie, Katell, Lin, Lisa, Mark, Niamh, Raman, Sally, Sinead and Susan, thanks for all the help motivation, good times and good fun. Special thanks must go to Joe who was always there as mentor, ideas man, slave driver and the only other guy in the big lab for a long time. And also to my bench buddy Ann Marie, it wouldn't have been the same without you. Fred and Katell were always there for help and ideas. And of course, the guiding presence of the leader himself, Thanks for everything Thorri.

I'd also like to thank all the staff in the Chemistry department, including John O Brien for countless NMRs, and many helpful discussions. Thanks to Martin, for all the assistance with the mass spec. To Paul Jensen, Tom McCabe and Woody for all the work acquiring crystal structures, as well as the technicians Fred, Ed, Patsy, Brendan, Mark and Peggy. Thanks to Theresa Mc Donald for keeping everything running smoothly, from orders to lights to water to big holes in the floor. And thank you to the secretaries Corrine, Tess and Helen.

Finally, thanks to all my friends who kept me laughing. Thank you Lisa, for everything. And a special thanks to my family, Louis, Margaret, Louise and Elizabeth, the foundation underneath it all.



"So I said to myself 'What would God do?'"
"Itaque ipse quaesii 'Quid facet Deus'"

H. J. Simpson

Abstract

This thesis entitled "Cyclen Based Lanthanide Complexes for the Detection of Ions and Molecules and the Hydrolysis of Phosphodiesters" is divided into five chapters. Chapter 1, the introduction, is divided into two parts. The first half introduces the principles of luminescent sensing before illustrating some examples of fluorescent sensors. Then the advantages of lanthanide luminescent signalling systems are discussed followed by a description of the mechanism by which lanthanide luminescence is produced. Finally, a review of various lanthanide luminescent chemosensors is presented. The second half of the introduction deals with the area of phosphodiester hydrolysis. It shall begin by looking at natural ribonucleases capable of hydrolysing RNA, followed by a look at the mechanism of hydrolysis. The use of metal ions to promote phosphodiester hydrolysis is then discussed, followed by a discussion on the use of metal complexes. A review of the acceleration of phosphodiester hydrolysis by binuclear metal complexes is then presented with special attention paid to the rate acceleration provided by the cooperative action of two metal ions. This shall be followed by a review of binuclear lanthanide complexes capable of producing this cooperative action. Chapter 2 details the synthesis, characterisation and photophysical studies of a lanthanide luminescent sensor, designed for the detection of Cu(II). The synthesis involves the incorporation of a 1,10-phenanthroline unit into a tris-alkylated cyclen molecule, followed by complexation with a Eu(III) ion. The resulting complex exhibits the characteristic Eu(III) emission bands after excitation of the phenanthroline chromophore under physiological conditions. This complex signals the presence of Cu(II) under physiological conditions by means of a quenching of the Eu(III) luminescence. The complex displays good selectivity over other physiologically prevalent ions and operates over the desired concentration range. Chapter 3 describes the synthesis, characterisation and photophysical studies of a range of lanthanide luminescent sensors, designed for the detection of aromatic carboxylates. The chapter begins with the development of co-ordinately unsaturated mononuclear Tb(III) and Eu(III) cyclen complexes before moving on to an unsaturated binuclear Tb(III) cyclen complex. Luminescent studies demonstrated the ability of the Tb(III) complexes to bind aromatic carboxylates *via* the displacement of the metal bound water molecules, which occupy the vacant coordination sites around the lanthanide ion. Furthermore, this binding event is signalled by and increase in the previously "silent" Tb(III) emission. Chapter 4 is concerned with the area of phosphodiester hydrolysis and details the synthesis,

characterisation and kinetic studies of a range of binuclear lanthanide complexes, designed for the acceleration of phosphodiester hydrolyisis. The incorporation of various pendant arms, as well as the effect of different spacer groups is investigated. A convenient method for the production of α–chloroamides in water is also presented. The ability of the binuclear lanthanide complexes to promote the hydrolysis of the **HPNP** phosphodiester, a model RNAcompound, shall be discussed with particular attention upon rate enhancement over corresponding mononuclear complexes. The trends that emerge from these studies shall be discussed, before a detailed investigation of the **Tb.117** complex, which was found to be by far the most active binuclear complex, reducing the half-life of **HPNP** to 28 minutes from 240 days, a 12,333 fold rate increase. This is comparable to the largest rate enhancements detailed within the literature. A discussion of the possible reaction mechanism shall also be presented. Chapter 5 outlines the experimental procedures, and presents the synthesis and characterisation of the compounds discussed within the thesis.

Abbreviations

A	adenine
Abs	absorbance
AcOH	acetic acid
Ala	alanine
Arg	argentine
Asn	Asparagine
Asp	aspartic acid
a.u.	arbitrary units
B	binding constant
bipy	bipyridine
BNPP	bis(p-nitrophenyl)phosphate
BOC	*tert*-butoxycarbonyl
Br	broad
C	cytosine
$CHCl_3$	chloroform
CH_2Cl_2	dichloromethane
CH_3CN	acetonitrile
CTACl	cetyltrimethylammonium chloride
Cyclen	1,4,7,10-tetraazacyclododecane
Cyclam	1,4,8,11-tetraazacyclotetradecane
Cys	cysteine
d	doublet
DCM	dichloromethane
DMF	dimethyl formamide
DMSO	dimethyl solfoxide
DNA	deoxyribonucleic acid
DTPA	diethylenetriamine pentaacetic acid
ε	molar extinction coefficient
EDTA	ethylenediamine tetraacetic acid
EPNP	ethyl-p-nitrophenyl phosphate
ES	electrospray

pH	$-\log[H_3O^+]$
pKa	$-\log[K_a]$ where K_a is the acidity constant
pM	-log[M]
Phe	Phenylalanine
Phen	phenanthroline
ppm	parts per million
Pro	praline
RNA	ribonucleic acid
rRNA	ribosomal RNA
S_0	Singlet ground state
S_1	First excited singlet state
Ser	serine
T	thymine
T_1	First excited triplet state
THF	tetrahydofuran
TMACl	tetramethyl ammonium chloride
TMAPCl	tetramethyl ammonium perchlorate
TMAOH	tetramethyl ammonium hydroxide
TNP	tris-p-nitrophenyl phosphate
TRIS	Tris(hydroxymethyl)aminomethane
Trif	triflate (trifluorosulfonate)
tRNA	transfer RNA
Thr	threonine
Trif	triflate
Trp	tryptophan
Tyr	tyrosine
U	uracil
UV	ultra violet
Val	valine
ν	frequency
μ	micro ($\times 10^{-6}$)
λ	wavelenght

Table of Contents

Chapter 1 - Introduction

1.0 Prelude 1
1.1.0 Introduction to Sensors 1
1.1.1 Fluorescent Sensors 2
1.1.2 Photophysics of Lanthanide Luminescence 5
1.1.3 Lanthanide Luminescent Sensors 10
1.1.4 Lanthanide Luminescent Probes as Cation Sensors 13
1.1.5 Lanthanide Luminescent Probes as Anion Sensors 15
1.1.6 Conclusion 20
1.2.0 Phosphodiester Hydrolysis 21
1.2.1 Acceleration of Phosphodiester Hydrolysis by Metal Cations 23
1.2.2 Phosphodiester Models 26
1.2.3 Phosphodiester Hydrolysis by Metal Complexes 27
1.2.4 Cooperative Action by Binuclear Transition Metal Ion Systems 29
1.2.5 Pertinent Factors for Double Lewis Acid Activation 33
1.2.6 Trinuclear complexes 37
1.2.7 Cooperative Action by Binuclear Lanthanide Systems 40
1.2.8 Hydrolysis by Hetrodinuclear Complexes 44
1.2.9 Functional Organic Pendant Groups 46
1.2.10 Antisense Approach 47
1.2.11 Project Aim 50

Chapter 2 – Lanthanide Luminescent Cu(II) Sensor

2.1 Introduction 52
2.1.1 Fluorescent Copper(II) Sensors 53
2.1.2 Requirements for Luminescent Sensor 55
2.2 Design of Lanthanide Luminescent Sensor 56
2.3 Synthesis 59
2.3.1 Synthesis of Tris Functionalised Cyclen 59
2.3.2 Synthesis of **Eu.104** 61
2.4 Characterisation of Eu.104 63
2.5 Photophysical Properties 65

2.5.1 Lanthanide Luminescence of **Eu.104** 66
2.5.2 pH Dependence of Absorption Spectrum 67
2.5.3 pH Dependence of Fluorescence Spectrum 69
2.5.4 pH Dependence of Eu(III) Luminescence 70
2.5.5 Determination of Metal Bound Water Molecules 74
2.6 Comparison to Model Receptor 75
2.6.1 Fluorescence Response of **106** to Cu(II) 78
2.7 Luminescent Studies of the Effect of Copper (II) upon Eu.104 80
2.7.1 Absorption Spectrum 80
2.7.2 Fluorescence Spectrum 81
2.7.3 Lanthanide Luminescence 82
2.8 Selectivity studies for other metal ions 86
2.8.1 Studies for Fe(III) 88
2.8.2 Studies for Fe(II) 89
2.8.3 Studies for Co(II) 89
2.9 Effect of Ionic Strength 91
2.10 Conclusion 92

Chapter 3 – Lanthanide Luminescent Sensing of Aromatic Carboxylates

3.1 Introduction 94
3.2 Synthesis of Heptadentate Tri-arm Cyclen 95
3.3 Complexation of the Heptadentate Cyclen Ligands 100 and 107 96
3.4 Determination of Metal Bound Water Molecules 97
3.5 Displacement of Metal Bound Water Molecules 100
3.6 Luminescence Measurements 100
3.7 Sensitisation by Salicylic Acid 104
3.8 Bis Terbium System 108
3.9 Synthesis 109

Chapter 4 – Ln(III) Complexes as Phosphodiester Cleaving Agents

4.1 Introduction 122
4.2 Design of Binuclear systems 123

4.3 Synthesis of Binuclear Lanthanide Complexes 124
4.3.1 Synthesis of α-Chloroacetamide Spacers 125
4.3.1.1 *N*-Acylation Reactions in Water 127
4.3.1.2 The Effect of Changing the Base 132
4.3.1.3 Conclusion 133
4.3.2 Selective Protection of Cyclen 133
4.3.3 Synthesis of Bis-Cyclen Framework 135
4.3.4 Synthesis of Acetamide-Based Bis-Cyclen Ligands **154-157** 138
4.3.5 Complexation of Acetamide-Based Bis-Cyclen Ligands 141
4.3.6 Changing the Pendant Arm 147
4.3.7 Synthesis of Glycine and Pyridine Pendant Arms 148
4.3.8 Synthesis of 3-Armed Cyclen Systems 148
4.3.9 Synthesis of Bis-Pyridine and Bis-Glycine Ligands 151
4.3.10 Complexation of Bis-Pyridine and Bis-Glycine Ligands 155
4.3.11 Synthesis of *p*-Xylyl Bridged Binuclear System 156
4.3.12 Summary 158
4.4 Phosphodiester Hydrolysis Studies 158
4.4.1 Hydrolysis of **HPNP** by Binuclear Acetamide Systems 160
4.4.2 pH Dependence of **HPNP** Hydrolysis by Binuclear Acetamide Systems 164
4.4.3 Hydrolysis of **HPNP** by Coordinately Saturated Complexes 167
4.4.4 Hydrolysis of **HPNP** by Binuclear Glycine Systems 168
4.4.5 pH Dependence of **HPNP** Hydrolysis by Binuclear Glycine Systems 171
4.4.6 Hydrolysis of **HPNP** by Binuclear Pyridine System 172
4.5 Trends in Activity 173
4.6 Changing the Spacer: Combining Rigid and Flexible Properties 175
4.6.1 Hydrolysis of **HPNP** by **Eu.117** 175
4.6.2 pH Dependence of **HPNP** Hydrolysis by **Eu.117** 177
4.7 Conclusion 181
4.8 Future Work 182

Chapter 5 – Experimental Procedures

5.1 General experimental details 184

5.2 Synthesis..... 184
5.3 Lanthanide Complexes – Photophysical Studies 218
5.4 Phosphodiester Hydrolysis Studies..... 219

Chapter 6 - References

6.0 References..... 220

Appendix

Publications

Delayed lanthanide luminescence sensing of aromatic carboxylates using heptadentate triamide Tb(III) cyclen complexes: The recognition of salicylic acid in water - *Chem. Commun.* **2002**, 2134.

The formation of luminescent supramolecular ternary complexes in water: Delayed luminescence sensing of aromatic carboxylates using coordinated unsaturated cationic heptadentate lanthanide ion complexes - *J. Supramolecular Chem.* **2003**, 505-519.

pH responsive Eu(III)-phenanthroline supramolecular conjugate: Novel " *off-on-off*" luminescent signalling in the physiological pH range - *J. Am. Chem. Soc.* **2003**, *125*, 12062.

Eu(III)-cyclen-phen conjugate as a luminescent copper sensor: The formation of mixed polymetallic macrocyclic complexes in water - *Chem. Commun.* **2004**, 782.



Chapter 1

Introduction

1.0 Prelude

The work within this thesis encompasses two different research areas; lanthanide luminescent sensing and phosphodiester hydrolysis. Each of these areas shall be introduced separately. As such, the first half of this introduction deals with luminescent sensing, detailing the advantages offered by lanthanide luminescent sensors over fluorescent devices, before examining how to go about provoking a lanthanide emission, followed by a look at some examples of lanthanide luminescent pH, cation and anion sensors. This will be followed by an introduction to the field of phosphodiester hydrolysis, focusing on the attainment of rate enhancements due to the cooperative action of two or more metal ions.

1.1.0 Introduction to Sensors

A sensor is a substance that provides information about a specific target within a specific matrix, for example, the concentration of a specific metal ion within blood or water, *etc.*[1] It must perform two functions; sensing/recognition and signalling. Recognition must be selective, therefore, within its chosen environment, the sensor must selectively recognise one target species out of all the possible species present. Recognition usually occurs through reversible binding.[1] Upon recognition the sensor must then be able to signal this event. A signalling event is usually heralded, after binding has occurred, by a modification of some property of the sensor such as a change in colour, a variation in the light emitting properties or an alteration in some other electronic, magnetic or thermal property (Scheme 1.1). The work within this thesis shall be confined to luminescent sensing, *i.e.* where the signal is observed as a variation in the light emitting properties of the sensor.

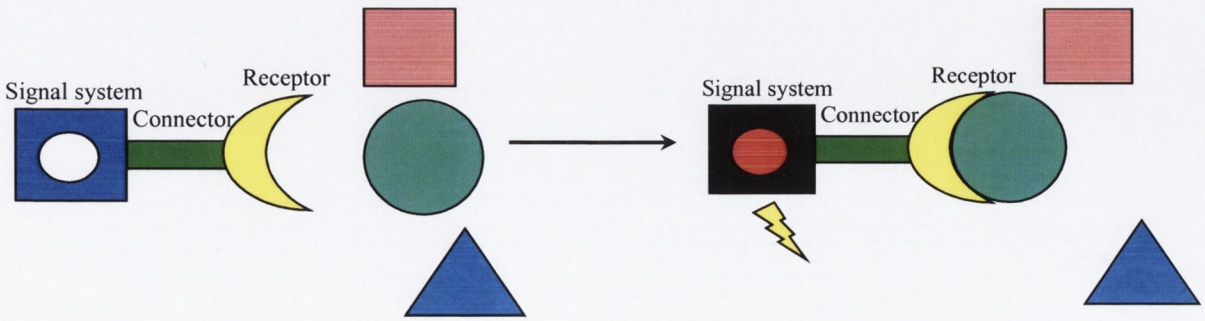

Scheme 1.1. Representation of a luminescent sensor showing selective binding of a substrate (recognition), followed by production of a light indication (signalling).

1.1.1 Fluorescent Sensors

Some of the classic examples of luminescent sensors utilise a fluorescent signalling moiety. The term fluorescence describes the emission of a photon of light from the first excited singlet state (S_1). When a molecule absorbs a photon of light an electron is excited from the singlet ground state (S_0) to the first excited singlet state (S_1). After relaxing to the lowest vibrational level within this state, the electron may then return to the ground state S_0, either by a non-radiative deactivation, or by emitting a photon of light with energy ($h\upsilon$) equal to the energy gap between the two states. The fluorescent emission of a photon from a S_1 state is an allowed process and is characterised by a very short lifetime, 10^{-9} seconds (ns).[2] Alternatively, the electron can enter the triplet excited state (T_1) by means of inter system crossing (ISC). The emission of a photon accompanying the transition of an electron to the ground state from the triplet state ($T_1 \rightarrow S_0$), is known as phosphorescence. However, this transition is spin forbidden and hence occurs over a longer timescale than fluorescence. These processes can be illustrated in a Jablonski diagram, which is a simplified depiction of the relative positions of the electronic energy levels of a molecule (Figure 1.1). Vibrational levels in a given electronic state lie above each other, but their relative horizontal locations bear no relation to the nuclear separation of the states.[2]

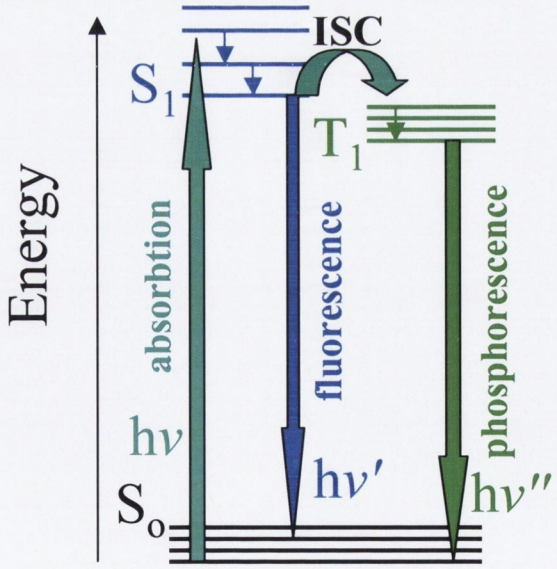

Figure 1.1. Jablonski diagram illustrating energy levels and states associated with fluorescence and phosphorescence[2]

There are numerous examples of sensors that employ organic molecules as fluorescent signalling moieties. One early such example developed by de Silva *et al.* are the "*off-on*"

sensors for H^+, **1**,[3] Na^+, **2a** and K^+, **2b**.[4] In these systems the anthracene moiety functions as the fluorophore, while the crown ether is the receptor, and they are attached by a methylene spacer. In the absence of any cations the fluorophore shows very little fluorescence as an electron transfer to the anthracene moiety, from nitrogen lone pair of the receptor, prevents any radiative decay (Scheme 1.2). However, upon binding H^+ in the case of **1**, Na^+ in the case of **2a**, or K^+ in the case of **2b**, the receptor is unable to participate in electron transfer due to the increased oxidation potential of the receptor's HOMO. As a result, the anthracene fluorophore can now fluoresce and shed its excited energy by emitting a photon, returning to the ground state. This is illustrated in Scheme 1.3.

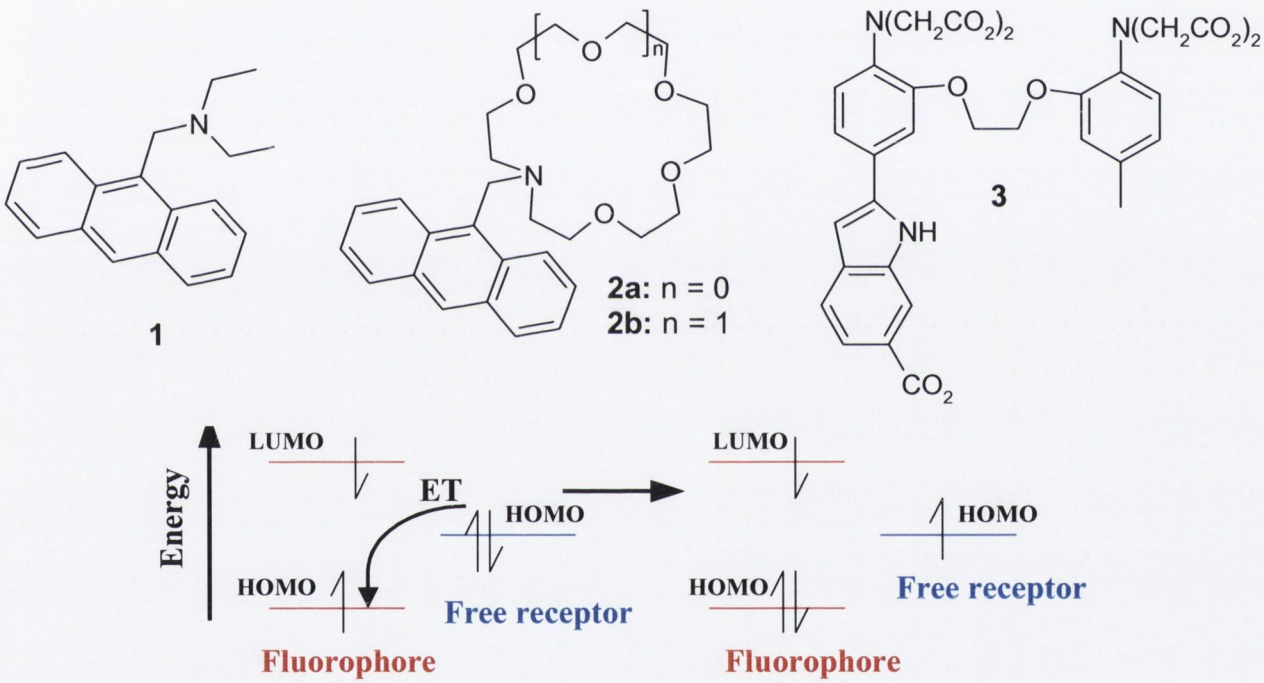

Scheme 1.2. Free Receptor – an electron transfer (ET) from the receptor prevents the fluororphore from losing its excited energy by radiative decay

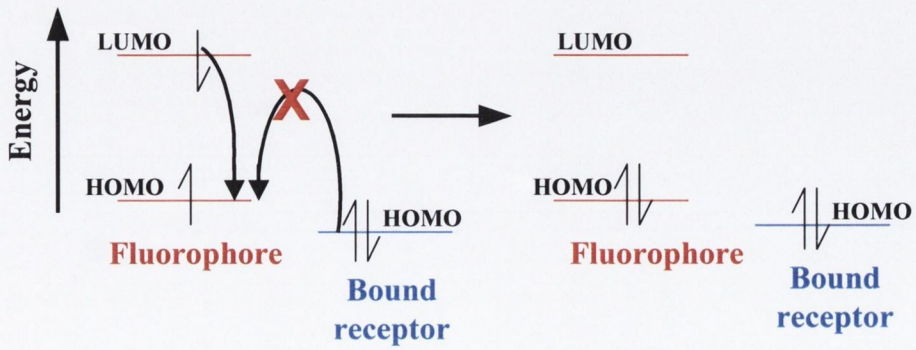

Scheme 1.3. Bound Receptor – the receptor is now lower in energy than the fluorophore and hence cannot participate in an electron transfer. Consequently the fluorescence is switched on as the fluorophore loses its energy by emitting a photon

Another example of an early fluorescent sensor was developed by Tsien and co-workers who synthesised the Ca^{2+} sensor **3**.[5] In its metal free state the nitrogen lone pairs are again involved in stabilizing the excited state of the chromophore giving rise to a long wavelength emission. Upon binding of a Ca^{2+} ion, however, the emission shifts to shorter wavelengths as the nitrogen lone pairs are now involved in the binding.

The above molecules are all classed as cation sensors, their signalling systems are based on fluorescent organic molecules and their receptors are selective for cations. Of equal importance is the area of anion sensing, especially anions with biological relevance. Gunnlaugsson *et al.*[6] have recently developed a range of "*on-off*" sensors **4** - **6**, which showed ideal PET behaviour in DMSO. In the absence of any ions the fluorescence is "switched on". The fluorescent emission is then quenched by the presence of AcO^-, $H_2PO_4^-$, and F^-, selectively over Cl^- and Br^-. These sensors operate in a manner similar to that described in Scheme 1.2, except that the unbound receptor is lower in energy and does not participate in electron transfer, while the bound receptor is higher in energy and does participate in electron transfer thereby quenching the anthracene fluorescence, *i.e.* the sensor is "switched on" in its free state and quenched, or "switched off", after binding the analyte.

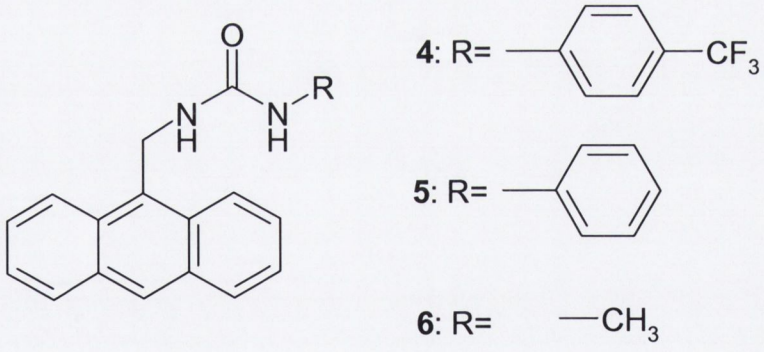

One of the major drawbacks of fluorescent sensors comes into play when working *in vivo* due to autofluorescence from biological systems. This is noise that is caused by short-lived background fluorescent emissions from the tissue itself, which can mask or drown out the fluorescent signal of the sensor.[7] The relatively new field of metal based luminescent sensors overcomes this problem due to the long lived nature of the light emission. The most common metal based luminescence systems utilise transition metals such as Ru(II) and Os(II).[8, 9] However, the focus of this thesis shall be upon lanthanide luminescent systems, which are the subject of the following section.

1.1.2 Photophysics of Lanthanide Luminescence

As mentioned above, the final signalling step performed by a luminescent sensor can be problematic when dealing with biological samples, as any light signal must compete against autofluorescence and light scattering, short lived background radiation with a ns timescale, from the body tissue itself. Lanthanide luminescent sensors may be employed here in order to circumvent these problems.

The fifteen elements from lanthanum to lutetium with access to their 4*f* shell are known as the lanthanides.[10] They are all hard, electropositive metals and the nature of their 4*f* shells imparts some unique properties to the lanthanides. The electronic shielding of the *f* electrons is quite weak and hence increasing atomic number or nuclear charge, causes a decrease in the radii of the atoms as one proceeds from La to Lu, which is known as the lanthanide contraction.[10] The lanthanides are easily oxidised and favour the 3^+ oxidation state with few exceptions.[11] The *f* orbitals are buried within the atom and hence interact with ligand orbitals only very weakly. As a result, $f \rightarrow f$ transitions, which occur in the visible region of the spectrum, give rise to very narrow bands and the lifetimes of their excited states are quite long lived (μs-ms).[11]

Systems which utilise emissive lanthanide conjugates as signalling moieties have some significant advantages over analogous fluorescent systems allowing them to overcome the autofluorescence and light scattering of body tissue.[12]

- Their long lived excited states (ms for Eu(III) and Tb(III)) allows the short-lived background fluorescence to disperse before the lanthanide emission occurs (Figure 1.2).[15]
- The long wavelengths (500-750 nm for Eu(III)) at which lanthanides emit occur beyond the absorbance of body tissue, this is important for signal quality.
- Their line-like emission bands (10 nm) also give a better signal to noise ratio compared to fluorescent bands (several hundred nm).

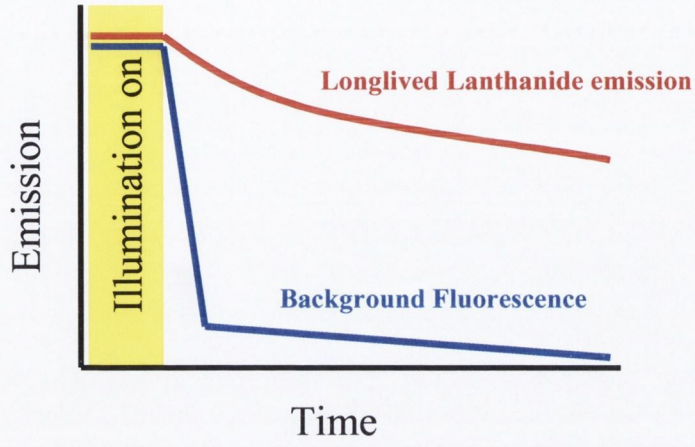

Figure 1.2. Lanthanide ions possess a long lived exited state which continues to emit long after background fluorescence has dispersed.

The long-lived lanthanide excited state allows the short-lived background fluorescence to disperse before the lanthanide emission is measured thus giving a much improved signal to noise ratio. However, before a lanthanide emission can occur, the lanthanide ion must first be elevated into this excited state. Direct excitation of a lanthanide ion is not easily achieved, as it requires a Laporte forbidden *f-f* transition (low extinction coefficient $\varepsilon \sim 5$-$10\ M^{-1}\ cm^{-1}$).[13, 14, 15] As a result lanthanides are usually photophysically "silent" and have low molar absorbencies.[15] However, this problem can be circumvented *via* indirect excitation by connecting a sensitising chromophore or "antenna" to the lanthanide ion (Figure 1.3).[16] Once excited, the antenna can then pass its excited energy onto the lanthanide ion by an energy transfer process, resulting in a lanthanide emission (high extinction coefficient $\varepsilon \sim 40K\ M^{-1}\ cm^{-1}$).[14, 15]

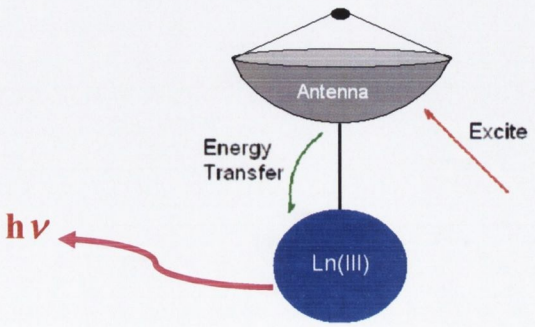

Figure 1.3. Indirect lanthanide excitation, involving, excitation of the antenna, followed by energy transfer to the lanthanide ion resulting in a lanthanide emission.

This indirect excitation of a lanthanide ion can be illustrated in a Jablonski diagram, (Figure 1.4). The sensitising antenna, denoted Ar, absorbs a photon of energy hν, and is excited to its singlet excited state, ^{1}Ar. From here the energy can be passed into the antennas triplet excited state, ^{3}Ar, *via* intersystem crossing (ISC). The lanthanide's excited state, *Ln, can now be populated from the antennas triplet state, by means of an intramolecular energy transfer (ET), provided that this triplet state is higher in energy than the lanthanide excited state.[17] The excited energy now resides within the lanthanide ion, and can be lost by emission of light, resulting in the characteristic lanthanide emission spectra as each transition will correspond to an emission band.

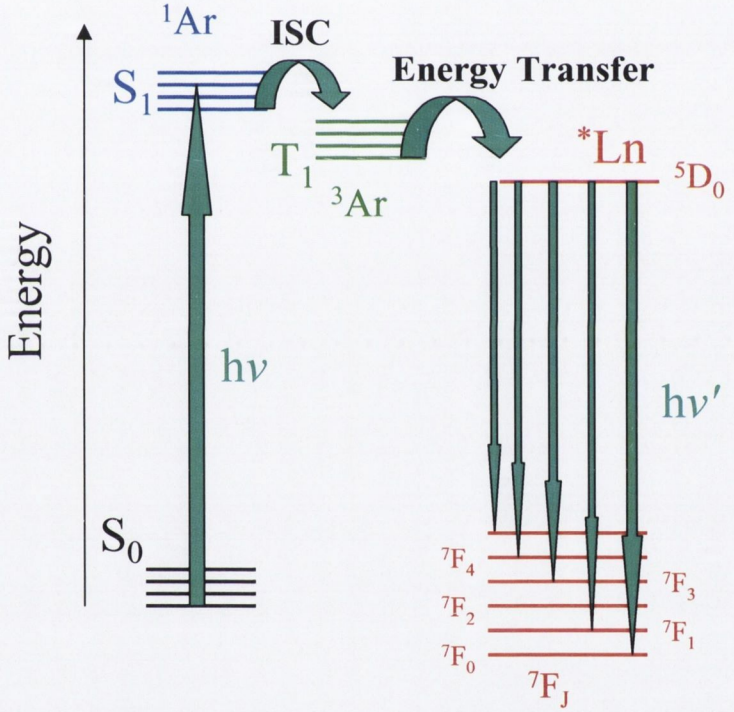

Figure 1.4. Jablonski Diagram illustrating sensitisation of a lanthanide ion. Other energy loss pathways have been omitted for clarity[18]

Singlet and triplet excited states share a common geometry where their potential energy curves intersect (Figure 1.5),[2] but intersystem crossing from a S_1 to T_1 state is a spin forbidden process. Nonetheless, when a mechanism for unpairing electrons exists the excited molecule may undergo intersystem crossing ISC to the triplet state. The presence of a heavy atom such as a lanthanide ion in the molecule, gives rise to a significant amount of spin-orbit coupling and it is this which provides a mechanism for intersystem crossing from the S_1 to T_1 state.[2, 19]

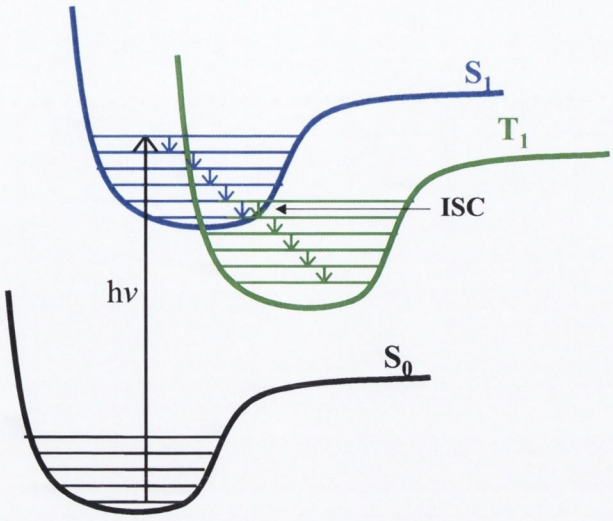

Figure 1.5. Potential energy wells showing vibrational levels. Note the overlapping common geometry of the T_1 and S_1 states. Intersystem crossing (ISC) from a singlet to a triplet excited state $S_1 \rightarrow T_1$ is made possible by spin-orbit coupling.[2]

The mechanism for energy transfer from the $^3Ar \rightarrow {}^*Ln$ state is somewhat debated. One possible mechanism is the Förster energy transfer mechanism,[20] which involves overlap of energy levels. In the Förster mechanism energy transfer occurs through space and has a r^{-6} distance dependence, where r is the distance between the metal ion and the excited chromophore. Consequently, the energy transfer process can be made more efficient by minimising the distance between the lanthanide ion and the chromophore or "antenna".

The alternative mechanism for the energy transfer is known as the Dexter mechanism and involves an electron exchange between the excited chromophore and the metal ion in a through bond interaction and should display a e^{-r} dependency.[21, 22] Again the process can be made more efficient by minimising the distance r.

Of course, the pathway shown in Figure 1.4 is not the only means by which the excited energy can be lost. This pathway must compete with other mechanisms through which the energy can be discarded (Scheme 1.4).[2] Energy can be lost from the singlet excited state ^1Ar through radiative decay *i.e.* fluorescence, or non-radiative decay by collisions and vibration interactions with the surrounding molecules. When a photon is emitted from the triplet ^3Ar state, this is known as phosphorescence. Phosphorescence has a longer lifetime than fluorescence owing to the fact that it is a spin forbidden process.[2] Triplet states may also be quenched by interactions with molecular oxygen.[15] The lanthanide excited state $^*Ln$ can also lose its energy through non-radiative decay by vibrational interactions with other molecules, such as water.[23]

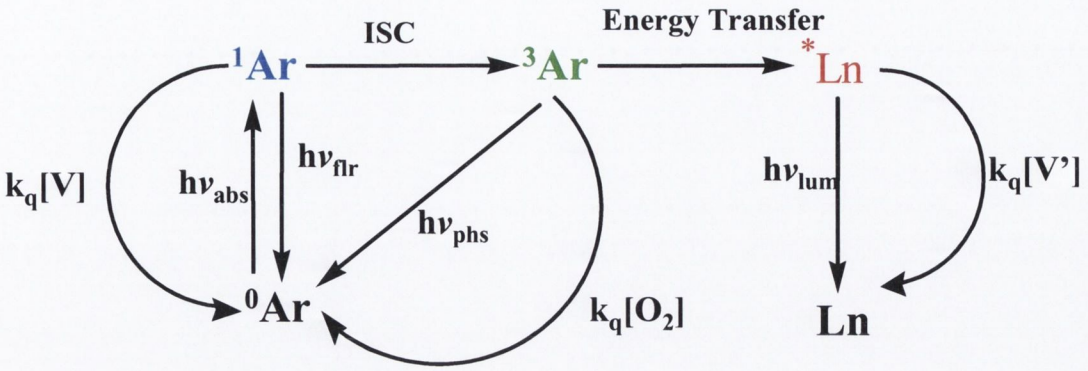

Scheme 1.4. Competing paths for energy loss include radiative decay through fluorescence $h\nu_{flr}$ and phosphorescence $h\nu_{phs}$, aswell as non-radiative quenching due to vibration, $K_q[V']$, and triplet quenching by O_2, $K_q[O_2]$[14, 15]

In order for the preferred pathway to operate *i.e.* population of the lanthanide excited state followed by a lanthanide emission, the design must minimise energy loss to other pathways. By maximising the efficiency of the intersystem crossing and energy transfer processes, it is possible to minimise the amount of time that the excited energy spends in the ^{1}Ar and ^{3}Ar states and therefore minimise the loss to deactivation pathways from these states. As stated before, ISC is made possible by spin-orbit coupling, which is increased by the presence of a heavy atom, so the very presence of a lanthanide ion itself will elegantly increase the efficiency of this process.[2]

Once in the lanthanides orbitals, the energy is somewhat isolated from its environment.[11] Back energy transfer is possible but minimised by having the ^{3}Ar state sufficiently higher above that of the *Ln state. Vibrational quenching by metal bound water molecules is now the main competing deactivation pathway.[23] The use of a tightly binding chelating ligand will reduce the number of metal bound water molecules, and thus minimise non-radiative quenching by O-H oscillators.[15]

So to summarise, in order to produce a lanthanide emission a conjugate must be designed such that an antenna with a triplet energy above that of the lanthanide excited state, is in close proximity to the lanthanide ion. Furthermore, the design requires the lanthanide ion to be tightly bound by a ligand to minimise the number of metal bound water molecules and maximise stability and solubility. The next section shall detail some examples where sensors have utilised lanthanide luminescence as a signalling moiety.

1.1.3 Lanthanide Luminescent Sensors

Numerous sensing systems have been designed that take advantage of luminescent lanthanide ions as signalling moieties.[14,15,24] One such system that was reported by de Silva *et al.* is the pentadentate terpyridyl ligand **7**.[25] When complexed to a lanthanide ion, this conjugate is designed to function as a pH sensor with the amino groups acting as the proton receptors, the pyridyl groups acting as the sensitising antenna and the lanthanide ion acting as the signalling moiety. The sensor functions in water but was not stable and thus a 100 fold excess of lanthanide ion was used to ensure the desired complex was present. Upon protonation of the amine receptors the lanthanide luminescence was observed to increase with enhancements of up to 16 times the original intensity. This was attributed to the suppression of electron transfer to the singlet excited state of the ligand due to the protonation of the aminoalkyl group.

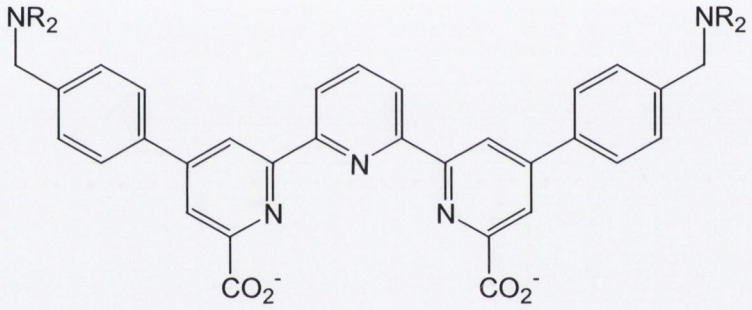

7

Another more stable example was reported by Gunnlaugsson *et al.*, who developed the lanthanide conjugate **8**, whose Eu(III) luminescence displayed a dependence upon pH, under highly acidic conditions.[26] In this case the *N*-(3-quinolyl)ethanamide functions as both the antenna and the receptor, as the quinoline nitrogen behaves as a H^+ acceptor. Under alkaline conditions (above pH 6), the Eu(III) luminescence of **8** was quenched, while between pH 6 and 3.5, the complex was found to be only weakly luminescent with the Eu(III) emission remaining almost constant over this pH range. However, between pH 3.5 and 1.5 and after excitation at 350 nm, the Eu(III) luminescence was "switched on" with an enhancement factor of *ca.* 300. This was attributed to the protonation of the quinoline moiety, which allowed the antenna to better transfer its excited energy to the lanthanide ion.

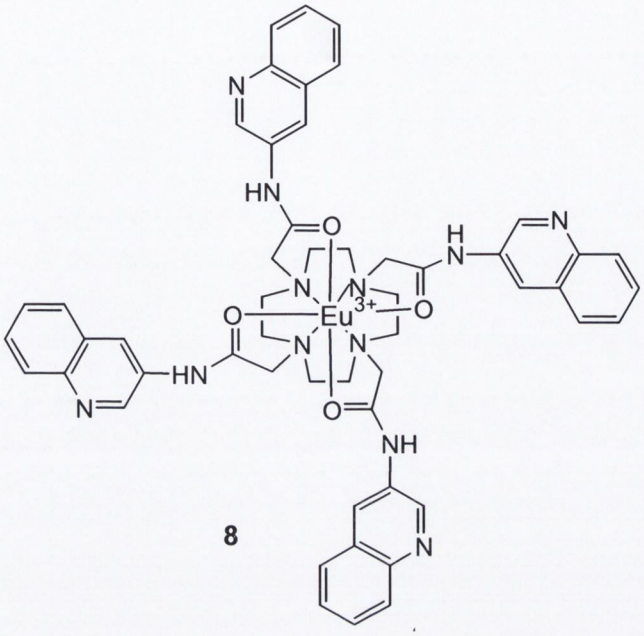

8

Woods and Sherry have also reported examples of lanthanide luminescent pH probes.[27] The aryl substituted tetraamide complexes **9**-**11**, take advantage of the $\Delta J2/\Delta J1$ intensity ratio. The Eu(III) $^5D_0 \rightarrow {}^7F_1$ ($\Delta J1$) transition is known to be insensitive to ligand field effects, while the $^5D_0 \rightarrow {}^7F_2$ ($\Delta J2$) transition is considered to be hypersensitive to the coordination environment of the Eu(III) ion.[28] After excitation (*via* the chromophore), the Eu(III) complex **9**, displays a Eu(III) emission, however, the $\Delta J2/\Delta J1$ intensity ratio of this emission is dependant upon the pH of the solution, reaching a maximum between pH 6 and 8. This particular method of measurement may offer a unique advantage as the results are independent of the Eu(III) complex concentration. The authors found it was possible to alter the pH window of operation by varying the ligand, for instance **10** demonstrates changes between pH 7 and 9. The authors attributed the changes in luminescence to the deprotonation of the amide groups followed by increased electron transfer to the easily oxidized Eu(III) ion.[14]

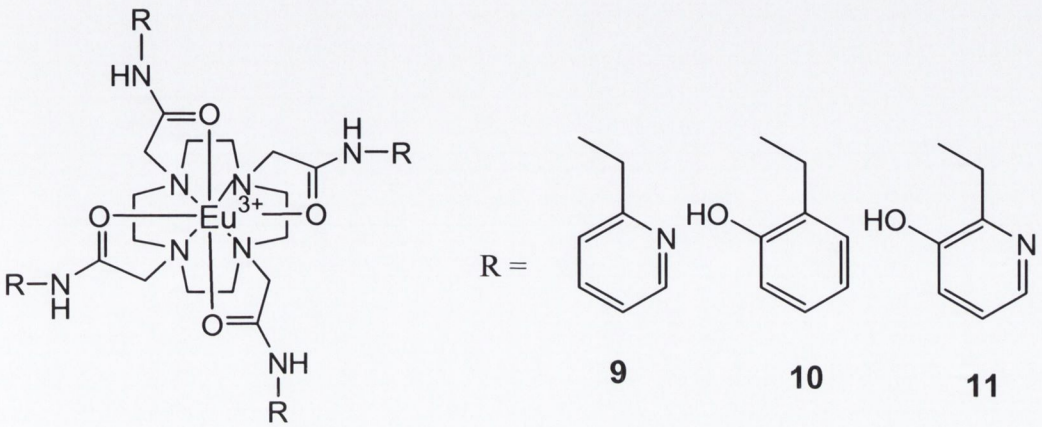

9 **10** **11**

Parker *et al.* described the charge neutral, Eu(III) complex of **12**, which employs a phenanthridine moiety as the sensitising antenna.[29] The complex was found to display significant pH dependence. After excitation at 340 nm, a 500 fold luminescent enhancement of the Eu(III) emission could be observed upon protonation of the phenanthridine nitrogen (pK_a = 4.45). Meanwhile, the *N*-methylated analogue **Eu.13**, was found to have its luminescence "switched on", independent of the pH. However, its luminescence was effectively quenched by the addition of Cl^-, Br^- or I^-. Interestingly the luminescence was unaffected by the presence of the anions of phosphate, citrate, lactate or bicarbonate and as such may have applications as an intracellular Cl^- sensor. Further examples of anion sensors shall be discussed in section 1.7.

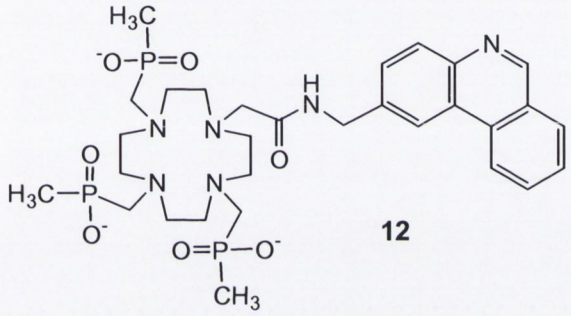

12

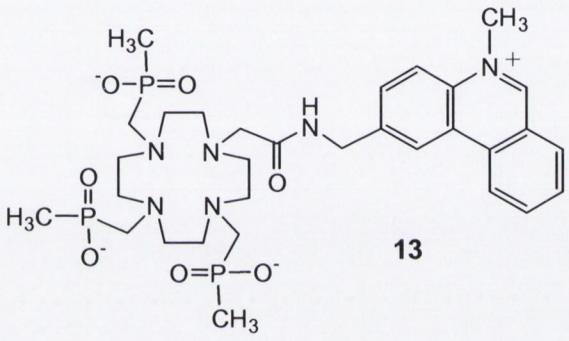

13

As stated earlier, the Tb(III) $^5D_4$ excited state is of higher energy than the Eu(III) $^5D_0$ state (20500 and 17200 cm^{-1} respectively),[15] and this higher energy state conveys some interesting properties to the Tb(III) complexes of **12** and **13**.[30] The triplet state energies of the phenanthridine antennae were estimated to be 22000 and 21300 cm^{-1} respectively. As the gap between the triplet states and the $^5D_4$ excited state is less than 1500 cm^{-1}, thermal back energy transfer from the lanthanide to the chromophore is possible and consequently, the luminescence becomes dependant upon the presence of molecular oxygen, which can effectively quench the chromophore triplet state.[17] The complex **Tb.13**, exhibited a strong luminescence in degassed solution, which was independent of the pH between 2 and 9. However, the presence of dissolved oxygen in the solution efficiently quenched the luminescence of **Tb.13**, which effectively acts as an oxygen sensor.[31]

Gunnlaugsson *et al.* have also developed luminescent sensors that act like pH probes as well as molecular logic gates.[32] The Eu(III) complex **Eu.14**, is an example of a pH chemosensor. When **Eu.14** was excited at 330 nm under ambient conditions in aqueous alkaline solution the Eu(III) emission was found to be "switched off". Nevertheless, the

Eu(III) emission could be gradually enhanced by increasing the acidity of the solution with luminescent enhancement factors of up to 250 fold. This increase in luminescence was attributed to the protonation of the quinolyl nitrogen moiety, which greatly enhanced sensitisation of the lanthanide ion, due to increased ease of populating the S_1 state of the antenna. The Eu(III) emission was found to be "switched on" over the pH 6.5 – 4.5 region. In contrast, the acidification of an aqueous solution of the Tb(III) complex **Tb.14**, gave rise to much smaller luminescent enhancements of *ca.* 1.7. This was ascribed to a quenching of the antenna's triplet state by the presence of molecular oxygen. Consequently, when the measurements were repeated in degassed acidic solution, the Tb(III) emission was "switched on" with a 50 fold luminescent enhancement factor. As the Tb(III) emission is governed by two molecular inputs, and is only "switched on" in the presence of H^+ and the absence of O_2, **Tb.14** can be described as a NAND or "inhibit" logic gate (a combination of the NOT and AND logic functions).

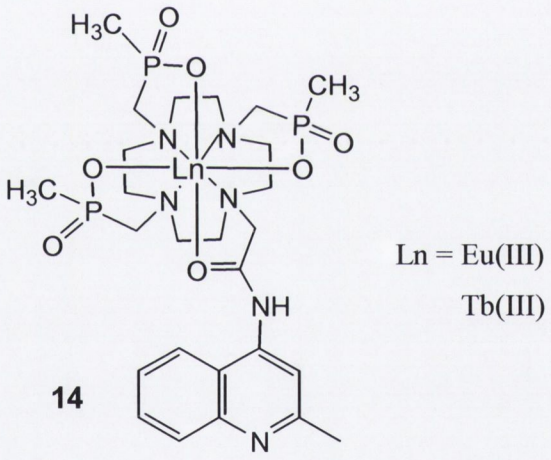

14

Ln = Eu(III)
Tb(III)

From these examples it can be seen that lanthanide luminescent sensors have great potential as *in vivo* probes as they are non-invasive causing minimal disturbance to the system under study, yet emit at long wavelengths offering better signal quality over fluorescent probes. The next section shall detail the use of lanthanide luminescent probes as cation sensors.

1.1.4 Lanthanide Luminescent Probes as Cation Sensors

Lanthanide luminescent probes have been shown to be effective tools for pH sensing however, by altering their receptors, such probes can be utilised as cation sensors. One

such system that utilises such probes for the sensing of Zn(II) cations was developed by Gunnlaugsson *et al.* Their zinc sensor **Eu.15** showed a 42% enhancement in luminescence upon 1:1 binding of Zn(II), while **Tb.16** showed a 60% increase in luminescence.[33,34] The increasing luminescence upon the coordination of Zn(II), was attributed to the suppression of photo-induced electron transfer from or to the intermediate singlet excited state, S_1.[35] Both sensors were selective for Zn(II) over Ca^{2+} and Mg^{2+}.

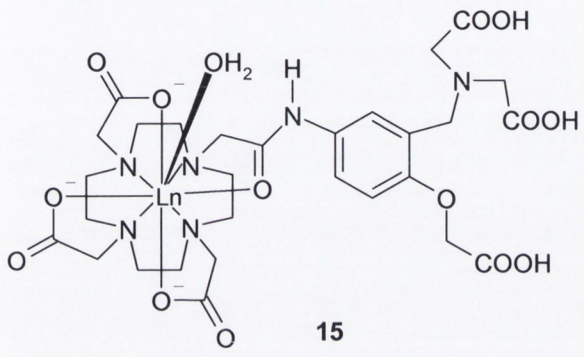

15

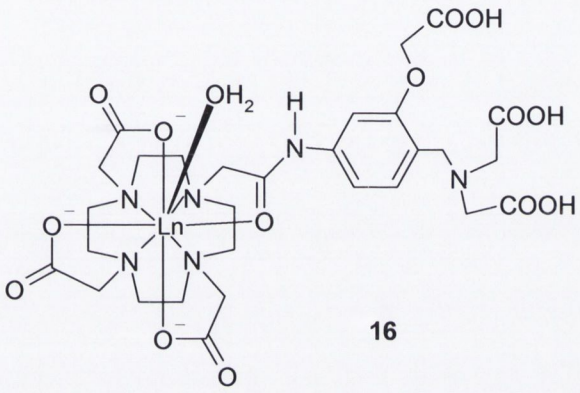

16

Nagano and Kikuchi reported another such sensor, the Eu(III) complex of a combination of diethylenetriaminepentaacetic acid (DTPA) and a quinoline containing TPEN ligand, **17**.[36] The quinoline antenna was chosen due to its longer absorption wavelength (>300 nm), which offers advantages for *in vivo* work. Upon addition of Zn(II) to an aqueous solution of **Eu.17** (50 μM), at pH 7.4, a 8.5 fold increase in the luminescence was observed after excitation at 320 nm. Further investigation revealed a 1:1 stoichiometry, with an apparent dissociation constant K_d of 59 nM for Zn(II). The presence of Na^+, K^+, Ca^{2+} or Mg^{2+} did not give rise to any enhancement in the luminescence and furthermore, the luminescence of the complex was found to be insensitive to pH between 3.6 and 8.8. Consequently, the Eu(III) complex **Eu.17**, can be considered as a useful probe for the biological detection of Zn(II).

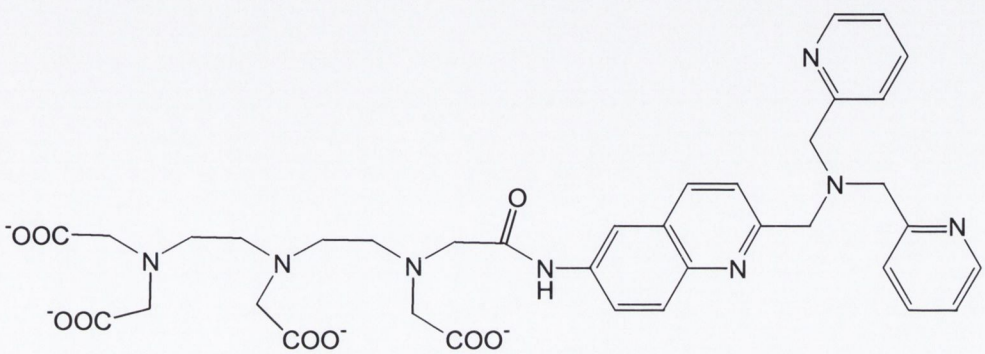

17

Wong and co-workers described the Tb(III) complexes of **18** and **19**.[37] The luminescent lifetime of **Tb.19** in H_2O was found to increase by 65 % upon the addition of NaCl 0.13 mM, from 1.81 ms to 3.02 ms, this was accompanied by a decrease in the hydration state *q* from one to zero. Further investigation showed that this effect was independent of the choice of anion. The effect was ascribed to the interaction between the crown ether and the Tb(III) centre resulting in the displacement of a metal bound water molecule. Interestingly, the Tb(III) complex **Tb.18**, did not respond to the presence of the alkali metal ions.

The authors also found that the luminescent intensities of both **18** and **19** increased substantially upon the addition of *p*-chlorobenzoate **20**, with luminescent enhancement factors of 49 and 5 respectively, after excitation at 246 nm in H_2O. Significantly, when the Na^+ cation in **20** was replaced by a tetrabutylammonium cation the luminescent enhancement decreased from 49 to 7. These studies suggested that the crown ether effectively binds the Na cation which facilitates the close approach of the benzoate anion to the Tb(III) complex, permitting it to act as a sensitising antenna, providing efficient energy transfer to the Tb(III) metal centre. This ion pair sensor leads nicely to the next section, which discusses the use of luminescent lanthanide probes as anion sensors.

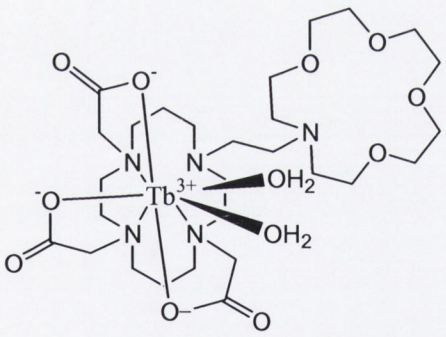

18

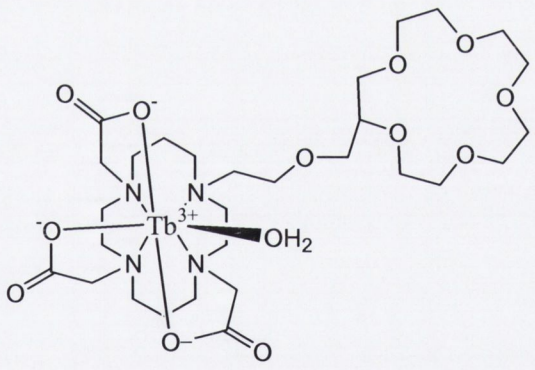

19

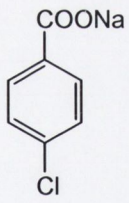

20

1.1.5 Lanthanide Luminescent Probes as Anion Sensors

The large positive charge of the lanthanide ions as well as the sensitivity of their emission spectra to their coordination environment, make lanthanide ions ideal sensors for the detection of anions. Charbonnière *et al.* developed lanthanide complexes of a bis-bipyridine-phosphine-oxide ligand **21**, as luminescent anion sensors.[38] The bipyridine (bipy) units were expected to coordinate to the lanthanide ion and function as sensitising antennae, while the strong coordinating ability of the P=O bond[39] would increase the

stability of the complex, despite the fact that it would remain coordinately unsaturated, with two solvent molecules occupying the final coordination positions. It was found that in aqueous solution neither **Eu.21** nor **Tb.21** gave rise to any luminescence, indicating that neither of the bipy units were coordinated to the lanthanide ions under these conditions. In MeCN solution, after excitation of the bipy absorption bands (310 nm), the triflate salt complexes were found to display the typical lanthanide luminescence bands. No change was observed upon the addition of fluoride or acetate ions, however, upon addition of tetrabutylammonium nitrate **Eu.21** and **Tb.21**, respectively, underwent an 11 and 7 fold increase in their luminescent intensities. The same trend was observed upon addition of chloride anions with a 5 and 2.5 fold increase in luminescent intensities, respectively. The reason for these dramatic changes in the luminescence spectra was ascribed to the coordination environment of the lanthanide ions. In MeCN the triflate counter anions do not bind directly to the lanthanide ion and hence two solvent molecules occupy the remaining open coordination positions. However, the addition of nitrate anions leads to an increased emission from the lanthanide ions as the nitrate ion displaces the metal bound solvent molecules and binds directly to the metal ion, thereby shielding the lanthanide from the solvent molecules and increasing the luminescence. The addition of a second equivalent of the nitrate anion displaces one of the bipy units. This leads to a further enhancement in the luminescence due to the resulting stronger electronic interaction between the lanthanide ion and the second bipy unit. Addition of a third nitrate ion to the metal ion decreases the luminescence as it displaces the final bipy unit and hence weakens the energy transfer mechanism.

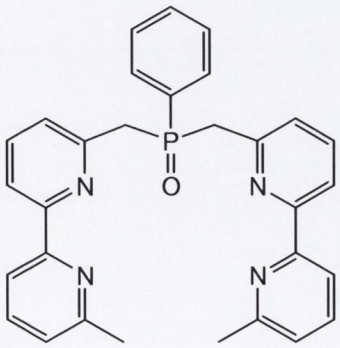

21

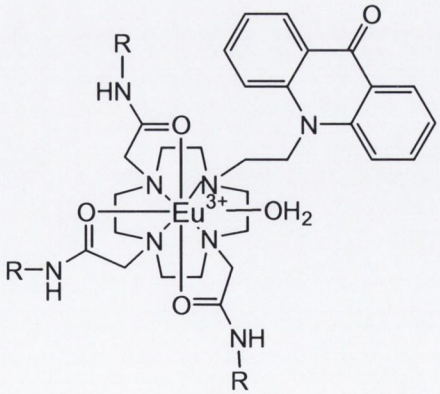

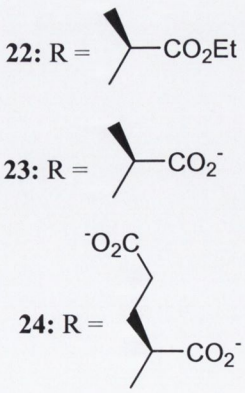

Other anion sensors have also been reported. Parker *et al.* developed a range of phosphate anion sensors **22** – **24**.[40] The acridone moiety of these complexes functions as the antenna, absorbing energy and passing it to the Eu(III) ion. Selectivity towards phosphates can be

tuned by varying the electrostatic gradient around the lanthanide ion,[41] achieved in this case by varying R. The binding of selected phosphates, as well as phosphorylated amino acids such as Ser-OP and Tyr-OP, were investigated by observing the emission spectra of the complexes **22** – **24** (0.1 mM) at 295 K, pH 7.4 (0.1 M MOPS) in the presence of a ten fold excess of phosphate. Job plot analysis revealed the formation of 1:1 adducts, which displayed subtlety different emission spectra, with Tyr-OP giving the lowest $\Delta J2/\Delta J1$ intensity ratio. As such phosphorylated tyrosine could be selectively detected by subtle changes in the Eu(III) luminescence.

Tsukube and co-workers reported the Eu(III) complex of tris(2-pyridylmethyl)amine **25**, as a luminescent sensor for nitrate, NO_3^-, while the corresponding Tb(III) complex displayed Cl^- selectivity.[42] The Eu(III) complexes of **25** and **26** display 1:1 stoichiometry and are stable enough for use in solution. In this case, the pyridine units fulfil the role of the sensitising antenna, absorbing at 260 nm before passing their energy to the lanthanide ion and inducing a lanthanide emission. However, the complexes are coordinately unsaturated and hence the metal bound solvent molecules effectively quench the luminescence. Nevertheless, upon the addition of 3 equivalents of NO_3^- to **Eu.25** in MeCN, or Cl^- in the case of **Tb.25**, the solvent molecules are displaced and the luminescence is increased by a factor of 4.9 and 5.4 respectively. Conversely, the addition of ions such as I^-, Br^-, F^-, ClO_4^-, SCN^- and HSO_4^- did not elicit a response. The achiral ligand **26** showed similar anion selectivity in MeCN, however, it displayed a lower sensitivity than the chiral analogue.

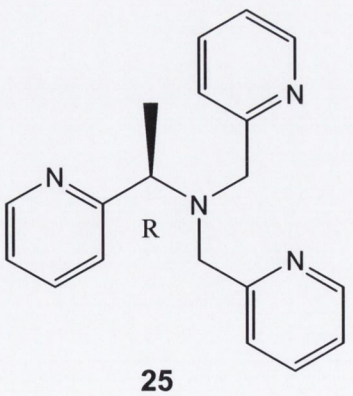

25

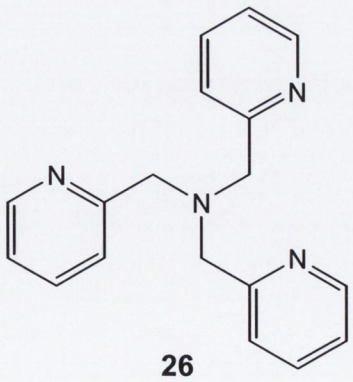

26

Michels and Reinhoudt described the Eu(III) and Tb(III) complexes of the EDTA-based β-cyclodextrin dimer **27,** which operate in H_2O at pH 7.0 as luminescent sensors for aromatic carboxylates.[43] As the ligand does not provide any sensitising antenna no luminescence

was observed. Nevertheless, upon the addition of **28**, the luminescence intensities of **Eu.27** and **Tb.27** increased by a factor of 350 and 310, respectively, after excitation of the aromatic chromophore at 250 nm. These large enhancements were ascribed to the hydrophobic binding contribution of the β-cyclodextrin units which can bind the aromatic unit thereby positioning the Ln(III) coordinating carboxyl group correctly to function as a sensitising antenna and allow efficient energy transfer to the lanthanide ion. The stoichiometry was reported to be 1:2 with a stability constant of $K = 5.0 \times 10^4\ M^{-1}$. As expected, the addition of the benzyl alcohol **29**, led to much smaller enhancements of *ca.* 2 fold. The authors explained this lower enhancement as owing to the lack of a carboxylate functionality through which the chromophore can bind to the lanthanide ion.

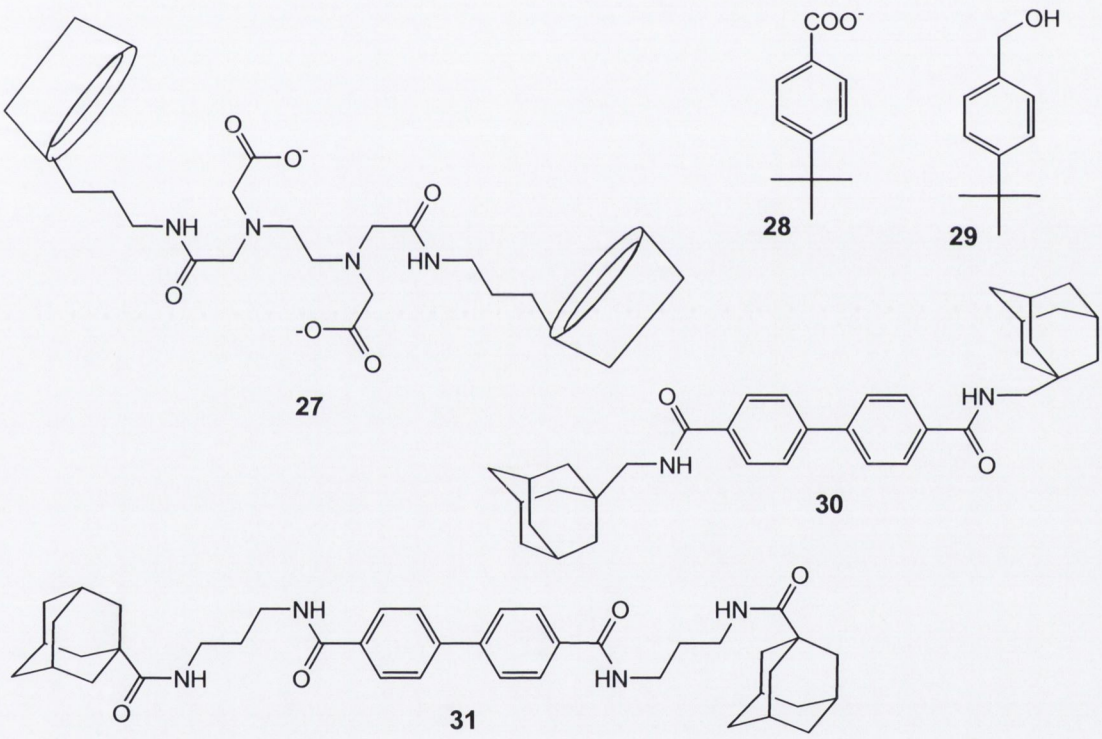

The interaction between **Eu.27** and bisadamantyl biphenyl sensitisers **30** and **31**, was also studied. Once again, upon excitation of the sensitisers at 285 nm, large increases in the Eu(III) luminescence was observed, *ca.* 300 and 360 fold for **30** and **31** respectively, in D_2O. A 1:1 binding stoichiometry was observed with stability constants K of 9.9×10^6 and $1.0 \times 10^7\ M^{-1}$ for the **Eu.27.30** and **Eu.27.31** conjugates respectively. The very high association constants suggest that both β-cyclodextrin cavities of **27** are involved in the binding of the bisadamantyl biphenyl sensitisers **30** and **31**.

Georges and Arnaud reported a method of salicylic acid detection using a combination of Tb(III) and ethylenediaminetetraacetic acid (EDTA).[44] The presence of the EDTA prevents

the formation of insoluble terbium hydroxides and also acts to exclude water molecules from the coordination sphere of the lanthanide ion, reducing quenching due to OH oscillators. A 1 x 10^{-4} M solution of **Tb.EDTA**, could detect salicylic acid with a limit of detection (LOD) of 5 x 10^{-9} M in water at pH 12, the high pH was required in order for the ternary luminescent chelates between salicylic acid and Tb(III) to form. In this case the analyte itself acts as the sensitising antenna, forming a ternary complex with **Tb.EDTA** and then passing its excited energy to the Tb(III) centre, provoking a lanthanide emission. The sensitivity increased in the presence of cetyltrimethylammonium chloride (CTACl) (LOD = 4 x 10^{-10} M) and the authors attributed this to the cationic surfactant forming micelles in solution. The use of organised materials such as micelles and cyclodextrins can greatly increase the efficiency of the intramolecular energy transfer and hence the overall luminescence.[24]

A similar method utilising ternary chelates of Tb(III) and trioctylphosphine oxide (TOPO) was reported by Pérez-Bendito and co-workers as a luminescent sensor for the determination of benzoic acid and saccharin in soft drinks.[45] This group also reported a kinetic method of determining salicylic acid and diflunisal (a salicylic acid derivative) based on lanthanide luminescence.[46] Coupled with the aid of a stopped-flow mixing technique, it again involved the formation of ternary chelates of salicylate (or diflunisal) and **Tb.EDTA**, this time in the presence of cetyltrimethylammonium bromide (CTAB), which acts as the cationic surfactant. They were able to determine between the two analytes due to the different rate of formation of the ion-association complex of CTAB and the anionic ternary complex. They used a similar method for the detection of bromadiolone (a coumarine derivative).[47]

In 2000, Parker *et al.* reported the heptadentate complex **32**.[48, 49] Lifetime studies revealed that the Eu(III) and Tb(III) complexes **Eu.32** and **Tb.32** each possessed two metal bound water molecules. The authors reported that in aqueous solution these water molecules could be displaced by anions such as phosphate lactate and carbonate, and that the formation of these 1:1 ternary complexes was signalled by changes in the lifetime of the Eu(III) and Tb(III) excited state.

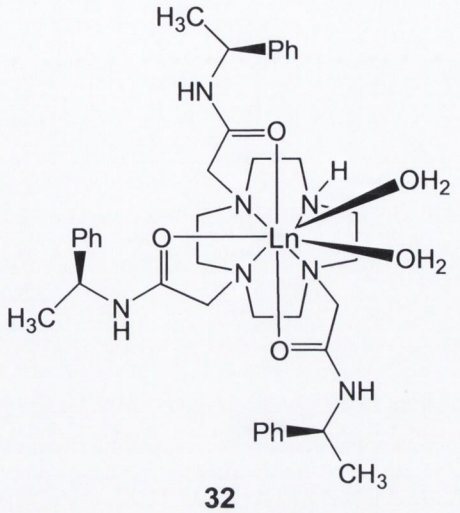

32

So far we have focused on the luminescence of the Eu(III) and Tb(III) complexes. They are by far the most popular ions due to their easily accessible excited states, their long lived excited nature and intense long wavelength emissions in the visible region of the spectrum.[24] Furthermore, these particular ions are not usually quenched by organic sensitiser molecules.[50] However, other lanthanide ions of interest are the near infrared emitting lanthanides of Yb(III) and Nd(III). Compared to Eu(III) and Tb(III), these ions posses lower energy emission states and hence can utilise chromophores with longer absorption wavelengths, offering improved detection limits for *in vivo* applications.[51] As these ions emit at wavelengths greater than 800 nm, specialised instruments are required for measuring them. The Faulkner group, and others, have detailed some elegant examples of sensitisation of Yb(III) and Nd(III) complexes by long wavelength absorbing chromophores.[51, 52, 53] However, as yet these systems have not been utilised as sensors.

1.1.6 Conclusion

It has been shown how a photonic, or light, response can be obtained from a lanthanide luminescent system by way of a sensitising antenna, and how this signalling moiety can be utilised for luminescent sensing, offering advantages over conventional fluorescent systems. We are concerned with the development of new luminescent sensors that employ lanthanide ion as signalling systems. The aim of this project is to construct a novel lanthanide luminescent system for the detection of the biologically relevant Cu(II) cation. The design, synthesis, photophysical properties and analysis of this system shall be the subject of Chapter 2. We shall also utilise lanthanide luminescent systems as anion

detectors, and Chapter 3 shall detail the development of sensors for aromatic caboxylates, focusing on *N,N*-dimethyl benzoic acid, salicylic acid and terephthalic acid.

1.2.0 Phosphodiester Hydrolysis

In recent years, there has been a sustained effort to develop synthetic molecules that cleave phosphodiester bonds efficiently.[54, 55, 56] Phosphodiester bonds perform an important task in nature, linking together the genetic code of the nucleic acids, deoxyribonucleic acid (DNA) and ribonucleic acid (RNA). In essence, the phosphodiester linking the nucleic acids together forms the backbone of both DNA and RNA. It was chosen by nature due to its incredible stability,[57] in order to preserve the genetic information. The negative charge on the phosphate drastically reduces the rate of hydrolysis and as a result, nucleic acids are very inert to cleavage under physiological conditions. It has been estimated that DNA has a half-life of 200 million years at pH 7 and 25 °C.[58] The major difference between DNA and RNA is the presence of the 2'-OH hydroxyl group on the ribose of RNA, which can act as an intramolecular nucleophile. As such, RNA can be hydrolysed with greater ease than DNA.[55] Despite this, RNA is still a very stable molecule, with a half-life thought to be of the order of hundreds of years, under physiological conditions.[59]

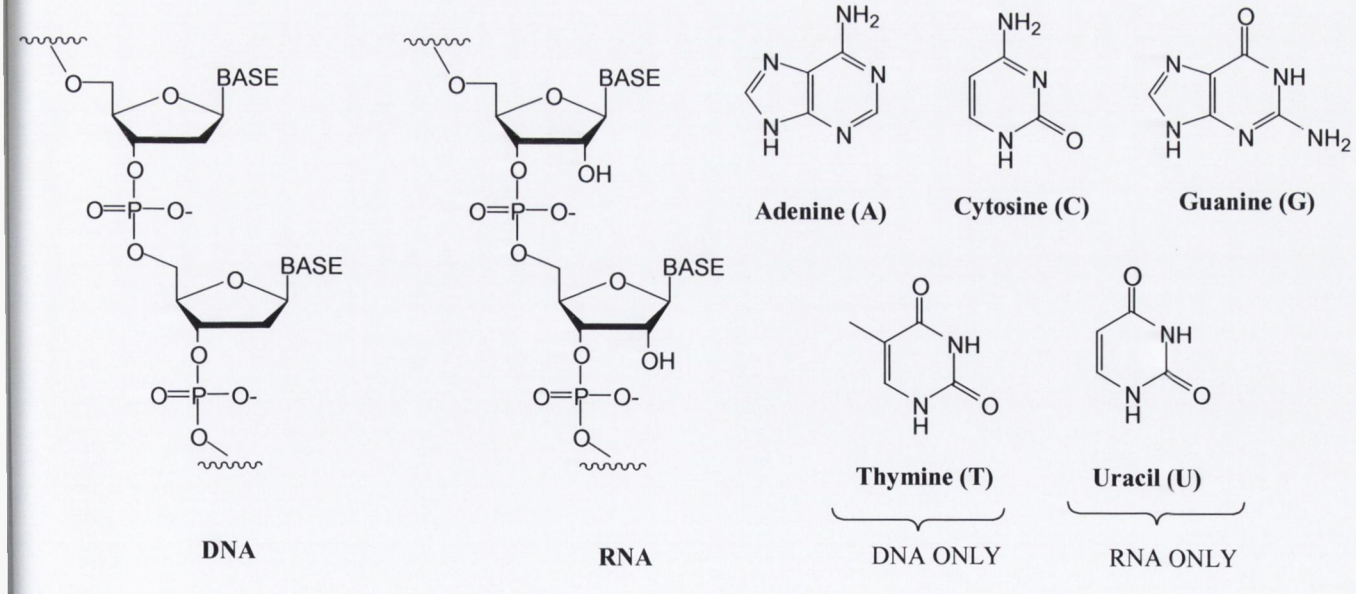

Figure 1.6. Illustrating the structural differences between the negatively charged phosphodiester backbone of DNA and RNA and nucleotide bases

The translation into proteins, of the genetic information encoded within DNA, is conducted by messenger RNA (mRNA).[60] The ability to selectively cleave this RNA would provide control over the production of undesirable proteins. Many diseases, including bacterial, viral, fungal and even some forms of cancer, could be targeted since they operate by producing harmful proteins.[54] The work within this thesis shall focus on RNA hydrolysis.

In nature, the hydrolysis of nucleic acids is carried out by a class of enzymes called hydrolases or ribozymes. [54,61] These enzymes frequently contain metal cations such as Ca^{2+}, Mg^{2+} and Zn(II), at their active sites.[55,62] The hammerhead ribozyme, for instance, which effectively cleaves RNA, is known to posses multiple Mg^{2+} metal cations at its active site.[63] The crystal structure of ribonuclease P1, which catalyses the hydrolysis of single stranded DNA and RNA, reveals the presence of three Zn(II) ions, at the active site (Figure 1.7).[64]

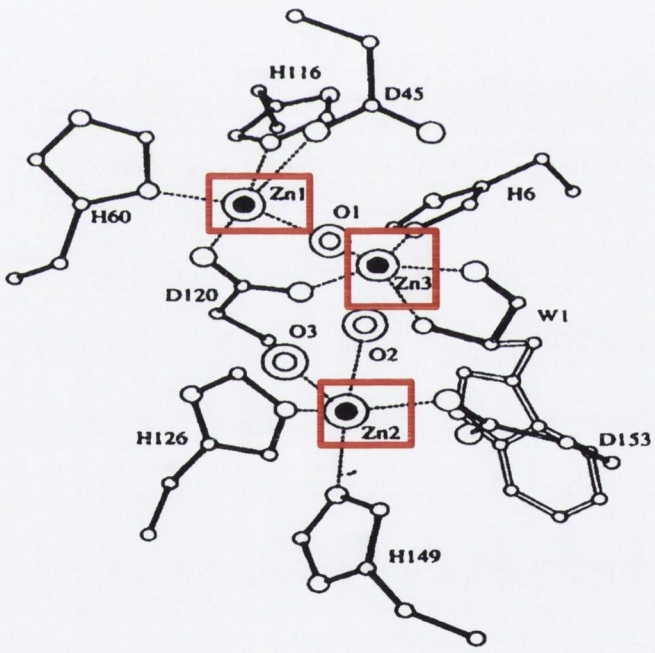

Figure 1.7. The active site of ribonuclease P1 possesses Zn(II) ions with bridging water molecules

The mechanism for the hydrolysis of RNA has been studied in detail.[57, 65] It is thought to proceed *via* a two step mechanism, which displays a pH dependence and can be catalysed by both general and specific acid/base catalysis (Scheme 1.5). In the first step, transesterfication, the 2'-OH group acts as a nucleophile and attacks the tetrahedral phosphodiester, giving a 5 coordinate phosphorane intermediate. The second step involves removal of the 5'-OH of the ribose from the phosphorous atom, *i.e.* hydrolysis of the

phosphorane. Nucleophilic attack on a negatively charged phosphodiester is unfavourable,[66] the five coordinate, doubly charged phosphorane intermediate is also unstable, however, both can be stabilized by protons, metal cations and/or a Lewis acid.[54] This has been cited as the reason why such a wide range of substances including protons, Cu(II), Zn(II) and lanthanide ions accelerate RNA cleavage.[54] The following section shall show and discuss how metal ions can accelerate the rate of phosphodiester cleavage.

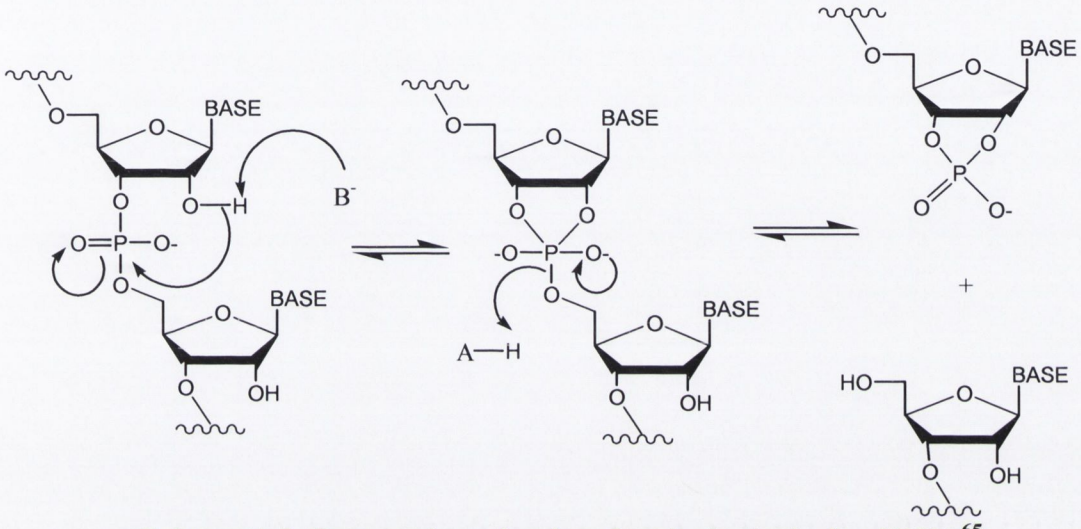

Scheme 1.5. Proposed mechanism for the hydrolysis of RNA[65]

1.2.1 Acceleration of Phosphodiester Hydrolysis by Metal Cations

It has been shown in numerous accounts that highly charged cations, particularly lanthanides, can greatly accelerate phosphodiester hydrolysis.[67,68,69] For instance, in 1993, Breslow *et al.* showed that metal cations accelerated the rate of hydrolysis of the RNA dinucleotide UpU[70] (Table 1.1). The lanthanide cation Eu(III), was found to promote the hydrolysis 15 times faster than Zn(II). This was attributed to the higher charge density of Eu(III) compared to Zn(II), which makes the lanthanide ion a stronger Lewis acid. Lewis acids accelerate the cleavage of phosphodiesters by binding to and stabilising the negatively charged phosphate ion, hence activating the phosphate towards nucleophilic attack. This is known as Lewis acid activation.[71] The authors found that a ten fold increase in Eu(III) concentration led to only a three fold rate increase, which suggests a kinetic saturation.

Catalyst	$k \times 10^3\ hr^{-1}$	k_{rel}
None	0.046 (± 0.004)	1
$ZnCl_2$ (1 mM)	1.46 (± 0.04)	32
$EuCl_2$ (1 mM)	22 (± 7)	475
$EuCl_2$ (10 mM)	67 (± 10)	1460

Table 1.1. Pseudo first order rate constants (k) and relative rate enhancements (k_{rel}) for the cleavage of UpU (3 mM) in 10 mM HEPES (pH 7.0) at 80 °C[70]

In addition to this, it was also shown that metal cations increased the rate of hydrolysis for simpler model phophodiesters such as 2-hydroxy *p*-nitrophenylphosphate (**HPNP**) (Table 1.2). The phosphodiester **HPNP**, is often utilised as an RNA model compound due to the ease of kinetic analysis, which can be followed by absorbance spectroscopy. It will be employed throughout this thesis, and discussed in greater detail later.

Catalyst	$k \times 10^2\ hr^{-1}$	k_{rel}
None	0.012 (± 0.001)	1
$CaCl_2$	0.032 (± 0.004)	3
$MgCl_2$	0.53 (± 0.20)	46
$ZnCl_2$	1.70 (± 0.12)	150
$PbCl_2$	32 (± 6)	2800
$EuCl_3$	88.9 (± 4.5)	7700
$TbCl_3$	110 (± 6)	9500
$YbCl_3$	109 (± 6)	9500

Table 1.2. Pseudo first order rate constants (k) and relative rate enhancements (k_{rel}) for the cleavage of HPNP (0.18 mM) in 10 mM HEPES (pH 7.0) at 37 °C with various metal ions (0.5 mM)[70]

The results shown in Table 1.2, clearly illustrate that lanthanide ions are by far the most effective at accelerating the hydrolysis of phosphodiesters. The cleavage of **HPNP** by Eu(III) was found to be 50 fold more effective than cleavage promoted by Zn(II). The Tb(III) ions were found to be slightly more active than the Eu(III) ions, which can be explained by their smaller size and hence greater Lewis acidity. However, the similarity between Tb(III) and Yb(III), suggests that ionic radius is not the only determining factor for the activity of the free ions, as Yb(III) is considerably smaller.[70]

Roigk and Schneider, investigating the effect of varying lanthanide concentrations upon hydrolysis of phosphate esters, found that the lanthanides displayed Michaelis-Menten saturation kinetics (*i.e.* the rate became independent of the concentration of metal ion at high concentrations).[69] Furthermore, it was found that the efficiency of the heavier lanthanide ions such as Lu(III) and Yb(III), actually decreased at higher concentration (0.1

– 0.5 mM). This decrease in efficiency was attributed to the formation, at higher concentrations, of aggregates of these ions. Indeed the lanthanides with the greatest Lewis acidity were only the most effective when applied at low concentrations (0.05 mM). It was also noted that the presence of NaCl or $MgCl_2$ reduced the rate of cleavage of phosphodiesters due to competitive binding with the substrate.

Despite these factors, metal ions, and lanthanide ions in particular, remain excellent promoters for phosphodiester hydrolysis. The reason behind the large enhancements provided by the metal ions is that they are Lewis acids and can promote hydrolytic cleavage in a number of ways, such as:[62,71]

- (a) Electrostatic activation of the substrate in the ground state
- (b) Stabilisation of the transition state
- (c) Stabilization of leaving group
- (d) Generation of nucleophile *via* proton abstraction (general base catalysis)
- (e) Stabilization of leaving group *via* proton donation (general acid catalysis)
- (f) Nucleophilic attack by metal coordinated hydroxide

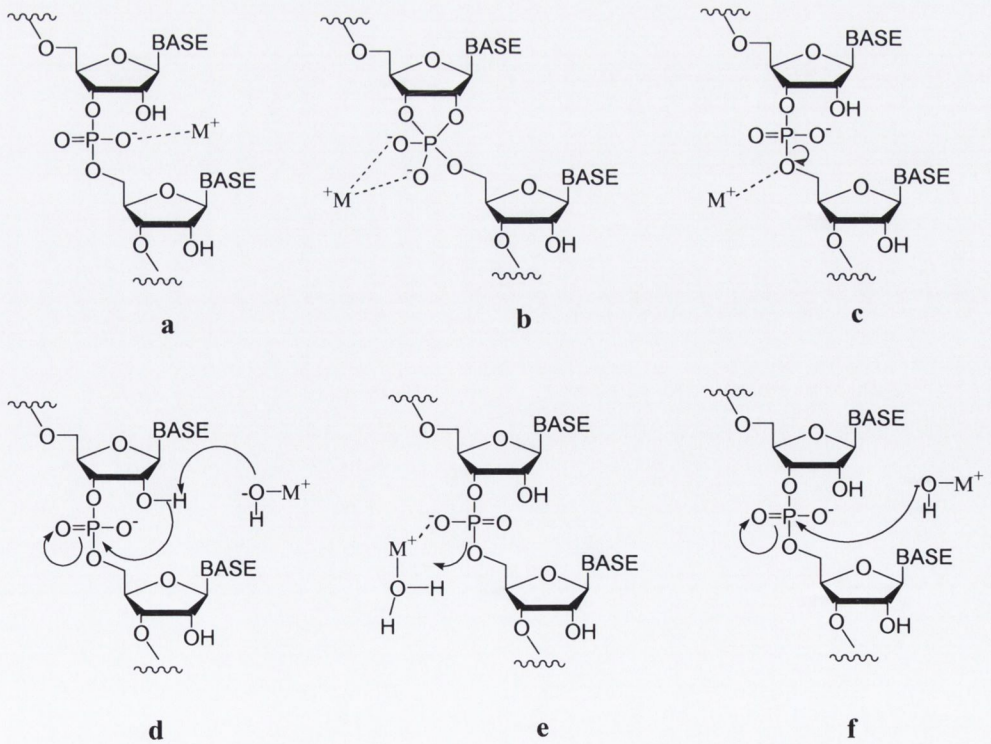

Figure 1.8. Showing three direct and three indirect, possible modes of Lewis acid activation[62, 71]

The reason lanthanide ions are so successful at accelerating phosphodiester hydrolysis stems from their large positive 3^+ charge combined with their relatively small ionic radius, which leads to a large charge density, thus making the lanthanide ions powerful Lewis acids. The next section shall detail some of the substrates often utilised as phosphodiester model compounds within the literature.

1.2.2 Phosphodiester Models

At this point it should be noted that instead of RNA, different researchers use various model compounds to test their cleaving agents.[54] This is mainly for convenience and to avoid the difficulties associated with the handling of RNA. The model compounds usually contain a phosphodiester with a good leaving group, which upon hydrolysis releases a product that can be observed by absorption spectroscopy. For instance 2-hydroxy *p*-nitrophenylphosphate (**HPNP**) is a phosphodiester, which, like RNA, has a hydroxyl group that can act as an intramolecular nucleophile. However, **HPNP** has the advantage that its hydrolysis kinetics can be followed by absorption spectroscopy, as **HPNP** absorbs at 300 nm, while the product of its cleavage, 4-nitophenolate (**34**), absorbs at 400 nm (Scheme 1.6).

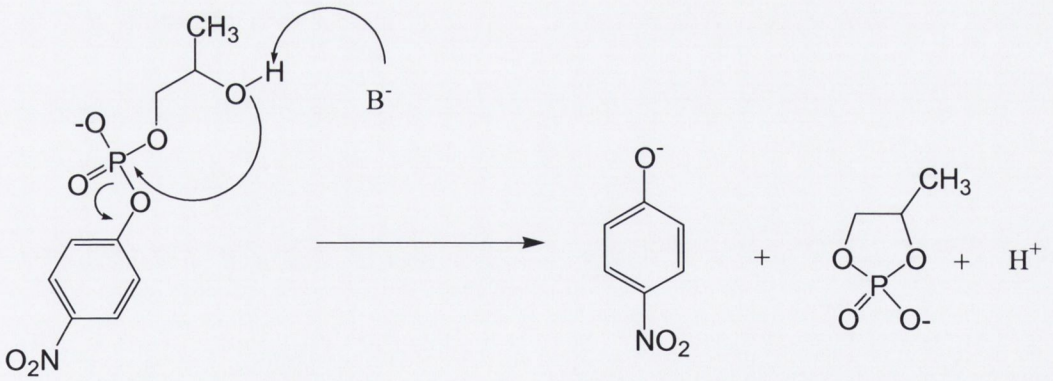

33 HPNP abs 300 nm **34** abs 400 nm **35**

Scheme 1.6. The hydrolysis of HPNP gives 34 (*p*-nitro phenolate) and a cyclic phosphate, 35, and can be monitored by absorption spectroscopy

Other model compounds often cited in the literature are displayed in Table 1.3. They too release **34** upon hydrolysis and as such, their kinetics can be followed by absorption

spectroscopy. However, apart from the RNA dinucleotide UpU, they do not contain an internal hydroxyl nucleophile and as such they more closely resemble DNA.

It is important to remember that although these model compounds can provide valuable information about phosphodiester hydrolysis, they do not precisely depict RNA or DNA hydrolysis. Indeed it has been found in some cases that cleaving agents, which were found to accelerate the hydrolysis of model compounds were inactive towards RNA cleavage and *vice versa*.[54] In general, however, they remain important indicators as to the activity of a cleaving agent. The next section will look at the development of metal complexes that can cleave model phosphodiesters, such as these as well as RNA and DNA.

Abbreviation	Name	Structure
BNPP	Bis(*p*-nitrophenyl) phosphate	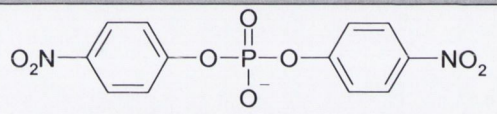
NPP	*p*-nitrophenyl phosphate	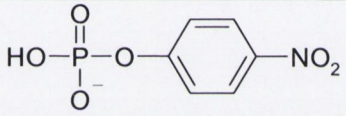
EPNP	Ethyl *p*-nitrophenyl phosphate	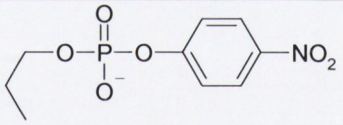
TNP	Tris *p*-nitrophenyl phosphate	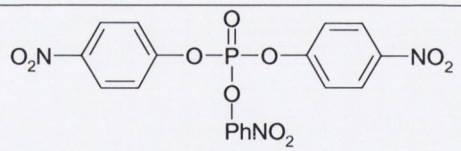
UpU	Uracil dinucleotide	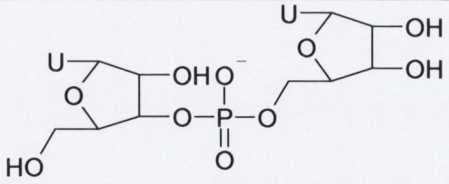

Table 1.3. DNA and RNA model compounds

1.2.3 Phosphodiester Hydrolysis by Metal Complexes

As previously mentioned, large rate enhancements for phosphodiester hydrolysis were obtained by Breslow *et al.*, using metal cations. The largest of these enhancements were obtained using lanthanide ions. In spite of this, the use of metal ions *in vivo* is undesirable, as they are often toxic and unselective, and can form hydroxides that precipitate out of solution.[72] In order to harness the potential offered by metal cations, for *in vivo*

applications, they must be incorporated into a stable coordination environment.[73] There are many examples in the literature of metal complexes accelerating the rate of phosphodiester hydrolysis.

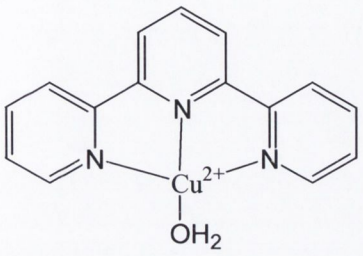

36

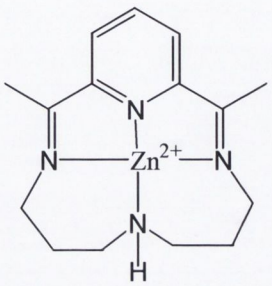

37

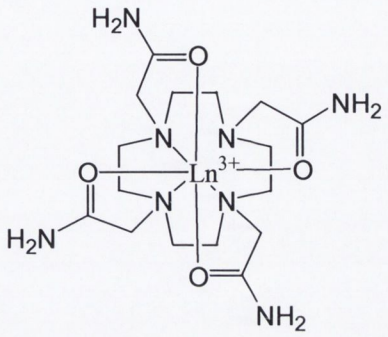

38

One such example is the Cu(II) complex **36**, reported by Chin *et al.*[74] A ten fold excess of complex **36** was found to cleave **HPNP** (0.2 mM) at pH 7.0 and 25 °C, with a pseudo first order rate constant of 5.74 x 10^{-6} s^{-1}, corresponding to a rate enhancement, k_{rel}, of 172 over the uncatalysed reaction. Zinc complexes have also been found to hydrolyse phosphodiester bonds. The Zn(II) complex **37** (0.5 mM) was reported by Breslow *et al.* to accelerate the rate of **HPNP** (0.19 mM) hydrolysis with a pseudo first order rate constant of 7.4 x 10^{-4} hr^{-1} corresponding to a 7 fold rate enhancement over the uncatalysed reaction at pH 7.0 and 37 °C.[75] Mirroring the trend set by the free metal ions themselves, lanthanide complexes have been found to be among the best at promoting phosphodiester hydrolysis. The La(III) complex **38** (0.18 mM) was reported by Morrow *et al.* to cleave **HPNP** (0.18mM) at pH 7.4 and 37 °C, with a pseudo first order rate constant of 5.8 x 10^{-2} hr^{-1}, a rate enhancement, k_{rel}, of 483 over the uncatalysed reaction.[76] Unfortunately, direct comparisons between these systems are not always possible as reported reaction conditions, such as temperature, pH, solvent and concentration often vary. The work conducted within this thesis shall employ the conditions utilised by Morrow *et al.* in order to allow comparison where possible.

To date, some of the greatest enhancements have been observed using lanthanide complexes. Gunnlaugsson *et al.* reported the complex **39**, which utilised extended pseudo peptide arms to form a hydrophobic cavity. [77] At pH 7.4 and 37 °C, the lanthanum complex **La.39** (0.18 mM) was reported to cleave **HPNP** (0.18 mM) with a pseudo first order rate constant of 0.410 (±0.026) hr^{-1}, corresponding to a half-life, $\tau_{1/2}$ = 1.70 hours, and a relative rate enhancement, k_{rel}, of 3417.

Morrow reported the europium complex **Eu.40**, as the first example of a metal complex, which exhibited catalytic turnover in the hydrolysis of RNA at 37 °C neutral pH. **Eu.40** (490 μM) was found to cleave 41 % of the dinucleotide ApUp (20 μM) after four hours.[78] The complex **Eu.40** (200 μM) was also reported to cleave 81 % of the RNA oligomer of adenylic acid ($A_{12} - A_{18}$) (190 μM) after four hours.

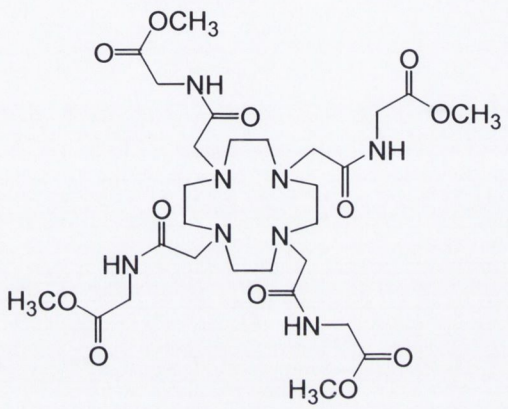

39

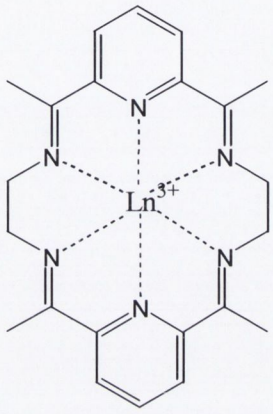

40

Previous work within the Gunnlaugsson laboratory has concentrated on mononuclear systems such a **39**, described above. The focus of this thesis, however, shall be upon the phosphodiester hydrolysis ability of binuclear systems. The following sections describe some of the binuclear systems already published within the literature.

1.2.4 Cooperative Action by Binuclear Transition Metal Ion Systems

X-ray crystallography, has shown that the natural enzymes which hydrolyse RNA often posses two or more metal ions at their active sites.[79] These findings strongly indicated that a bimetallic system should lead to greater catalytic efficiency. The synthesis of many elegant binuclear transition metal ion complexes has been achieved,[80, 81] and numerous accounts have now been reported, showing that the presence of a second metal ion, can lead to large rate enhancements of phosphodiester hydrolysis over similar mononuclear systems.[82] One of the first reports of this greater efficiency, achieved by cooperating metal ions came from Breslow *et al.* They synthesised a binuclear Zn(II) complex, **41**, which at pH 8.0 hydrolysed the neutral ester diphenyl *p*-nitrophenyl phosphate (DPNP) 4.4 times faster than the corresponding mononuclear complex.[83]

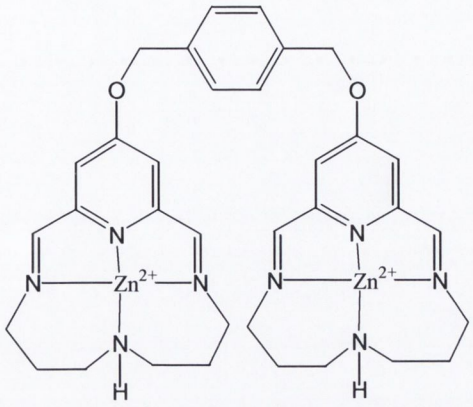

41

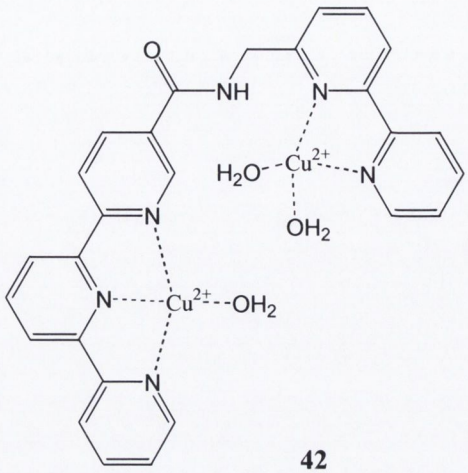

42

Since then, numerous examples of this increased efficiency by binuclear systems have been reported.[56,71,84] Hamilton *et al.* reported the binuclear Cu(II) system **42**, based on a covalently linked terpyridine and bipyrindine ligand system.[85] This binuclear complex exhibited a notable base selectivity, and 2.0 mM of **42**, was found to hydrolyse the RNA dinucleotide ApA, (0.1 mM) 11 times faster than the similar mononuclear complex **36**, with a first order rate constant of 1.52 x 10^{-4} s^{-1} at pH 7.5 and 25 °C. The selectivity towards adenine bases was attributed to strong π–π stacking interactions with the bipyridine unit. Komiyama reported the dinuclear Zn(II) complex **43**.[86] A solution containing 2.5 mM, of **43**, at 50 °C, pH 7.0, was found to hydrolyse ApA (0.1 mM), with a pseudo first order rate of 7 x 10^{-5} s^{-1}, whereas, the mononuclear complex, was found to be inactive towards ApA hydrolysis.

Chin *et al.* reported the dinuclear Cu(II) complex **44**, 1 mM of which, was found to cleave **HPNP** (50 μM) at 25 °C and pH 7.0 with a pseudo first order rate constant of 2.1 x 10^{-3} s^{-1}, a 52 fold increase over the rate obtained for the analogous mononuclear system.[87]

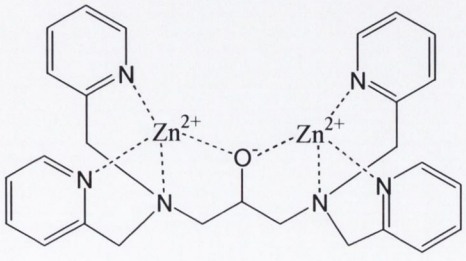

43

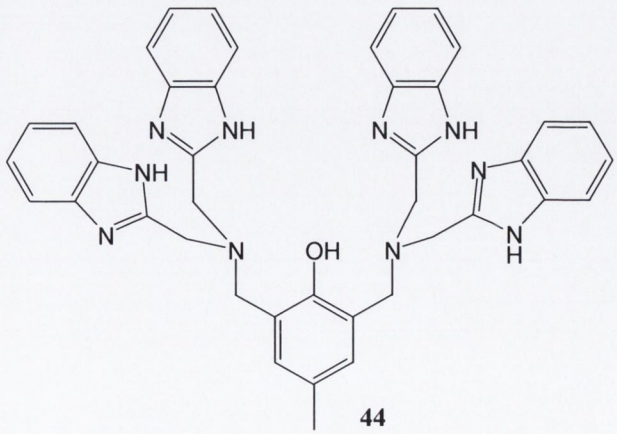

44

Similar findings were reported by Morrow *et al.* who described the binuclear Cu(II) complexes **45** and **46** (0.5 mM), which were respectively found to cleave GpppG (30 μM),

a model of the 5'-cap mRNA structure, 46 and 32 times faster per metal centre, than the mononuclear Cu(II) system, with pseudo first order rate constants of 5.6 x 10^{-5} s^{-1} and 3.9 x 10^{-5} s^{-1}, respectively, at pH 7.3 and 37 °C.[88]

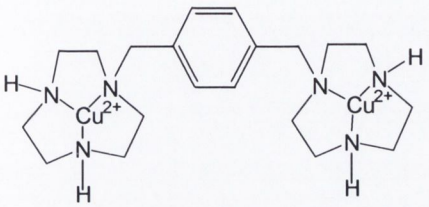

45

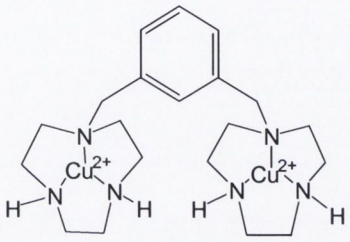

46

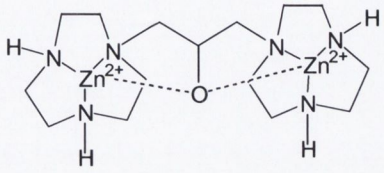

47

The binuclear Zn(II) complex **47** was reported as one of the best dinuclear zinc catalysts for **HPNP** cleavage with the highest reported second order rate constant (0.25 M^{-1} s^{-1}) in 100 % aqueous solution at pH 7.6, 25 °C.[89] This represented a 120 fold increase over the mononuclear system. The complex **47**, was also reported to cleave 90 % of a oligoribonucleotide containing six adenosines (A_6), after 24 hours. Interestingly, the Cu(II) complex of **47** was reported to be inactive in the cleavage of **HPNP**. This was tentatively attributed to a decrease in the available coordination sites on the Cu(II) ion in comparison to the Zn(II) analogue.

Further examples of large rate enhancements due to the presence of a second metal ion were reported by Bianachi *et al.*[90] The dinuclear Zn(II) complex **48** was found to cleave **BNPP** 10 times faster than its mononuclear analogue. The binuclear Cu(II) complex of **49**, was reported by Chin *et al.* to cleave ApA 300 times faster than the mononuclear system at pH 6.0.[91] This complex was reported to have a Cu – Cu distance of approximately 4.5 Å. Interestingly, this is similar to the distance between metal ion centres in natural enzymes, reported to be between 3 and 5 Å.[92]

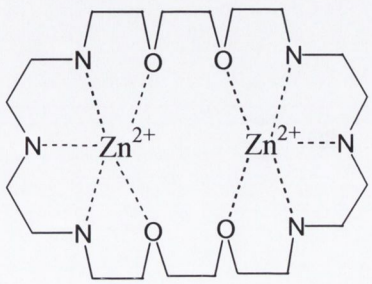

48

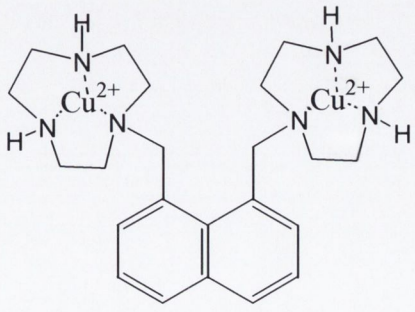

49

These large rate enhancements over the mononuclear systems are far greater than can be explained by a simple increase in metal ion concentration. It is widely accepted that the rate enhancements are due to a cooperative action between the two metal centres. Binuclear complexes can utilise a double Lewis acid activation mechanism Figure 1.9 a,[93,94,95] whereby,

- One metal ion can bind and activate the incoming nucleophile (the 2'-OH)
- The second metal ion can bind to the leaving group (the 5'-OH),
- While both metals can bind to the phosphate activating it towards nucleophilic attack and stabilizing the developing negatively charged transition state.

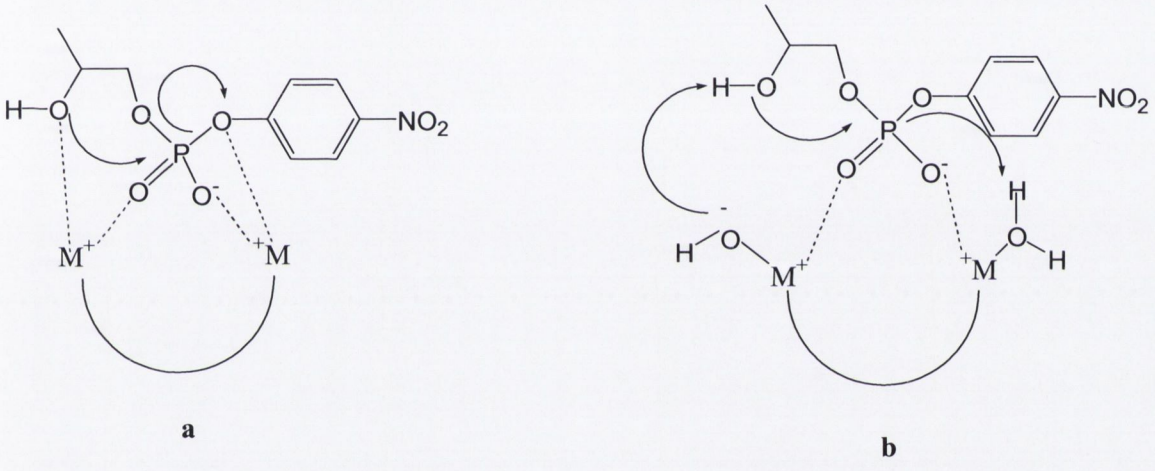

Figure 1.9. (a) Proposed mechanism for the cooperative action of two metal centres in the hydrolysis of HPNP[93] (b) Alternate mechanism involving metal bound water molecules[56]

An alternate mechanism involving metal bound water molecules is also possible Figure 1.9 b, whereby a metal bound hydroxide functions as a general base catalyst deprotonating the 2'-OH, while a metal bound water molecule functions as a general acid catalyst for the 5'-OH leaving group.[56]

From the examples detailed so far, it can be seen that there is a wide divergence between binuclear systems. Some are only moderately superior to their corresponding mononuclear complex; for example **41** was only 4.4 times faster. Others show more than an order of magnitude improvement upon their mononuclear systems, for instance **44** exhibited a 52 fold enhancement. The factors affecting the extent of the binuclear cooperation shall be the subject of the next section.

1.2.5 Pertinent Factors for Double Lewis Acid Activation

A crucial factor for efficient cooperative action between the metal ions is the spacer group employed. Investigating the effect of the spacer group, Breslow *et al.* reported a series of Zn(II) complexes **50** – **53**.[96]

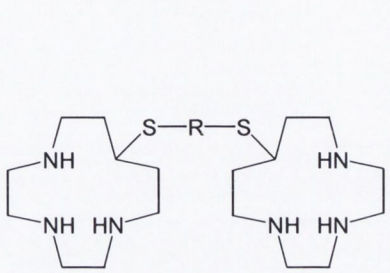

50: R = 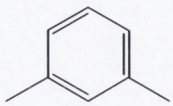

51: R = 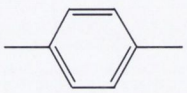

52: R = 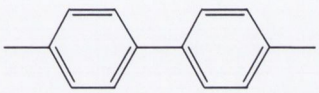

53: R = —$(CH_2)_5$—

They found all the binuclear complexes to be more active than the corresponding mononuclear systems (Table 1.4). It was also shown that the shorter spacers of **Zn.50** and **Zn.51** were more active in the hydrolysis of monoesters, while the longer biphenyl spaced **Zn.52** was the most active for phosphodiesters. The biphenyl spaced **Zn.52**, was shown to be 10 times more active than its corresponding mononuclear system. This highlights the importance of the spacing between metal centres as well as the ability to adopt a suitable geometry for a specific substrate. The authors reported the flexible pentamethylene spaced **Zn.53** to be a poor promoter compared to the more rigid complexes. It has since been reported that the rate enhancement observed for the **Zn.52** complex was not due to the cooperative action of the two metal ions but to an increased hydrophobic binding contribution from the biphenyl spacer.[97]

Complex	k x 10^{-5} s^{-1}	k_{rel}
Zn.50	8.1	450
Zn.51	10.0	556
Zn.52	19.3	1072
Zn.53	8.0	444
Zn.Mono[a]	3.5	194

Table 1.4. Pseudo first order rate constants (k) and relative rate enhancements (k_{rel}) for the cleavage of HPNP (454 mM) in 50 mM TRIS (pH 8.4) at 30 °C with various Zn(II) complexes (227 mM). [a](454 mM)[96]

The flexibility of the system is also an important feature. Czarnik reported the synthesis of both the very flexible and rigid binuclear Co(III) complexes, **Co.54**[98] and **Co.55**.[99] The flexible binuclear complex **Co.54**, promoted the hydrolysis of **BNPP** 6.4 fold faster than the mononuclear analogue, with a rate constant of 7 x 10^{-5} s^{-1}, at pH 7.0 and 25 °C. In contrast, the rigid binuclear **Co.55** complex did not give rise to any cooperative rate enhancement for the hydrolysis of **BNPP**, as it could not accommodate the geometry required. This highlights the need for an element of flexibility within the design of the molecule.

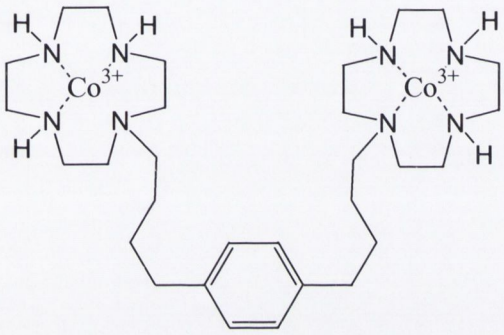

54

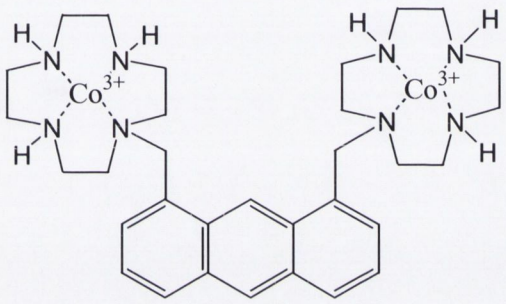

55

In general, however, rigidly spaced molecules that are preorganised to interact with a substrate show greater activity than more flexible spaced analogues. For example, the same rigid complex **Co.55** (1 mM) gave rise to a large cooperative rate enhancement for the hydrolysis of the phosphate monoester NPP (25 μM), which at pH 7.0 and 25 °C, was cleaved with pseudo first order rate constant of 1.33 x 10^{-2} s^{-1}, corresponding to a 20 fold increase over that observed for the corresponding mononuclear analogue.

Clearly, the type of spacer group employed can have dramatic consequences upon the extent of the cooperativity between the metal ions and hence the extent of the enhancement achieved. In summary it can be concluded that:

- Binuclear systems with rigid spacer groups without a favourable geometry do not give rise to any cooperative rate enhancement
- Binuclear systems with flexible spacer groups exhibit weak cooperative enhancements of the order of 4 – 6 fold

- Complexes with semi-rigid spacer groups with a preorganised geometry that accommodates the substrate, give the largest cooperative rate enhancements, of the order of 10 – 100 fold

Canary *et al.* reported the binuclear ligands **56** and **57**, whose ability to cleave **BNPP** (2.0 mM) was evaluated in a 30 % DMSO solution at 55 °C, with 0.4 mM $Cu(ClO_4)_2$ and 0.2 mM of the binuclear ligand, respectively.[100] The first order rate constants were calculated by the initial rate method. The complex **$Cu_2$56** was found to cleave **BNPP**, exhibiting a maximum activity at pH 8.4 with a pseudo first order rate constant 1.14×10^{-6} s^{-1} a 10^4 fold rate enhancement over the uncatalysed reaction and a ~ 10 fold rate enhancement over the analogous mononuclear system. The hydrolysis by the complex exhibited a bell shaped pH dependence, which is common for binuclear systems. This bell shaped pH dependence was explained by the formation of the active species. Each Cu(II) ion possesses one metal bound water molecule, whose ionisation state is determined by the pH of the solution.

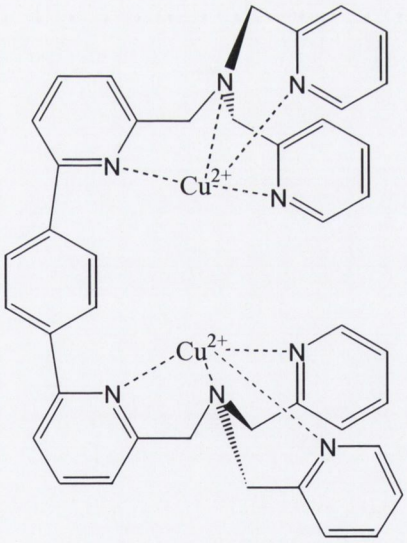

56

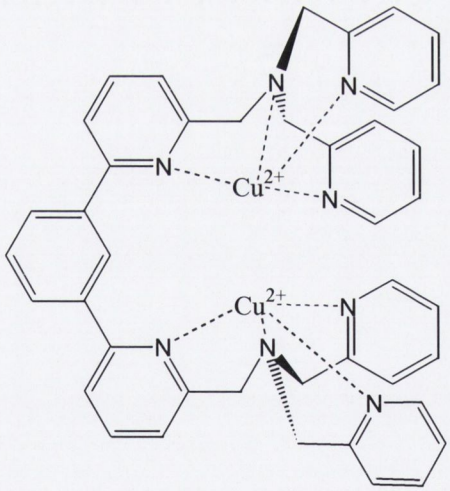

57

The active species is believed to be the $[\mathbf{Cu_2}\mathbf{56}(OH^-)(H_2O)]^{3+}$ species, as this species provides a potent nucleophile in the form of the metal bound hydroxide, while also providing Lewis acid activation through the other metal ion, which can bind to the phosphodiester *via* displacement of a metal bound water molecule. In contrast, the di-aqua species cannot provide a nucleophile, while the di-hydroxide species is known to inhibit coordination to the phosphodiester due to the tightly bound hydroxide molecules.[103]

Interestingly, the binuclear conjugate **57** gave no rate enhancement over the mononuclear system. One possible reason for this may be the shorter intermetal distance, which may prevent the two Cu(II) centres from adopting a favourable orientation for binuclear cooperativity.[101]

To date, one of the greatest rate enhancements has been achieved by Reinhoudt *et al.* who reported the synthesis of a calix[4]arene based, binuclear Zn(II) complex, **58**.[102] In a 50:50 MeCN:aqueous buffered solution at pH 7.0 and 25 °C, the complex **58** (0.48 mM), was reported to cleave **HPNP** (0.19 mM) with a pseudo first order rate constant of 6.3 x 10^{-4} s^{-1} corresponding to a half-life of 18 minutes, calculated by the initial rates method. This represents a remarkable 23,000 fold rate enhancement over the uncatalysed system. The complex also exhibited catalytic turnover and was reported to be 50 times more active than the corresponding mononuclear complex.

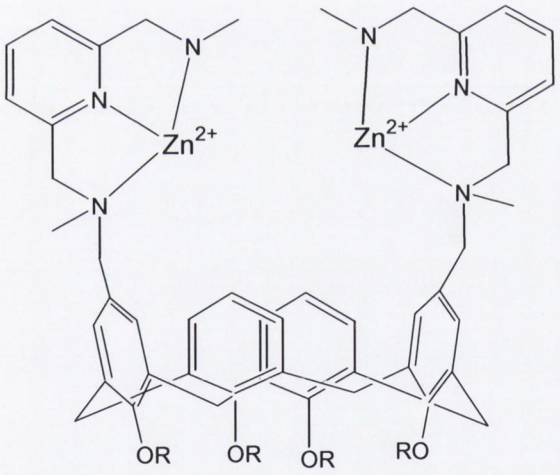

58

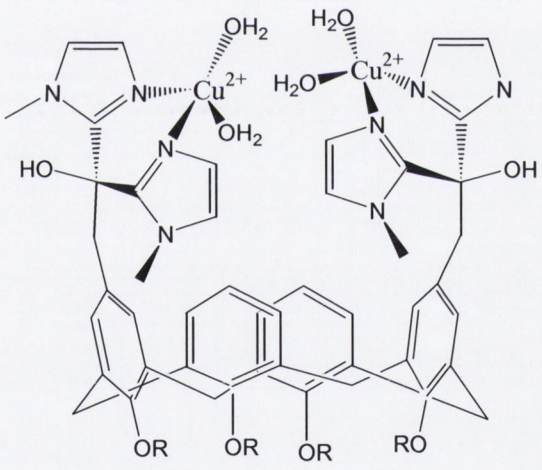

59

Reinhoudt *et al.* also reported the binuclear Cu(II) complex **59**, which under similar conditions in a 35:75 EtOH:H_2O solution, buffered at pH 6.2, cleaved **HPNP** with a pseudo first order rate constant of 2.9 x 10^{-4} s^{-1} corresponding to a half-life of 40 minutes and a rate enhancement, k_{rel}, 10,000.[103] The complex was found to be 22 times more active than its mononuclear system and also exhibited catalytic turnover cleaving a four fold excess of **HPNP** with no loss of activity. The authors attributed the activity to the cooperative action of the two preorganised but still dynamic metal cations, which are held in a somewhat rigid fashion by the calixarene moiety.

The authors also noted a higher binding affinity for phosphate by the binuclear systems over the mononuclear analogue. This increase is often observed for binuclear systems, and reflects the stronger electrostatic stabilization offered by the highly cationic, dinuclear complex.[104] The remarkable activity of the complexes was attributed to a moderate turnover combined with a strong binding affinity for the case of **Zn.58**, or a high turnover rate combined with a moderate binding affinity, in the case of **Cu.59**.

It appears that metal centres linked by very flexible scaffolds display a smaller cooperative activity compared to more rigid scaffolds.[96] Nevertheless, molecules that are too rigid have also shown poor cooperative activity.[105] A balance between preorganised rigidity and a certain degree of flexibility is required for optimum activity.[56,103] The intermetal distance as well as the overall geometry also play important roles.

1.2.6 Trinuclear complexes

A number of natural enzymes, such as ribonuclease P1, possess three metal ions at their active site,[64] and hence it was suggested that the incorporation of a third metal into a phosphodiester cleavage agent would further improve upon the rate of hydrolysis obtained. This hypothesis was further supported by the trinuclear Zn(II) complex **60**, which was developed as a receptor for phosphate dianions, and showed a greater binding affinity (Log K = 5.8) for nitrophenylphosphate (NPP), than the corresponding dinuclear Zn(II) complex (Log K = 4.0).[106] In 1997 Komiyama *et al.* reported the trinuclear Zn(II) complex **61**, which was found to hydrolyse ribonucleotide dimers (0.1 mM) at pH 6.9 at elevated temperature *ca.* 50 °C.[107] A concentration of 5 mM **61** was found to hydrolyse CpA with a pseudo first order rate constant of 7.2 x 10^{-4} s^{-1}, and ApA with a rate constant of 4.6 x 10^{-4} s^{-1}. This corresponded to half-lives of 16 and 23 minutes, respectively. A similar dinuclear Zn(II) complex was found to cleave CpA and ApA with pseudo first order rate constants of 0.6 and 0.5 x 10^{-4} s^{-1}, corresponding to half-lives of 183 and 250 minutes, respectively. Clearly, these trinuclear complexes are efficient and active phosphodiester cleavage agents.

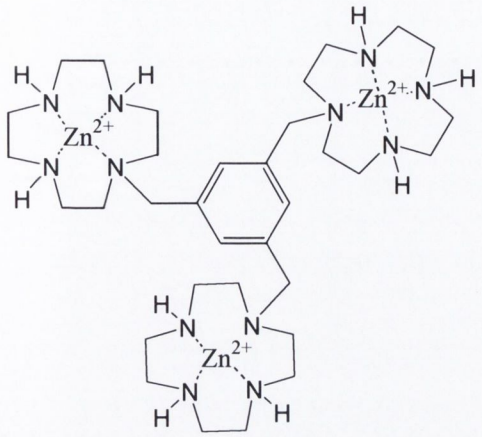

60

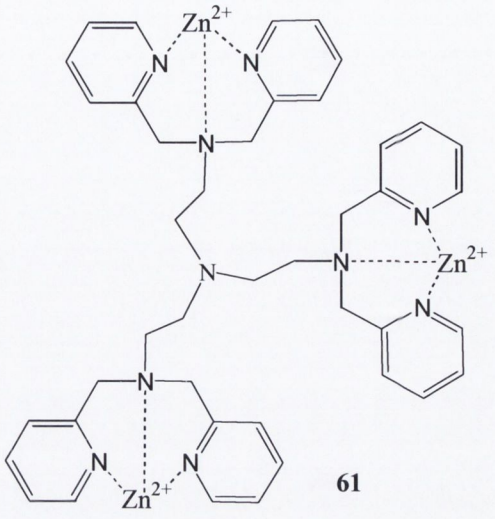

61

In 2002 Komiyama *et al.* reported the trinuclear Cu(II) complex **62**, which was found to hydrolyse ribonucleotide dimers (0.1 mM) at pH 7.0 and 50 °C.[108] It was reported to be the first complex to distinguish between 2'–5' and 3'–5' phosphodiester linkages. The hydrolysis of the 2'–5' UpU dimer was 56 fold more rapid than the 3'–5' isomer (Table 1.5). Interestingly, the specificity was reversed in the case of ApA. The rigidified analogue **63**, was found to have a lower activity than that of **62**, showing that flexibility is essential for efficient trinuclear complexes.

Ribonucleotide	2'-5'	3'-5'
UpU	28 (0.6)	0.5 (0.7)
GpG	0.3 (0.2)	0.3 (0.4)
ApA	0.5 (2.0)	24 (6.0)
CpC	–	7.0 (2.0)

Table 1.5. Pseudo first order rate constants (10^{-4} min^{-1}) for the hydrolysis of (2'–5') and (3'–5')-diribonucleotides (0.1 mM), by 62 (2 mM) at pH 7.0, 50 °C. Parentheses shows the values for the dinuclear complex (3 mM)

Molenveld and Reinhoudt reported the trinuclear Zinc complex **64**.[105] In 50 % MeCN aqueous solution buffered at pH 7.0 and 25 °C, **64** (0.48 mM) was found to cleave **HPNP** (0.19 mM) with a pseudo first order rate constant of 8.55 x 10^{-4} s^{-1}, corresponding to a rate acceleration of 32,000 over the uncatalysed reaction, and a 1.4 fold rate enhancement over the dinuclear zinc complex **58**, which was discussed in the previous section.

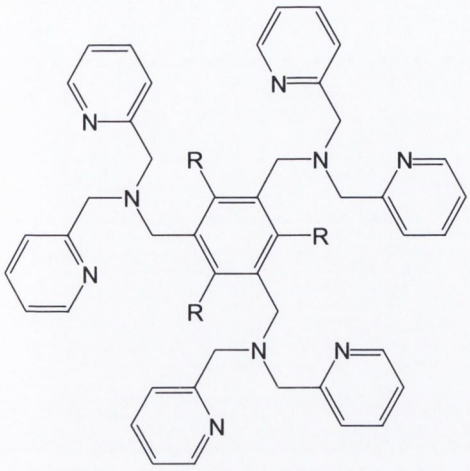

62: R=H **63:** R=CH_2CH_3

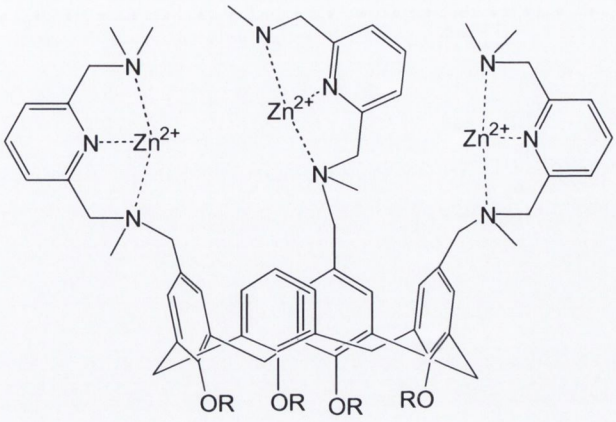

64

Furthermore, the complex exhibited catalytic turnover cleaving a four fold excess of **HPNP** with a 40 % loss of activity after each turnover. In a further study the trinuclear Zinc complex (0.9 mM) was found to efficiently hydrolyse RNA dinucleotides (3'– 5' NpN) (0.09 mM) in a 35 % EtOH aqueous solution buffered at pH 8.0 and 50 °C (Table 1.6).[109] The rate accelerations over the uncatalysed reaction are of the order of 10^4–10^5, and once again the trinuclear complex exhibits catalytic turnover, cleaving a three fold excess of UpU. The trinuclear complex **64**, is a factor of 10, 19, and 160 times more active than the dinuclear complex for the cleavage of CpC, UpU and GpG, respectively. The greater reactivity towards GpG hydrolysis was explained by an enhanced binding coupled with a higher conversion rate.

Substrate	GpG	UpU	CpC	GpA	ApG	ApA
64	72	8.5	6.1	4.6	2.7	0.44
58	0.45	0.45	0.58	N/A	N/A	0.28

Table 1.6. Observed pseudo first order rate constants (10^{-5} s^{-1}) for the cleavage of RNA dinucleotides (0.09 mM) by Zn(II) complexes (0.9 mM), in 35 % EtOH aqueous solution buffered at pH 8.0, 50 °C

Until now, we have only discussed multinuclear complexes of transition metal ions, however, the focus of this thesis shall be on binuclear lanthanide complexes, and these will be the subject of the next section.

1.2.7 Cooperative Action by Binuclear Lanthanide Systems

The cooperative action and rate enhancements detailed above have also been observed in binuclear lanthanide systems.[71] Chin *et al.* reported the formation of a La(III) dimer which self assembles in solutions above pH 8.5 and rapidly cleaves RNA.[110] From potentiometric titrations, it was proposed that the dimer was bridged by five hydroxide ions, **65**.

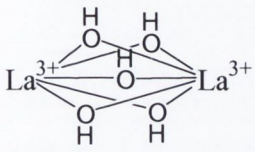

65

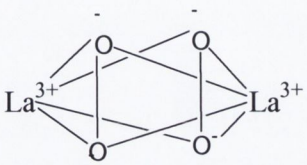

66

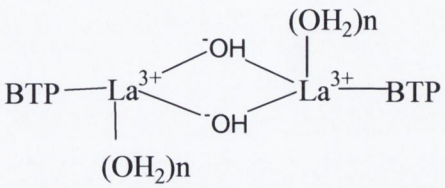

67

The La(III) dimer **65** (1 mM), was reported to cleave ApA with a half-life of 13 seconds at pH 8.5, 25 °C. This represents a 10^4 fold increase in activity over the mononuclear lanthanide ions. Chin *et al.* also reported the peroxide bridged La(III) dimer **66**, which demonstrated a 10^9 fold rate acceleration for the hydrolysis of **BNPP** at pH 7.0, 25 °C.[111] However, the use of peroxide in biological systems is undesirable, as oxidative cleavage of DNA and RNA produces unselective diffusible free radicals, which can cause damage to surrounding cells.[112] Hydrolytic, rather than oxidative, cleavage is preferred for biological uses.

There are numerous examples of binuclear and even higher order lanthanide complexes within the literature, as many elegant multinuclear Gd(III) complexes have been developed for use as medicinal chemical contrast agents.[113, 114] However, few if any, of these complexes have demonstrated an ability to accelerate the rate of phosphodiester hydrolysis. Indeed, despite the large rate accelerations demonstrated by lanthanide ions,[70] mononuclear lanthanide complexes[73] and lanthanide ion dimers,[110] there are relatively few examples of rate accelerations provided by cooperative binuclear lanthanide complexes. As explained earlier, metal ions must be incorporated into a stable ligand framework if they are to be of use for pharmaceutical applications. One possible reason for the lack of reported binuclear lanthanide complexes may stem from their large coordination number requirement, which necessitates the use of stable, multidentate ligands, often requiring complex synthesis.

Moving in this direction, Yatsimirsky *et al.* reported that a combination of BisTris Propane (BTP) (20 mM) and $LaCl_3$ (4 mM) cleaved **BNPP** (0.04 mM) with a pseudo first order rate

constant of approximately 6.8 x 10^{-4} s^{-1} at pH 9.0, 25 °C.[115] From potentiometric titrations, they proposed the active species to be the binuclear La(III) structure, $M_2(BTP)_2(OH)_2^{4+}$ **67**. This, however, is not a stable complex and mass spectral analysis revealed the presence of numerous other species in solution including the free metal ion, which itself is an active catalyst.

A similar hydroxy bridged complex utilising BisTris as a ligand, has also been reported by Park and co-workers.[116] The active species in solution at pH 9.8 and above, was reported to be a BisTris La(III) dimer bridged by four hydroxy molecules $La_2(BisTris)_2(OH)_4^{2+}$. The activity of this compound was found to be similar to that of the La(III) dimer **64**. A 1:1 mixture of $LaCl_3$ and BisTris (0.5 mM) with two equivalents of NaOH was found to cleave **BNPP** with a pseudo first order rate constant, k, of 7.3 x 10^{-3} s^{-1}. These results indicate that lanthanide complexes can act in a cooperative fashion to provide large rate enhancements for phosphodiester hydrolysis. However, the high pHs required for the formation of these dimers, not to mention the low stability of the resulting complexes negates their use for medicinal purposes.

Schneider *et al.* reported one of the relatively few examples of a cooperative binuclear lanthanide complex for phosphodiester hydrolysis in 1996.[117] The 2:1 Eu(III) complex of **71** was found to be 5 times more active towards **BNPP** hydrolysis than the 1:1 complex. The complex **Eu.71** (1 mM) at pH 7.0 and 50 °C, in a 5 % DMSO solution, was reported to reduce the half-life of **BNPP** (33.5 μM) from 75 years to 8 minutes. Furthermore the Pr(III) complex **Pr.71** (1mM), was reported to cleave 77 % of double stranded, plasmid DNA (19.5 μM in base pairs) at pH 7.0 and 37 °C, after two hours. Nevertheless, the addition of EDTA was found to decrease the rate by approximately 70 % indicating that the complexes were not kinetically stable. Schneider *et al.* also reported the binuclear complexes **68** – **70**, however, these complexes were found to give only moderate rate enhancements at best. Their disappointing activity was attributed to the shorter metal to metal distance of the complexes, as mentioned earlier, efficient binuclear cooperativity requires a certain separation of the metal centres in order to facilitate Lewis acid stabilisation of a bound phosphate at one end, with concomitant activation of nucleophile at the other.[118]

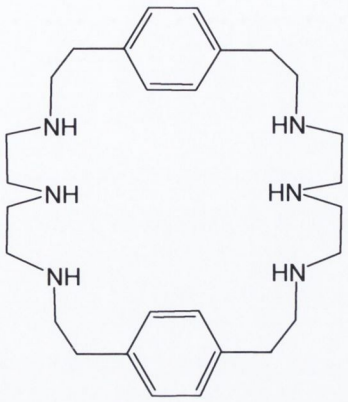

68

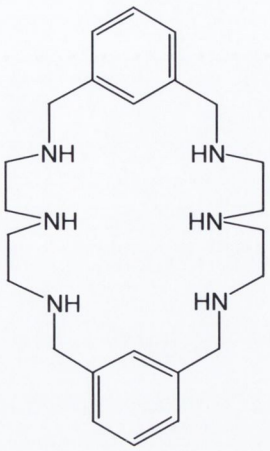

69

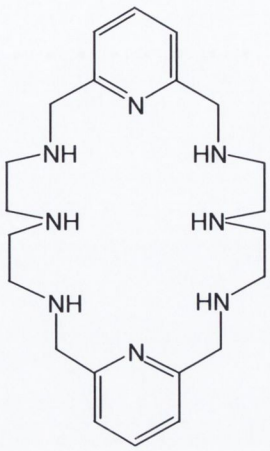

70

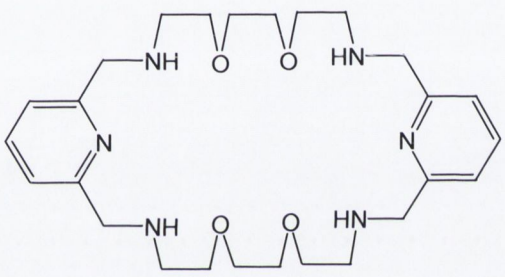

71

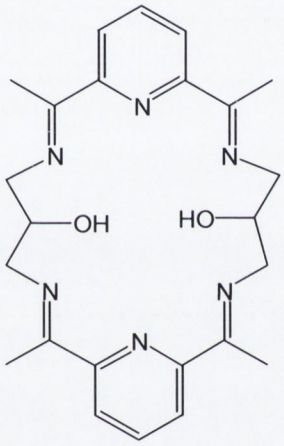

72

In 1999, Zhu *et al.* described the more kinetically stable complex **72**. The 2:1 Er(III) complex, **Er.72** (0.7 mM), was reported to cleave plasmid DNA (1 μg) to both nicked and linear forms, after one hour, in yields of 42 % and 11 % respectively, under neutral conditions at 37 °C.[119] The authors reported the pseudo first order rate constant for the cleavage of the plasmid DNA to be 2.8 x 10^{-2} min^{-1}. The kinetic inertness was studied using excess Cu(II) as a trapping agent. The drawback to these systems, however, is the lack of a handle to further functionalise the molecule. This is important, as the incorporation of catalytically active groups has been shown to greatly increase the activity of ribozyme mimics. Some examples of this shall be detailed in section 1.10.

In 2000 Jurek and Martell, reported the synthesis of the binuclear La(III) complex of **73**.[120] Measurements with this complex were conducted in a 75:25 EtOH:H_2O solution with 0.1 M KCl at 35 °C. The pH was kept constant by addition of dilute KOH and the rate constants were determined using the initial rates method. A species diagram showed the presence of multiple species, however, only $\mathbf{[La_2 73(OH)]^{3+}}$ and $\mathbf{[La_2 73(OH)_2]^{2+}}$ are

believed to contribute significantly to the hydrolysis. The 2:1 La(III) complex of **73** (0.486 mM) reportedly cleaved **BNPP** (0.539 mM) at pH 8.25, with a rate constant of 7.3 x 10^{-8} M^{-1} s^{-1}. The cooperativity between the two La(III) ions in this binuclear complex was evidenced by the much lower activity displayed by the mononuclear 1:1 La(III) complex of **73** (0.487 mM), which was found to cleave **BNPP** (0.500 mM) at pH 8.00, with a rate constant of 8.0 x 10^{-10} M^{-1} s^{-1}, corresponding to a 90 fold decrease in activity. An apparent third order dependence upon concentration, observed in the case of the binuclear La(III) complex, was attributed to the mechanism for the hydrolysis of **BNPP**, which is believed to proceed *via* the aggregation of three binuclear complexes and one molecule of **BNPP**.

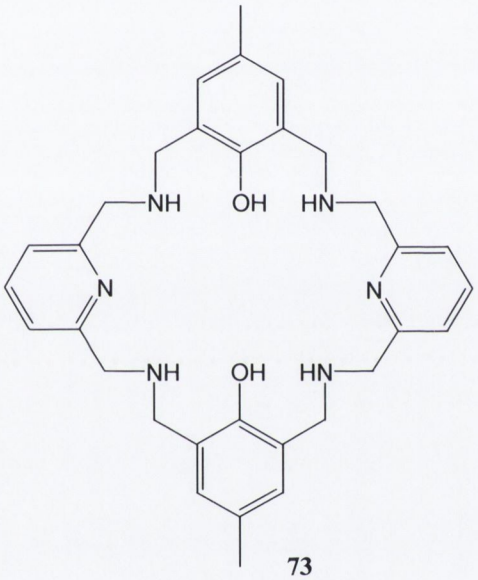

73

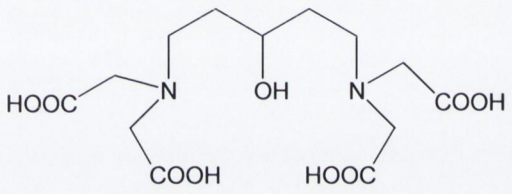

74

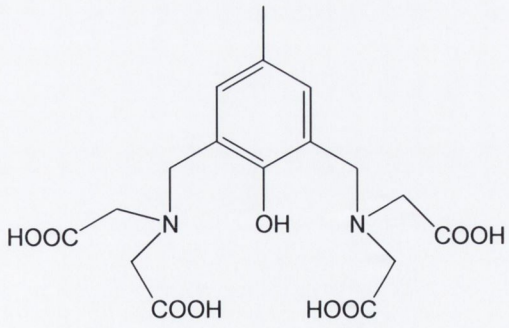

75

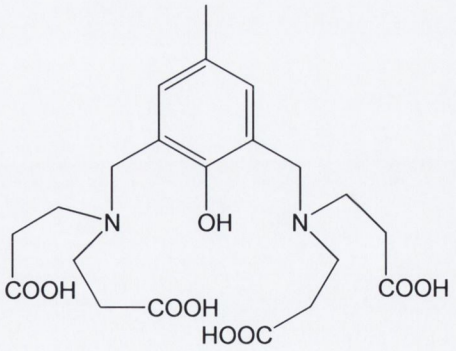

76

In 2001, one final example of a dinuclear lanthanide complex capable of hydrolysing DNA, was reported by Que *et al.*[121] The dicerium complexes of ligands **74** – **76**, were found to promote the hydrolysis of double stranded DNA. Plasmid DNA (0.1 $\mu g/\mu L$) was incubated for at pH 8.0 and 37 °C, in the presence of the dicerium complex **75** (100 μM). After 12 hours the mixture contained 17 % supercoiled, 63 % nicked and 20 % linear

DNA. The dicerium complexes of **74** and **76** were found to be less active, as under the same conditions after 12 hours the mixtures contained, 55 % supercoiled, 42 % nicked, and 3 % linear DNA. Of the other lanthanide ions, only Yb(III) formed a dinuclear complex capable of hydrolysing DNA under these conditions, though its activity was found to be half that of the dicerium complex. The cleavage of DNA by free cerium ions is known to proceed through an oxidative pathway.[122] In order to confirm that the mechanism operating here was hydrolytic rather than oxidative, the authors investigated the cleavage products, and found them to be predominantly due to hydrolytic cleavage. The dicerium complex of **75** (0.1 mM) was also found to cleave **BNPP** (1 mM) with a second order rate constant of 0.10 M^{-1} s^{-1} or 1.0 x 10^{-5} s^{-1} at 37 °C.

1.2.8 Hydrolysis by Hetrodinuclear Complexes

Another class of complexes worth discussing are the hetrodinuclear complexes.[123] Inspired by the work of Komiyama *et al.*, who reported efficient cleavage of both **BNPP** and ApA, by the cooperation of free La(III) and Fe(III) ions,[124] Manseki *et al.*, detailed the hetrodinuclear complex **77**, which cleaved NPP (0.5 mM) with a rate constant of 2 x 10^{-5} s^{-1}, representing a 2.8 fold enhancement over the mononuclear La(III) complex, which gave a rate constant of 7 x 10^{-6} s^{-1}.[125] Significantly, neither the mononuclear nor the dinuclear Cu(II) complexes promoted the hydrolysis of NPP. All of these measurements were carried out in a 1:9 H_2O:DMF solution at pH 7.0 and 37 °C, and the rates were determined by the initial rates method.

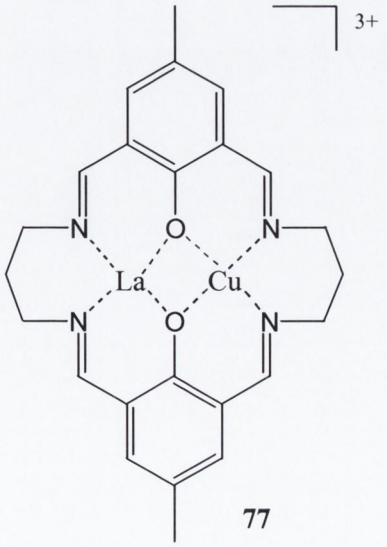

77

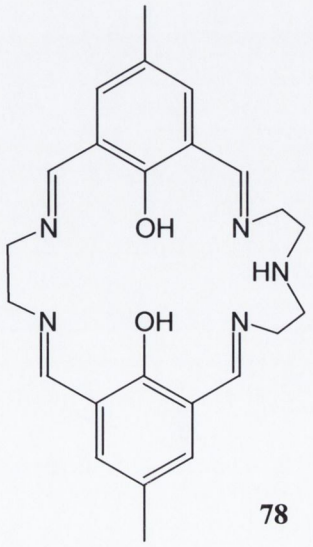

78

Mixed transition metal systems have also been reported. In 1998 Ōkawa *et al.*, described the synthesis of the hetrodinuclear Zn(II)Pb(II) complex of **78**.[126] This complex (1 mM) was found to cleave TNP (10 mM) in 100 % DMSO solution. The rate constant was not reported, however, at 25 °C, the hydrolysis of TNP was found to be completed after 5 minutes.

Komiyama *et al.*, reported the hetrodinuclear Fe(III)Zn(II) complex of **79**.[127] The hydrolysis of ApA (5 mM) in 5 % MeCN at pH 5.6, 50 °C, by various combinations of metals and ligands were reported and are shown in Table 1.7. A 1:1:1 mixture of Fe(III), Zn(II) and **79**, was found to efficiently hydrolyse ApA, while in contrast, 2:1 mixtures of Fe(III) or Zn(II), with **79** showed only poor activity. The results were attributed to the bimetallic synergism between the Fe(III) and Zn(II). The mechanism is believed to involve base catalysis by a Zn(II)-bound hydroxide ion, which activates the 2'-OH of the ribose, and acid catalysis by the Fe(III), which can stabilize the intermediate and promote removal of the 5'-OH.

[Fe(III)] M	[Zn(II)] M	[79] M	Rate Const (10^{-3} h^{-1})
2.5	0.0	2.5	0.2
5.0	0.0	2.5	0.2
0.0	5.0	2.5	0.3
2.5	2.5	2.5	4.1
5.0	2.5	2.5	0.7

Table 1.7. Pseudo first order rate constants for the hydrolysis of ApA (5 mM) in 5 % MeCN at pH 5.6, 50 °C

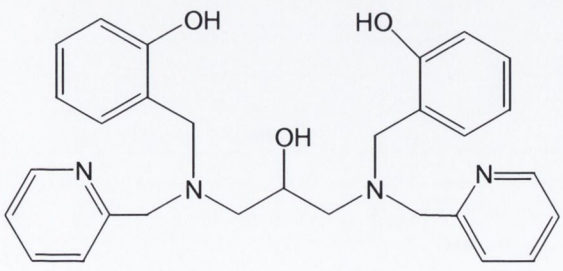

79

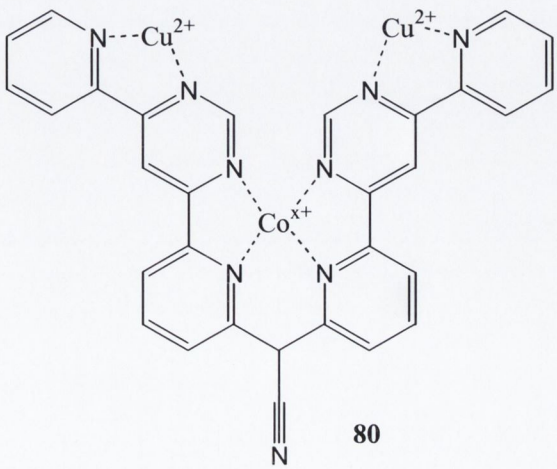

80

In 2003 Krämer *et al.* reported the hetro trinuclear complex **80**.[128] The $Cu(II)_2/Co(III)$ complex (7×10^{-4} M) was reported to cleave **HPNP** (5×10^{-4} M) in buffered water/DMSO 3:1 at pH 7.0 and 20 °C with an initial rate of *ca.* 6×10^{-4} s^{-1}. In contrast a dinuclear Cu(II) complex of 4,6-di(2-pyridyl)pyridine was found to cleave **HPNP** under the same conditions with an initial rate of 8×10^{-6} s^{-1}, a 62 fold decrease in activity.

1.2.9 Functional Organic Pendant Groups

Both general and specific acid/base catalysis is involved in the mechanism of phosphodiester hydrolysis.[65, 122, 129] It has been shown that introducing a pendant group, which can act as an acid or base, can promote the rate of phosphodiester hydrolysis.[75] Hamilton *et al.* have shown that the incorporation of pendant tertiary amine groups increases the activity of the complexes **81** and **82** by nearly 3 and 7 fold, respectively, over **36** (Table 1.8).[130] This increase in activity was ascribed to the tertiary amine providing general base catalysis. This demonstrates how functionalisation of metal complexes with organic, catalytic groups can lead to more efficient ribozyme mimics.[62]

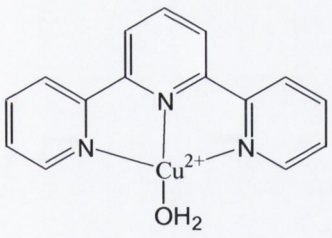

36

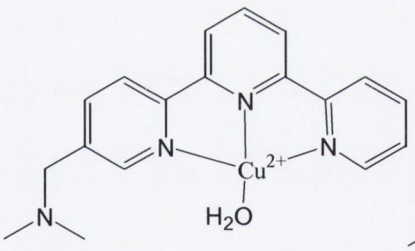

81

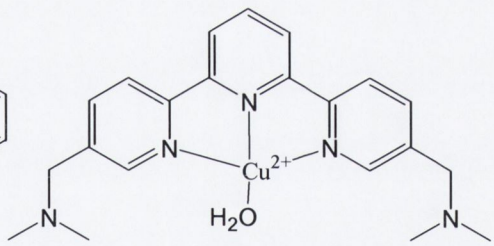

82

Complex	k x10^{-5} s^{-1}	k_{rel}
36	0.58	174
81	1.53	459
82	3.89	1167

Table 1.8. Pseudo first order rate constants (k) and relative rate enhancements (k_{rel}) for the cleavage of HPNP (0.2 mM) in 50 mM HEPES (pH 7.0) at 25 °C with various Cu(II) complexes (2.0 mM).

Breslow *et al.* observed the same effect upon adding additional catalytic groups to the Zn(II) complex **37**.[131] The addition of thiophenol, **83**, or imidazole, **84**, groups to the

molecule led to a 9 and 20 fold rate enhancement, respectively, for the hydrolysis of **HPNP**, over the original system **37**, under the same conditions, in 10 % DMSO aqueous solution with 10 mM HEPES, at pH 7.0 and 37 °C (Table 1.9).

Complex	k x 10^{-2} h^{-1}	k_{rel}
37	0.074	1
83	0.690	9
84	1.50	20

Table 1.9. Pseudo first order rate contanats (k) and relative rate enhancements (k_{rel}) for the cleavage of HPNP (0.19 mM) in 10 % DMSO in water with 10 mM HEPES (pH 7.0) at 37 °C with various Cu(II) complexes (0.5 mM).

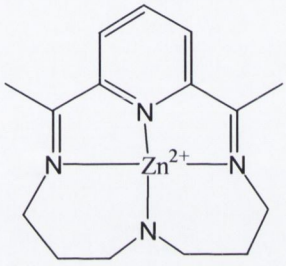

37

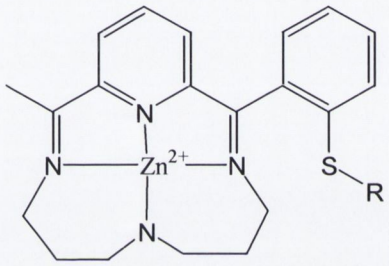

83: R=H

84: R=

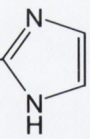

1.2.10 Antisense Approach

In order to be of use as a potential ribozyme mimic, the metal complexes described above must be engineered to cleave RNA in a sequence specific manner. It has been proposed that this sequence specificity can be obtained by covalently connecting a catalytically active complex to a DNA oligonucleotide.[54] The oligonucleotide would be specific for its complementary RNA sequence due to the Watson-Crick hydrogen bonding.[132] This is known as the antisense approach and should serve to increase the overall efficiency of RNA cleavage by both increasing binding and specificity.[133]

One of the first examples of this specificity was presented by Komiyama *et al.*, who showed that a Lu(III) complex that had been covalently bound to a DNA oligomer could selectively hydrolyse RNA at the target site.[134] The hydrolysis of the RNA (0.3 μM) was conducted at pH 8.0 and 37 °C, and under these conditions, a mixture of 1:1 DNA-IDA and $LuCl_3$ (10 μM), was found to cleave 17 % of the RNA outside the duplex, after 8 hours.

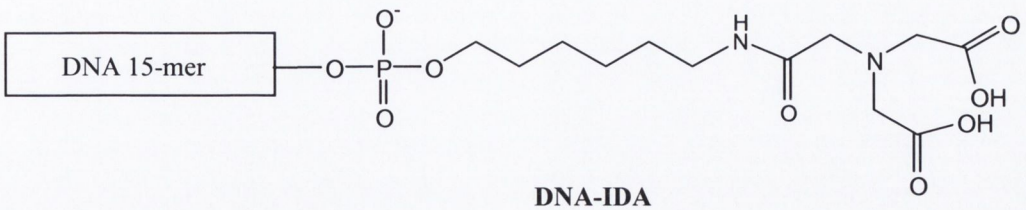

DNA-IDA

It is known that DNA-RNA hybrids are much more inert towards hydrolysis than single stranded RNA.[135] Consequently, cleavage usually occurs outside the DNA-RNA duplex, as in the above case. However, the high affinity of complimentary strands hinders product release, thus impeding catalytic turnover.[112] Positioning the cleaving moiety in the centre of the antisense oligomer leads to smaller product fragments, which are more easily released. Furthermore, the use of slightly non complementary antisnese oligomers, leads to "bulges" of single stranded RNA within the DNA-RNA hybrid which have been shown by Komiyama and Kalesse, to be cleaved with far greater ease.[136, 137]

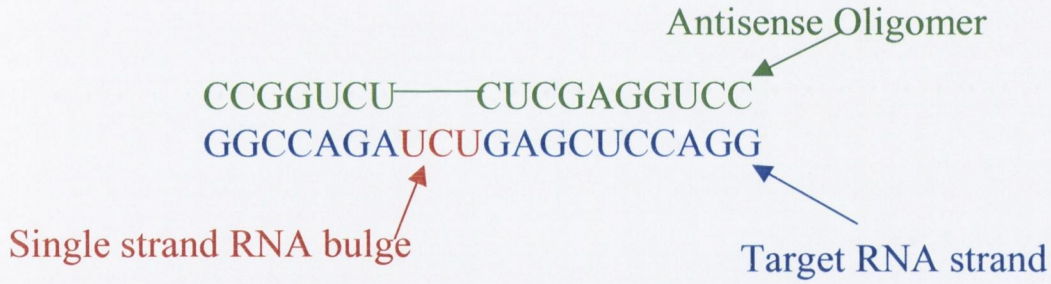

Figure 1.10. Formation of single stranded RNA bulge

Hovinen *et al.*, demonstrated that a 5 fold excess of **84**, an oligonucleotide with a histamine conjugate tethered at 3'-terminus, promoted the hydrolysis of the complementary RNA 16-mer (0.5 μM) in the presence of Zn(II) (50 μM).[138] The cleavage was predominantly observed at one site, and between 2 % and 5 % of the RNA was cleaved after 19 hours at room temperature in water buffered at pH 7.0.

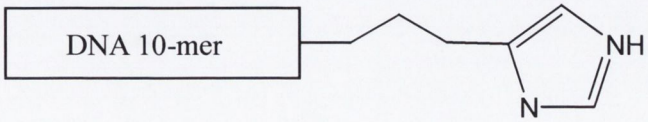

85

An alternate strategy to cleaving the RNA strand itself, is to cleave or modify the 5'-cap structure of the mRNA. The 5'-cap structure is a N7 methylated guanosine residue that is

linked to the 5'-terminus of mRNA by a triphosphate linkage. It acts as a protein recognition element in several processes of mRNA metabolism. It is believed that its alteration will result in the inhibition of gene expression.[139] Baker, Morrow and co-workers reported the 15-mer DNA tethered Eu(III) complex **86**, where the cleaving agent was attached such that upon binding its complementary RNA fragment, it would be in proximity to the 5'-cap structure of the target mRNA. The antisense oligonucleotide **86**, granted 50 % inhibition of protein expression (IC_{50}), of its target RNA 43-mer, ICAM-1 (0.25 nM), at a concentration of 18 nM in water buffered at pH 7.4, in the presence of KCl (150 mM) and NaCl (10 mM). The antisense oligonucleotide without the Eu(III) complex had a much higher IC_{50} of 64 nM. Investigation of the hydrolysis products confirmed that **86** had cleaved the 5' cap structure, however the reaction did not go to completion, due to dissociation of the Eu(III) ion from the tethered complex.

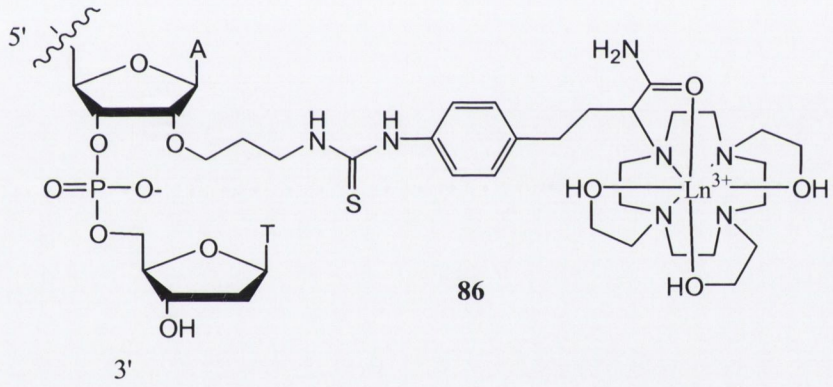

86

To date, the most active antisense oligonucleotide conjugate has been the dinuclear Cu(II) complex **87**.[140] It was found to cleave at only one nucleotide site, and offered a 130 fold rate enhancement over its mononuclear analogue. It cleaved RNA catalytically, with a rate constant of 1.8 x 10^{-4} s^{-1}, corresponding to a 6.7 x 10^4 fold rate enhancement over the uncatalysed reaction. This result further highlights the importance of developing binuclear complexes for the hydrolysis of RNA.

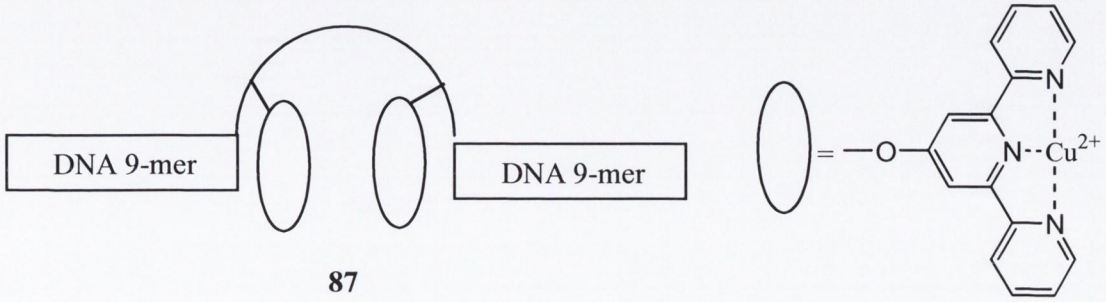

87

1.2.11 Project Aim

Metal ions, in particular lanthanide ions, have been shown to be extremely successful at accelerating the hydrolysis of phosphodiester bonds including those of RNA. For pharmaceutical applications these ions must be complexed as they can be toxic and unselective. Two or more complexed metal ions have been shown to function in a cooperative manner providing rate accelerations many times above that of similar mononuclear systems. However, relatively few examples of cooperative rate enhancements by binuclear lanthanide complexes exist. With the ultimate aim of efficient and selective RNA hydrolysis for the reasons of disease control mentioned earlier, the aim of this project is to design and synthesise binuclear lanthanide complexes, which can cleave phosphodiesters by utilising the cooperative action between two metal ions. These complexes should show large rate enhancements over similar mononuclear systems and offer possibilities for further functionalisation.

As such the design shall be based on a bis-cyclen template **88**, which allows for functionalisation with various R groups. It has been previously observed that modification of the cyclen pendant arms, can lead to large increases in phosphodiester hydrolysis activity.[73] Therefore, a number of different pendant arms, including amide, glycine and pyridine pendants, shall be employed in order to allow comparison to similar mononuclear systems and investigate the effect of varying pendant groups for binuclear lanthanide complexes.

Particular attention shall be focused upon the choice of spacer group employed, as it will play a vital role in determining the intermetal distance, as well as the overall flexibility and geometry of the binuclear complexes, and thus it will have a large input into determining whether the two metal ions function in a cooperative manner or not. As already discussed, it appears that metal centres linked by very flexible scaffolds display a smaller cooperative activity compared to more rigid scaffolds.[96] Nevertheless, molecules that are too rigid have also shown poor cooperative activity.[105] Consequently, a range of rigid and flexible spacers, or bridging groups shall be investigated, and their phosphodiester cleaving ability will be compared. Comparisons shall also be drawn against similar mononuclear systems. This work shall be discussed in Chapter 4.

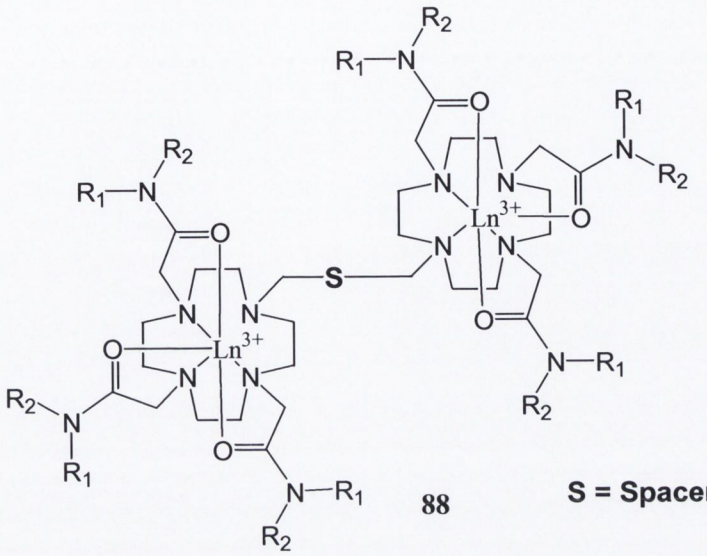

88 **S = Spacer**



Chapter 2

Lanthanide Luminescent Cu(II) Sensor

2.1 Introduction

Copper is a tough and ductile metal from group 11 of the periodic table. Loss of an electron leads to the diamagnetic Cu(I) ion, which has a $3d^{10}$ electronic configuration.[11] Biologically however, the most important oxidised form of copper is Cu(II), which is paramagnetic due to its $3d^9$ electronic configuration, and characteristically prefers a distorted octahedral or square planar coordination environment.[141] Copper plays a vital role in the human body. It is one of relatively few metals essential for human health and is a vital component of many enzymes including, ceruloplasm, superoxide dimutase, cytochrome oxidase, tyrosinase, monoamine oxidase, lysyl oxidase and phenylalanine hydroxylase.[142, 143] Copper is found in all the organs and tissues of the human body, with the highest concentrations present in the liver, brain, heart and kidneys.[141] The distribution of copper ranges from 1.4 – 2.1 mg/kg for the average human or 12 – 21 μM.[144] In blood copper is bound in its Cu(II) oxidation state to albumin or transcuprin as well as other chelating peptides and amino acids.[142, 143] Copper is also the main oxidation catalyst for one electron reactions occurring outside the cell.[145] While trace amounts are essential, excessive amounts are extremely toxic and can result in fatal liver damage.[142]

There are a number of genetic disorders that affect copper utilisation, the most serious of which are associated with Menkes syndrome and Wilson disease.[146] Wilson disease involves a fault in copper transport throughout the body and results in accumulation of copper in the liver and brain of affected individuals.[142, 147] Menkes syndrome is a fatal copper transport disorder that kills infants before the age of three if not treated. A defect in the absorption of copper through the gut leads to a deficiency of copper in the body, and hence to both mental and physical deterioration.[141, 142]

The common methods for the quantification of copper are neutron activation analysis (NAA), atomic absorption spectroscopy (AAS) and inductively coupled plasma-mass spectrometry (ICP-MS), which are all based on expensive and sophisticated instruments.[148,149] As such, a stable and selective Cu(II) sensor which functions under physiological conditions, without causing harm to the host is desirable. Chapter 1 highlighted various examples of luminescent sensors for the detection of cations such as Na(I), Ca(II) and Zn(II). The following section shall detail some examples of luminescent Cu(II) sensors.

2.1.1 Fluorescent Copper(II) Sensors

Recently, there have been a number of examples of fluorescent Cu(II) sensors detailed within the literature.[150] One such example is the two component chemosensor developed by Fabbrizzi *et al.*, which utilises a fluorescent anthracene chromophore as a signalling moiety and a tetrathia-macrocycle as the receptor.[151] In anhydrous EtOH, after excitation at 368 nm, the compound **89** (1 μM), exhibited a strong fluorescence band centred at 470 nm. Upon addition of Cu(II) however, the intensity of the emission gradually decreased and was fully quenched by one equivalent of Cu(II). The authors attributed this to the quenching of the charge transfer excited state of the anthracene by an electron transfer to the Cu(II) ion. The sensor was also reported to be selective for Cu(II) in the presence of the ions of Mn(II), Fe(II) , Co(II) and Zn(II).

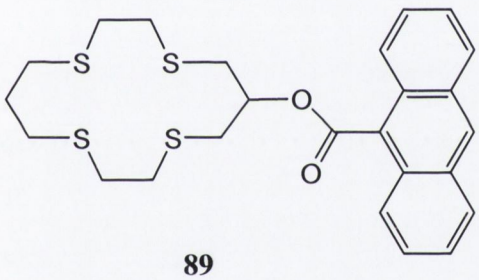

89

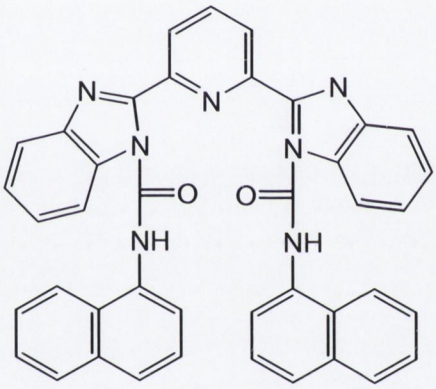

90

Zhou *et al.* reported another example of a fluorescent Cu(II) sensor, the *N*-substituted 2,6-bis(benzimidazol-2-yl)pyridine **90**.[152] In DMF, after excitation at 320 nm, **90** (10 μM), showed a broad fluorescence peak at 380 nm. This fluorescence was found to be quenched after the addition of one equivalent of Cu(II), while the presence of the divalent ions Co(II), Ni(II) and Zn(II) did not effect the fluorescence of **90**.

The examples discussed above, operate in non aqueous media, however, as the main applications envisaged for successful copper sensors would be analysis of environmental or biological samples, the ability to operate in water at pH ~ 7 is vital.[153] Gunnlaugsson *et al.* have developed a colorimetric Cu(II) sensor, which functions in water at pH 7.4.[154] Under these conditions the azobenzene based chemosensor **91**, has a deep red colour due to the internal charge transfer (ICT) from the electron donating amine to the electron withdrawing nitro group. Upon the binding of Cu(II), however, the amine can no longer participate in the ICT process and the colour of the solution is observed to change to

yellow. The process was found to be reversible as the addition of EDTA returned the solutions colour to a deep red. Group I and II metals such as Na^+, Ca^{2+} and Mg^{2+} had no effect upon the sensor, while Cd(II) and Zn(II) were found to elicit the same response, albeit in a different concentration range. Interestingly, for compound **92**, no response towards transition metals was observed, and this was attributed to the lack of the *o*-methoxy group.

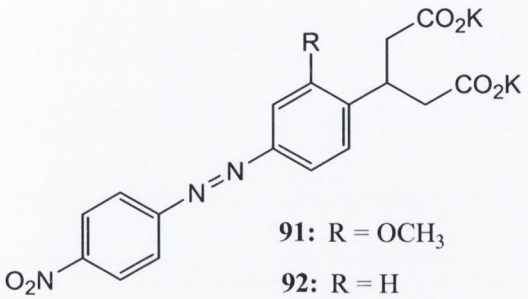

91: R = OCH_3

92: R = H

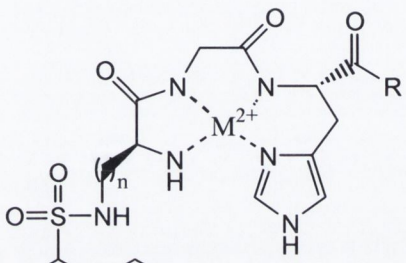

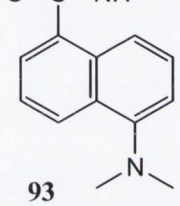

93

R =

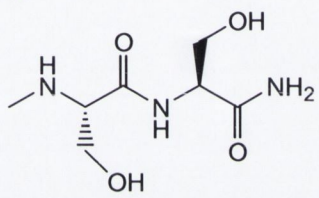

There have also been examples of fluorescent Cu(II) sensors that operate under these aqueous conditions. Imperiali *et al.* reported the chemosensor **93**, which utilises a Gly-Gly-Hys tripeptide as a binding receptor.[155] In buffered water at pH 7.0 (150 mM NaCl), after excitation at 333 nm, the compound **93** (10 μM), was found to have a broad fluorescence band at ~ 550 nm. The addition of Mn(II), Co(II), Mg(II), Ca(II), Zn(II) or Cd(II) had no effect upon the fluorescence, nevertheless, the addition of one equivalent of Ni(II) was found to quench the fluorescence to 15 – 35 % of the original intensity, while one equivalent of Cu(II) quenched the fluorescence to 7 % of its initial value. The addition of EDTA reversed the quenching, reinstating the fluorescence.

Beltramello *et al.* reported another example, which was based on a triamino-trihydroxy-cyclohexane scaffold.[156] The compound **94** (5 μM), in water at pH 7.0 displayed a broad fluorescence band at 425 nm after excitation at 330 nm. Addition of one equivalent of Cu(II) quenched the fluorescence to 15 % of its original value, while Ni(II), Co(II), Zn(II), Pb(II), Cd(II) and Mn(II) had no effect, although Fe(II) and Hg(II) did quench the fluorescence by ~ 20 %.

One other example is the anthracene based ligand **95**, reported by Czarnik *et al.*, which signals the presence of Cu(II) or Hg(II) in water.[157] Under aqueous conditions at pH 7.0, the compound **95** (4 μM), after excitation at 368 nm, showed a broad fluorescent band which was unaffected by the presence of Ca(II), Cr(III), Ni(II), Co(II), Zn(II), Pb(II),

Cd(II), Mn(II) and Fe(III). Upon addition of Hg(II) or Cu(II), however, the fluorescence was found to be reduced by 18 fold and 4 fold respectively.

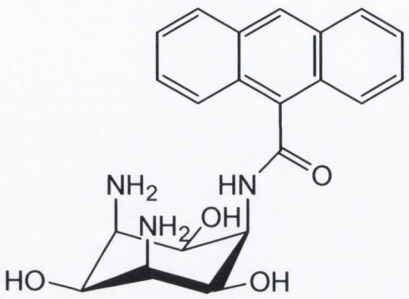

94

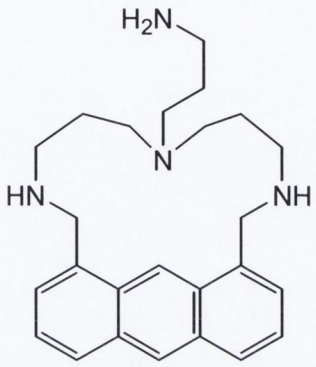

95

As mentioned in Chapter 1, the drawback to all of these fluorescent systems comes into play when working with biological samples, where the fluorescent signal has to compete against the autofluorescence of the biological sample itself. The aim of this project is to synthesise a lanthanide luminescent Cu(II) sensor, which can overcome the autofluorescence issue due to the long-lived nature of the lanthanide emission, as discussed in Chapter 1.

2.1.2 Requirements for Luminescent Sensor

If the sensor is to be used as a diagnostic tool for medicinal purposes there are a number of requirements that it must fulfil.

- The sensor should not be toxic as it may need to be administered directly to the patient, as such it should be kinetically and thermodynamically stable.
- It is essential that the sensor function under physiological conditions (*i.e.* aqueous environment, pH 7.4, high ionic strength).
- The sensor must also be selective for a specific target as it will be in the presence of numerous other ions.
- It should also be sensitive for a specific concentration range.
- Finally, the sensor must be able, after recognition of a specific target species, to somehow signal this presence.

As stated before the final signalling step is not a trivial problem when dealing with tissue samples due to the short lived background radiation (ns time scale) from the body tissue

itself. Lanthanide luminescent sensors may be employed here in order to circumvent this problem.

As stated in Chapter 1, lanthanide luminescent systems have some significant advantages over analogous fluorescent systems.

- They are able to overcome the autofluorescence and light scattering of body tissue.[158,186]
- Their long lived excited states (ms) allows the short-lived background fluorescence to disperse before the lanthanide emission occurs.
- The long wavelengths (500-750 nm for Eu(III)) at which lanthanides emit occur beyond the absorbance of body tissue, this is important for signal quality.
- Their line-like emission bands (10 nm) also give a better signal to noise ratio compared to fluorescent bands (several hundred nm).

With these requirements and conditions in mind we set about designing and synthesising a luminescent sensor for Cu(II).

2.2 Design of Lanthanide Luminescent Sensor

Free lanthanide ions are not very soluble in water and tend to form hydroxide gels at high concentration, which precipitate out of solution.[159] They are also toxic due to their similarity in both charge and size to Mg(II) and Ca(II).[160] In addition to this, protic solvents quench lanthanide luminescence by non-radiative vibrational decay through the O-H oscillators.[161] In order to overcome these drawbacks the lanthanide ions must be complexed *i.e.* incorporated into a ligand. This increases their stability,[162] and provides shielding from water molecules hence increasing the luminescence. There are many such examples of this in the literature.[163,180,181] The cyclen macrocycle, or 1,4,7,10-tetraazacyclododecane, is a good example of this, which when suitably functionalised virtually encapsulates the lanthanide ion forming complexes that are inert to dissociation in water at 37 °C, neutral pH.[162,186,187] Europium (III) was selected as the lanthanide ion, because it emits in the red (700 nm) *i.e.* beyond the absorbance of body tissue. Lanthanide ions have a high coordination number requirement, nine for Eu(III). This high coordination requirement will be fulfilled by the four donor nitrogen atoms from the cyclen macrocycle, and four donor oxygen atoms from the pendant amide arms. The remaining coordination site will be filled by a water molecule.

In order for a lanthanide to emit it must first be excited. As explained in Chapter 1, directly exciting a lanthanide ion is not feasible, as it requires a Laporte forbidden *f-f* transition.[164,176] This problem is solved by connecting a sensitising chromophore or "antenna" to the lanthanide ion, which can pass its excited energy onto the lanthanide ion by an energy transfer process, resulting in a lanthanide emission.

It is worth recalling the Jablonski diagram from Chapter 1, which illustrates this indirect excitation (Figure 2.1).[165]

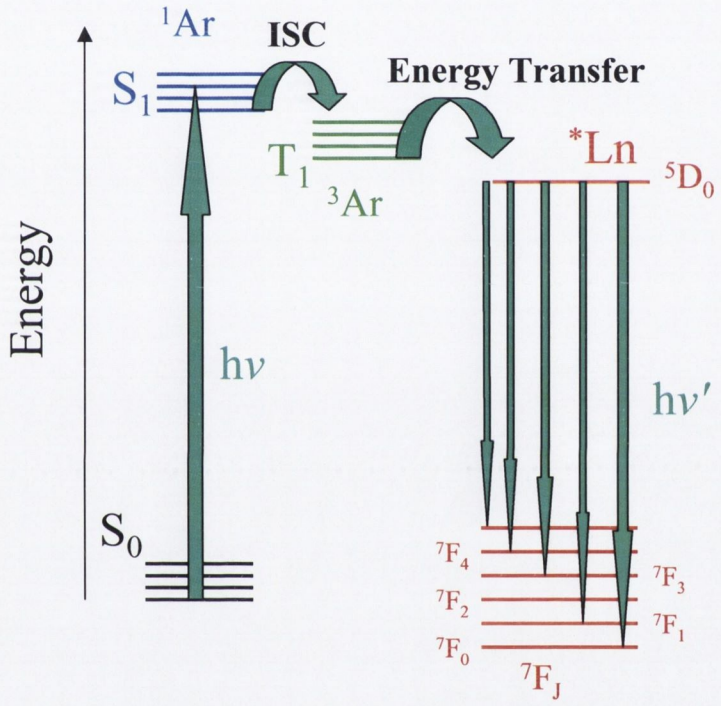

Figure 2.1. Jablonski Diagram illustrating sensitisation of a lanthanide ion. Other energy loss pathways have been omitted for clarity[166]

The sensitising antenna, denoted Ar, absorbs a photon, hν, and is excited to its singlet excited state, ^{1}Ar. From here the energy can be passed into the antennas triplet excited state, ^{3}Ar, *via* intersystem crossing (ISC). The lanthanide's excited state, *Ln, can now be populated from the antennas triplet state, by means of an intramolecular energy transfer (ET), provided that this triplet state is higher in energy than the lanthanide excited state. The excited energy now resides on the lanthanide ion, and can be lost by emission of light, resulting in the characteristic lanthanide emission spectra as each transition will correspond to an emission band.

As explained in Chapter 1, the pathway shown in Figure 2.1 is not the only path by which the excited energy can be lost. This pathway must compete with other mechanisms through which the energy can be discarded (Scheme 2.1).[165] Energy can be lost through radiative

decay *i.e.* fluorescence and phosphorescence, or non-radiative decay by collisions and vibration interactions with the surrounding molecules. The lanthanide excited state *Ln can also lose its energy through non-radiative decay by vibrational interactions with molecules such as water.[167]

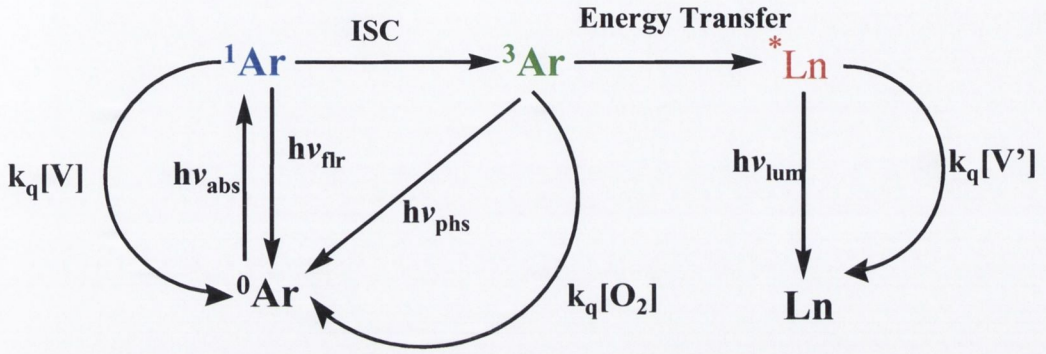

Scheme 2.1. Competing paths for energy loss include radiative decay through fluorescence $h\nu_{flr}$ and phosphorescence $h\nu_{phs}$, aswell as non-radiative quenching due to vibration, $K_q[V']$, and triplet quenching by O_2, $K_q[O_2]$[176]

In order for our preferred pathway to operate *i.e.* population of the lanthanide excited state followed by a lanthanide emission, our design must minimise energy loss to other pathways. By maximising the efficiency of the intersystem crossing and energy transfer processes, it is possible to minimise losses to other deactivation pathways. As stated before, ISC is made possible by spin-orbit coupling, which is increased by the presence of a heavy atom, so the very presence of a lanthanide ion will increase the efficiency of this process.[165]

Once in the lanthanides orbitals, the energy is somewhat isolated from its environment.[11] Back energy transfer is possible but minimised by having the ^{3}Ar state sufficiently higher above that of the *Ln state. Vibrational quenching by metal bound water molecules is now the main competing deactivation pathway. By minimising the number of these this non-radiative quenching can be minimised.

So to recap the design requires a lanthanide ion, Eu(III), tightly bound by a ligand to minimise metal bound water molecules and maximise stability and solubility. This will be accomplished using the cyclen macrocycle functionalised with amide arms. The design also requires a sensitising chromophore or antenna, which has a triplet state energy level higher than that of the Eu(III)'s $^{5}D_0$ excited state. The distance between this antenna and the lanthanide ion must be minimised. Finally a suitable receptor to bind Cu(II) ions is a necessity.

Phenanthroline was chosen as the antenna (Figure 2.2). Phenanthroline has a triplet energy above that of Eu(III)'s $^5D_0$ excited state and is known to be able to populate this state and hence stimulate a lanthanide emission.[168,169] The elegance of this system is that the antenna will also function as the receptor. Phenanthroline has two nitrogen atoms which can bind Cu(II).[170] The binding of the Cu(II) will interfere with the energy transfer process by changing the redox potential of the antenna, lowering its triplet state below that of the lanthanides excited state, thereby quenching the luminescence. So this will be an "*on-off*" system.

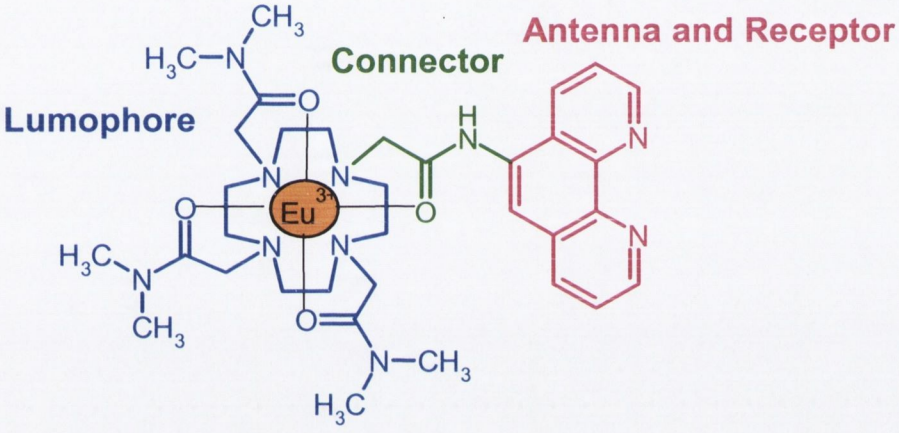

Figure 2.2. Copper Sensor showing various parts.

2.3 Synthesis

The aim was to synthesise a lanthanide luminescent sensor for Cu(II), where europium would play the part of the signalling system. As mentioned before lanthanide ions tend to be toxic and have a high coordination number requirement and so to circumvent both of these problems a cyclen macrocycle functionalised with pendant amide arms was employed. The eight donor atoms would satisfy the high coordination requirement while also forming a stable complex.

2.3.1 Synthesis of Tris Functionalised Cyclen

The cyclen macrocycle was functionalised with three pendant amide arms, according to the literature procedure[171] by reacting three equivalents of the α-chloroamide, 2-chloro-*N,N*-dimethyl-acetamide, **98a**, with cyclen, **99**, in the presence of $NaHCO_3$ in refluxing MeCN for three days (Scheme 2.2). After the inorganic salts were filtered off, the solvent was

removed and the residue purified by alumina column chromatography gradient elution 100 → 80:20 CH_2Cl_2:MeOH(NH_3). The desired product 2-(4,7-Bis-dimethylcarbamoylmethyl-1,4,7,10tetraaza-cyclododec-1-yl)-*N,N*-dimethyl-acetamide, **100**, was yielded as a white foam 8.63 g, in 35 % yield.

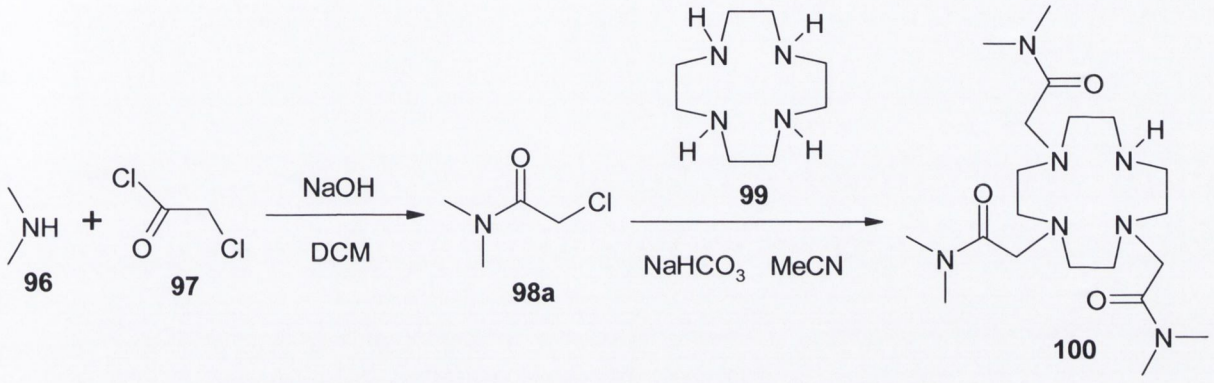

Scheme 2.2. Synthesis of tris functionalised cyclen[171]

The spectral data for this product was in agreement with the published characterisation.[171] The ^{1}H NMR showed the presence of 1 NH proton at 9.99 ppm and also the peaks corresponding to the CH_2 protons from the pendant amide arms at 3.59 and 3.58 ppm (2 peaks due to C_2 symmetry).

The α-chloroamide arms were formed by adding a solution of chloro acetylchloride, **97**, in CH_2Cl_2 to an aqueous solution of *N, N* dimethylamine, **96**, and NaOH at –15 °C.[172] The reaction was left to stir at room temperature overnight. The resulting solution was then filtered and the organic layer separated and washed repeatedly with 0.1M HCl. The organic layer was then dried over K_2CO_3 and the solvent was removed under reduced pressure to yield an oil in 46 % yield. The spectral data for this product was in agreement with the published characterisation.[172]

The pendant amide arms were chosen due to their stability and their ability to form strong complexes. Amides have the ability to form a resonance structure (Scheme 2.3). This resonance form hinders rotation about the N=C double bond, makes the amide molecule planar and very stable towards nucleophilic attack or hydrolysis.[173] It also increases the donor ability of the oxygen towards Lewis acids.

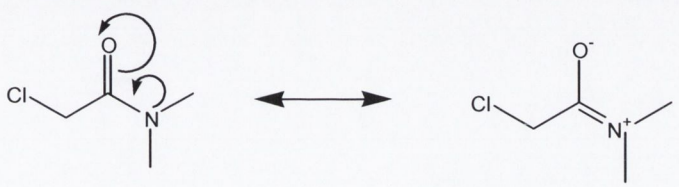

Scheme 2.3. Resonance forms of α-chloroamide

2.3.2 Synthesis of Eu.104

Phenanthroline was to play a dual role as both antenna and receptor. In order to link it to the cyclen macrocycle framework it was to be modified with a short α-chloroamide connector. This was synthesised from 5-nitro-[1,10]-phenanthroline, **101**, which was reduced by refluxing with Pd/C 5 % and hydrazine hydrate in absolute ethanol to yield 5-amino-[1,10]-phenanthroline, **102**.[174] The resulting yellow solid was triturated with ether and dried under vacuum to give a yellow solid in 93% yield (Scheme 2.4). The spectral data for this product agreed well with the published characterisation.[174] The ^{1}H NMR showed the presence of a doublet at 9.18 ppm corresponding to the H_2 proton, while the H_9 proton was seen as a doublet at 8.95 ppm. The clearest indication of the formation of the product however, was the appearance in the spectrum of the two NH protons at 6.15 ppm.

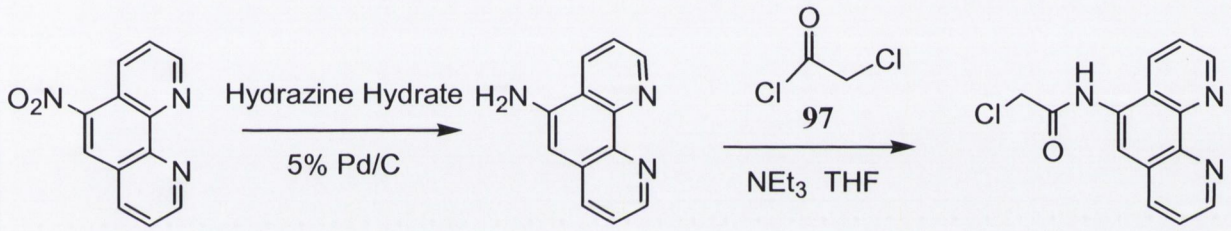

101 **102** **103**

Scheme 2.4. Synthesis of the phenanthroline antenna/receptor

The 5-amino-[1,10]-phenanthroline, **102**, was next acylated by refluxing with chloroacetyl chloride, **97**, in a solution of THF and triethylamine under argon for 18 hours. The product, 2-chloro-*N*-[1,10]phenanthrolin-5-yl-acetamide, **103**, a brown solid, was isolated in 59 % yield. This was characterised by high resolution mass spectrometry and NMR. The ^{1}H NMR spectrum of **103** showed the presence of a single amide NH proton at 8.91 ppm. The appearance of a new peak at 4.43 ppm corresponding to the two CH_2 protons was also observed. The product was also readily identifiable from the ^{13}C NMR spectrum by the appearance of the carbonyl peak at 164.2 ppm as well as the CH_2 peak at 42.8 ppm.

This antenna was then connected to the macrocycle framework. **100** and **103** were reacted together in DMF in the presence of Cs_2CO_3 and refluxed for 12 hours under argon (Scheme 2.5). The resulting brown oil was purified by alumina column chromatography using gradient elution 100 → 90:10 CH_2Cl_2:MeOH, to give the desired product 2-[4,7-Bis-dimethylcarbamoylmethyl-10-([1,10]phenanthrolin-5-ylcarbamoylmethyl)-1,4,7,10 tetraaza-cyclododec-1-yl]-*N,N*-dimethyl-acetamide, **104**, as a pale solid in 38 % yield. This

was characterised by conventional methods, ^{1}H, ^{13}C NMR, ESMS, IR and high resolution mass spectroscopy.

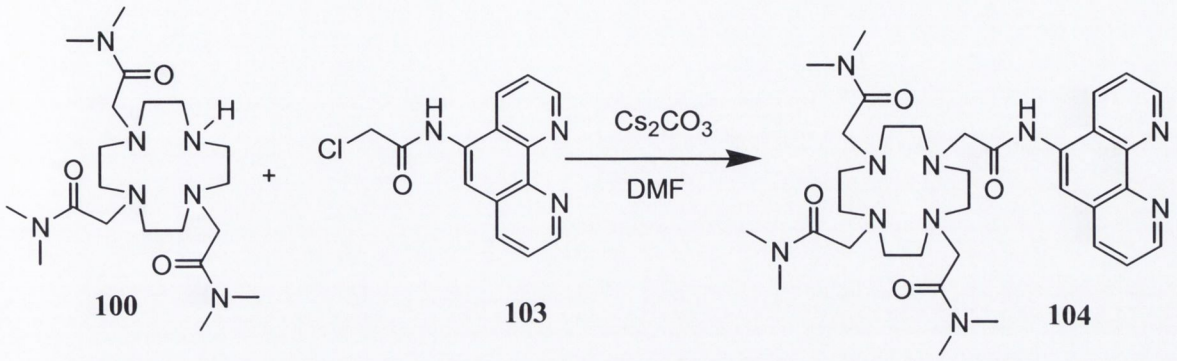

Scheme 2.5. Ligand Formation

The ^{1}H NMR spectrum of **104** (Figure 2.3) showed the presence of 1 NH proton at 11.35 ppm as well as the seven phenanthroline resonances. The cyclen and CH_2 resonances were observed as a broad signal at ~ 2.57 ppm due to the fast relaxing nature of the molecule.The ^{13}C NMR spectrum showed three quaternary carbonyl peaks (due to the C_2 symmetry plane through the cyclen) and four quaternary aromatic peaks. The seven aromatic peaks of the phenanthroline are also visible as well as seven CH_2 and two CH_3 peaks.

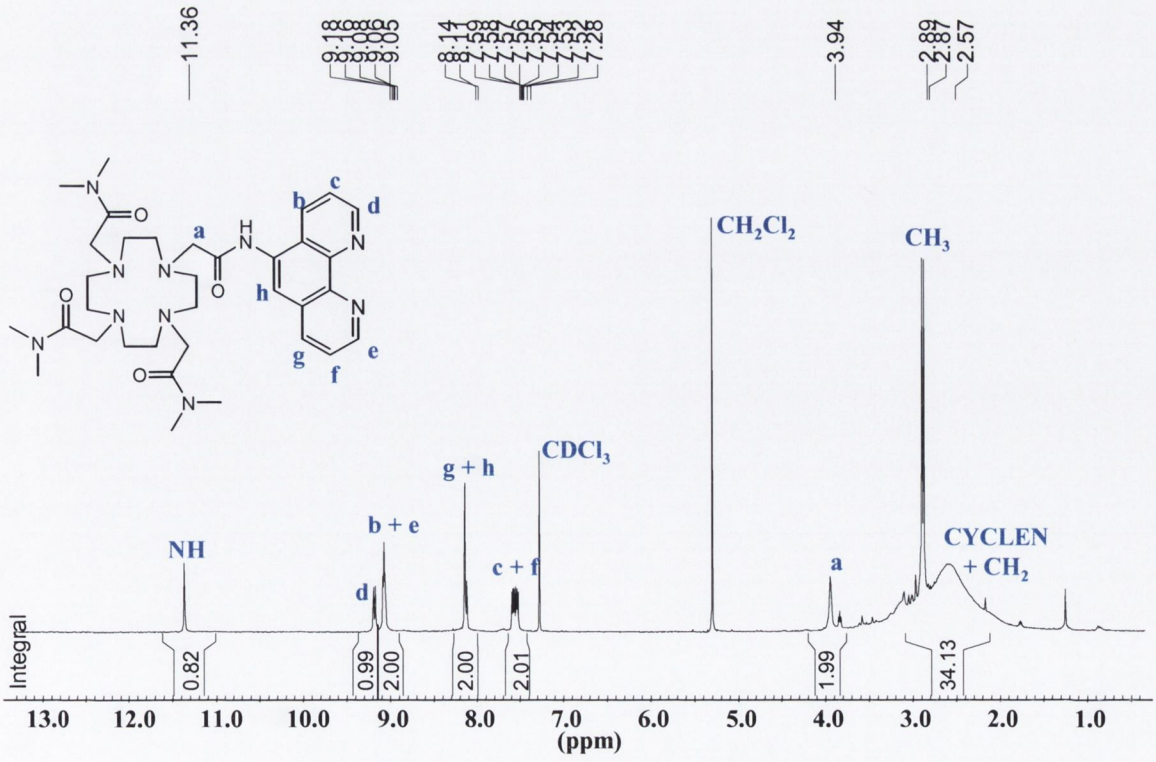

Figure 2.3. 400 MHz ^{1}H NMR of 104 in $CDCl_3$

Finally the lanthanide complex **Eu.104** was formed by refluxing the ligand with 1.1 equivalents of $Eu(CF_3SO_3)_3$ (Europium triflate) under argon in MeCN for 18 hours. The complex was precipitated from ether and then from CH_2Cl_2 before being collected by filtration and dried under vacuum to give a brown solid in 90 % yield. The characterisation of this sample will be discussed in the next section.

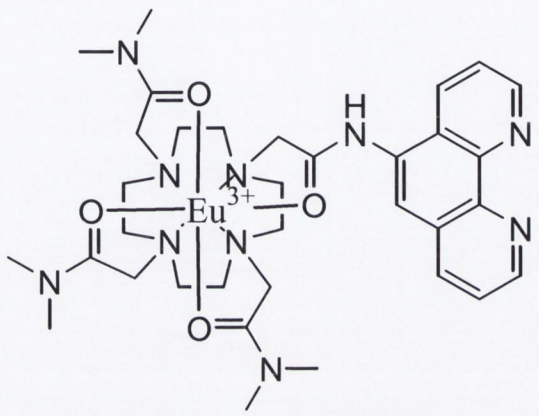

Eu.104

2.4 Characterisation of Eu.104

The complex was characterised by ^1H NMR, ESMS, IR, and high resolution mass spec. Lanthanides are shift reagents.[175] Protons in close proximity to the paramagnetic lanthanide ion will experience an extra magnetic field and will be shifted in the NMR spectrum accordingly. In this case the axial and equatorial protons of the cyclen ring as well as the acetamide CH_2 protons will be shifted by the Eu(III) ion. Lanthanide complexes also give rise to fast relaxation times and broadens the peaks of the spectrum. This shall be discussed in greater depth in Chapter 4.

Normally an NMR spectrum is run from 0 to 20 ppm however, as europium is a NMR shift reagent, a much larger spectral width is employed from 50 to –50 ppm (Figure 2.4).Notice the peaks at 28, –3, –8, –12, and –15. These are europium shifted axial and equatorial CH_2s. This is indicative of the geometry in solution; which is mono capped square antiprismatic.[176] The broad spectrum is what we would expect for a europium complex due to its fast relaxation properties along with the presence of other geometries in solution due to stereochemical nonrigidity.[177]

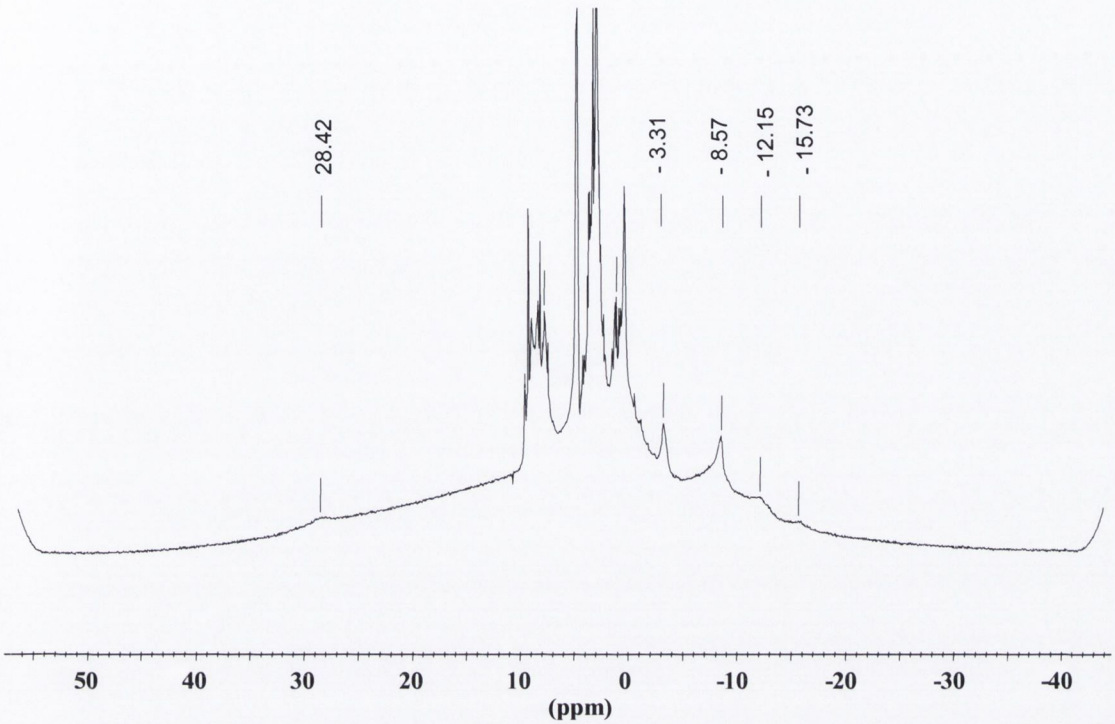

Figure 2.4. ^{1}H NMR of Eu.104 showing the effect of the paramagnetic europium metal ion

The mass spectrum for the complex showed two peaks. One at 406.9 corresponding to the M+2H/2 species. The other at 481.8 corresponds to the M+Triflate/2 species. The distinctive isotope distribution pattern (Figure 2.5), is due to the presence of the two europium isotopes. High resolution mass spectrometry confirmed the characterisation of the molecule.

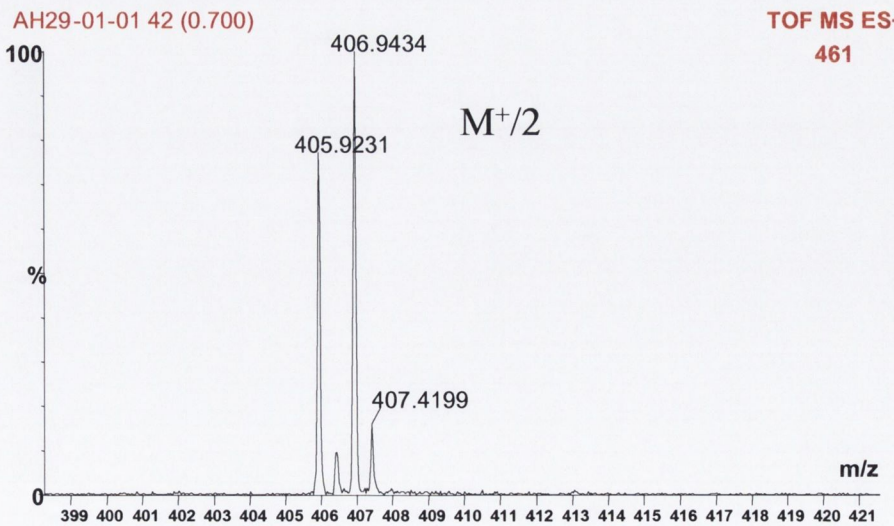

Figure 2.5. Mass spectrum of Eu.104 showing europium isotope pattern

As mentioned before lanthanides have a very high coordination number.[176] When a ligand cannot totally accomplish this high coordination number, solvents, such as water molecules, will often fill the extra coordination positions. In this case one metal bound water molecule was expected to be present as europium has a coordination number of nine.[178] In order to confirm this, the luminescent lifetimes (τ) of the lanthanide-excited states were measured in D_2O and H_2O, by direct excitation of the Eu(III) ion at 395 nm. From these measurements the number of metal bound water molecules, or q value, was evaluated using the following equation.[179, 180, 181]

$$(i) \qquad q^{Eu(III)} = 1.2\,[(1/\tau_{H2O} - 1/\tau_{D2O}) - 0.25 - 0.075x]$$

Here the prefix 1.2 is a proportionality constant that mirrors the sensitivity of the europium ion to quenching by metal bound water molecules. The correction term – 0.25 represents quenching by second sphere water molecules, while – 0.075x represents the quenching by *N-H* oscillators, where x is the number of such oscillators directly bound to the complex. From this the q value was indeed determined to be 1 (Table 2.1).

Complex	τ_{H2O} (ms)	k_{H2O} (1/ms)	τ_{D2O} (ms)	k_{D2O} (1/ms)	q (±0.5)
Eu.104	0.328	3.050	0.528	1.892	1.00

Table 2.1. Determination of q value shows there is one metal bound water molecule

The following section will detail studies performed to evaluate the molecules ability to operate as a sensor for Cu(II). Of particular interest, will be the complexes lanthanide luminescence behaviour, both as a function of pH and of metal ion concentration.

2.5 Photophysical Properties

The design of the sensor envisaged indirect excitation of the europium ion by a covalently attached antenna, which could absorb a photon of light and then pass its excited energy to the lanthanide excited state *via* its own triplet state. To test whether the molecule functioned as it was designed, a series of measurement were carried out in water at pH 7.4 (buffered with 0.1 M HEPES) under ambient conditions. These conditions were selected due to their similarity to the physiological environment that the sensor should function in.

The 1, 10-phenanthroline molecule is known to have an absorption peak at ~ 265 nm.[182] The absorption spectrum of **Eu.104** showed two peak maxima at 266 nm (log ϵ = 3.66) and 230 nm (log ϵ = 3.90). After excitation at 266 nm the complex had a broad fluorescent band at 425 nm. This fluorescence band is due to the only fluorophore in the molecule, the phen antenna. This is important as it shows that the antenna's singlet state S_1 is being populated. The question now was whether this energy would be transferred to the lanthanide excited state and result in a lanthanide emission (Scheme 2.6).

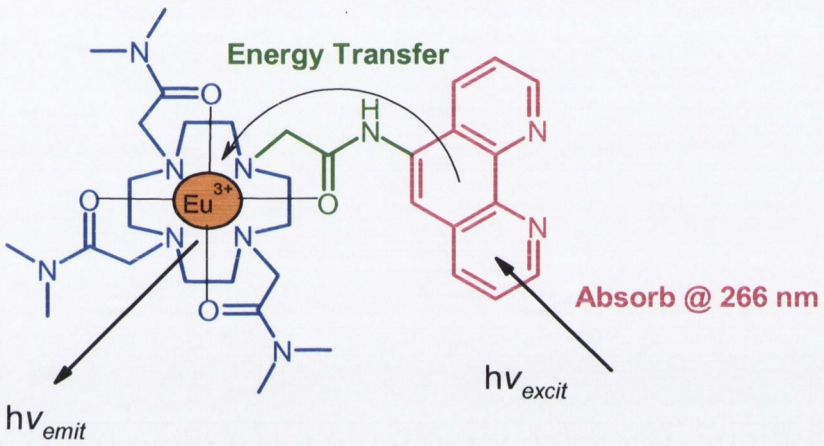

Scheme 2.6. The antenna absorbs a photon of light. It then passes its excited energy to the lanthanide *via* a energy transfer mechanism. The europium ion losses this energy with a characteristic emission spectrum

2.5.1 Lanthanide Luminescence of Eu.104

After excitation of the antenna at 266 nm, the lanthanide luminescent spectrum of **Eu.104**, showed the characteristic Eu(III) emission (Figure 2.6). This shows that the antenna is indeed able to sensitise the lanthanide ion and "switch on" the luminescence. This was an important aspect of the design as the luminescence needed to be "switched on" in order to be able to signal the presence of Cu(II) ions by a quenching of the luminescence.

There are a number of things to note here. Firstly, the lifetime of this emission is in the ms time scale, important as this negates the autofluorescence problem. Secondly it emits in the red 700 nm, which is beyond the absorbance of body tissue. Thirdly the line like emission bands (ca. 10 nm) which improve the signal to noise ratio.

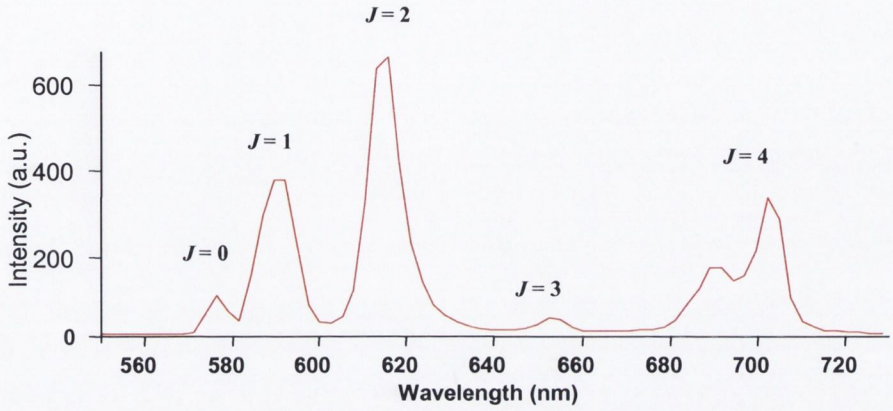

Figure 2.6. Luminescent spectrum of Eu.104, after excitation at 266 nm, showing characteristic europium emission

So far the molecule is functioning as desired. The phen moiety is acting as an antenna, absorbing energy and entering its singlet excited state. Some of this energy is being lost due to fluorescence, however, the luminescence spectra shows that the antenna is passing its energy, through its triplet excited state to the Eu(III) ion, where it is lost in the form of a photon or light emission.

It was next necessary, to determine the pH behaviour of the complex. It was foreseen that the nitrogen atoms of the phen moiety could be protonated, and that the amide nitrogen could possibly be deprotonated. A pH titration was carried out in order to ascertain whether these protonations would affect the spectral properties of the complex. The pH titrations were carried out in water with TMACl or TMAPCl (0.1 M) in order to maintain high ionic strength.

2.5.2 pH Dependence of Absorption Spectrum

At neutral pH the complex had two absorption bands with λ_{max} = 266 nm and 230 nm. As the pH was increased the absorption spectrum showed a bathochromic shift in the absorbance band at 266 nm, which was shifted to 278 nm. This bathochromic shift was again observed upon moving to alkaline pH's, along with a concomitant hypochromic effect (Figure 2.7). The shifts in absorbance correlate well with the pK_a's for the protonation of the phen nitrogen at low pH, and the deprotonation of the amide nitrogen at high pH, which will be shown later.

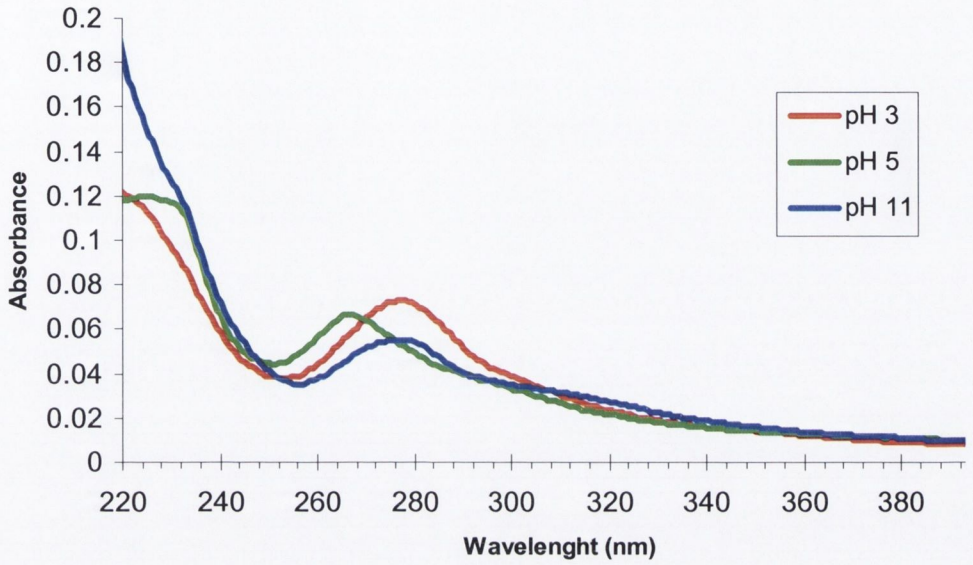

Figure 2.7. Absorption spectrum of Eu.104 showing effect of varying pH on absorbance. Note there was no clear isosbestic point

By plotting the change in pH against absorbance it is clear that the actual absorbance does not change significantly (Figure 2.8). As such the complex should function under physiological conditions or in the pH 4 – 9 region, and any major changes in luminescence cannot be ascribed to changes in the absorption spectrum.

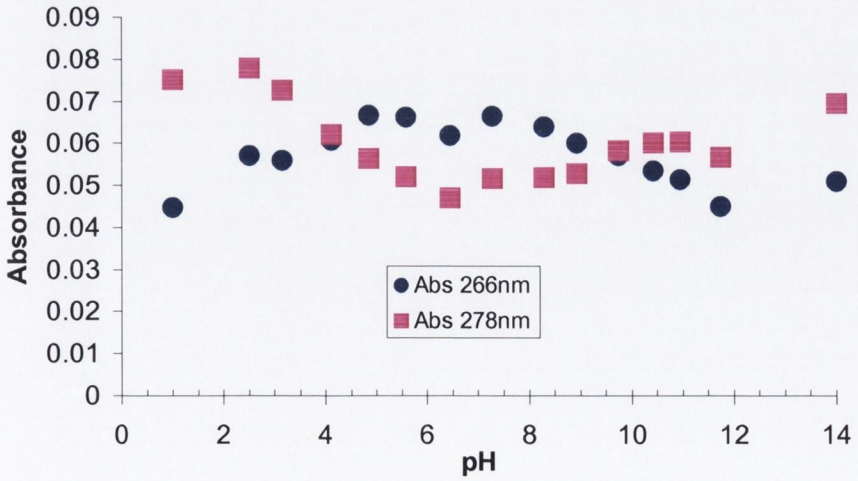

Figure 2.8. Plot of pH Vs Absorbance of Eu.104 illustrates that only small changes were observed upon protonation and deprotonation

2.5.3 pH Dependence of Fluorescence Spectrum

The changes in the fluorescence spectrum with respect to pH was also investigated in an identical manner. When the complex was irradiated at 266 nm (corresponding to the maximum absorbance of the phen antenna), a broad fluorescecne emission band, centred at 425 nm, was observed. There was a small change in the fluorescence intensity over the pH scale ~ 38 % (Figure 2.9). However, over the physiologically important pH 4 – 8 range, the change was only 15 %. The fluorescence shows that the singlet excited state of the antenna is still being populated at both acidic and alkaline pH's.

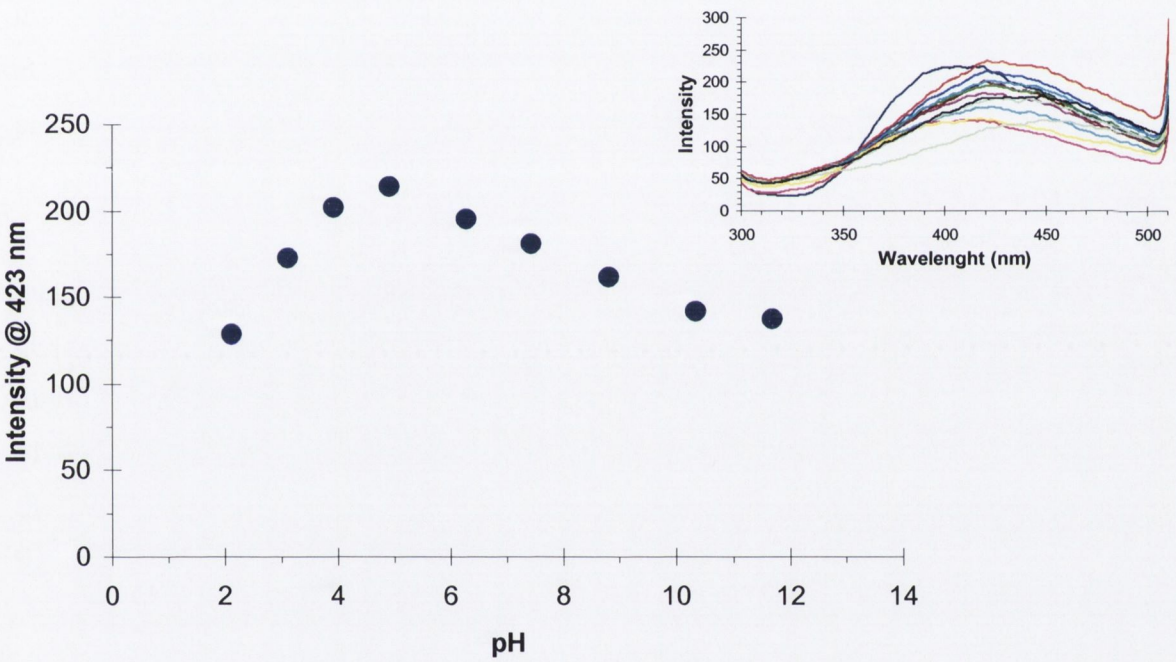

Figure 2.9. Plot showing the change in fluorescence emission of Eu.104 at 423 nm as a function of pH. Excite at 266 nm. Inset shows fluorescence spectrum

The changes in fluorescence intensity mirror those of the absorption spectra at 266 nm. This may indicate that the lower intensity in emission, at a particular pH, is due to the lower intensity of absorbance at that pH. It is clear that the protonation and deprotonation events are affecting the spectral properties, however, the overall change in absorbance and emission are relatively small. The antenna is still absorbing energy and populating its singlet excited state. Whether this energy would continue to be transferred to the Eu(III) ion, *via* the triplet excited state, shall be investigated in the next section.

2.5.4 pH Dependence of Eu(III) Luminescence

The pH dependence of the Eu(III) luminescence was also investigated in an identical manner. It was found that the changes in the Eu(III) emission, with respect to pH, were much greater than observed for the fluorescence or absorbance spectra. Furthermore, unlike the examples discussed previously in Chapter 1, such as **8**, reported by Gunnlaugsson *et al.* the lanthanide emission of **Eu.104** was not a simple "*off-on*" pH switch. In order to clearly ascertain the effect of pH upon the luminescence the results shall be discussed in two parts, the effect of base, and the effect of acid. Figure 2.10 shows the effect on the luminescence of **Eu.104** over the pH range 5.5 to 12.5. As the pH was increased a gradual decrease in the luminescence intensity was observed. This was attributed to the deprotanation of the amide moiety interfering with the energy transfer process (Scheme 2.7). Recall that the changes in absorbance and fluorescence over this pH range were relatively minor and that the singlet excited state of the antenna is still being populated. As such, there are two possible explanations for the deprotonation event quenching the Eu(III) emission. Fistly, when the amide is deprotonated this allows an electron transfer form the amide to the Eu(III) ion. The resulting Eu(II) ion is not emissive in the same area and hence the luminescence is quenched. Alternatively, the deprotonation of the amide moiety, changes the oxidation potential of the antennas excited state, moving the triplet state below the lanthanides excited state and hence prohibiting the population of the lanthanides excited state.

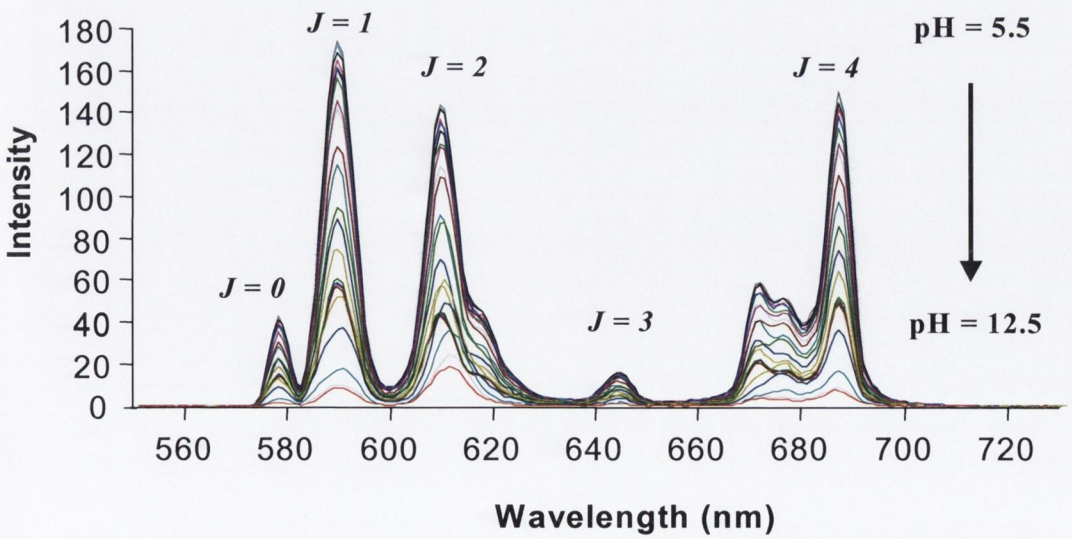

Figure 2.10. Base titration of Eu.104 showing gradual quenching of the luminescence with increasing pH. Excitation at 266nm

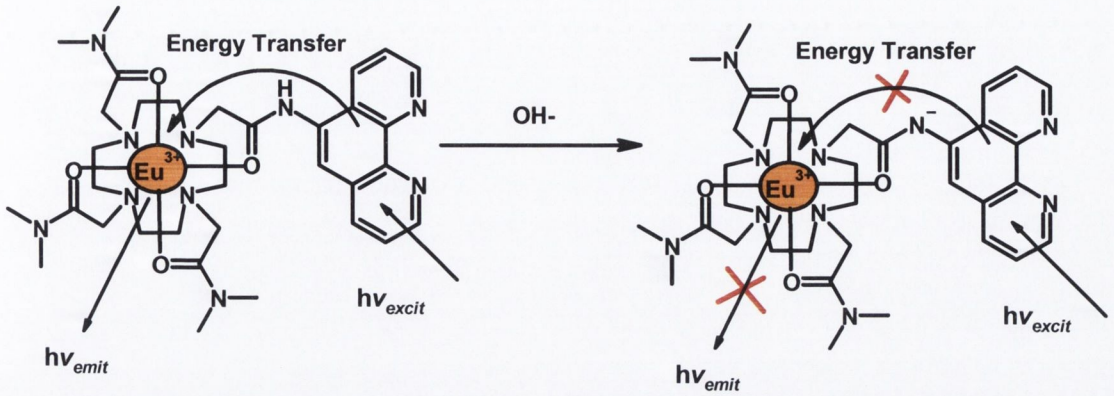

Scheme 2.7. Deprotanation of the amide interferes with the energy transfer process and hence quenches the luminescence of Eu.104

Figure 2.11 shows the effect on the luminescence of **Eu.104** over the pH range 5.5 to 1.3. Upon moving from neutral to more acidic pHs, the luminescence was found to be gradually quenched. Once again this is a drastic change compared to the changes is absorption and fluorescence discussed earlier, which showed that the singlet excited state is still being populated under these conditions of pH.

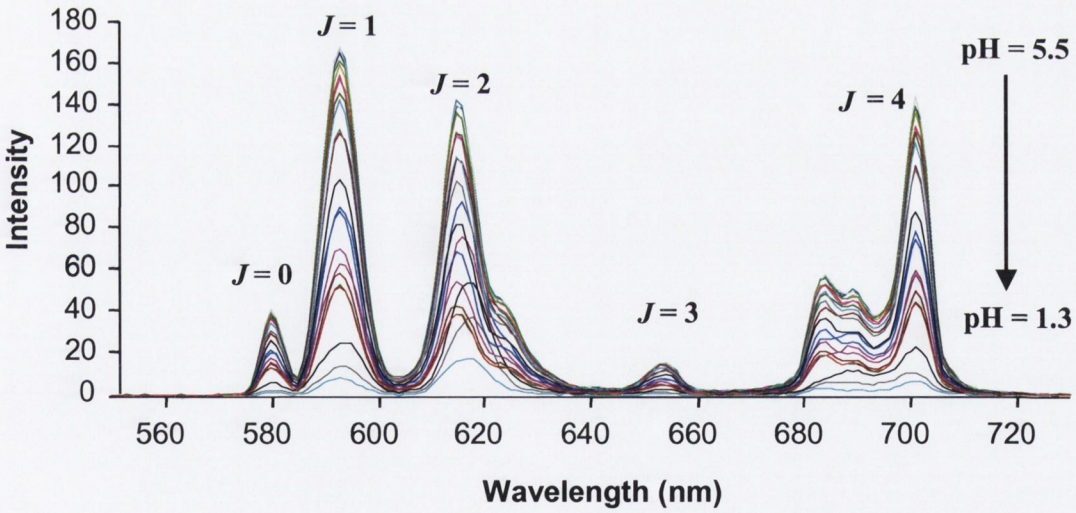

Figure 2.11. Acid titration of Eu.104 showing gradual quenching of the luminescence with decreasing pH. Excitation at 266nm

The quenching of the Eu(III) luminescence here can be attributed to the protonation of the phen nitrogen interfering with the energy transfer process to the lanthanide ion (Scheme 2.8). The reason for this is that as the phen is protonated the oxidation potential of the phen is changed.[183] This lowers the energy level of the triplet excited state below that of the lanthanide excited state and hence no energy transfer can occur (Scheme 2.9).

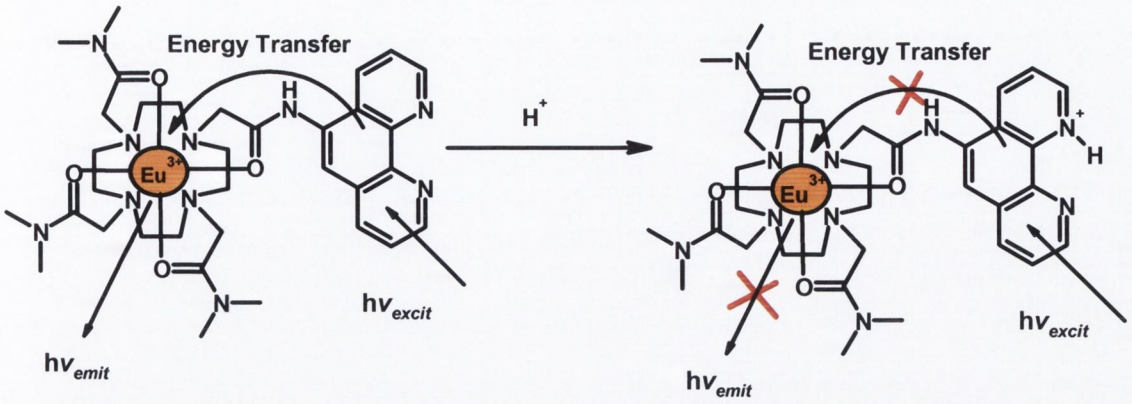

Scheme 2.8. Protonation of the phen interferes with the energy transfer process and hence quenches the luminescence of Eu.104

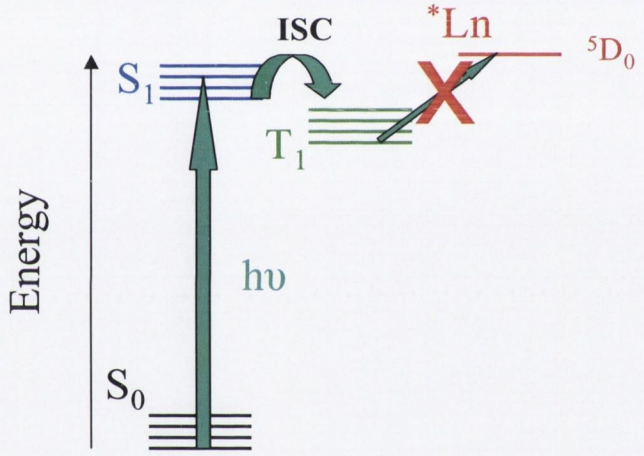

Scheme 2.9. Protonation of the phen nitrogen lowers the triplet excited energy level, T_1, below that of the lanthanide excited state which, therefore can not be populated

Combining the two titrations and plotting the luminescence intensity at 592 nm (J = 1 transition), as a function of pH gives a bell shaped pH dependent graph reminiscent of many pH driven enzymes, such as those involved in phosphodiester hydrolysis, discussed in Chapter 1 (Figure 2.12).[184] The luminescence is quenched under alkaline and acidic conditions. Crucially the luminescence is switched "on" within the physiological pH range 4 – 8. As such, this pH behaviour gives rise to an "*off-on-off*" system, which is switched "on" under physiological conditions, but switched "off" under acidic and alkaline conditions. This switching process was found to be fully reversible, and the same solution could be used to go from acid to base and back again. Furthermore the luminescence was found to be almost independent of pH between 5 and 7. This is important as small fluctuations within this pH window will not give rise to changes in the luminescence spectra and hence any changes that do occur, must be attributed to some other factor.

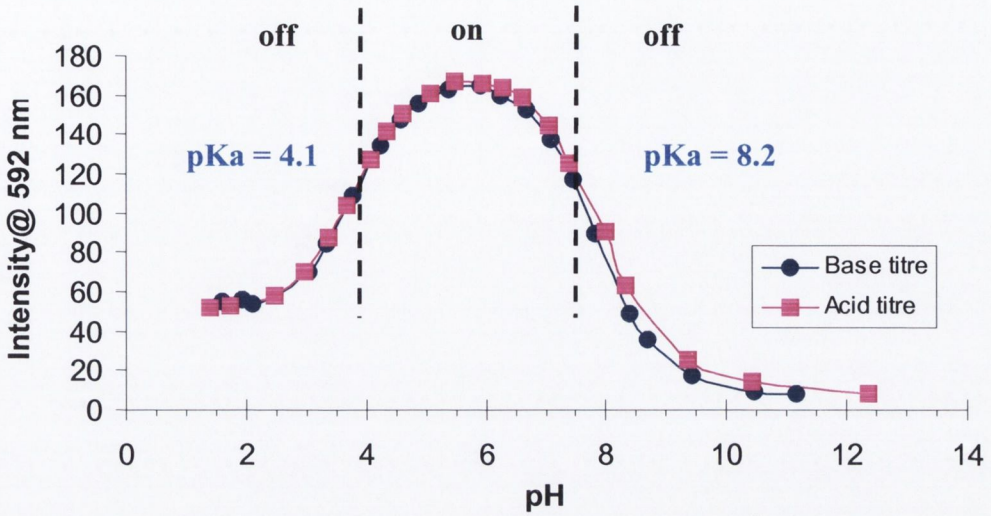

Figure 2.12. pH profile of Eu.104 showing fully reversible *off-on-off* pH dependence

It should be noted that the pH profile consists of two sigmoidal curves. From these it is possible to deduce two pK_a values; 4.1 (± 0.2) for the protonation of the phen nitrogen and 8.2 (± 0.2) for the deprotonation of the amide.

These pK_a values were confirmed by potentiometric titration of **Eu.104** (21.48 μM) with NaOH (93.92 mM) (standardised against KHphtalate) (Figure 2.13). The measurements were carried out in triply distilled water purged with argon. The starting pH was adjusted to the desired value (*e.g.* pH 3.86) using conc. HCl.

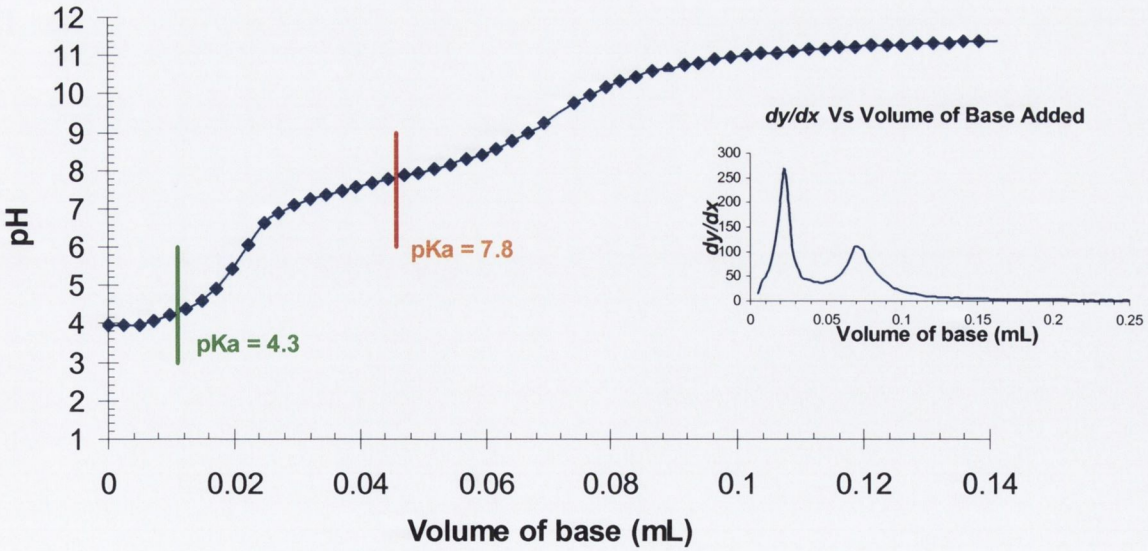

Figure 2.13. Potentiometric plot for Eu.104 shows pK_a values of 4.3 (± 0.2) and 7.8 (± 0.2). The plot of *dy/dx* (insert) shows the equivalence points at the maxima

For potentiometric plots the pK_a's are found by plotting volume of base added against *dy/dx,* where y = pH, x = volume of base added. The equivalence points will be shown as

maxima here. The first pK_a will be the pH at half the x value at the first equivalent point. Subsequent pK_a's will be the pH at half the x value between equivalence points.[185]

The complex was extensively studied to determine its stability in solution. It was found that when stored in buffered aqueous solution at pH 7.4, no discernable decrease in the luminescent intensity was observed over a six month period.

2.5.5 Determination of Metal Bound Water Molecules

Metal bound water molecules decrease the luminescence from lanthanide ions as they offer alternative pathways to losing excited energy through O-H vibrations instead of radiative decay. As a result increasing the number of metal bound water molecules on a lanthanide ion will lead to a decrease in luminescence, while decreasing the number of metal bound water molecules will lead to an increase in luminescence.[163,186,187] In order to rule out any possibility that the pH dependence displayed by **Eu.104** was due to a change in the number of metal bound water molecules, it was decided to evaluate the q values of **Eu.104** at varying pH. This was done by measuring the excited state lifetime τ, in D_2O and H_2O, at different pH's. The pH, or pD, was adjusted using HCl and NaOH in the case of H_2O, and DCl and NaOD in the case of D_2O. The pD was obtained by measuring the pH and applying the formula; $pD = pH_{measured} + 0.4$.[188] In all cases the q value was found to be 1 (Table 2.2).

pH	$1/\tau_{H2O}$ (ms^{-1})	$1/\tau_{D2O}$ (ms^{-1})	q (± 0.5)
1.4	2.320	1.270	0.87
3.0	2.443	1.133	1.18
4.0	2.643	1.554	0.92
5.3	2.559	1.160	1.29
7.1	3.050	1.892	1.00
7.9	3.359	1.930	1.32
10.1	3.709	2.695	0.83

Table 2.2. Determination of q values showed there to be one metal bound water molecule at all pHs.

In conclusion the Eu(III) luminescence is modulated by the pH to a much greater extent than either the fluorescence or absorbance spectra. The number of metal bound water

molecules remains constant over the pH range and as such, cannot be held responsible for any change in luminescence. The changes in luminescence correspond well with the pK_a values determined for the protonation and deprotonation of the phen and amide moieties respectively, indicating that these processes are responsible for a disruption of the energy transfer mechanism needed to produce a luminescent signal.

The luminescence is switched "on" in the physiological pH range and this is essential to the design of the sensor which envisages a quenching of the luminescence by the presence of Cu(II) ions under physiological conditions. Before testing whether the complex could detect and signal the presence of Cu(II), it was decided to investigate the properties and functions of a phen type model receptor in order to allow comparative analysis. The following sections will detail the properties and response to Cu(II) of this model receptor.

2.6 Comparison to Model Receptor

A model receptor, consisting of an acylated 1, 10-phenanthroline unit was synthesised according to literature proceedure.[174] This model would have similar properties to the recognition, or "receptor" part, of the **Eu.104** complex and as such, would allow comparative analysis to be drawn.

The receptor *N*-[1,10]phenanthrolin-5-yl-acetamide, **106**, was synthesised by refluxing a solution of 5-amino-[1,10]-phenanthroline, **102**, in MeOH overnight, with acetic anhydride in the presence of $NaHCO_3$ (Scheme 2.10). The desired product was isolated as an off white powder in 64 % yield. The spectral data for the product agreed well with the published characterisation.[174] The ^1H NMR showed the presence of a doublet at 8.63 ppm, corresponding to the H_4 proton, while the H_7 proton was seen as a doublet at 8.44 ppm. The clearest indication of the formation of the product however, was the appearance in the spectrum of the three CH_3 protons at 2.24 ppm.

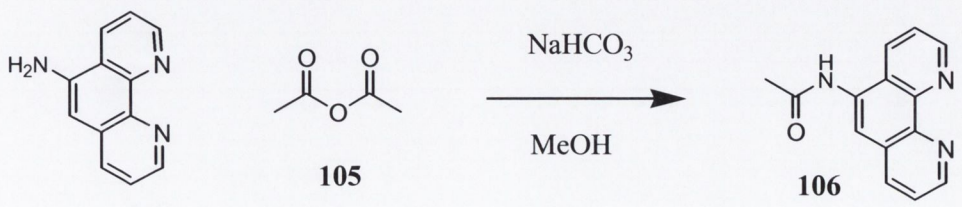

Scheme 2.10. Synthesis of model receptor 106

The absorption spectrum of **106** showed two peaks with λ_{max} at 231 nm (log ϵ = 4.51) and 267 nm (log ϵ = 4.44). Upon excitation at 267 nm the compound **106**, gave a strong fluorescent band centred at 427 nm, similar to that seen for **Eu.104**. As in the case of **Eu.104** the pH behaviour of the compound was investigated. The absorbance peak at 231 nm seemed to be more sensitive to the protonation of the amide than the absorbance at 267 nm, indicating that the peak at 231 nm is due to the n → π^* transition for C=O and the peak at 267 nm is due to the π → π^* transition for the phen. Recall the 1, 10 phenanthroline unit, is known to have an absorption peak at ~ 265 nm.[182] From the changes in the absorption spectrum at 267 nm and 231 nm respectively, it was possible to assign two pK_a values; 4.6 (± 0.2) for the protonation of the phen and 9.3 (± 0.2) for the protonation of the amide (the absorption changes for the band at 266 nm are shown in Figure 2.14, while the absorption changes for the band at 231 nm are shown in the appendix). The known literature pK_a value for 1,10 phenanthroline is 4.6.[189] The pK_a value for the protonation of the phen nitrogen also compares well with the value calculated for **Eu.104**. However, the pK_a value of the amide is vastly different. This is to be expected due to the vastly different environment of the respective amides. The amide of **Eu.104** is coordinated to the positively charged Eu(III) cation. As such it is donating electron density towards the metal ion. This increases the δ^+ nature of the amide nitrogen, which results in lowered affinity for the bound proton and hence, a lowering of the pK_a.

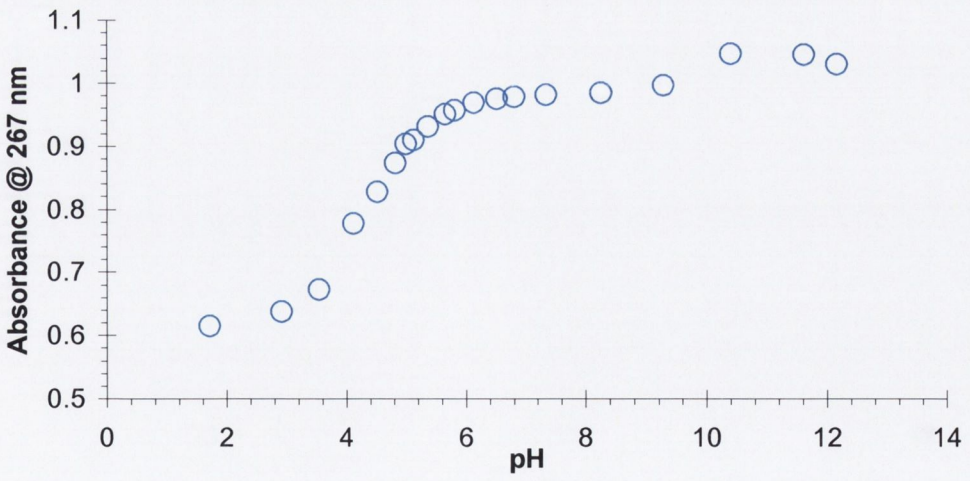

Figure 2.14. Effect of pH on absorption of 106 at 267 nm, showing hypochromic shift upon protonation of phen nitrogen pK_a 4.6.

Protonation of phen moiety results in a bathochromic shift in the 267 nm band between pH 5.6 → 278 nm at pH 3.6. However, the same protonation of the phen moiety results in a

hypsochromic shift in the band centred at 231 nm → 222 nm. In contrast to **Eu.104** protonation of the amide nitrogen does not shift the absorbance peaks of **106**.

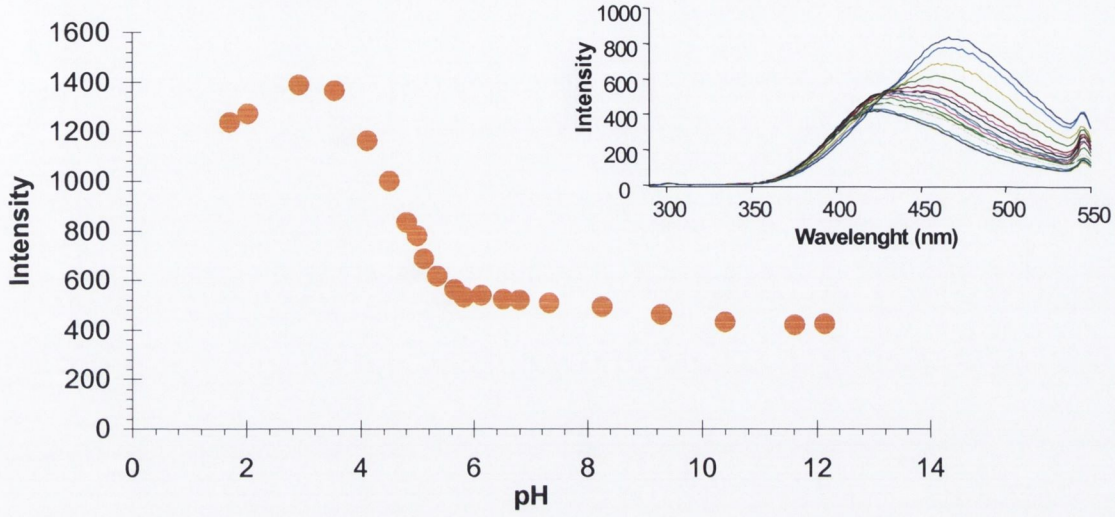

Figure 2.15. Changes in fluorescence of 106 with respect to pH

Analysing the changes in fluorescence intensity, as a function of pH revealed that the fluorescence was at its most intense when the phen moiety was protonated and protonation of the amide did not seem to affect the fluorescence (Figure 2.15).

In order to evaluate the model systems response to the presence of Cu(II) ions, measurements were carried out in water at pH 7.4 (buffered with 0.1 M HEPES) in order to resemble physiological conditions. $CuCl_2$ was gradually titrated into a 40.5 μM solution of **106**. A clear change was recorded in the absorption spectrum, indicating that Cu(II) was indeed binding to the phenanthroline receptor (Figure 2.16).

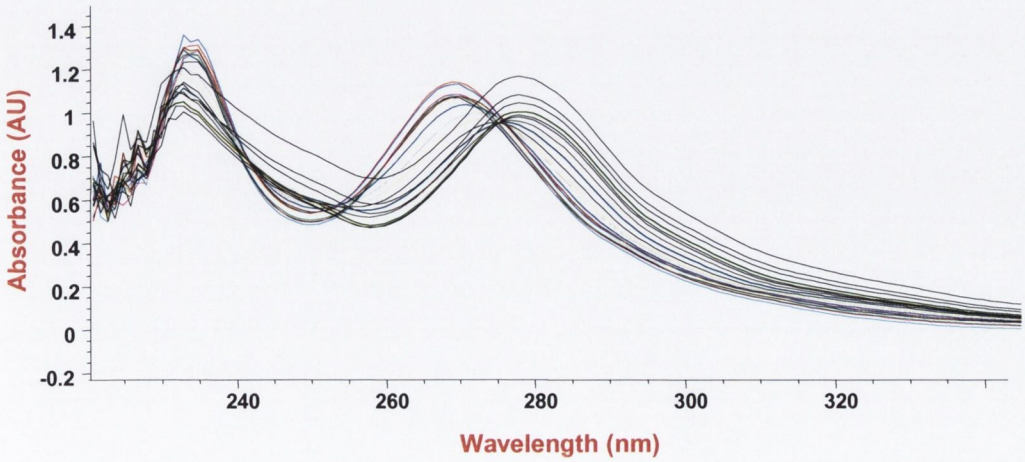

Figure 2.16. Absorption spectrum of 106 showing changes upon addition of Cu(II)

Upon addition of Cu(II) to **106**, the absorption band at 231 nm underwent a hypochromic shift. This hypochromic effect was also observed in the 267 nm band along with a concomitant bathochromic shift to 280 nm. Upon addition of excess Cu(II) a hyperchromic effect was observed in the 280 nm band, this was attributed to the absorbance by Cu(II) at 280 nm. A plot of p[Cu(II)] against absorbance, where p is the negative Log of concentration, revealed that the hypochromic effect occurred over one log unit p 5.5 → 4.4 (Figure 2.17).

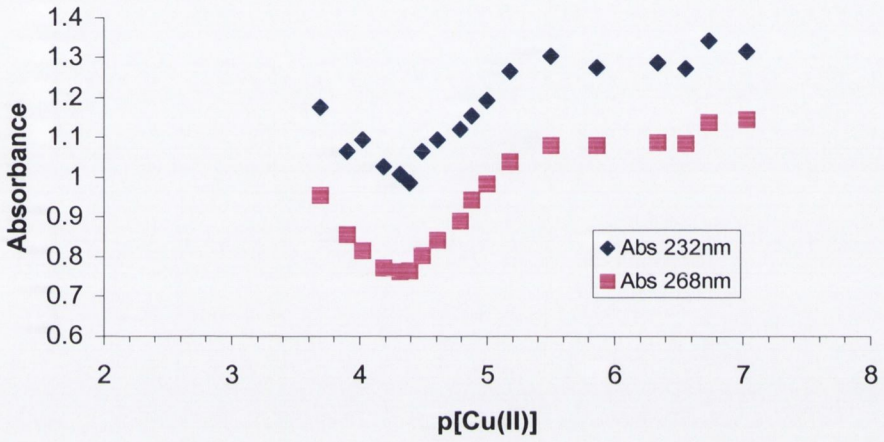

Figure 2.17. Changes in absorption of 106 as a function of -Log[Cu(II)]

2.6.1 Fluorescence Response of 106 to Cu(II)

The effect of increasing Cu(II) concentration upon fluorescence was also monitored. As the concentration of Cu(II) was increased a concomitant decrease in the fluorescence of **106** was observed. The fluorescence was quenched after 0.6 equivalents of Cu(II) had been added (Figure 2.18), which suggested that a 2:1 binding mode was in operation.

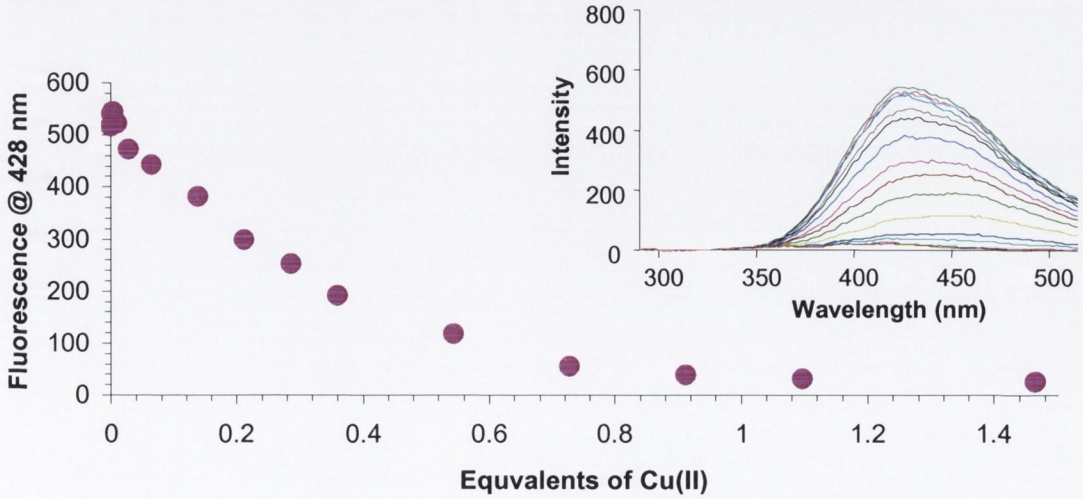

Figure 2.18. Equivalents plot against fluorescence of 106 shows quenching after 0.6 equivalents of Cu(II). Inset shows changes in fluorescence. Excite at 266 nm

A plot of p[Cu(II)] against fluorescence revealed that the binding occurred over 1 log unit (Figure 2.19).

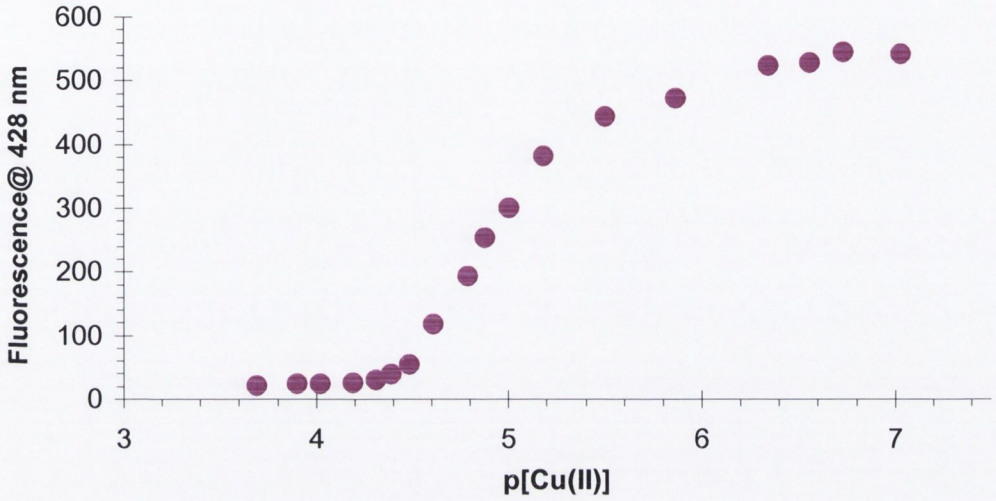

Figure 2.19. p[Cu(II)] Vs Fluorescence of 106 shows quenching over 1 log unit

In order to confirm the binding mode mass spectrometry was employed. Three equivalents of **106** were dissolved in MeOH and one equivalent of $Cu(ClO_4)_2$ was added. The solution was left to stand and green crystals were obtained. The mass spectrum of the solution revealed peaks with the correct isotope distribution pattern corresponding to 268.4 [2M+Cu/2], 387.1 [3M+Cu/2], 537.0 [2M+Cu], 637.9 [2M+Cu+ClO_4]. It is clear that at least two binding methods are possible.

The studies on the model receptor revealed that it does indeed bind Cu(II) and that this binding event modulates the absorption spectrum as well as the fluorescence spectrum, with quenching of the fluorescence observed after 0.6 equivalents of Cu(II) had been added. The binding of Cu(II) clearly quenches the singlet excited state of the phenanthroline receptor. The spectroscopic studies suggest a to a 2:1 binding mode, however, physical studies employing mass spectroscopy, revealed that a 3:1 binding mode is also possible. The pK_a value for the protonation of the phen nitrogen was found to be similar to the value obtained for the **Eu.104** complex. This might suggest that this "receptor" part of both molecules may operate in a similar fashion. This data will allow comparisons to be drawn when investigating the **Eu.104** complexes response to the presence of Cu(II), which is the subject of the next section.

2.7 Luminescent Studies of the Effect of Copper (II) upon Eu.104

The design of the **Eu.104** system factored that the phenanthroline moiety would function like a sensitising antenna, absorbing light and passing on its excited energy onto the lanthanide ion, resulting in a lanthanide emission. As shown the antenna effect was achieved and the system functions like an "*off-on-off*" pH switch with its luminescence "switched on" over the physiological pH range. So far the system functions as designed and operates under the conditions desired. However, the design envisaged a dual role for the phen moiety with it also operating as the receptor. The phen ligand itself has been shown to bind Cu(II) before. The question now was whether the phen moiety within the complex would function as a receptor, bind to Cu(II) and whether this event would cause a change in the luminescent properties of the complex.

2.7.1 Absorption Spectrum

To investigate the systems response to the presence of Cu(II) ions, measurements were carried out in water at pH 7.4 (buffered with 0.1 M HEPES). $CuCl_2$ was gradually titrated into a 35.8 μM solution of **Eu.104**. The absorption spectrum showed that as the concentration of Cu(II) was increased a gradual hypochromic effect in the absorbance at 230 nm and 266 nm, as well as a slight bathochromic shift in the 266 nm band ensued (Figure 2.20). Note the isosbestic point at 280 nm.

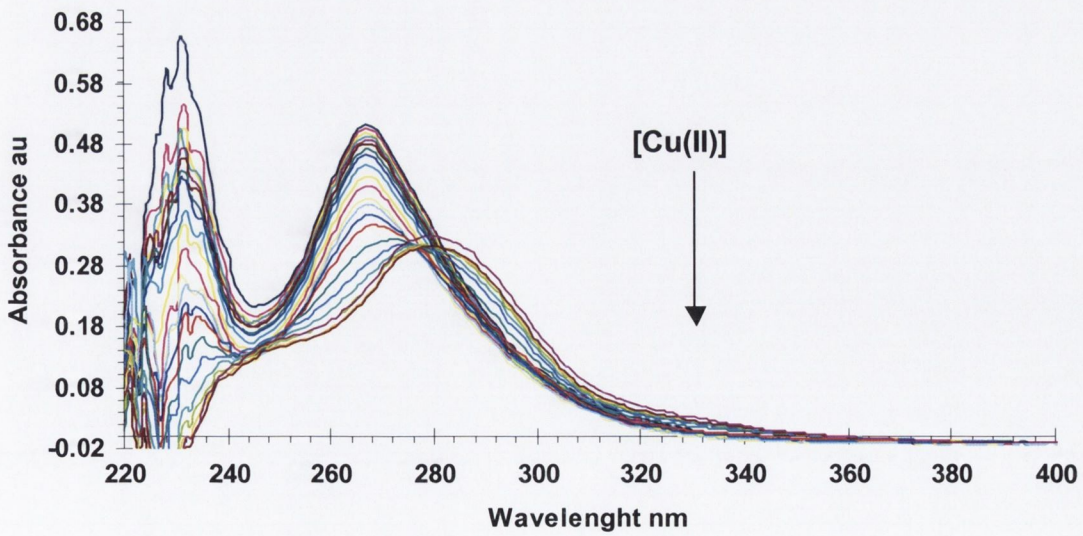

Figure 2.20. Absorption spectrum of Eu.104 showing decrease in absorbance along with bathochromic shift upon gradual addition of Cu(II)

The shift to longer wavelengths in the absorption spectrum, upon addition of Cu(II), implies that a change in the oxidation potential of the phen is occurring.

2.7.2 Fluorescence Spectrum

After excitation at 266 nm, or at the isosbestic point at 280 nm, a fluorescent band was observed at 440 nm. The fluorescence spectrum showed a gradual decrease in the fluorescence of the compound as the concentration of Cu(II) was increased. By plotting p[Cu(II)] against the relative intensity it is possible to compare the responses to Cu(II) of both the complex **Eu.104** and the model receptor **106** (Figure 2.21). The results were in good agreement. It is immediately clear that the two systems operate in similar fashions quenching over 1 log unit in the same concentration range, p 5.5 → 4.5.

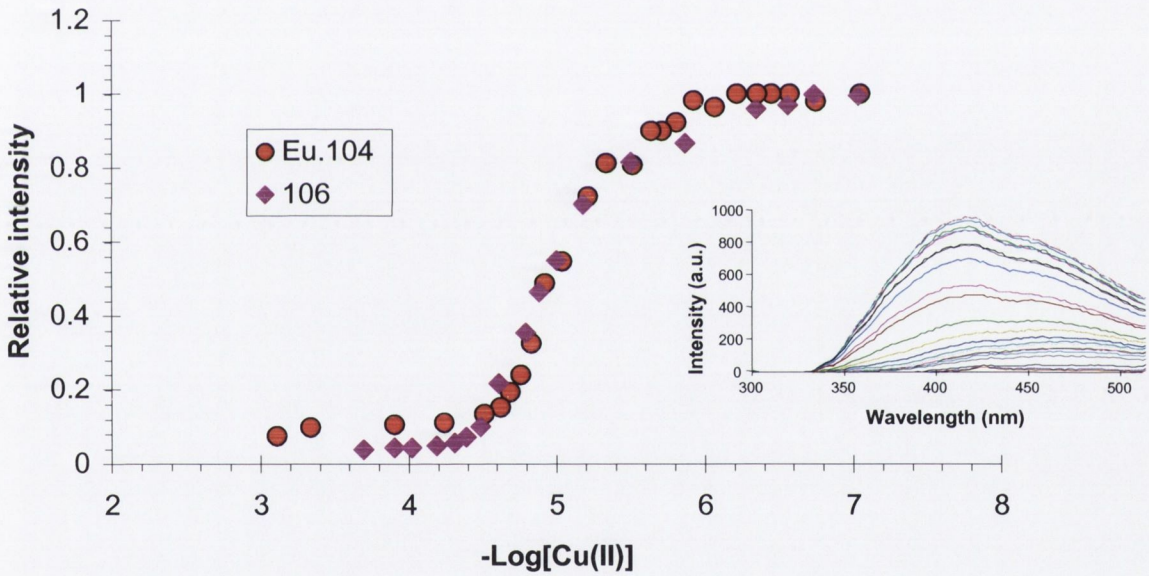

Figure 2.21. Quenching of fluorescence occurs over 1 log unit. Inset shows Eu.104 fluorescent spectra quenching upon addition of Cu(II). Excite at 266 nm

The fluorescence spectrum gives an insight into what is happening in the singlet excited state of the antenna. If the singlet state is being quenched, then it will not be able to transfer its excited energy to the triplet excited state and hence should be unable to populate the lanthanide excited state and therefore a quenching of the Eu(III) luminescence is also expected to occur (Scheme 2.11). Note that binding of Cu(II) is also expected to lower the energy levels of the phen hence impeding energy transfer to the *Ln

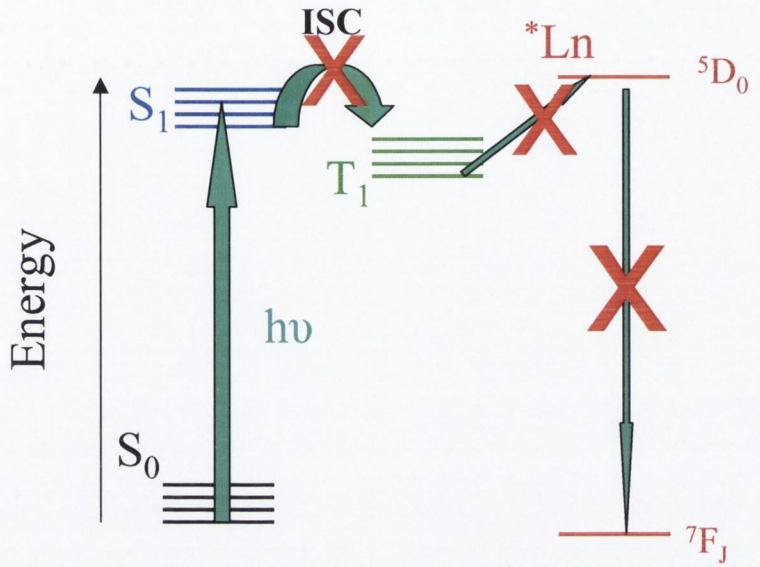

Scheme 2.11. Jablonski diagram illustrating how if the singlet state is being quenched then it will be not be able to populate the lanthanide excited state *Ln

2.7.3 Lanthanide Luminescence

As stated above, the binding of Cu(II) quenches the singlet excited state and is also expected to interfere with the energy transfer process and hence quench the Eu(III) luminescence (Scheme 2.12). This was indeed found to be the case. The Eu(III) luminescence spectrum showed a gradual decrease in the intensity as the concentration of Cu(II) was increased, until the luminescence was completely quenched at ~ 20 μM [Cu(II)] (Figure 2.22).

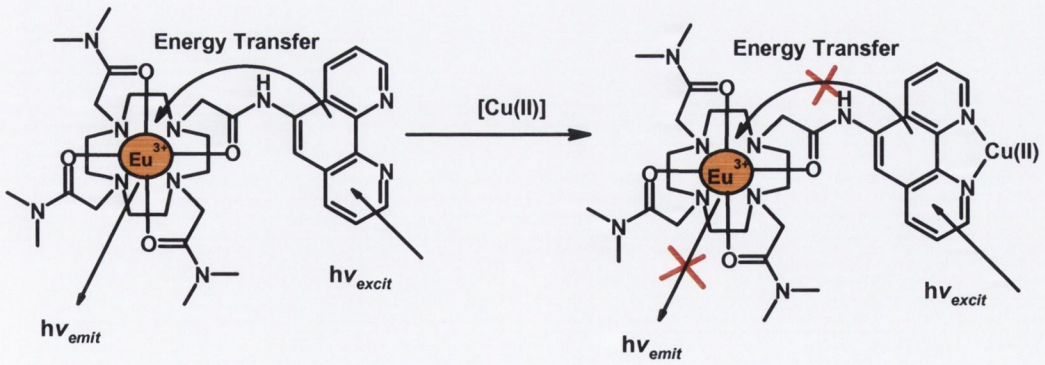

Scheme 2.12. As the Cu(II) ion is bound by the phen receptor of Eu.104 it should interfere with the energy transfer process and hence quench the luminescence

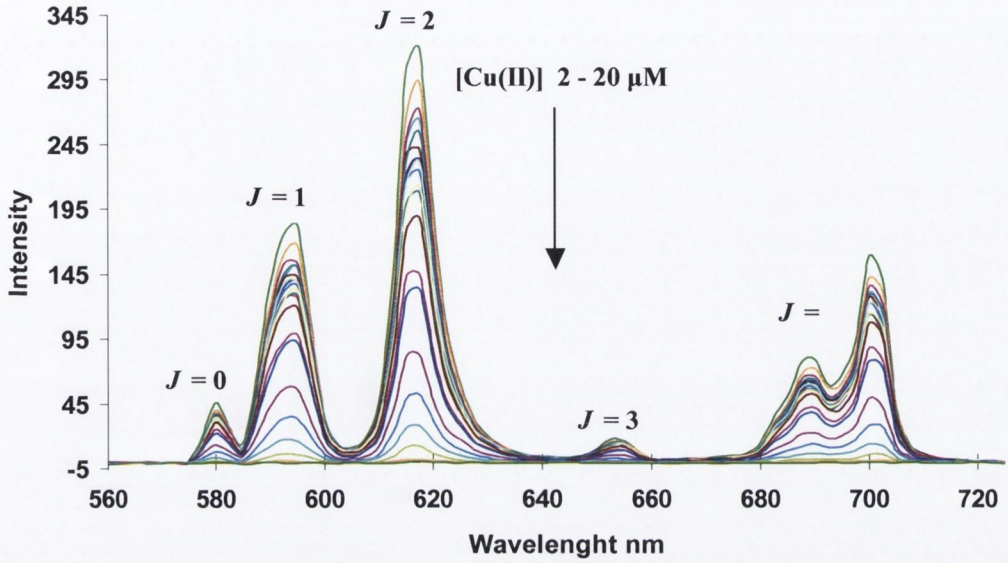

Figure 2.22. Luminescence spectra of Eu.104 showing quenching of luminescence upon addition of Cu(II). Excite at 266nm, Conc 35.8 μM

Once again any of the bands can be used to analyse the data as each gives the same result. A plot of the luminescent intensity at 620 nm ($J = 2$ band) clearly shows that the quenching of the luminescence occurs over one log unit (Figure 2.23). The response range here is significant, p 5.8 → 4.7, which corresponds to a 2.5 ~ 20 μM Cu(II) concentration range. The normal range of Cu(II) in serum is 12.5 – 21 μM Cu(II).[144]

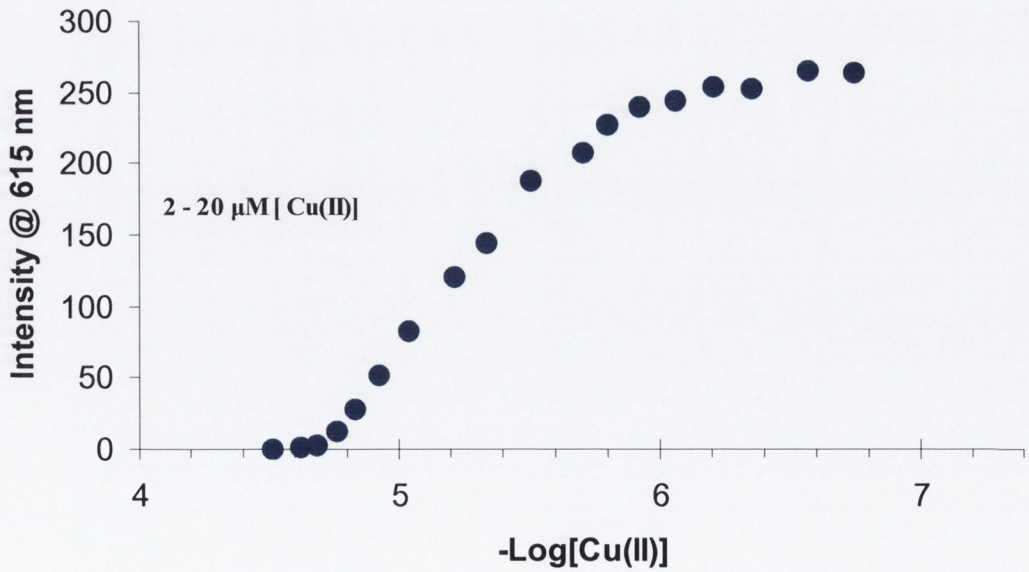

Figure 2.23. Quenching of Eu(III) luminescence of Eu.104 by Cu(II) occurs over one log unit

Cu(II) d^9 is well known for its distorted square planer geometry due to the Jahn Teller effect of its single unpaired electron. However, for strong field ligands such as phen, Cu(II) often prefers a distorted octahedral geometry.[170,190] As such a 2:1 or 3:1 binding mode was expected. The equivalents plot indicated that the biding mode operating in this case was 2:1, as the quenching of the luminescence occurs just after 0.5 equivalents of Cu(II) has been added (Figure 2.24).

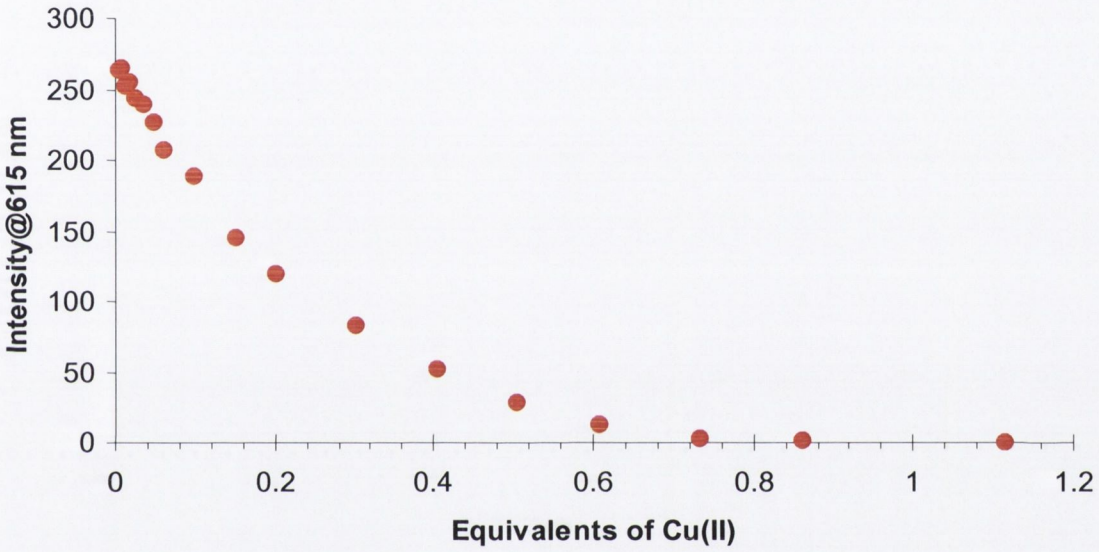

Figure 2.24. Equivalent plot for Cu(II) showing quenching of luminescence of Eu.104 after 0.6 equivalents of Cu(II)

An investigation of the mass spectrum, similar to that carried out for **106**, did not reveal any useful information about the binding due to the extreme complexity of the spectrum. In order to further investigate the binding mode a Job plot analysis was carried out. To do this measurements were conducted as the mole fraction ([G]/[G]+[H]) was varied, while the overall concentration of [G]+[H] was kept constant at 5.6 μM.[191] Where G denotes the guest, Cu(II), and H denotes the host, **Eu.104**. Under these conditions the absorption band at 267 nm exhibited its maximum, at a mole fraction of 0.33 (Figure 2.25). Furthermore, a minimum was observed in the Eu(III) luminescence intensity, again at a mole fraction of 0.33. This is shown in the appendix. This figure implies that the binding mode operating in this case, is indeed 2:1 as 0.33/(1-0.33) = 2.0, *i.e.* two **Eu.104** complexes binding to one Cu(II) ion.[191]

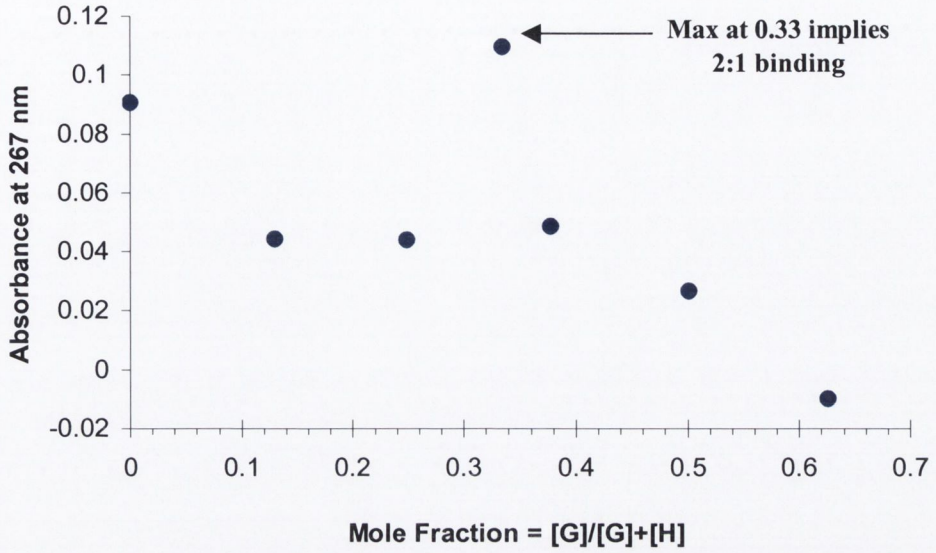

Figure 2.25. Absorption Job plot where [G] is the concentration of guest *i.e.* Cu(II) and [H] the concentration of host

As stated before 0.5 equivalents of Cu(II) quenches the Eu(III) luminescence of **Eu.104**. However, upon addition of EDTA the luminescence was "switched" back "on". This switching effect can be seen in the appendix and shows that the binding of Cu(II) by the phenanthroline receptor is reversible. This is an important property of any sensor.

In order to evaluate the systems ability to function at high ionic strength measurements were conducted in water at pH 7.4 (buffered with 0.1 M HEPES) in the presence of 0.1M TMACl. As previously, $CuCl_2$ was gradually titrated into a 35.8 μM solution of **Eu.104**.

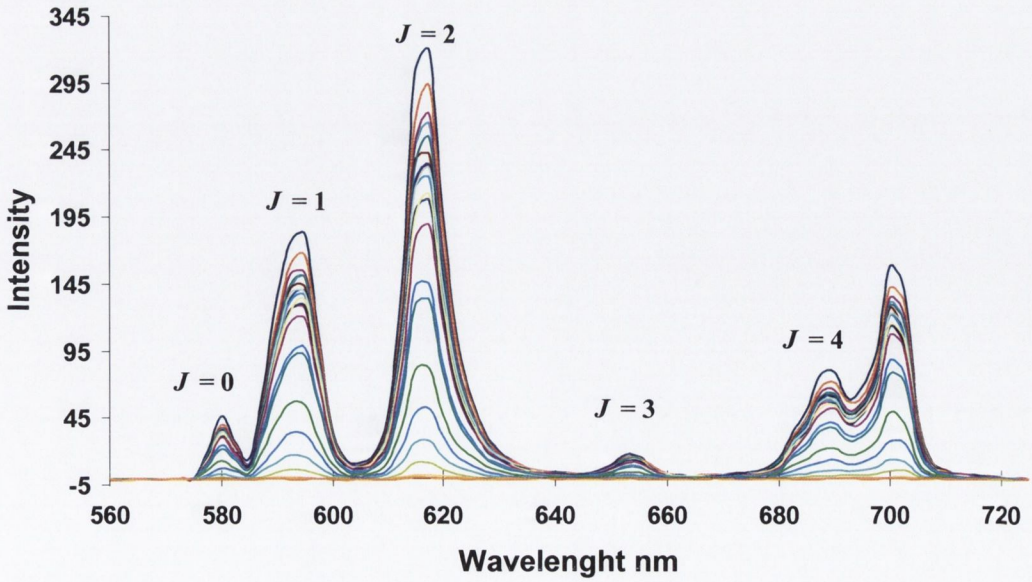

Figure 2.26 Luminescence titration of Eu.104 with Cu(II) in pH 7.4 buffered solution at high ionic strength (0.1M TMACl). Excite 266 nm, 35.8 μM

Once again the system responded with a gradual decrease in the luminescence finally quenching after 0.5 equivalents of Cu(II) had been added (Figure 2.26). However, there were some interesting points to note here. For instance throughout the titration in high ionic strength the $J = 1$ and $J = 2$ bands are closer in intensity (J2/J1 = 1.4), while for the original titration the $J = 2$ band was significantly larger (J2/J1 = 1.7). It is thought that these changes are due, under the conditions of high Cl^- ion concentration, to the displacement of the metal bound water molecule by a Cl^- ion, as the J = 2 band is known to be sensitive to its coordination environment.[192]

The systems response to the counter anion was also investigated. When $Cu(OOCH_3)_2$ was used instead of $CuCl_2$ the **Eu.104** complex, responded in an identical manner to that described above, quenching after 0.5 equivalents of Cu(II) or ~ 20μM.

It can be seen that under the physiological conditions applied (*i.e.* aqueous solution pH 7.4, high salt concentration) the conjugate **Eu.104**, can detect and signal the presence of Cu(II) ions. The recognition occurs through reversible binding to the phen moiety, while signalling is accomplished by quenching of the long lived Eu(III) emission. The sensor is stable and sensitive to an important concentration range (2.5 – 20 μM). However, the systems selectivity towards Cu(II) over other ions must now be investigated.

2.8 Selectivity studies for other metal ions

Following the success in the detection of Cu(II), the systems response to various other biologically prevalent metal ions was investigated (Table 2.3).

Metal	Extra cellular concentration	Test concentration	Response
Na^+	150 mM	100 mM	No change
K^+	5 mM	10 mM	No change
Ca^{2+}	2 mM	10 mM	No change
Mg^{2+}	10 mM	10 mM	No change
Zn^{2+}	2 mM	10 mM	No change

Table 2.3. Response of Eu.104 to biologically prevalent metal ions

The system gave no response to Zn(II) or to the group I and II metals. However, a response was observed for the transition metal ions of Co(II), Fe(II) and Fe(III). To confirm the sensors insensitivity to group I/II ions, a titration was carried out in a simulated biological

buffer with 150 mM NaCl, 10 mM KCl, 5 mM $CaCl_2$ and 5 mM $MgCl_2$ at pH 7.4. As seen previously the Eu(III) emission was quenched upon the addition of 0.5 equivalents of Cu(II). The same pattern was observed if the sample was excited at its isosbestic point 280 nm (Figure 2.27). The luminescence could again be switched on by addition of EDTA.

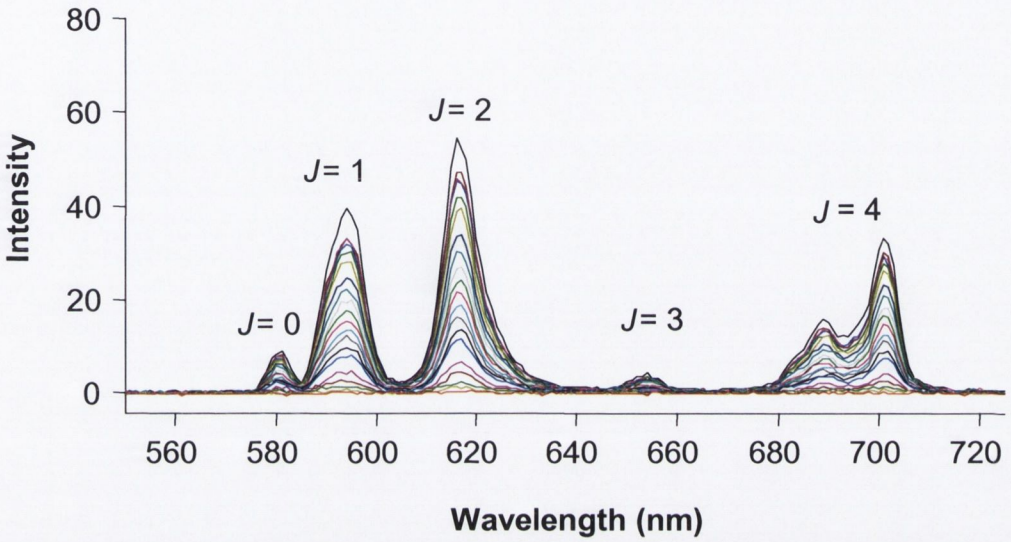

Figure 2.27. Luminescence titration of Eu.104 with Cu(II) in simulated biological background pH 7.4. Excited at the isosbestic point 280 nm

Note that the luminescence intensity is lower when the sample is excited at the isosbestic point. This is due to the lower absorbance value at 280 nm (Figure 2.20).

Thus far the studies performed have shown the sensor is stable, functions under physiological conditions, detects and signals the presence of Cu(II) ions, deals with the autofluorescence problem and is sensitive to a specific concentration range. The final requirement which the sensor must fulfil, is to be selective for a specific target, in this case Cu(II). As shown, the sensor was not responsive to the presence of the group I and II metal ions. This is crucial as they are present in high concentrations in blood samples.

The sensor elicits no response for Zn(II) ions however, as mentioned, a response was observed for the transition metal ions of Co(II), Fe(II) and Fe(III). In nature these biologically important ions are usually taken up or complexed by porphyrins. However, a small amount of the free or uncomplexed ions may be present in the blood and as such may impede the selectivity and accuracy of the sensor. In order to elucidate the effect these ions would have, selectivity studies were performed to determine the response to these transition metal ions.

2.8.1 Studies for Fe(III)

Of the three metal ions Fe(III), $3d^5$, showed the lowest affinity for the sensor. $Fe(III)Cl_3$ was titrated into a 35.8 μM solution of **Eu.104** in buffered water at pH 7.4. The luminescence spectrum shows that the addition of Fe(III) quenched the Eu(III) luminescence in a similar manner to that previously observed with Cu(II) (Figure 2.28).

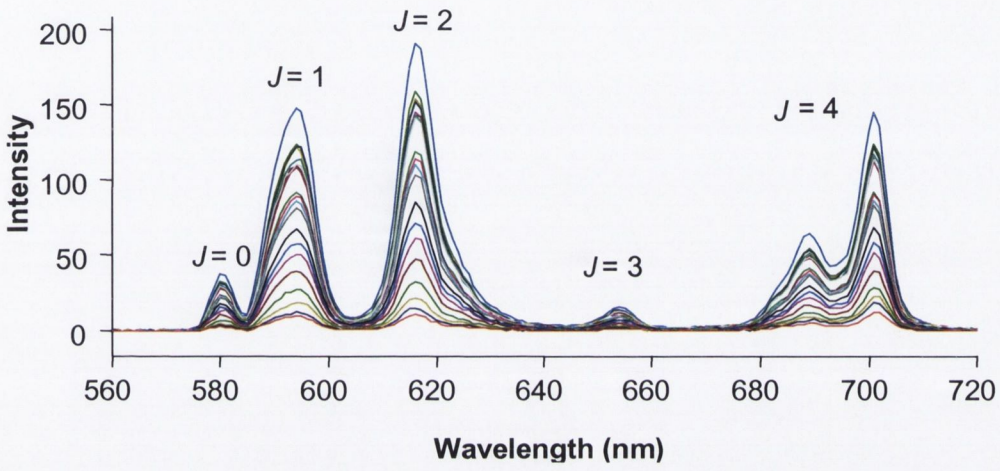

Figure 2.28. Luminescence spectra of Eu.104 in pH 7.4 buffered solution is quenched upon addition of Fe(III). Excited at 266 nm

Nevertheless, the quenching of the luminescence by Fe(III) occurs over a vastly different concentration range (20 μM → 3 mM), compared to the quenching by Cu(II) (3 → 20 μM). This can be highlighted by plotting p[Fe(III)] against intensity (Figure 2.29). The quenching by Fe(III) occurs over 4 log units. Recall the biding of Cu(II) occurs over a narrow concentration range p[Cu(II)] 5.8 → 4.7, as such Cu(II) can be detected selectively over Fe(III).

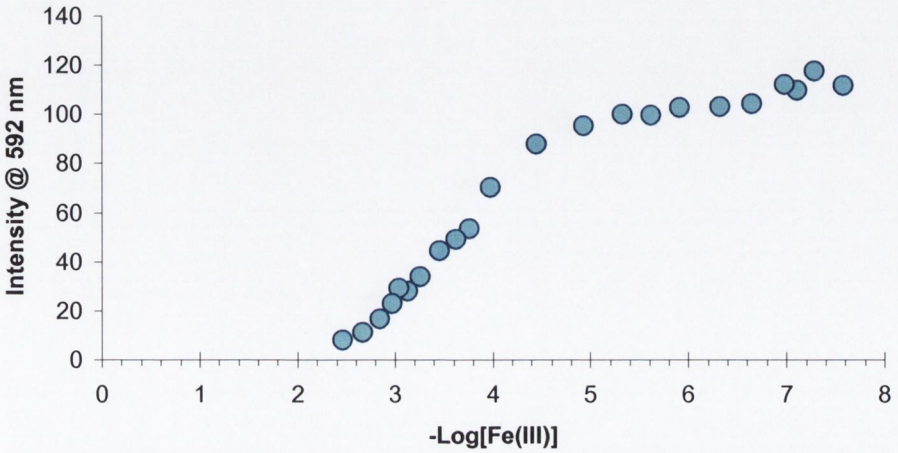

Figure 2.29.Quenching of Eu(III) luminescence of Eu.104 by Fe(III) over 4 log units

2.8.2 Studies for Fe(II)

The response of the sensor **Eu.104**, towards Fe(II) ($3d^6$), was also investigated. $Fe(II)Cl_2$ was titrated into a 35.8 μM aqueous solution of **Eu.104** buffered at pH 7.4. The luminescence was quenched upon addition of Fe(II) similar to the quenching of the luminescence by Fe(III) (Figure 2.28). However, the concentration range was again different *ca.* 3 → 600 μM. In this case, the binding of Fe(II) occurs over 3 log units p[Fe(II)] 6→ 3 (Figure 2.30). Once again Cu(II) can be detected selectively over Fe(II). The luminescence spectra for the Fe(II) and Co(II) titrations can be found in the appendix.

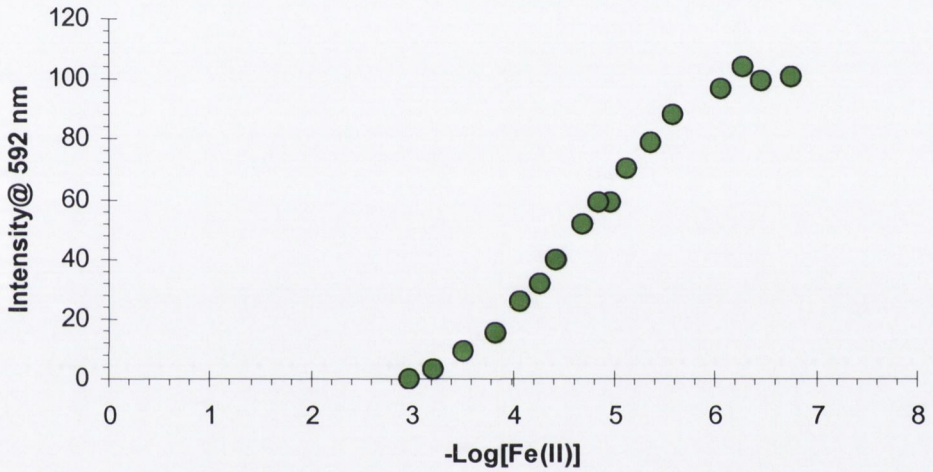

Figure 2.30. Quenching of Eu(III) luminescenceof Eu.104 by Fe(II) occurs over 3 log units

2.8.3 Studies for Co(II)

Cobalt is another biologically relevant ion. Its concentration in the human body (20 mg/ 1000 Kg) is far less than that of Cu(II) (1000 mg/ 1000 Kg).[141] It is usually taken up in porphyrins and the concentration of the free ion in the blood should be very low. Nevertheless, the effect of Co(II) ($3d^7$), upon the luminescence of **Eu.104**, was investigated in an identical manner to that above. $Co(II)Cl_2$ was titrated into a 35.8 μM aqueous solution of **Eu.104** buffered at pH 7.4. The luminescence was found to be quenched over a similar concentration range to that of Fe(II) (Figure 2.31). As stated before this is much removed from the concentration range for Cu(II) and as such Cu(II) can be detected selectively over Co(II).

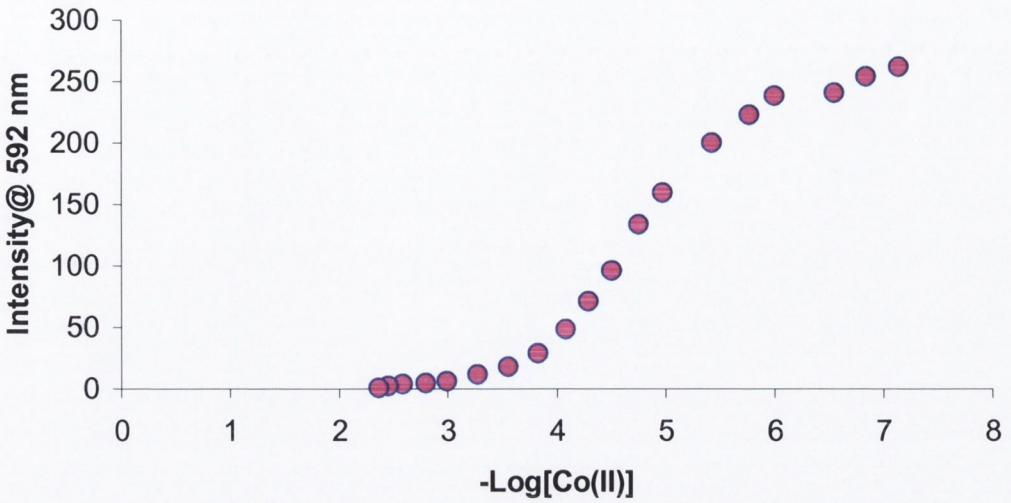

Figure 2.31. Quenching of Eu(III) luminescence of Eu.104 by Co(II)

By plotting the relative intensities of the various metal ions a direct comparison of the sensor's sensitivity to each metal ion is possible. The plot of the relative intensities clearly reveals that the sensor can selectively detect Cu(II) in the concentration range in which we are interested namely 2.5 → 20 μM (Figure 2.32).

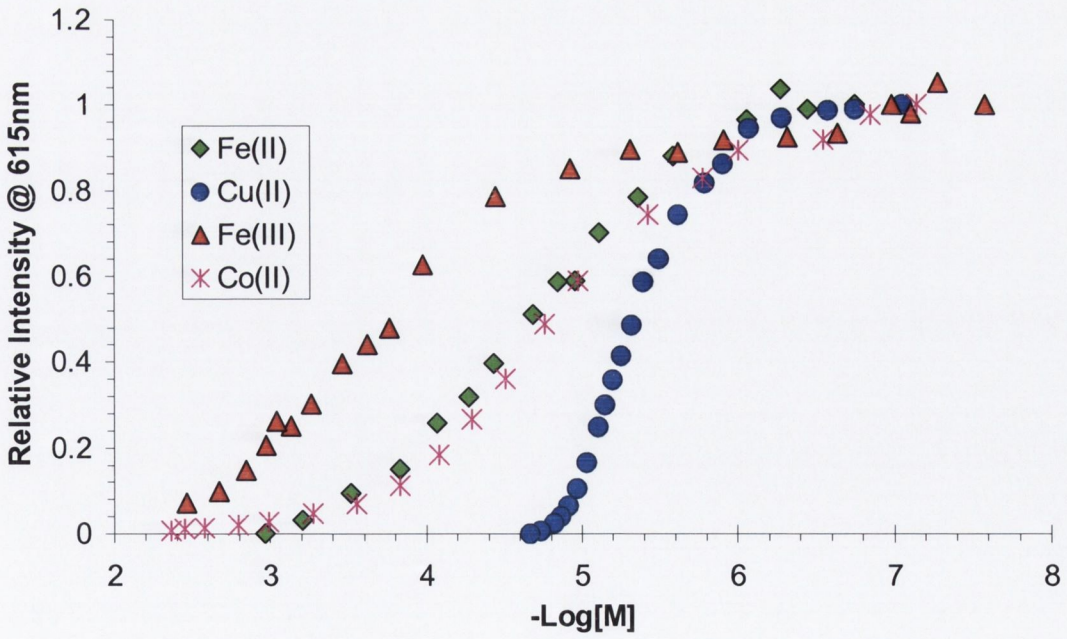

Figure 2.32. Plot of –Log[M] V relative luminescent intensities of Eu.104 showing selective detection of Cu(II)

At this point it can be seen that the sensor is fulfilling the requirements needed.

- It is stable in water at pH 7.4.
- It functions under physiological conditions (*i.e.* aqueous environment, pH 7.4, high ionic strength).
- It is selective for Cu(II).
- It senses in the desired concentration range.

One final series of measurements were required to confirm this ideal behaviour, under physiological conditions.

2.9 Effect of Ionic Strength

The sensor has been shown to be selective for Cu(II) in water at pH 7.4. However, as mentioned earlier the sensor must function under conditions of high ionic strength. As such, it was decided to investigate the effect of ionic strength upon the sensors sensitivity towards the other metal ions. The above titrations were repeated and each of the metal ions titrated into a 35.8 μM aqueous solution of **Eu.104** buffered at pH 7.4 with high ionic strength (0.1 M TMACl).

The high ionic strength seemed to have very little effect upon the Fe(III) titration. However, it clearly effected both the Fe(II) and Co(II) titration but in different ways. Under conditions of high ionic strength the sensitivity of the sensor towards Fe(II) was reduced p[Fe(II)] 5 → 3. Indeed it now resembled the Fe(III) titration more accurately. On the other hand the sensitivity towards Co(II) increased dramatically p[Co(II)] 6.5 → 4.5. Once again by plotting the relative intensities against p[M], a direct comparison can be drawn (Figure 2.33). From the relative intensities plot it can clearly be seen how the sensitivity of Fe(II) now more closely resembles that of the Fe(III) titration. Unfortunately the increase in sensitivity towards Co(II) now means that it has a similar detection range as that of Cu(II) although its shape is still different as it quenches over three log units p[Co(II)] 7 → 4.

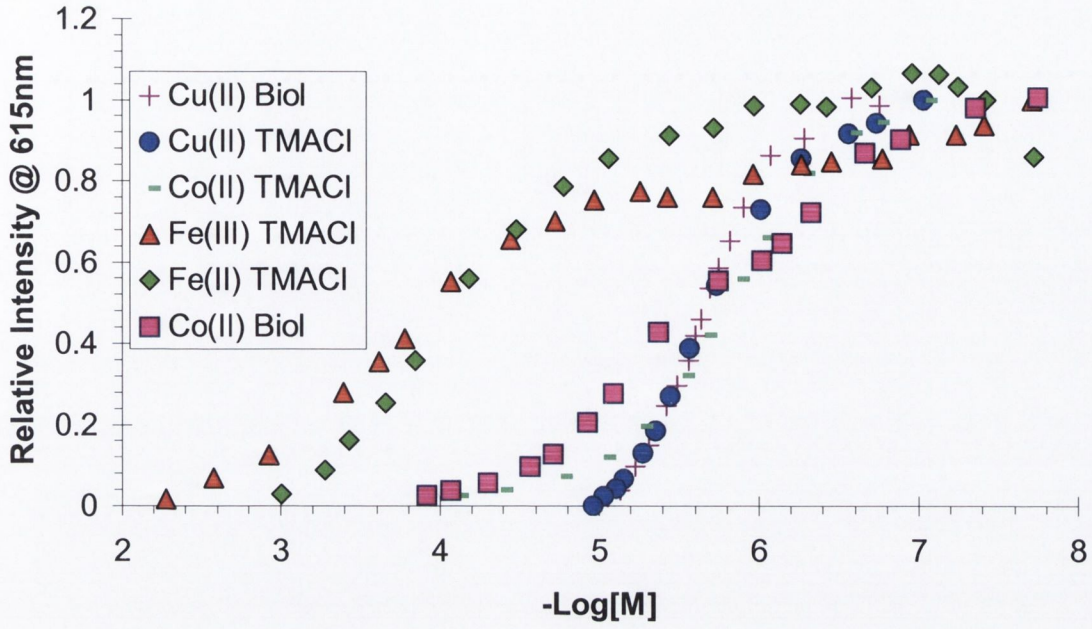

Figure 2.33. Plot of p[M] Vs Relative Intensities of Eu.104 showing change in sensitivity towards metal ions under conditions if high ionic strength

It should be noted how the profile for the quenching in high ionic strength (TMACl), mirrors that of the quenching in the simulated biological solution (Biol) for both Cu(II) and Co(II) titrations.

It is hoped that the **Eu.104** conjugate, may still be useful as a diagnostic tool for the detection of Cu(II) in blood samples as the concentration of Co(II) is so much smaller than that of Cu(II), 20 ppb and 1000 ppb, respectively.[141]

2.10 Conclusion

The purpose of this project was to develop a lanthanide luminescent system which could detect and signal for the presence of Cu(II) under physiological conditions in a concentration range similar to that expected in blood serum samples, but which could overcome the autofluorescence issue by time gating techniques. To this end the synthesis and characterisation of **Eu.104** was accomplished. This is the first example of a lanthanide luminescent system which senses for the presence of Cu(II) cations.

Photophysical analysis of **Eu.104** showed that it was stable in solution, and able to produce a Eu(III) emission after excitation of the phenanthroline chromophore, which acts like a sensitising antenna, absorbing energy and transferring it to the lanthanide ion. The luminescence of **Eu.104**, was also determined to have a strong bell shaped pH dependence where the luminescence was switched "on" within the physiological pH range 4 – 8, but

quenched under more alkaline or acidic conditions. As such, the luminescence gives rise to an "*off-on-off*" system, which is switched "on" under physiological conditions, but switched "off" under acidic and alkaline conditions. This switching process was found to be fully reversible and almost independent of pH between 5 and 7.

At pH 7.4, both the fluorescence and the Eu(III) luminescence of **Eu.104**, was found to be quenched by the presence of Cu(II) ions. The sensor detected Cu(II) within the 3 - 20 μM concentration range, which was comparable to the concentration range desired (12 – 21 μM).[144] The binding mode was determined to be 2:1 **Eu.104**:Cu(II). This was inferred through Job plot analysis and equivalence plots as well as comparison to the model receptor **Eu.106**. The geometry around the Cu(II) ion is expected to be a distorted square planar geometry due to the Jahn Teller effect of the Cu(II), ($3d^9$), single unpaired electron. However, there are two possible supramolecular isomers, the cis and trans isomers.

The sensor was selective for Cu(II) in the presence of group I and II metal ions, and was also selective over other biologically prevalent transition metal cations. The sensors sensitivity did show a dependence upon ionic strength, however, and under conditions of high ionic strength its sensitivity towards Co(II) was similar to that of Cu(II). Despite this, the prevalence of Co(II) in the body is much smaller than that of Cu(II), 20 ppb and 1000 ppb, respectively.[141] As such, it is envisaged that **Eu.104** may still be useful as a diagnostic tool for the detection of Cu(II) within blood serum samples.

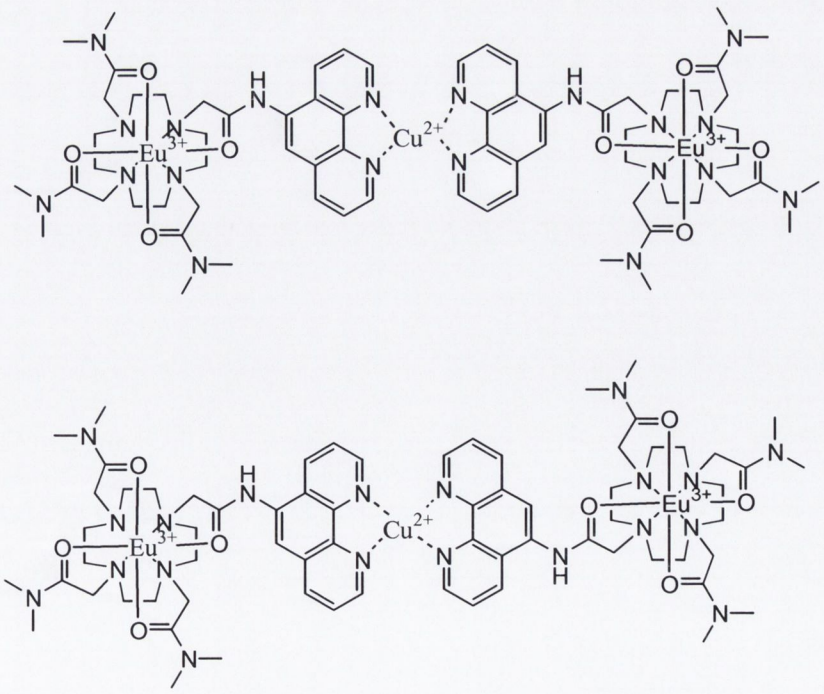

Figure 2.34. Showing cis and trans structural isomers for the 8^+ supramolecular ternary complex



Chapter 3

Lanthanide Luminescent Sensing of Aromatic Carboxylates

3.1 Introduction

The previous chapter dealt with the sensing of Cu(II), a transition metal cation, however, the sensing of anions is also an active area of research.[193] As mentioned in Chapter 1 metal complexes, including lanthanide complexes, have great potential as anion sensors as they can interact with anions through columbic attractions that are much stronger than the hydrogen bonding interactions, which are often exploited for anion recognition.[194] Chapters 1 and 2 have already detailed the advantages of lanthanide luminescent systems as signalling moieties for sensors, as well as how to elicit a lanthanide emission *via* the use of a sensitising chromophore or antenna. Some examples of lanthanide luminescent probes as anion sensors were presented in section 1.7, and most of them function by the conventional method, discussed in Chapter 2, utilising a covalently attached sensitising antenna to populate the lanthanide excited state. However, an alternative method, which uses the analyte itself as the antenna has also been described. In this case, the analyte, usually an aromatic chromopohre, coordinates to the sensor, either directly to the metal centre itself or in close proximity to it, and subsequently behaves as the sensitising antenna, populating the lanthanide excited state and inducing a lanthanide emission.

Some examples of this indirect excitation were detailed in section 1.7, including the sensitisation of a Tb(III) EDTA complex by salicylic acid in water at pH 12, described by Georges and Arnaud, and the aromatic carboxylate sensors **Tb.27** and **Eu.27**, which were reported by Michels and Reinhoudt, at the same time as the work to be described in this Chapter.

The aim of this project was to design and develop a sensor for aromatic carboxylates, whereby the target analyte, *i.e.* the aromatic carboxylate would bind directly to a coordinately unsaturated lanthanide ion that was part of a kinetically stable cyclen complex, *via* the displacement of two metal bound water molecules by the carboxylate moiety. The lanthanide complex itself, does not contain a sensitising antenna and thus in the absence of the analyte, remains photophysically silent *i.e.* does not give rise to any luminescence. Once bound, however, and assuming a suitable triplet state energy level was available, the analyte would then function as a sensitising antenna, in an analogous manner to that discussed in Chapter 2, absorbing energy and transferring it to the lanthanide ion, thereby populating the lanthanides excited state and inducing a lanthanide emission (Scheme 3.1). Furthermore, it was desirable that this sensor function under physiological conditions, *i.e.* in water at pH 7.4 and high ionic strength, in order to allow for *in vivo*

applications. The work upon the mononuclear lanthanide systems, presented in this Chapter, was conducted in collaboration with Dr. Joseph Leonard.

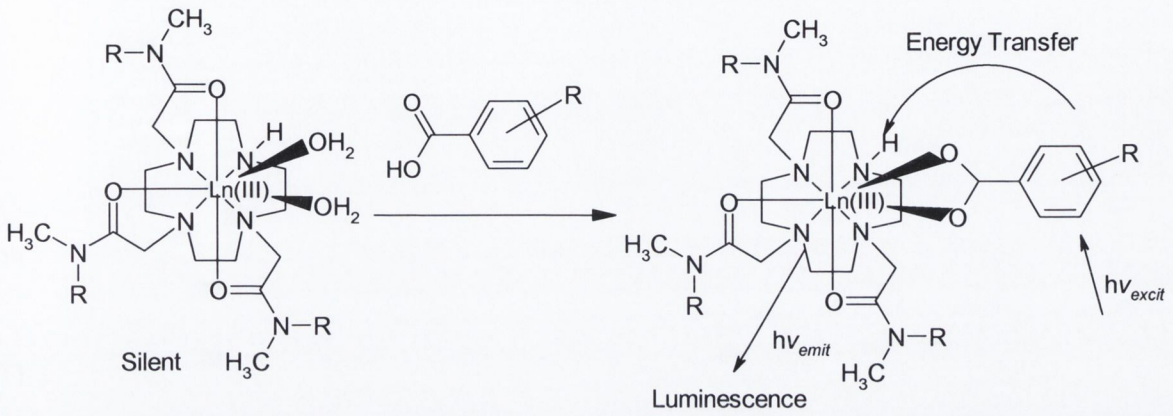

Scheme 3.1. Proposed mechanism for aromatic sensing; analyte displaces the metal bound water molecules and functions as a sensitising antenna, absorbing light before passing it to the lanthanide ion by means of a energy transfer mechanism, resulting in a lanthanide emission

In order for the analyte to function as a sensitising antenna, it must posses a carboxyl group in order to displace the metal bound water molecules and hence bind to the lanthanide ion. Furthermore, the analyte must contain a chromophore and have access to an excited triplet state energy level above that of the lanthanides excited state (20,400 cm^{-1} for Tb(III) and 17,200 cm^{-1} for Eu(III)).

3.2 Synthesis of Heptadentate Tri-arm Cyclen

The aim of the project was to synthesise a lanthanide luminescent sensor for aromatic carboxylates, where the lanthanide would play the part of the signalling system. As mentioned before lanthanides tend to be toxic and have a high coordination number requirement and so to circumvent both of these problems a cyclen macrocycle, functionalised with three pendant amide arms, was employed. The large number of donor atoms would be capable of forming a stable complex,[195] but should leave the lanthanide complex co-ordinately unsaturated, which is important in order to allow for later binding of the analyte. Furthermore, the ligand does not contain a chromophore capable of sensitising a lanthanide ion and hence any lanthanide complex of the ligand should remain photophysically silent.

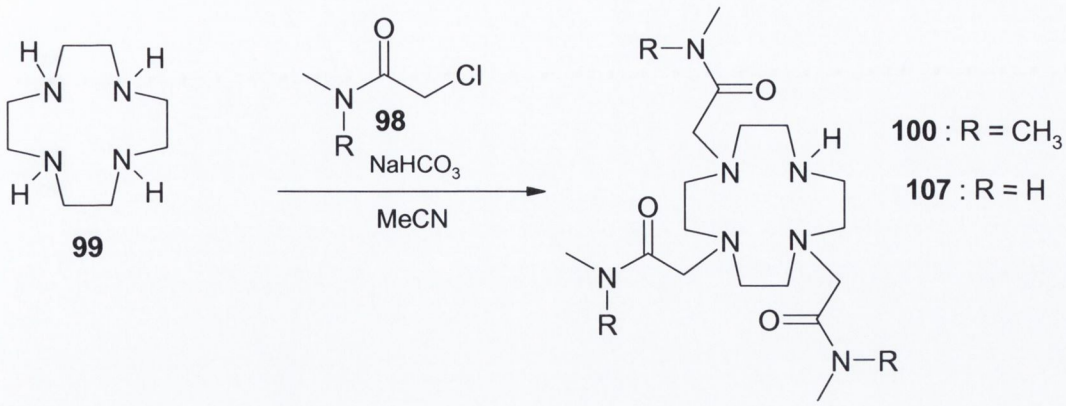

Scheme 3.2. Synthesis of heptadentate 3 arm cyclen ligands[196]

The synthesis was carried out according to the literature procedure,[196] by reacting the α-chloroamides of *N,N*-dimethyl acetamide **98b** and *N*-methyl acetamide **98a** respectively with cyclen, **99**, in dry CH_3CN (3:1 molar ratio) at 65 °C for three days in the presence of $NaHCO_3$, (Scheme 3.2). The synthesis of **100** was discussed in detail in Chapter 2. The compound 2-(4,7-bis-methylcarbamoylmethyl-1,4,7-10-tetraaza-cyclododec-1-yl)-*N*-methyl-acetamide, **107**, was synthesised in a similar manner and purified by precipitation from dry diethyl ether and obtained in 58 % yield. The ^1H NMR spectrum corresponded with the published characterisation showing the presence of 1 NH proton at 7.59 ppm and 2 NH protons at 7.30 ppm, due to the C_2 plane of symmetry through the molecule. Resonances corresponding to the CH_2 protons from the pendant amide arms appeared at 3.06 and 2.96 ppm. The mass spectrum contained two signals at *m/z* = 386.3 and 408.4 corresponding to the [M+H] and [M+Na] species, respectively. High resolution mass spectrometry confirmed the presence of the desired molecule.

These two ligands would be capable of forming stable lanthanide complexes and hence the next step was to insert the lanthanide metal ions.

3.3 Complexation of the Heptadentate Cyclen Ligands 100 and 107

The Eu(III) and Tb(III) complexes of **100** and **107**, were synthesised by J. P. Leonard, by refluxing together an equivalent amount of **100** or **107** with either Eu(III) or Tb(III) triflate ($(CF_3SO_3)_3$) in dry CH_3CN, under inert atmosphere for 24 hours (Scheme 3.3).[197] Upon cooling to room temperature the solution was poured into a stirring solution of dry diethyl ether, which resulted in oily residues that were isolated by decanting the organic layers and rinsing the resulting residues with CH_2Cl_2. The complexes were isolated after exhaustive drying under vacuum over P_2O_5.

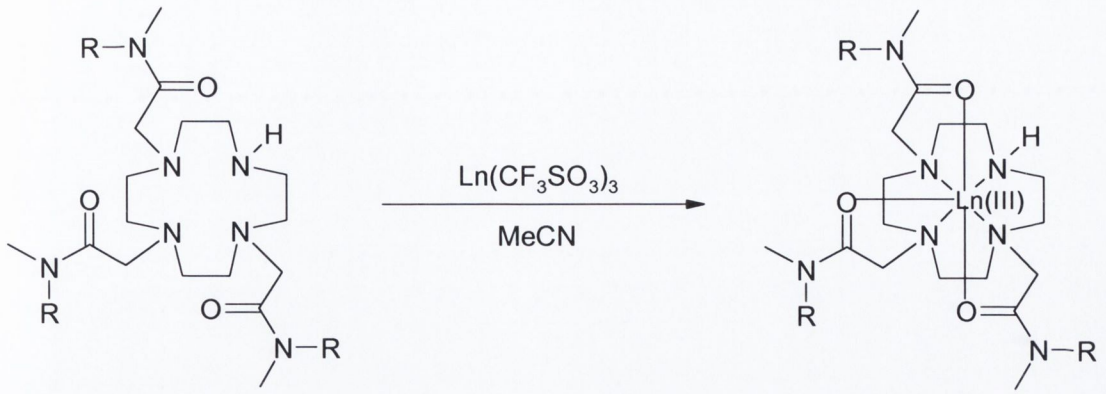

100: R = CH_3
107: R = H

Ln.100 : R = CH_3
Ln.107 : R = H

Scheme 3.3. Complexation of heptadentate cyclen ligands[197]

The complexes were characterised by conventional means ^{1}H NMR spectroscopy, high resolution mass spectroscopy, ESMS, IR and elemental analysis.[197] The ^{1}H NMR spectrum showed that the complexes had formed, evidenced by the large shift in the positions of the peaks due to the paramagnetic nature of the metal ions. This will be discussed in greater detail in section 4.3.5. High resolution mass spectra were obtained for all of the complexes and each showed the correct characteristic isotope distribution pattern.

3.4 Determination of Metal Bound Water Molecules

As previously shown in Chapter 2, lanthanides have a very high coordination number requirement, usually nine for Eu(III) and Tb(III), which if left unfulfilled are usually occupied by metal bound water molecules.[198] The heptadentate macrocyclic framework employed here leaves the lanthanide ion coordinatively unsaturated and therefore the complexes of **100** and **107** were expected to possess two metal bound water molecules (Figure 3.1). The metal bound water molecules are an essential part of the design, as they shall be displaced by the incoming analyte.

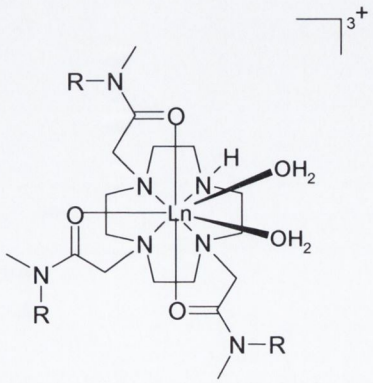

Figure 3.1. Showing two metal bound water molecules

In order to confirm this, the luminescent lifetimes (τ) of the lanthanide-excited states were measured in D_2O and H_2O after direct excitation of the metal ion. Using these, the number of metal bound waters, *i.e. q* value, was evaluated from the following equations. [199 ,200]

(i) $$q^{Eu(III)} = 1.2\ [(1/\tau_{H2O}-1/\tau_{D2O}) - 0.25 - 0.075x]$$

(ii) $$q^{Tb(III)} = 5\ [(1/\tau_{H2O}-1/\tau_{D2O}) - 0.06]$$

Here the prefixes 1.2 and 5 are proportionality constants that mirror the sensitivity of the corresponding ions to quenching by metal bound water molecules. The correction terms –0.25 and –0.66 represent quenching by second sphere water molecules, whereas –0.075x in equation *(i)* represents the quenching by *N-H* oscillators, where *x* is the number of such oscillators directly bound to the complex. In all cases the *q* value was determined to be two (Table 4). In addition, X-ray crystal structures of three of the four complexes, namely **Eu.100**, **Eu.107** and **Tb.100** (Figure 3.2), were obtained.[201] These clearly showed that there were indeed two water molecules attached to the metal centre.

Complex	τ_{H2O} (ms)	k_{H2O} (1/ms)	τ_{D2O} (ms)	k_{D2O} (1/ms)	*q(±0.5)*
Eu.100	0.281	3.55	0.855	1.17	2.55
Eu.107	0.315	3.17	0.936	1.07	1.95
Tb.100	0.720	1.38	1.080	0.92	2.01
Tb.107	0.869	1.15	1.386	0.72	1.85

Table 3.1. Measured lifetimes and rate constants for Eu.100, Eu.107, Tb.100 and Tb.107 and the corresponding hydration number (*q*±0.5)

In each case, the geometry of the crystal structure was found to be a square antiprism with the lanthanide ion coordinating to the four moacrocyclic ring nitrogens and the three pendant amide oxygens. As expected, two metal bound water molecules completed the high coordination environment. The average La(III)···N and La(III)···O distances for the complexes were found to be 2.64 Å and 2.37 Å, respectively (Table 3.2). The OW1···La(III)···OW2 angle was found to be 71.80°, 72.17° and 70.86° for **Tb.100**, **Eu.100** and **Eu.107**, respectively. It is important that these bite angles are similar to the bite angles of the carboxylate anions that will displace them. Parker *et al.* and Dickins *et al.* recently reported similar three-arm cyclen complexes, which form adducts with various carboxylate anions with bite angles of between 54° and 69°.[202, 203]

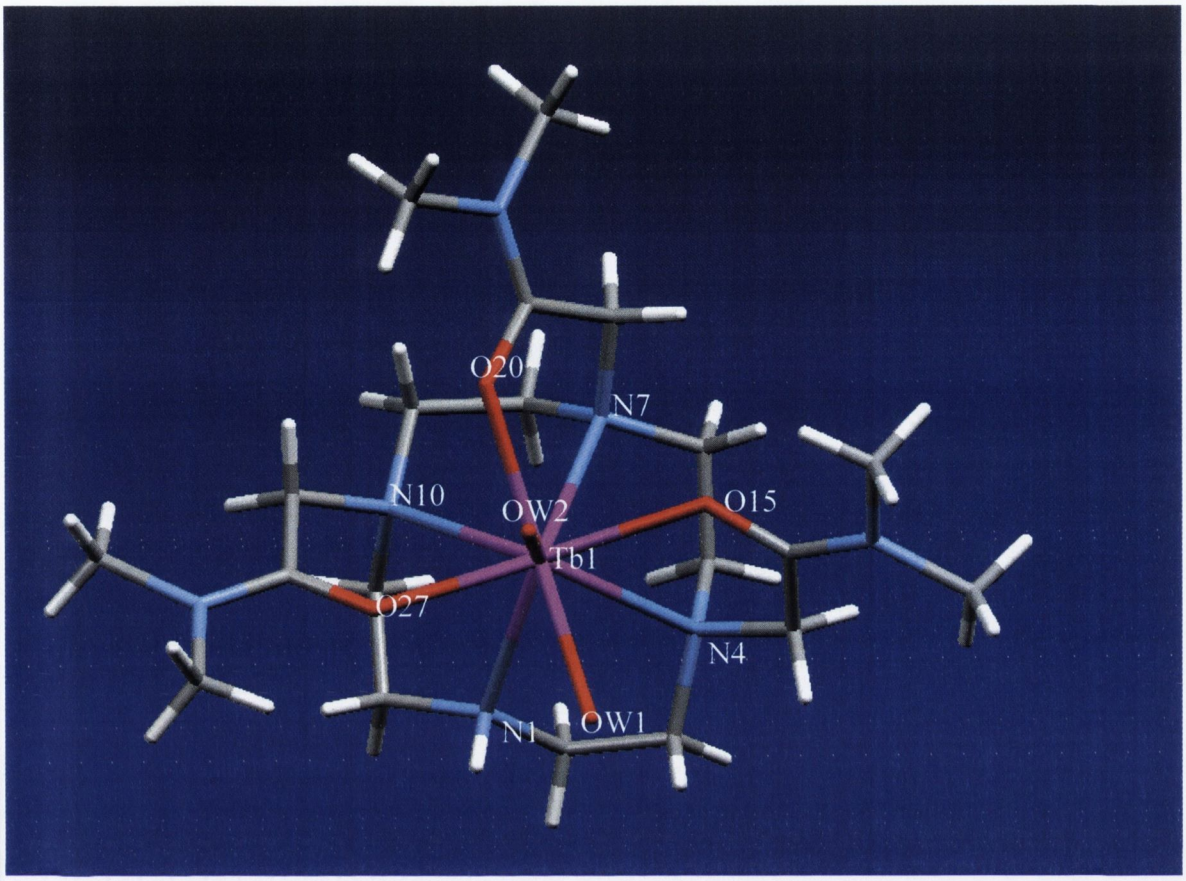

Figure 3.2 View from the top of Tb.100 showing the binding of Tb(III) to 100 and the two water molecules. Anions and solvent molecules have been removed for clarity[197]

Bond Label	Tb.100	Eu.100	Eu.107
Ln-O15 (Å)	2.348	2.342	2.378
Ln-O27 (Å)	2.325	2.364	2.394
Ln-O20 (Å)	2.368	2.378	2.399
Ln-O1W(water) (Å)	2.429	2.418	2.449
Ln-O2W(water) (Å)	2.441	2.421	2.485
Ln-N1 (Å)	2.601	2.605	2.673
Ln-N10 (Å)	2.656	2.624	2.617
Ln-N7 (Å)	2.637	2.625	2.67
Ln-N4 (Å)	2.641	2.647	2.677
OW1-Ln-OW2 (°)	71.80	72.17	70.86

Table 3.2. Selected lengths and angles for Tb.100 taken from Mercury 1.1 CIF file

3.5 Displacement of Metal Bound Water Molecules

No significant luminescence was observed from the complexes *i.e.* they were photophysically "silent". As explained before, this was due to the difficulty in directly exciting a lanthanide ion, combined with the lack of a sensitising antenna and the effective quenching mechanism provided by the two metal bound water molecules *via* their OH oscillations. The design of the sensor envisaged the metal bound water molecules being displaced by a suitable antenna. This would reduce the quenching of the lanthanide excited state by displacing the OH oscillators while offering an alternate indirect route to lanthanide sensitisation and as such, should lead to large enhancements in the luminescence. As discussed in Chapter 1, Parker *et al.*[202] and Dickins *et al.*[203] have shown related three-arm cyclen complexes that can form bidentate adducts with organic anions such as acetate, citrate and lactate by displacing these metal bound waters.

In considering a suitable antenna a number of factors needed to be addressed. Firstly, the antenna must posses a carboxyl group in order to displace the metal bound water molecules and hence bind to the lanthanide metal ion. Secondly, the antenna must have access to an excited triplet state and the energy of this state must be above that of the lanthanides excited singlet state (20,400 cm^{-1} for Eu(III) and 17,200 cm^{-1} for Tb(III)). Finally, the antenna must be able to transfer its energy to the lanthanide efficiently, as such the distance between the chromophore (in this case an aromatic group) and the metal must be short.

3.6 Luminescence Measurements

Dimethylaminobenzoic acid (**DMABA**), **108**, was chosen as the antenna as it fulfilled the above requirements. It contains a carboxyl group through which it may bind to the lanthanide ion by displacing the metal bound water molecules. It also contains an aromatic ring, with a suitable triplet energy level, which can act as a sensitising chromophore.[204] Also the distance between the two components is short, which should promote efficient energy transfer.

To investigate the complexes response to **DMABA**, measurements were carried out in water, at pH 7.4 (buffered with 0.1 M TRIS), at high ionic strength (0.1 M TMACl), in order to resemble physiological conditions. **DMABA** was gradually titrated into a 16 μM solution of the corresponding lanthanide complex. The complexes themselves did not absorb in the visible region, however, upon addition of **DMABA** the appearance of an absorption band at 288 nm was observed corresponding to the λ_{max} of the chromophore.

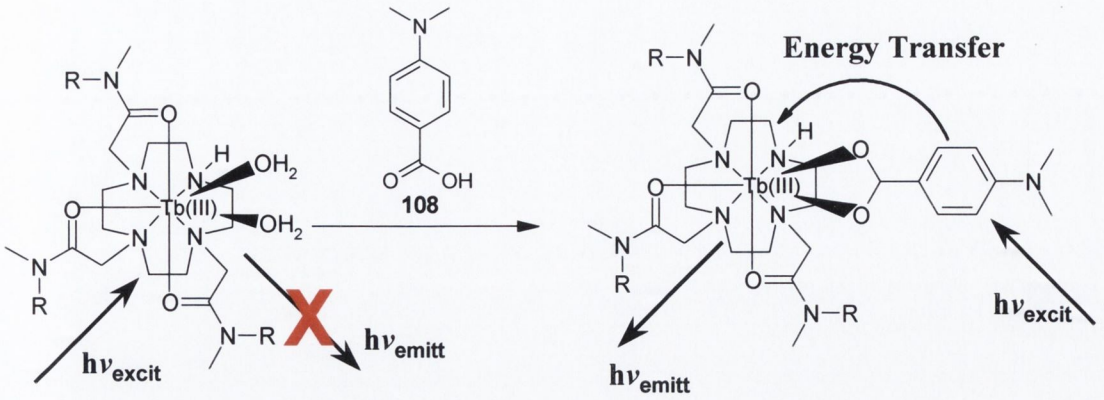

No Tb(III) Emission **Tb(III) Emission "switched on"**

Scheme 3.4. Upon binding the antenna the previously silent lanthanide complex is 'switched on' as its excited state is populated by an energy transfer from the antenna

The luminescent spectrum was also investigated. As noted earlier, the lanthanide complexes are photophysically silent prior to addition of the antenna. It was found that when the antenna **DMABA**, was excited at its λ_{max} = 288 nm, in the presence of **Tb.100**, a Tb (III) emission was observed (Scheme 3.4). Furthermore the luminescence intensity increased with increasing concentration of **DMABA**, reaching a maximum at ~ 2 equivalents, with a luminescence enhancement factor of *ca.* 220 (Figure 3.3).

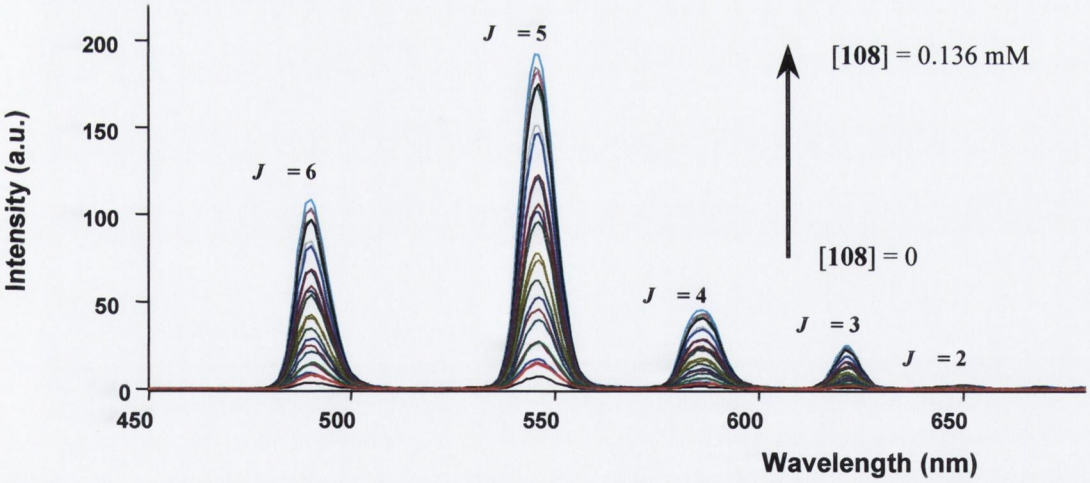

Figure 3.3. Luminescence spectra of Tb.100, showing increase in Tb(III) emission with increasing[DMABA] (108). Tris buffer pH 7.4, 0.1M TMACl, excite at 288 nm

Unexpectedly, the luminescence began to decrease upon further addition of **DMABA**, and was quenched after about 60 equivalents had been added (Figure 3.4). The pH of the solution remained constant over these measurements and consequently the decrease in luminescence can be directly attributed to the increased concentration of **DMABA**. One

possible explanation for the observed quenching of the luminescence may be the inner filter effect, caused by the presence of such an excess of antenna, as only the small percentage of the analyte directly bound to the Tb(III) ion may function as a sensitiser.[205]

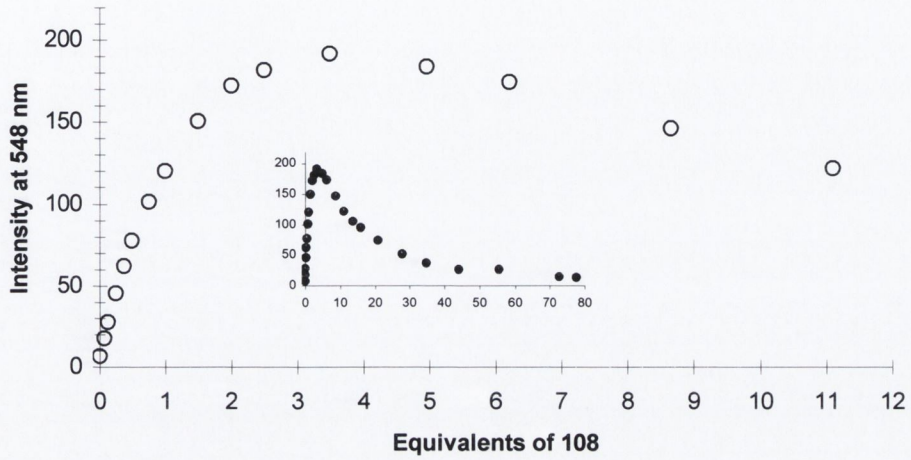

Figure 3.4. The changes in the intensity of the $J = 5$ transition of Tb.100 as a function of added equivalents of DMABA (108)

The appearance of the characteistic Tb(III) spectral bands can be explained by the use of a Jablonski diagram (Figure 3.5). Once bound to the lanthanide ion the analyte, denoted Ar, absorbs a photon of light and enters its singlet excited state, S_1. From here the energy can be transferred to the analytes triplet excited state, T_1, by means of intersystem crossing, ISC.

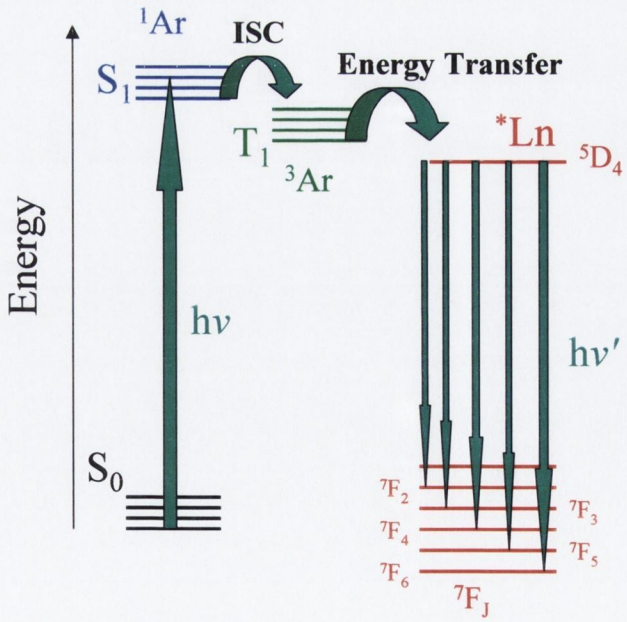

Figure 3.5. Jablonski diagram illustrating indirect excitation of Tb(III) ion by the bound analyte, Ar, which functions as a sensitising chromophore. Each transition $^5D_4 \rightarrow {}^7F_J$ will correspond to an emission band

As this state is higher in energy than the Tb(III) excited state, *Ln, it is possible for the analyte to pass its energy onto the lanthanide ion by means of the energy transfer mechanism, which was discussed in the introduction. The excited energy now resides on the Tb(III) ion, and can be lost by emission of light, resulting in the characteristic Tb(III) emission spectra as each transition will correspond to an emission band, $J = 6$ *etc.* The Tb(III) emission differs from the Eu(III) emission due to the different nature of the corresponding energy levels. The Tb(III) $^5D_4$ excited state is at 20,400 cm^{-1}, while the Eu(III) $^5D_0$ excited state is at 17,200 cm^{-1}.

A plot of p[**108**], where p is the negative log of concentration, against intensity of any of the bands, in this case the $J = 5$ band, revealed that the luminescence was switched on over two log units, p 6.2 → 4.2, which is indicative of 1:1 binding (Figure 3.6).[206]

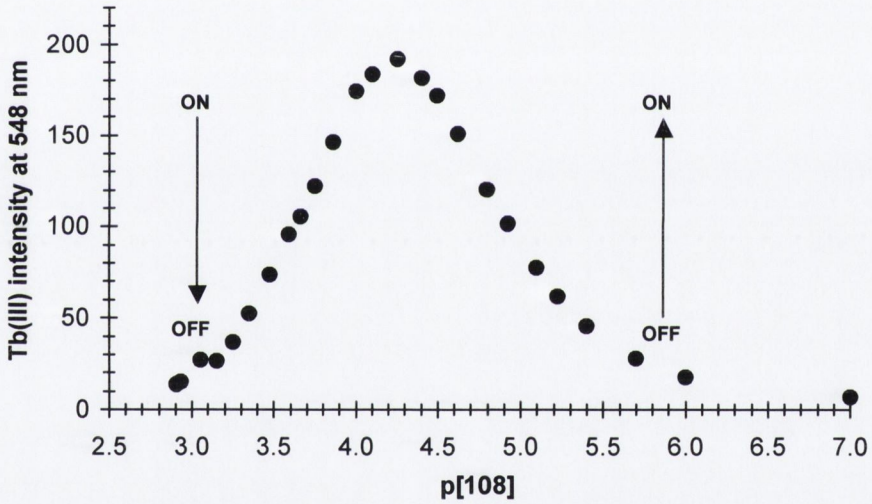

Figure 3.6. Plot of p[108] against Intensity reveals binding occurs over two log units, where p is the negative Log of concentration

The above measurements were repeated for **Tb.107** and again positive sensitisation occurred, although the enhancement factor was somewhat smaller *ca.* 80. This was attributed to additional quenching of the Tb(III) excited state by the presence of additional N-H oscillators in **Tb.107**.[199] These results indicate that for both **Tb.100** and **Tb.107** the carboxyl group was binding to the Tb(III) metal centre and successfully populating their excited states. Nevertheless, when these measurements were repeated for the europium compounds **Eu.100** and **Eu.107**, no sensitisation was observed. Lifetime measurements were carried out, this time in the presence of four equivalents of **DMABA (108)**, in an attempt to elucidate whether the analyte/antenna was displacing the metal bound water

molecules and binding to the metal ion as had been envisaged in the design (Table 5). From these measurements a q value of zero for the terbium complexes, and a q value of two for the europium complexes was determined. This inferred that **108** was not binding to the europium metal ion as neither of the metal bound water molecules were being displaced. The q value of zero for the terbium complexes indicated that the water molecules had been successfully displaced by **108** and that the ligand was binding through both the oxygens of its carboxyl group. This agrees with previous findings by Dickins and Parker, who found that oxyanion ternary complexes of Tb(III) complexes in water, were an order of magnitude more stable than their Eu(III) analogues.[207] This can be attributed to the enhanced Lewis acidity of Tb(III) over Eu(III).

Complex	τ_{H2O} (ms)	k_{H2O} (1/ms)	τ_{D2O} (ms)	k_{D2O} (1/ms)	$q(\pm 0.5)$
Eu.100	0.235	4.25	0.438	2.28	2.07
Eu.107	0.276	3.62	0.733	1.35	1.80
Tb.100	1.593	0.62	1.795	0.55	0.06
Tb.107	1.626	0.61	1.895	0.52	0.14

Table 3.3. Measured lifetimes and rate constants for Eu.100, Eu.107, Tb.100 and Tb.107 and the corresponding hydration number in the *presence* of four equivalents of *N,N*-dimethylaminobenzoic acid (108)

Further luminescence measurements were performed for the ester **109**, and ketone **110**, derivatives of **DMABA**. The excitation wavelength was chosen as the λ_{max} of **109** and **110**, respectively. However, neither one could sensitise the complexes. This seemed to confirm that both oxygens were required to successfully bind to the complex.

As remarked in Chapter 1, Georges and Arnaud have previously used salicylic acid as a sensitising chromophore for Tb(III) EDTA complexes in water at pH 12. It was decided to investigate whether the heptadentate complexes of **100** and **107** could also function as salicylic acid sensors under the physiological conditions employed above, *i.e.* in water at pH 7.4, and high ionic strength.

3.7 Sensitisation by Salicylic Acid

Aspirin® (**112**) is a well-known non-steroidal, anti-inflammatory drug that has many pharmacological actions. The active form of the drug is salicylic acid **111**, which is formed *in vivo* after hydrolysis of the ester group by enzymes.[208] Salicylic acid, **111**, is often used as a painkiller but can cause gastric bleeding due the free phenolic group.[208] This is

prevented by transforming the phenolic group to an ester to form the well known drug aspirin (**112**). Salicylic acid (**111**) is also an apt contender to be an antenna as it has a carboxylic group attached to an aromatic ring and is known to have a suitable triplet energy state above that of the Tb(III) excited state (Figure 3.9).[209]

Luminescence studies were carried out using salicylic acid. As found previously, no sensitisation was observed for the europium complexes. However, upon addition of **111** to a 16 μM solution of **Tb.100**, after excitation at 296 nm, sensitisation was observed with enhancement factors of *ca.* 40 and 30 (in H_2O and in Tris buffer, pH 7.4, respectively) (Figure 3.7). Again the intensity increased with increasing concentration of **111**, reaching its maximum at 10 equivalents before being slowly quenched with further increases in concentration (Figure 3.8). The plot of p[**111**] against intensity revealed that the luminescence was switched on over two log units, p 5.5 → 3.5, indicative of 1:1 binding (Figure 3.8).

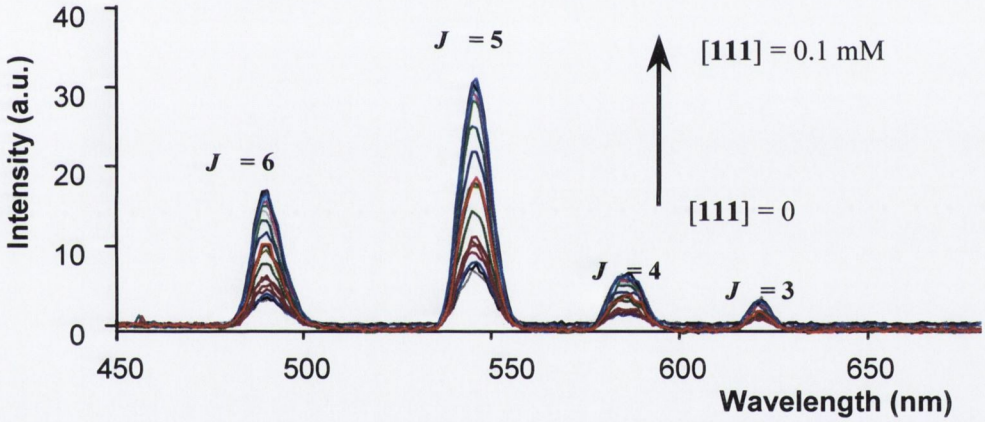

Figure 3.7. Luminescence spectra showing changes in Tb.100 emission upon addition of salicylic acid (111) in Tris buffer pH 7.4, 0.1M TMACl, excite at 296 nm

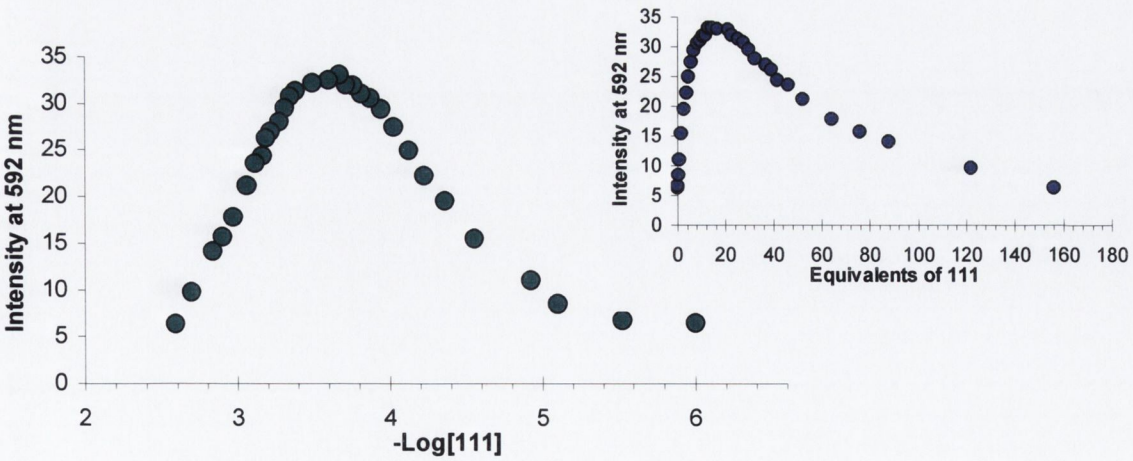

Figure 3.8. Plot of p[111] against Intensity showing switching on of Tb(III) luminescence over two log units. Inset showing equivalents plot for 111

Sensitisation was also observed for **Tb.107**, but the enhancement was much less than that of **Tb.100** and hence was not investigated further as the increases in luminescence were too small to be of practical use. The smaller enhancement was once again attributed to additional quenching of the Tb(III) excited state by the presence of the extra N-H oscillators in **Tb.107**.[199]

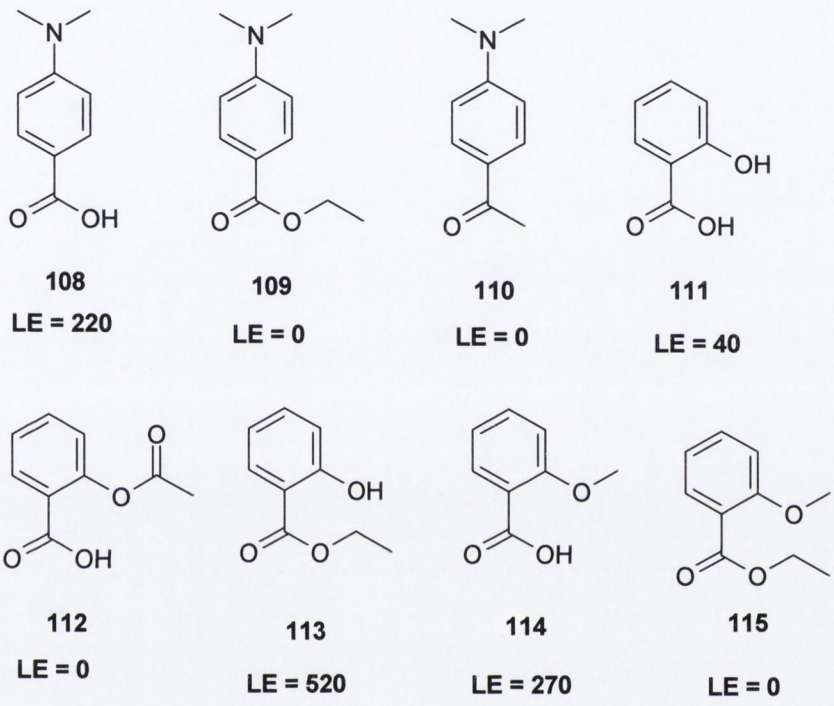

Figure 3.9. Compounds evaluated for ability to sensitise lanthanide complexes and their enhancement factors (LE) for Tb.100

Subsequently, aspirin (**112**) was evaluated as a sensitiser. Measurements were conducted in an identical manner to that described above. Surprisingly though, **112** was found to be unable to sensitise the lanthanide complexes, and in all cases, the luminescence remained switched "off". This was unexpected as the molecule contains a free carboxylic group attached to an aromatic ring and thus was expected to bind to the lanthanide centre and function as a sensitising antenna. Lifetime measurements were conducted and the q value for **Tb.100**, in the presence of aspirin (**112**) was determined to be two. This result revealed that the metal bound water molecules had not been displaced and therefore, aspirin (**112**) was not binding to the metal centre and as a result, was unable to sensitise the Tb(III) ion. Furthermore, competition experiments showed that **Tb.100** could selectively detect **111**, in the presence of **112**, *i.e.* when **111** was added to a photophysically silent solution of

Tb.100 and **112** (four equivalents), the luminescence was found to be "switched on" in an identical manner to that previously observed. The inability of **112** to bind to the lanthanide centre may have been due to steric factors from the increased bulk of the ester or it may point to a different binding mode (Figure 3.10). In order to investigate further, tests were carried out on the salicylic acid analogues **113**, **114** and **115**.

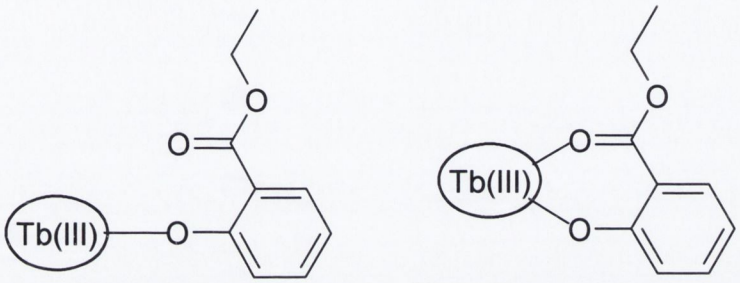

Figure 3.10 . Possible binding modes for Tb.100 with 113

In each case, the excitation wavelength was chosen as the λ_{max} of the antenna. As expected **115** did not sensitise any of the lanthanide complexes, as both of the hydroxyl binding sites are protected. The characteristic Tb(III) emission was observed for **114**, with luminescence enhancements of *ca.* 270. Surprisingly **113**, which does not have a free carboxylic acid group with which to bind, gave the greatest enhancements with luminescence increasing by a factor of *ca.* 520. This discrepancy points to the possibility of different binding modes, both in this case and in the case of salicylic acid **111**. To sensitise the **Tb.100** complex, **113** must bond to the metal either *via* its phenolic oxygen or through a 6 membered ring using the carboxyl oxygen as well. In order to establish which bonding mode was operating, lifetime measurements were carried out to determine the *q* value. The *q* values for **Tb.100** in the presence of **113**, **114** and **115** were all measured and found to be between zero and one ($q \pm 0.5$). This suggested that only one of the metal bound water molecules was being replaced upon the binding of these compounds. It is also possible that a mixture of these binding modes were operating. Nevertheless, whichever binding mode is in operation, we can conclude that **Tb.100** can selectively bind and sense salicylic acid (**111**) over aspirin (**112**).

In order to be viable as a *in vivo* sensor, **Tb.100** must function in the presence of other biological anions such as, phosphate, lactate and carbonate. As mentioned in the introduction, Parker *et al.*[210, 211] demonstrated that the similar heptadentate Eu(III) and

Tb(III) complexes **Eu.100** and **Tb.100**, which each possessed two metal bound water molecules, form 1:1 ternary complexes with these anions. When measurements were repeated upon **Tb.100** in the presence of 0.1 M carbonate (Na_2CO_3) or ($NaHCO_3$), the luminescence remained "switched off" even after the addition of four equivalents of **111**. The preferential binding of carbonate by **Tb.100**, indicates that the sensor would be impractical for *in vivo* applications.

In summary, four novel unsaturated lanthanide complexes **Eu.100**, **Eu.107**, **Tb.100** and **Tb.107**, have been prepared and each of them has been shown to possess two metal bound water molecules. In the case of the two Tb(III) complexes the addition of aromatic carboxylate anions such as **DMABA** (**108**) and salicylic acid (**111**) gave rise to significant enhancements in the luminescence of the complexes, due to the self assembly of ternary complexes in aqueous solution under ambient conditions, *i.e.* in water at pH 7.4 at high ionic strength (0.1M TMACl). The complexes themselves do not contain a chromophore and require the formation of the ternary complex, with the analyte, in order to allow indirect sensitisation by the analyte/antenna to lead to a lanthanide emission. For the Eu(III) complexes, no increase in luminescence was observed, as under these conditions they did not form ternary complexes with the analyte and hence could not be sensitised. This was confirmed by lifetime measurements in the presence of excess analyte.
In the case of the **DMABA** analyte, the binding is believed to proceed through both carboxyl oxygens *via* the formation of a four-membered bidentate ring, with both metal bound waters being displaced. The binding mode for **111** is less certain and may operate in a monodentate or bidentate fashion. The sensors did not function in the presence of 0.1 M carbonate, indicating that they may be unsuitable for *in vivo* applications.

3.8 Bis Terbium System

The success of **Tb.100** as a sensor for aromatic carboxylates, encouraged us to pursue this work further. It was of interest whether the incorporation of a second metal ion into the design would impact upon the properties of the sensor. It was envisaged that a binuclear Tb(III) conjugate could bind bis-carboxylates and signal this event through a change in the luminescence. Therefore the aim of the project was to synthesise a bis-lanthanide luminescent sensor for aromatic carboxylates and investigate its luminescent response to antennae, with the goal of sensing aromatic bis-carboxylates. The synthesis and characterisation of this compound shall be the subject of the following section.

3.9 Synthesis

Building upon the previous design it was decided to link two **Tb.100** complexes together by a short xylene bridge. The **Tb.100** unit was chosen as it had given the best results to date. The synthesis was carried out as shown in Scheme 3.5. The ligand **100** was refluxed in MeOH with α,α-dichloro-*p*-xylene **116**, in a 2:1 molar ratio, in the presence of Cs_2CO_3 and KI for four days. The solvent was then evaporated and the residue was suspended in $CHCl_3$ and filtered. The volume was then reduced and the solution was left to stand at 4 °C. The resulting crystals were filtered and washed with cold $CHCl_3$, yielding the product 2-{4,7-bis-dimethylcarbamoylmethyl-10-[4-(4,7,10-tris-dimethylcarbamoylmethyl-1,4,7,10-tetra-aza-cyclododec-1-ylmethyl)-benzyl]-1,4,7,10-tetraaza-cyclododec-1-yl}-*N,N*-dimethyl-acetamide, **117**, in 10 % yield.

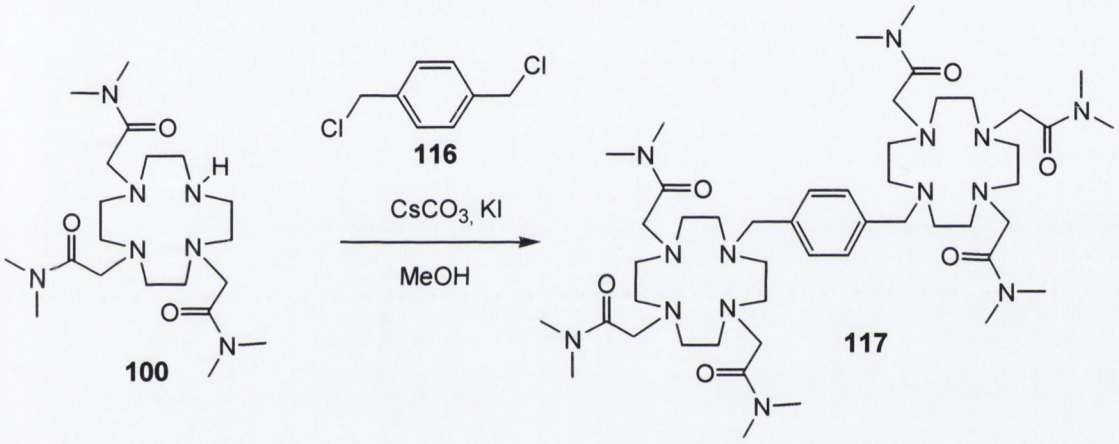

Scheme 3.5. Synthesis of 117 was carried out with 10 % yield

The bis-cyclen ligand **117**, had not been previously reported and was fully characterised. The ^1H NMR spectrum in D_2O of **117** revealed the high degree of symmetry inherent in the molecule. The four aromatic protons resonanced at 7.30 ppm while the four benzyl protons were observed at 3.95 ppm (Figure 3.11).

The ^{13}C NMR spectrum showed two carbonyl resonances at 172.5 and 172.1 ppm. The aromatic signals were visible at 136.5 (quaternary) and 129.8 ppm, while seven CH_2 resonances were visible at 57.7, 54.5, 53.8, 50.8, 50.3, 49.7 and 48.3 ppm respectively. Three CH_3 resonances were observed at 35.5, 35.1 and 34.8 ppm, due to a syn and anti relationship with the amide carbonyl group (Figure 3.12).

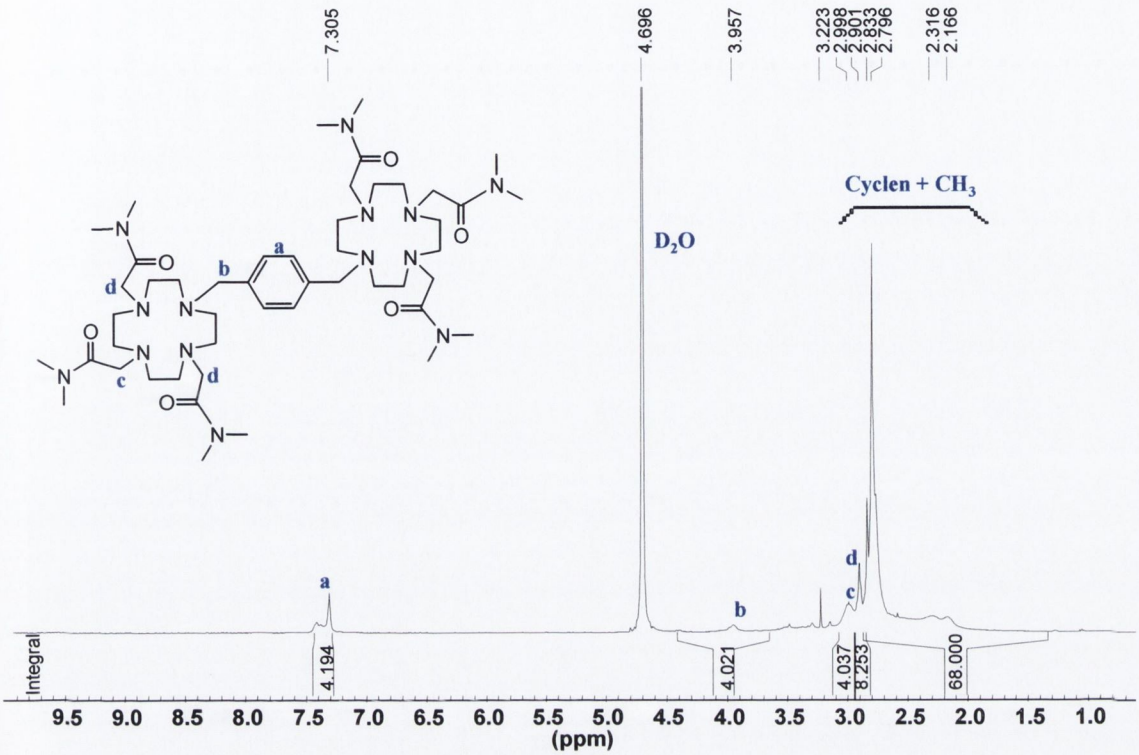

Figure 3.11. 400 MHz ^{1}H NMR in D_2O of 117

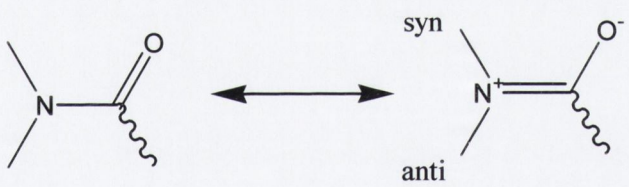

Figure 3.12. The lack of rotation around the N=C double bond leads to the syn methyl group "experiencing" the electric field of the oxygen, to a greater extent than the anti methyl group

The mass spectrum contained three signals at *m/z* = 479.1, 490.0 and 500.9, corresponding to the [M+H]/2, [M+Na]/2 and [M+K]/2 species respectively. Elemental analysis and high resolution mass spectrometry confirmed that the ligand had been synthesised. A crystal structure corresponding to the sodium complex of the ligand was also obtained (Figure 3.13). Sodium is known to have a similar coordination geometry to that of terbium. The sodium complex was seen to have two metal bound water molecules.

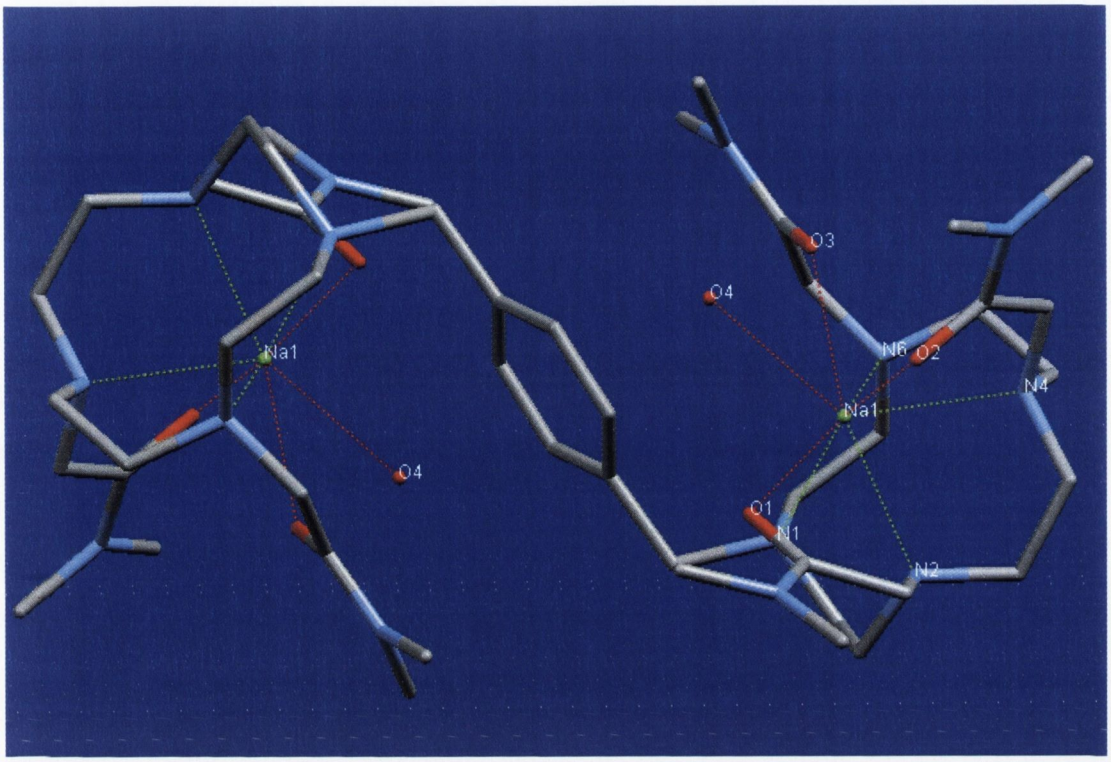

Figure 3.13. Sodium complex of 117 M.2Na.2H_2O. 8$CHCl_3$.2I. Hydrogen, solvent and anions have been removed for clarity

Atom1	Atom2	Length (Å)
Na1	N1	2.729
Na1	N2	2.43
Na1	N4	2.492
Na1	N6	2.534
Na1	O1	2.484
Na1	O2	2.489
Na1	O3	2.373
Na1	O4	3.461

Angle Label	Angle (°)
O1-Na1-N2	67.04
O2-Na1-N4	66.52
O3-Na1-N6	67.75
O4-Na1-O3	61.17
O4-Na1-O2	57.04
O4-Na1-O1	60.25

Table 3.4. Selected lengths and angles taken from Mercury 1.2.1 CIF file

The ligand adopts a square antiprism geometry around the sodium ion, which coordinates to the four macrocyclic ring nitrogens as well as the three pendant amide oxygens with average Na···N and Na···O distances of 2.55 Å and 2.45 Å, respectively. This geometry is also common for octadentate lanthanide cyclen complexes.[212] The similarity in geometry stems from the fact that, like the lanthanide ions, sodium prefers a high coordination environment. The crystal structure also shows the presence of two metal bound water molecules with a Na to water (O4) distance of 3.461 Å, while the Na···Na distance was found to be 8.688 Å.

The corresponding terbium complex was formed by refluxing **117** with two equivalents of $Tb(CF_3SO_3)_3$ in MeOH overnight (Scheme 3.6). The complex was precipitated from ether and washed with CH_2Cl_2 to give the desired product **Tb.117**, in 41 % yield. The ^1H NMR spectrum revealed that the complex was present, evidenced by the large shift in the proton signals due to the paramagnetic metal ion (Figure 3.14). This effect shall be described in greater detail in section 4.3.5. The spectrum showed signals ranging from 120.25 to –122.88. The mass spectrum contained signals at m/z = 573.5 and 284.8 corresponding to the [M+3 triflate]/3 and [M+1 triflate]/5 species. The IR spectrum showed that the carbonyl stretching frequency had decreased from 1639 cm^{-1} to 1624 cm^{-1}, again indicating that the complex had been formed. Elemental analysis confirmed the characterization of the complex.

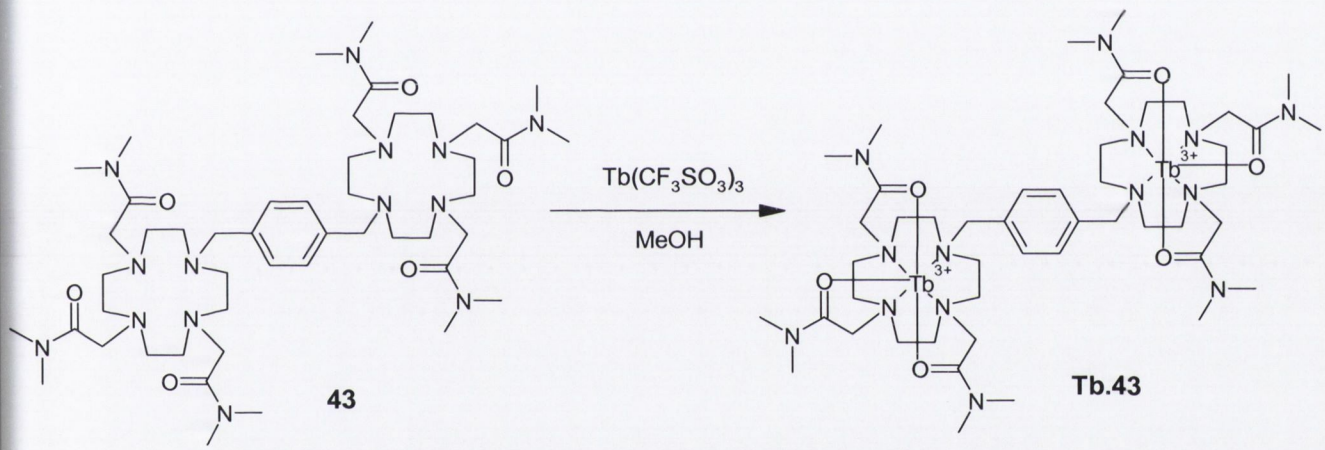

Scheme 3.6. Complexation of 117 proceeded in 41 % yield

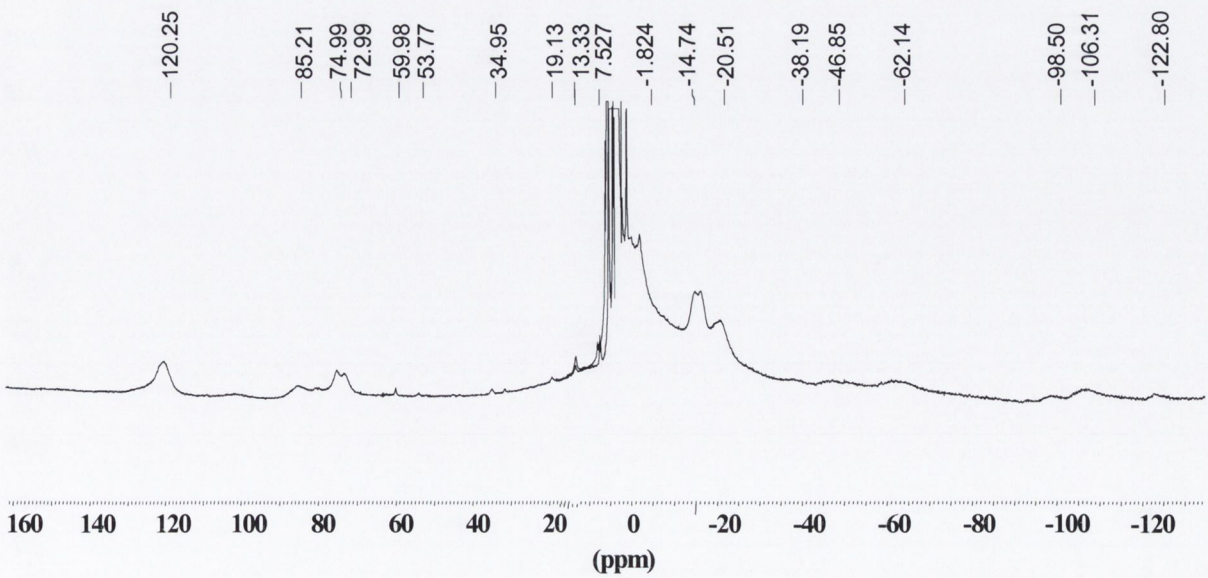

Figure 3.14. 400MHz ^1H NMR of Tb.117

Once again, the number of metal bound water molecules was deduced by measuring the luminescent lifetimes (τ) of the Tb(III) excited state, after direct excitation, in both D_2O and H_2O. As in the case of the mononuclear system, the number of metal bound water molecules on each metal centre was found to be two (Table 3.5).

Complex	τ_{H2O} (ms)	k_{H2O} (1/ms)	τ_{D2O} (ms)	k_{D2O} (1/ms)	q (±0.5)
Tb.117	0.730	1.35	1.071	0.93	1.93

Table 3.5. Measured lifetimes and rate constants for Tb.117 and the corresponding hydration number *q*

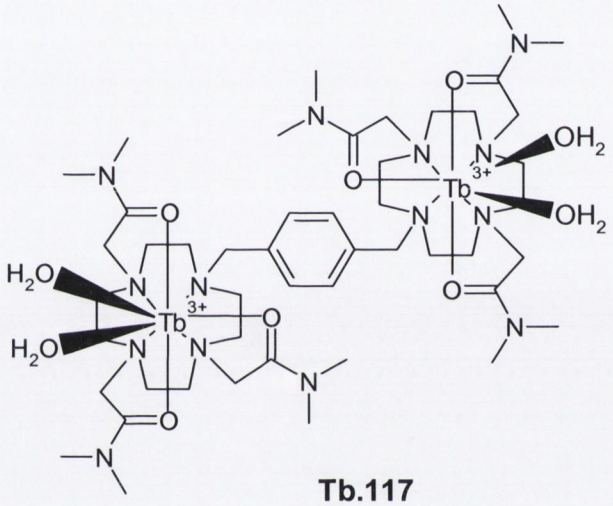

Tb.117

Figure 3.15. Showing metal bound water molecules

Interestingly the lifetime and rate constant values were very similar to the corresponding mononuclear complex, **Tb.100**. As such, the relative binding was expected to operate in a similar fashion. In contrast to the mononuclear system, however, **Tb.117** now possesses its own xylene chromophore and thus is no longer photophysically silent.

3.10 Photophysiclal Studies of Tb.117

The complex, **Tb.117**, absorbed in the UV with λ_{max} at 237 nm. When excited at 237 nm the characteristic Tb(III) emission was observed, showing that the xylene bridge can act as an antenna and populate the Tb(III) excited state. The systems response to the original antenna **DMABA**, **108**, was investigated, in order to compare it to the mononuclear system **Tb.100**. Measurements were conducted in water at pH 7.4 (buffered with 0.1 M HEPES),

at high ionic strength (0.1 M TMACl). **DMABA** was gradually titrated into a 16 μM solution of the lanthanide complex, **Tb.117**.

Upon addition of **DMABA** the appearance of a band at 288 nm was observed. A fluorescent band was also observed at 356 nm after excitation at 288 nm (see appendix). Both the absorption and fluorescent transitions, were seen to increase in intensity with increasing concentration of **DMABA** and they can be directly attributed to the antenna. The luminescent spectrum of **Tb.117** was also investigated as a function of **DMABA** concentration. When excited at 288 nm, prior to addition of **DMABA**, the complex, **Tb.117**, was found to have a very weak luminescence (20 a.u.). However, upon the addition of the antenna **DMABA 108**, and after excitation at 288 nm, a large increase in the Tb (III) emission was observed (Figure 3.16).

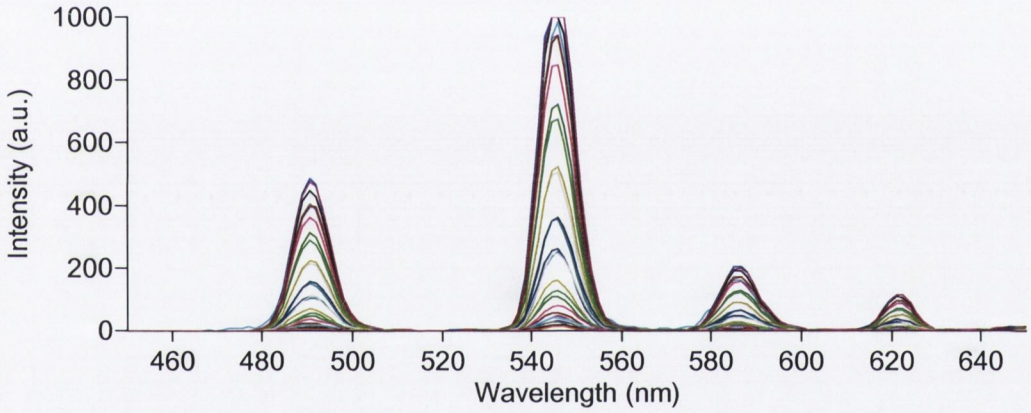

Figure 3.16. Luminescence spectrum of Tb.117 (16 μM), showing increase in luminescent intensity upon addition of DMABA. Excite at 288 nm, pH 7.4, 0.1 M TMACl

Furthermore the luminescence intensity increased with increasing concentration of **DMABA 108**, reaching a maximum at ~ 2 equivalents, with a luminescence enhancement factor of *ca.* 1000 (Figure 3.17). As noted for **Tb.100**, the luminescence began to decrease upon further addition of **DMABA** and was fully quenched after about 70 equivalents had been added (Figure 3.17). Once again, the pH of the solution remained constant over the course of these measurements and thus the quenching can be directly attributed to the high concentration of the free antenna compared to the relatively small percentage of bound antenna in the ternary complex.

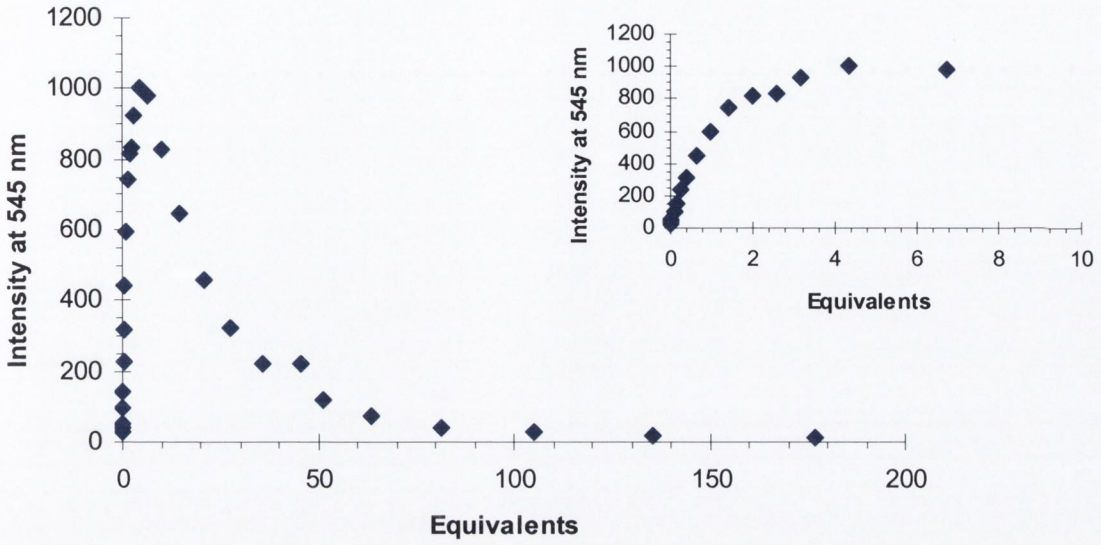

Figure 3.17. The change in intensity of the luminescent band at 545 nm, with respect to the equivalents of DMABA added

By plotting p[**DMABA**] against the relative intensity at 545 nm, a direct comparison to the mononuclear system **Tb.100**, is possible. The plot of p[**108**] against intensity revealed that the luminescence was switched on over two log units, p 5.9 → 4.2 (Figure 3.18).

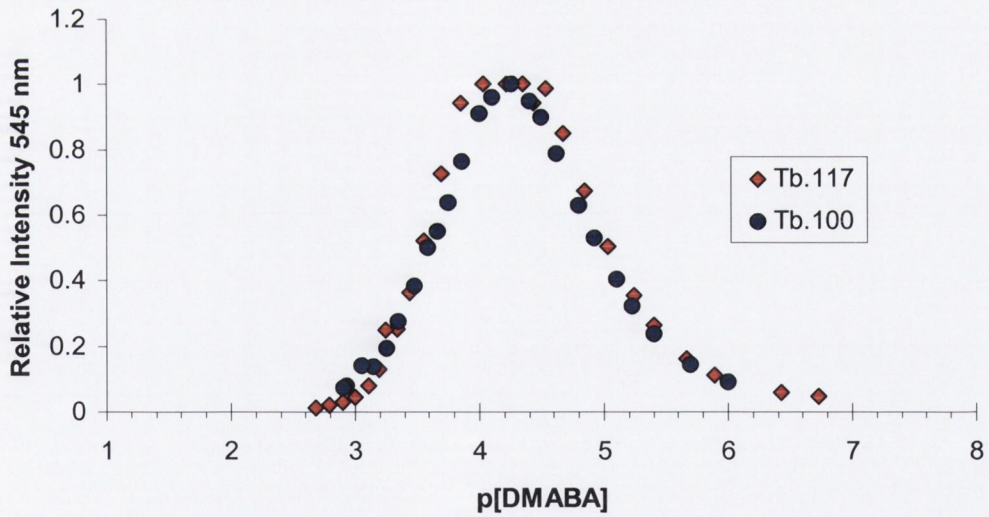

Figure 3.18. Plot of p[DMABA] against Relative intensity

It can clearly be seen that both titrations behave similarly over similar concentration ranges, clearly quenching over two log units p 6.2 → 4.2. As they are both at 16 uM, **Tb.117** has twice as many metal centres as **Tb.100**. This is evidenced by the much larger luminescent enhancement viewed for **Tb.117** ~ 1000 *ca.* 220. It may have been expected that the **Tb.117,** having twice as many metal centres would behave differently. However,

the two metal centres seem to be acting independently of each other and as such, this can be viewed as a 1 antenna: 1 metal centre, binding motif (Figure 3.19), similar to the 1:1 binding motif of the mononuclear **Tb.100** complex.

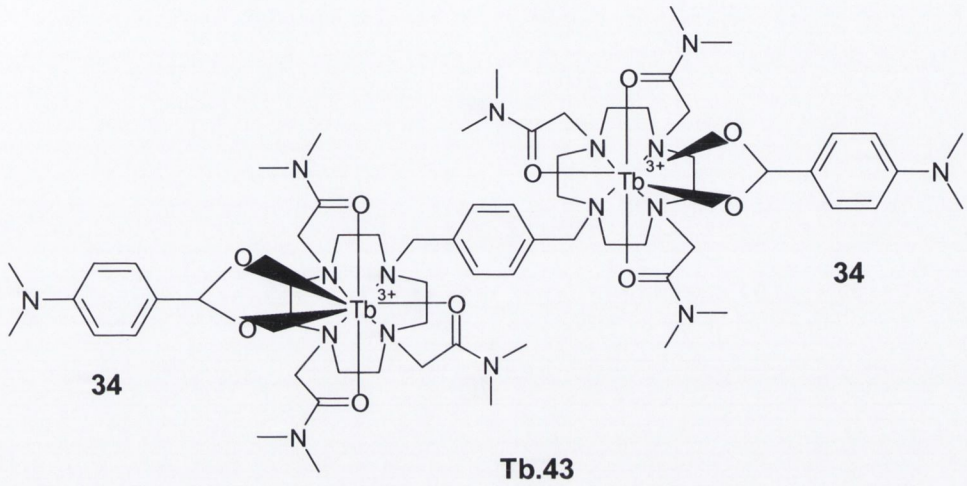

Figure 3.19. Showing possible binding mode for 108 with Tb.117

Luminescent lifetime measurements were carried out upon **Tb.117** in the presence of four equivalents of **DMABA**. The lifetime values were similar to those observed for **Tb.100** in the presence of **DMABA**, and again corresponded to a hydration value, q, of zero (Measured lifetimes and rate constants for Tb.117 and the corresponding hydration number in the *presence* of four equivalents of *N,N*-dimethylaminobenzoic acid (108)). This further supported the theory that the two metal bound water molecules on each Tb(III) ion were displaced by **DMABA**.

Complex	τ_{H2O} (ms)	k_{H2O} (1/ms)	τ_{D2O} (ms)	k_{D2O} (1/ms)	q (±0.5)
Tb.117	1.315	0.761	1.504	0.665	0.18
Tb.100	1.593	0.62	1.795	0.55	0.06

Table 3.6. Measured lifetimes and rate constants for Tb.117 and the corresponding hydration number in the *presence* of four equivalents of *N,N*-dimethylaminobenzoic acid (108)

In summary, a novel binuclear Tb(III) complex, **Tb.117**, has been synthesised, which was found to possess two metal bound water molecules per Tb(III) ion. The addition of the aromatic carboxylate **DMABA (108)**, to a solution of **Tb.117**, gave rise to large enhancements in the Tb(III) emission intensity, due to the self assembly of ternary complexes in aqueous solution under ambient conditions, *i.e.* in water at pH 7.4 at high

ionic strength (0.1M TMACl), whereby the **DMABA** acts as a sensitising antenna for the Tb(III) ion.

Luminescent lifetime measurements in the presence of excess **DMABA**, revealed that both metal bound water molecules had been displaced, indicating that the binding of the **DMABA** anion is proceeding through both carboxyl oxygens *via* the formation of a four membered ring, giving rise to a one **DMABA** to one Tb(III) ion, or two **DMABA** to one **Tb.117** ternary complex.

3.11 Sensitisation with dicarboxylates

Following the response to the **DMABA** carboxylate a series of measurements were conducted to determine whether the binuclear Tb(III) complex **Tb.117**, could be sensitised by aromatic dicarboxylates. Terephthalic acid, **118**, was chosen as a sensitiser as it is a bis carboxylic acid, has a complementary geometry to that of **Tb.117**, and is known to have a suitable triplet energy state above that of the Tb(III) excited state.[204]

Luminescence studies were conducted in an identical manner to that described previously using **118**. The analyte, **118**, absorbs in the UV with a λ_{max} at 240 nm. This is very close to the λ_{max} of the **Tb.117** complex itself (237 nm), and indeed upon excitation of **Tb.117,** at 240 nm, in the absence of any antenna, the characteristic terbium emission was observed.

Upon addition of **118** to a 16 μM solution of **Tb.100**, after excitation at 240 nm, sensitisation was observed with enhancement factors greater than 1000 (*i.e.* off the scale). As a result the fluorimeter settings were altered and the emission slit width was changed from 5 nm to 2.5 nm, all other settings remained unchanged. Under these settings luminescent enhancements of *ca.* 350 were obtained (Figure 3.20).

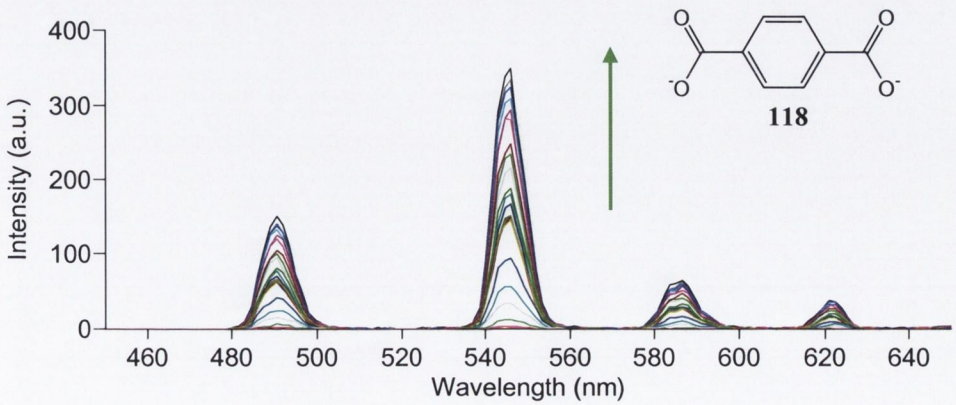

Figure 3.20. Changes in luminescence of Tb.117 upon addition of 118 at pH 7.4, 0.1 M TMACl, excite at 240 nm. Note emission slit reduced to 2.5 nm

As expected, the intensity increased with increasing concentration of **118**, reaching its maximum at ~ 3 equivalents before being quenched with further increases in concentration (Figure 3.21).

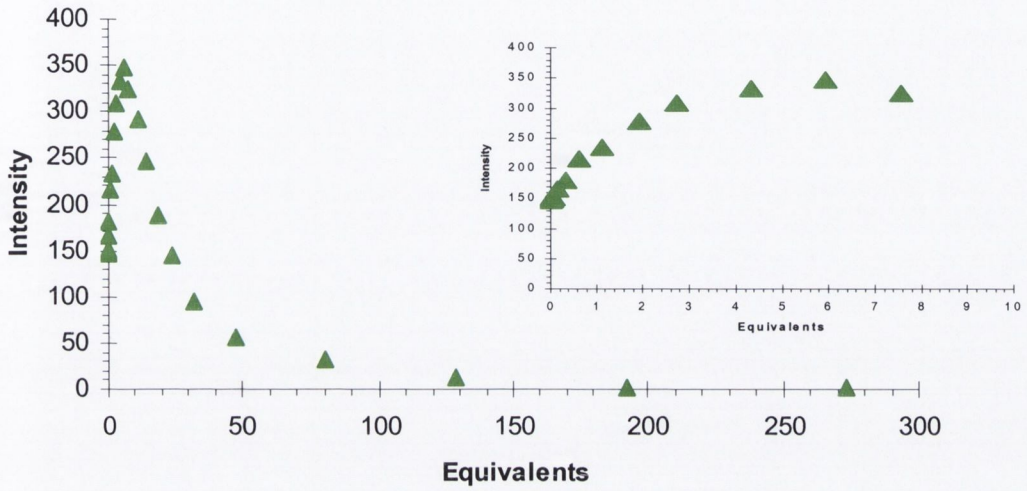

Figure 3.21. Plot of equivalents of 118 against Intensity at 545 nm for Tb.117 at pH 7.4, 0.1 M TMACl, excite at 240 nm

The plot of p[**118**] against intensity revealed that the luminescence was switched on over two log units, p 5.9 → 4.0, indicative of 1:1 binding (Figure 3.22).

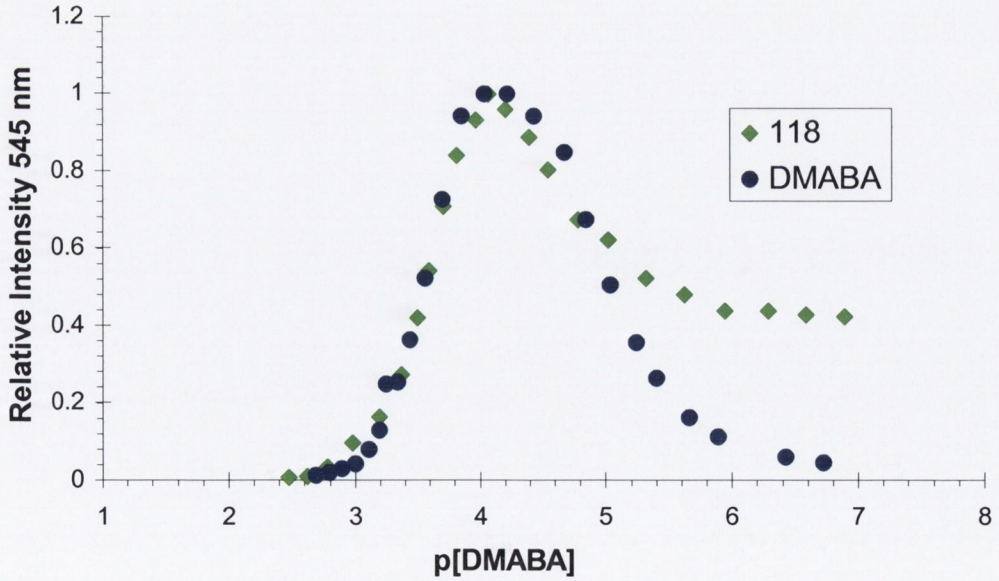

Figure 3.22. Relative intensities plot showing the effect of 118 and DMABA upon Tb.117 at pH 7.4, 0.1 M TMACl

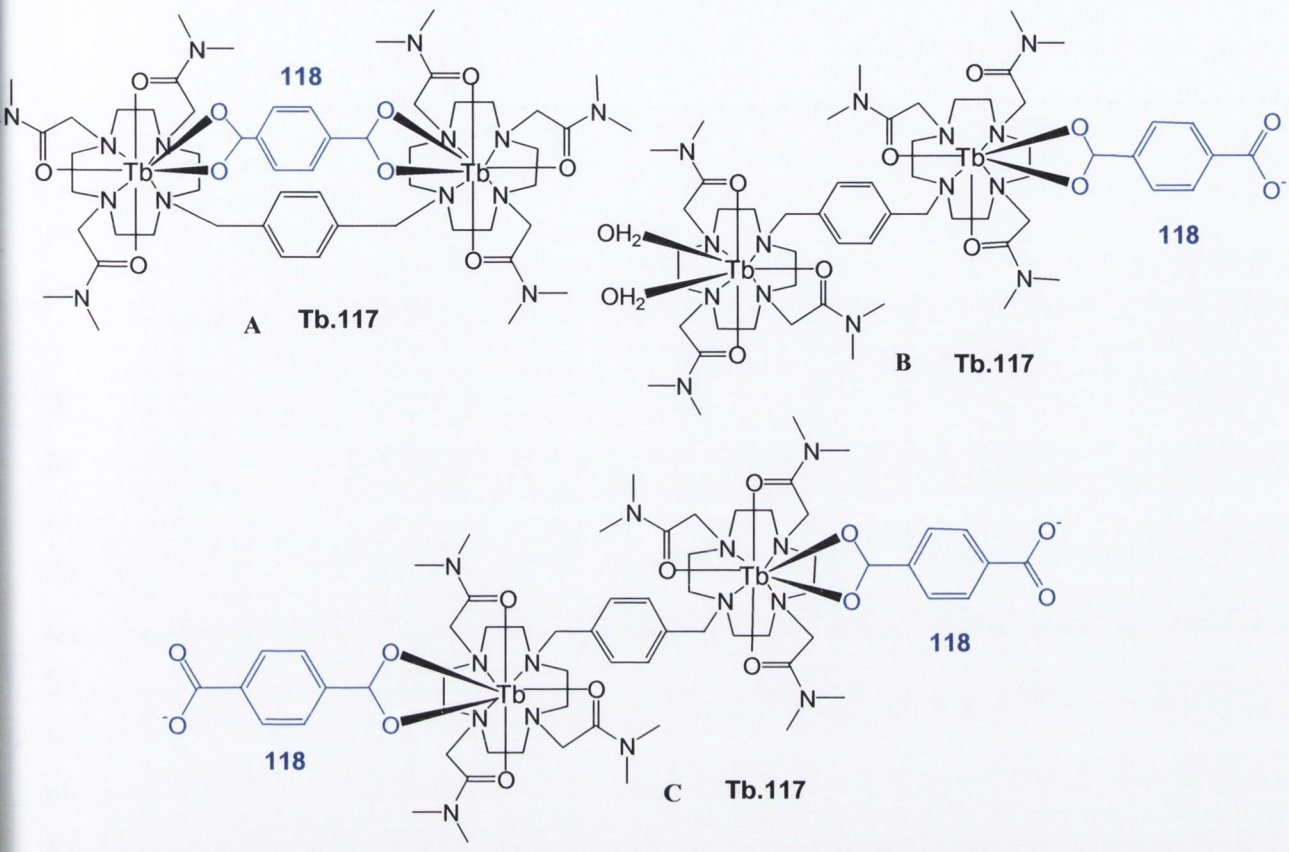

Figure 3.23. Possible binding modes for Tb.117 and the sensitising antenna 118

As yet, it was unclear whether the **Tb.117**: **118** binding mode operating was **A**: a two Tb(III) ion to one **118**, **B**: a one Tb(III) ion to one **118**, or **C**: a one **Tb.117** to two **118**, interaction (Figure 3.23). In order to elucidate more clearly, lifetime measurements were once again conducted upon **Tb.117** in the presence of four equivalents of **118**. From the lifetime values obtained the hydration number was ascertained to be zero (Table 3.7). This immediately ruled out the 1:1 binding interaction **B**, as in that case, the hydration number would be higher as one of the Tb(III) ions would retain two metal bound water molecules. Whether both Tb(III) ions are binding to the same **118** unit, **A**, or are acting independently, **C**, is still unclear, and work is continuing within the Gunnlaugsson laboratory to solve this conundrum. Nevertheless, whichever binding mode is in operation, we can conclude that **Tb.117** can bind, recognise and signal the presence of terephthalic acid (**118**).

Complex	τ_{H2O} (ms)	k_{H2O} (1/ms)	τ_{D2O} (ms)	k_{D2O} (1/ms)	q (±0.5)
Tb.117	1.315	0.761	1.452	0.689	0.06

Table 3.7. Measured lifetimes and rate constants for Eu.100, Eu.107, Tb.100 and Tb.107 and the corresponding hydration number (q±0.5) in the *presence* of four equivalents of terephthalic acid (118)

As in the case of the mononuclear system, when the measurements were repeated upon **Tb.117** in the presence of 0.1 M carbonate (Na_2CO_3), the luminescence remained "switched off" even after the addition of four equivalents of **DMABA** or **118**. The preferential binding of carbonate at high concentrations, indicates that the sensor would be impractical for *in vivo* applications.

3.13 Conclusion

In summary, lanthanide complexes have been prepared that can sense for aromatic carboxylates by means of self-assembling ternary complexes. It has been shown both through x-ray crystallography and lifetime measurements that each lanthanide ion possesses two metal bound water molecules. These metal bound waters can be displaced by aromatic carboxylates, which can then act as 'antennae', passing their energy to the lanthanide excited state and thereby inducing a luminescent emission from the previously photophysically silent lanthanide complex. Of the four mononuclear complexes studied, **Eu.100**, **Eu.107**, **Tb.100** and **Tb.107**, the Eu(III) complexes did not give rise to the formation of such self-assembling complexes. It was concluded that this was due to the lower affinity of europium complexes towards the carboxylate antennae. Other researchers have made similar observations.[202] The effective binding of **DMABA (108)** to both **Tb.100** and **Tb.107** was observed with large increases in luminescence and proceeded *via* the formation of a four-membered bidentate ring, with both metal bound waters being displaced. The binding of salicylic acid (**111**) however, could operate through either a mono or bidentate fashion. This was shown by probing the bonding modes of **113**, **114** and **115**. All of these processes occur under ambient conditions *i.e.* in water at pH 7.4 at high ionic strength (0.1M TMACl).

A novel binuclear Tb(III) complex, **Tb.117**, has also been synthesised. The crystal structure of the sodium complex of **117** indicated that metal bound water molecules would be present and lifetime measurement confirmed that each Tb(III) ion possesses two metal bound water molecules. This complex also exhibited large increases in its luminescence *ca.* 1000, after the formation of a ternary complex with the **DMABA** antenna, over an identical concentration range to that observed for **Tb.100**. Lifetime measurements in the presence of the **DMABA** antenna indicated that each of the Tb(III) ions was binding one carboxylate anion, as all the metal bound water molecules had been displaced, $q = 0$ (± 0.5).

Furthermore the addition of the bis-carboxylate, terephthalic acid, gave rise to even stronger luminescent enhancements. The effective binding of **118**, occurred over an identical region to that of **DMABA**. Lifetime measurements in the presence of **118** confirmed that all metal bound water molecules had been displaced, $q = 0$ (± 0.5). Further work is necessary to determine the precise binding mode as whether it is 1:2 or 1:1 is still undetermined.

In the presence of 0.1 M Na_2CO_3, the luminescence of both the mononuclear and binuclear systems was quenched and the addition of increasing concentrations of antenna had no effect. This was attributed to the coordination of the carbonate anion by the Tb(III) ion, preventing binding of the analyte. In conclusion a new general class of sensor for aromatic carboxylates such as **DMABA**, salicylic acid, **111**, and terephthalic acid, **118**, have been successfully developed. They operate under ambient conditions through the formation of ternary complexes, which give rise to large increases in the Tb(III) luminescence.



Chapter 4

Lanthanide Complexes as Phosphodiester Cleaving Agents

4.1 Introduction

Phosphodiester bonds play an important role in nature. The very stable 3',5'-phosphodiester is used to link together the genetic code of the nucleic acids, DNA and RNA. The large stability of this molecule stems from the negative charge on the phosphate, which drastically reduces the rate of hydrolysis.[213] As mentioned in Chapter 1, the ability to selectively cleave the RNA phosphodiester, could lead to the targeting and control of specific diseases, which operate by the production of harmful proteins.[214] As such, efforts to develop ribozyme mimics that cleave phosphodiester bonds efficiently are currently underway.[214, 215, 216]

Nature utilises a class of enzymes known as ribozymes, to efficiently cleave unwanted nucleic acids. As previously discussed in Chapter 1, these enzymes often contain metal ions as well as catalytically active cofactors like histidine, at their active sites. Drawing upon nature's ideas, these components are being studied and utilised in the design of ribozyme mimics. Metal ions, and lanthanide ions in particular, have been shown to greatly accelerate the hydrolysis of phosphodiesters.[217, 218] However, as they can be both toxic and unselective, they must be incorporated into a ligand framework to be of use for *in vivo* applications.[219] Chapter 1 detailed some examples of phosphodiester hydrolysis accelerated by coordinated metal ion complexes. To date, work in the Gunnlaugsson group has focused on the use of mononuclear lanthanide systems and their ability to promote phosphodiester hydrolysis.[220]

The focus of this thesis, however, is the rate enhancement provided by the cooperative action of two metal ions. As discussed in Chapter 1, binuclear metal ion systems can promote phosphodiester cleavage many times more rapidly than similar mononuclear systems. The work herein concentrates solely on binuclear lanthanide complexes, which to date, despite large rate enhancements reported for mononuclear lanthanide systems, have been largely overlooked.[216, 221] With the goal of obtaining large rate enhancements above those of similar mononuclear systems, this chapter shall detail the synthesis of some binuclear lanthanide complexes. It will then discuss the phosphodiester cleavage ability of such compounds, comparing them to similar mononuclear systems from the literature and the Gunnlaugsson laboratory.

4.2 Design of Binuclear systems

The objective of this project was to design and synthesise binuclear lanthanide metal ion systems that would improve upon the rate of hydrolysis of RNA and RNA mimic compounds currently attained by mononuclear complexes. As previously stated, lanthanides are toxic to biological systems, because of their similarity to Ca(II) and Mg(II), and hence, for pharmaceutical applications, must to be incorporated into stable macrocyclic ligands.[219] The overall charge on the ligand must remain neutral so as not to depress the hard Lewis acid character of the lanthanide metal ions.[222, 223] For example negatively charged ligands such as EDTA, which are known to strongly bind lanthanide ions, have been found to be unable to promote the cleavage of RNA.[223] However, in order to form a stable complex the neutral ligand must go some way towards fulfilling the lanthanide ions high coordination number requirement, which commonly reach nine or ten and sometimes higher.[224, 223]

The cyclen macrocycle was chosen as the basic template for the ligand in order to allow comparison with mononuclear lanthanide systems previously reported, such as those described earlier, in Chapter 1. Cyclen offers a number of advantages for coordinating lanthanide ions, over other systems. It provides a handle for further functionalisation, and this allows organic catalytically active groups to be incorporated into the design. Cyclen also provides four donor nitrogen atoms, however, additional coordinating donor groups can be incorporated into the macrocycle which, when properly functionalised, is known to virtually encapsulate lanthanide ions forming lanthanide (III) complexes that are inert to dissociation at 37 ^{o}C in water at neutral pH. [224]

In order to form a stable lanthanide complex the ligand must provide numerous donor atoms to satisfy the high coordination requirement of the lanthanide ions. Nevertheless, studies have shown that the best hydrolysis rates are achieved when the ion is left coordinatively unsaturated with one or more metal bound water molecules occupying the vacant sites.[225] As such, it was decided to functionalise the cyclen macrocycle with four pendant amide arms. The carboxyl oxygen of the amide groups would help satisfy the high coordination requirement of the lanthanide ion, forming a stable complex. This would ensure that the overall charge of the metal complex would remain positive, thereby maintaining the strong Lewis acid character of the metal ion. In addition, the eight donor sites of the ligand will leave the lanthanide metal ion coordinatively unsaturated.[252]

The desired molecule will be comprised of four parts (Figure 4.1):

- A spacer or linker to link the two metal binding sites
- The two cyclen macrocycles
- The neutral pendant amide arms
- Two lanthanide metal ions

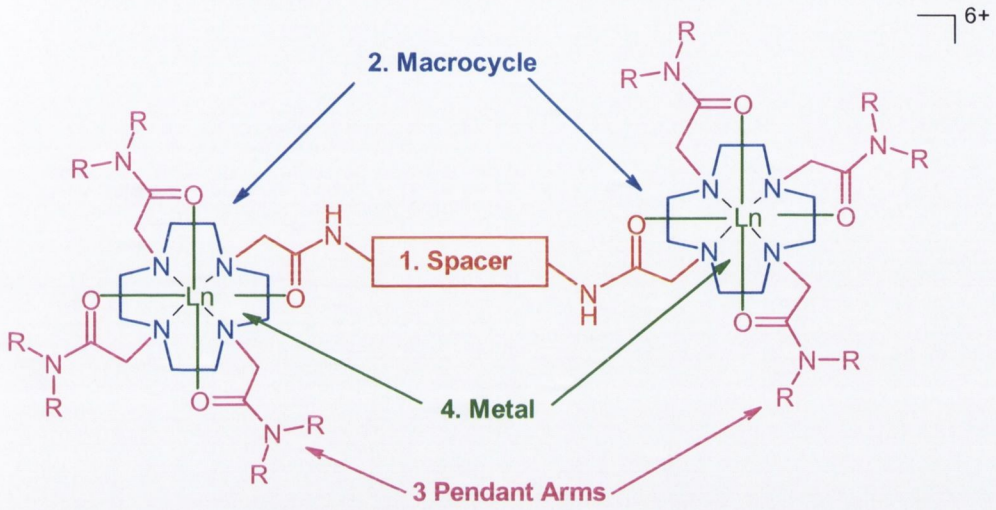

Figure 4.1. Showing component parts of the intended target molecule a cationic dinuclear complex with overall charge of 6^+

4.3 Synthesis of Binuclear Lanthanide Complexes

As discussed in Chapter 1, the choice of spacer group has been noted in the literature, as one of the critical factors in the development of cooperative binuclear complexes.[226] Very flexible spacer groups have been shown to give only moderate rate enhancements, of the order of 3 – 6 fold, over mononuclear systems,[227] as observed by Czarnik who reported the flexible binuclear Co(III) complex **54**, which promoted the hydrolysis of **BNPP** 6.4 fold faster than the mononuclear analogue. Systems that employ more rigid spacer groups have been found to exhibit a larger cooperative rate enhancement. For example, Morrows xylyl bridged binuclear Cu(II) complex **45** was found to cleave GpppG, a model of the 5'-cap mRNA structure, 46 times faster than the corresponding mononuclear Cu(II) system.[228] However, if the spacer group is too rigid it may be unable to match the desired geometry required for a cooperative mechanism to take effect. For example Canarys binuclear Cu(II) complex **57**, did not give rise to any cooperative enhancement over the corresponding mononuclear system. The spacer must possess enough flexibility to allow both metals to interact with the phosphodiester.[229] The most effective examples to date have utilised rigid

scaffolds, such as calixarenes, that offer a degree of flexibility.[226] It was decided to test a range of spacers, including flexible, alkyl chain spacers and more rigid, aromatic xylylene spacers. The following section will deal with the synthesis of these spacers.

4.3.1 Synthesis of α-Chloroacetamide Spacers

The spacers were synthesised from diamine precursors by reaction with two equivalents of chloroacetyl chloride. This was done to facilitate their incorporation into the macrocycle structure *via* a S_N2 reaction, where the chlorine atom would act as the leaving group. Initially, the acylation of *p*-xylylenediamine **119**, to yield 1,4-bis-(2-chloro-acetylamino)-xylyene, **120**, was carried out in $CHCl_3$ with Et_3N present as a base. However, as this method led to low yields (11 %) and involved a tedious work up, it was decided to try and optimise the reaction by use of an alternative method (Scheme 4.1).

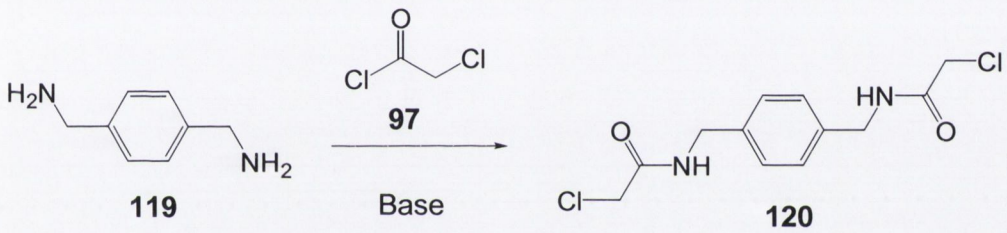

Scheme 4.1. Acylation of *p*-xylylenediamine to yield 1,4–bis (2–chloro-acetylamino) xylylene (120)

Various solvents and conditions were examined, including CH_2Cl_2 and THF, however, no significant improvement was observed (Table 4.1). The problem seemed to stem from the insolubility of **119**, which was only fully soluble in alcohols and water. Alcohols react with chloroacetyl chloride to produce esters and so an alternative was sought.

The formation of amides by the reaction of an amine and acid chloride results in the production of an equivalent of HCl, which must be neutralised. Under the classic Schotten-Baumann conditions this HCl is neutralised with NaOH by employing a two phase system consisting of water and CH_2Cl_2. The solvents chosen are immiscible so that the amine and acid chloride remain in the lower CH_2Cl_2 layer, while the NaOH remains in the upper aqueous layer. [230]

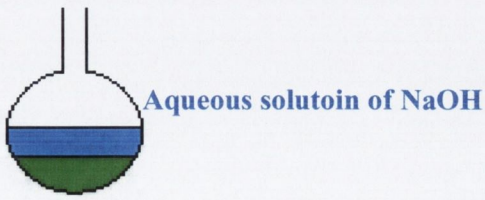

Figure 4.2: Schotten-Baumann two phase system

However, as previously stated, the diamine **119**, is poorly soluble in CH_2Cl_2, and so in this case, it was decided to modify the reaction by carrying out the acylaction under purely aqueous conditions. The diamine **119**, along with four equivalents of NaOH were dissolved in H_2O and cooled in an acetone/ice bath. Four equivalents of chloroacetyl chloride were added dropwise over one hour. The solution was left to stir overnight and the desired product **120**, precipitated out of solution and was isolated by filtration in yields of up to 75 % with no need for further purification.

Solvent	Base	Temperature	Yield
CH_2Cl_2	Et_3N	-5 – 20 °C	~5 >13 %
THF	Et_3N	-5 – 20 °C	~5 >13 %
BuOH	Et_3N	-5 – 20 °C	10 %
MeCN	Et_3N	-5 – 20 °C	0 %
EtOAc	Et_3N	-5 – 20 °C	10 %
EtOAc	DMAP	-5 – 20 °C	.1 %
Toluene	Et_3N	-5 – 20 °C	~10 %
H_2O	NaOH	-10 – 20 °C	75 %

Table 4.1. Effect of various reaction conditions for the synthesis of 120

The reaction was found to be temperature dependant as the yield dropped to 18 % when the reaction was carried out at room temperature. It is believed that this phenomena is due to the chloroacetyl chloride reacting with the H_2O at higher temperatures, thereby competing against the desired reaction (Scheme 4.2).[230]

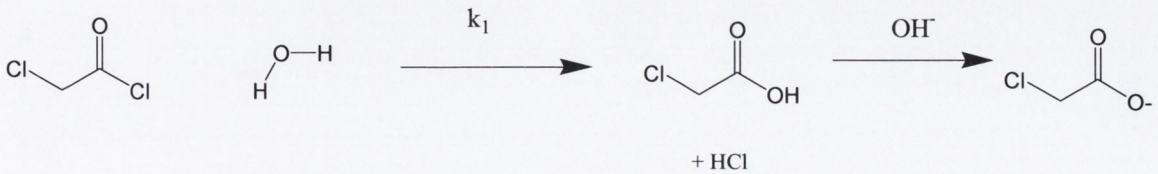

Scheme 4.2. The reaction of chloroacetyl chloride with H_2O leads to undesired side products

The ^{1}H NMR (DMSO) of the compound displayed four resonances including the NH proton at 8.72 ppm, the four aromatic protons at 7.22 ppm, the four benzyl protons at 4.26 ppm and the four acetamide protons at 4.11 ppm (Figure 4.3). The ^{13}C NMR (DMSO) revealed five peaks including the carbonyl signal at 165.9 ppm, the aromatic signals at 137.5 and 127.3ppm, as well as two CH_2 signals at 42.6 and 42.2 ppm respectively. High resolution mass spectrometry and elemental analysis confirmed that the desired compound had been successfully synthesised.

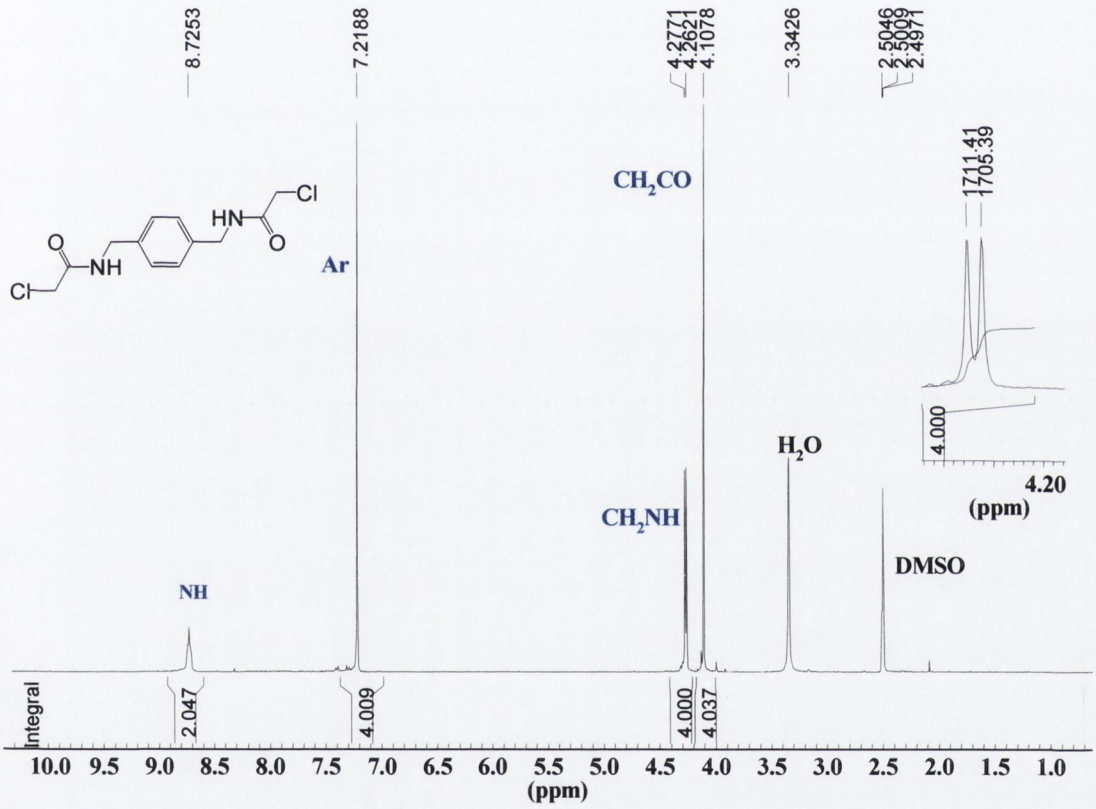

Figure 4.3. 400 MHz ^{1}H NMR of 120 in DMSO

4.3.1.1 *N*-Acylation Reactions in Water

Due to the success and simplicity of the above reaction, it was decided to investigate its range and suitability for other *N*–acylation type reactions. Under the same conditions as employed for **120**, the α–chloroamides **121** – **124**, were synthesised from their corresponding aromatic diamines (Figure 4.4).

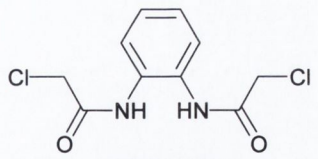

60 % yield

121

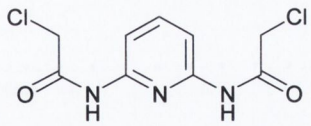

9 % yield

122

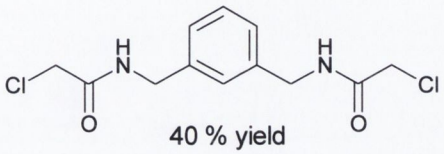

40 % yield

123

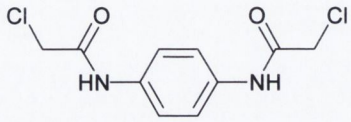

98 % yield

124

Figure 4.4. Compounds 121 – 124 were synthesised from their corresponding aromatic diamines

At this point, it was decided to investigate whether the scope of this reaction could be extended beyond aromatic amines, towards aliphatic amines.

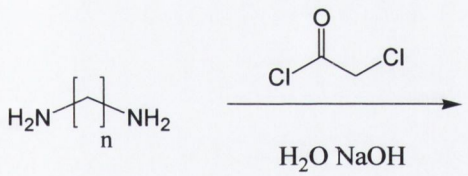

H_2O NaOH

n=3 **125**, 30 % yield
n=4 **126**, 39 % yield
n=5 **127**, 42 % yield
n=6 **128**, 42 % yield

Scheme 4.3. Synthesis of alkyl α–chloroamides and yields after combined CH_2Cl_2 extraction

The compounds **125** – **128,** were synthesised under the same conditions, previously described. Once again the desired products were found to precipitate out of solution however, the yields of these alkyl α–chloroamides were lower than the aromatic α–chloroamides. The alkyl α–chloroamides were found to be more soluble in H_2O than the aromatic analogues and hence, in order to increase the yield a CH_2Cl_2 extraction of the aqueous solution was carried out. Combining the extracted product with that obtained from filtration was found to increase the yield (Table 4.2).

Name	n	% yield a	% yield b
125	3	10	30
126	4	32	39
127	5	36	42
128	6	32	42

Table 4.2. Showing % yields before (a) and after (b) combined extraction with CH_2Cl_2

The versatility of the reaction was investigated further, by introducing more functional groups into the starting materials to observe whether this would effect the overall reaction. Compounds **129** – **136** were synthesised from their corresponding aromatic amines, using the above general procedure. From Figure 4.5 it can be seen that despite introducing various functional groups onto the benzene ring the reactions proceeded satisfactorily and the overall procedure is a versatile and adaptable way of conducting *N*–acylation reactions. The advantage of the reaction is the ease of the work up, all the compounds in Figure 4.5 were isolated by simple filtration, with no further need for purification.

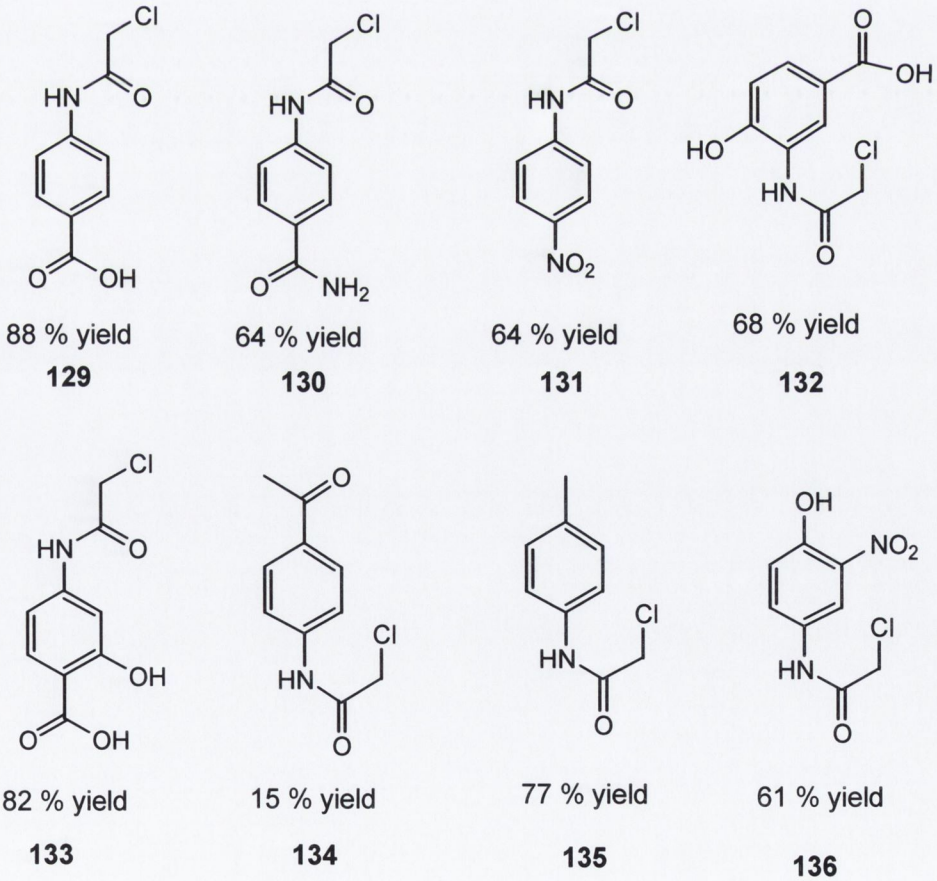

Figure 4.5. The products and yields using various functionalised aromatic amines

It should be noted that in general all the starting materials were soluble in aqueous solution, and that all the products precipitated out of solution. However, the starting materials for **131** and **134** were not soluble in aqueous solution. Despite this the reaction still proceeded and the desired products **131** and **134** were isolated, by filtration, in 64 % and 15 % yields respectively. For **131** the starting material, a suspended solid, was observed to undergo a colour change from yellow to white as the reaction proceeded. This highlights the versatile nature of the procedure, as it can even be utilised for insoluble starting materials.

This versatility was further highlighted by the synthesis of **137**, **138** and **139**. These compounds as well as their amine starting materials are hydrophobic (Figure 4.6). The aromatic amine precursors are liquids at room temperature, and are immiscible with H_2O. However, upon the addition of chloroacetyl chloride, the products precipitated out of the aqueous solution, as white solids, which were again isolated by filtration.

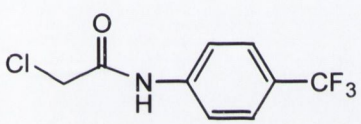

31 % yield

137

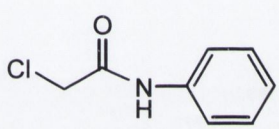

58 % yield

138

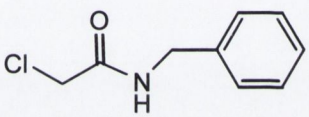

43 % yield

139

Figure 4.6. Synthesised hydrophobic α–chloroamides and their yields

In the case of the more hydrophilic pyridine α–chloroamides **140** and **141,** the reaction was less useful. **140** and **141** were successfully synthesised, however, they did not precipitate from solution, as they were highly soluble in H_2O. They were isolated after a tedious work up that included the removal of solvent under reduced pressure, followed by suspension of the residue in EtOH before filtration to remove the salt. The EtOH was then evaporated and the residue suspended in acetone and filtered to remove the chloroacetyl chloride. The solid was then dissolved in EtOH and this solution was added slowly to swirling ether to further purify the compounds.

One of the major advantages of the reaction so far has been the ease of work up. The loss of this advantage coupled with the fact that the pyridine systems have an easier, known synthesis in acetone with higher yields,[231] negates the practicality of this reaction, for these particular systems.

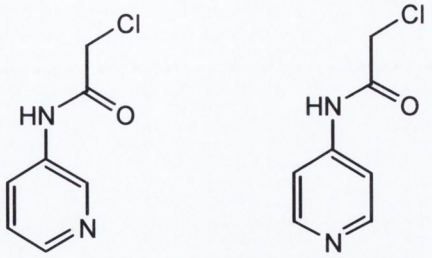

48 % yield — **140**

40 % yield — **141**

Figure 4.7. Synthesised pyridine α–chloroamides and their yields

The reaction procedure was less successful when more extended ring systems were employed. The *N*–acylation reaction was attempted upon the amines of anthracene, phenanthroline and methyl–quinoline under the aqueous conditions. However, the reactions did not proceed to completion and the desired α–chloroamide products could not be isolated.

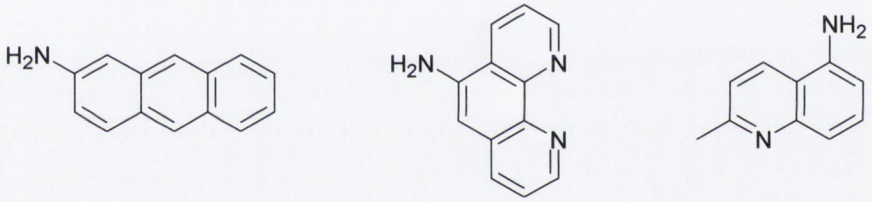

142 **102** **143**

Figure 4.8. The *N*–acylation reaction was unsuccessful under the aqueous conditions for the extended ring systems

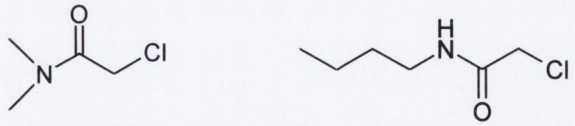

5 % yield — **98a**

42 % yield — **144**

Figure 4.9. Synthesised alkyl amides and their yields

For **144** and **98a,** under the same general reaction conditions employed, no precipitate was observed. However, the desired products were isolated, in 42 % and 5 % yield respectively, after a CH_2Cl_2 extraction of the solution. It is notable that the yields tend to be linked to the solubility of the product in H_2O, with less soluble products giving higher yields.

In order to further test the flexibility of the reaction, an acylation with acetic anhydride was attempted under the similar aqueous conditions. In the presence of four equivalents of acetic anhydride and NaOH, *p*–amino phenol was found to undergo acylation at both the N and O position (Scheme 4.4). This is further evidence of the adaptability of this reaction.

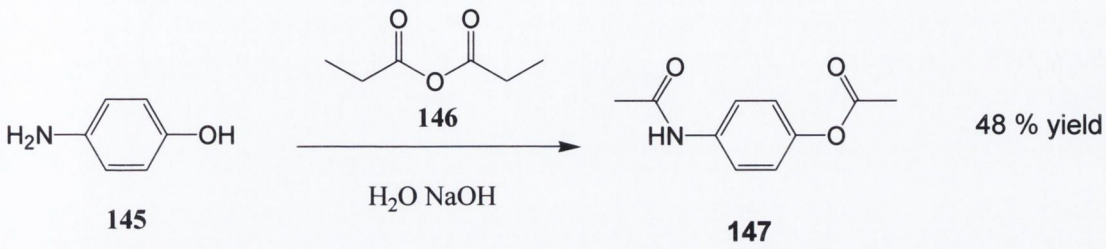

Scheme 4.4. Acylation of *p*–amino phenol with acetic anhydride under aqueous conditions

4.3.1.2 The Effect of Changing the Base

An investigation was conducted in order to determine whether the choice of base employed had an effect upon the reaction. Four reactions from the above section, with a range of yields were chosen. From Table 4.3 it can clearly be seen that the choice of base does have an impact upon the yield for the reaction. While no immediate trend for the effect is visible it is clear that the reaction yields are dependant upon the choice of base. Recall that the temperature too can be used to optimise the reaction.

Name	NaOH	NEt_3	$NaHCO_3$	No Base
128	32 %	27 %	7 %	13 %
130	64 %	69 %	85 %	74 %
122	8 %	28 %	14 %	0 %
120	70 %	39 %	17 %	9 %

Table 4.3. Effect of changing base upon the yields for *N*-acylation

The reason for the large changes in yield is that there are, at least, two possible mechanisms at work (Scheme 4.5). Varying the temperature and base, can change which mechanism is favoured.

In order for the desired product to be formed in good yield, k_2 must proceed faster than k_1. Recall for **120** that the yield was found to be lower when the reaction was carried out at higher temperatures. This implies that, for **120**, k_2 is thermodynamically favoured while k_1

is kinetically favoured. While in depth temperature studies were not performed on the other compounds, it was noted that some compounds displayed a similar dependence. The strength and nature of the base will also influence whether k_2 or k_1 is the preferred pathway. Strong bases such as NaOH will increase the rate of k_1, however this may be offset by a larger increase in the rate of k_2, depending on the nature of the amine present. As such no simple trend for the effect of the base was observed.

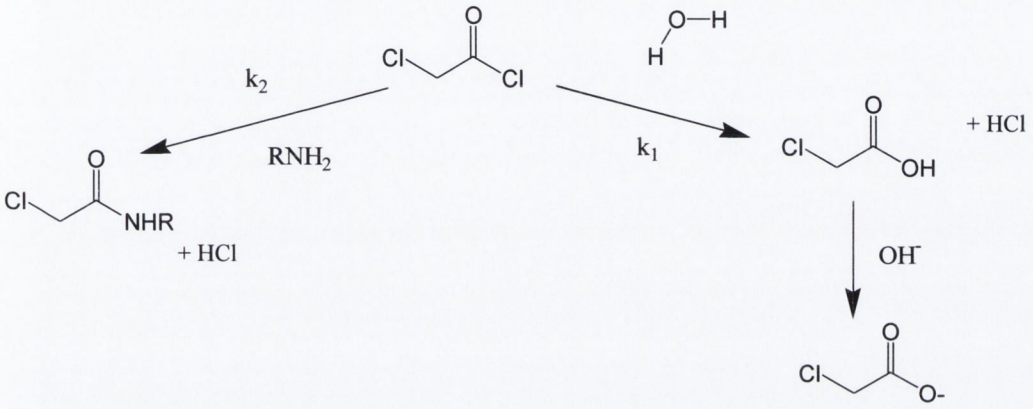

Scheme 4.5. Competing pathways within the reaction

4.3.1.3 Conclusion

A versatile method for *N*–acylation of amines has been shown to function under purely aqueous conditions. It differs from the well known Schotten Bauman method, in that no organic solvent is required. Its usefulness stems from the fact that the solvent, H_2O, is cheap and environmentally friendly and as such, would be favoured by industry. The simplicity of the reaction as well as the ease of work up are also major advantages. The reaction has been shown to be successful for a range of amines and diamines, both aromatic and aliphatic. It has also been shown that optimisation of the reaction can be achieved by tuning the temperature and the base employed for each reaction. Some of the bis α–chloroamides synthesised here will be used as spacers in the next section.

4.3.2 Selective Protection of Cyclen

Having successfully synthesised the bridging moieties, the next step was to introduce them into the cyclen framework. Various methods were explored for the attachment of the cyclen macrocycles to the spacer. Directly reacting the cyclen with the spacer was unsatisfactory due to the formation of numerous possible side products and polymers. a

variety of methods for the mono alkylation of cyclen have been described in the literature,[232, 233] most proceed *via* the protection of three of the cyclen nitrogens, leaving the fourth available for alkylation. A number of these methods were attempted in this project including *tert*-butyl-carbonate (Boc) protection[234] and formyl (CHO) protection methods (Scheme 4.6).[235]

The tris Boc protected cyclen, 1,4,7,10-tetraaza-cyclododecane-1,4,7-tricarboxylic acid tri-tert-butyl ester, **148**, was synthesised by stirring cyclen with three equivalents of di-*tert*-butyl-dicarbonate (Boc_2O), in $CHCl_3$ in the presence of Et_3N.[234] The desired product **148**, was obtained in 57 % yield after purification by flash silica column chromatography using EtOAc:Hexane 5:1 as the eluent. The alternative tris protected compound, 1,4,7,10-tetraaza-cyclododecane-1,4,7-tricarbaldehyde, **149**, was synthesised by stirring cyclen with six equivalents of chloral-hydrate in EtOH at 60 °C for three hours.[235] The desired product, **149**, was obtained in 87 % yield after purification by flash silica column chromatography using DCM:MeOH 9:1 as the eluent. The advantage of these protecting groups is that they are labile and can be easily removed, they are not air sensitive and hence, can be stored and used later. Normally, alkylation of **148** and **149** is carried out in MeCN,[234,235] however, the spacer **120**, was insoluble in MeCN, and so the reactions were carried out in DMF in the presence of Cs_2CO_3. Unfortunately, under these conditions the reaction did not proceed (Scheme 4.6).

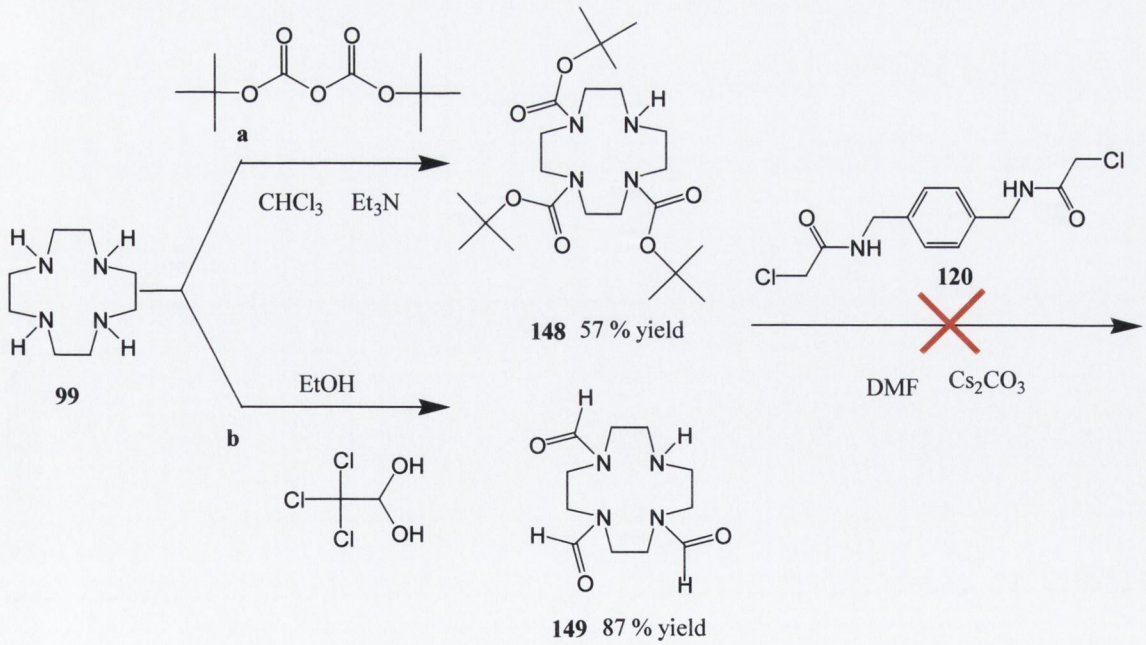

Scheme 4.6. Synthesis of tris protected cyclen derivatives 148 and 149

An alternative method for the protection of cyclen using molybdenum hexacarbonyl[236] was found to be the most consistently effective method, despite the drawback that the product **150**, is known to be air sensitive. The protection was conducted according to the literature procedure.[236] The cyclen and molybdenum hexacarbonyl were suspended in dry dibutyl ether and freeze-pump-thawed three times in order to remove any oxygen. The suspension was then refluxed for two hours under argon. The product, 1,4,7-molybdenum tris carbonyl-(1,4,7,10-tetraaza-cyclododecane) **150**, a bright yellow solid, was then isolated by filtration in 88 % yield using the special suction filtration apparatus shown in Figure 4.10. This reaction required scrupulously anhydrous conditions and all glassware joints had to be sealed with parafilm. The compound **150**, was treated as a reaction intermediate due to its air sensitive nature and was not characterised, but reacted on immediately. The following section will discuss the bridging of two of these protected cyclen molecules by the spacer.

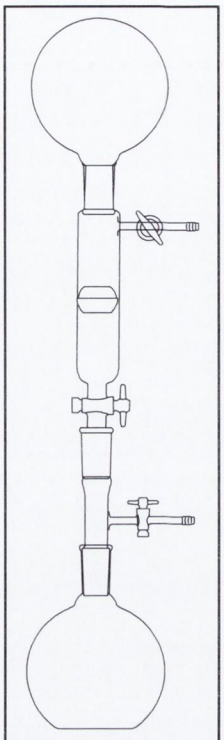

Figure 4.10

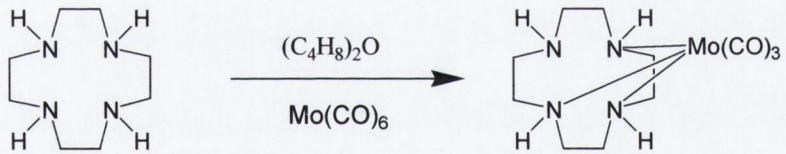

99 **150**

Scheme 4.7. Protection of cyclen with molybdenum hexacarbonyl

4.3.3 Synthesis of Bis-Cyclen Framework

Coupling the macrocycles to the spacer involved freeze-pump-thawing **120** with two equivalents of **150**, two equivalents of Cs_2CO_3 and two equivalents of KI in DMF. The solution was then stirred at 85 °C for 40 hours and then filtered. The DMF was removed under reduced pressure and the resulting residue was left stirring overnight in an aqueous solution of HCl (15 % v/v), in order to deprotect the cyclen (Scheme 4.8). The acidic solution was then filtered and washed with CH_2Cl_2, before being basified (pH ~ 13) with

KOH and extracted with CH_2Cl_2. The CH_2Cl_2 was removed under reduced pressure and the desired product 2-(1,4,7,10-teraaza-cyclododec-1-yl)-*N*-{4-[(2-1,4,7,10-tetraaza-cyclododec-1-yl-acetylamino)-methyl]-benzyl}-acetamide **152**, was isolated as a yellow oil in 41 % yield. Once again the reaction required scrupulously anhydrous conditions and all glassware joints had to be sealed with parafilm. Even still, the reaction was problematic and very sensitive to the conditions employed and frequently the desired compound could not be isolated.

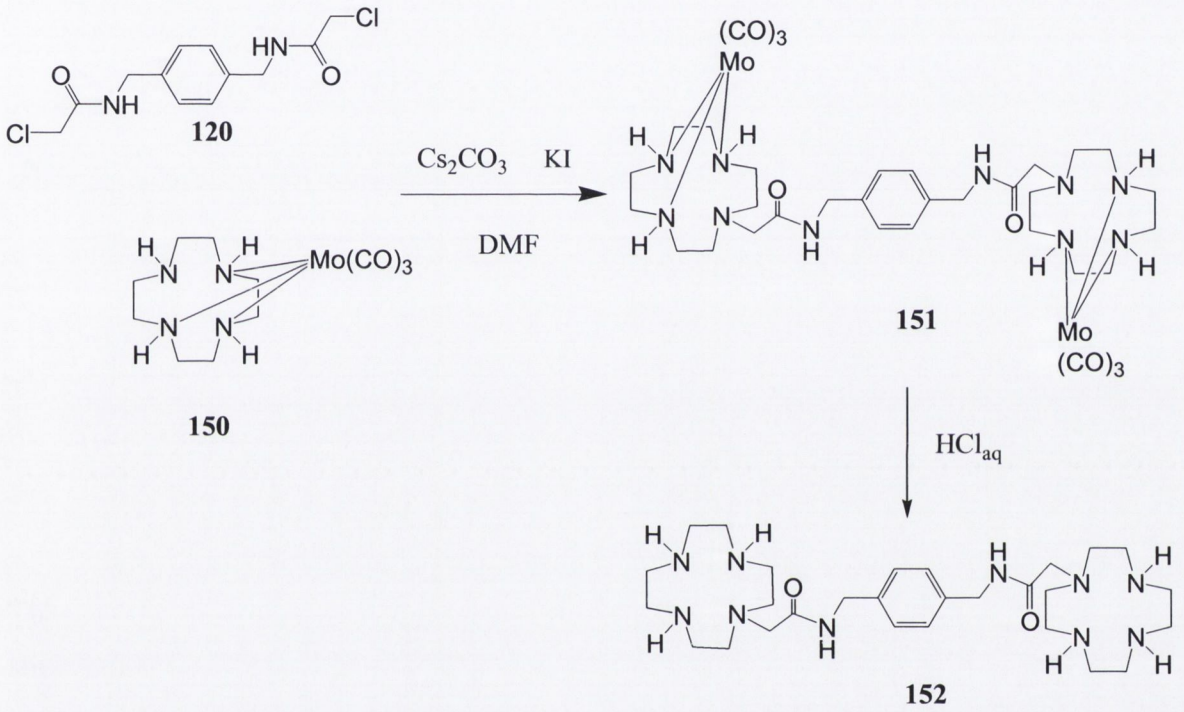

Scheme 4.8. Synthesis of 152 proceeded with 41 % yield

The inherent symmetry of **152** was evident in the ^1H NMR (Figure 4.11) as well as the ^{13}C NMR spectra. The aromatic protons were clearly visible as a singlet at 7.25 ppm, however, their position obscured the $CDCl_3$ signal. The four benzyl protons were observed at 4.38 ppm, while the four acetamide protons were observed at 3.19 ppm. The ^{13}C NMR spectra showed the presence of one carbonyl group at 171.1 ppm, while the aromatic signals were observed at 137.2 and 127.7 ppm respectively. The mass spectrum presented signals at *m/z* 561.4, 583.4, 599.4 and 281.2 corresponding to the [M+H], [M+Na], [M+K] and [M+H]/2 species respectively. A high resolution mass spectrum of **152** was obtained, confirming the synthesis of the product, although, the hygroscopic nature of the compound meant that elemental analysis could not be successfully obtained.

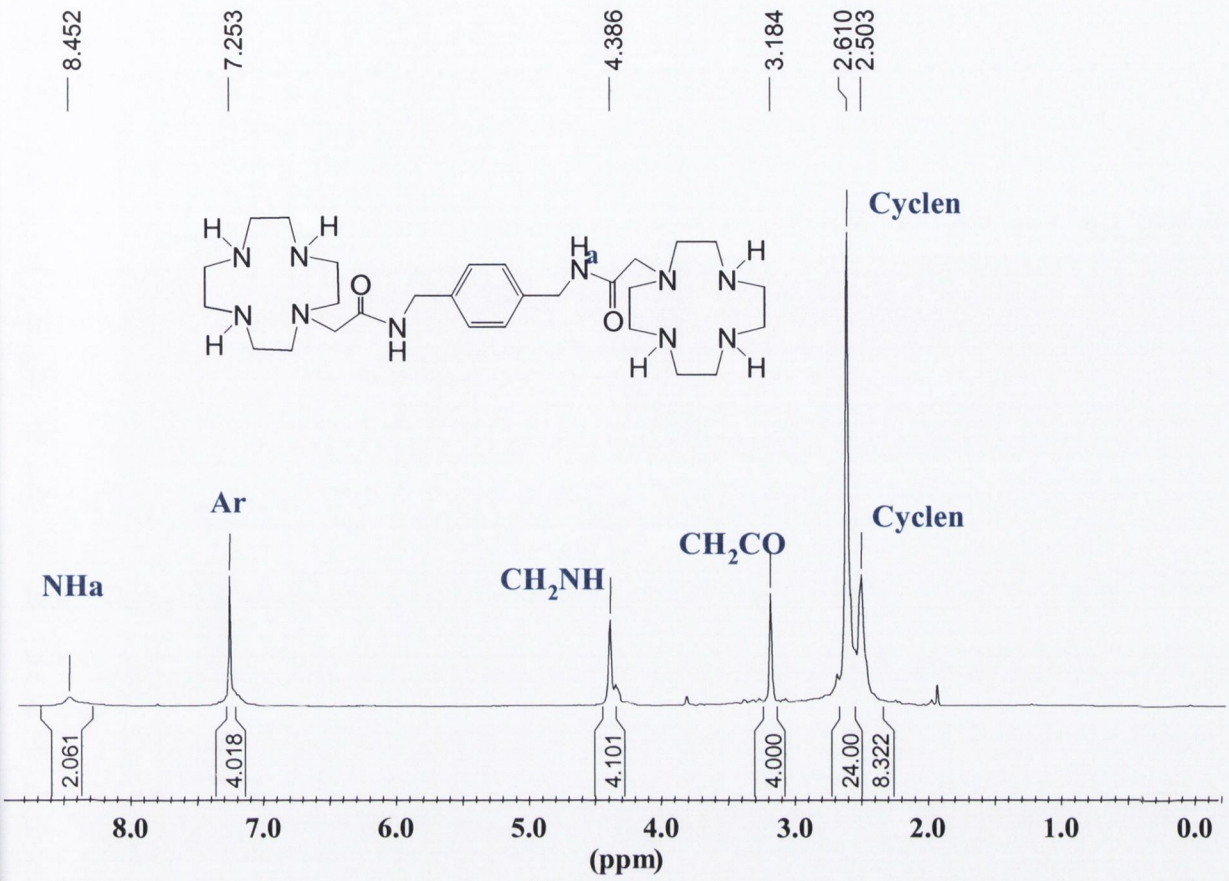

Figure 4.11. 400 MHz ^{1}H NMR of 152 in $CDCl_3$

The hexane spacer (**128**) analogue of **152** was also synthesised under similar conditions by stirring **128** with two equivalents of **150** in DMF at 85 °C for 40 hours, in the presence of two equivalents of Cs_2CO_3 and two equivalents of KI. The procedure was similar to that of **152**, however the desired product 2-(1,4,7,10tetraaza-cyclododec-1-yl)-*N*-[6-(2-1,4,7,10tetraaza-cyclododec-1-yl-acetylamino)-hexyl]-acetamide **153**, was isolated as its HCl salt in 37 % yield after precipitation from a EtOH:conc. HCl 5:1 solution.

Again the ^{1}H NMR in D_2O was relatively simple due to the high degree of symmetry in the molecule. The four acetamide protons were observed at 3.31 ppm, while the cyclen protons resonated two signals at 3.06 ppm and 2.88 ppm respectively. The three sets of methylene protons from the alkyl spacer were observed at 2.88 ppm (overlapping with 8 cyclen protons), 1.39 ppm and 1.20 ppm respectively. The ^{13}C NMR showed the presence of a carbonyl signal at 172.4 ppm along with eight methylene resonances. The mass spectrum contained two signals at *m/z* 541.6 and 271.4 corresponding to the [M+H] and [M+2H/2] species. Elemental analysis confirmed the presence of the six HCl molecules.

Two basic templates for a binuclear system had now been synthesised. One contained a rigid aromatic xylylene spacer, while the other contained a flexible alkyl spacer. However,

in their present form, they would not satisfy the high coordination requirement of the lanthanide ions. Consequently, further functionalisation was required, and that will be the subject of the next section.

4.3.4 Synthesis of Acetamide-Based Bis-Cyclen Ligands 154-157

In order to accommodate the lanthanide ions high coordination number requirement, 9 and 10 for Eu(III) and La(III) respectively,[224, 223] the incorporation of further donor atoms into the bis-cyclen ligands **152** and **128**, was necessary. This was accomplished by functionalising the cyclen moieties with pendant amide arms *via* a S_N2 alkylation reaction. Initially simple acetamide arms were investigated in order to probe the validity of the bis lanthanide systems as cleaving agents for phosphodiester hydrolysis as they would allow comparison with analogous mononuclear lanthanide systems previously reported by Morrow *et al.*[223]

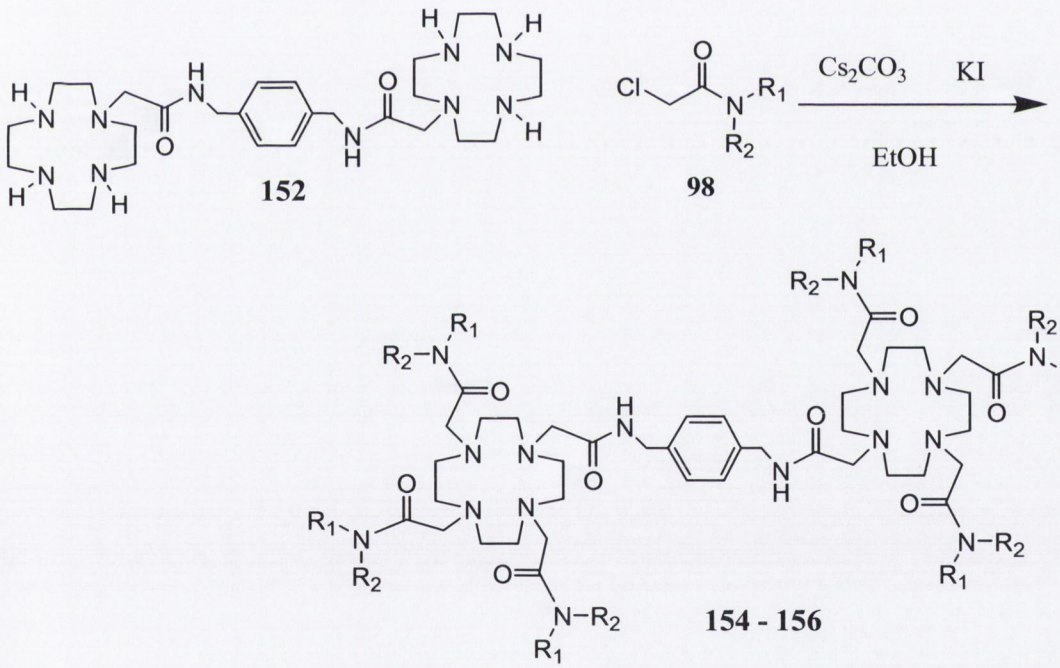

Compound	R group	Yield
154	$R_1, R_2 = H$	57 %
155	$R_1 = H, R_2 = CH_3$	30 %
156	$R_1, R_2 = CH_3$	38 %

Scheme 4.9. General synthesis of acetamide-based bis-cyclen ligands 154, 155 and 156

The three pendant arms employed in this case were, 2-bromo-acetamide, **98c**, 2-chloro-*N*,*N*-dimethyl-acetamide, **98a**, and 2-chloro-*N*-methyl-acetamide, **98b**. The bis-cyclen ligand **152**, was only sparingly soluble in solvents such as MeCN, CH_2Cl_2 and $CHCl_3$ and using these solvents, the reaction did not proceed. Consequently, the reactions were carried out in refluxing EtOH in the presence of Cs_2CO_3 and KI, as the above compounds were all soluble in this solvent.

The primary amide 2-{4,10-bis-carbamoylmethyl-7-[(4-{[2-(4,7,10-tris-carbamoylmethyl-1,4,7,10-tetraaza-cyclododec-1-yl)-acetylamino]-methyl}-benzylcarbamoyl)-methyl]-1,4,7,10-tetraaza-cyclododec-1-yl}- acetamide, **154**, was isolated in 57 % yield, after precipitation from CH_2Cl_2, followed by recrystalisation from boiling EtOH. The secondary amide 2-{4,7-bis-methylcarbamoylmethyl-10-[(4-{[2-(4,7,10-tris-methylcarbamoylmethyl-1,4,7,10-tetraaza-cyclododec-1-yl)-acetylamino]-methyl}-benzylcarbamoyl)-methyl]-1,4,7,10-tetraaza-cyclododec-1-yl}-acetamide, **155**, was isolated in a similar fashion in 30 % yield. The tertiary amide 2-{4,10-bis-dimethylcarbamoylmethyl-7-[(4-{[2-(4,7,10-tris dimethylcarbamoyl-methyl-1,4,7,10-tetraaza-cyclododec-1-yl)-acetylamino]-methyl}-benzylcarbamoyl)-methyl]-1,4,7,10-tetraaza-cyclododec-1-yl}-*N*,*N*-dimethyl-acetamide, **156**, was found to be soluble in CH_2Cl_2 and so was isolated in 38 % yield after washing with H_2O and 0.1 M HCl.

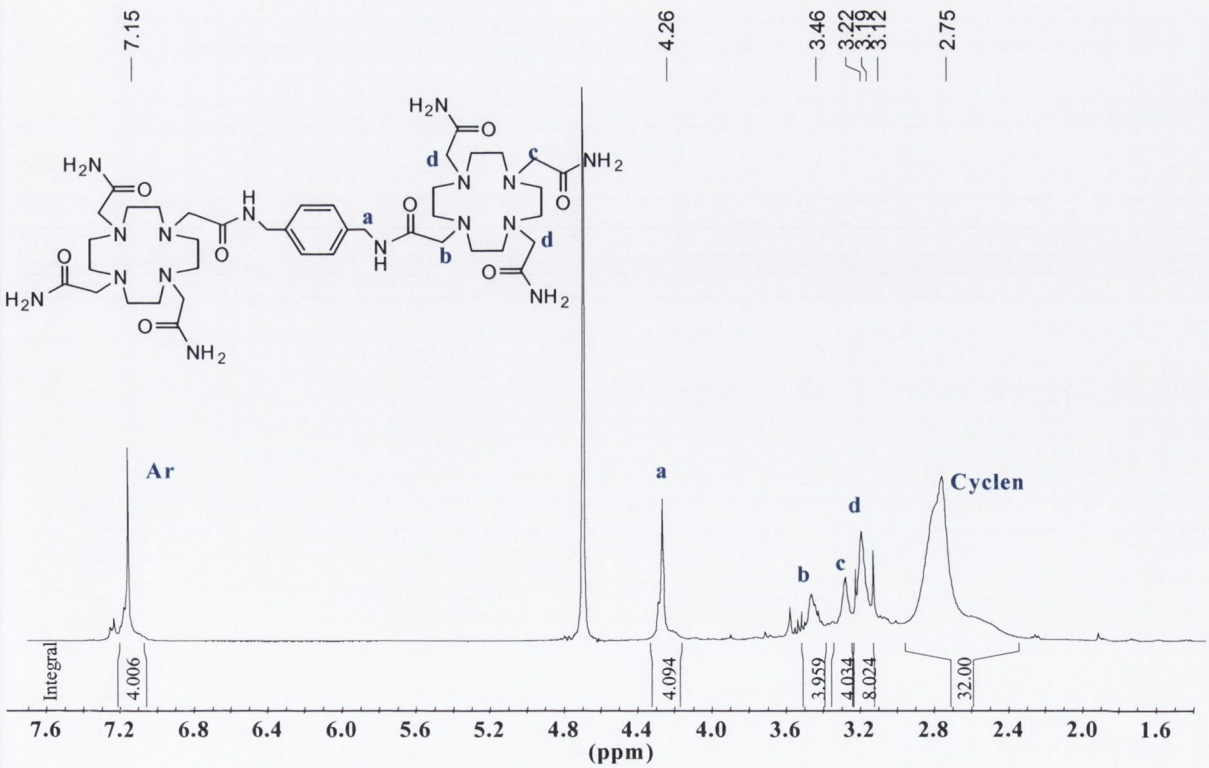

Figure 4.12. 400 MHz ^{1}H NMR of 154 in D_2O

The ^{1}H NMR in D_2O of **154** revealed the high degree of symmetry in the molecule. The four aromatic protons resonanced at 7.16 ppm while the four benzyl protons were observed at 4.26 ppm (Figure 4.12). The ^{13}C NMR revealed the presence of three carboxyl signals at 173.8, 173.4 and 170.2 ppm respectively, while the aromatic carbon signals were observed at 136.6 and 127.1 ppm, respectively. Eight methylene signals were also observed at 58.1, 56.9, 56.7, 56.1, 55.5, 55.3, 50.2 and 42.2 ppm respectively. High resolution mass spectrometry and elemental analysis confirmed that the product had been formed. Characterisation of **155** and **156** yielded similar results.

The hexane linker analogue of **154,** was also synthesised by refluxing **153** in EtOH, with seven equivalents of bromo acetamide in the presence of fourteen equivalents of Et_3N (Scheme 4.10). A large excess of Et_3N was needed, as **153** was present as a hexa-HCl salt. The desired product 2-[4,7-bis-carbamoylmethyl-10-({6-[2-(4,7,10-tris-carbamoylmethyl-1,4,7,10-tetraaza-cyclododec-1-yl)-acetylamino]-hexylcarbamoyl}-methyl)-1,4,7,10-tetraaza-cyclododec-1-yl]-acetamide **157,** was isolated in 83 % yield, after precipitation from CH_2Cl_2 followed by precipitation from *i*-propanol:EtOH 3:1.

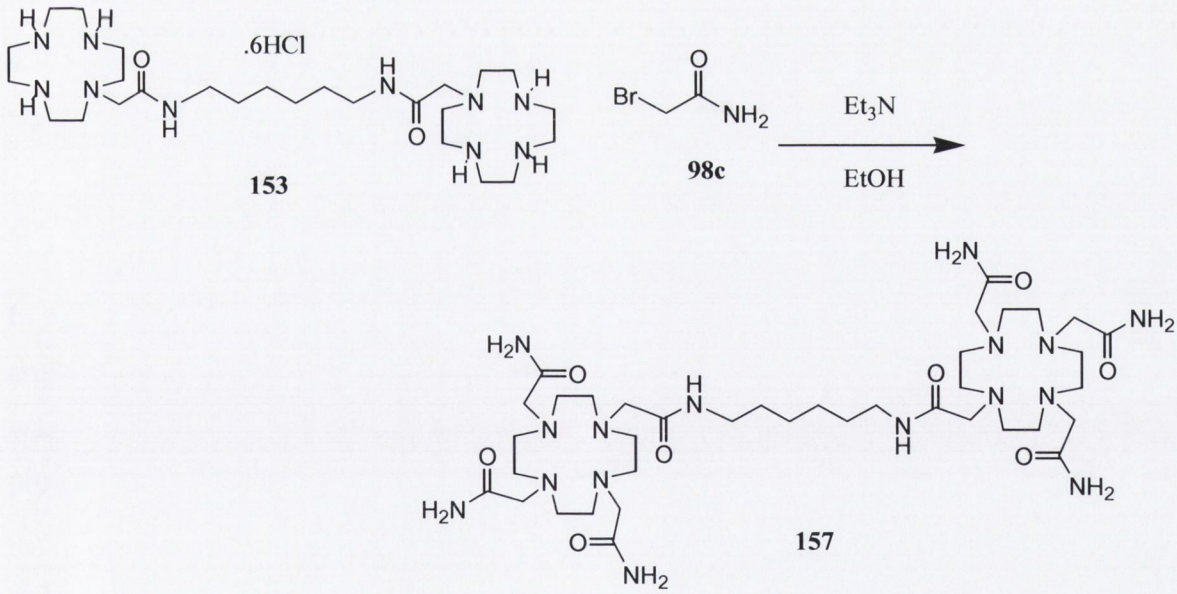

Scheme 4.10. Synthesis of hexyl spaced acetamide bis-cyclen ligand 157

The ^{1}H NMR (D_2O) revealed the high degree of symmetry inherent in the molecule (Figure 4.13), as four of the methylene resonances of the alkyl chain appeared at 1.38 and 1.19 ppm respectively. The ^{13}C NMR revealed three carbonyl peaks at 174.2, 173.5 and 169.7 ppm as well as eight methylene resonances at 56.1, 55.6, 50.1, 49.8, 48.9, 38.9, 27.8 and 25.3 ppm respectively (only two cyclen signals, confirmed by CHCOSY). The mass

spectrum consisted of two peaks *m/z* 883.7 and 442.5 corresponding to the [M+H] and [M+2H/2] signals. Elemental analysis confirmed the characterisation of the molecule.

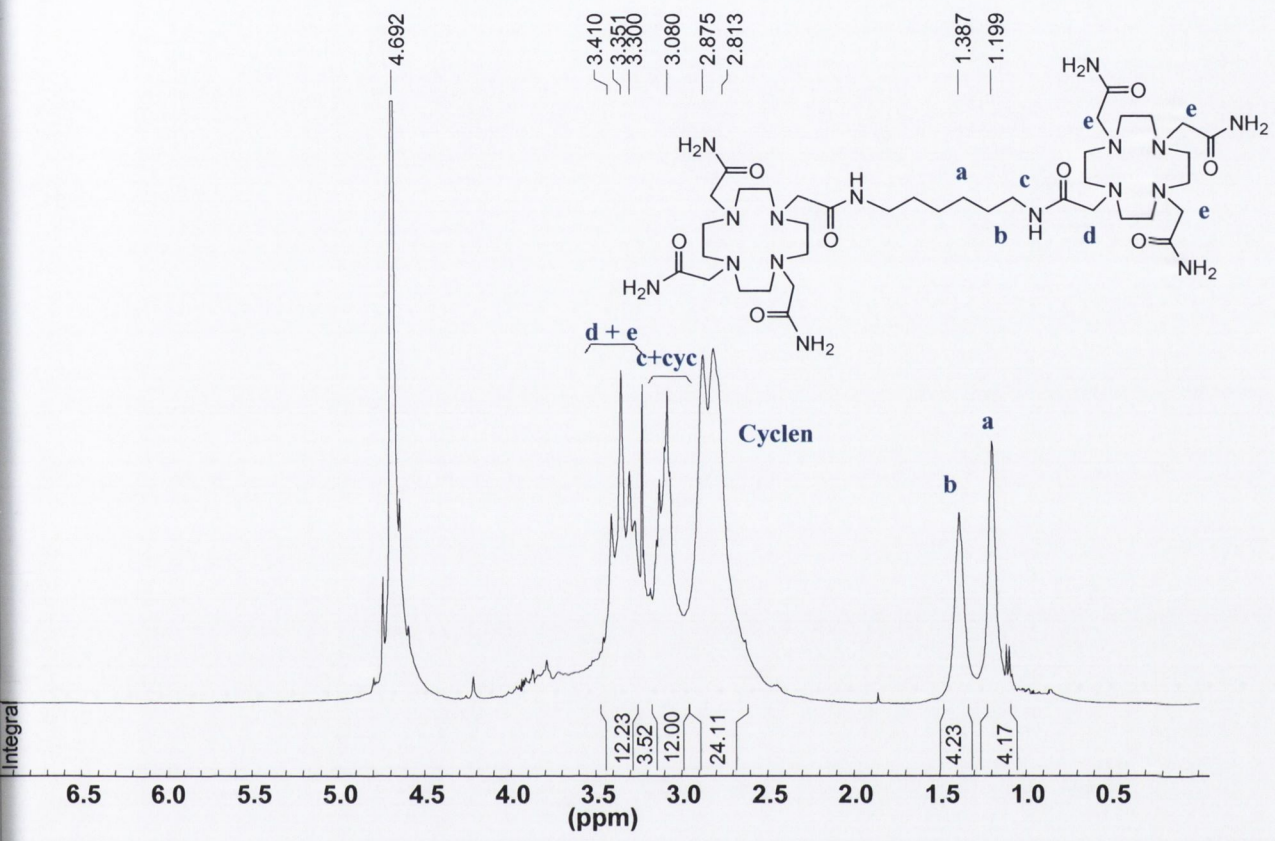

Figure 4.13. 400 MHz ^{1}H NMR of 157 in D_2O

In summary, four new ligands **154**, **155**, **156** and **157**, incorporating three different pendant arms and two different spacer groups, have been made and characterised. The next step was to synthesise the corresponding lanthanide complexes from these ligands, in order to produce potential ribozyme mimics. This process is described in the next section.

4.3.5 Complexation of Acetamide-Based Bis-Cyclen Ligands

Europium and lanthanum were chosen as the lanthanide ions in order to allow comparison to similar mononuclear systems previously reported.[237] The lanthanide complexes of the ligands **154**, **155**, **156** and **157** were prepared by refluxing each ligand with two molar equivalents of the relevant lanthanide triflate in MeOH for 16 hours (Scheme 4.11). The resulting solution was filtered and reduced in volume to ~ 5 mL. This solution was added dropwise to swirling ether and the resulting precipitate was collected by filtration. The complexes **Eu.154, La.154, Eu.155, La.155, Eu.156** and **La.157** were further purified by

precipitation from CH_2Cl_2, and isolated by suction filtration. This gave the complexes in pure form.

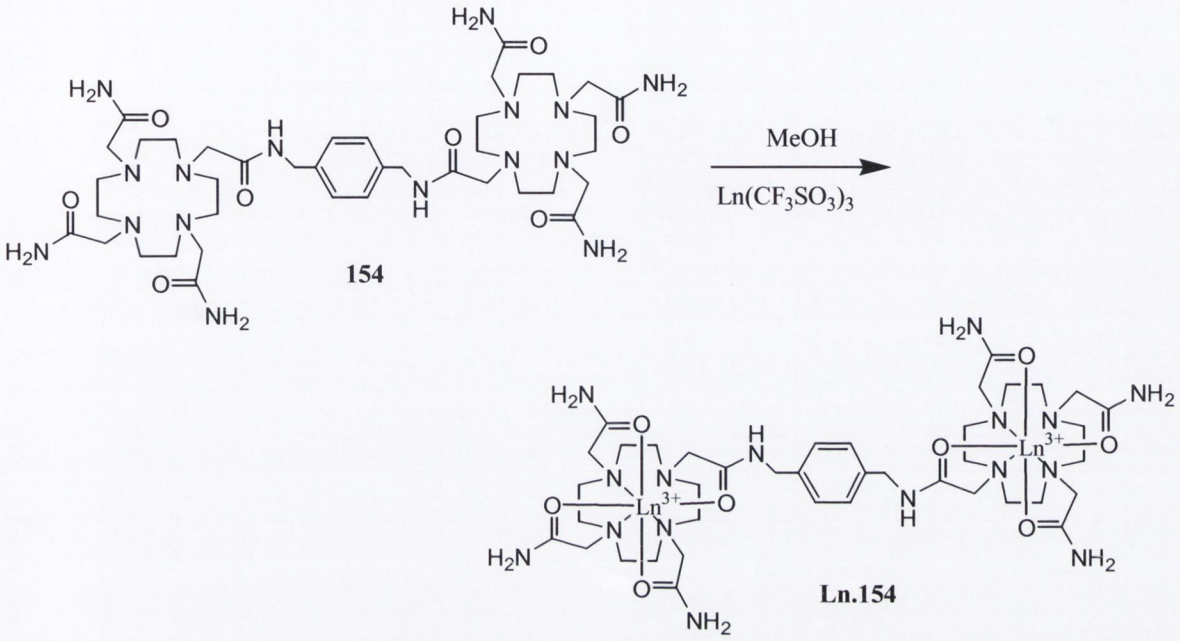

Compound	R group	Yield
Eu.154	R_1, R_2 = H	80 %
La.154	R_1, R_2 = H	88 %
Eu.155	R_1 = H, R_2 = CH_3	81 %
La.155	R_1 = H, R_2 = CH_3	69 %
Eu.156	R_1, R_2 = CH_3	47 %
La.157 $(CH_2)_6$	R_1, R_2 = H,	87 %

Scheme 4.11. Complexation of 154

Paramagnetic lanthanide ions, like Eu(III), are known to be NMR shift reagents.[238] In this case the methylene resonances of the acetamide and the cyclen ring protons experience an extra magnetic field due to the proximity of the paramagnetic Eu(III) ion. This extra magnetic field causes a shift in the position of the affected protons signal, the extent of which is determined by the protons proximity to the metal centre.[239, 241] This can be seen from the Figure 4.14, as the axial protons, H_{ax}, will experience the magnetic field of the metal ion to a

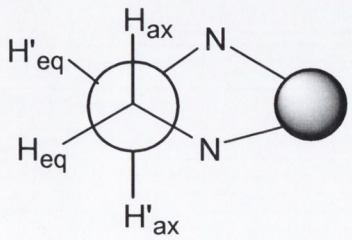

Figure 4.14: Different proton positions with respect to the metal ion

greater extent than the equatorial protons, H_{eq}. In the case of **Eu.154** the shifted methylene protons came between 26.16 and – 13.56 ppm. [240] The ^{1}H NMR spectra of the complexes consisted of broad signals due to the fast relaxation times induced by the paramagnetic metal ion, which precluded full characterisation.

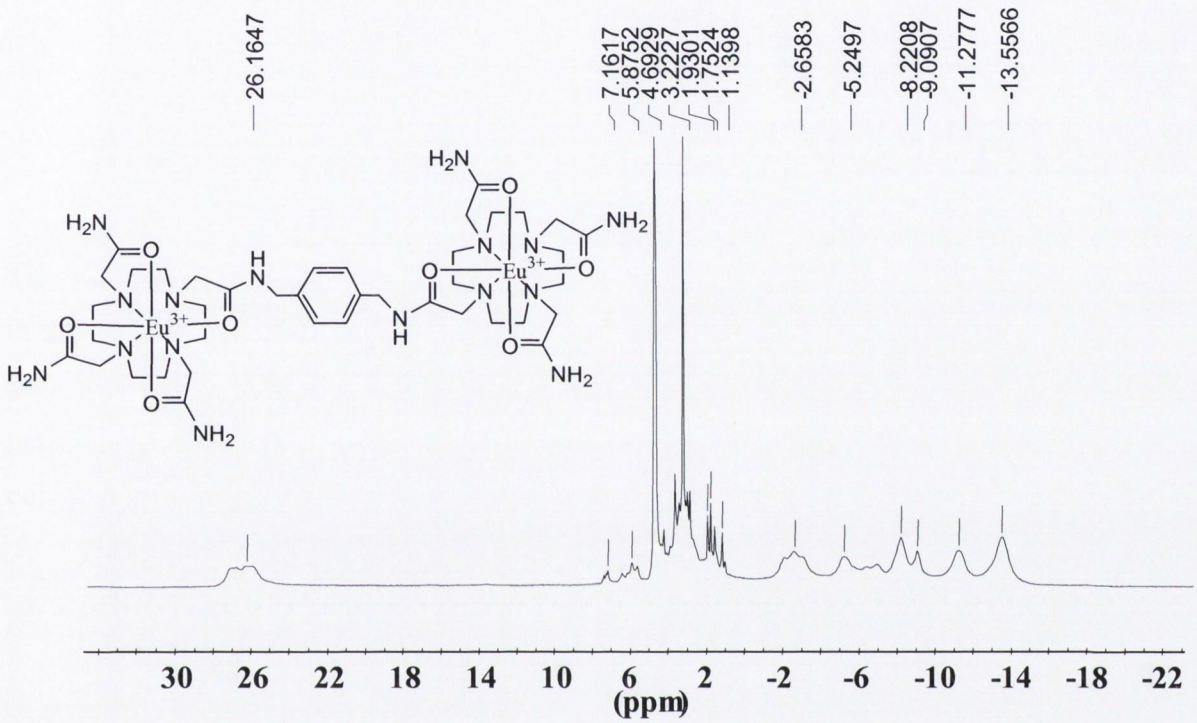

Figure 4.15. 400 MHz ^{1}H NMR spectrum in D_2O of Eu.154. Shifted peaks show Eu(III) complexation has occurred

The ^{1}H NMR spectrum of **Eu.154** (D_2O) (Figure 4.15) showed peaks at 26.16, –2.66, –5.25, –9.09, –11.28, and –13.56 ppm. These peaks are indicative of the Eu(III) shifted, axial and equatorial protons of the cyclen and acetamide CH_2's.[241] This was clear evidence that the europium had complexed to the cyclen ligand. The ESMS (Figure 4.16) also showed that complexation had occurred. It revealed a number of peaks all of which related to the desired complex, as seen by the characteristic europium isotope distribution pattern observed. The range of peaks seen were due to the method of ionisation and corresponded to the *m/z* of the complex with differing numbers of triflate counter ions *i.e.* the signals at *m/z* = 901.1 and 376.5 corresponded to the [M+4Trif]/2 and[M+2Trif]/4 species respectively. Elemental analysis confirmed the characterisation of this complex.

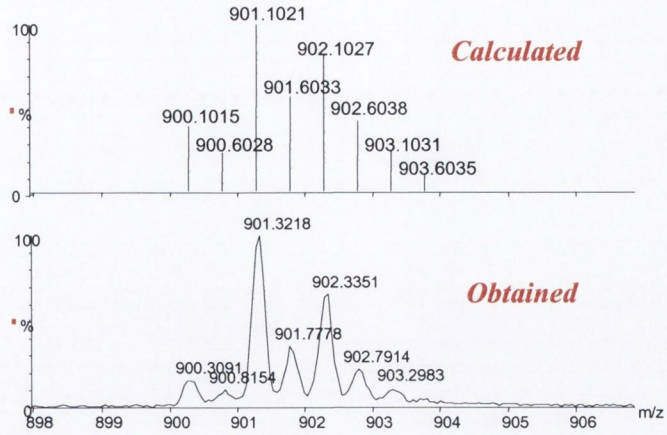

Figure 4.16. Europium isotope distribution pattern. [M+4triflates]/2

The europium complexes, **Eu.155** and **Eu.156,** gave similar results. Their ^{1}H NMR spectra in D_2O again showed the expected shifted cyclen resonances at ~ 30, –1, –5, –8, –12 and –16 ppm, clear evidence that complexation had occurred. The europium isotope distribution pattern could again be observed in the mass spectrum for peaks corresponding to the complex with numerous triflate counter ions.

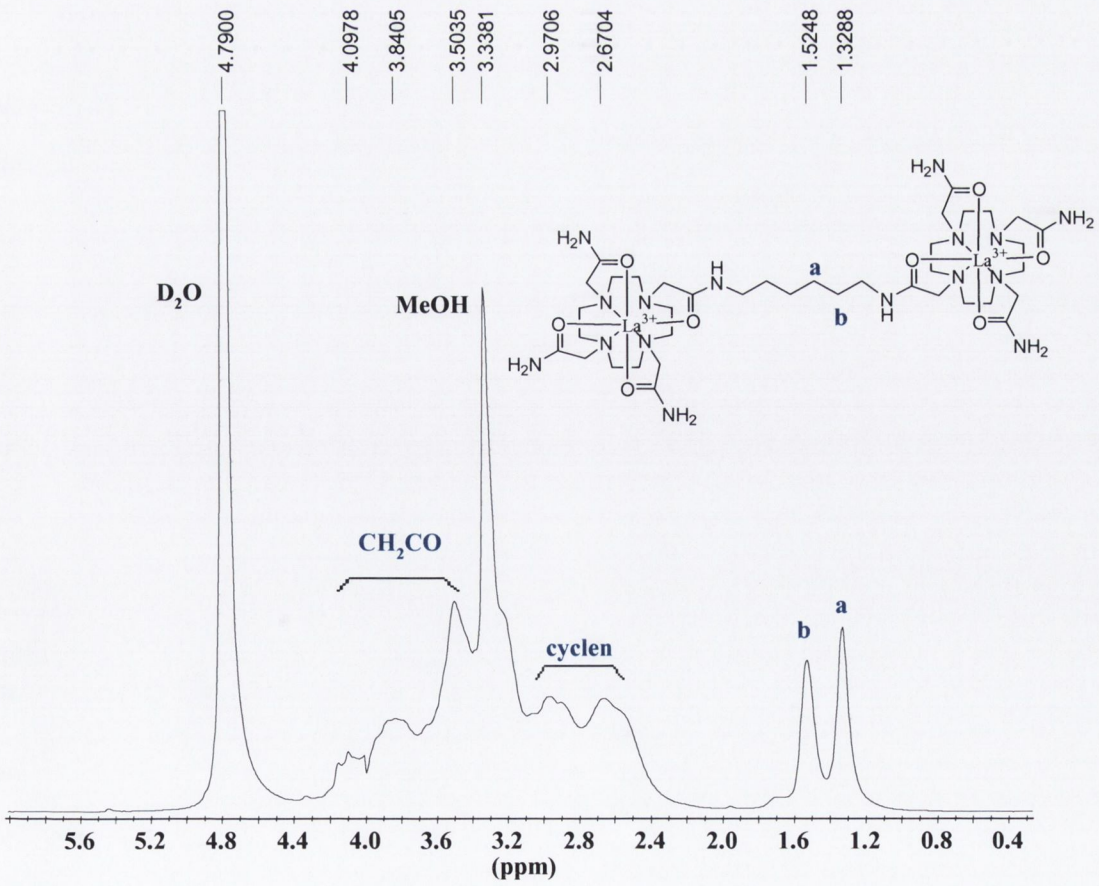

Figure 4.17. ^{1}H NMR of La.157 in D_2O showing broadened peaks

The lanthanum ion is not paramagnetic and as a result the shifted peaks observed in the ^{1}H NMRs of the Eu(III) complexes were not observed for the La(III) complexes. However, lanthanide ions are known for their fast NMR relaxation properties. Indeed, it is this property that is utilised for medicinal purposes in MRI contrast agents such as [Gd(DOTA)(H_2O)].[241] The strong relaxation properties of the La(III) ion result in broadened spectral peaks in the NMR of its complexes. This can be seen in the ^{1}H NMR of **La.157** (Figure 4.17).

The ^{1}H NMR of the lanthanum complexes, **La.154** and **La.155** showed similar broadened peaks. The La(III) complexes were also characterised by other conventional methods, ESMS, IR and elemental analysis.

Infrared (IR) spectroscopy is a useful method in determining whether a complex has been formed as the vibrational bands associated with the bonds involving the coordinating atoms, usually move to lower frequency (*i.e.* lower energy), upon complexation of a metal ion.[242] In this case the ligands carbonyl bond is expected to donate electron density to the metal centre, resulting in an increase in the bond length and a concomitant decrease in the IR stretching frequency. This was indeed found to be the case for the ligands **154** – **157**, as upon complexation of a metal ion, the IR stretching frequency of the carbonyl band was changed (Table 4.4).

Compound	Ligand (cm^{-1})	La Complex (cm^{-1})	Eu Complex (cm^{-1})
154	1678	1634	1665
155	1657	1638	1638
156	1647	–	1621
157	1670	1635	–

Table 4.4. IR carbonyl stretching frequencies decrease upon complexation of metal ion

For the amide bis-cyclen Eu(III) complexes **Eu.154, Eu.155** and **Eu.156**, the octadentate ligands were expected to leave one free coordination site, and as such, each Eu(III) metal centre was expected to posses one metal bound water molecule, in a similar manner to that previously observed for the analogous mononuclear systems.[223] In order to confirm this, the luminescent lifetimes (τ) of the complexes excited states were measured in D_2O and

H_2O, after direct excitation of the Eu(III) ion at 395 nm. The lifetimes were used to determine the number of metal bound water molecules, or q value, using equation (*i*), previously discussed in Chapter 2.[243,244,245]

$$(i) \qquad q^{Eu(III)} = 1.2\,[(1/\tau_{H2O} - 1/\tau_{D2O}) - 0.25 - 0.075x]$$

As discussed in Chapter 2, the prefix 1.2, is a proportionality constant that reflects the sensitivity of the europium ion to quenching by metal bound water molecules. The correction term – 0.25 represents quenching by second sphere water molecules, while – 0.075x represents the quenching by *N-H* oscillators, where x is the number of such oscillators bound to the complex.[239] In the cases of **Eu.154, Eu.155** and **Eu.156**, the number of coordinated amide NH groups x, were seven, four and one respectively.
The results of these measurements are shown in Table 4.5. As expected, each of the Eu(III) complexes were found to have one metal bound water molecule per Eu(III) ion.

Complex	x	τ_{H2O} (ms)	k_{H2O} (1/ms)	τ_{D2O} (ms)	k_{D2O} (1/ms)	q (±0.5)
Eu.154	7	0.507	1.971	2.265	0.440	0.91
Eu.155	4	0.553	1.808	2.451	0.408	1.02
Eu.156	1	0.553	1.808	1.851	0.541	1.13

Table 4.5. Lifetime measurements revealed that each Eu(III) ion possessed one metal bound water molecule

Unfortunately the q values for La(III) complexes can not be measured in the same way, however, it is reasonable to assume that the coordination environment of the binuclear La(III) systems is similar to the mononuclear systems, and that each La(III) ion possesses two metal bound water molecules.[223]

In summary this section has described the synthesis of six novel binuclear lanthanide complexes **Eu.154, La.154, Eu.155, La.155, Eu.156** and **La.157**. Lifetime studies have revealed that each of the Eu(III) complexes possesses one metal bound water molecule per Eu(III) ion, while the La(III) complexes are expected to possesses two. The ability of these complexes to promote the hydrolysis of phosphodieters, shall be investigated later in this chapter. At this point it was of interest to see whether changing the pendant arm from the

simple acetamide groups to more complex functionalities, would impact upon the rate of phosphodiester hydrolysis attained by the complexes. The synthesis and characterisation of binuclear complexes incorporating different pendant arms shall be the subject of the following section.

4.3.6 Changing the Pendant Arm

The nature of the ligand itself is known to play a role in modulating the properties of the metal ion. For instance, the Lewis acidity of a metal ion will be modulated by the nature of the ligand and mirrored by a change in the pK_a of any metal bound water molecules.[246] Previous investigations carried out using mononuclear lanthanide systems have highlighted the importance of the nature, of the pendant arms.[220, 249] Natural ribozymes, such as RNaseA, are known to utilise groups such as histidine, which can provide acid-base catalysis to promote hydrolysis of RNA.[247] Introducing a pendant group, which can function as an acid or a base, into the ligand of a ribozyme mimic can also promote the rate of phosphodiester hydrolysis. This has been demonstrated by several researchers including Hamilton *et al.* who demonstrated that incorporating pendant tertiary amine groups increased the activity of **82** by providing general base catalysis.[248] The pyridine functional group can act as a general base catalyst and complexes incorporating pyridine pendant arms, such as **Ln.158**, have been shown to be highly successful cleaving agents by Gunnlaugsson *et al.*[249] The synthesis of binuclear systems incorporating these pendant arms was desired, in order to improve upon the accelerations already obtained by mononuclear systems.

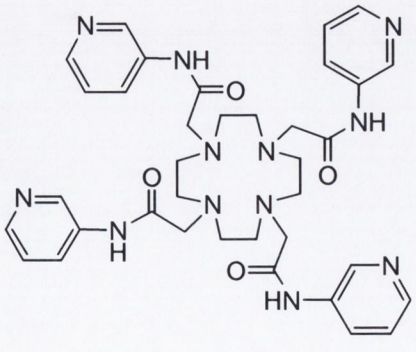

158

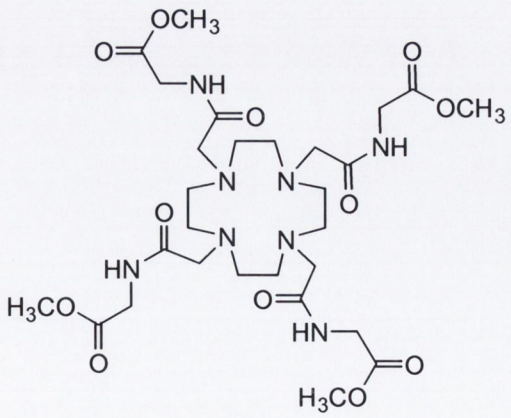

39

Amino acids such as His and Arg, are utilised by natural ribozymes,[247] and indeed amino acids such as poly(Leu-Lys) have been shown to promote the cleavage of ApAp.[250] Gunnlaugsson *et al.* have shown that ribozyme mimics incorporating pseudo dipeptide

pendant arms (Ala, Gly, Leu. *etc.*), increased the rate of hydrolysis of phosphodiesters. Of these systems, the 4-armed glycine methyl ester complex **La.39**, was found to give the greatest rate enhancement and this was attributed to the ability to form hydrophobic cavities.[251, 252].

The following sections shall describe the synthesis of binuclear lanthanide systems incorporating glycine methyl ester and pyridine pendant arms.

4.3.7 Synthesis of Glycine and Pyridine Pendant Arms

The α-chloroamide arm, (2-chloro-acetylamino)-acetic acid methyl ester, **159**, was synthesised according to the literature procedure,[253] by stirring the HCl salt of glycine methyl ester with one equivalent of chloroacetyl chloride, in an ice bath, overnight, in the presence of Et_3N in CH_2Cl_2. The desired product was isolated as an oil in 60 % yield after aqueous work up. The ^1H NMR of **159** agreed well with the published characterisation, showing four signals including the NH proton as a singlet at 7.11 ppm, and the "Gly" methylene resonances as a doublet (J = 6.0 Hz) at 3.95 ppm. The three methoxy protons were observed at 3.64 ppm.

Of the three possible pyridine isomers, previous investigations in the Gunnlaugsson group had revealed the mononuclear 3-pyridine isomer was the most effective at accelerating the rate of phosphodiester hydrolysis of **HPNP**,[249] and hence it was decided to utilise this isomer in the synthesis of the binuclear system. The α-chloroamide pyridine arm, 2-chloro-*N*-pyridin-3-yl-acetamide, **140,** was also synthesised according to the literature procedure,[231] by stirring 3–aminopyridine with chloroacetyl chloride in acetone overnight at room temperature. The desired product precipitated out of solution as its HCl salt in 86 % yield. The characterisation agrees with the literature, M.P. 134 - 135.6 °C (Lit M.P. 134 - 135 °C).[231]

The next section shall describe the introduction of these α-chloroamide arms into the cyclen ligand framework.

4.3.8 Synthesis of 3-Armed Cyclen Systems

Initially, an attempt was made to functionalise the bis-cyclen ligand, **152**, with the pendant arms **159** and **140**, as illustrated in Scheme 4.12, however, this proved unsuccessful, as the reactions did not proceed. Various solvent conditions were employed including EtOH, MeOH and DMF, however, no trace of the desired compound was detected. Solvent had

been previously noted as a key factor in the formation of the mononuclear 4-armed ligand **39**, as the reaction only proceeded in MeCN.[237] The bis-cyclen ligand **152,** was however, insoluble in MeCN and hence, yet again the reaction did not proceed.

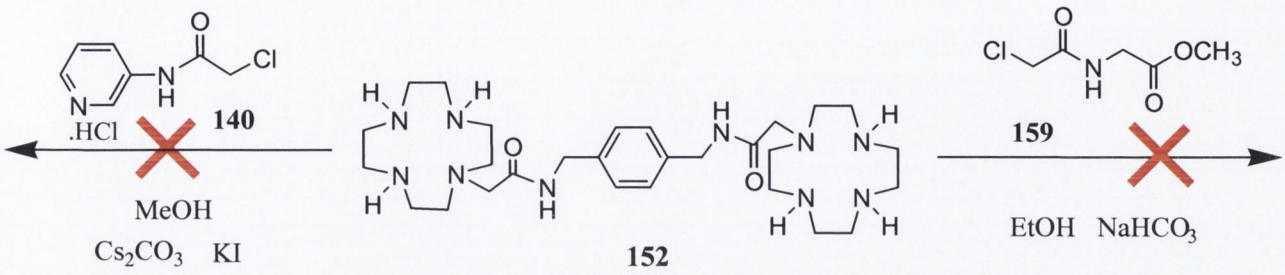

Scheme 4.12. Attempted synthesis of Glycine and Pyridine bis-cyclen

An alternative approach was attempted, involving the synthesis of the 3-armed cyclen ligand by stirring three equivalents of **159** in MeCN at 60 °C, with one equivalent of cyclen, in the presence of three equivalents of $NaHCO_3$ (Scheme 4.13). The reaction, had previously been described by Ann Marie Fanning,[290] and was monitored by mass spectrometry, which showed the formation of three new species, the di, tri and tetra functionalised cyclen moieties. The desired 3-armed ligand, (2-{4,7-bis-[(methoxycarbonylmethyl-carbamoyl)-methyl]-1,4,7,10-tetraaza-cyclododec-1-yl}-acetylamino)-acetic acid methyl ester, **160**, was isolated from this mixture by alumina column chromatography using CH_2Cl_2/MeOH(NH_3) gradient elution, 0 → 10 %, to give a white foam in 27 % yield.

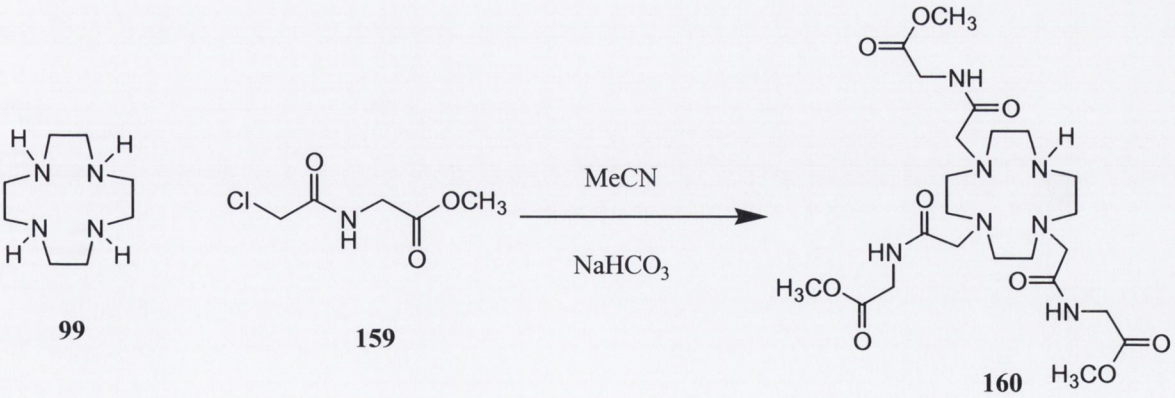

Scheme 4.13. Formation of 3-armed glycine cyclen 160, proceeded with 27 % yield

The mass spectrum of the compound **160**, showed one peak at *m/z* 560.2 corresponding to the M+H species. The $CDCl_3$ ^1H NMR (Figure 4.18) clearly showed the presence of a C_2 plane of symmetry running through the molecule with the amine proton visible as a broad singlet at 9.38 ppm, while two amide NH signals were observed at 8.69 and 8.38 ppm

respectively. The ^{13}C NMR showed four carbonyl peaks at 172.2, 171.1, 170.5 and 169.6 ppm, while the methoxy signals were observed at 51.7 and 51.2 ppm. Elemental analysis confirmed the characterisation of the product.

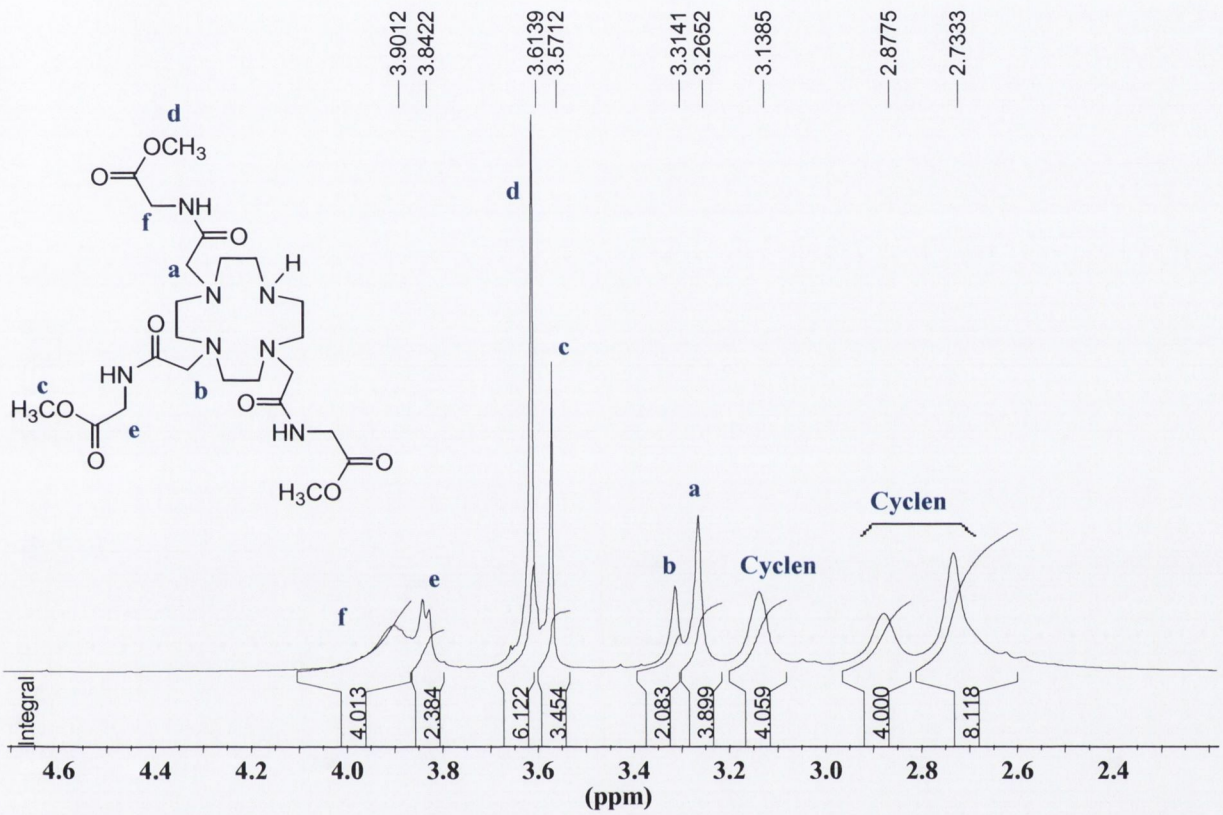

Figure 4.18. 400 MHz ^1H NMR in $CDCl_3$ of 160 exhibiting C_2 plane of symmetry

The 3-armed pyridine system, 2-[4,7-bis-(pyridin-3-yl-carbamoylmethyl)-1,4,7,10-tetraaza-cyclododec-1-yl]-*N*-pyridin-3-yl-acetamide, **161** was synthesised in a similar fashion by refluxing cyclen with three equivalents of **140** in MeOH for 36 hours, with Cs_2CO_3 and KI. The desired compound was isolated by alumina column chromatography using CH_2Cl_2/MeOH(NH_3) gradient elution, 0 → 10 %, to give a white solid in 29 % yield. The mass spectrum showed two peaks at *m/z* 597.3 and 575.3 corresponding to M+Na and M+H, respectively. Again the ^1H NMR showed there was a C_2 plane of symmetry through the molecule as there were two signals for each pyridine position. The ^{13}C NMR revealed two carbonyl signals at 171.4, and 170.9 ppm. Again there were two signals for each pyridine position and six methylene resonances were also observed. High resolution mass spectrometry confirmed the that the desired product had been obtained.

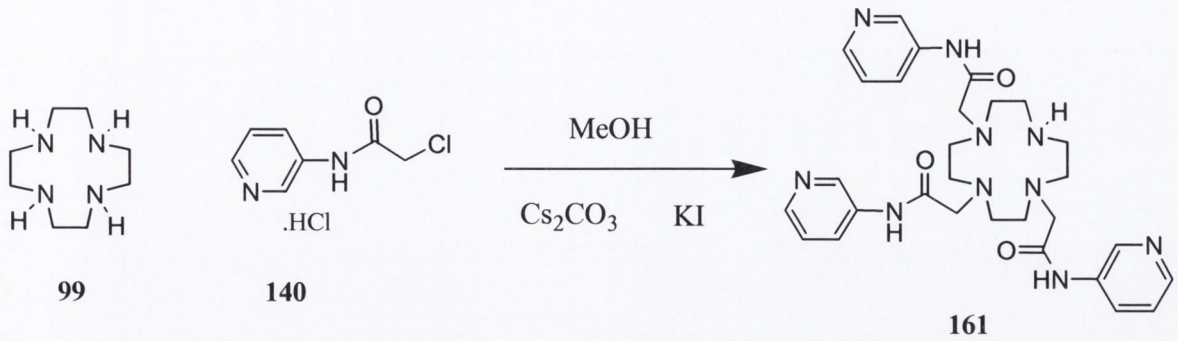

99 **140** **161**

Scheme 4.14. Synthesis of 3-armed pyridine cyclen proceeded with 29 % yield

Once the two 3-armed cyclen systems incorporating the different pendant arms had been synthesised, the next step was to use them to make binuclear systems, by bridging two of the molecules with an appropriate spacer group. The following section will detail how this was achieved.

4.3.9 Synthesis of Bis-Pyridine and Bis-Glycine Ligands

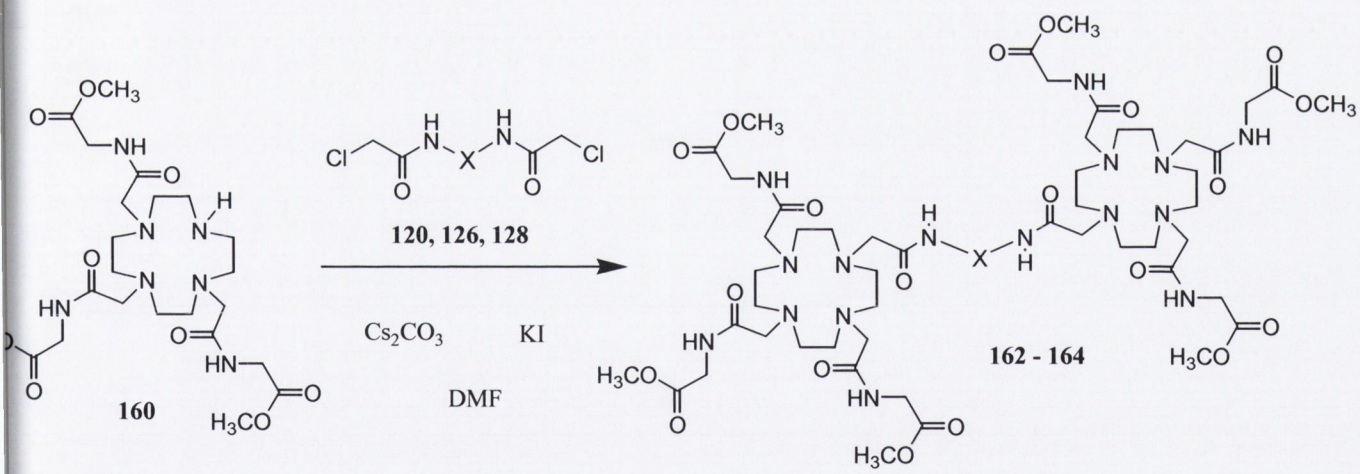

160 **162 - 164**

Compound	X	Yield
162	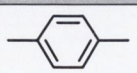	41 %
163	$(CH_2)_4$	41 %
164	$(CH_2)_6$	52 %

Scheme 4.15. General synthesis of glycine-bis-cyclen systems

In order to form the desired binuclear systems, the 3-armed cyclen systems had to be linked together with a spacer group. Initially, the 3-armed glycine system **160**, was bridged with the aromatic xylylene spacer **120**. This was achieved by stirring **160** together with half an equivalent of **120**, at 80 °C in DMF, in the presence of Cs_2CO_3 and KI, for five days. The desired product, {2-[4,7-bis-[(methoxycarbonylmethyl-carbamoyl)-methyl]-10-({4-[(2-{4,7,10-tris-[(methoxycarbonylmethyl-carbamoyl)-methyl]-1,4,7,10-tetraaza-cyclo dodec-1-yl}-acetylamino)-methyl]-benzylcarbamoyl}-methyl)-1,4,7,10-tetraaza-cyclododec -1-yl]-acetylamino}-acetic acid methyl ester, **162**, was isolated by precipitation from acetone in 41 % yield (Scheme 4.15).

The ^{1}H NMR of **162** in D_2O, exhibited quite broad peaks, however, once again the high degree of symmetry was evident (Figure 4.19). The four aromatic protons were observed at 7.16 ppm, while the four benzyl protons could be resonated at 4.28 ppm. The methoxy CH_3's and "Gly" CH_2's resonated between 3.64 and 3.56 ppm, while the cyclen protons were observed at 2.71 ppm. The ^{13}C NMR showed three carbonyl signals at 175.3, 171.3 and 171.1 ppm. The aromatic signals were observed at 136.5 and 127.0 ppm and the two methoxy CH_3's resonanced at 52.3 and 52.2 ppm, while ten methylene resonances were also observed.

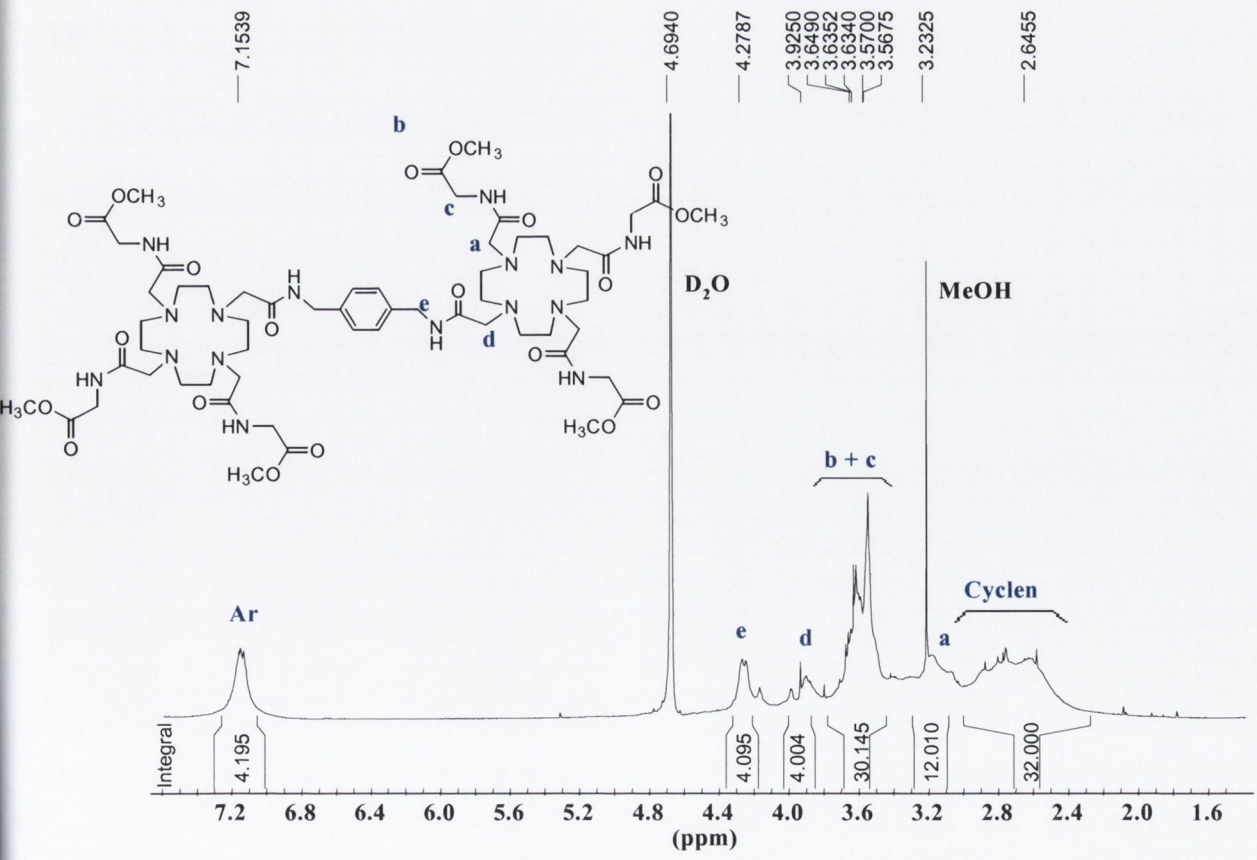

Figure 4.19. 400 MHz ^{1}H NMR of 162 in D_2O. Broad signals, due to fast relaxation

Both [2-(4,7-bis-[(methoxycarbonylmethyl-carbamoyl)-methyl]-10-{[4-(2-{4,7,10-tris-[(methoxycarbonylmethyl-carbamoyl)-methyl]-1,4,7,10-tetraaza-cyclododec-1-yl}-acetyl-amino)-butylcarbamoyl]-methyl}-1,4,7,10-tetraaza-cyclododec-1-yl)-acetylamino]-acetic acid methyl ester, **163** and [2-(4,7-bis-[(methoxycarbonylmethyl-carbamoyl)-methyl]-10-{[6-(2-{4,7,10-tris-[(methoxycarbonylmethyl-carbamoyl)-methyl]-1,4,7,10-tetraaza-cyclododec-1-yl}-acetylamino)-hexylcarbamoyl]-methyl}-1,4,7,10-tetraaza-cyclododec-1-yl)-acetylamino]-acetic acid methyl ester, **164,** were synthesised, using the butane spacer **126**, and hexane spacer **128**, respectively, under the same reaction conditions, in 41 % and 52 % yield, respectively. Three new glycine bis-cyclen ligands **160**, **163** and **164**, with different spacer groups have now been synthesised

In a similar manner the 3-armed pyridine cyclen **161** was coupled to the spacer **120** by heating in DMF at 85 °C, in a 2:1 molar ratio, in the presence of Cs_2CO_3 and KI for 5 days, after which, the solution was filtered and the DMF removed under reduced pressure (Scheme 4.16). The desired product, 2-[4,7,10-tris-(pyridin-3-ylcarbamoylmethyl) -1,4,7,10-tetraaza-cyclododec-1-yl]-*N*-[4-({2-[4,7,10-tris-(pyridin-3-ylcarbamoylmethyl)-1,4,7,10-tetraaza-cyclododec-1-yl]-acetylamino}-methyl)-benzyl]-acetamide, **165**, was isolated in 41 % yield after precipitation from ether, to remove any DMF, followed by precipitation from acetone, to further purify the ligand.

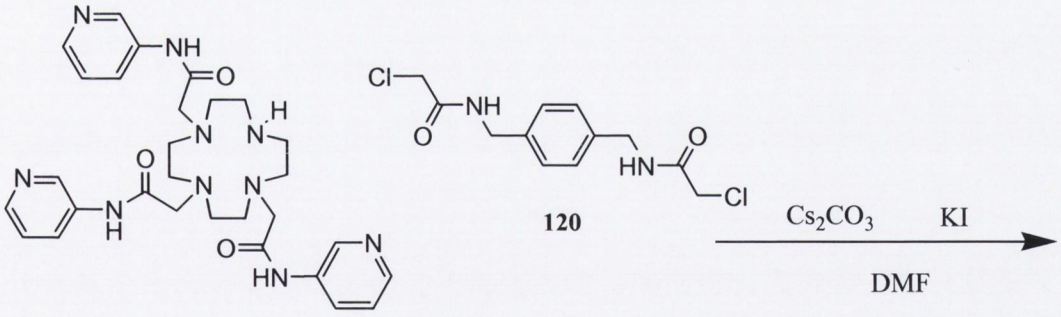

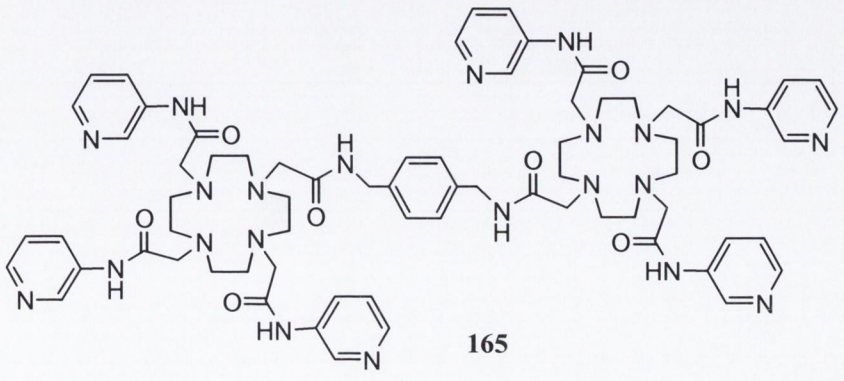

Scheme 4.16. Synthesis of pyridine bis-cyclen 165, 41 % yield

The ^{1}H NMR in CD_3OD revealed the symmetry of the molecule, as there were two sets of pyridine resonances (Figure 4.20). Two pyridine H2` protons resonated at 8.62 ppm, while the four pyridine H2 protons were observed at 8.47 ppm. The multiplet at 8.03 ppm corresponded to the twelve H4 and H6 pyridine protons. The four benzene protons were visible as a singlet at 7.12 ppm, while the six pyridine H5 protons were seen at 6.90 ppm as a double doublet (J = 6.0 Hz, J = 6.0 Hz). The methylene resonances were observed as a broad multiplet integrating for 48H at 2.64 ppm. The ^{13}C NMR revealed five CH_2 signals including one broad signal for the cyclen carbons at 50.1 ppm. Twelve aromatic signals along with three carbonyl signals were also observed. Elemental analysis confirmed the characterisation of the molecule. Unfortunately, due to time constraints, the more flexible analogues of this binuclear pyridine system were not synthesised.

This section has described the development of four new ligands **162, 163 164** and **165**, incorporating two different pendant arms and three different spacer groups. The next step was to introduce the lanthanide ions into these ligands to form the corresponding complexes, in order to produce potential ribozyme mimics. This process shall be detailed in the following section.

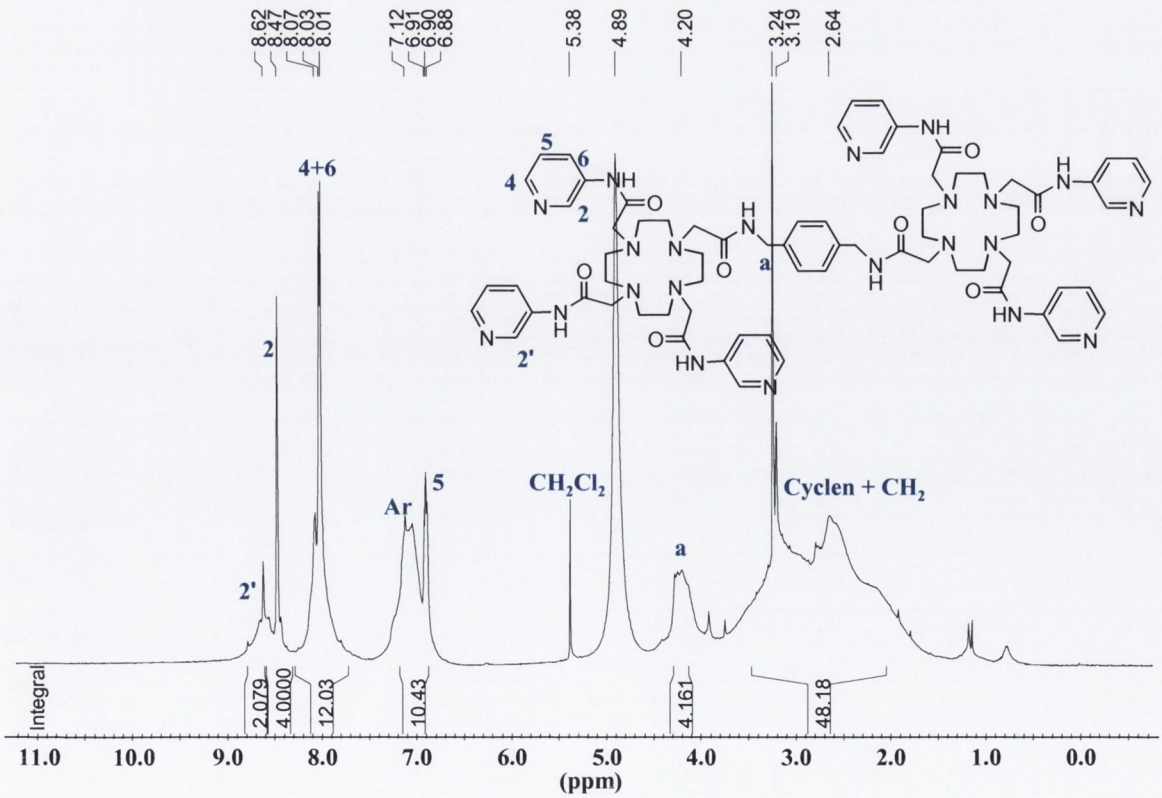

Figure 4.20. 400 MHz 1H NMR of 165 in MeOD

4.3.10 Complexation of Bis-Pyridine and Bis-Glycine Ligands

The lanthanum complex of **162** was formed by refluxing two equivalents of $La(CF_3SO_3)_3$ with **162** in MeOH overnight. The product **La.162**, was isolated in 90 % yield, after precipitation from ether followed by precipitation from CH_2Cl_2. Similarly, the lanthanum complexes of the bis-glycine cyclen ligands, **163, 164** and **165** were synthesised in 72 %, 85 % and 83 % yield, respectively. The europium complex of **164** was also synthesised, in 66 % yield. Again time constraints meant that only one of the ligands was complexed with europium. The resulting lanthanum complexes each showed the characteristic broadening in their ^1H NMR spectra, while the **Eu.164** ^1H NMR showed the characteristic Eu(III) shifted peaks. The changes in the IR carbonyl stretching frequency were also notable, showing that complexation had occurred (Table 4.6). Unfortunately, the mass spectrum of these complexes could not be obtained. The hygroscopic nature of the glycine complexes precluded the obtainment of elemental analysis, nevertheless, elemental analysis was obtained for the pyridine complex **La.165**, and confirmed that the complex had been successfully synthesised.

Compound	Ligand (cm^{-1})	La Complex (cm^{-1})	Eu Complex (cm^{-1})
GBC 162	1663	1627	-
GBB 163	1655	1638	-
GBH 164	1662	1638	1638
PBC 165	1685	1654	-

Table 4.6. Showing changes in IR carbonyl stretching frequencies upon lanthanide complexation

This section has described the synthesis of five novel binuclear lanthanide complexes **La.162, La.163, La.164, Eu.164** and **La.165** incorporating two types of pendant arm, namely glycine methyl ester and pyridine arms. The general base catalytic ability of the pyridine cofactors, and the hydrophobic nature of the glycine cofactors may lead to greater acceleration of phosphodiester hydrolysis. Lifetime studies again revealed that the Eu(III) complex **Eu.164**, possesses one metal bound water molecule per Eu(III) ion, while the La(III) complexes are expected to possesses two. The ability of these complexes to promote the hydrolysis of phosphodieters, shall be investigated later in this chapter. At this point, the synthesis of one final complex, which utilised an alternative bridge, was desired.

It was of interest to see whether the use of a shorter xylyl bridge, would impact upon the rate of phosphodiester hydrolysis attained by the complexes. The synthesis and characterisation of this system is the subject of the following section.

4.3.11 Synthesis of *p*-Xylyl Bridged Binuclear System

As mentioned earlier the coordination of metal bound water molecules plays an important role in the hydrolysis of phosphodiesters. The shorter xylylene bridge was chosen, in order to investigate the effect of leaving the lanthanide ion coordinatively unsaturated. As this spacer group lacks the acetamide functionality, the complex should gain one extra free coordination site per Eu(III) ion, which in turn should provide the complex with a better ability to bind and accelerate phosphodiester hydrolysis.[225, 254] The synthesis and characterisation of the ligand 2-{4,7-bis-dimethylcarbamoylmethyl-10-[4-(4,7,10-tris-dimethylcarbamoylmethyl-1,4,7,10-tetraaza-cyclododec-1-ylmethyl)-benzyl]-1,4,7,10-tetraaza-cyclododec-1-yl}-*N,N*-dimethyl-acetamide, **117**, was discussed in Chapter 3. The europium complex of **117** was produced by refluxing **117** and two equivalents of $Eu(CF_3SO_3)_3$ in MeOH for sixteen hours (Scheme 4.17). The complex **Eu.117**, was soluble in acetone however, precipitation from CH_2Cl_2 yielded the desired product in 59 % yield. The ^1H NMR (d-acetone) showed the characteristic, shifted axial and equatorial peaks at 36.02, 26.52, 19.14, 17.02, 12.88, 11.32, 8.30, 4.72, 3.70, 2.85, 1.24, 0.83, –0.18, –1.40, –2.69, –6.45, –8.68, –12.48, –14.39, –20.64, –22.99, –25.01 and –25.90 ppm (Figure 4.22). The IR spectrum revealed a shift in the carbonyl stretching frequency from 1639 cm^{-1} for **117** to 1626 cm^{-1} for **Eu.117**.

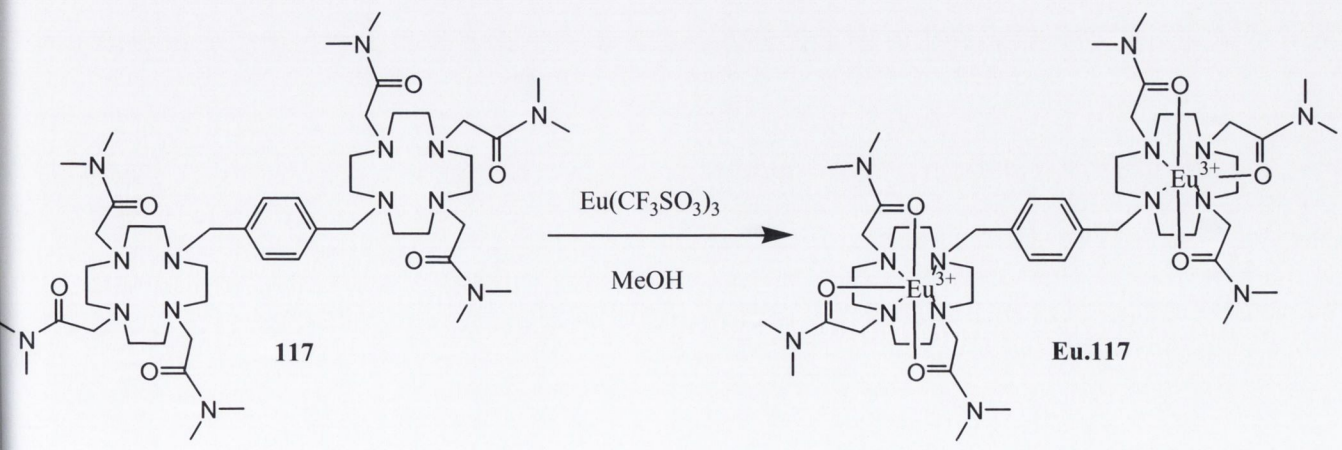

Scheme 4.17. Complexation of 117 proceeded with 59% yield

At this point it is worth recalling the crystal structure of the corresponding sodium complex discussed in Chapter 3 (Figure 3.10), as sodium is known to have a similar coordination geometry to that of europium. The sodium complex exhibited a square antiprism geometry around the sodium ion and was seen to have two metal bound water molecules.

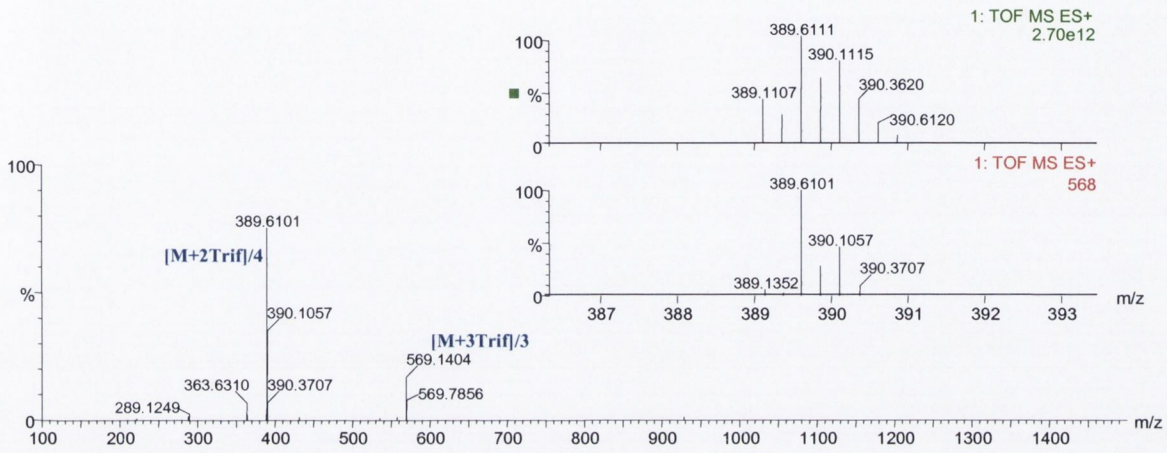

Figure 4.21. Mass spectrum of Eu.117 and inset showing europium isotope distribution pattern and expected pattern above

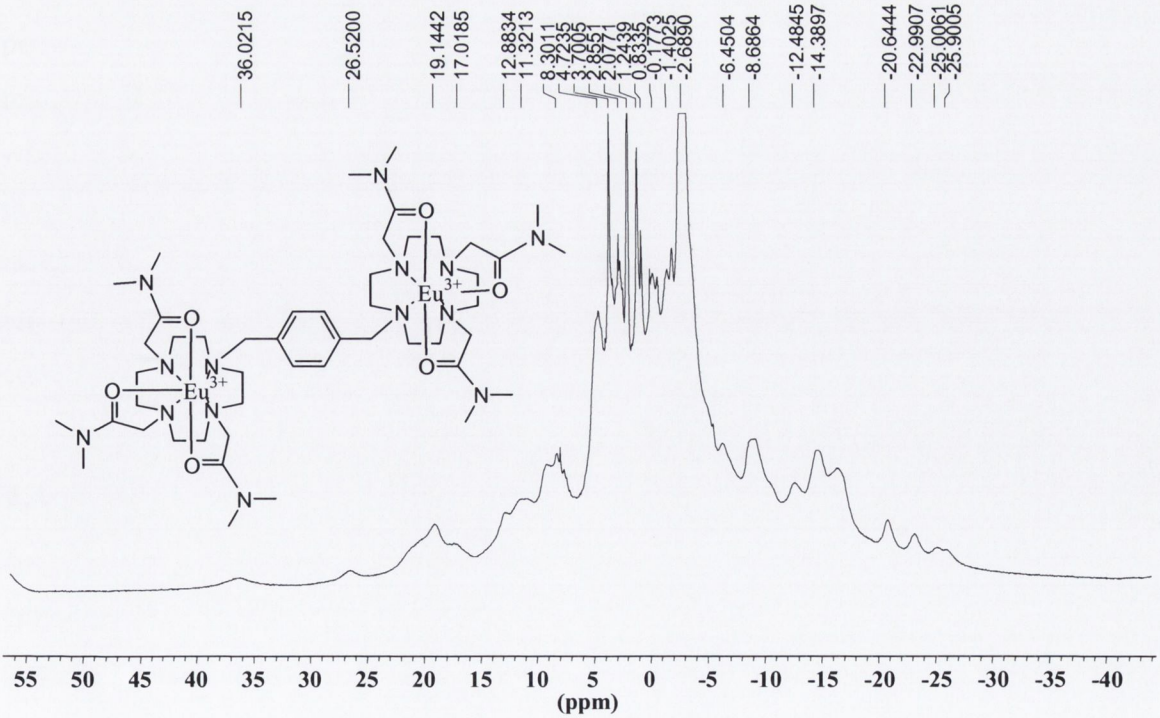

Figure 4.22. 400 MHz ^{1}H NMR in d-acetone of Eu.117

Previously, the Tb(III) complex **Tb.117**, was found to possess two metal bound water molecules per Tb(III) ion. As Eu(III) occupies a similar coordination environment to Tb(III), **Eu.117** was also expected to possess two metal bound water molecules.

Complex	τ_{H2O} (ms)	k_{H2O} (1/ms)	τ_{D2O} (ms)	k_{D2O} (1/ms)	q (±0.5)
Eu.117	0.443	2.258	1.356	0.737	1.52

Table 4.7. Measured lifetimes and rate constants for Eu.117 and the corresponding hydration number *q*

The q value for **Eu.117** was found to be 1.52 ± 0.5, however, as **Tb.117** was found to possess two metal bound water molecules it is reasonable to assume that **Eu.117** will display a similar coordination environment.

4.3.12 Summary

This section has described the development of twelve new complexes, **Eu.154, La.154, Eu.155, La.155, Eu.156, La.157, La.162, La.163, La.164, Eu.164, La.165** and **Eu.117**, which have been designed to accelerate the rate of phosphodiester cleavage as discussed in Chapter 1. These complexes utilise four different bridging groups and five different pendant arms. The selection of pendant arms will allow comparison to similar mononuclear lanthanide systems previously reported, while the various bridging groups will allow for comparison between the binuclear systems. Lifetime studies have indicated that the Eu(III) complexes are nine coordinate, where the ninth site is occupied by a single metal bound water molecule. In the case of the heptadentate binuclear ligand **Eu.117**, the ion is expected to possess two metal bound water molecules. The ability of these complexes to cleave phosphodiesters shall be discussed in the following sections.

4.4 Phosphodiester Hydrolysis Studies

As previously discussed in Chapter 1, most research groups employ phosphodiester model compounds, instead of RNA, when evaluating potential ribozyme mimics, due to the convenience offered by such molecules, such as the ability to follow the hydrolysis kinetics by absorption spectroscopy. Throughout this chapter the model compound, **HPNP** (2-hydroxypropyl *p*-nitrophenylphosphate), **33**, shall be utilised in order to assess the complexes' ability to promote phosphodiester hydrolysis. Like RNA, **HPNP** is a phosphodiester, which has a hydroxyl group that can act as an intramolecular nucleophile,

in the 2' position. However, **HPNP** has the advantage that its hydrolysis can be followed by absorption spectroscopy. **HPNP** absorbs at 300 nm, while the product of its cleavage, 4-nitophenolate, **34**, absorbs at 400 nm (Scheme 4.18). By following the rise in the peak at 400 nm, over the course of the hydrolysis, the rate constant (k) can be determined.

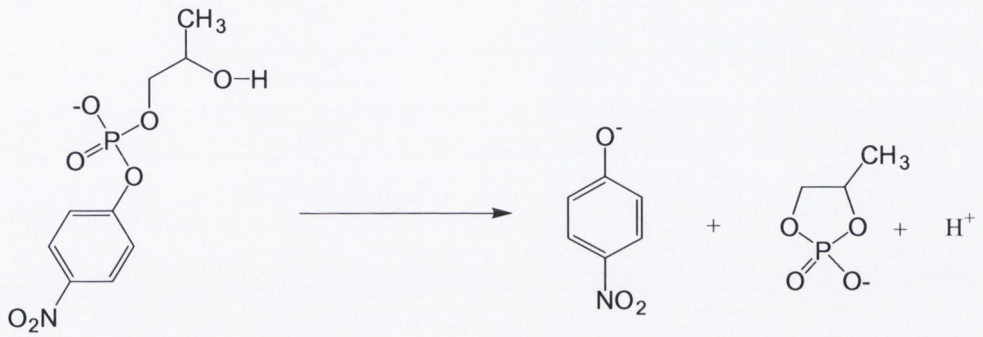

33 HPNP abs 300 nm **34** abs 400 nm **35**

Scheme 4.18: Hydrolysis of HPNP (33) (abs @ 300 nm) to give *p*-nitrophenolate (34) (abs @400nm)

As seen in Chapter 1, it can be difficult to directly compare different reported ribozyme mimics due to the differing conditions employed. In order to facilitate comparison between systems the conditions employed here were chosen to mimic those reported by Morrow *et al.*[258] Consequently, the measurements were conducted using a 0.18 mM solution of **HPNP** (Abs = 1.22 at 300 nm), in buffered aqueous solution (50 mM HEPES) pH 7.4, at 37 °C. To this was added one equivalent of the complex. The kinetics were then followed by absorption spectroscopy over sixteen hours with constant stirring, by measuring the absorbance at 400 nm (ϵ = 6430 M^{-1} cm^{-1}).[255] The rate constant (k) values were determined by fitting the data to first order rate kinetics[256]. The half-life was then calculated from the rate constant obtained ($\tau_{1/2} = \ln 2/k$). The relative rate enhancement, k_{rel}, is the ratio between k and the rate constant of the 'uncatalysed' hydrolysis of **HPNP**, (k_{uncat}) which has been measured to be 0.00012 h^{-1}, $\tau_{1/2}$ = 5.78 x 10^3 h, at pH 7.4.[257] Every rate is an average of two to three measurements agreeing to within a 10 % error. Another reason for choosing these conditions was their similarity to physiological conditions, pH ~ 7.4, 37 °C. The following sections shall detail the results of these measurements beginning with the binuclear acetamide systems.

4.4.1 Hydrolysis of HPNP by Binuclear Acetamide Systems

The simple acetamide bis systems were tested first. The measurements were conducted as described above. The changes in the absorbance spectra of **HPNP** in the presence of **Eu.154** can be seen in Figure 4.23. The peak at 300 nm, corresponding to [**HPNP**] was found to decrease over time, while a new peak at 400 nm appeared, indicating the formation of **34**. By plotting the changes in absorbance as a function of time (Figure 4.24), it can be seen that the decrease in absorbance at 300 nm is smaller than the increase in absorbance at 400 nm. This is due to the absorbance at 300 nm by the products of cleavage. By fitting the change in absorbance at 400 nm to first order rate kinetics, the rate constant was determined. This can also be determined manually by plotting the natural log of the absorbance at 400 nm against time, an example of which is shown in the appendix. The complex **Eu.154**, was found to cleave **HPNP** with a 'pseudo first order' rate constant of 0.099 (±0.011) hr^{-1}, corresponding to a half-life of 7.08 hours. This is a rate enhancement (k_{rel}) of *ca.* 822 over the uncatalysed reaction.[257]

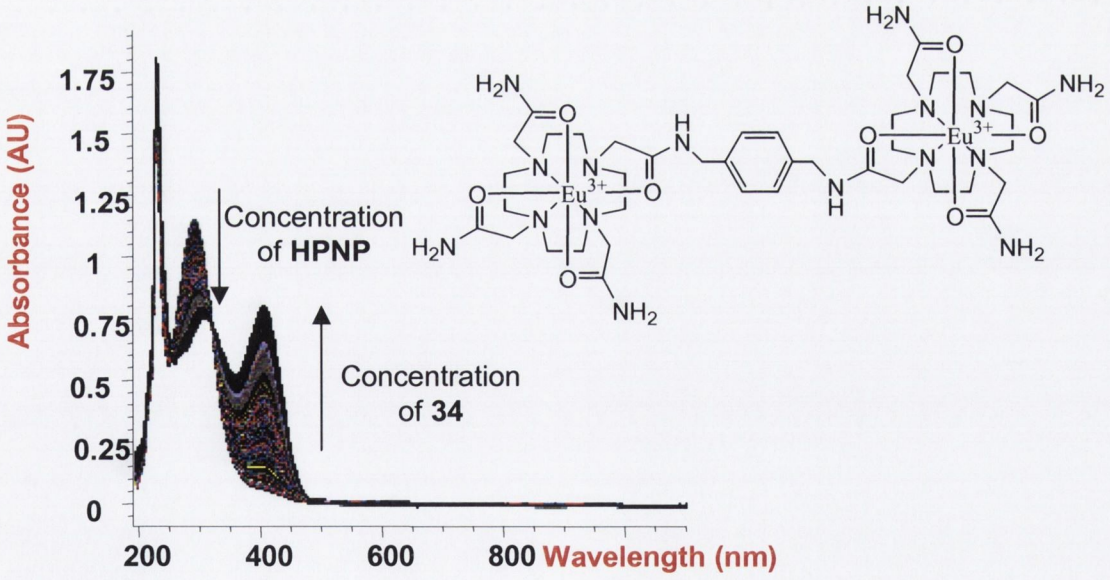

Figure 4.23. Changes in absorbance spectra for Eu.154 and HPNP showing increase in abs at 400 nm corresponding to [34] over time, as well as decrease in abs at 300 nm corresponding to [HPNP]

Significantly, under identical conditions, the analogous mononuclear 4-armed complex **Eu.38,** was reported not to accelerate the rate of hydrolysis at all.[258] This inactivity was attributed to the reduced number of metal bound water molecules (one for **Eu.38**,

compared to two for **La.38**).[258] As the binuclear system **Eu.154**, now provides two metal bound water molecules (one from each ion), this may no longer be such a limiting factor.

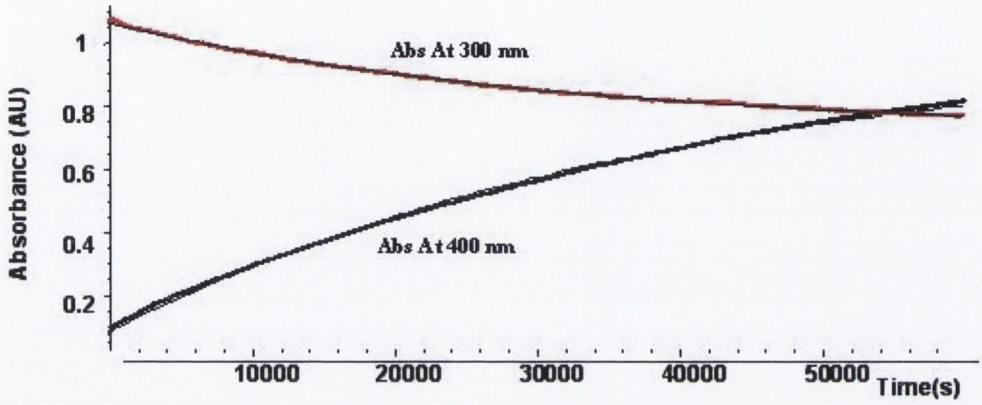

Figure 4.24. Kinetics profile for Eu.154. Top line corresponding to abs at 300 nm by [HPNP], Bottom line corresponding to abs at 400 nm by [34]

The La(III) analogue **La.154**, was next evaluated. Under identical conditions to those previously described, **La.154** was found to cleave **HPNP** with a 'pseudo first order' rate constant (k) of 0.088 (±0.012) hr^{-1}, corresponding to a half-life of 7.85 hours. This is a rate enhancement (k_{rel}) of *ca.* 736 over the uncatalysed reaction.[257] The rate constant for the analogous mononuclear 4-armed complex, **La.38,** was found to be 0.058 hr^{-1}, $\tau_{1/2}$ = 11.59 hours, (k_{rel}) of *ca.* 483.[258] The binuclear system does show an increase in activity at pH 7.4 over the mononuclear system, however, in this case it is less than a two fold increase. This type of increase is consistent with the relative increase in concentration of the metal ion[259] and as such, can be viewed as a cumulative rather than cooperative effect. The rigid xylylene spacer may be inhibiting the cooperative action of the metals by preventing them from approaching one another.

Comparing the two binuclear systems **La.154** and **Eu.154**, it can be seen that the Eu(III) analogue is slightly faster than the La(III) one, although when the errors are taken account of the difference is quite small. Previous mononuclear systems reported by Morrow[258] and Gunnlaugsson[251, 252] have typically found the La(III) complexes to be significantly faster than the Eu(III) analogues, due to lanthanum's larger coordination environment, which facilitates the presence of an extra metal bound water molecule and thus an extra coordination site to bind the phsphodiester. In this case however, the binuclear system **Eu.154**, provides two metal bound water molecules (one from each ion), and hence the number of metal bound water molecules may no longer be the most significant factor.

Having evaluated the complexes of **154**, identical measurements were carried out upon the other acetamide binuclear complexes, **Eu.155, La.155, Eu.156** and **La.157**. The results of these complexes are shown in Table 4.8. All of the complexes were found to accelerate the rate of phosphodiester hydrolysis to some extent. However, some interesting trends can be deduced from the results.

Comparing the three Eu(III) complexes of **154, 155, 156** it can be seen that the rate of phosphodiester hydrolysis seems to decrease upon addition of *N* methyl groups (Table 4.8). A similar trend is evident for the La(III) complexes of **154** and **155**. This trend may be due to the hydrogen bonding ability of the amide ligand gradually being diminished as the number of methyl groups increases.[260] Of the mononuclear systems only **La.38** had been shown to accelerate **HPNP** hydrolysis by a measurable amount.[258,261] The term cooperativity is often used when a mononuclear complex is inactive, but the binuclear complex displays activity. This is incorrect however, as cooperativity requires demonstration.[262] As the rate accelerations produced by the binuclear complexes of **155** and **156** can not be directly compared to their mononuclear analogues no conclusion upon cooperative action can be drawn.

Complex	R	Rate k (h^{-1})	$t_{1/2}$ (h)	k_{rel}
None		0.0001	5730	1
Eu.38	$R_1, R_2 = H$	N/A	N/A	N/A
La.38	$R_1, R_2 = H$	0.058	11.59	483
Eu.154	$R_1, R_2 = H$	0.099 (±0.011)	7.08	822
La.154	$R_1, R_2 = H$	0.088 (±0.012)	7.85	736
Eu.155	$R_1 = CH_3$ $R_2 = H$	0.043 (±0.015)	17.72	432
La.155	$R_1 = CH_3$ $R_2 = H$	0.065 (±0.004)	10.66	545
Eu.156	$R_1, R_2 = CH_3$	0.027 (±0.012)	25.67	230
La.157	$R_1, R_2 = H$, $X = (CH_2)_6$	0.247 (±0.026)	2.80	2058

Table 4.8. Pseudo first order rate constants (k), half lives (τ) and relative rates (k_{rel}) for the cleavage of HPNP 0.18 mM in 50 mM Hepes (pH 7.4) at 37 °C with various complexes

Thus far, although the binuclear systems discussed have shown improved rate enhancements over their analogous mononuclear systems, no evidence of a cooperative enhancement has been observed. Consequently, it was decided to test a binuclear complex with a more flexible spacer *i.e.* **La.157**. Of the simple acetamide systems, **La.157**, the hexane linked analogue of **154,** promoted the hydrolysis of **HPNP** to the greatest extent.

Comparing the kinetics profile of **La.157** (Figure 4.25) to that of **Eu.154**, highlights the extent of the rate acceleration.

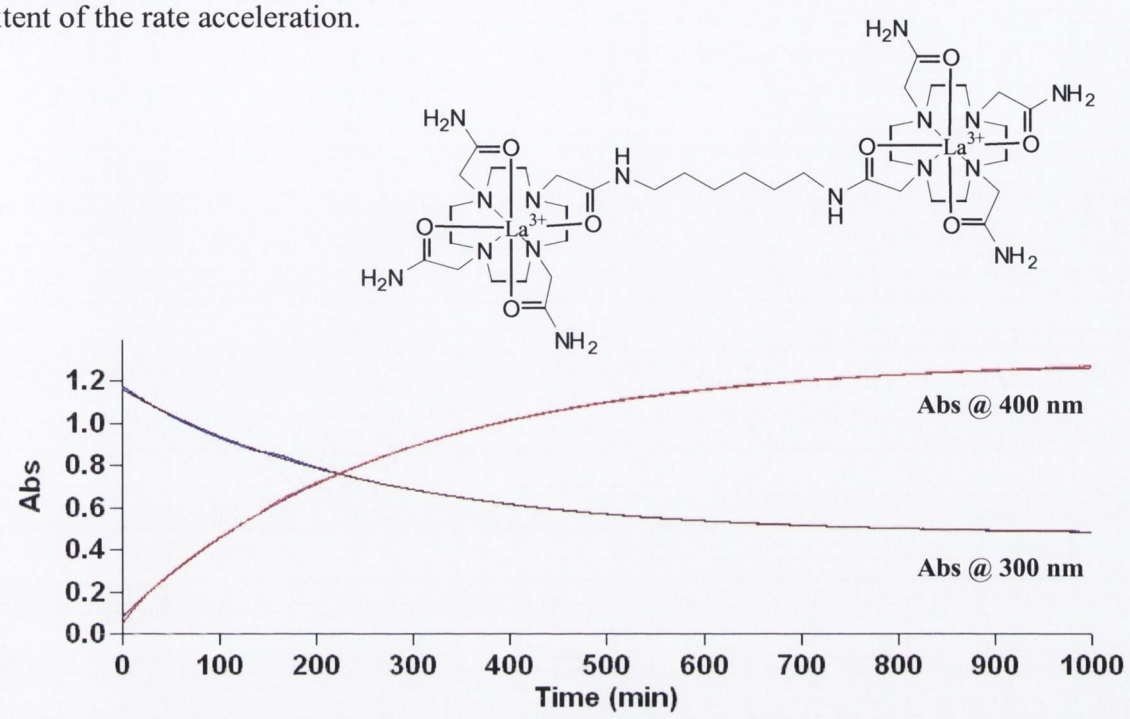

Figure 4.25. Kinetics profile for the hydrolysis of HPNP by La.157 at pH 7.4 37°C

The complex **La.157** was found to cleave **HPNP** with a 'pseudo first order' rate constant (k) of 0.247 (±0.026) hr^{-1}, corresponding to a half-life of 2.80 hours. It was found to be almost three fold more active than the original binuclear system, **La.154,** and four fold more active than the analogous mononuclear system at pH 7.4. This increase is more than can be explained by a simple cumulative effect. The complex **La.157** is providing a cooperative rate enhancement, and the four fold rate increase over the mononuclear system is in line with the cooperative activity displayed by other binuclear systems with flexible spacer groups.[227]

At this point it can be seen that the flexible alkyl bridged binuclear system **La.157** is more effective than the rigid xylylene bridged binuclear conjugates, although, all measurements so far have been conducted at one pH *i.e.* pH 7.4. As mentioned in the introduction, however, the rate of hydrolysis by such compounds, is known exhibit a pH dependence. Consequently, the effect of pH upon the hydrolysis was investigated and shall be detailed in the next section.

4.4.2 pH Dependence of HPNP Hydrolysis by Binuclear Acetamide Systems

It has previously been observed that the rate of phosphodiester hydrolysis can be dependant upon the pH.[220] Studies were therefore, carried out to investigate the effect of pH upon the rate of hydrolysis by these complexes. The measurements were conducted at various pHs, in an analogous manner to that already described. The results are presented here in two graphs, one showing the Eu(III) complexes and the other showing the La(III) complexes. The tertiary amide complex **Eu.156** was the poorest of the acetamide systems and hence its pH dependence was not investigated. The pH profile of the Eu(III) complexes **Eu.154** and **Eu.155** are shown in Figure 4.26. The first item to note is that the maximum activity of the complexes is at pH 7.0 for **Eu.154** and pH 7.2 for **Eu.155**, respectively. The second item of note is the "pseudo" bell shaped pH dependence displayed by both complexes.

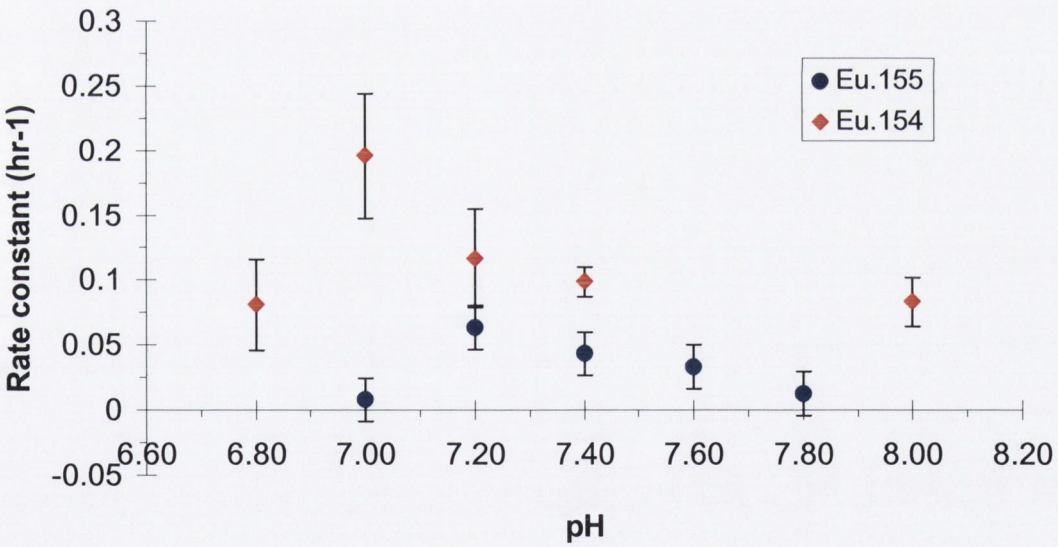

Figure 4.26. pH profiles for the hydrolysis of 0.18 mM HPNP at 37 °C by acetamide based Eu(III) complexes

A similar pseudo bell shaped pH dependence was observed for the La(III) complexes, shown in Figure 4.27. It is also of interest that the La(III) complexes exhibit their maximum activity at a slightly higher pH than the Eu(III) complexes (pH 7.6 for both **La.154** and **La.157**). The point of maximum activity is important, as if the complexes are to be utilised as ribozyme mimics they will be required to function under physiological

conditions, pH ~ 7.4. The pH dependence of the complexes can be explained in terms of the protonation state of the metal bound water molecules.

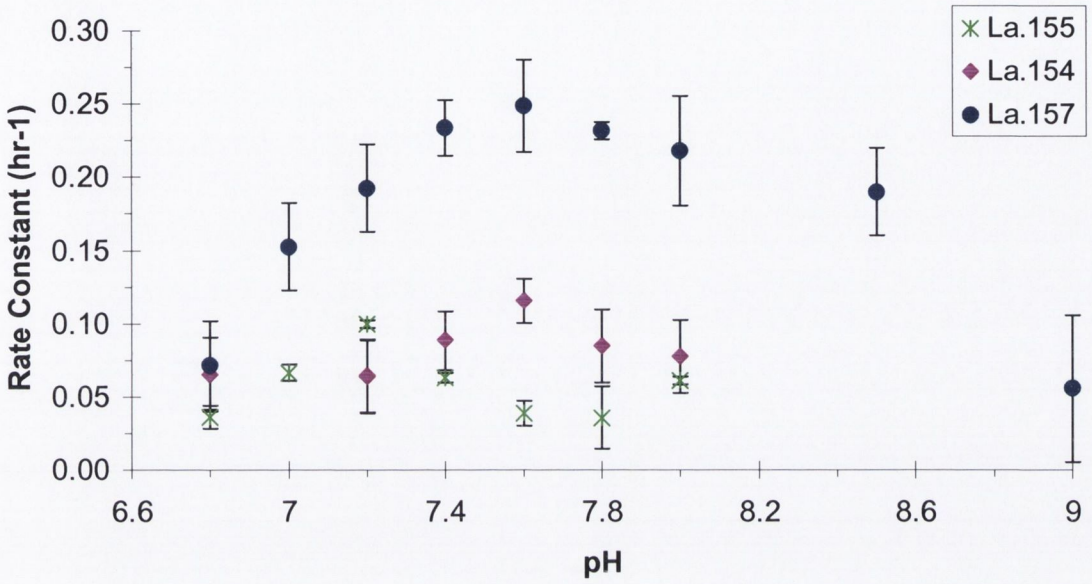

Figure 4.27. pH profiles for the hydrolysis of 0.18 mM HPNP at 37 °C by acetamide based La(III) complexes

A bell shaped pH rate profile is usually taken as evidence that the reaction is catalysed by both acid and base, however, it can also indicate a change in the rate determining step.[263] As discussed in the introduction, the hydrolysis of phosphodiesters proceeds *via* a two step mechanism.[264] The first step, transesterfication, is catalysed by base, while the second step, hydrolysis of the phosphorane intermediate, is catalysed by acid. The reaction is bifunctional since both acid and base catalysts are involved. However, each step involves only one catalytic species, so overall the reaction is pseudo first order no matter which step is rate limiting, even if the two steps are of comparable rate.[265] With an excess of the base catalyst, the second step is rate limiting. With an excess of the acid catalyst, the first step is rate limiting. The maximum rate is obtained when both catalysts are present and both steps are accelerated, so the pH rate profile is bell shaped.[265]

This bell shaped pH dependence has previously been observed for mononuclear systems. Its presence is linked to the protonation state of the metal bound water molecules. Metal bound hydroxide is known to be a potent base catalyst,[266] while metal bound water molecules can act as acid catalysts and also facilitates binding of the phophodiester. The maximum rate is obtained when the balance between binding and cleaving is optimum. For mononuclear La(III) complexes the optimum active species is believed to be the $M(H_2O)(OH^-)$.[267] It offers a potent hydroxyl base catalyst as well as the metal bound water

molecule, which can act as an acid catalyst and also be displaced in order to bind the phosphodiester. The $M(OH^-)_2$ species is known to be less active, as the two tightly bound hydroxide molecules inhibit the coordination of the anionic phosphodiester.[268] A proposed mechanism for the hydrolysis of **HPNP** by a mononuclear La(III) complex can be seen in Scheme 4.19.

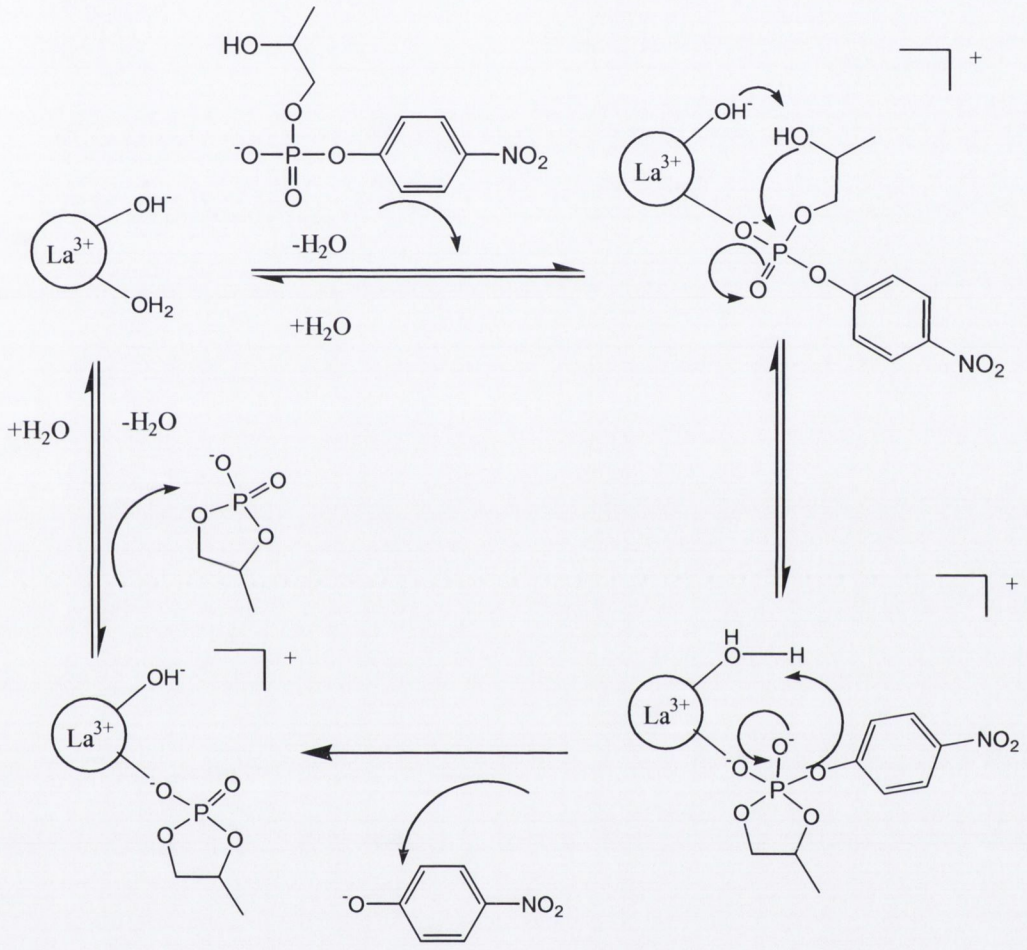

Scheme 4.19. Proposed mechanism for the hydrolysis of HPNP by mononuclear La(III) complex

The situation is more complicated for binuclear systems, however the same principles apply. As yet the minimum number of metal bound water molecules or binding sites required for a cooperative binuclear system, has not been established.[259] These requirements may differ from mononuclear complexes, as highlighted by **Eu.154**. However, mechanisms involving two, three or even four metal bound water molecules can be envisaged for cooperative binuclear systems. This shall be discussed further in section 4.6.3.

It is clear from the pH rate profiles that **La.157**, with its more flexible bridge, is by far the most effective system for the promotion of phosphodiester hydrolysis (Figure 4.27).

This seemed to confirm that the lack of flexibility afforded by the original linker group **120,** was inhibiting the promotion of hydrolysis. The flexibility granted by the alkyl chain allows the two metal centres to act in a more cooperative manner, hence the larger rate enhancements in the hydrolysis of **HPNP**.

In general, all of the binuclear acetamide complexes accelerated the rate of **HPNP** hydrolysis to some extent, displayed a pseudo bell shaped pH dependence, and were found to be significantly more active than the corresponding mononuclear systems. Nevertheless, the rate acceleration provided by the very rigid xylylene spaced systems could be attributed to a simple cumulative effect. However, the most active complex, the more flexible alkyl linked **La.157,** produced a rate enhancement, which was larger than a relative metal ion concentration effect could explain. The four fold rate improvement can be tentatively assigned to the double Lewis acid activation provided by the cooperative action of two metals.[269]

4.4.3 Hydrolysis of HPNP by Coordinately Saturated Complexes

At this point it should be noted that the Cu(II) and Zn(II) complexes of **152** were also synthesised, and their hydrolytic ability tested against the **HPNP** phosphodiester. Neither **Cu.152** nor **Zn.152** were found to be active. It is believed that the fully saturated coordination spheres of the metal ions prohibits them from interacting with the phosphodiester and hence minimizes their cleavage ability. Similar observations have been made by Fry *et al.* who reported the four coordinate binuclear Cu(II) complex **Cu.166**, to be inactive.[270] This highlights the important role played by metal bound water molecules and the need to provide coordinatively unsaturated ligand environments.

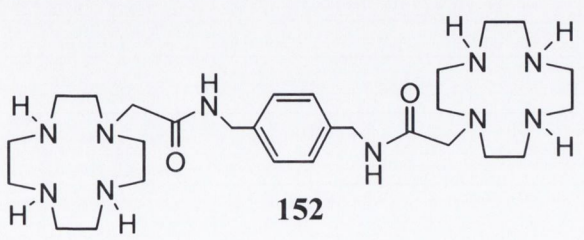

152

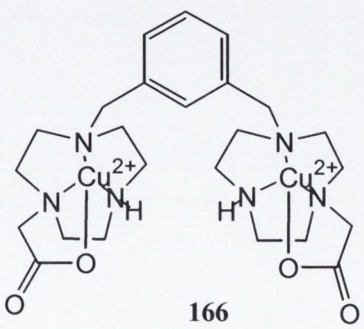

166

4.4.4 Hydrolysis of HPNP by Binuclear Glycine Systems

To date, one of the largest rate enhancements for the hydrolysis of **HPNP**, provided by a mononuclear lanthanide complex, was reported by Gunnlaugsson *et al.* Utilising the hydrophobic nature of the pseudo peptide, glycine methyl ester pendant arms, they reported the La(III) complex **La.39**, which was found to cleave **HPNP** at pH 7.4 37 °C, with a 'pseudo first order' rate constant of 0.410 (±0.026) hr^{-1}, corresponding to a half-life $\tau_{1/2}$ of 1.70 hours, k_{rel} 3417.[251, 252] This enhancement is even greater than that achieved by the cooperative binuclear complex **La.157**, already discussed. The ability to provide these large rate enhancements was attributed to the capability of the complex to form a hydrophobic cavity.

The synthesis of a binuclear lanthanide complex incorporating these "glycine" cofactors was desired in order to improve upon the rate of hydrolysis already obtained by utilising the cooperative effect of two metal ions in conjunction with the glycine pendant arms, which would more closely mimic the hydrophobic nature at the active sites of natural ribonucleases. The synthesis of four new binuclear glycine complexes was discussed earlier in section 4.3.9. This section shall look at the ability of these complexes to promote the hydrolysis of **HPNP**, beginning with the rigid xylylene spaced conjugate **La.162**.

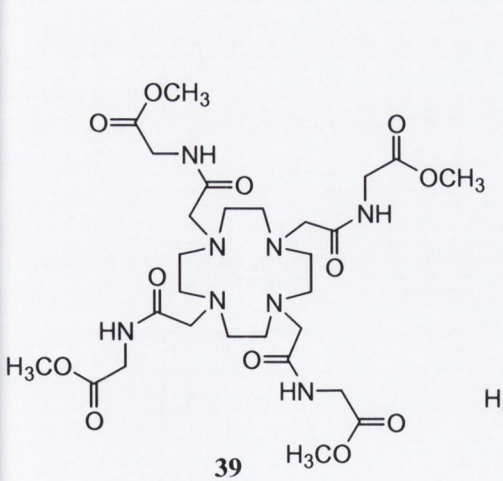

39

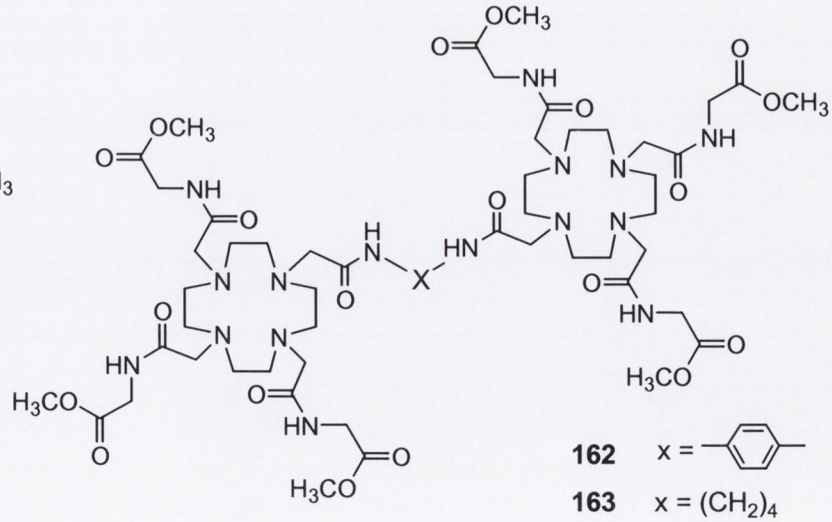

162 x =

163 x = $(CH_2)_4$

164 x = $(CH_2)_6$

The "glycine" complexes ability to promote the hydrolysis of **HPNP** was evaluated in an identical manner to that already described. The kinetics rate profile for **La.162** can be seen in Figure 4.28.

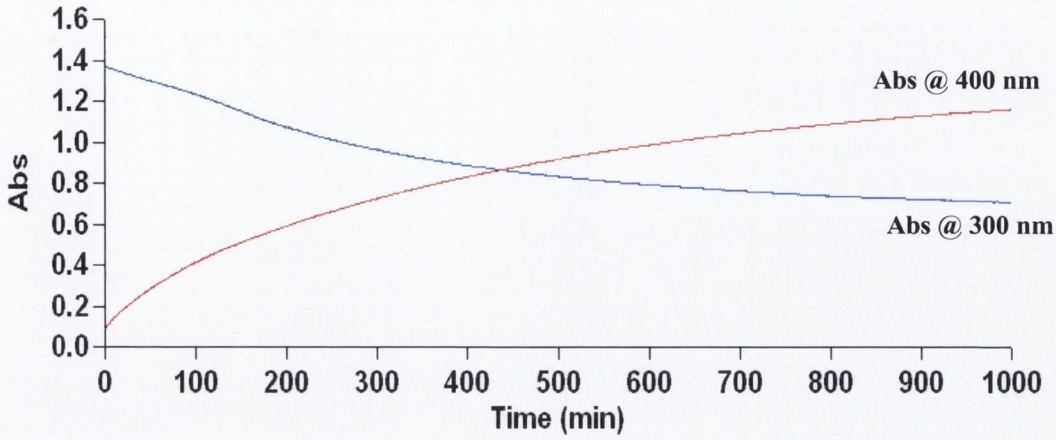

Figure 4.28. Kinetics profile for the hydrolysis of HPNP (0.18 mM) by La.162 at pH 7.4 37°C

At pH 7.4, 37 °C, **La.162** was found to cleave **HPNP** with a 'pseudo first order' rate constant of 0.157 (±0.012) hr^{-1}, corresponding to a half-life of 4.42 hours, giving a rate enhancement (k_{rel}) of *ca.* 1308 over the uncatalysed reaction.[257] This increase in activity represents a large improvement over the xylylene spaced binuclear acetamide complexes **Ln.154, Ln.155** and **Ln.156**, discussed earlier, showing that the effect of the pendant group is quite important. However, this rate acceleration was actually less than that provided by the analogous mononuclear 4-armed complex, **La.39,** reported to be 0.410 (±0.026) hr^{-1}, $\tau_{1/2}$ 1.70 hours, k_{rel} of 3417, at the same pH (7.4).[251] A pH profile was carried out to determine whether the pH was a contributing factor.

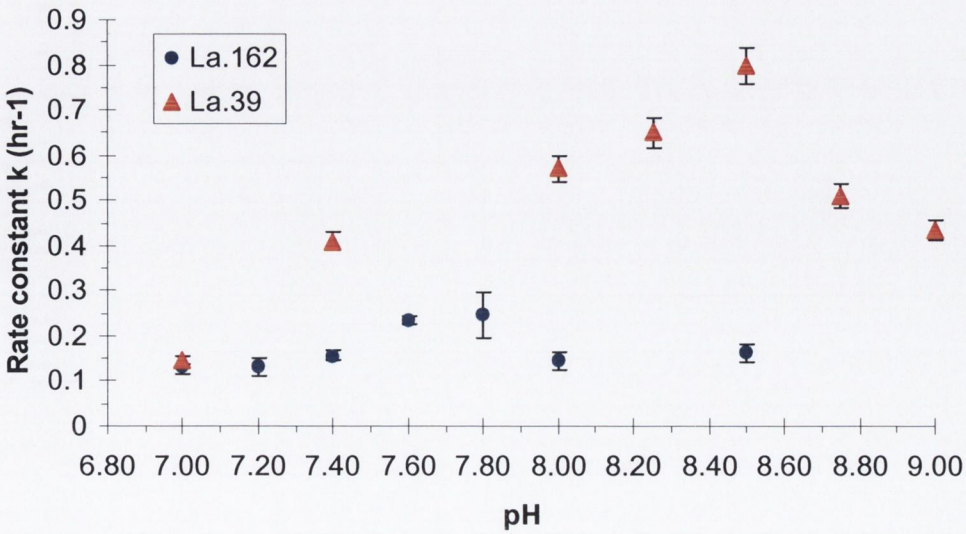

Figure 4.29. pH profile comparing rate constant *k* for the hydrolysis of 0.18 mM HPNP by La.162 and La.39[237]

Comparing the pH profile of **La.162** to the mononuclear complex it can be seen that in this case the mononuclear system is significantly faster than the binuclear system at all pHs (Figure 4.29). Just as in the case of the rigid xylylene binuclear acetamide systems, no evidence of a cooperative effect was observed for **La.162**.

Having evaluated the complex **La.162**, identical measurements were carried out on the other glycine binuclear complexes, **La.163, La.164** and **Eu.164**. The results for these complexes are shown in Table 4.9. All of the complexes were found to promote the hydrolysis of **HPNP** and the kinetic profiles for these three complexes can be seen in the appendix section.

Section 4.11 has shown how changing the spacer moiety can drastically alter the rate of phosphodiester hydrolysis. In the case of the "glycine" systems, once again the more flexible alkyl linked binuclear systems were found to promote the cleavage of **HPNP** to a greater extent than the original, rigid, xylylene linked system (Table 4.9). Nevertheless, in the case of the La(III) complexes the changes were relatively small and not as dramatic as those observed for the binuclear acetamide complexes.

Complex	Rate constant k (h^{-1})	$\tau_{1/2}$ (h)	(k_{rel})
Eu.39	0.153 (0.013)	4.53	1250
La.39	0.410 (±0.026)	1.70	3147
La.162	0.157 (±0.012)	4.42	1308
La.163	0.182 (±0.014)	3.82	1517
La.164	0.201 (±0.045)	3.53	1675
Eu.164	0.477 (±0.034)	1.45	3978

Table 4.9. Hydrolysis of 0.18 mM HPNP at pH 7.4, 37 °C by "glycine" complexes

The results from Table 4.9 show that the greatest increase in activity by the binuclear systems, was observed for **Eu.164**, which showed an almost three fold increase in activity over **La.162** as well as a three fold increase over the corresponding mononuclear complex **Eu.39** at pH 7.4.[220] This three fold increase is right at the limit of what can be considered a cooperative effect.[259] It confirms similar results in the literature, which found that very flexible spacers tend to generate only weak cooperative effect between metal ion centres.[229] The results are somewhat atypical and hence, it was decided to investigate the pH dependence of all the binuclear complexes.

4.4.5 pH Dependence of HPNP Hydrolysis by Binuclear Glycine Systems

An investigation into to pH behaviour of the complexes was conducted by measuring the rate of hydrolysis of **HPNP** at various pHs, in an analogous manner to that already described. The results are shown in Figure 4.30. The pH rate profile of **La.163** is similar to that of **La.164** and can be seen in the appendix. A full pH rate profile for the mononuclear **Eu.39** system was not carried out, although the point at pH 7.4 was reported to be a local maximum.[220] It is also of note that the **Eu.164** complex displays its maximum at pH 7.2 – 7.4. This is important as a ribozyme mimic must function under physiological conditions and thus, it is desirable for the mimic to exhibit its maximum cleaving ability at pH 7.4 to grant the most efficient cleavage.

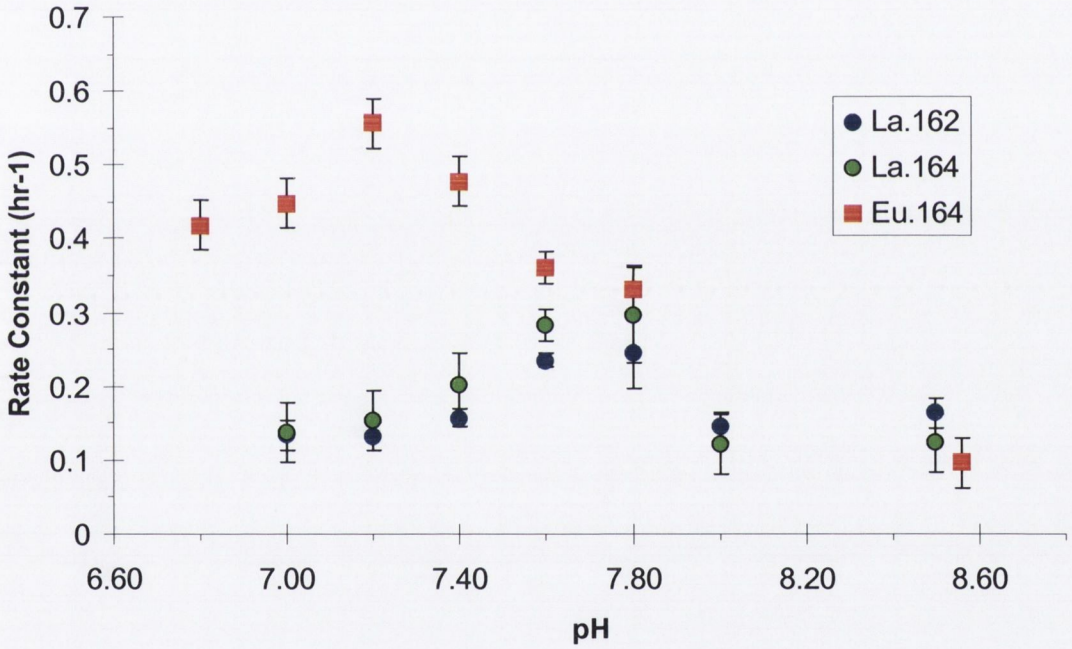

Figure 4.30. pH profile for the hydrolysis of 0.18 mM HPNP at 37 °C by binuclear "Gly" ligands

Once again, pseudo bell shaped pH rate profiles were obtained for each of the complexes, and the more flexible spacers were found to be more active than the rigid xylylene spaced system. Interestingly, the Eu(III) complex was found to be the most active of the binuclear systems. This is in contrast to previous results for the mononuclear systems, which found La(III) complexes to be more active. The larger size of the La(III) ion allows it one extra coordination site, usually occupied by a metal bound water molecule, which aids in the phosphodiester hydrolysis. [220,258] As the binuclear systems now also provide two metal bound water molecules (one from each ion), the dominant factor may become the larger

Lewis acidity of the Eu(III) ion compared to La(III) ion.[218] Yet, as this work is only in its infancy, the scope of it was not to investigate the effect of the metal ion, but to obtain a cooperative effect between the metals, which lead to large rate enhancements over mononuclear systems. Nonetheless, in this case, it was clear that the mononuclear La(III) system was still the most active (Figure 4.29).

A number of factors could be responsible for the decrease in activity. The large rate enhancement observed for the 4-armed **La.39** system was attributed to the formation of a hydrophobic cavity.[251,252] Such a cavity may be prevented from forming here by the steric environment forced upon the complex by the spacer. Also the increased steric bulk of the pendant arms, as well as the relative rigidity of the spacer, in the case of **La.162,** may prevent the two metal centres from approaching one another, thus prohibiting the desired cooperative action and contributing to the lower than expected activity.

4.4.6 Hydrolysis of HPNP by Binuclear Pyridine System

As previously discussed, natural ribozymes are known to utilise groups, which can provide acid-base catalysis to promote the hydrolysis of RNA.[247] The incorporation of pendant groups such as pyridine, which can provide base catalysis, into ribozyme mimics has been shown to improve the rate of phosphodiester hydrolysis.[249] The synthesis of a binuclear lanthanide complex incorporating pyridine pendant arms was discussed in Chapter 4. The ability of this complex to promote the hydrolysis of **HPNP** was evaluated in an identical manner to that described earlier. The kinetics profile of **La.165** can be seen in Figure 4.31.

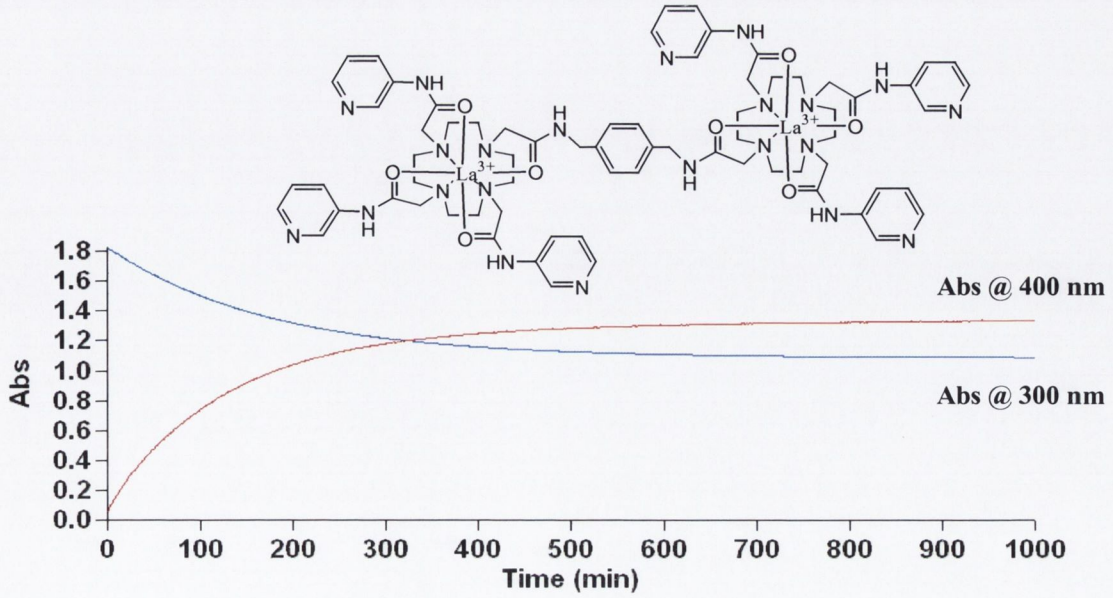

Figure 4.31. Kinetics profile for the hydrolysis of HPNP (0.18 mM) by La.165 at pH 7.4 37°C

The pyridine moiety absorbs at 300 nm and hence the higher absorbance at this point ~ 1.8. At pH 7.4, 37 °C, the binuclear pyridine system **La.165,** was found to cleave **HPNP** with a 'pseudo first order' rate constant of 0.440 (± 0.029) hr^{-1}, corresponding to a half-life of 1.57 hours, giving a rate enhancement (k_{rel}) of *ca.* 3666 over the uncatalysed reaction.[257] This is almost a seven fold increase over the enhancement of **La.155**, again showing the importance of the pendant group. The rate constant for the analogous mononuclear 4-armed complex, **La.158**, was reported to be 0.189 (±0.003) hr^{-1}, $\tau_{1/2}$ of 3.66 hours, k_{rel} of 1578.[249] The hydrolysis of **HPNP** by **La.165** was evaluated as a function of pH (Figure 4.32). It can be seen that **La.165** has its maximum activity at pH 8.0, with a 'pseudo first order' rate constant of 0.611 (±0.005) hr^{-1}, $\tau_{1/2}$ of 1.13 hours, k_{rel} of 5096. This is the largest rate enhancement provided by the binuclear conjugates described here, so far. Pyridine seemed to be an extremely effective pendant group for the hydrolysis of phosphodiesters, however, the two fold rate enhancement over the mononuclear system, while promising, seemed to be cumulative rather than cooperative. Unfortunately, time constraints prevented the synthesis and testing of the more flexible analogues of this system.

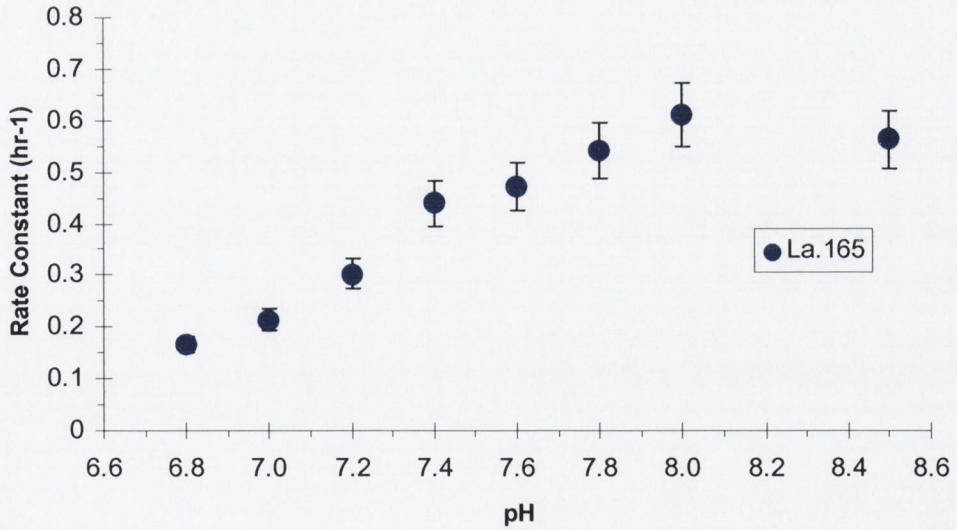

Figure 4.32. pH profile for the hydrolysis of 0.18 mM HPNP by La.165

4.5 Trends in Activity

At this point it is useful to review the activities of the binuclear complexes tested so far. Figure 4.33 compares the rate constant for the hydrolysis of **HPNP** at pH 7.4. It is immediately clear that the choice of pendant arm has a dramatic effect upon the activity of

the complex. It is also evident that larger rate enhancements are observed for the more flexible alkyl bridged complexes. Indeed, so far the rigid xylyene spaced binuclear systems have failed to demonstrate any cooperative effect. One likely explanation for this may be the rigid nature of this spacer, which may prevent the two metal centres from adopting a favourable orientation for binuclear cooperativity.[271, 272]

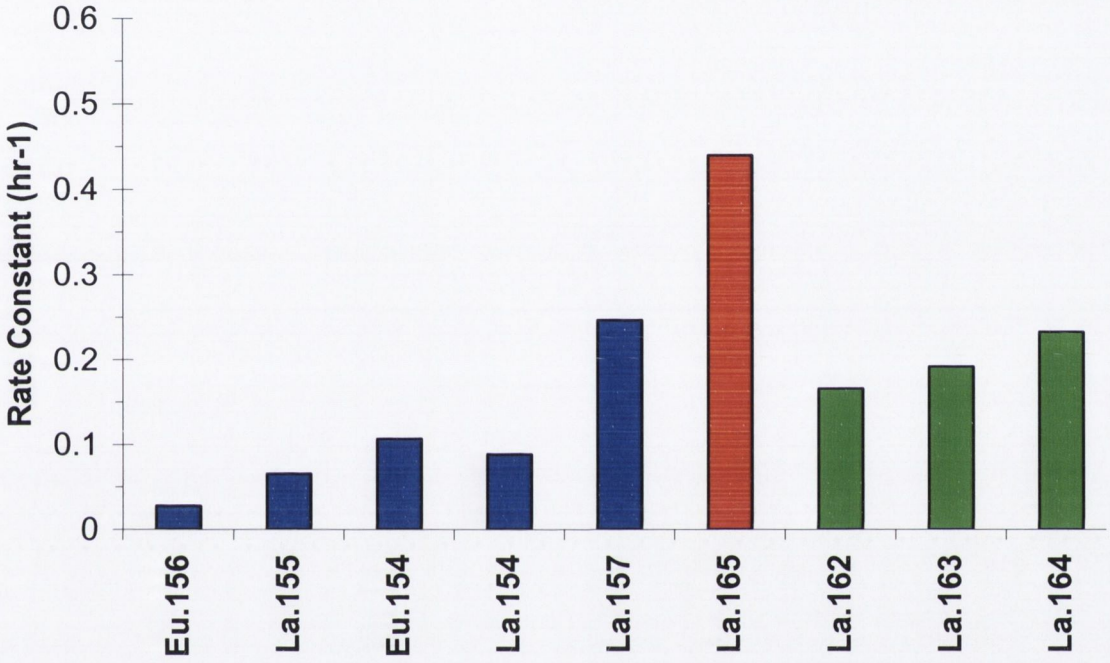

Figure 4.33. Hydrolysis of 0.18 mM HPNP at pH 7.4, 37 °C

By comparing the hydrolysis as a function of pH it can be seen that La(III) and Eu(III) complexes display their maximum activity at different pHs (Figure 4.30). This is due to the differing pK_as of their metal bound water molecules. Although these values have not yet been determined, it is known that the lanthanide contraction causes the heavier lanthanides to have a smaller ionic radius. This results in an increased charge density, which makes the heavier lanthanides stronger Lewis acids. It also results in a decrease in the pK_a of any metal bound water molecules.[273] As such, **Eu.164** was found to peak at a lower pH (7.2) than the **La.164** complex (pH 7.8). Of course the nature of the ligand will also impact upon the Lewis acidity of the metal ion and hence the resulting pK_a of any metal bound water molecules.

4.6 Changing the Spacer: Combining Rigid and Flexible Properties

Up until now, the complexes with the very rigid xylylene spacer **120,** have shown no cooperative enhancement effects. Those with the very flexible alkyl spacers have shown weak cooperative effects with 3 – 4 fold rate enhancements. The spacers seem to be either too rigid or too flexible, to provide the desired cooperativity. A balance between the two extremes is required. Work by Morrow[228] and Breslow,[229] has shown that binuclear Cu(II) and Zn(II) complexes, which utilise a shorter *p*-xylyl spacer that lacks the acetamide functionality, can provide large cooperative rate enhancements over similar mononuclear systems. It was decided to utilise this shorter *p*-xylyl spacer in a binuclear lanthanide system. It would combine the rigid and flexible qualities desired and would also offer another advantage.

It had been noted in the Gunnlaugsson group that leaving the lanthanide ion coordinatively unsaturated was important for phosphodiester hydrolysis. Reducing the number of donor groups, by for example, removing one of the pendant amide arms, resulted in an increase in the number of metal bound water molecules, which in turn led to an increase in the rate of phosphodiester hydrolysis. This was explained by the presence of an extra metal bound water molecule, which in turn provided a better ability to bind and accelerate phosphodiester hydrolysis.[225, 258, 274] As the shorter *p*-xylyl spacer lacks the acetamide functionality, the complex should gain one extra free coordination site.

4.6.1 Hydrolysis of HPNP by Eu.117

The binuclear complex **Eu.117**, was synthesised as described in section 4.3.11. It contained the same dimethyl acetamide pendant arms as the **Eu.156** conjugate discussed in section 4.4.1, however, it differed from the original binuclear system in that it had a shorter bridge, and also left each metal ion with one extra open coordination site. Its ability to promote phosphodiester hydrolysis was tested against the phosphodiester **HPNP** in an analogous manner to that described earlier.

At pH 7.4 and 37 ^{o}C, **Eu.117** was found to cleave **HPNP** with a 'pseudo first order' rate constant of 1.48 (± 0.08) hr^{-1}, corresponding to a half-life of 0.47 hours or 28 minutes (Figure 4.34). This gives an unprecedented rate enhancement (k_{rel}) of *ca.* 12,333 over the uncatalysed reaction.[257]

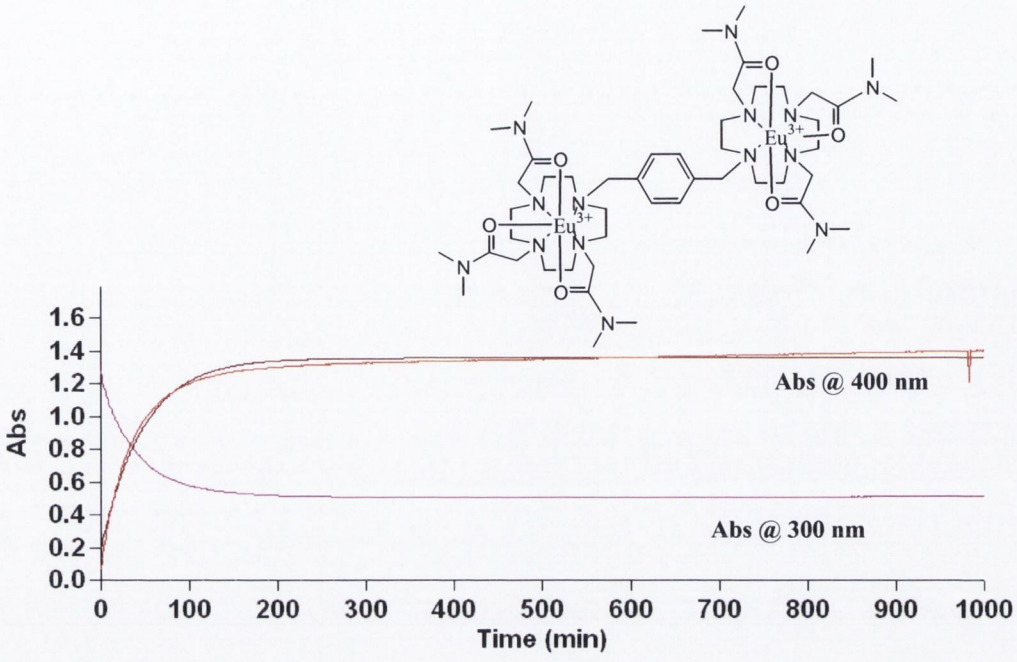

Figure 4.34. Hydrolysis of 0.18 mM HPNP at pH 7.4, 37 °C by Eu.117, $\tau_{1/2}$ 28 minutes

The octadentate mononuclear 4-armed Eu(III) complex was found not to accelerate the rate of hydrolysis to any measurable extent. However, as **Eu.117** possesses one extra coordination site per metal ion than mononuclear 4-armed complex, a more reasonable comparison can be drawn with the heptadentate mononuclear 3-armed Eu(III) complex which, was reported to give a moderate rate enhancement effect, with a rate constant k of 0.052 (± 0.021) hr^{-1}, corresponding to a half-life of 13.32 hours, k_{rel} of *ca.* 243, [275] Therefore, the acceleration provided by the binuclear **Eu.117** complex, represents a 28.5 fold increase over the mononuclear 3-armed system. This is the largest rate enhancement over both the uncatalysed reaction as well as the mononuclear complex, which has yet been observed in the Gunnlaugsson laboratory.

Comparing **Eu.117** to the similar binuclear dimethyl acetamide conjugate **Eu.156**, discussed in section 4.5.1, highlights the importance of the role of the spacer group. Recall that the **Eu.156** conjugate, cleaved **HPNP** with a 'pseudo first order' rate constant of 0.027 (± 0.012) hr^{-1}, corresponding to a half-life of 25.67 hours, k_{rel} of *ca.* 230. The shorter xylene bridged **Eu.117** complex, shows a 75 fold rate increase over the similar **Eu.156** system. The only major differences between the structures are the linking bridge and the increased number of metal bound water molecules. The xylene bridge of **Eu.117** is shorter and more flexible than the very rigid linker **120**. It is believed that this allows the two metal centres to approach each other to a greater extent and hence adopt a favourable orientation for the metal ions to act in a cooperative fashion allowing the double Lewis

acid activation discussed earlier. The shorter spacer also lacks the amide functionality, which leaves an extra coordination site open to be occupied by a metal bound water molecule. As such, each Eu(III) ion was expected to have two metal bound water molecules. Extra metal bound water molecules have previously been shown to accelerate hydrolysis.[274] Although the co-ordinately unsaturated nature of the metal ion undoubtedly plays a role in the enhancement, its effect should not be overestimated as the coordinatively unsaturated analogous 3–armed mononuclear system was reported to have only a moderate rate enhancement effect.

Thus far, all the complexes tested herein, have displayed a significant pH dependence. Consequently, the pH dependence of **Eu.117**, was investigated and shall be detailed in the next section.

4.6.2 pH Dependence of HPNP Hydrolysis by Eu.117

The pseudo first order rate constants for the hydrolysis of **HPNP** by **Eu.117**, at various pHs were evaluated in the manner previously described. The results are presented here in Figure 4.35. Comparing the complex to the binuclear methyl acetamide system **Eu.155**, highlights just how effective the **Eu.117** system is at accelerating the rate of phosphodiester hydrolysis. Recall from section 4.4.1 that a pH profile for the dimethyl acetamide conjugate **Eu.156**, was not investigated as it displayed the poorest activity of the acetamide systems however, it would be expected to have a similar, if smaller, rate profile to that of **Eu.155**.

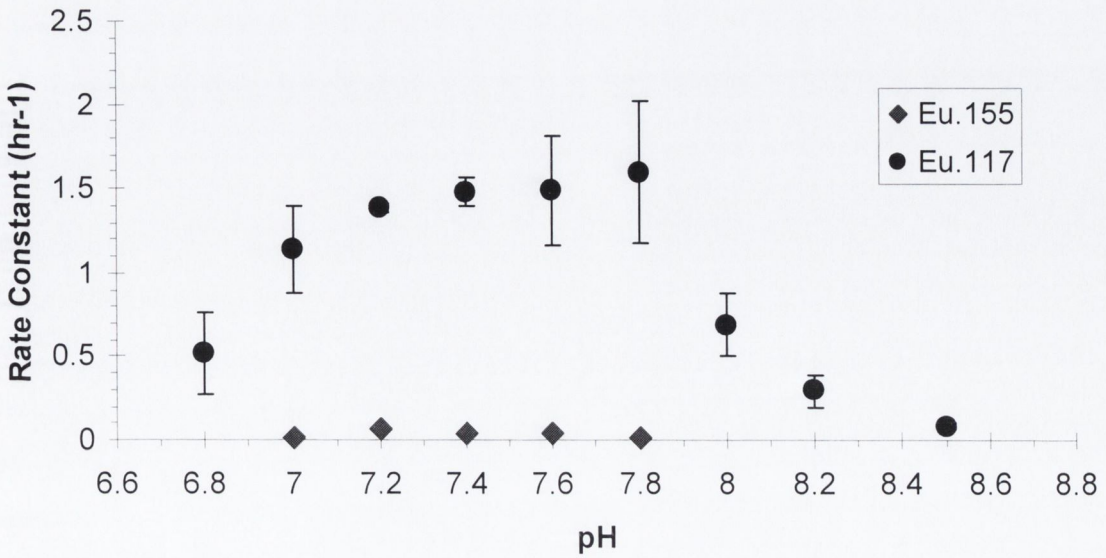

Figure 4.35. pH profile for the hydrolysis of 0.18 mM HPNP by Eu.117

The binuclear complex **Eu.117**, was found to exhibit a pseudo bell shaped pH dependence and boasted its maximum rate enhancement at pH 7.8 with a 'pseudo first order' rate constant of 1.60 (± 0.40) hr^{-1}, corresponding to a half-life of 26 minutes, k_{rel} of *ca.* 13,333. To the best of our knowledge, this is one of the largest reported rate enhancements for the hydrolysis of **HPNP** under aqueous conditions.

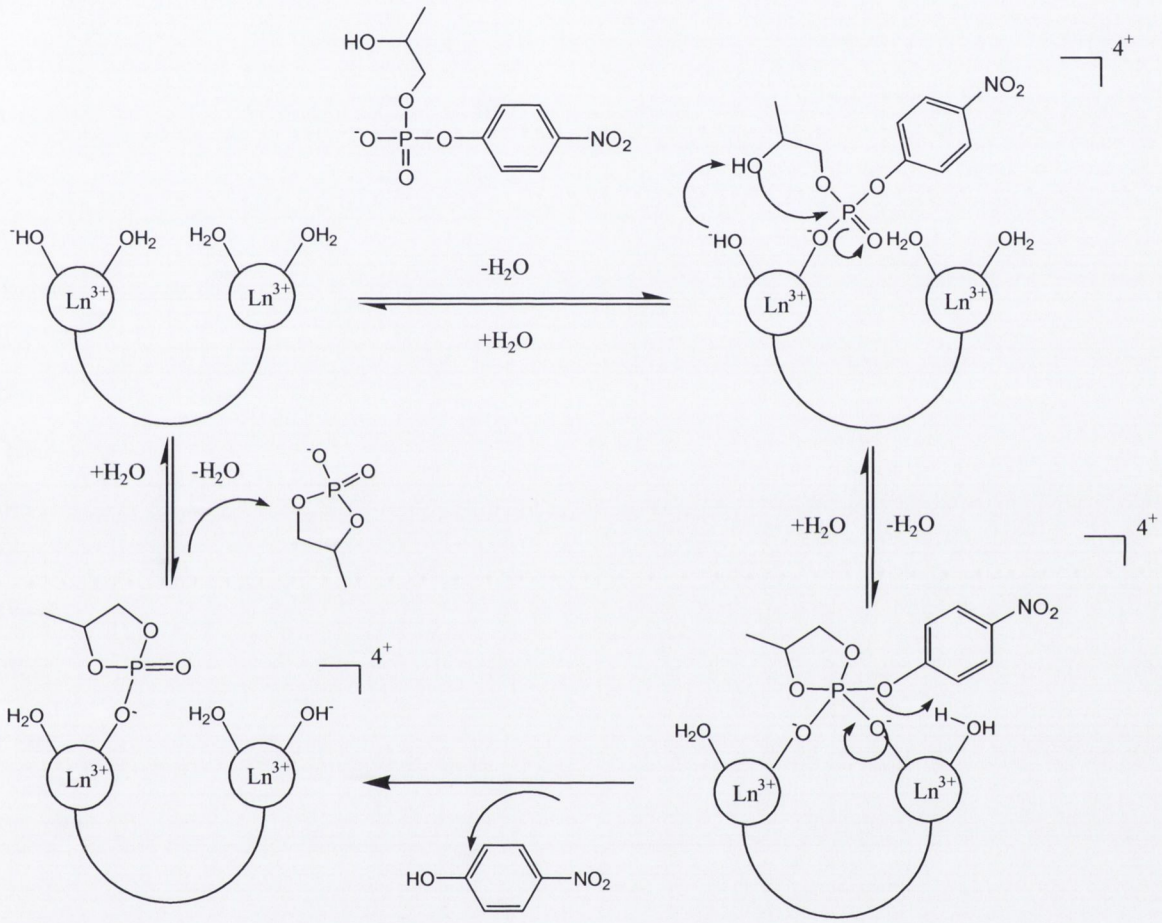

Scheme 4.20. Proposed mechanism for double Lewis acid activation provided by the cooperative action of a binuclear lanthanide system

The reason for this huge increase over the mononuclear system can be attributed to the double Lewis acid activation provided by the cooperative action of the two metal centres. [276, 277, 278] A possible mechanism for the hydrolysis of **HPNP** by a binuclear Ln(III) complex with two metal bound water molecules per ion, is shown in Scheme 4.20. The first step involves binding of **HPNP** to the metal ion by displacement of one of the metal bound water molecules. This activates the phosphodiester towards nucleophilic attack by neutralising the negative charge. A metal bound hydroxide can provide general base catalysis by abstracting a proton from the OH, which in turn acts as an intramolecular

nucleophile and attacks the phosphorous. The resulting five coordinate, negatively charged phosphorane transition state can now be stabilised by double Lewis acid activation using both metal ions. A metal bound water molecule can now provide general acid catalysis, thereby stabilising the leaving group. The final step is the release of the cyclic phosphate with displacement by water. This step must proceed if the process is to be catalytic.

The effect of varying concentration of **Eu.117**, upon the first order rate constant k, is shown in Figure 4.36. A second order rate constant of 2.82 (± 0.22) M^{-1} s^{-1} for the hydrolysis of **HPNP** by **Eu.117** was obtained by calculating the slope of the linear plot of rate constant k, against concentration, [**Eu.117**].[259] This is significantly faster than the second order rate constant of 0.25 M^{-1} s^{-1} for the dinuclear Zn(II) complex **47**, which was reported by Morrow *et al.* to be one of the highest rate constants for the cleavage of **HPNP**.[259] Despite the considerably large second order rate constants, the cleavage of **HPNP** by **Eu.117**, was not catalytic. While, a 2.5 fold excess of **HPNP** was cleaved with a "pseudo first order" rate constant of 0.26 hr^{-1} a four fold excess of **HPNP** could not be fully hydrolysed. The lack of catalytic turnover combined with the considerably large rate constants, points to a strong binding interaction.[259] It is believed that after the cleavage event, the resulting cyclic phosphate is not being released and hence is inhibiting catalytic turnover. In order to elucidate further, ^{31}P NMR studies were conducted.

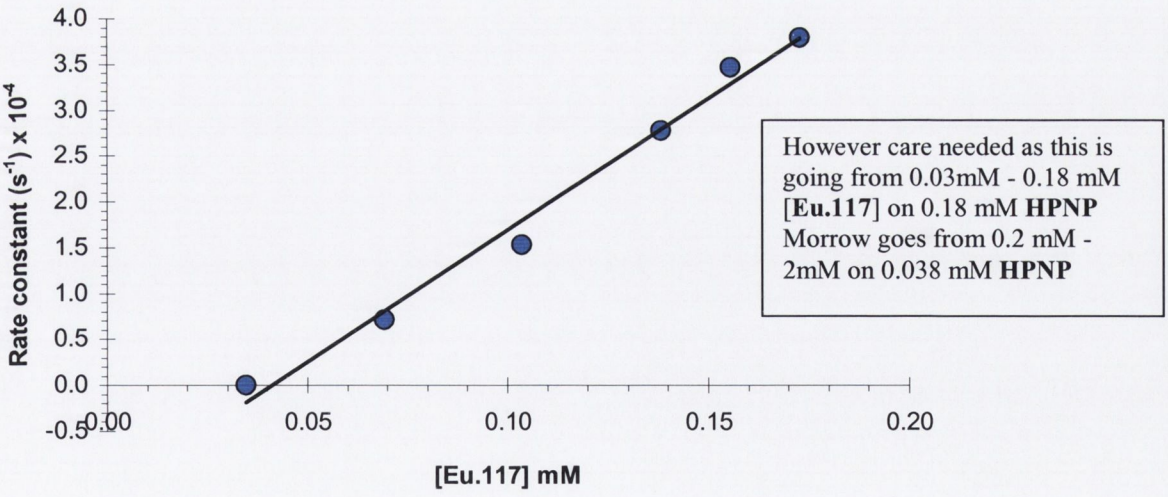

Figure 4.36. Dependence of pseudo first order rate constant for the hydrolysis of HPNP (0.18 mM) on concentration of Eu.117 at pH 7.4 37 °C

The ability of **Eu.117** to bind diethyl phosphate was investigated by ^{31}P NMR. Diethyl phosphate was chosen as it can interact with **Eu.117** in a similar fashion as **HPNP**, but

cannot undergo cleavage itself. Increasing equivalents of diethyl phosphate were added to a 10 mM solution of **Eu.117** in H_2O, and the resulting change in the ^{31}P NMR signal was monitored. The results of this are depicted in Figure 4.37. It can be seen that after the addition of four equivalents of phosphate the plot began to plateau, indicating that binding was complete at this point. What is most striking however, is the drastic change in the ppm of the phosphate signal *ca.* 28.98 ppm. Similar studies upon mononuclear lanthanide complexes in the Gunnlaugsson group, observed the changes in the ^{31}P NMR signal to occur over approximately one ppm. The dramatic changes observed in the case of **Eu.117** indicate a demonstrably strong binding interaction with phosphates, and lends credence to the theory of poor product release, inhibiting catalytic turnover. A higher binding affinity for phosphate by the binuclear systems has previously been observed, and is believed to reflect the stronger electrostatic stabilisation offered by highly cationic, dinuclear complexes.[259, 279]

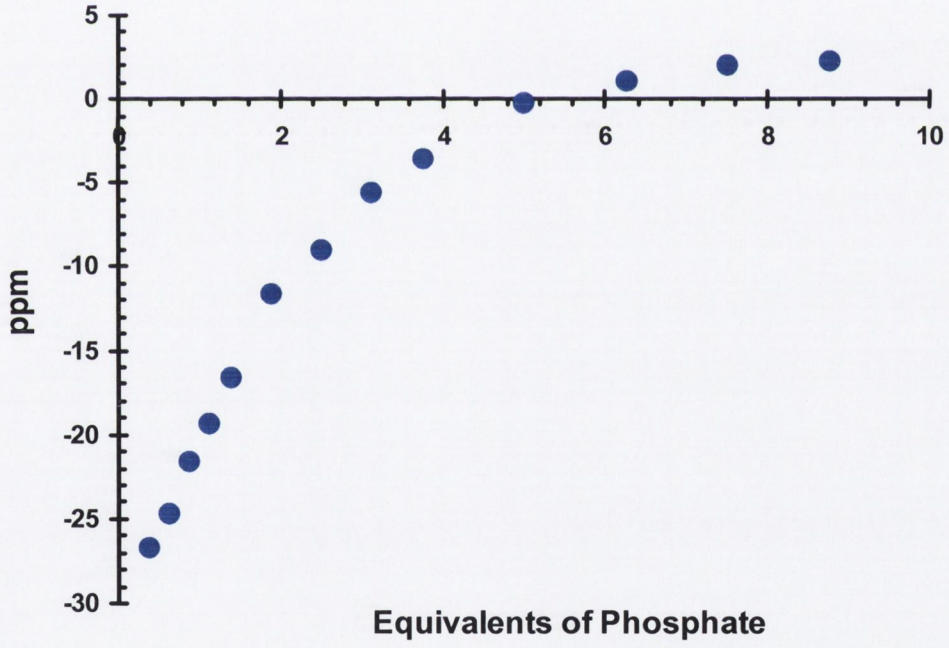

Figure 4.37. Changes in ^{31}P NMR as a function of molar equivalents of diethyl phosphate added to Eu.117

The tetratdendate ligand, EDTA, is known to strongly bind lanthanide ions, however the resulting complexes have been found to be unable to promote the cleavage of phosphodiesters.[223] In order to confirm that the large rate enhancements achieved by **Eu.117**, was not due to the presence of free lanthanide ions in solution, the hydrolysis measurements were repeated in the presence of EDTA. Under similar conditions at pH 7.4,

37 °C, with 0.22 equivalents of EDTA present, the reaction still went to completion, however, the rate constant fell to 0.634 hr^{-1}, corresponding to a half-life of 1.1 hours or 65.5 minutes. With one equivalent of EDTA present again the reaction went to completion but the rate constant was reduced to 0.280 hr^{-1}, giving a half-life of 2.5 hours or 148 minutes. Although the hydrolysis of **HPNP** by **Eu.117** in the presence of 0.22 or 1 equivalent of EDTA is still being promoted by a large extent, the respective 2 fold and 5 fold reduction in activity may indicate that the complex is not stable to exchange with EDTA. However, as each molecule possesses four binding sites, it is possible that the EDTA could be coordinating to the complex itself, and thus reducing the activity by this manner. Further work is needed to confirm the stability of the complex.

The promising results obtained with the cooperative action of the binuclear lanthanide system **Eu.117**, emphasise the importance of this work and highlight the need for future development of the binuclear lanthanide complex area. This shall be further discussed in the next section.

4.7 Conclusion

In conclusion, new bimetallic lanthanide complexes for the cleavage of phosphodiesters have been synthesised, characterised and tested for phosphodiester hydrolysis ability. A wide variety of factors can be seen to effect the activity of the Ln(III) complex cleavage agents, including the choice of metal ion, pH, the choice of pendant arm and, crucially, the spacer group. Examining the choice of metal ion, it was observed that the Eu(III) complexes were at their most active at lower pHs (7.2 for **Eu.164**) then the corresponding La(III) complexes (pH 7.8 for **La.164**). This could be an important factor when tuning for the greatest activity under biological conditions.

The choice of pendant arm was found to also be an extremely important factor in obtaining the greatest rate enhancements. The simple acetamide pendant arms showed only moderate rate enhancements, while better enhancements were observed for the more complex arms, the greatest being observed for the pyridine pendant arms. This improvement can be assigned to the basic nature of the pyridine group allowing it to operate as a general base catalyst.

The choice of spacer group was found to be the central factor in the promotion of hydrolysis. The cooperative action sought between the two metals was prevented by the very rigid nature of the original spacer group **120**. Employing more flexible alkyl chains as

bridging groups, did lead to a modest cooperative rate enhancement, in line with similar results using flexible bridged binuclear systems reported earlier.[227] The alkyl bridged **La.157** was found to be four fold more active than its analogous mononuclear complex.

The largest rate enhancement was provided by the **Eu.117** system which cleaved **HPNP** at pH 7.4 37 °C, with a pseudo first order rate constant of 1.48 hr^{-1}, corresponding to a half-life of 0.47 hours and a rate enhancement k_{rel} of 12,333. Under these conditions, this is one of the largest rate enhancements reported in the literature. It is believed that this large rate enhancement is due to the cooperative action of the two metal centres working in unison. The coordinately unsaturated nature of the metal ion undoubtedly plays a part, nevertheless, it should not be overestimated as the coordinatively unsaturated analogous 3-armed mononuclear system was found to have only a moderate rate enhancement effect.

The **Eu.117** complex did not exhibit catalytic turnover and this was attributed to the strong binding of the substrate resulting in poor product release. The exceptionally strong binding of phosphate by **Eu.117** was demonstrated by the large change in the ^{31}P NMR signal, *ca.* 29 ppm, upon addition of diethyl phosphate.

In summary, **Eu.117** cleaves **HPNP** with a rate constant of 1.48 (± 0.08) hr^{-1}, corresponding to a half-life of 0.47 hours or 28 minutes, an unprecedented rate enhancement (k_{rel}) of *ca.* 12,333, while the corresponding mononuclear 3-armed system was reported to cleave **HPNP** with a rate constant k of 0.052 (± 0.021) hr^{-1}, corresponding to a half-life of 13.32 hours, k_{rel} of *ca.* 243. Further optimisation is possible and shall be discussed as future work in the final section.

4.8 Future Work

It is clear that the acceleration of phosphodiester hydrolysis, by the binuclear compounds discussed throughout this thesis provided by both the nature of the pendant groups and the linker are significant in the acceleration of hydrolysis. In order for cooperative action between two metals to function a rigid spacer with some flexibility must be employed. Future work should concentrate on finding the correct combination of pendant arm and linker to further accelerate the hydrolysis. The significance of the linker cannot be overstated as the fastest rate enhancement was observed with simple amide arms that had previously given the worst result. The ability of similar type spacer groups, such as *o*-xylyl, *m*-xylyl and biphenyl groups, to provide large cooperative enhancements should be investigated. Whether this type of cooperative rate enhancement can be achieved using

more complicated pendant arms, such as the pyridine pendant arms, is also of interest. The pyridine pendant arms should be combined with the shorter *p*-xylyl spacer group. It is imperative that the ability of this compound to cleave the RNA phosphodiester is tested and established. The effect of the metal ion should also be investigated to determine whether preliminary results, which indicated that the Lewis acidity of the metal ion is now more important than the size, are accurate. Determination of pK_a values should also be investigated.



Chapter 5

Experimental Procedures

5.1 General experimental details

Melting points were determined using an Electrothermal IA9000 digital melting point apparatus. Infrared spectra were recorded on a Mattson Genesis II FTIR spectrophotometer equipped with a Gateway 2000 4DX2-66 workstation. Oils were analysed using NaCl plates, solid samples were dispersed in KBr and recorded as clear pressed discs. ^{1}H NMR spectra were recorded at 400 MHz using a Bruker Spectrospin DPX-400 instrument. Tetramethylsilane (TMS) was used as an internal reference standard, with chemical shifts expressed in parts per million (ppm or δ) downfield from the standard. ^{13}C NMR were recorded at 100 MHz using a Bruker Spectrospin DPX-400 instrument. Mass spectrometry was carried out using HPLC grade solvents. Mass spectra were determined by detection using Electrospray on a Micromass LCT spectrometer, using a Shimadzu HPLC or Water's 9360 to pump solvent. The whole system was controlled by MassLynx 3.5 on a Compaq Deskpro workstation. High resolution mass spectra were determined relative to a standard of leucine enkephaline. Elemental analysis was performed in the Microanalytical Laboratory, University College Dublin. Starting materials were obtained from Sigma Aldrich, Strem Chemicals and Fluka. Columns were run using Silica gel 60 (230-400 mesh ASTM) or Aluminum Oxide (activated, Neutral, Brockmann I STD grade 150 mesh). Solvents were used at GPR grade unless otherwise stated.

5.2 Synthesis

2-(4,7-bis-dimethylcarbamoylmethyl-1,4,7,10-tetraaza-cyclododec-1-yl)-*N,N*-dimethyl-acetamide (100) [171]

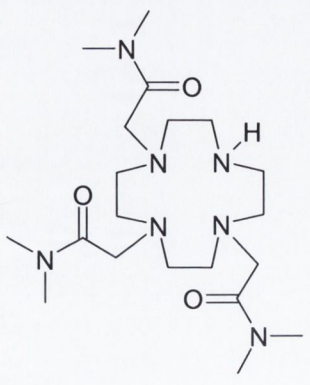

1, 4, 7, 10-tetraazacyclododecane, **99**, (10.00 g, 58.04 mmol) and $NaHCO_3$ (21.10 g, 174.13 mmol) were placed in a 150 mL RBF with MeCN (40 mL). The RBF was placed in a ice bath and allowed to cool. **98a** (14.60 g, 174.13 mmol) in MeCN (10 mL) was added quickly and the solution was stirred at 0 °C for 5 minutes and then refluxed for 96 hours. The solution was filtered and the solvent was then removed. The residue was suspended in CH_2Cl_2, filtered and then purified by alumina column chromatography using gradient elution 100 → 80:20 CH_2Cl_2:MeOH(NH_3). This yielded a white foam, 8.63 g, 35 %. Calculated for $C_{20}H_{42}N_7O_3$ [M+H] m/z = 428.3344. Found m/z = 428.3349. δ_H (400 MHz, $CDCl_3$) 9.99 (s, 1H, NH),

3.59 (s, 2H, CH_2CO), 3.58 (s, 4H, CH_2CO), 3.09 (s, 8H, CH_2), 3.04 (s, 3H, CH_3), 2.97 (s, 6H, CH_3), 2.89 (s, 9H, CH_3), 2.84 (s, 8H, $CH_{2cyclen}$). δ_C (100 MHz, $CDCl_3$) 169.9, 169.8, 55.2, 53.3, 51.2, 50.5, 49.3, 45.7, 36.4, 36.0, 34.9. Mass Spectrum: (MeOH, ES+) *m/z* Expected: 427.3 Found: 428.3 [M+H], 450.4 [M+Na]. IR υ_{max} (cm^{-1}) 3434, 2927, 2852, 1637, 1508, 1475, 1402, 1338, 1261, 1103, 1064, 1022, 881, 806, 769, 667, 649, 574, 484.

2-(4,7-bis-methylcarbamoylmethyl-1,4,7,10-tetraaza-cyclododec-1-yl)-*N*-methyl-acetamide (107)[171]

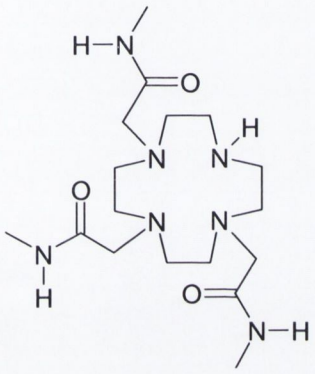

1, 4, 7, 10-tetraazacyclododecane (0.37 g, 2.13 mmol) and $NaHCO_3$ (0.54 g, 6.39 mmol) were placed in a 150 mL RBF with MeCN (15 mL). The RBF was placed in a ice bath and allowed to cool. **98b** (0.71 g, 6.60 mmol) in MeCN (3 mL) was added quickly and the solution was stirred at 65 °C for 72 h. The solution was filtered through celite and the solvent was removed. The residue was suspended in EtOH, filtered and then precipitated from ether and the desired product was isolated as a cream foam, 0.48 g, 58 %. Calculated for $C_{17}H_{36}N_7O_3$ [M+H] m/z = 386.2880. Found m/z = 386.2874. δ_H (400 MHz, $CDCl_3$) 7.59 (s, 1H, NH), 7.30 (s, 2H, NH), 3.06 (s, 4H, CH_2CO), 2.96 (s, 2H, CH_2CO), 2.75 (d, 6H, J = 4.5 Hz, CH_3), 2.76 (d, 3H, J = 4.5 Hz, CH_3), 2.60 (s, 4H, CH_2), 2.58 (s, 4H, CH_2), 2.53 (s, 4H, CH_2), 2.49 (s, 2H, CH_2). δ_C (100 MHz, $CDCl_3$) 171.5, 171.4, 59.5, 57.5, 53.3, 52.6, 51.8, 46.1, 25.9, 25.7. Mass Spectrum: (MeOH, ES+) *m/z* Expected: 385.5 Found: 386.3 [M+H], 408.4 [M+Na]. IR υ_{max} (cm^{-1}) 3430, 2846, 2103, 1643, 1567, 1456, 1415, 1367, 1311, 1257, 1164, 1111, 989, 482.

Procedure 1: General procedure for the synthesis of compounds 98[172]

The relevant amine was placed in a RBF with NaOH (1 equivalent) and CH_2Cl_2 (25 mL). The solution was cooled to –15 °C. Chloroacetyl chloride (1 equivalent) was dissolved in CH_2Cl_2 (20 mL) and added dropwise over 1 hour and the solution was left stirring at room temperature overnight. The organic and aqueous layers were then separated and the aqueous layer was washed with CH_2Cl_2 (2 x 15 mL). The organic extracts were combined and washed with 0.1 M HCl (3 x 10 mL). The organic layer was then dried over K_2CO_3 and the solvent was removed.

2-chloro-*N*,*N*-dimethyl-acetamide (98a)[172]

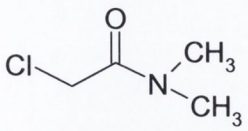

98a was synthesised by following Procedure 1, using *N, N*-dimethylamine 60 % aqueous solution (6.30 g, 0.14 mol), along with NaOH (5.60 g, 0.14 mol), CH_2Cl_2 (50 mL) and chloroacetyl chloride (15.82 g, 0.14 mol). The product was obtained as a clear oil, 7.88 g, 46 %. δ_H (400 MHz, $CDCl_3$) 4.02 (s, 2H, CH_2), 3.02 (s 3H, CH_3), 2.90 (s 3H, CH_3). δ_C (100 MHz, $CDCl_3$) 166.0, 40.7, 37.0, 35.3.

2-chloro-*N*-methyl-acetamide (98b)[172]

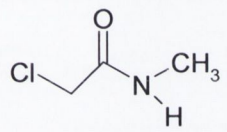

98b was produced according to Procedure 1, using *N*-methylamine 40 % aqueous solution (10.00 g, 0.32 mol), NaOH (12.9 g, 0.32 mol), CH_2Cl_2 (25 mL) and chloroacetyl chloride (36.4 g, 0.32 mol). **98b** was isolated as a clear oil which solidified upon cooling, 10.60 g, 30 %. δ_H (400 MHz, $CDCl_3$) 6.67 (bs, 1H, NH), 4.03 (s, 2H, CH_2), 2.87 (s, 3H, CH_3). δ_C (100 MHz, $CDCl_3$) 166.0, 42.1, 26.0.

5-amino-[1,10]-phenanthroline (102)[174]

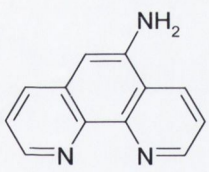

5-Nitro-[1,10]-phenanthroline (**101**) (0.50 g; 2.22 mmol) and Pd/C (5%; 0.12 g; 1.11 mmol) were placed in a tri necked round bottomed flask, dried under vacuum and put under argon. Absolute ethanol (150 mL) was added via syringe. Hydrazine mono hydrate (0.35 g; 11.1 mmol; 0.35 mL) was then added dropwise. The solution turned yellow and was refluxed for forty hours after which, it was filtered through celite to remove the palladium. The filtrate was then evaporated at reduced pressure. The resulting yellow solid was triturated with ether (3 x 15 mL) and dried under vacuum. 0.41 g; 93% yield. Melting point 250 °C (lit m.p. 245 – 246 °C).[174] δ_H(400 MHz, $CDCl_3$) 9.18 (d, 1H, J = 4.0 Hz, H_2), 8.95 (d, 1H, J = 4.0 Hz, H_9), 8.29 (d, 1H, J = 8.0 Hz, H_4), 8.01 (d, 1H, J = 8.0 Hz, H_7), 7.68 (dd, 1H, J = 8.0 Hz, 4.0 Hz, H_3), 7.53 (dd, 1H, J = 8.0 Hz, 4.0 Hz, H_8), 6.87 (s, 1H, H_6), 6.15 (s, 2H, NH_2). δ_c (100 MHz, $CDCl_3$) 149.3, 144.8, 142.6, 132.7, 130.8, 130.5, 123.2, 122.1, 121.8, 101.7.

2-chloro-*N*-[1,10]phenanthrolin-5-yl-acetamide (103)

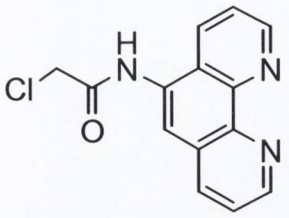

5-Amino-[1,10]–phenanthroline, **102**, (0.30 g, 1.54 mmol) was placed in a round bottomed flask under argon. THF (dry, 55 mL) and triethylamine (0.16 g, 1.58 mmol, 0.22 mL) were added and the suspension was stirred for 30 mins. The mixture was cooled to 0 °C before chloroacetyl chloride (0.213 g, 1.89 mmol, 0.22 mL) in THF (5 mL) was added dropwise. The mixture was left to stir overnight at room temperature. The solution was washed with a 5% $NaHCO_3$ aqueous solution and the organic layer was collected, evaporated, and the residue washed with water and ether to yield a brown solid, 0.241 g, 59 %. M.P. 240 °C. Calculated for $C_{14}H_{10}N_3OCl$: C, 61.89; H, 3.71; N, 15.47. Found: C, 60.84; H, 3.71; N, 14.84. Calculated for $C_{14}H_{11}N_3OCl$: [M+H] *m/z* = 272.0579. Found: *m/z* = 272.0591. δ_H (400 MHz, $CDCl_3$) 9.27 (d, 1H, *J* = 4.0 Hz, H_2), 9.18 (d, 1H, *J* = 4.0 Hz, H_9), 8.91 (s broad, 1H, NH), 8.39 (s, 1H, H_6), 8.33 (d, 1H, *J* = 8.0 Hz, H_4), 8.27 (d, 1H, *J* = 8.0 Hz, H_7), 7.74 (dd, 1H, *J* = 8.0 Hz, *J* = 4.0 Hz, H_3), 7.67 (dd, 1H, *J* = 8.0 Hz, *J* = 4.0 Hz, H_8), 4.43 (s, 2H, CH_2). δ_c (100 MHz, $CDCl_3$) 164.2, 150, 149.8, 146.1, 144.2, 138.9, 137.2, 135.6, 128.5, 127.6, 123.2, 122.6, 119.2, 42.8. Mass Spectrum: (MeOH, ES+) *m/z* Expected: 272.0. Found: 272.0 [M+H]. IR υ_{max} (cm^{-1}) 1687, 1541, 1422, 1318, 1250, 1153, 1130, 896, 804, 739, 653.

N-[1,10]phenanthrolin-5-yl-2-(4,7,10-tris-dimethylcarbamoylmethyl-1,4,7,10 teraaza-cyclododec-1-yl)-acetamide (104)

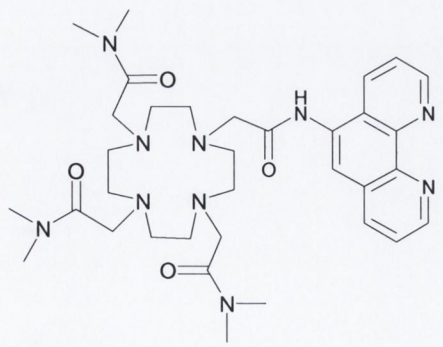

2-(4,7-Bis-dimethylcarbamoylmethyl-1,4,7,10 tetraazacyclododec-1-yl)-*N,N*-dimethyl-acetamide, **100**, (0.23 g, 0.53 mmol), 2-chloro-*N*-[1,10]phenanthrolin-5-yl-acetamide, **103**, (0.17 g, 0.64 mmol) and Cs_2CO_3 (0.21 g, 0.64 mmol) were dissolved in DMF (10 mL) and refluxed overnight under argon. The mixture was allowed cool and then filtered through celite. The solvent was then evaporated under reduced pressure and the resulting brown oil purified by alumina column chromatography using gradient elution 100 → 95:5 CH_2Cl_2:MeOH. This successfully yielded a pale brown solid, 0.135 g, 38 %. Calculated for $C_{34}H_{51}N_{10}O_4$: [M+H] *m/z* = 663.4069. Found: *m/z* = 663.4095. δ_H (400 MHz, $CDCl_3$) 11.12 (s, 1H, NH),

9.09 (d, 1H, J = 8.2 Hz, H_{2phen}), 8.98 (m, 2H, $H_{4+9phen}$), 8.04 (m, 2H, $H_{6+7phen}$), 7.45 (m, 2H, $H_{3+8phen}$) 3.86 (broad s, 2H, CH_2), 3.02-2.05 (broad m, 42H, CH_2, CH_3). δ_c (100 MHz, $CDCl_3$) 172.2, 170.5, 170.4, 149.1, 148.6, 145.7, 144.2, 135.0, 133.9, 132.6, 127.9, 122.3, 121.8, 119.2, 56.4, 54.4, 54.3, 52.9, 51.2, 50.5, 50.0, 35.5, 34.9. Mass Spectrum: (MeOH, ES+) *m/z* Expected: 663.4. Found: 663.4 [M+H]. IR υ_{max} (cm^{-1}) 3413, 2968, 2825, 2361, 1647, 1536, 1507, 1456, 1408, 1347, 1299, 1262, 1226, 1151, 1104, 1062, 1004, 951, 901, 828, 742, 630.

Eu.104.$(CF_3SO_3)_3$.(H_2O)

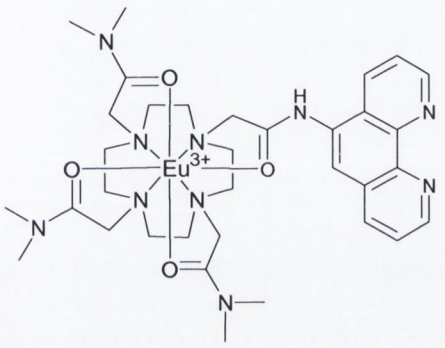

104 (16.00 mg, 24.1 μmol) and $Eu(CF_3SO_3)_3$ (Europium triflate) (15.90 mg, 26.5 μmol) were dissolved in acetonitrile (5 mL). The solution was freeze-pump-thawed twice in order to remove any oxygen. The reaction was refluxed under argon overnight. The complex was precipitated from ether and then from CH_2Cl_2, before being collected by filtration and dried under vacuum. The isolated product was a light brown hydroscopic solid, 27.60 mg, 90 %. Calculated for $C_{35}H_{51}N_{10}O_7F_3SEu$: *m/z* = 965.2876. Found: *m/z* = 965.2827. [M+1Trif]. δ_H(400 MHz, D_2O) 28.3, 9.1, 8.1, 7.6, 3.21, 2.8, 1.0, 0.2, -3, -8, -12, -15. Mass Spectrum: (MeOH, ES+) *m/z* Expected: 813.8 Found: 406.9 [M^+/2], 481.8 [M+Triflate/2]. IR υ_{max} (cm^{-1}) 3362, 2945, 2833, 1656, 1449, 1414, 1278, 1257, 1114, 1028.

N-[1,10]phenanthrolin-5-yl-acetamide (106)[174]

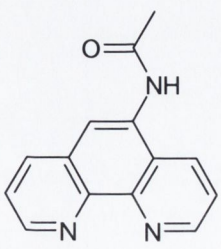

5-Amino-[1,10]-phenanthroline, **102**, (0.10 g, 0.51 mmol) was placed in a round bottomed flask with acetic anhydride (0.11 g, 1.00 mmol), $NaHCO_3$ (0.05 g, 0.59 mmol) and MeOH (15 mL). The solution was refluxed overnight. The solvents were removed and the residue was suspended in CH_2Cl_2 (25 mL) and filtered. The CH_2Cl_2 was then washed with water (2 x 10 mL). The solvent was then removed yielding a white solid, 0.08 g, 64 %. M.P. 236 °C (lit M.P. 231 – 233 °C). δ_H (400 MHz, DMSO) 10.17 (s,1H, NH), 9.11 (s, 1H, H_2), 9.02 (s,1H, H_9), 8.63 (d, 1H, *J* = 8.0 Hz, H_4), 8.44 (d, 1H, *J* = 8.0 Hz, H_7), 8.16 (s, 1H, H_6), 7.82 (dd, 1H, *J* = 8.0 Hz, 4.5

Hz, H_3), 7.74 (dd, 1H, J = 8.0 Hz, 4.5 Hz, H_8), 2.24 (s, 3H, CH_3). Mass Spectrum: (MeOH, ES+): *m/z* Expected: 236.0 Found: 236.9 [M+H].

2-{4,7-bis-dimethylcarbamoylmethyl-10-[4-(4,7,10-tris-dimethylcarbamoylmethyl-1,4,7,10-tetraaza-cyclododec-1-ylmethyl)-benzyl]-1,4,7,10-tetraaza-cyclododec-1-yl}-*N*,*N*-dimethyl-acetamide (117)

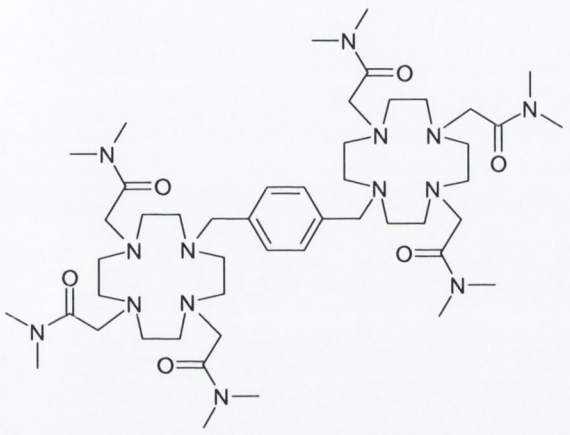

Tris dimethylacetamide cyclen (**100**) (0.22 g, 0.51 mmol), α,α-dichloro-*p*-xylene (**118**) (0.04 g, 0.24 mmol) and Cs_2CO_3 (0.12 g, 0.37 mmol) and KI (0.08 g, 0.49 mmol) were dissolved in MeOH (25 mL) and refluxed for 120 hours. The solvent was evaporated and the residue was then suspended in $CHCl_3$ and filtered. The volume was then reduced and the solution was left to stand. The resulting crystals were filtered and washed with cold $CHCl_3$. The desired product was isolated as off white crystals, 0.04 g, 10 %. M.P. decomp above 118 °C. Calculated for $C_{48}H_{88}N_{14}O_6Na_2.(H_2O)_2.CHCl_3$: C, 50.79; H, 8.09; N, 16.92. Found: C, 50.82; H, 7.95; N, 17.13. Calculated for $C_{48}H_{90}N_{14}O_6$ [M+2H] m/z = 958.7168. Found m/z = 958.7117 (- 5.3 ppm). δ_H (400 MHz, D_2O) 7.30 (s, 4H, Ar), 3.95 (s, 4H, Ar-CH_2), 3.22 (s, 4H, CH_2), 2.99 (s, 8H, CH_2), 2.79 (bm, 68H, cyclen + CH_3). δ_C (100 MHz, D_2O) 172.5, 172.1, 136.5, 129.8, 57.7, 54.5, 53.8, 50.8, 50.3, 49.7, 48.3, 35.5, 35.1, 34.8. Mass Spectrum: (MeOH, ES+) *m/z* Expected: 956.7 Found: 479.1 [M+H]/2, 490.0 [M+Na]/2, 500.9 [M+K]/2. IR υ_{max} (cm^{-1}) 3442, 2937, 2829, 1639, 1507, 1453, 1404, 1348, 1262, 1102, 1006, 819, 631.

Tb.117.$(CF_3SO_3)_6.(H_2O)_4$

117 (26.00 mg, 27.2 μmol) and $Tb(CF_3SO_3)_3$ (33.00 mg, 54.4 μmol) were placed in a 50 mL RBF. MeOH (15 mL) was added and the solution was refluxed at 75 °C overnight. The solution was filtered and the solvent was then removed. The residue was triturated with CH_2Cl_2 (3 x 20 mL). The residue was then dissolved in MeOH (5 mL) and added dropwise to ether (150 mL). The resulting precipitate was filtered, allowing the collection of a pale

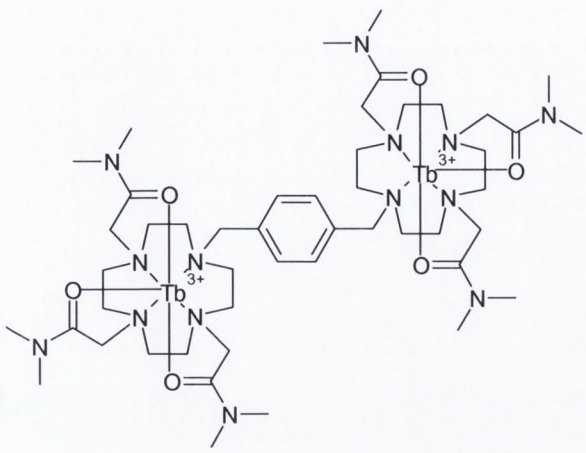

yellow solid, 24.00 mg, 41 %. M.P. decomp above 170 °C. Calculated for $C_{47}H_{93}N_{14}O_6Tb_2.(CF_3SO_3)_6.(H_2O)_2.(CH_2Cl_2)_4$ C, 27.06; H, 3.86; N, 7.75. Found: C, 26.68; H, 3.74; N, 7.59. δ_H (400 MHz, D_2O) 120.25, 85.41, 74.99, 72.99, 59.79, 34.95, 31.35, 19.33, 13.33, 7.48, 5.44, 3.54, 3.31, 3.12, 1.17, –14.75, –15.76, –20.76, –37.78, –46.99, –61.40, –98.04, –106.25, –122.88. Mass Spectrum: (MeOH, ES+) m/z Expected: 1274.5. Found: 573.5 [M+3 triflate]/3. IR υ_{max} (cm^{-1}) 3460, 2939, 1624, 1508, 1458, 1409, 1259, 1165, 1082, 1031, 959, 826, 639, 574, 517, 468.

Eu.117.$(CF_3SO_3)_6.(H_2O)_4$

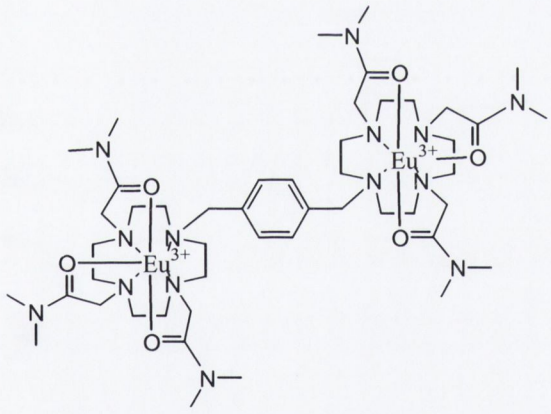

117 (50.00 mg, 52.30 μmol) and $Eu(CF_3SO_3)_3$ (65.80 mg, 109.83 μmol) were placed in a 50 mL RBF. MeOH (15 mL) was added and the solution was refluxed overnight. The solution was filtered and the solvent was removed. The residue was suspended in EtOH (2 mL) and added dropwise to swirling CH_2Cl_2 (75 mL). The resulting precipitate was filtered and triturated with CH_2Cl_2 (2 x 20 mL). The desired product was isolated as a pale yellow solid, 69.00 mg, 59 %. Calculated for $C_{50}H_{88}N_{14}O_{12}F_6S_2{}^{151}Eu^{153}Eu$ [M+2Triflate] m/z = 1558.4463. Found m/z = 1558.4404 (–3.8 ppm). δ_H (400 MHz, d-acetone) 36.02, 26.52, 19.14, 17.02, 12.88, 11.32, 8.30, 4.72, 3.70, 2.85, 1.24, 0.83, –0.18, –1.40, –2.69, –6.45, –8.68, –12.48, –14.39, –20.64, –22.99, –25.01, –25.90. Mass Spectrum: (MeOH, ES+) m/z Expected: 1262.5. Found: 569.14 [M+3 triflate]/3, 389.61 [M+2 triflate]/4. IR υ_{max} (cm^{-1}) 3458, 2941, 2351, 1626, 1410, 1257, 1168, 1082, 1031, 959, 825, 762, 638, 575.

Procedure 2: General experimental procedure for bis systems 120-124.

The relevant aromatic diamine was placed in a 100 mL RBF with NaOH (4 equivalents) and dissolved in H_2O. The solution was placed in an acetone/ice bath and allowed to cool. Chloroacetyl chloride (4 equivalents) was then added dropwise over 1 hour. The solution was left to stir overnight. The solution was then filtered and the precipitate washed with water and ether.

1,4-bis-(2-chloro-acetylamino)-xylyene (120)

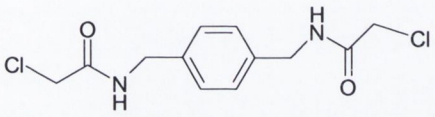

120 was synthesised according to Procedure 2, using *p*-xylylenediamine (**119**) (0.50 g, 3.67 mmol), NaOH (0.59 g, 14.70 mmol), H_20 (10 mL) and chloroacetyl chloride (1.66 g, 14.70 mmol). The product was isolated as white solid, 0.79 g, 75% yield. M.P. 206 - 207 °C. Calculated for $C_{12}H_{14}N_2O_2Cl_2$: C, 49.85; H, 4.88; N, 9.69. Found: C, 49.64; H, 4.75; N, 9.55. Calculated for $C_{12}H_{14}N_2O_2Cl_2Na$ [M+Na] *m/z* = 311.0330. Found *m/z* = 311.0339 (+ 2.8 ppm). δ_H (400 MHz, DMSO) 8.72 (b.s, 2H, N-H), 7.22 (s, 4H, Ar-H), 4.26 (d, 4H, *J* = 6.0 Hz, CH_2NH), 4.11 (s, 4H, CH_2Cl). δ_C (100 MHz, DMSO) 165.9, 137.5, 127.3, 42.6, 42.2. Mass Spectrum: (MeOH, ES+): *m/z* Expected: 288.0. Found: 311.0 [M+Na], 326.9 [M+K]. IR υ_{max} (cm^{-1}) 3280, 3072, 2952, 1656, 1549, 1415, 1267, 1235, 1066, 1001, 831, 769, 680, 547, 416.

1,2 –bis–(2-chloro-acetylamino)-benzene (121)

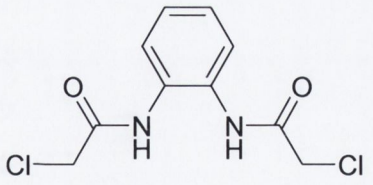

121 was produced according to Procedure 2, using *o*-diamino benzene (2.00 g, 18.50 mmol), NaOH (2.96 g, 74.00 mmol), H_2O (80 mL) and chloroacetyl chloride (12.50 g, 110.00 mmol) The desired product was found to be a grey solid, 2.87 g, 60% yield. M.P. = 198 °C. Calculated for $C_{10}H_{11}N_2O_2Cl_2$ [M+H] *m/z* = 261.0198. Found *m/z* = 261.0195 (– 0.9 ppm). δ_H (400 MHz, $CDCl_3$) 8.67 (s, 2H, N-H), 7.55 (s, 2H, Ar-H), 7.33 (s, 2H, Ar-H), 4.25 (s, 4H, CH_2Cl). δ_C (100 MHz, $CDCl_3$) 164.7, 129.2, 126.8, 125.1, 42.3. Mass Spectrum: (MeOH, ES+): *m/z* Expected: 260.0. Found: 260.9 [M+H], 282.9 [M+Na], 300.8 [M+K]. IR υ_{max} (cm^{-1}) 3255, 1667, 1655, 1596, 1550, 1516, 1451, 1411, 1339, 1283, 1230, 1143, 766, 706, 536.

2,5–bis–(2-chloro-acetylamino)-pyridine (122)

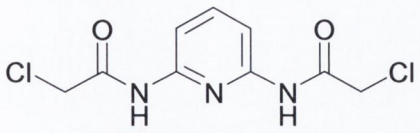

122 was synthesised following Procedure 2, using *m*-diamino pyridine (1.50 g, 13.70 mmol) with NaOH (2.20 g, 55.00 mmol), H_2O (100 mL) and chloroacetyl chloride (15.55 g, 138.00 mmol). This yielded the desired product as a grey solid, 0.29 g, 8 % yield. M.P. 156 °C. Calculated for $C_9H_{10}N_3O_2Cl_2$ [M+H] *m/z* = 262.0150. Found *m/z* = 262.0160 (+ 3.9 ppm). δ_H (400 MHz, DMSO) 8.66 (s, 2H, NH), 7.98 (d, 2H, *J* = 8.0 Hz, Ar-H), 7.81 (dd, 1H, *J* = 8.0 Hz, 8.0 Hz, Ar-H), 4.22 (s, 4H, CH_2Cl). δ_C (100 MHz, DMSO) 163.9, 148.1, 140.7, 109.8, 42.3. Mass Spectrum: (MeOH, ES+): *m/z* Expected: 261.0. Found: 261.9 [M+H], 283.9 [M+Na], 299.9 [M+K]. IR υ_{max} (cm^{-1}) 3336, 3010, 1715, 1648, 1452, 1164, 803.

1,3-bis-(2-chloro—acetylamino)-xylylene (123)

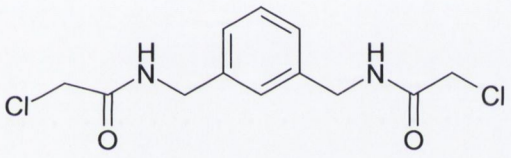

123 was synthesised according to Procedure 2, using *m*-xylylenediamine (1.00 g, 7.30 mmol), NaOH (0.88 g, 22.00 mmol), H_2O (40 mL). and chloroacetyl chloride (2.49 g, 22.03 mmol). The product was collected and was a white solid, 0.83 g, 40 %. M.P. 153 – 154 °C. Calculated for $C_{12}H_{14}N_2O_2Cl_2Na$ [M+Na] *m/z* = 298.9756. Found *m/z* = 298.9756 (+ 2.2 ppm). δ_H (400 MHz, DMSO) 8.75 (s, 2H, NH), 7.27 (t, 1H, *J* = 8 Hz, Ar-H_5), 7.15 (s, 2H, Ar-$H_{4,6}$), 7.14 (s, 1H, Ar-H_2), 4.28 (d, 4H, *J* = 5 Hz, CH_2), 4.11 (s, 4H, CH_2Cl). δ_C (100 MHz, DMSO) 165.9, 138.9, 128.4, 126.3, 125.9, 42.6, 42.4. Mass Spectrum: (MeOH, ES+): *m/z* Expected: 288.0. Found: 311.0 [M+Na]. IR ν_{max} (cm^{-1}) 3285, 3083, 3009, 2954, 2882, 2795, 2360, 1658, 1547, 1489, 1447, 1416, 1360, 1330, 1230, 1171, 1094, 1065, 1024, 922, 898, 780, 710, 599, 484.

1,4–bis–(2-chloro-acetylamino)-benzene (124)

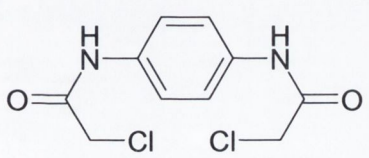

124 was synthesised similarly, following Procedure 2, using *p*–diamino benzene (1.50 g, 13.90 mmol), NaOH (2.20 g, 55.00 mmol), H_2O (100 mL) and chloroacetyl chloride (9.40 g, 83.30 mmol). This successfully produced the desired product as a brown solid, 3.57 g, 98% yield. M.P. decomp above 320 °C. Calculated for $C_{10}H_{10}N_2O_2Cl_2K$ [M+K] *m/z* = 298.9756. Found *m/z* = 298.9756 (– 0.1

ppm). δ_H (400 MHz, DMSO) 10.30 (s, 2H, N-H), 7.55 (s, 4H, Ar-H), 4.23 (s, 4H, CH_2Cl). δ_C (100 MHz, DMSO) 164.4, 134.4, 119.8, 43.5. Mass Spectrum: (MeOH, ES+): *m/z* Expected: 260.0. Found: 298.9 [M+K]. IR υ_{max} (cm^{-1}) 3261, 3176, 3095, 1891, 1754, 1667, 1585, 1515, 1406, 1345, 1292, 1242, 1201, 1127, 1017, 963, 922, 851, 831, 751, 684, 518.

Procedure 3: General experimental procedure for bis systems 125-128.

The relevant diamino alkane was placed in a 100 mL RBF with NaOH (three equivalents) and dissolved in H_2O. The solution was placed in an ice bath at 0 °C and allowed to cool. Chloroacetyl chloride (three equivalents) was then added dropwise over one hour. The solution was left to stir overnight. The solution was then filtered and the precipitate was washed with ether. The solution was then extracted with CH_2Cl_2 (4 x 20 mL) and the solvent was subsequently evaporated and the residue suspended in ether and filtered.

2-chloro-*N*-[3-(2-chloro-acetylamino)-propyl]-acetamide (125)

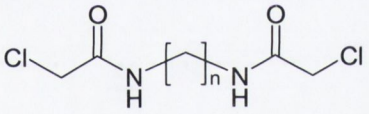

n = 3, **125**
n = 4, **126**
n = 5, **127**
n = 6, **128**

125 was synthesised following Procedure 3, using 1,3 diamino propane (0.44 g, 6.00 mmol), with NaOH (0.72 g, 18 mmol) and H_2O (25 mL), and chloroacetyl chloride (1.65 g, 15.00 mmol). The product was isolated as a white solid, 0.28 g, 20 %. M.P. 128 – 129 °C. Calculated for $C_7H_{12}N_2O_2Cl_2Na$ [M+Na] *m/z* = 249.0174. Found *m/z* = 249.0168 (– 2.2 ppm). δ_H (400 MHz, $CDCl_3$) 7.17 (s, 2H, NH), 4.09 (s, 4H, CH_2Cl), 3.38 (dt, 4H, *J* = 6 Hz, *J* = 6 Hz, CH_2NH), 1.73 (quintet, 2H, *J* = 6 Hz, CH_2). δ_C (100 MHz, $CDCl_3$) 166.3, 42.2, 35.9, 28.9. Mass Spectrum: (MeOH, ES+): *m/z* Expected: 226.0. Found: 249.0 [M+Na]. IR ν_{max} (cm^{-1}) 3283, 3078, 3005, 2970, 2953, 2879, 2361, 1675, 1638, 1554, 1464, 1448, 1401, 1316, 1292, 1269, 1249, 1194, 1128, 923, 759, 626, 574, 469, 414.

2-chloro-*N*-[4-(2-chloro-acetylamino)-butyl]-acetamide (126)

126 was synthesised according to Procedure 3, using 1,4 diaminobutane (0.50 g, 5.68 mmol) NaOH (0.68 g, 17.00 mmol) H_2O (25 mL) and chloroacetyl chloride (2.25 g, 19.89 mmol). The product was isolated as a white solid, 0.58 g, 42 % yield. M.P. 129 – 131 °C (lit[280] M.P. 133 °C). Calculated for $C_8H_{14}N_2O_2Cl_2Na$ [M+Na] *m/z* = 263.0330. Found *m/z* = 263.0336 (+ 2.3 ppm). δ_H (400 MHz, DMSO) 8.22 (s, 2H, NH), 4.03 (s, 4H, CH_2Cl), 3.07

(d, 4H, J = 6 Hz, CH_2NH), 1.40 (d, 4H, J = 6 Hz, $\underline{CH_2}CH_2NH$). δ_C (100 MHz, DMSO) 165.8, 42.6, 38.5, 26.2. Mass Spectrum (MeOH ES+) *m/z* Expected: 240.0. Found: 241.1 [M+H], 263.1 [M+Na]. IR υ_{max} (cm^{-1}) 3321, 2947, 2859, 1640, 1551, 1455, 1433, 1398, 1365, 1321, 1263, 1190, 1081, 987, 921, 770, 738, 618, 567, 462.

2-chloro-*N*-[5-(2-chloro-acetylamino)-pentyl]-acetamide (127)

127 was similarly produceded according to Procedure 3, using 1,5 diamino pentane (0.17 g, 1.74 mmol), $NaHCO_3$ (0.43g, 5.13 mmol), H_2O (25 mL) and chloroacetyl chloride (0.58 g, 5.10 mmol). The product was isolated as a white solid, 0.17 g, 39 %. M.P. 117 – 119 °C. Calculated for $C_9H_{16}N_2O_2Cl_2Na$ [M+Na] *m/z* = 277.0487. Found *m/z* = 277.0492 (+ 2.0 ppm). δ_H (400 MHz, DMSO) 8.19 (s, 2H, NH), 4.03 (s, 4H, CH_2Cl), 3.04 (dt, 4H, J = 7 Hz, J = 6 Hz, CH_2NH), 1.39 (t, 4H, J = 7 Hz, $\underline{CH_2}CH_2NH$), 1.24 (t, J = 7 Hz, 2H, CH_2). δ_C (100 MHz, DMSO) 165.7, 42.7, 38.8, 28.4, 23.6. Mass Spectrum: (MeOH, ES+): *m/z* Expected: 254.0. Found: 277.0 [M+Na]. IR ν_{max} (cm^{-1}) 3276, 3079, 3005, 2969, 2929, 2859, 2362, 1638, 1549, 1463, 1445, 1401, 1379, 1313, 1270, 1247, 1222, 1193, 1138, 1080, 1004, 940, 935, 769, 751, 569, 489.

2-chloro-*N*-[6-(2-chloro-acetylamino)-hexyl]-acetamide (128)

128 was synthesised following Procedure 3, using 1,6 diamino hexane (0.50 g, 4.30 mmol) NaOH (0.43 g, 10.80 mmol), H_2O (25 mL) and chloroacetyl chloride (1.46 g, 12.90 mmol). The desired product was isolated as a white solid, 0.37 g, 32 %. M.P. 129 – 131 °C. Calculated for $C_{10}H_{18}N_2O_2Cl_2Na$ [M+Na] *m/z* = 291.0643. Found *m/z* = 291.0641 (– 0.7 ppm). δ_H (400 MHz, $CDCl_3$) 8.11 (s, 2H, NH), 3.94 (s, 4H, CH_2Cl), 2.97 (dt, 4H, J = 6 Hz, J = 6 Hz, CH_2NH), 1.31 (t, 4H, J = 6 Hz, $CH_{2(2,5)}$) 1.16 (s, 4H, $CH_{2(3,4)}$). δ_C (100 MHz, $CDCl_3$) 165.7, 42.7, 38.8, 28.7, 25.9. Mass Spectrum (MeOH ES+) *m/z* Expected: 268.1. Found: 269.1 [M+H], 291.1 [M+Na]. IR υ_{max} (cm^{-1}) 3270, 3083, 2936, 2856, 1663, 1560, 1462, 1403, 1338, 1240, 1055, 926, 780, 728, 588, 517, 419.

Procedure 4:General experimental procedure for the synthesis of compounds 129-136

The relevant functionalised aromatic amine was dissolved in H_2O (40 mL) along with NaOH (3 equivalents). The solution was placed in an ice bath at 0 °C and allowed to cool. Chloroacetyl chloride (3 equivalents) was then added dropwise over 1 hour. The solution

was left to stir overnight. The solution was then filtered and the resulting precipitate was washed with water and ether.

4-(2-chloro-acetylamino)-benzoic acid (129)

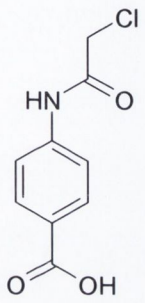

129 was synthesised according to Procedure 4, using 4-amino-benzoic acid (0.50 g, 3.60 mmol), H_2O (50 mL), NaOH (0.29 g, 7.30 mmol) and chloroacetyl chloride (1.24 g, 10.90 mmol). The product was successfully isolated as a white solid, 0.69 g, 88 %. M.P. 263 – 265 °C (lit[281] M.P. 259 °C). δ_H (400 MHz, DMSO) 12.77 (s, 1H, OH), 10.61 (s, 1H, NH), 7.91 (d, 2H, J = 9 Hz, Ar-$H_{2,6}$), 7.69 (d, 2H, J = 9 Hz, Ar-$H_{3,5}$), 4.30 (s, 2H, CH_2Cl). δ_C (100 MHz, DMSO) 165.8, 165.1, 142.5, 130.5, 125.7, 118.6, 43.6.

4-(2-chloro-acetylamino)-benzamide (130)

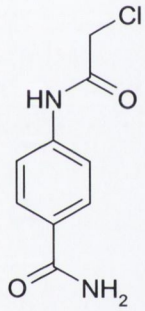

130 was produced according to Procedure 4, using 4-amino-benzamide (0.50 g, 3.67 mmol), H_2O (25 mL), NaOH (0.44 g, 11.00 mmol) and chloroacetyl chloride (1.25 g, 11.00 mmol). The product was successfully isolated as a white solid, 0.49 g, 64 %. M.P. 242 –243 °C (lit[282] M.P. 241 – 242 °C). δ_H (400 MHz, DMSO) 10.51 (s, 1H, NH), 7.88 (s, 1H, NH_2), 7.84 (d, 2H, J = 7 Hz, Ar-$H_{2,6}$), 7.64 (d, 2H, J = 7 Hz, Ar-$H_{3,5}$), 7.28 (s, 1H, NH_2), 4.29 (s, 2H, CH_2Cl). δ_C (100 MHz, DMSO) 167.2, 164.9, 141.0, 129.4, 128.4, 118.4, 43.6.

2-chloro-*N*-(4-nitro-phenyl)-acetamide (131)

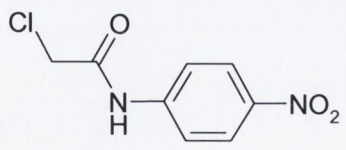

131 was synthesised by Procedure 4, using 4-nitroaniline (0.50 g, 3.62 mmol), H_2O (40 mL), NaOH (0.29 g, 7.20 mmol) and chloroacetyl chloride (1.22 g, 10.80 mmol). The product was successfully isolated as a white solid, 0.51 g, 64 %. M.P. = 178 °C (lit[283] M.P. 181 - 183 °C). δ_H (400 MHz, DMSO) 10.91 (s, 1H, NH), 8.24 (d, 2H, J = 9 Hz, Ar-$H_{3,5}$), 7.83 (d, 2H, J = 9 Hz, Ar-$H_{2,6}$), 4.34 (s, 2H, CH_2Cl). δ_C (100 MHz, DMSO) 165.0, 144.6, 142.6, 125.0, 119.0, 43.5.

3-(2-chloro-acetylamino)-4-hydroxy benzoic acid (132)

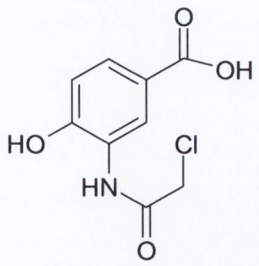

132 was synthesised according to Procedure 4, using 4-amino-4-hydroxybenzoic acid (0.30 g, 1.96 mmol), H_2O (25 mL), NaOH (0.78 g, 19.50 mmol) and chloroacetyl chloride (0.24 g, 2.15 mmol). The product was successfully isolated as a white solid, 0.36 g, 79 %. M.P. 275.5 °C. Calculated for $C_9H_8NO_4Cl$: C, 47.08; H, 3.51; N, 6.10. Found: C, 46.79; H, 3.46; N, 6.22. Calculated for $C_9H_8NO_4ClNa$ [M+Na] *m/z* = 252.0040. Found *m/z* = 252.0050 (+ 4.1 ppm). δ_H (400 MHz, DMSO) 10.95 (s, 1H, OH), 9.54 (s, 1H, NH), 8.54 (d, 1H, *J* = 2 Hz, Ar-H_2), 7.59 (dd, 1H, *J* = 8 Hz, *J* = 2 Hz, Ar-H_6), 6.94 (d, 1H, *J* = 8 Hz, Ar-H_5), 4.39 (s, 2H, CH_2Cl). δ_C (100 MHz, DMSO) 167.0, 164.9, 151.8, 126.9, 125.3, 123.0, 121.3, 114.7, 43.3. . Mass Spectrum: (MeOH, ES+): *m/z* Expected: 288.0. Found: 311.0 [M+Na]. IR υ_{max} (cm^{-1}) 3366, 3077, 2878, 2008, 1678, 1596, 1555, 1514, 1461, 1402, 1374, 1286, 1234, 1200, 1124, 996, 911, 837, 772, 699, 631, 578, 535, 444.

4-(2-chloro-acetylamino)-2-hydroxy-benzoic acid (133)

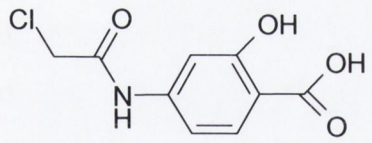

133 was produced following Procedure 4, using 4-amino salicylic acid (0.50 g, 3.26 mmol), H_2O (40 mL), NaOH (0.13 g, 3.20 mmol) and chloroacetyl chloride (1.80 g, 15.92 mmol). The product was successfully isolated as a white solid, 0.62 g, 82 %. M.P. 236 °C (lit[284] M.P. 235 - 236 °C). δ_H (400 MHz, DMSO) 10.58 (s, 1H, NH), 7.75 (d, 1H, *J* = 9 Hz, Ar-H_6), 7.33 (s, 1H, Ar-H_3), 7.06 (d, 1H, *J* = 9 Hz, Ar-H_5) 2.50 (s, 2H, CH_2Cl). δ_C (100 MHz, DMSO) 171.5, 165.3, 162.0, 144.7, 131,2, 110.3, 108.2, 106.2, 43.6.

N-(4-acetyl-phenyl)-2-chloro-acetamide (134)

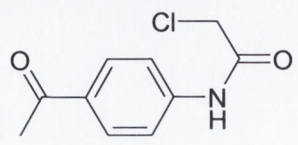

134 was synthesised according to Procedure 4, using 4-amino-acetophenone (0.30 g, 2.22 mmol), H_2O (40 mL), NaOH (0.18 g, 4.44 mmol) and chloroacetyl chloride (0.42 g, 3.78 mmol). The product was successfully isolated as a white solid, 0.07 g, 15 %. M.P. = 148 – 150 °C (lit[285] M.P. 150 – 151 °C). δ_H (400 MHz, DMSO) 10.64 (s, 1H, NH), 7.95 (d, 2H, *J* = 8 Hz, Ar-H), 7.72 (d, 2H, *J* = 8 Hz, Ar-H), 4.31 (s, 2H, CH_2Cl) 2.54 (s, 3H, CH_3). δ_C (100 MHz, DMSO) 196.6, 165.2, 142.7, 132.2, 129.5, 118.7, 43.5, 26.4.

2-chloro-*N*-*p*-tolyl-acetamide (135)

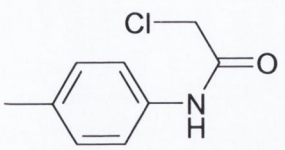

135 was produced according to Procedure 4, using *p*-toluidine (0.30 g, 2.80 mmol), H_2O (40 mL), NaOH (0.22 g, 5.60 mmol) and chloroacetyl chloride (0.63 g, 5.60 mmol). The product was successfully isolated as a white solid, 0.39 g, 77 %. M.P. 163 °C (lit[286] M.P. 163 °C). δ_H (400 MHz, DMSO) 10.20 (s, 1H, NH), 7.44 (d, 2H, J = 8 Hz, Ar-H), 7.11 (d, 2H, J = 8 Hz, Ar-H), 4.21 (s, 2H, CH_2Cl) 2.24 (s, 3H, CH_3). δ_C (100 MHz, DMSO) 164.3, 135.9, 132.8, 129.2, 119.3, 43.5, 20.4.

2-chloro-*N*-(4-hydroxy-3-nitro-phenyl) acetamide (136)

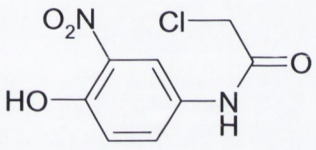

136 was synthesised by Procedure 4, using 4-amino-2-nitrophenol (0.30 g, 1.95 mmol), H_2O (25 mL), NaOH (0.78 g, 19.50 mmol) and chloroacetyl chloride (0.44 g, 3.89 mmol). The product was successfully isolated as an off white solid, 0.35 g, 78 %. M.P. 131 – 133 °C. Calculated for $C_8H_7N_2O_4Cl$: C, 41.67; H, 3.06; N, 12.15. Found: C, 41.72; H, 2.95; N, 12.09. δ_H (400 MHz, $CDCl_3$) 10.42 (s, 1H, NH), 8.37 (d, 1H, J = 2 Hz, Ar-H_2), 8.29 (s, 1H, OH), 7.79 (dd, 1H, J = 9 Hz, J = 2 Hz, Ar-H_6), 7.19 (d, 1H, J = 9 Hz, Ar-H_5), 4.24 (s, 2H, CH_2Cl). δ_C (100 MHz, $CDCl_3$) 163.6, 151.9, 129.9, 128.8, 124.4, 120.1, 115.7, 42.2. IR υ_{max} (cm^{-1}) 3346, 3288, 3086, 1670, 1591, 1555, 1517, 1485, 1411, 1320, 1284, 1239, 1174, 1125, 943, 884, 853, 782, 761, 635, 545.

Procedure 5: General experimental procedure for compounds 137-139

The relevant aromatic amine and NaOH (2.5 equivalents) were placed in a RBF to which H_2O was added. The solution was cooled to 0 °C. Chloroacetyl chloride (2 equivalents) was then added dropwise over 1 hour. The solution was left to stir overnight, and the resulting precipitate was filtered and rinsed with H_2O, hexane and cold $CHCl_3$.

2-chloro-*N*-(4-trifluoromethyl-phenyl)-acetamide (137)

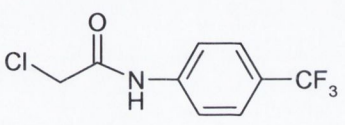

137 was synthesised according to Procedure 5, using trifluoromethyl aniline (0.64g, 3.98 mmol) with NaOH (0.79g, 9.95 mmol) H_2O (25 mL) and chloroacetyl chloride (0.90g, 7.97 mmol). The product was isolated as a white solid, 0.29 g, 31 % yield. M.P.

158 – 160 °C. . Calculated for $C_9H_7NOClF_3$: C, 45.49; H, 2.97; N, 5.89. Found: C, 45.50; H, 2.95; N, 5.80. δ_H (400 MHz, $CDCl_3$) 8.39 (s, 1H, NH), 7.73 (d, 2H, J = 8.5 Hz, Ar-H), 7.65 (d, 2H, J = 8.5 Hz, Ar-H), 4.24 (s, 2H, CH_2Cl). δ_C (100 MHz, $CDCl_3$) 163.6, 139.2, 126.4, 126.0, 125.95, 119.2, 42.3. IR υ_{max} (cm^{-1}) 3281, 3212, 3141, 3093, 1687, 1614, 1556, 1520, 1413, 1320, 1259, 1195, 1155, 1103, 1066, 1023, 845, 729, 595.

2-chloro-*N*-phenyl-acetamide (138)

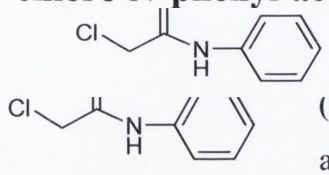

(0.50g, 5.37 mmol), NaOH (0.43g, 10.75 mmol), H_2O (40 mL), and chloroacetyl chloride (0.90g, 7.97 mmol). The desired product was isolated as a white solid, 0.53 g, 58 %. M.P. 134 – 135 °C (lit M.P. 134 – 135 °C).[287] δ_H (400 MHz, $CDCl_3$) 8.26 (s, 1H, NH), 7.58 (d, 2H, J = 7.5 Hz, Ar-$H_{(2,6)}$), 7.40 (dd, 2H, J = 7.5 Hz, J = 7.5 Hz, Ar-$H_{(3,5)}$), 4.21 (s, 2H, CH_2Cl). δ_C (100 MHz, $CDCl_3$) 163.3, 136.2, 128.7, 124.8, 119.6, 42.4.

N-benzyl-2-chloro-acetamide (139)

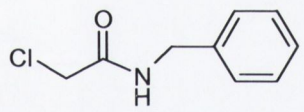

139 was synthesised following Procedure 5, using benzylamine (0.58 g, 5.47 mmol) along with NaOH (0.55 g, 13.67 mmol), H_2O (25 mL), and chloroacetyl chloride (1.23 g, 10.93 mmol). The product was found to be a white solid, 0.37 g, 43 %. M.P. 93 °C (lit[288] M.P. 92 – 93 °C). δ_H (400 MHz, $CDCl_3$) 6.91 (s, 1H, NH), 7.35 (m, 5H, Ar-H), 4.52 (d, 2H, J = 5.5 Hz, CH_2NH), 4.13 (s, 2H, CH_2Cl). δ_C (100 MHz, $CDCl_3$) 191.1, 154.0, 128.4, 127.4, 127.3, 43.4, 42.2.

Procedure 6: General experimental procedure for compounds 140-141

The relevant amino pyridine was placed in a 100 mL RBF with NaOH (2 equivalents) and dissolved in H_2O. Chloroacetyl chloride (2 equivalents) was then added dropwise over 1 hour. The solution was then stirred at room temperature overnight. The solvent was removed under reduced pressure and the residue suspended in EtOH and filtered. The EtOH was evaporated and the residue suspended in acetone and filtered. The solid was dissolved in EtOH (5 mL) and this solution was added slowly to swirling ether (100 mL). The resulting precipitate was collected by filtration.

2-chloro-*N*-pyridin-3-yl-acetamide (140)[231]

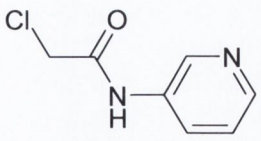

140 was synthesised according to Procedure 6, using 3-amino pyridine (0.50 g, 5.32 mmol) along with NaOH (0.43 g, 10.64 mmol), H_2O (10 mL), and chloroacetyl chloride (1.20 g, 10.64 mmol). The product was isolated as a white solid, 0.44 g, 48 %. δ_H (400 MHz, D_2O) 9.16 (d, J = 3 Hz, 1H, Ar-H_2), 8.44 (d, 1H, J = 6 Hz, Ar-H_6), 8.39 (d, 1H, J = 9 Hz, Ar-H_4), 7.91 (dd, 1H, J = 9 Hz, 6 Hz, Ar-H_5) 4.26 (s, 2H, CH_2Cl). δ_C (100 MHz, D_2O) 168.0, 136.9, 136.5, 132.6, 127.1, 42.2.

2-chloro-*N*-pyridin-4-yl-acetamide (141)[231]

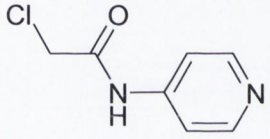

141 was synthesised following Procedure 6, using 4-amino pyridine (0.35 g, 3.72 mmol) with NaOH (0.29 g, 7.40 mmol), H_2O (10 mL), and chloroacetyl chloride (0.84 g, 7.40 mmol). The desired product was successfully isolated as a white solid, 0.26 g, 40 %. δ_H (400 MHz, D_2O) 7.83 (d, J = 8 Hz, 1H, Ar-H_2), 7.75 (d, 2H, J = 7 Hz, Ar-H_6), 6.70 (d, 2H, J = 7 Hz, Ar-H_4), 4.60 (s, 2H, CH_2Cl). δ_C (100 MHz, D_2O) 166.5, 150.3, 146.8, 113.9, 43.54.

Procedure 7: General experimental procedure for compounds 98a and 144

The relevant amine was placed in a 100 mL RBF with NaOH and dissolved in H_2O. The solution was placed in an ice bath at 0 °C and allowed to cool. Chloroacetyl chloride was then added dropwise over 1 hour. The solution was then stirred at room temperature overnight. The solution was then extracted with CH_2Cl_2 (5 x 20 mL). The CH_2Cl_2 was washed with 0.1M HCl (2 x 15 mL) and H_2O (2 x 15 mL). The organic layer was subsequently dried over K_2CO_3 and filtered before the solvent was removed.

2-chloro *N,N*-dimethylacetamide (98a)

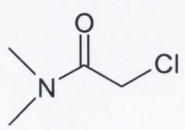

98a was synthesised according to Procedure 7, using *N,N*-dimethylacetamide (7.20 g, 0.16 mol) with NaOH (6.80 g, 0.17 mol), H_2O (25 mL) and chloroacetyl chloride (18.50 g, 0.16 mol). The product was isolated as a white solid, 0.89 g, 4.6 %. δ_H (400 MHz, $CDCl_3$) 4.01 (s, 2H, CH_2), 3.01 (s, 3H, CH_3), 2.89 (s, 3H, CH_3). δ_C (100 MHz, $CDCl_3$) 165.9, 40.8, 37.0, 35.4.

N-butyl-2-chloro acetamide (144)

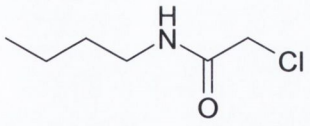

144 was synthesised following Procedure 7, using butylamine (0.30 g, 4.10 mmol) along with NaOH (0.33 g, 8.25 mmol), H_2O (25 mL) and chloroacetyl chloride (1.16 g, 10.27 mmol). The product was found to be a clear oil, 0.26 g, 42 %. δ_H (400 MHz, $CDCl_3$) 6.93 (s, 1H, NH), 3.91 (s, 2H, CH_2Cl), 3.14 (t, 2H, $J = 6$ Hz, CH_2NH), 1.37 (tt, 2H, $J = 8$ Hz, $J = 6$ Hz, CH_2), 1.21 (m, 2H, $J = 8$ Hz, $\underline{CH_2}CH_3$), 0.79 (t, 3H, $J = 8$ Hz, CH_3). δ_C (100 MHz, $CDCl_3$) 165.6, 42.1, 39.0, 30.7, 19.4, 13.1.

1-acetoxy-4-acetylamino-benzene (147)

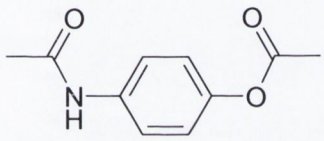

4-aminophenol (**145**) (0.50 g, 4.59 mmol) was placed in a 100 mL RBF with NaOH (1.83 g, 4.59 mmol) and dissolved in H_2O (40 mL). Acetic anhydride (**146**) (2.5 equiv, 1.17 g, 11.4 mmol, 2 mL) was then added dropwise over one hour. The solution was then stirred at room temperature for 2hours. The reaction was filtered and the precipitate was washed with water and then ether, isolating the desired product as a white solid, 0.3 g, 33 %. M.P. 149 – 150 °C (lit[289] M.P. 148 - 151°C) δ_H (400 MHz, DMSO) 7.50 (d, 2H, $J = 9$ Hz, Ar-H), 7.28 (s, 1H, NH), 7.04 (d, 2H, $J = 9$ Hz, Ar-$H_{2,6}$), 2.31 (s, 3H, $CH_{3\ 2,6}$), 2.19 (s, 3H, $CH_{3\ 3,5}$). δ_C (100 MHz, $CDCl_3$) 169.2, 167.7, 146.3, 135.0, 121.5, 120.3, 24.1, 20.6.

1,4,7,10-tetraaza-cyclododecane-1,4,7-tricarboxylic acid tri-tert-butyl ester (148)[234]

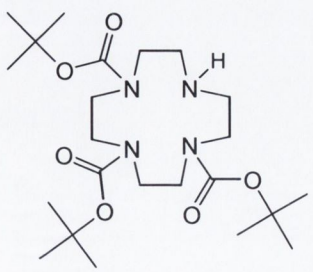

Cyclen (**99**) (0.80 g, 4.65 mmol) and Et_3N (1.45 g, 14.42 mmol) were placed in a 100 mL RBF and dissolved in $CHCl_3$ (30 mL). Di-*tert*-butyl-dicarbonate (Boc_2O), (3.14 g, 14.42 mmol) in $CHCl_3$ was then added very slowly and the solution was left stirring overnight. The solvent was evaporated to give an oil, which was then purified by flash silica column chromatography using hexane:EtOAc 1:5, as eluent. The product was isolated as white foam, 1.24g, 57 %. δ_H (400 MHz, $CDCl_3$) 3.57 (s, 4H, CH_2), 3.23 (s, 8H, CH_2), 2.79 (s, 4H, CH_2) 1.41 &1.39 (2s, 27H, CH_3). δ_C (100 MHz, $CDCl_3$) 155.0, 154.9, 78.7, 50.5, 49.3,

48.9, 48.3, 45.4, 44.4, 28.1, 27.9. Mass Spectrum: (MeOH, ES+) *m/z* Expected: 472.3 Found: 473.0 [M+H].

1,4,7,10-tetraaza-cyclododecane-1,4,7-tricarbaldehyde (149)[235]

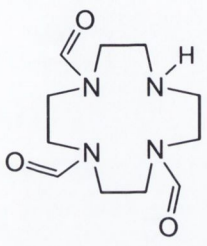

Cyclen (**99**) (0.50 g, 2.90 mmol) and chloral hydrate (2.87 g, 17.40 mmol) were placed in a 50 mL RBF. EtOH (10 mL) was added and the solution was heated to 60 °C and stirred for 3 hours. The solvent was removed to give a clear oil, which was then dissolved in CH_2Cl_2. The product was purified by flash silica column chromatography using CH_2Cl_2 : MeOH, 9:1, as eluent, (R_f = 0.7). This yielded a clear oil, 0.65 g, 87 %. δ_H (400 MHz, $CDCl_3$) 7.96 (m, 3H, CHO), 3.36 (m, 12H, CH_2), 2.74 (m, 4H, CH_2). Mass Spectrum: (MeOH, ES+) *m/z* Expected: 256.1 Found: 257.0 [M+H].

1,4,7, Molybdenum tris carbonyl-(1,4,7,10-tetraaza-cyclododecane) (150)[236]

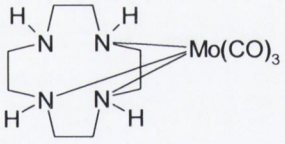

To a 100 mL RBF, cyclen (**99**) (1.75 g, 10 mmol) and molybdenum hexacarbonyl (2.74 g, 10 mmol) were added. The system was placed under argon. Dry dibutylether (65 mL) was added. The solution was freeze-pump-thawed twice and then refluxed for 2 hours under argon. The solution was filtered and the resulting pale yellow solid was collected and dried under vacuum, 3.10 g, 88 %.

2-(1,4,7,10 teraaza-cyclododec-1-yl)-N-{4-[(2-1,4,7,10-tetraaza-cyclododec-1-yl-acetylamino)-methyl]-benzyl}-acetamide (152)

Method 1

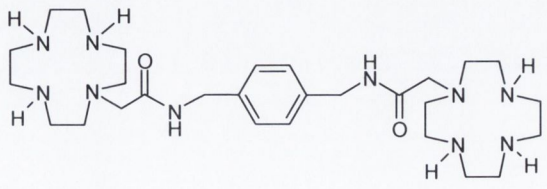

148 (0.74 g, 1.57 mmol), **120** (0.21 g, 0.60 mmol), Cs_2CO_3 (0.61 g, 1.87 mmol) and KI (0.10 g, 0.60 mmol) were placed in a 100 mL RBF. DMF (50 mL) was added and the solution was then heated to 75 °C and left to stir for 120 hours under argon. The solution was filtered off and the DMF removed under reduced pressure. The residue was suspended in EtOAc and separated by flash silica column chromatography,

using EtOAc, 100 %, as eluent. However, the NMR revealed that the majority was **148** and that the reaction had not proceeded.

Method 2

149 (0.12 g, 0.46 mmol), **120** (0.06 g, 0.23 mmol), Cs_2CO_3 (0.07 g, 0.23 mmol) and KI (0.04 g, 0.23 mmol) were placed in a 100 mL RBF. DMF (50 mL) was added and the solution was then heated to 75 °C and left to stir for 48 hours under argon. The solution was filtered off and the DMF removed under reduced pressure. The residue was suspended in EtOAc and separated by flash silica column chromatography, using EtOAc, 100 %, as eluent. However, the NMR and mass spec again revealed that the reaction had not proceeded.

Method 3

150 (1.08 g, 3.07 mmol), 1,4–bis–(2-chloro-acetylamino)-xylyene (**120**) (0.44 g, 1.5 mmol), Cs_2CO_3 (1.00 g, 3.07 mmol) and KI (0.49 g, 3.07 mmol) were placed in a 100 mL RBF. DMF (50 mL) was added under vacuum and the solution was freeze-pump-thawed three times. The solution was then heated to 85 °C and left to stir for 40 hours under argon. The cream precipitate was filtered off and the DMF removed under reduced pressure. The residue was dissolved in HCl (15 % v/v; 25 mL) and left stirring overnight. This aqueous solution was filtered and washed with CH_2Cl_2 (3 x 20 mL). The aqueous layer was then basified to pH >13 with KOH pellets and was subsequently filtered and extracted with CH_2Cl_2 (5 x 20 mL). The organic extracts were combined and dried over K_2CO_3 and filtered. The solvent was removed to yield a yellow oil, 0.35 g, 41 %. Calculated for $C_{28}H_{53}N_{10}O_2$: [M+H] *m/z* = 561.4353. Found: *m/z* = 561.4340 (- 2.4 ppm). δ_H (400 MHz, $CDCl_3$) 8.45 (s, 2H, NH), 7.25 (s, 4H, Ar-H), 4.39 (d, 4H, CH_2NH), 3.18 (s, 4H, CH_2CO), 2.61 (s, 24H, cyclen CH_2), 2.50 (s, 8H, cyclen CH_2). δ_C (100 MHz, $CDCl_3$) 171.1, 137.2, 127.7, 58.6, 52.8, 46.6, 46.2, 45.1, 42.4. Mass spectrum (MeOH, ES+) *m/z* Expected: 560.4. Found: 561.4 [M+H], 583.4 (M+Na), 599.4 (M+K), 281.2 [M+H]/2. IR υ_{max} (cm^{-1}) 3194, 2724, 2362, 1640, 1543, 1269, 1170, 1076, 1020, 972, 941, 722.

Bis-copper 2-(1,4,7,10 teraaza-cyclododec-1-yl)-*N*-{4-[(2-1,4,7,10-tetraaza -cyclododec-1-yl-acetylamino)-methyl]-benzyl}-acetamide (Cu.152)

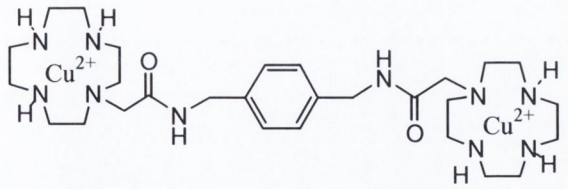

152 (0.11 g, 0.19 mmol) and copper perchlorate hexa hydrate (0.15 g, 0.41 mmol) were placed in a 50 mL RBF with MeOH (20 mL). The solution was refluxed overnight. The solution was filtered and the solvent removed under reduced pressure. The residue was suspended in EtOH and filtered to yield a blue solid, 0.11 g, 53 %. M.P. decomp above 121 °C. Calculated for $C_{28}H_{52}N_{10}O_{10}Cl_2Cu_2$: $[M+2ClO_4]$ *m/z* = 884.1837. Found: *m/z* = 884.1862 (+ 2.9 ppm). Mass spectrum (MeOH, ES+) *m/z* Expected: 686.3 Found: 984.6 $[M+ 3ClO_4]$, 442.8 $[M+2ClO_4]/2$. IR υ_{max} (cm^{-1}) 3279, 2941, 2350, 1847, 1651, 1568, 1361, 1293, 1089, 805, 625.

Bis-zinc 2-(1,4,7,10-tetraaza-cyclododec-1-yl)-*N*-{4-[(2-1,4,7,10-tetraaza-cyclododec-1-yl-acetylamino)-methyl]-benzyl}-acetamide (Zn.152)

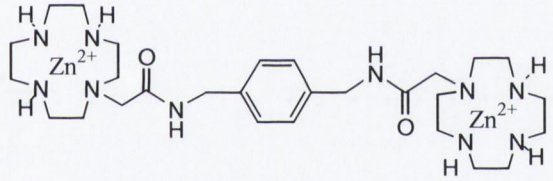

152 (0.11 g, 0.20 mmol) and $Zn(CF_3SO_3)_2$ (0.16 g, 0.44 mmol) were placed in a 50 mL RBF and dissolved in MeOH (15 mL). The solution was refluxed overnight. The volume of MeOH was reduced (~5 mL) and added dropwise onto ether (100 mL). The resulting precipitate was filtered and dissolved in MeOH (5 mL). This was added dropwise onto CH_2Cl_2 (100 mL) and the resulting precipitate was then filtered and dried to yield a brown hydroscopic solid, 0.15 g, 59 %. M.P. decomp above 136 °C. δ_H (400 MHz, D_2O) 7.23 (s, 4H,ArH), 4.39 (s, 4H, CH_2N), 3.46 (s, 4H, CH_2CO), 2.73 (m, 32H, cyclen CH_2). δ_C (100 MHz, D_2O) 172.6, 136.0, 127.3, 54.4, 45.9, 44.4, 44.3, 42.8. IR υ_{max} (cm^{-1}) 3521, 3289, 3111, 2941, 2887, 2285, 1651, 1568, 1463, 1257, 1166, 1091, 1030, 960, 854, 814, 760, 638, 574, 518.

2-{4,10-bis-carbamoylmethyl-7-[(4-{[2-(4,7,10-tris-carbamoylmethyl-1,4,7,10-tetraaza-cyclododec-1-yl)-acetylamino]-methyl}-benzyl-carbamoyl)-methyl]- 1,4,7,10-tetraaza-cyclododec-1-yl}- acetamide (154)

152 (0.11 g, 0.19 mmol), bromo acetamide (0.19 g, 1.36 mmol) and Et_3N (0.19 g, 1.95 mmol) were placed in a 50 mL RBF. EtOH (20 mL) was added and the solution was refluxed at 85 °C for 40 hours. The solution was filtered and then reduced in volume (5 mL) before it was added dropwise to a solution of CH_2Cl_2 (150 mL). The resulting

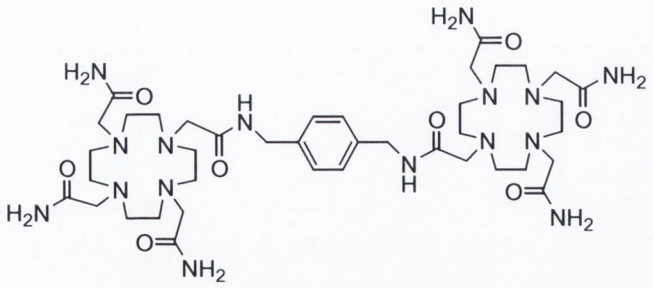

precipitate was filtered, dissolved in hot EtOH (5 mL) and left to stand. The resulting precipitate was filtered, yielding a pale yellow solid, 0.10 g, 57 %. M.P. decomp above 163 °C. Calculated for $C_{40}H_{70}N_{16}O_8.(CH_2Cl_2)_2.(H_2O)_2.MeOH$: C, 45.26; H, 7.24; N, 19.64. Found: C, 45.19; H, 6.89; N, 19.51. Calculated for $C_{40}H_{72}N_{16}O_8$: [M+2H] *m/z* = 904.5719. Found: *m/z* = 904.5726 (+ 0.8 ppm). δ_H (400 MHz, D_2O) 7.16 (s, 4H, Ar-H), 4.26 (s, 4H, CH_2NH), 3.46 (bs, 4H, CH_2CO), 3.27 (s, 4H, $CH_2C{=}O$), 3.19 (s, 6H, $CH_2C{=}O$), 3.12 (s, 2H, $CH_2C{=}O$), 2.75 (bs, 32H, cyclen CH_2). δ_C (100 MHz, D_2O) 173.8, 173.4, 170.2, 136.6, 127.1, 58.1, 56.9, 56.7, 56.1, 55.5, 55.3, 50.2, 42.2. Mass Spectrum: (MeOH, ES+) *m/z* Expected: 902.6. Found: 902.7 (M+), 924.7 (M+Na), 451.9 (M+2H)/2, 301.7 (M+3H)/3. IR υ_{max} (cm^{-1}) 3336, 2949, 2831, 2074, 1959, 1678, 1551, 1420, 1288, 1117, 971, 902, 806, 647, 469.

2-{4,7-bis-methylcarbamoylmethyl-10-[(4-{[2-(4,7,10-tris-methyl-carbamoylmethyl-1,4,7,10-tetraaza-cyclododec-1-yl)-acetylamino]-methyl}-benzylcarbamoyl)-methyl]- 1,4,7,10-tetraaza-cyclododec-1-yl}-acetamide (155)

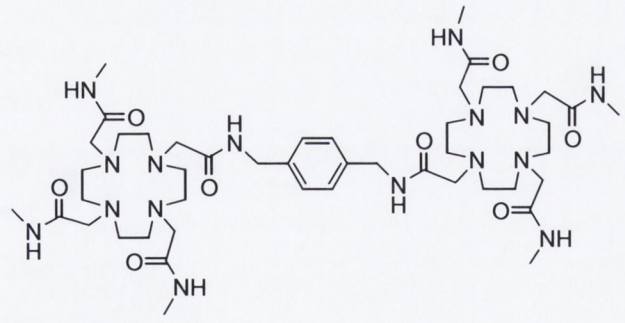

152 (0.28 g, 0.50 mmol), K_2CO_3 (0.25 g, 1.85 mmol) and 2-chloro-*N*-methyl-acetamide (0.35 g, 2.25 mmol) were placed in a 100 mL RBF. EtOH (30 mL) was added and the solution was refluxed at 85 °C for 40 hours. The solution was filtered to remove the cream precipitate and the EtOH was removed under reduced pressure. The residue was suspended in CH_2Cl_2 (30 mL) and filtered. The solid was dissolved in EtOH (5 mL) and added to CH_2Cl_2/Ether 25:7. The resulting precipitate was filtered and then dissolved in a small volume of EtOH (<10 mL) and left to sit overnight. The resulting precipitate was filtered and was then dissolved in DMF and filtered, before being precipitated from ether to yield a yellow solid, 0.15 g, 30 %. M.P. decomp above 139 °C. Calculated for $C_{46}H_{82}N_{16}O_8.CH_2Cl_2.H_2O.EtOH$: C, 51.79; H, 8.16; N, 19.72. Found: C,

51.72; H, 7.48; N, 19.67. Calculated for $C_{46}H_{84}N_{16}O_8$ [M+2H] *m/z* = 988.6658. Found *m/z* = 988.6623. (- 3.6 ppm). δ_H (400 MHz, D_2O) 7.12 (s, 4H, Ar-H), 4.22 (s, 4H, CH_2NH), 3.21 (s, 4H, CH_2CO), 2.86 (bs, 12H, CH_2CO), 2.57 (s, 8H, cyclen CH_2), 2.52 (s, 18H, CH_3), 2.43 (s, 24H, cyclen CH_2). δ_C (100 MHz, D_2O) 173.6, 172.9, 136.7, 127.1, 62.8, 57.4, 51.3, 41.9, 25.0. Mass Spectrum: (MeOH, ES+): *m/z* Expected: 986.6. Found: 987.9 [M+H], 1024.9 [M+K], 531.9 [M+2K]/2, 512.9 [M+K]/2, 494.0 [M+2H]/2. IR υ_{max} (cm^{-1}) 3453, 3276, 3080, 2943, 2820, 2067, 1657, 1549, 1449, 1412, 1371, 1308, 1245, 1152, 1116, 972, 870, 707, 587.

2-{4,10-bis-dimethylcarbamoylmethyl-7-[(4-{[2-(4,7,10-tris dimethyl-carbamoy lmethyl-1,4,7,10-tetraaza-cyclododec-1-yl)-acetylamino]-methyl}-benzylcarba moyl)-methyl]- 1,4,7,10-tetraaza-cyclododec-1-yl}-*N,N*-dimethyl-acetamide (156)

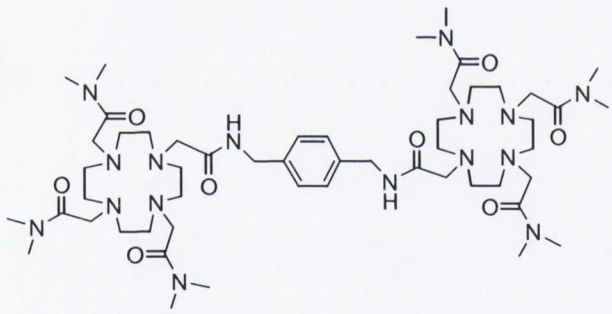

152 (0.15 g, 0.26 mmol), Cs_2CO_3 (0.30 g, 0.92 mmol), 2-chloro-*N,N*-dimethyl-acetamide (0.21 g, 1.70 mmol) and KI (0.13 g, 0.92 mmol) were placed in a 100 mL RBF and dissolved in EtOH (20 mL). The solution was refluxed at 85 °C for four days. The solution was filtered to remove cream precipitate and the solvent removed under reduced pressure. The residue was dissolved in CH_2Cl_2 (30 mL) and filtered. The CH_2Cl_2 was extracted with 0.1 M HCl (4 x 20 mL), which was then washed with CH_2Cl_2 (4 x 15 mL). The pH was adjusted to 7 using K_2CO_3 (10 %) and the solution extracted with CH_2Cl_2 (4 x 15 mL). The solvent was then removed to give a clear oil which solidified after drying in vacuum desicator over P_2O_5, 0.11 g, 38 %. M.P. decomp above 124 °C. Calculated for $C_{52}H_{96}N_{16}O_8$ [M+2H] *m/z* = 1072.7597. Found *m/z* = 1072.7567 (– 2.8 ppm). δ_H (400 MHz, $CDCl_3$) 7.17 (s, 4H, Ar-H), 4.31 (s, 4H, CH_2NH), 3.49 (s, 4H, CH_2CO), 3.09 (bm, 12H, CH_2CO), 2.89 (bm, 68H, cyclen and CH_3). δ_C (100 MHz, $CDCl_3$) 170.8, 170.4, 169.4, 139.8, 126.7, 63.6, 59.8, 55.6, 50.3, 48.3, 42.1, 36.5, 35.7, 35.3, 34.9. Mass Spectrum: (MeOH, ES+) *m/z* Expected: 1070.7. Found: 1071.9 [M+H], 535.9 [M+2H]/2, 357.9 [M+3H]/3. IR υ_{max} (cm^{-1}) 3448, 3279, 3055, 2933, 2817, 1647, 1542, 1508, 1450, 1403, 1348, 1301, 1262, 1102, 1062, 1006, 950, 900, 822.

Procedure 8: General procedure for synthesis of lanthanide complexes

Lanthanide complexes were prepared by refluxing each ligand with the relevant lanthanide triflate (2.1 equivalents) in MeOH (15 mL) for 16 hours. The resulting solution was filtered and reduced in volume to ~ 5 mL. This solution was added dropwise to swirling ether (100 mL) and the resulting precipitate was collected by filtration. The complexes were further purified by precipitation from CH_2Cl_2 (75 mL), and isolated by filtration. The complexes were dried in a vacuum desicator over P_2O_5. The ^1H NMR spectra of the complexes consisted of broad signals due to fast relaxation times from the paramagnetic metal ion, which precluded full characterisation. The fast relaxation times also precluded the acquisition of ^{13}C spectra. Spectral widths were set at 100 ppm (*i.e.* ± 50 ppm). Additional spectral widths were obtained by adjusting the central offset (*i.e.* – 150 to – 50 ppm, 0 to + 150 ppm). Note that the lanthanide ions were expected to have metal bound water molecules, one for each europium and two for each lanthanum ion.

Eu.154.$(CF_3SO_3)_6$.$(H_2O)_2$

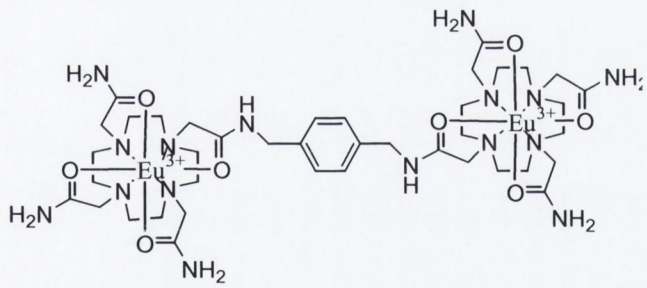

Eu.154 was prepared according to Procedure 8, using **154** (0.13 g, 0.15 mmol) and $Eu(CF_3SO_3)_3$ (0.20 g, 0.33 mmol) yielding a pale yellow solid upon drying, 0.25 g, 80 %. M.P. decomp above 215 °C. Calculated for $C_{40}H_{70}N_{16}O_8.Eu_2.(CF_3SO_3)_6(H_2O)_2$: C, 25.85; H, 3.49; N, 10.48. Found: C, 26.31; H, 3.48; N, 10.03. Calculated for $C_{42}H_{70}N_{16}O_{14}F_6S_2{}^{151}Eu^{153}Eu$ [M+2triflate] m/z = 1504.3014. Found m/z = 1504.3027 (+ 0.9 ppm). δ_H (400 MHz, D_2O) 27.10, 26.28, 7.33, 7.16, 5.87, 4.20, 3.61, 3.22, 2.87, 1.93, 1.75, 1.55, 1.14, 1.04, –2.65, –5.25, –8.22, –9.09, –11.28, –13.55. Mass Spectrum: (MeOH, ES+): m/z Expected: 1208.4. Found: 901.1 [M+4Trif]/2, 376.5 [M+2Trif]/4. IR υ_{max} (cm^{-1}) 3374, 1665, 1459, 1252, 1150, 1082, 1029, 989, 638.

La.154.$(CF_3SO_3)_6.(H_2O)_4$

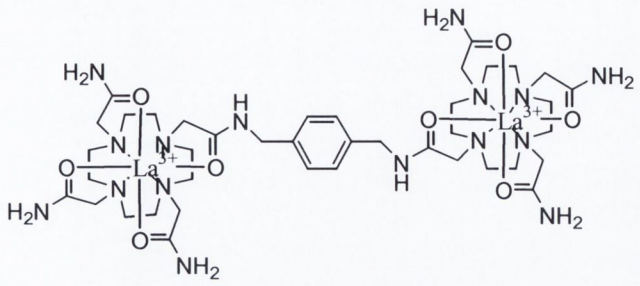

La.154 was synthesised according to Procedure 8, using **154** (41.0 mg, 45.40 μmol) and $La(CF_3SO_3)_3$ (53.2 mg, 90.80 μmol) giving a yellow oil which became a yellow solid upon drying in dessicator, 83 mg, 88 %. M.P. decomp above 227 °C. Calculated for $C_{40}H_{70}N_{16}O_8.La_2.(CF_3SO_3)_6.(H_2O)_4.(MeOH)_4$: C, 26.39; H, 4.16; N, 9.85. Found: C, 26.26; H, 3.76; N, 9.51. Calculated for $C_{43}H_{70}N_{16}O_{17}F_9S_3{}^{139}La_2$ [M+3 triflate]/3 *m/z* = 1627.2250. Found *m/z* = 1627.2285 (+ 2.1 ppm). δ_H (400 MHz, D_2O) 7.26, 4.36, 3.54, 3.52, 3.37, 3.22. Mass Spectrum: (MeOH, ES+): *m/z* Expected: 542.4. Found: 542.4 [M+3Trif]/3, 885.11 [M+4Trif]/2. IR υ_{max} (cm^{-1}) 3401, 2872, 1669, 1634, 1466, 1253, 1169, 1084, 1029, 913, 639, 575, 518.

Eu.155.$(CF_3SO_3)_6.(H_2O)_2$

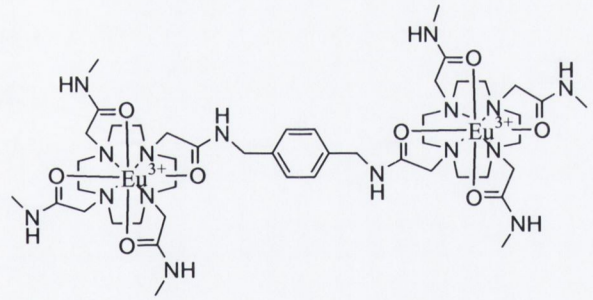

Eu.155 was prepared by following Procedure 8, using **155** (36.40 mg, 36.88 μmol) and $Eu(CF_3SO_3)_3$ (46.40 mg, 77.45 μmol). This yielded a pale yellow solid 66.00 mg, 81 %. M.P. decomp above 215 °C. Calculated for $C_{45}H_{79}N_{16}O_8Eu_2.(CF_3SO_3)_6.(H_2O)_2.(CH_2Cl_2)_5$: C, 25.87; H, 3.66; N, 8.47. Found: C, 25.75; H, 3.29; N, 8.31. δ_H (400 MHz, D_2O) 26.81, 8.41, 5.62, 3.51, 2.60, 2.04, 1.03, 0.78, –2.47, –6.26, –8.14, –11.88, –13.76. Mass spectrum: (MeOH, ES+): *m/z* Expected: 1292.5. Found: 944.3 [M+ 4Trif]/2, 580.0 [M+ 3Trif]/3. IR υ_{max} (cm^{-1}) 3504, 3324, 3134, 2951, 1638, 1419, 1256, 1168, 1083, 1029, 978, 639, 575, 517.

La.155.$(CF_3SO_3)_6.(H_2O)_4$

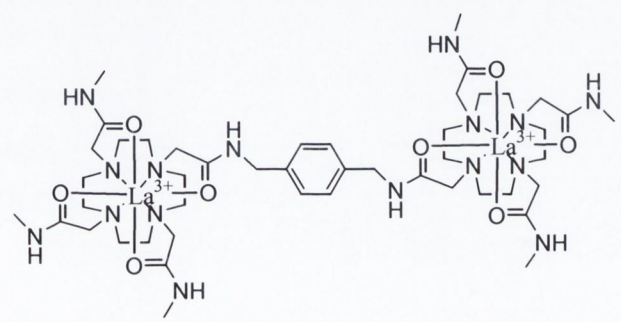

La.155 was synthesised according to Procedure 8, using **155** (35.20 mg, 35.66 μmol) and $La(CF_3SO_3)_3$ (42.00 mg, 71.67 μmol). The resulting

yellow/brown precipitate was dried in a dessicator, 53 mg, 69 %. M.P. decomp above 215 °C. Calculated for $C_{46}H_{82}La_2N_{16}O_8.(CF_3SO_3)_6.(H_2O)_4.(CH_2Cl_2)_5$: C, 25.77; H, 3.79; N, 8.44. Found: C, 26.17; H, 3.39; N, 8.35. δ_H (400 MHz, D_2O) 7.26, 4.37, 3.23, 2.74. Mass spectrum: (MeOH, ES+): *m/z* Expected: 1264.4 Found: 930.5 [M+ 4Trif]/2, 570.4 [M+ 3Trif]/3, 390.9 [M+ 2Trif]/4. IR υ_{max} (cm^{-1}) 3518, 3326, 3131, 2955, 1638, 1417, 1255, 1168, 1086, 1029, 761, 639, 575, 517.

Eu.156.$(CF_3SO_3)_6.(H_2O)_2$

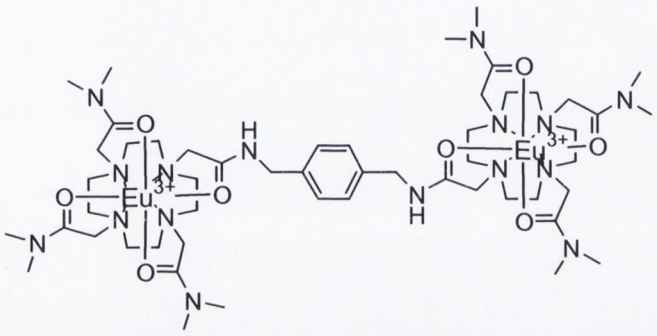

Eu.156 was synthesised by following Procedure 8, using **156** (58.00 mg, 54 μmol) and $Eu(CF_3SO_3)_3$ (90.00 mg, 120 μmol, 2.2 equivalents). The product was successfully isolated as a yellow solid, 58.00 mg, 47 %. M.P. decomp above 235 °C. Calculated for $C_{52}H_{94}N_{16}O_8Eu_2.(CF_3SO_3)_6.(H_2O)_2.(CH_2Cl_2)_6$: C, 27.30; H, 3.94; N, 7.96;. Found: C, 27.02; H, 3.61; N, 8.33. δ_H (400 MHz, D_2O) 31.63, 9.90, 3.21, 2.81, 2.56, 1.51, 1.14, 1.00, 0.76, 0.24, –1.04, –5.89, –7.44, –7.94, –12.30, –13.22, –16.19. Mass spectrum: (MeOH, ES+) *m/z* Expected: 1376.6. Found: 985.1 [M+4trif]/2, 607.1 [M+3trif]/3, 557.1 [M+2trif]/3, 343.1. IR υ_{max} (cm^{-1}) 3465, 2872, 2350, 1621, 1463, 1253, 1163, 1081, 1029, 957, 911, 824, 758, 638, 574, 427.

2-(1,4,7,10-tetraaza-cyclododec-1-yl)-*N*-[6-(2-1,4,7,10-tetraaza-cyclododec-1-yl-acetylamino)-hexyl]-acetamide (151)

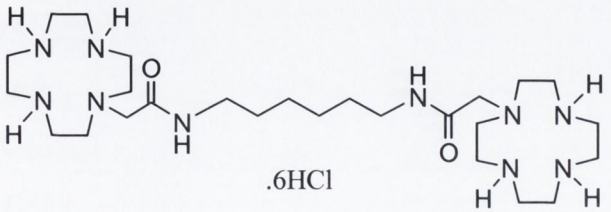

1,6-bis-(2-chloro-acetylamino)-hexane (**128**) (0.40 g, 1.49 mmol), molybdenum cyclen (**150**) (1.05 g, 2.97 mmol), Cs_2CO_3 (1.45 g, 4.46 mmol) and KI (0.20 g, 0.12 mmol) were placed in a 100 mL RBF. DMF (35 mL) was added under vacuum and the suspension was freeze-pump-thawed three times. The reaction was heated to 85 °C and left to stir for 120 hours under argon. The solution was filtered and the DMF was removed under reduced pressure. The residue was suspended in HCl (15 % ; 25 mL) and left stirring overnight. The solution

was filtered and then washed with CH_2Cl_2 (3 x 20 mL). The aqueous solution was basified with KOH and extracted with CH_2Cl_2 (4 x 20 mL). The CH_2Cl_2 was dried over K_2CO_3, filtered and the solvent removed. The residue was dissolved in EtOH (15 mL) and conc. HCl (3 mL) was added and the solution. The resulting precipitate was filtered and washed with EtOH to yield a brown solid, 0.42 g, 37 %. M.P. decomp above 178 °C. Calculated for $C_{26}H_{62}N_{10}O_2Cl_6$.MeOH: C, 40.97; H, 8.40; N, 17.69. Found: C, 41.14; H, 7.97; N, 17.77. δ_H (400 MHz, D_2O) 3.31 (s, 4H, CH_2CO), 3.06, (s, 24H, cyclen CH_2), 2.88 (bs, 12H, cyclen CH_2 & CH_2NCO), 1.39 (bs, 4H CH_2), 1.20 (s, 4H, CH_2). δ_C (100 MHz, D_2O) 172.4, 54.9, 49.2, 43.9, 42.2, 41.8, 39.1, 27.6, 25.3. Mass Spectrum: (MeOH, ES+) *m/z* Expected: 540.5. Found: 541.6 [M+H], 271.4 [M+2H/2]. IR υ_{max} (cm^{-1}) 3427, 2935, 2648, 1647, 1554, 1444, 1375, 1271, 1175, 1075, 1009, 947, 728, 574, 489.

2-[4,7-bis-carbamoylmethyl-10-({6-[2-(4,7,10-tris-carbamoylmethyl-1,4,7,10-tetraaza-cyclododec-1-yl)-acetylamino]-hexylcarbamoyl}-methyl)-1,4,7,10-tetraaza-cyclododec-1-yl]-acetamide (157)

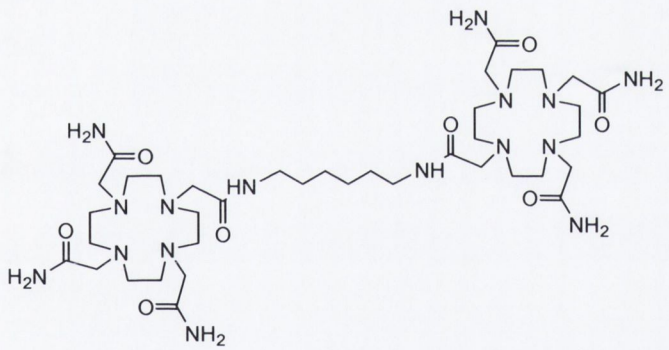

151 (0.10 g, 0.14 mmol), bromo acetamide (0.13 g, 0.97 mmol) and Et_3N (0.21 g, 2.07 mmol) were placed in a 100 mL RBF and dissolved in EtOH (35 ml). The solution was heated at 70 °C for 96 hours. The solvent was removed under reduced pressure and the residue was triturated with CH_2Cl_2. The residue was dissolved in EtOH (2 mL) and added dropwise to swirling CH_2Cl_2 (100 mL). The resulting precipitate was filtered. This was then dissolved in boiling *i*-propanol : EtOH 3:1 (5 mL) and left to stand. The resulting precipitate was filtered, isolating a pale yellow solid, 0.10 g, 83 %. M.P. decomp above 147 °C. Calculated for $C_{38}H_{74}N_{16}O_8$.$(CH_2Cl_2)_3$.MeOH: C, 43.12; H, 7.24; N, 19.16. Found: C, 43.12; H, 7.61; N, 19.55. δ_H (400 MHz, D_2O) 3.35 (m, 12H, CH_{2acet}), 3.12 (bm, 4H, CH_2CO_{bridge}) 3.08 (bm, 12H, 4 x $CH_{2cyclen}$ + 2 x $CH_{2(1,6)}$), 2.87 (bs, 24H, $CH_{2cyclen}$), 1.38 (s, 4H, $CH_{2(2,5)}$), 1.19 (s, 4H, $CH_{2(3,4)}$). δ_C (100 MHz, D_2O) 174.2, 173.5, 169.7, 56.1, 55.6, 50.1, 49.8, 48.9, 38.9, 27.8, 25.3. Mass Spectrum: (MeOH, ES+) *m/z* Expected: 882.6. Found: 883.7 [M+H],

442.5 [M+2H/2]. IR υ_{max} (cm^{-1}) 3388, 3187, 2935, 2851, 1670, 1551, 1457, 1407, 1288, 1161, 1118, 1088, 974, 888, 772, 592.

La.157.$(CF_3SO_3)_6$.$(H_2O)_4$

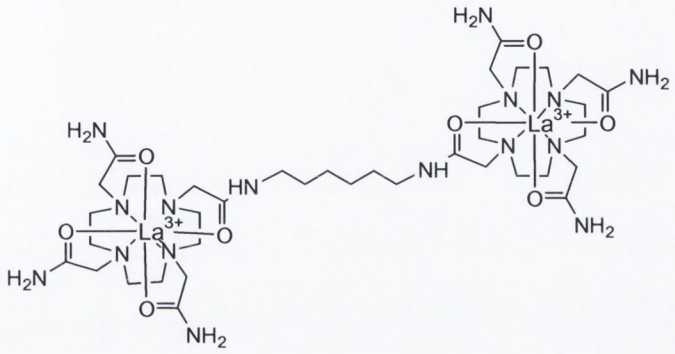

La.157 was prepared according to Procedure 8, using **157** (65.00 mg, 74.06 μmol) $La(CF_3SO_3)_3$ (91.00 mg, 155.53 μmol). The residue was triturated with acetone and dried under vacuum, yielding a yellow solid, 13.70 mg, 87 %. M.P. decomp above 127 °C. Calculated for $C_{38}H_{74}N_{16}O_8$ $La_2.(CF_3SO_3)_6(H_2O)_4.(CH_2Cl_2)_4$. $(MeOH)_4$: C, 24.07; H, 4.12; N, 8.64. Found: C, 24.05; H, 4.22; N, 8.38. δ_H (400 MHz, D_2O) 4.03, 3.76, 3.43, 3.27, 2.89, 2.59, 1.45, 1.25. Mass Spectrum: (MeOH, ES+) *m/z* Expected: 1160.4. Found: 535.7 [M+3Trif]/3, 364.5 [M+2Trif]/4. IR υ_{max} (cm^{-1}) 3377, 2975, 2868, 1669, 1635, 1466, 1270, 1169, 1085, 1030, 974, 913, 819, 762, 639, 576, 517, 434.

(2-chloro-acetylamino) acetic acid methyl ester (159) [253]

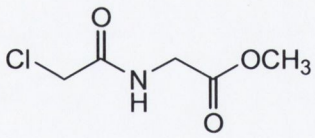

Glycine methyl ester.HCl (2.00 g, 15.94 mmol) and Et_3N (3.22 g, 31.87 mmol) were placed in a 100 mL RBF and dissolved in CH_2Cl_2 (15 mL). The solution was cooled to 0 °C, and chloroacetylchloride (1.80 g, 15.94 mmol) in CH_2Cl_2 (20 mL) was added dropwise over one hour. The reaction was left stirring overnight. The solution was washed with 0.1M HCl (4 x 20 mL) and then with H_2O. The solvent was removed to yield the product as a brown oil, 1.57 g, 60 %. δ_H (400 MHz, $CDCl_3$) 7.11 (s, 1H, NH), 3.99 (s, 2H, CH_2Cl), 3.95 (d, 2H, J = 6.0 Hz, CH_2NH), 3.64 (s, 3H, OCH_3). δ_C (100 MHz, $CDCl_3$) 169.3, 166.2, 51.9, 41.8, 40.8. Mass Spectrum: (MeOH, ES+) *m/z* Expected: 165.5 Found: 166.4 [M+H].

(2-{4,10-Bis-[(methoxycarbonylmethyl-carbamoyl)-methyl]-1,4,7,10-tetraaza-cyclododec-1-yl}-acetylamino)-acetic acid methyl ester (160)[290]

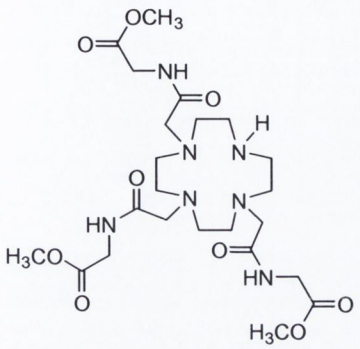

Cyclen (**99**) (0.94 g, 5.45 mmol), and $NaHCO_3$ (1.60 g, 19.07 mmol) were placed in a 100 mL RBF to which was added MeCN (15 mL). **159** (2.84 g, 17.16 mmol) was dissolved in MeCN (35 mL) and added dropwise over 2 hours. The solution was left stirring overnight at room temperature and then heated to 60 °C and left for 96 hours. The solution was filtered and the solvent removed. The residue was dissolved in CH_2Cl_2 and purified by alumina column chromatography using gradient elution 100 → 80:20 CH_2Cl_2:MeOH(NH_3) to give a white foam, 0.84 g, 27 %. Calculated for $C_{23}H_{41}N_7O_9.CH_2Cl_2$: C, 44.72; H, 6.72; N, 15.21. Found: C, 45.08; H, 6.86; N, 15.63. δ_H (400 MHz, $CDCl_3$) 9.38 (bs, 1H, NH), 8.69, (s,1H, NH), 8.38 (s, 2H, NH), 3.90 (s, 4H, NCH_2CO), 3.83 (d, 2H, J = 5.5 Hz, $NHCH_2CO$), 3.61 (s, 6H, OCH_3), 3.57 (s, 3H, OCH_3), 3.31 (s, 2H, CH_2CO), 3.21 (s, 4H, CH_2CO), 3.14 (s, 4H, cyclen CH_2), 2.88 (s, 4H, cyclen CH_2), 2.73 (s, 8H, cyclen CH_2). δ_C (100 MHz, $CDCl_3$) 172.2, 171.1, 170.5, 169.6, 60.6, 55.5, 54.8, 53.0, 52.7, 51.7, 51.2, 46.6, 40.3, 40.1. Mass Spectrum: (MeOH, ES+) *m/z* Expected: 559.3. Found: 560.2 [M+H]. IR υ_{max} (cm^{-1}) 3431, 3066, 2840, 1744, 1659, 1540, 1437, 1370, 1216, 1121, 1034, 982, 708, 582.

Procedure 9: General procedure for synthesis Bis Glycine systems

The 3-armed glycine cyclen ligand **160,** was placed in a 100 mL RBF with the relevant linker (0.5 equivalents), Cs_2CO_3 (1.5 equivalents) and KI (0.5 equivalents). DMF (30 mL) was added. The suspension was heated to 80 °C and left stirring for 120 hours. The solution was filtered and the DMF removed under reduced pressure. The residue was triturated with ether and acetone. The residue was precipitated from ether (100 mL) and, subsequently, from acetone (75 mL). The precipitate was then triturated with CH_2Cl_2 and dried under vacuum over P_2O_5.

{2-[4,7-bis-[(methoxycarbonylmethyl-carbamoyl)-methyl]-10-({4-[(2-{4,7,10-tris-[(methoxycarbonylmethyl-carbamoyl)-methyl]-1,4,7,10-tetraaza-cyclododec-1-yl}-acetylamino)-methyl]-benzylcarbamoyl}-

methyl)-1,4,7,10-tetraaza-cyclododec-1-yl]-acetylamino}-acetic acid methyl ester (162)

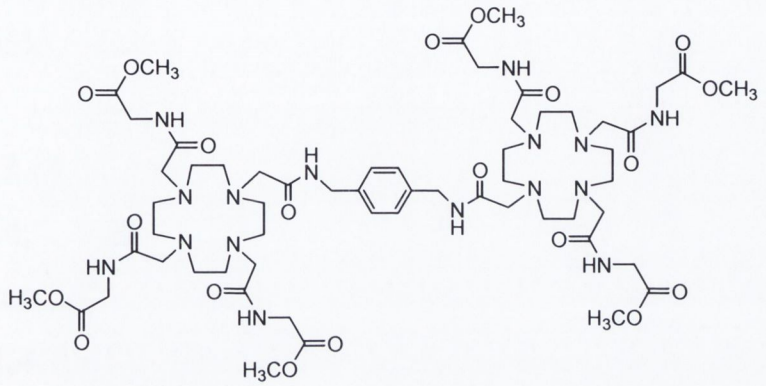

162 was prepared according to Procedure 9, using **120** (65.00 mg, 0.24 mmol), **160** (265.00 mg, 0.12 mmol), Cs_2CO_3 (232.00 mg, 0.71 mmol) and KI (0.20 g, 0.12 mmol). The desired product was yielded as a brown solid, 0.13 g, 41 %. M.P. decomp above 107 °C. δ_H (400 MHz, D_2O) 7.16 (s, 4H, Ar-H), 4.28, (d, J = Hz, CH_2-Ar), 3.92 (bs, 4H, CH_2CO_{bridge}) 3.64-3.56 (bm, 30H, OCH_3 + 6x CH_{2gly}), 3.20 (bs, 12H, CH_{2acet}), 2.71 (bs, 32H, $CH_{2cyclen}$). δ_C (100 MHz, D_2O) 175.7, 175.3, 171.8, 171.3, 171.1, 136.5, 127.0, 57.1, 56.5, 56.1, 55.1, 52.3, 52.2, 50.1, 49.9, 42.7, 42.6, 42.1, 40.67. IR υ_{max} (cm^{-1}) 3362, 3074, 2952, 2837, 1743, 1663, 1606, 1543, 1437, 1386, 1305, 1216, 1116, 1033, 974, 679, 569.

[2-(4,7-Bis-[(methoxycarbonylmethyl-carbamoyl)-methyl]-10-{[4-(2-{4,7,10-tris-[(methoxycarbonylmethyl-carbamoyl)-methyl]-1,4,7,10-tetraaza-cyclododec-1-yl}-acetylamino)-butylcarbamoyl]-methyl}-1,4,7,10-tetraaza-cyclododec-1-yl)-acetylamino]-acetic acid methyl ester (163)

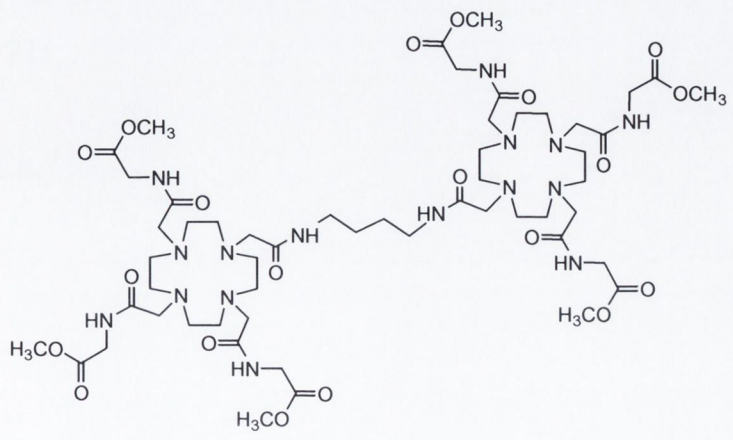

163 was synthesised according to Procedure 9, using **126** (64.00 mg, 0.26 mmol), **160** (0.30 g, 0.53 mmol), Cs_2CO_3 (0.26 g, 0.79 mmol) and KI (0.05 g, 0.30 mmol) the residue was then triturated with MeCN and dried under vacuum to give a brown solid, 0.14 g, 41 %. M.P. decomp above 108 °C. δ_H (400 MHz, D_2O) 3.94 (bm, 12H,

CH_{2gly}), 3.64 (s, 6H, OCH_3), 3.61 (s, 12H, OCH_3), 3.42 (bs, 8H, CH_2CO), 3.14 (bm, 20H, CH_2CO, $CH_{2cyclen}$), 2.63 (bm, 24H, CH_2). δ_C (100 MHz, D_2O) 173.3, 171.1, 168.9, 165.6, 164.1, 60.4, 56.8, 52.3, 50.0, 49.2, 42.7, 40.6, 38.5, 25.4. IR υ_{max} (cm^{-1}) 3407, 3088, 2949, 2854, 2362, 1735, 1655, 1542, 1438, 1387, 1308, 1222, 977, 569.

[2-(4,7-bis-[(methoxycarbonylmethyl-carbamoyl)-methyl]-10-{[6-(2-{4,7,10-tris-[(methoxycarbonylmethyl-carbamoyl)-methyl]-1,4,7,10-tetraaza-cyclododec-1-yl}-acetylamino)-hexylcarbamoyl]-methyl}-1,4,7,10-tetraaza-cyclododec-1-yl)-acetylamino]-acetic acid methyl ester (164)

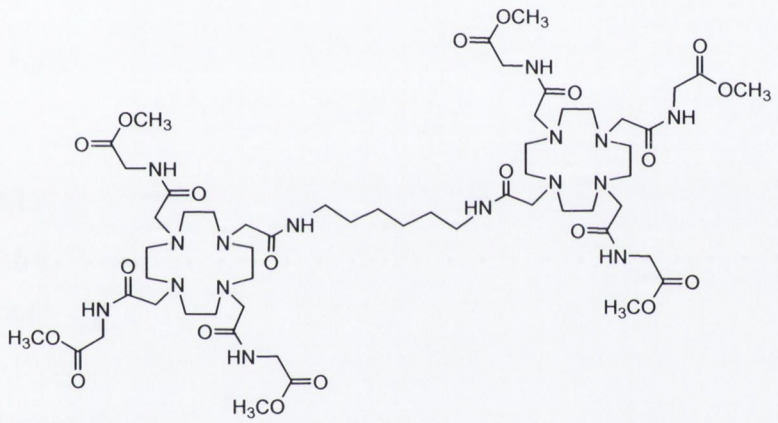

164 was prepared by following Procedure 9, using **128** (0.13 g, 0.48 mmol), **160** (0.57 g, 0.96 mmol), Cs_2CO_3 (0.46 g, 1.43 mmol) and KI (0.05 g, 0.30 mmol), yielding a brown solid, 0.33 g, 52 %. M.P. decomp above 114 °C. δ_H (400 MHz, D_2O) 3.97 (bs, 12H CH_{2gly}), 3.66 (s, 6H, OCH_3), 3.65 (s, 12H, OCH_3), 3.50 (bm, 20H, CH_2CO, CH_2NH), 2.80 (bm, 32H, $CH_{2cyclen}$), 1.41 (s, 4H, $NHCH_2\underline{CH_2}$), 1.21 (s, 4H, $NHCH_2CH_2\underline{CH_2}$). δ_C (100 MHz, D_2O) 171.3, 171.1, 165.0, 164.8, 164.2, 60.4, 57.0, 56.8, 56.4, 52.3, 52.2, 49.6, 49.0, 42.8, 40.7, 40.6, 38.8, 27.8, 25.3. IR υ_{max} (cm^{-1}) 3406, 2941, 2859, 1943, 1739, 1662, 1542, 1439, 1385, 1307, 1221, 1119, 1033, 979, 904, 768, 670, 583.

La.162.$(CF_3SO_3)_6$.$(H_2O)_4$

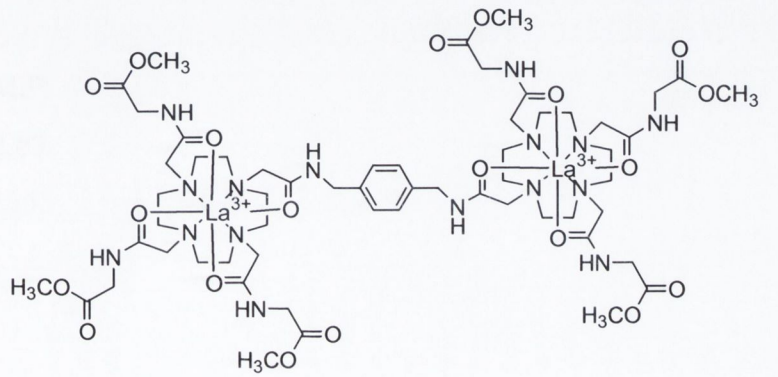

La.162 was prepared according to Procedure 8, using **162** (72.00 mg, 54.35 μmol) and $La(CF_3SO_3)_3$ (64.00 mg, 108.69 μmol) yielding a brown solid,

0.13 g, 90 % yield. M.P. decomp above 239 °C. δ_H (400 MHz, D_2O) 7.20, 4.30, 4.03, 3.95, 3.64, 3.54, 2.81, 2.54. IR υ_{max} (cm^{-1}) 3423, 3126, 2956, 2925, 2326, 1742, 1627, 1439, 1420, 1260, 1167, 1080, 1031, 763, 642, 576, 519.

La.163.$(CF_3SO_3)_6$.$(H_2O)_4$

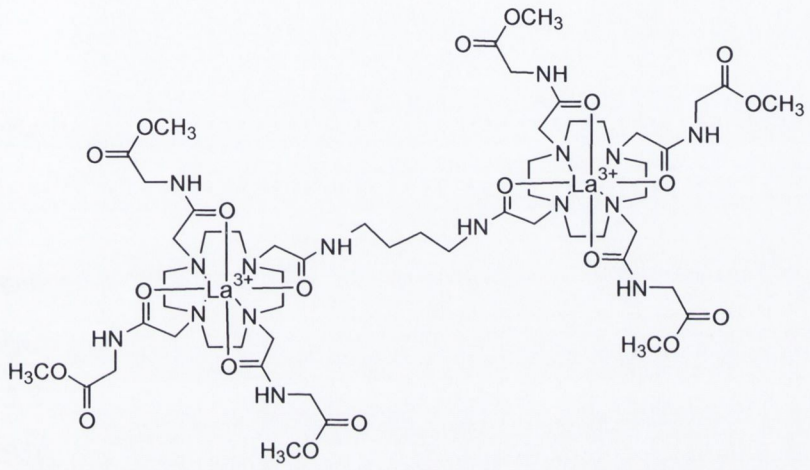

La.163 was prepared by following Procedure 8, using **163** (77.00 mg, 59.87 μmol) and $La(CF_3SO_3)_3$ (71.00 mg, 119.75 μmol). The residue was then triturated with acetone to yield a brown solid, 0.13 g, 85 %. M.P. decompasition above 221 °C. δ_H (400 MHz, D_2O) 4.08, 4.02, 3.67, 3.64, 3.44, 3.23, 2.83, 2.74, 1.42. IR υ_{max} (cm^{-1}) 3405, 2958, 2870, 2569, 1742, 1638, 1443, 1412, 1259, 1170, 1081, 1031, 969, 897, 763, 641, 576, 517.

La.164.$(CF_3SO_3)_6$.$(H_2O)_4$

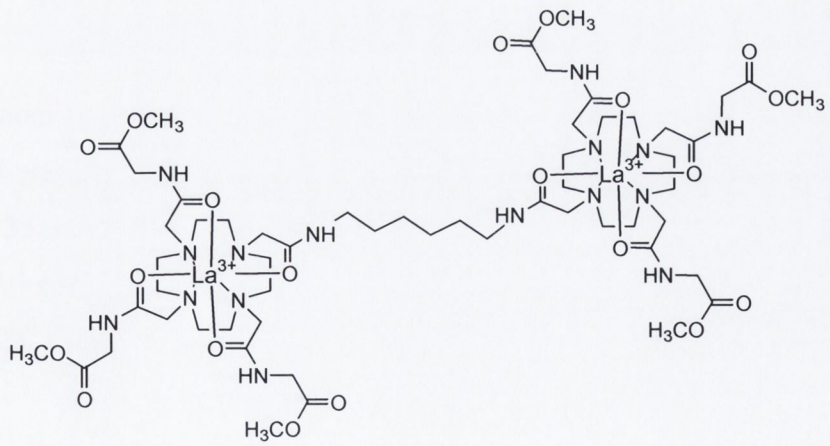

La.164 was prepared according to Procedure 8, using **164** (92.00 mg, 70.01 μmol) and $La(CF_3SO_3)_3$ (82.00 mg, 140.03 μmol) yielding a brown solid, 0.13 g, 72 %. M.P. decomposition above 224 °C. δ_H (400 MHz, D_2O) 4.01, 3.94, 3.67, 3.63, 3.41, 2.99, 2.83, 2.74, 1.39, 1.21. IR υ_{max} (cm^{-1}) 3399, 2954, 2866, 2565, 1742, 1638, 1442, 1411, 1255, 1170, 1082, 1031, 969, 896, 763, 640, 576, 517.

Eu.164.$(CF_3SO_3)_6.(H_2O)_2$

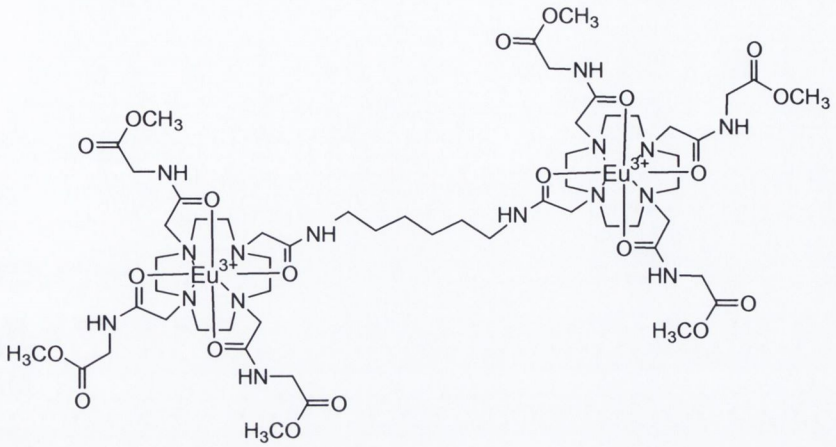

Eu.164 was synthesised according to Procedure 8, using **164** (90 mg, 68.87 μmol), and $Eu(CF_3SO_3)_3$ (82.00 mg, 137.70 μmol). The residue was then triturated with acetone to give a brown solid, 0.12 g, 66 %. M.P. decomp above 225 °C. δ_H (400 MHz, D_2O) 25.74, 24.85, 23.61, 8.05, 4.27, 4.01, 3.74, 3.49, 2.92, 1.48, 1.29, 0.85, –2.09, –3.10, –3.87, –6.11, –6.89, –8.35, –9.13, –11.48, –12.03, –13.27. IR υ_{max} (cm^{-1}) 3380, 3135, 2956, 2868, 2564, 1743, 1638, 1443, 1412, 1278, 1249, 1443, 1412, 1278, 1249, 1168, 1080, 1030, 761, 639, 574, 517.

2-chloro-*N*-pyridin-3-yl-acetamide (140)[231]

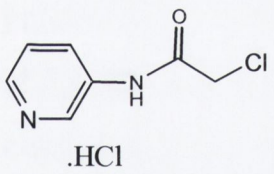

.HCl

3–amino pyridine (6.35 g, 67.55 mmol) was dissolved in acetone (70 mL). The solution was placed in an ice bath (0 °C). Chloroacetyl chloride (15.22 g, 135.10 mmol) was then added dropwise over 1 hour. The solution was left stirring overnight at room temperature. The white precipitate that formed was filtered and washed with acetone. It was then dried at 80 °C for 30 minutes to yield a white solid, 12.04 g, 86 %. M.P. 134 - 135.6 °C (Lit M.P. 134 - 135 °C).[231] δ_H (400 MHz, D_2O) 9.16 (d, J = 3Hz, 1H, H_2), 8.44 (d, J = 6Hz, 1H, H_4), 8.39 (d, J = 9Hz, 1H, H_6), 7.91 (dd, J = 6Hz, J = 9Hz, 1H, H_5), 4.26 (s, 4H, CH_2). δ_C (100 MHz, D_2O) 168.0, 136.9, 136.5, 132.9, 132.6, 127.1, 42.2.

2-[4,7-bis-(pyridin-3-ylcarbamoylmethyl)-1,4,7,10tetraaza-cyclododec-1-yl]-*N*-pyridin-3-yl-acetamide (161)

Cyclen (**99**) (0.70 g, 4.09 mmol) **140** (2.54 g, 12.28 mmol) Cs_2CO_3 (4.00 g, 12.28 mmol) and KI (0.5 g, 3.00 mmol) were placed in a 100 mL RBF to which MeOH (35 mL) was added. The solution was refluxed for 36 hours. The orange solution was then filtered and

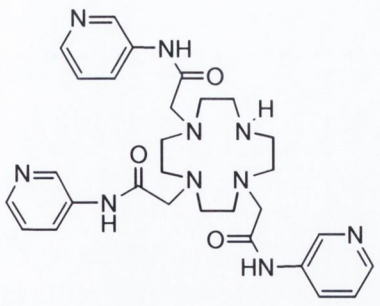

the volume reduced (~5 mL). CH_2Cl_2 (10 mL) was added. The solution was filtered and the compound purifed by alumina column chromatography, using gradient elution 100 → 80:20 CH_2Cl_2:MeOH(NH_3), to give a white solid, 0.69 g, 29 %. Calculated for $C_{29}H_{37}N_{10}O_3$ [M+H] *m/z* = 573.307. Found *m/z* = 573.3050 (– 3.7 ppm). δ_H (400 MHz, MeOH) 8.71 (s, 1H, H2`), 8.63 (s, 2H, H2), 8.26 (d, 1H, *J* = 5 Hz, H4`), 8.19 (d, 2H, *J* = 5 Hz, H4), 8.15 (s, 1H, H6`), 7.96 (s, 2H, H6), 7.29 (dd, 1H, *J* = 5 Hz, *J* = 3.5 Hz, H5`), 7.03 (dd, 2H, *J* = 5 Hz, *J* = 3.5 Hz, H5), 3.56 (s, 4H, CH_2CO), 3.41 (s, 2H, CH_2CO), 3.15 (s, 4H, $CH_{2cyclen}$), 3.01 (s, 4H, $CH_{2cyclen}$), 2.91 (s, 4H, $CH_{2cyclen}$), 2.79 (s, 4H, $CH_{2cyclen}$). δ_C (100 MHz, MeOH) 171.4, 170.9, 143.2, 143.1, 140.1, 139.6, 135.6, 135.0, 127.2, 126.9, 123.4, 123.3, 57.3, 56.1, 51.3, 48.1, 44.9, 44.6. Mass Spectrum: (MeOH, ES+) *m/z* Expected: 574.3. Found: 575.3 [M+H], 597.3 [M+Na]. IR υ_{max} (cm^{-1}) 3244, 3171, 3049, 2828, 1685, 1617, 1550, 1483, 1420, 1284, 1202, 1117, 953, 807, 706.

2-[4,7,10-tris-(pyridin-3-ylcarbamoylmethyl)-1,4,7,10-tetraaza-cyclododec-1-yl]-*N*-[4-({2-[4,7,10-tris-(pyridin-3-ylcarbamoylmethyl)-1,4,7,10-tetraaza-cyclododec-1-yl]-acetylamino}-methyl)-benzyl]-acetamide (165)

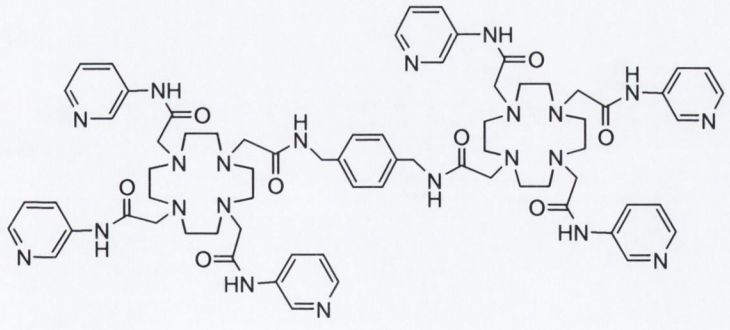

120 (0.16 g, 0.55 mmol), **161** (0.63 g, 1.10 mmol), Cs_2CO_3 (0.41 g, 1.27 mmol) and KI (0.10 g, 0.60 mmol) were placed in a 100 mL RBF to which DMF (30 mL) was added. The suspension was heated at 85 °C for 120 hours. The solution was filtered and the DMF was evaporated at reduced pressure. The residue was dissolved in MeOH (5 mL) and added dropwise to swirling ether (100 mL). The resulting precipitate was filtered, dissolved in MeOH (5 mL) and dropped onto swirling acetone (80 mL). The resulting precipitate was filtered and triturated with CH_2Cl_2. This allowed the isolation of the desired product as a yellow solid, 0.33 g, 41 %. M.P. decomp above 143 °C. Calculated for

$C_{70}H_{88}N_{22}O_8.(H_2O).(CH_2Cl_2)_3.(MeOH)_2$: C, 52.91; H, 6.16; N, 18.10. Found: C, 52.97; H, 5.77; N, 17.92. δ_H (400 MHz, MeOD) 8.62 (s, 2H, H2`), 8.47 (s, 4H, H2) 8.03 (m, 12H, H4&H6), 7.12 (s, 4H, Ar-H), 6.90 (dd, 6H, J = 6Hz, J = 6Hz, H5), 4.20 (s, 4H, $CH_{2acetbridge}$), 2.64 (bm, 48H, CH_{2acet}, $CH_{2cyclen}$, CH_2NH). δ_C (100 MHz, MeOD) 170.0, 169.7, 169.4, 141.9, 141.7, 138.6, 138.3, 136.0, 134.2, 134.1, 125.8, 125.5, 124.1, 122.1, 121.9, 56.1, 54.7, 51.7, 50.1, 40.5. IR υ_{max} (cm^{-1}) 3257, 3057, 2969, 2826, 1992, 1685, 1607, 1544, 1483, 1423, 1362, 11310, 1203, 1105, 1024, 952, 898, 807, 744, 706, 620, 569.

La.165.$(CF_3SO_3)_6.(H_2O)_4$

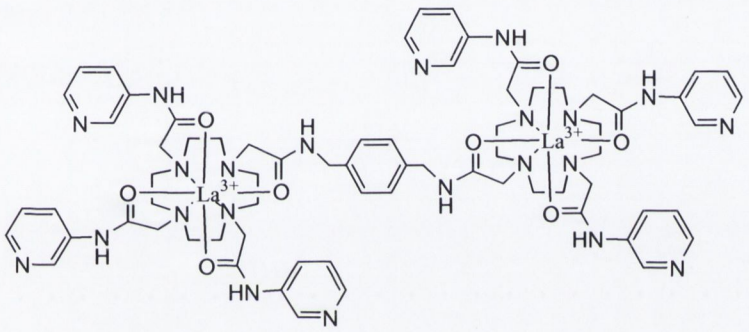

La.165 was prepared according to Procedure 8, using **165** (96.00 mg, 70.34 μmol) and $La(CF_3SO_3)_3$ (82.40 mg, 140.69 μmol). This yielded a brown solid upon drying, 0.15 g, 83 %. M.P. decomp above 196 °C. Calculated for $C_{70}H_{88}N_{22}O_8.(CF_3SO_3)_6(H_2O).(CH_2Cl_2)_5.((CH_3)_2CO)_2$: C, 24.07; H, 4.12; N, 8.64. Found: C, 24.05; H, 4.22; N, 8.38.δ_H (400 MHz, MeOD) 8.68, 8.33, 8.04, 7.23, 4.27, 4.09, 3.69, 3.32, 3.18, 2.81, 2.58. IR υ_{max} (cm^{-1}) 3474, 3290, 3099, 2925, 2871, 2362, 1654, 1562, 1486, 1437, 1279, 1253, 1167, 1085, 1029, 963, 8872, 809, 705, 639, 574, 517.

2-hydroxypropyl *p*-nitrophenylphosphate HPNP (33) [28]

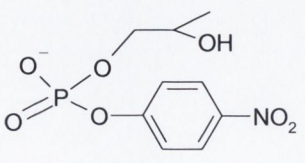

A solution of disodium *p*-nitrophenylphosphate (1.32 g, 5.00 mmol) in water (10 mL) was passed through a column of amberlite IR-120 (+) (H^+) resin and the acid effluent brought to pH 8 with aqueous ammonia. To this solution propylene oxide (20 mL) was added and the reaction mixture was refluxed at 35 °C for 66 hours. The solution was then distilled under vacuum to remove propylene oxide. The remaining solution was passed through IR-120 H^+ resin and the pH adjusted to 6-7 with $Ba(OH)_2$ solution. The solution was reduced to (~10 mL) and EtOH (20 mL) was added. Starting material precipitated out and was filtered off. The solution was then reduced and added to

10 % EtOH in acetone solution. A white precipitate was collected, 0.25 g, 15 %. δ_H (400 MHz, D_2O) 8.14 (d, 2H, J = 9Hz, Ar-H), 7.23 (d, 2H, J = 9 Hz, Ar-H), 3.85 (d, 2H, J = 20 Hz, CH_2), 3.68 (m, 1H, CH), 3.51 (q, 3H, J = 7 Hz, CH_3). Mass Spectrum: (MeOH, ES+) *m/z* Expected: 276.0 Found: 299.0 [M+Na]. UV λ_{max} 299 nm.

5.3 Lanthanide Complexes – Photophysical Studies

All photophysical studies were carried out in aqueous solution or in aqueous solution buffered at pH 7.4 and high ionic strength (0.1 M TMACl or 0.1M TMAPCl) as indicated. Complex concentrations were at ~ 36 μM for Chapter 2 and 16 μM for Chapter 3. Luminescence measurements were made on a Varian Carey Eclipse Fluorescence spectophotometer with the settings displayed below unless otherwise indicated. All scans were saved in CSV format and processed using Microsoft Excel to produce all graphs.

Luminescence Settings

Mode: Phosphorescence	**Total Decay**: 0.02 ms
Flash: 1	**Delay**: 0.1 ms
Gate: 10 ms	**PMT Voltage**: High
Excitation slit width: 10 or 5 nm	**Emission slit width**: 5 nm

Lifetime studies were performed in H_2O and D_2O with ~ 3 mg in 2 mL of the relevant complex. The settings for the Varian Carey Eclipse Fluorescence spectophotometer are displayed below.

Lifetime Settings

Direct excitation: Eu(III) – 395 nm, Tb(III) – 366 nm

Emission: Eu(III) – 615 nm, Tb(III) – 545 nm

No. Cycles: 1000	**Total Decay**: 10 - 15 ms
Flash: 1	**Delay**: 0.1 ms
Gate: 0.1 ms	**PMT Voltage**: High
Excitation slit width: 5 nm	**Emission slit width**: 5 nm

5.4 Phosphodiester Hydrolysis Studies

Kinetic measurements were carried out using an Agilent 8453 spectophotometer or a Varian Carey Eclipse 100, fitted with a circulating temperature controlled water bath, and a mechanical stirrer. The rate constant k, for the hydrolysis of **HPNP** was determined by fitting the data to first order rate kinetics.

The measurements were conducted in aqueous solution buffered at the relevant pH (50 mM HEPES). The concentration of **HPNP** was 0.18 mM (Abs 1.22 at 300 nm). The solution (2.4 mL) was incubated at 37 ^{o}C for 10 minutes. One equivalent of the relevant lanthanide complex, prepared in 100 μL of methanol, was then added to the **HPNP**, and the reaction monitored by absorption spectroscopy over 16 hours.



Chapter 6

References

[1] Fabbrizzi, L.; *Coord. Chem. Rev.* **2000**, 205, 1.
[2] Atkins, P. W. *Physical Chemistry*, sixth edn., Oxford, England, **1999**.
[3] Bissell, R. A.; Bryan, A. J.; Prosanna, deSilva, A.; McCoy, C. P.; *Chem. Commun.* **1994**, 405.
[4] De Silva, A. P.; de Silva, S. A.; *Chem. Commun.* **1986**, 1709.
[5] Tsien, R. Y.; Fluorescent and photochemical probes of dynamic biochemical signals inside living cells: Fluorescent chemosensors for Ion and Molecule Recognition. *ACS symposioum series* 538, **1993**.
[6] Gunnlaugsson, T.; Davis, A. P.; Glynn, M.; *Chem. Commun.* **2001**, 2556.
[7] Lakowicz, J. R.; **1999**, *Kluwer Academic* ISBN 0306460939.
[8] Barigelletti, F. Flamigini, L.; Calogero, G.; Hammarstrom, L.; Sauvage, J. P.; Collin, J. P.; *Chem. Commum.* **1998**, 2333.
[9] Xu, X. H. N.; Jeffers, R. B.; Gao, J. S.; Logan, B.; *Analyst,* **2001**, *126*, 1285.
[10] Cotton, F. A.; Wilkinson, G.; Gaus, P. L.; *Basic Inorganic Chemistry* 2nd Ed. **1987**, John Wiley and Sons, Inc. Canada.
[11] Shriver, D. F.; Atkins, P. W.; Langford, C. H; *Inorganic Chemistry,* **1990** Oxford University Press.
[12] Parker, D.; Gunnlaugsson, T.; Reany, O.; *J. Chem. Soc., Perkin Trans. 2,* **2000,** 1819.
[13] Plancherel, D.; *Inorg. Chem. Acta*, **1987**, *139*, 297.
[14] Parker, D.; Dickins, R. S.; Puschmann, H.; Cossland, C.; Howard, J. A. K. *Chem. Rev.* **2002**, *102*, 1977.
[15] Parker, D.; *Coord. Chem. Rev.* **2000**, *205*, 109.
[16] Parker, D.; Williams, J. A. G.; *J. Chem. Soc. Dalton Trans.,* **1996**, 3613.
[17] Sabbatini, M.; Guardigli, M.; Lehn, J.-M.; *Coord. Chem. Rev.* **1993**, *123*, 201.
[18] Richardson, F. S.; *Chem. Rev.* **1982**, *82*, 5, 541.
[19] Dadabhoy, A.; Faulkner, S.; Sammes, P. G.; *J. Chem. Soc. Perkin2,* **2002**, 348.
[20] Förster, T.; *Ann. Phys.* (*Leipzig*) **1984**, *2*, 55.
[21] Barigelletti, F.; Flamigini, L.; Balzani, V.; Collin, J. P.; Sauvage, J. P.; Sour, A.; Constable, E. C.; Cargill Thompson, A. M. W.; *Coord. Chem. Rev.* **1994**, *132*, 209.
[22] Dexter, D.; *J. Phys. Chem.* **1953**, *21*, 836.
[23] Aime, S.; Botta, M.; Fasano, M.; Terreno, E.; *Chem. Soc. Rev.* **1998**, *27*, 19.
[24] Georges, J.; *Analyst*, **1993**, *118*, 1481.
[25] De Silva, A. P.; Gunarante, H. Q. M.; Rice, T. E.; *Angew. Chem. Int. Ed. Engl.* **1996**, *35*, 201.
[26] Gunnlaugsson, T.; *Tetrahedron. Lett.* **2001**, *42*, 8901.
[27] Woods, M.; Sherry, D.; *Inorg. Chem.* **2003**, *42*, 4401.
[28] Bunzli, J.-C. G.; *Lanthanide Probes in Life, Chemical and Earth Sciences*, Elsevier, Amsterdam **1989**.
[29] Parker, D.; Senanayake, K.; Williams, J. A. G.; *Chem.Commun.* **1997**, 1777.
[30] Parker, D.; Williams, J. A. G.; *Chem.Commun.* **1998**, 246.
[31] Parker, D.; Senanayake, P. K.; Williams, J. A. G.; *J. Chem. Soc. Perkin2,* **1998**, 2129.
[32] Gunnlaugsson, T.; Mac Donaill, D. A.; Parker, D.; *J. Am. Chem. Soc.* **2001**, *123*, 12866.
[33] Parker, D.; Gunnlaugsson, T.; Reany, O.; *Chem. Commun.* **2000**, 473.
[34] Parker, D.; Gunnlaugsson, T.; Reany, O.; *J. Chem. Soc., Perkin Trans. 2*, **2000**, 1819.
[35] De Silva, A. P.; Fox, D. B.; Huxley, A. J. M.; McClenaghan, N. D.; Rioron, J.; *Coord. Chem. Rev.* **1999**, *185/6*, 297.
[36] Hanaoka, K.; Kikuchi, K.; Kojima, H.; Urano, Y. Nagano, T.; *J. Am. Chem. Soc.* **2004**, *126*, 39, 12470.
[37] Cong Li,; Wing-Tak Wong; *Chem. Commun.* **2002**, *18*, 2034.

[38] Charbonnière, L. J.; Ziessel, R.; Montalti, M.; Prodi, L.; Zaccheroni, N.; Boehme, C.; Wipff, G.; *J. Am. Chem. Soc.,***2002**, *124*, 7779.
[39] Baaden, M.; Berney, F.; Boehme, C.; Muzet, N.; Schurhammer, R.; Wipff, G. J.; *Alloys Compd.* **2000**, *303*, 104.
[40] Atkinson, P.; Bretonniere, Y.; Parker, D.; *Chem. Commun.* **2004**, 438.
[41] Adams, J. A.; *Chem. Rev.* **2001**, *101*, 2271.
[42] Yamada, T.; Shinoda, S.; Tsukube, H.; *Chem. Commun.* **2002**, 1218.
[43] Michels, J. J.; Huskens, J.; Reinhoudt, D. N.; *J. Am. Chem. Soc.* **2002**, *124*, 9, 2056.
[44] Arnaud, N.; Georges, J.; *Analyst*, **1999**, *124*, 1075.
[45] Aguilar-Caballos, M. P.; Gómez-Hens, A.; Pérez-Bendito, D.; *Analyst*, **1999**, *124*, 1079.
[46] Panadero, S.; Gómez-Hens, A.; Pérez-Bendito, D.; *Anal. Chim. Acta.* **1996**, *329*, 135.
[47] Sendra, B.; Panadero, S.; Gómez-Hens, A.; *Anal. Chim. Acta.* **1997**, *355*, 145.
[48] Bruce, J. I.; Dickins, R. S.; Govenlock, L. J.; Gunnlaugsson, T.; Lopinski, S.; Lowe, M. P.; Parker, D.; Peacock, R. D.; Perry, J. J. B.; Aime, S.; Botta, M.; *J. Am. Chem. Soc.* **2000**, *122*, 9674.
[49] Dickins, R. S.; Gunnlaugsson, T.; Parker, D.; Peacock R. D.; *Chem. Commun.* **1998**, 1643.
[50] Filipescu, N.; Mushrush, G. W.; *J. Phys. Chem.* **1968**, *72*, 3516.
[51] Pope, S. J. A.; Coe, B. J.; Faulkner, S.; Bichenkova, E. V.; Yu, X.; Douglas, K. T.;
[52] Klink S. I.; Hebbink, G. A.; Grave, L.; Peters, F. G. A.; van Veggel, F. C. J. M.; Reinhoudt, D. N.; Hofstraat, J. W. *Eur. J. Org. Chem.* **2000**, 1923.
[53] Hebbink, G. A.; Klink S. I.; Grave, L.; Alink, P. G. B. O.; van Veggel, F. C. J. M. *Chem. Phys. Chem.* **2002**, *3*, 1014.
[54] Bashkin, J.; Daniher, A.; Trawick, B. *Chem. Rev.* **1998**, *98*, 936.
[55] Hegg, E. L.; Burstyn, J. N. *Coord. Chem. Rev.* **1998**, *173*, 133.
[56] Reinhoudt, D. N.; Molenveld, P.; Engbersen, J. F. *J. Chem. Soc. Rev.* **2000**, *29*, 75.
[57] Komiyama, M.; Takeda, N.; Shigekawa, H. *Chem. Commum.* **1999**, 1443.
[58] Sigman, D. S.; Mazumder, A.; Perrin, D. M. *Chem. Rev.* **1993**, *93*, 2295.
[59] Chin, J.; Williams, N. H. *Chem. Commun.* **1996**, 131.
[60] Cambell, N. A. *Biochemistry*, 6th Ed. Benjamin/Cummings, Menlo Park, Workingham, **1996**.
[61] Dixon, M.; Webb, E. C. *Enzymes*, 3rd Ed., Academic Press, New York, **1979**.
[62] Kramer, R. *Coord. Chem. Rev.* **1999**, *182*, 243.
[63] Verma, S.; Vaish, N. K. Eckstein, F. *Curr. Opin. Chem. Biol.* **1997**, *1*, 532.
[64] Wilcox, D. E. *Chem. Rev.* **1996**, *96*, 2435.
[65] Anslyn, E. V.; Perreault, D. M. *Angew. Chem. Int. Ed. Engl.* **1997**, *36*, 432.
[66] Westheimer, F. H.; *Science*, **1987**, *235*, 1173.
[67] Kaliappa, G. Ragunathan; Hans-Jorg Schneider, *Angew. Chem. Int. Ed. Engl.* **1996**, *35*, 1219.
[68] Morrow, J. R.; Chin, K. O. A. *Inorg. Chem.* **1994**, *33*, 5036.
[69] Schneider, H. J.; Roigk, A.; Hettich, R. *Inorg. Chem.* **1998**, *37*, 4, 751.
[70] Breslow, R.; Huang, D. L. *Proc. Natl. Acad. Sci. USA,* **1991**, *88*, 4080.
[71] Chin, J.; *Curr. Opin. Chem. Biol.* **1997**, *1*, 514.
[72] Morrow, J. R.; Kolasa, K. A.; Amin, S.; Chin, K. O. A. *Mechanistic Bioinorganic Chemistry*, **1995**, 431.
[73] Gunnlaugsson, T.; Davies, R. J. H.; Nieuwehuyzen, M.; O'Brien, J. E.; Stevenson, C. S.; Viguier, R.; Mulready, S. *Polyhedron,* **2003**, *22*, 711.
[74] Linkletter, B.; Chin, J. *Angew. Chem. Int. Ed. Engl.* **1995**, *34*, 472.
[75] Breslow, R.; Burger, D.; Huang, D. L. *J. Am.Chem. Soc.* **1990**, *112*, 3686.

[76] Morrow, J. R.; Amin, S.; Lake, C. H.; Churchhill, M. R. *Angew. Chem. Int. Ed. Engl.* **1994**, *33*, 7, 773.
[77] Gunnlaugsson, T.; Davies, R. J. H.; Nieuwehuyzen, M.; Stevenson, C. S.; Viguier, R.; Mulready, S. *Chem. Comm.* **2002**, 2136.
[78] Morrow, J. R.; Buttrey, L. A.; Shelton, V. M.; Berback, K. A. *J. Am. Chem. Soc.* **1992**, *114*, 1903.
[79] Komiyama, M.; Yashiro, M.; Kawahara, R.; Kamitani, J. *Chem. Letters*, **1998**, 1047.
[80] Lindoy, L. F. *Adv. in Inorg. Chem.* **1998**, *45*, 75.
[81] Gavrilova, A. L.; Bosnich, B. *Chem. Rev.* **2004**, *104*, 349.
[82] Yamada, K.; Takahashi, Y-I.; Yamamura, H.; Araki, S.; Saito, K.; Kawai, M. *Chem. Commum.* **2000**, 1315.
[83] Breslow, R.; Singh, S. *Bioorg. Chem.* **1988**, *16*, 408.
[84] Gajda, T.; Diipre, Y.; Torok, I.; Harmer, J.; Schweiger, A.; Sander,J.; Kuppert, D.; Hegetschweiler, K. *Inorg. Chem.* **2001**, *40*, 4918.
[85] Hamilton, A. D.; Liu, S. *Chem. Commun.* **1999**, 587.
[86] Komiyama, M.; Yashiro, M.; Ishikubo, A. *Chem. Commun.* **1995**, 1793.
[87] Chin, J.; Wall, M.; Hynes, R. C. *Angew. Chem. Int. Ed. Engl.* **1993**, *32*, 11, 1633.
[88] Morrow, J. R.; McCue, K. P. *Inorg. Chem.* **1999**, *38*, 6136.
[89] Iranzo, O.; Elmer, T.; Richard, J. P.; Morrow, J. R. *Inorg Chem.* **2003**, *42*, 7737.
[90] Bazzicalupi, C.; Bencini, A.; Bianchi, A.; Fusi, V.; Giorgi, C.; Paoletti, P.; Valtancoli, B.; Zanchi, D. *Inorg. Chem.* **1997**, *36*, 2784.
[91] Young, M. J.; Chin, J. *J. Am. Chem. Soc.* **1995,** *117*, 10577.
[92] Vallee, B. L.; Auld, S. *Proc. Natl. Acad. Sci. USA.,* **1993**, *90*, 2715.
[93] Morrow, J. R.; McCue, K. P.; Voss, Jr., D. A.; Marks, C. *J. Chem. Soc., Dalton Trans.* **1998**, 2961.
[94] Chin, J.; Williams, N. *Chem. Commun.* **1996**, 131.
[95] Moleveld, P.; Engbersen, J.F.J.; Reinhoudt, D. *Eur. J. Org. Chem.* **1999**, 3269.
[96] Breslow, R.; Chapman, W. H. Jr. *J. Am. Chem. Soc.* **1995**, *117*, 5462.
[97] Leivers, M.; Breslow, R. *Bioorg Chem,* **2001**, *29*, 345.
[98] Czarnik, A. W.; Chung, Y.; Akkaya, E. U.; Venkatachalam, T. K. *Tetrahedron. Lett.* **1990**, *31*, 38, 5413.
[99] Vance, D. H.; Czarnik, A. W. *J. Am. Chem. Soc.* **1993,** *115*, 12165.
[100] Zhu, L.; dos Santos, O.; Wan Koo, C.; Rybstein, M.; Pape, L. Canary, W. *Inorg. Chem.* **2003**, *42*, 7912.
[101] Jurek, P.; Martell, A. E. *Inorg. Chim. Acta.* **1999**, *287*, 47.
[102] Reinhoudt, D. N.; Molenveld, P.; Kapsabelis, S.; Engbersen, J. F. J. *J. Am. Chem. Soc.*, **1997**, *119*, 2948.
[103] Reinhoudt, D. N.; Molenveld, P.; Engbersen, J. F. J.; Kooijman, H.; Spek, A. L. *J. Am. Chem. Soc.* **1998**, *120*, 6726.
[104] Iranzo, O.; Kovalevsky, Y.; Morrow, J. R.; Richard, J. P. *J. Am. Chem. Soc.* **2003**, *125*, 1988.
[105] Reinhoudt, D. N.; Molenveld, P.; Stikvoort, W. M. G.; Engbersen, J. F. J.; Kooijman, H.; Spek, A. L. *J. Org. Chem.* **1999**, *64*, 3896.
[106] Kimura, E.; Aoki, S.; Koike, T.; shiro, M. *J. Am.Chem. Soc.* **1997**, *119*, 3068.
[107] Komiyama, M.; Yashiro, M.; Ishikubo, A. *Chem. Commun.* **1997**, 83.
[108] Komiyama, M.; Kina, S.; Matsumura, K.; Sumaoka, J.; Tobey, S.; Lynch, V. M.; Anslyn, E. *J. Am.Chem. Soc.* **2002**, *124*, 13731.
[109] Reinhoudt, D. N.; Molenveld, P.; Engbersen, J. F. J. *Angew. Chem. Int. Ed.* **1999**, *38*, 21, 3189.

[110] Chin, J.; Hurst, P.; Takasaki, B. K. *J. Am. Chem. Soc.* **1996**, *118*, 9982.
[111] Takasaki, B. K.; Chin, J. *J. Am. Chem. Soc.* **1993**, *115*, 9337.
[112] Franklin, S. J. *Curr. Opin. Chem. Biol.* **2001**, *5*, 201.
[113] Caravan, P.; Ellison, J. J.; McMurry, T. J.; Lauffer, R. B. *Chem. Rev.* **1999**, *99*, 2293.
[114] Ranganathan, R. S.; Fernandez, M. E.; Kang, S. I.; Nunn, A. D.; Ratsep, P. C.; Pillai, K. M. R.; Zhang, X.; Tweedle, M. F. *Investigative Radiology*, **1998**, *33*, 11, 779.
[115] Gómez-Tagle, P.; Yatsimirsky, A. K. *Inorg. Chem.* **2001**, *40*, 15, 3786.
[116] Oh, S. J.; Choi, Y-S.; Hwangbo, S.; Bae, S. C.; Ku, J. K.; Park, J. W. *Chem. Commum.* **1998**, 2189.
[117] Schneider, H. J.; Ragunathan, K. G. *Angew. Chem. Int. Ed. Engl.* **1996**, *35*, 11, 1219.
[118] Chin, J. *Acc. Chem. Res.* **1991**, *24*, 145.
[119] Zhu, B.; Zhao, D.Q.; Ni, J.Z.; Zeng, Q.H.; Huang, B.Q.; Wang, Z.L. *Inorg. Chem. Comm.* 2, **1999**, 351.
[120] Jurek, P. E.; Jurek, A. M.; Martell, A. E. *Inorg. Chem.* **2000**, *39*, 1016.
[121] Branum, M. E.; Tipton, A. K.; Zhu, S.; Que, L. Jr. *J. Am. Chem. Soc.*, **2001**, *123*, 1898.
[122] Komiyama, M.; Takeda, N.; Shigekawa, H. *Chem. Commun.* **1999**, 1443.
[123] Lisowski, J.; Starynowicz, P. *Inorg. Chem.* **1999**, *38*, 1351.
[124] Komiyama, M.; Takeda, N.; Irisawa, M. *Chem. Commun.* **1994**, 2773.
[125] Manseki, K.; Nakamura, O.; Horikawa, K.; Sakamoto, M.; Sakiyama, H.; Nishida, Y.; Sadaoka, Y, Okawa, H. *Inorg. Chem. Commun.* **2002**, *5*, 56.
[126] Yamami, M.; Furutachi, H.; Yokoyama, T.; Ōkawa, H. *Inorg Chem.* **1998**, *37*, 6832.
[127] Komiyama, M.; Yashiro, M.; Kamitani, J.; Kawahara, R. *Chem. Lett.* **1998**, 1047.
[128] Fritsky, I. O.; Ott, R.; Pritzkow, H.; Krämer, R. *Inorg. Chim. Acta.* **2003**, *346*, 111.
[129] Komiyama, M.; Yashiro, M.; Ishikubo, A. *Chem. Commun.* **1995**, 1793.
[130] Hamilton, A. D.; Liu, S. *Tetrahedron. Lett.* **1997**, *38*, 7, 1107.
[131] Breslow, R.; Berger, D. Huang, D. L.; *J. Am. Chem. Soc.*, **1990**, *112*, 3686.
[132] Komiyama, M.; Yashiro, M.; Ishikubo, A.; Matsuda, S.; Kuzuya, A. *Angew. Chem. Int. Ed.* **1998**, *37*, 23, 3284.
[133] Morrow, J. R.; Iranzo, O. *Curr. Opin. Chem. Biol.* **2004**, *8*, 192.
[134] Komiyama, M.; Matsumura, K.; Endo, M. *Chem. Commun.* **1994**, 2019.
[135] Morrow, J. R.; Kolasa, K. A.; Sharma, A. P. *Inorg. Chem.* **1993**, *32*, 3983.
[136] Komiyama, M.; Kuzuya, A.; Akai, M. *Chem. Lett.* **1999**, 1035.
[137] Kalesse, M.; Michaelis, K. *Angew. Chem. Int. Ed.* **1999**, *38*, 15, 2243.
[138] Hovinen, J.; Guzaev, A,; Azhayeva, E.; Azhayev, A.; Lönnberg, H. *J. Org. Chem.* **1995**, *60*, 2205.
[139] Morrow, J. R.; Baker, B. F.; Lot, S. S.; Kringel, J.; Cheng-Flournoy, S.; Villet, P.; Sasmor, H. M.; Siwkowski, A. M.; Chappell, L. L. *Nucleic Acids Research*, **1999**, *27*, 6, 1547.
[140] Sakamoto, S.; Tamura, T.; Furukawa, T.; Komatsu, Y. Ohtsuka, E.; Kitamura, m. Inoue, H. *Nucleic Acids Res.* **2003**, *31*, 1416.
[141] Sarkar, B. *Handbook on Metals in Clinical and Analytical Chemistry*, Marcel Dekker Inc. New York, **1994**.
[142] Sarkar, B. *Chem. Rev.* **1999**, *99*, 2535.
[143] Lindar, M. C.; Hazegh-Azam, M. *Am. J. Clinical Nutrition*, **1996**, *63*, 821S.
[144] Pešák, J.; Opavský, J. *Acta Univ. Palacki. Olomuc., Fac. Med.* **2000**, *143*, 71.
[145] Kendrick, M. J.; May, M. T.; Plishka, M. J.; Robinson, K. D. *Metals in Biological Systems*, Ellis Horwood, England, **1992**.
[146] http://www.who.int.docstore/water_sanitation_health/GDWQ/Chemicals/copperfull.html.

[147] Wilson, S. A. K. *Brain*, **1912**, *34*, 295.
[148] Jianjun, Xia; Wanzhi, Wei; Yanbo, Hu; Han, Tao; Ling, Wu. *Analytical sciences*, **2004**, *20*, 1037.
[149] Stoytcheva, M.; Shakova, V.; Panayotova, M. *Anal. Chim. Acta*, **1998**, *364*, 195.
[150] Prodi, L.; Bolletta, F.; Montalti, M.; Zaccheroni, N. *Coord. Chem. Rev.* **2000**, *205*, 59.
[151] De santis, G.; Fabbrizzi, L.; Licchelli, M.; Mangano, C.; Sacchi, D.; Sardone, N. *Inorg. Chim. Acta.* **1997**, *257*, 69.
[152] Zhou, L-L.; Sun, H.; Zhang, X-H.; Wu, S.-K. *Spectrochimica Acta A.* **2004**, *61*, 61.
[153] Klein, G.; Kaufmann, D.; Schürch, S.; Reymond, J.-L. *Chem. Commun.* **2001**, 561.
[154] Gunnlaugsson, T.; Leonard, J. P.; Murray, N. *Org, Lett.* **2004**, *6*, 1557.
[155] Torrado, A.; Walkup, G. K.; Imperiali, B. *J. Am. Chem. Soc.* **1998**, *120*, 609.
[156] Beltramello, M; Gatos, M.; Mancin, F.; Tecilla, P.; Tonellato, U. *Tetrahedron. Lett.* **2001**, *42*, 9143.
[157] Yoon, J.; Ohler, N. E.; Vance, D. H.; Aumiller, W. D.; Czarnik, A. W. *Tetrahedron. Lett.* **1997**, *38*, 3845.
[158] Parker, D.; Gunnlaugsson, T.; Reany, O. *J. Chem. Soc., Perkin Trans. 2,* **2000,** 1819.
[159] Caravan, P.; Ellison, J. J.; Murray, T. J.; Lauffet, R. B. *Chem. Rev.*, **1999**, *99*, 9982.
[160] Franklin, S. J. *Curr. Opin. Chem. Biol.* **2001**, *5*, 201.
[161] Stein, G.; Wurzberg, E. *J. Chem. Phys.* **1975**, *62*, 208.
[162] Morrow, J. R.; Chin, K. O. A. *Inorg. Chem.* **1994**, *33*, 5036.
[163] Parker, D.; Williams, J. A. G. *J. Chem. Soc. Dalton Trans.,* **1996**, 3613.
[164] Plancherel, D. *Inorg. Chem. Acta*, **1987**, *139*, 297.
[165] Atkins, P. W. *Physical Chemistry*, sixth edn., Oxford, England, **1999**.
[166] Richardson, F. S. *Chem. Rev.* **1982**, *82*, 5, 541.
[167] Aime, S.; Botta, M.; Fasano, M.; Terreno, E. *Chem. Soc. Rev.* **1998**, *27*, 19.
[168] Bora, You; Joong, Kim; No, Gill, Park; Young, Sik, Kim. *Bull. Korean Chem. Soc.* **2001**, *22*, 9,1005.
[169] Balzani, V.; Brghmans, E.; Lehn, J.-M.; Sabbatini, N.; Terode, R.; Ziessel, R. *Helv. Chim. Acta*, **1990**, *73*, 2083.
[170] Potocnák, M.; Pohlová, M.; Wagner, C; Jäger. L. *Acta Cryst.* **2002**. *58*, 595.
[171] Gunnlaugsson, T.; Leonard, J. P.; Mulready, S. Nieuwenhuyzen, M. *Tetrahedron*, **2004**, *60*, 105.
[172] Parker, D.; Williams, J. A. G. *J. Chem. Soc. Perkin Trans. 2,* **1995**, 1305.
[173] Carey, F. A. *Organic Chemistry*, third edn., Mc Graw Hill, USA, **1996**.
[174] Garcia-Fesnadillo, D.; Orellana, G. *Helv. Chm. Acta*. **2001**, *84*, (9), 2708.
[175] Emeleus, H.J.; Bagnall, K. W. *Lanthanides and actinides, MTP international review of science. Inorganic Chemistry*. Series two. Vol. 7, Butterfield, London, **1975**.
[176] Parker, D.; Dickins, R. S.; Puschmann, H.; Cossland, C.; Howard, J. A. K. *Chem. Rev.* **2002**, *102*, 1977. Parker, D.; *Coord. Chem. Rev.* **2000**, *205*, 109.
[177] Cotton, F. A.; Wilkinson, G.; Gaus, P. L. *Basic Inorganic Chemistry*, second edn., John Wiley & Sons, New York, **1987**.
[178] Joseph Leonard; PhD Thesis, Trinity College Dublin, **2003**.
[179] Horrocks, W. D.; Sundick, D. R. *Acc. Chem. Res.* **1981**, *14*, 384.
[180] Beeby, A.; Clarkson, I. M.; Dickins, R. S.; Faulkner, S.; Parker, D.; Royle, L.; de Sousa, A. S.; Williams, J. A. G.; Woods, M. *J. Chem. Soc. Perkin Trans. 2.* **1999**, 493.
[181] Beeby, A.; Dickins, R. S.; Faulkner, S.; Parker, D.; Williams, J. A. G. *Chem. Commun.* **1997**, 1401.
Dickins, R. S.; Parker, D, de Sausa, A. S.; Williams, J. A. G. *Chem. Commun.* **1996**, 697.

[182] Bing Yan; Hongjie Zhang; Shubin Wang; Jiazun Ni. *Monatshefte für Chemie, Chemical Monthly*, **1998,** *129*, 567.
[183] Gunnlaugsson, T.; Mac Donaill, D. A.; Parker, D. *J. Am. Chem. Soc.* **2001**, *123*, 12866.
[184] Stryer, L. Biochemistry, 3rd . ed. Feeman, New York, **1988**.
[185] Harris, D. C. *Quantitative Chemical Analysis.*
[186] Gunnlaugsson, T.; Harte, A. J.; Leonard, J. P.; Nieuwenhuyzen, M. *Chem. Commun.* **2002**, 2134.
[187] Gunnlaugsson, T.; Harte, A. J.; Leonard, J. P.; Nieuwenhuyzen, M. *J. Supramolecular. Chem.* **2003**, 505.
[188] Wang, Y. M.; Wang, Y. J.; Wu, Y. L.; *Polyhedron*, **1998,** *18*, 109.
[189] Vani, P.; Krishna Kishore, K.; Rambabu, R.; Dikshitulu, L. S. A. *Proc. Indian Acad. Sci. (Chem. Sci.)*, **2001**, *113*, 4, 351.
[190] Cotton, F. A.; Wilkinson, G. A*dvanced Inorganic Chemistry*, fifth edn., John Wiley & Sons, New York, **1988**.
[191] Schneider, H.-J.; Yatsimirsky, A. *Principles and Methods in Supramolecular Chemistry*, Wiley, England, **2000**.
[192] Bunzli, J.-C. G. *Lanthanide Probes in Life, Chemical and Earth Sciences*, Elsevier, Amsterdam **1989**.
[193] Beer, P. D.; Cadman, J. *Coord Chem. Rev.* **2000**, *205*, 131.
[194] De Santis, G.; Fabbrizzi, L.; Licchelli, M.; Poggi, A.; Taglietti, A. *Angew. Chem. Int. Ed. Engl.* **1996**, *35*, 202.
[195] Parker, D. *Coord. Chem. Rev.* **2000**, *205*, 109; Parker. D.; Williams, J. A. G. *Chem. Commun.* **1998**, 245;
de Silva, A. P.; Gunaratne, H. Q. N.; Rice T. E.; Stewards, S. *Chem. Commun.* **1997**, 1891.
Sabbatini, N.; Guardigli M.; Lehn, J.-M. *Coord. Chem. Rev.* **1993**, *123*, 201.
[196] Gunnlaugsson, T.; Leonard, J. P.; Mulready, S. Nieuwenhuyzen, M. *Tetrahedron*, **2004**, *60*, 105.
[197] Gunnlaugsson, T.; Harte, A. J.; Leonard, J. P.; Nieuwenhuyzen, M. *Supramolecular Chem.* **2003**, *15*, 505.
[198] Bruce, J. I.; Dickins, R. S.; Govenlock, L. J.; Gunnlaugsson, T.; Lopinski, S.; Lowe, M. P.; Parker, D.; Peacock, R. D.; Perry, J. J. B.; Aime, S.; Botta, M. *J. Am. Chem. Soc.* **2000**, *122*, 9674.
[199] Beeby, A.; Clarkson, I. M.; Dickins, R. S.; Faulkner, S.; Parker, D.; Royle, L.; de Sousa, A. S.; Williams, J. A. G.; Woods, M. *J. Chem. Soc. Perkin Trans. 2*. **1999**, 493.
[200] Beeby, A.; Dickins, R. S.; Faulkner, S.; Parker, D.; Williams, J. A. G. *Chem. Commun.* **1997**, 1401;
Dickins, R. S.; Parker, D, de Sausa, A. S.; Williams, J. A. G. *Chem. Commun.* **1996**, 697.
[201] Joesph Leonard PhD Thesis Trinity College Dublin, **2003**.
[202] Dickins, R. S.; Gunnlaugsson, T.; Parker, D.; Peacock R. D. *Chem. Commun.* **1998**, 1643.
[203] Dickins, R. S.; Love, C. S.; and Puschmann, H. *Chem. Commun.* **2001**, 2308.
[204] Murov, S. L.; Carmichael, I.; Hug, G. L. *Handbook of photochemistry*, Marcel Dekker, New York, **1993**.
[205] IUPAC Compendium of Chemical Terminology 2nd edition **1997**.
[206] Skoog, D. A.; West, D. M.; Holler, F. J. *Fundamentals of Analytical Chemistry* 5th Ed. Saunders College Publishing, New York, **1988**.
[207] Dickins, R. S.; Aime, S.; Batsanov , A. S.; Beeby, A.; Botta, M.; Bruce, J. I.; Howard, J. A. K.; Love, C. S.; Parker, D.; Peacock, R. D.; Puschmann, H. *J. Am. Chem. Soc.* **2002**, *124*, 12697.

[208] *An Introduction to Medicinal Chemistry*, Patrick, G. L.; Oxford University Press, Oxford **1997**.
[208] Parker, D.; Williams, J.A.G. *J.Chem. Soc., Perkin Trans. 2,* **1995**, 1305.
[209] Arnaud, N.; Georges, J. *Analyst*, **1999**, *124*, 1075.
[210] Bruce, J. I.; Dickins, R. S.; Govenlock, L. J.; Gunnlaugsson, T.; Lopinski, S.; Lowe, M. P.; Parker, D.; Peacock, R. D.; Perry, J. J. B.; Aime, S.; Botta, M. *J. Am. Chem. Soc.* **2000**, *122*, 9674.
[211] Dickins, R. S.; Gunnlaugsson, T.; Parker, D.; Peacock R. D. *Chem. Commun.* **1998**, 1643.
[212] Howard, J. A. K.; Kenwright, A. M.; Maloney, J. M.; Parker, D.; Port, M.; Navet, M.; Rousseau, O.; Woods, M. *Chem. Commun.* **1998**, 1381.
[213] Cowan, J. A.; *Curr. Opin. Chem. Biol.* **2001**, *5*, 634.
[214] Bashkin, J.; Daniher, A.; Trawick, B.; *Chem. Rev.* **1998**, *98*, 936.
[215] Hegg, E. L.; Burstyn, J. N.; *Coord. Chem. Rev.* **1998**, *173*, 133.
[216] Reinhoudt, D. N.; Molenveld, P.; Engbersen, J. F. J.; *Chem. Soc. Rev.* **2000**, *29*, 75.
[217] Ragunathan K. G.; Schneider, H.-J.; *Angew. Chem. Int. Ed. Engl.* **1996**, *35*, 11, 1219.
[218] Breslow, R.; Huang, D. L. *Proc. Natl. Acad. Sci. USA,* **1991**, *88*, 4080.
[219] Morrow, J. R.; Kolasa, K. A.; Amin, S.; Chin, K. O. A. *Mechanistic Bioinorganic Chemistry*, **1995**, 431.
[220] Sinead Mulready PhD Thesis Trinity College Dublin, **2003**.
[221] Schneider, H. J.; Ragunathan, K. G. *Angew. Chem. Int. Ed. Engl.* **1996**, *35*, 1219.
[222] Morrow, J. R.; Chin, K. O. A.; Lake, C. H.; Churchhill, M. R. *Inorg. Chem.* **1994**, *33*, 656.
[223] Morrow, J. R. Amin, S.; Lake, C. H.; Churchhill, M. R. *Angew. Chem. Int. Ed. Engl.* **1994**, *33*, 7, 773.
[224] Morrow, J. R.; Chin, K. O. A. *Inorg. Chem.* **1994**, *33*, 5036.
[225] Kirby, A. J. *Angew. Chem., Int. ed. Engl.* **1996**, *35*, 707; Wilcox, D. E.; *Chem. Rev.* **1996**, *96*, 2435.
[226] Reinhoudt, D. N.; Molenveld, P.; Engbersen, J. F. J. *Chem. Soc. Rev.* **2000**, *29*, 75.
[227] Vance, D. H.; Czarnik, A. W. *J. Am. Chem. Soc.* **1993**, *115*, 12165.
[228] Morrow, J. R.; McCue, K. P. *Inorg. Chem.* **1999**, *38*, 6136.
[229] Breslow, R.; Chapman, W. H. Jr. *J. Am.Chem. Soc.* **1995**, *117*, 5462.
[230] Clayden, Greeves, Warren and Wothers, *Organic Chemistry*, Oxford University Press, New York, **2001**.
[231] Abdel, Rahman, A. E.; El-Sherief, H. A.; Mahmoud, A. M. *J. Indian Chem. Soc.* **1981**, *58*, 171.
[232] Handel, H.; Chuburu, F.; Le Baccon, M. *Tetrahedron.* **2001**, *57*, 2385.
[233] des Abbayes, H.; Patinec, V.; Yaouanc, J. J.; Clement, J. C.; Handel, H. *Tetrahedron. Lett.* **1995**, *36*, 1, 79.
[234] Kimura, E.; Aoki, S.; Koike, T.; Shiro, M. *J. Am.Chem. Soc* **1997**, *119*, 13, 3068.
[235] Boldrini, V.; Giovenzana, G. B.; Pagliarin, R.; Sisti, M. *Tetrahedron. Lett.* **2001**, *41*, 6527.
[236] Parker, D. *Macrocycle synthesis a practical approach.*
[237] Sinead Mulready PhD Thesis Trinity College Dublin, **2003**.
[238] Emeleus, H. J.; Bagnall, K. W. *Lanthanide and Actinides, MTP international review of science. Inorganic Chemistry.* Series Two. Vol. 7, London, Butterfield,**1975**.
[239] Merbach, A. E.; Toth, E.; *The Chemistry of Contrast Agents in Medicinal Magnetic Resonance Imaging,* Wiley, New York, **2001**.

[240] Spectral width was set at 100 ppm (*i.e.* ± 50 ppm). Additional spectral widths were obtained by adjusting the central offset (*i.e.* – 150 to – 50 ppm, 0 to + 150 ppm).
[241] Parker, D.; Dickins, R. S.; Puschmann, H.; Cossland, C.; Howard, J. A. K. *Chem. Rev.* **2002**, *102*, 1977.
Caravan, p.; Ellison, J. J.; McMurray, T. J.; Lauffer, R. B. *Chem. Rev.* **1999**, *99*, 283.
[242] Kazuo Nakamoto, *Infrared and Ramen Spectroscopy of Inorganic and Coordination Compounds*, 3rd edition, Wiley.
[243] Horrocks, W. D.; Sundick, D. R. *Acc. Chem. Res.* **1981**, *14*, 384.
[244] Beeby, A.; Clarkson, I. M.; Dickins, R. S.; Faulkner, S.; Parker, D.; Royle, L.; de Sousa, A. S.; Williams, J. A. G.; Woods, M. *J. Chem. Soc. Perkin Trans. 2*. **1999**, 493.
[245] Beeby, A.; Dickins, R. S.; Faulkner, S.; Parker, D.; Williams, J. A. G. *Chem. Commun.* **1997**, 1401.
Dickins, R. S.; Parker, D, de Sausa, A. S.; Williams, J. A. G. *Chem. Commun.* **1996**, 697.
[246] Bonfá, L.; Gatos, M.; Mancin, F.; Tecilla, P.; Tonellato, U. *Inorg. Chem.* **2003**, *42*, 3943.
[247] Cornish-Bowden, A.; Wharton, C. W. *Enzyme Kinetics*, IRL press, **1990**.
[248] Hamilton, A. D.; Liu, S. *Tetrahedron. Lett.* **1997**, *38*, 7, 1107.
[249] Ann-Marie Fanning, Transfer Report, Trinity College Dublin, **2004**.
[250] Barbier, B.; Brack, A. *J. Am. Chem. Soc.* **1988**, *110*, 6880.
[251] Gunnlaugsson, T.; Davies, R. J. H.; Nieuwehuyzen, M.; Stevenson, C. S.; Viguier, R.; Mulready, S. *Chem. Commun.* **2002**, 2136.
[252] Gunnlaugsson, T.; Davies, R. J. H.; Nieuwehuyzen, M.; O'Brien, J. E.; Stevenson, C. S.; Viguier, R.; Mulready, S. *Polyhedron.* **2003**, *22*, 711.
[253] Zlatoidsky, P.; Malier, T. *Eur. J. Med. Chem.* **1999**, *34*, 1023.
[254] Aime, S.; Barge, A.; Botta, M.; Howard, J. A. K.; Kataky, R.; Lowe, M. P.; Moloney, J. M.; Parker, D.; de Sousa, A. S. *Chem. Commun.* **1999**, 1047.
[255] Schneider, H. J.; Roigk, A.; Hettich, R. *Inorg. Chem.* **1998**, *37*, 4, 751.
[256] The rate constant (k) values were determined by fitting the data to first order rate kinetics using Biochemical Analysis Software for Agilent Chem. Station, or Varian Cary 100 Eclipse.
[257] Breslow, R.; Huang, D. L. *Proc. Natl. Acad. Sci. USA,* **1991**, *88*, 4080.
[k_{rel} is the ratio between k and the rate constant of the 'uncatalysed' reaction, (k_{uncat}) which has been measured to be 0.00012 h^{-1}, $\tau_{1/2} = 5.78 \times 10^3$ h, at pH 7.4].
[258] Morrow, J. R. Amin, S.; Lake, C. H.; Churchhill, M. R. *Angew. Chem. Int. Ed. Engl.* **1994**, *33*, 7, 773.
[259] Iranzo, O.; Elmer, T.; Richard, J. P.; Morrow, J. R. *Inorg Chem.* **2003**, *42*, 7737.
[260] Chin, J.; Wall, M.; Hynes, R. C.; Linkletter, B.; Williams, D.; Lebuis, A. M. *J. Am.Chem. Soc.* **1999**, *121*, 4710.
[261] Unpublished work Gunnlaugsson, T.; Mulready, S.
[262] Cowan, J. A. *Curr. Opin. Chem. Biol.* **2001**, *5*, 634.
[263] Breslow, R.; Labelle, M. *J. Am.Chem. Soc.* **1986**, *108*, 2655.
[264] Anslyn, E. V.; Perreault, D. M. *Angew. Chem. Int. Ed. Engl.* **1997**, *36*, 432.
[265] Breslow, R.; Anslyn, E. *J. Am.Chem. Soc.* **1989**, *111*, 4473.
[266] Gómez-Tagle, P.; Yatsimirsky, A. K. *Inorg. Chem.* **2001**, *40*, 15, 3786.
[267] Reinhoudt, D. N.; Molenveld, P.; Engbersen, J. F. J. *J. Org. Chem.* **1999**, *64*, 17, 6337.
[268] Zhu, L.; dos Santos, O.; Koo, C. W.; Rybstein, M.; Pape, L.; Canary, J. *Inorg. Chem.* **2003**, *42*, 7912.
[269] Morrow, J. R.; McCue, K. P.; Voss, Jr., D. A.; Marks, C. *J. Chem. Soc., Dalton Trans.* **1998**, 2961.

[270] Fry, F. H;, Spiccia, L.; Jensen, P.; Moubaraki, B.; Murray, K. S.; Tiekink, E. R. T. *Inorg. Chem.* **2003**, *42*, 5594.
[271] Jurek, P.; Martell, A. E. *Inorg. Chim. Acta.* **1999**, *287*, 47.
[272] Zhu, L.; dos Santos, O.; Wan Koo, C.; Rybstein, M.; Pape, L. Canary, W. *Inorg. Chem.* **2003**, *42*, 7912.
[273] Franklin, S. J. *Curr. Opin. Chem. Biol.* **2001**, *5*, 201.
[274] Aime, S.; Barge, A.; Botta, M.; Howard, J. A. K.; Kataky, R.; Lowe, M. P.; Moloney, J. M.; Parker, D.; de Sousa, A. S. *Chem. Commun.* **1999**, 1047.
[275] Unpublished work Gunnlaugsson, T.; Leonard J. P.
[276] Morrow, J. R.; McCue, K. P.; Voss, Jr., D. A.; Marks, C.; *J. Chem. Soc., Dalton Trans.* **1998**, 2961.
[277] Chin J.; Williams N. *Chem. Commun.* **1996**, 131.
[278] Moleveld, P.; Engbersen, J.F.J. ; Reinhoudt, D. N. *Eur. J. Org. Chem.* **1999**, 3269.
[279] Reinhoudt, D. N.; Molenveld, P.; Engbersen, J. F. J.; Kooijman, H.; Spek, A. L.; *J. Am. Chem. Soc.*, **1998**, *120*, 6726.
[280] Vera, Montserrat; Rodriguez-Galan, Alfonso; Puiggali, Jordi. *Macromolecular Rapid Communications* **2004,** *25*, (7), 812.
[281] Ronwin; Horn; *J. Org. Chem. 30*, **1965**, 2821.
[282] Jacobs; Heidelberger; *J. Am. Chem. Soc.* **1917**, *39*, 1437.
[283] *International Journal of Peptide & Protein Research*, **1995**, *45*(3), 257.
[284] Rosina; Lastowskii; *Zh. Obshch .Khim.* **1954**, *24*, 2063; engl. Ausg. S. 2029.
[285] Hinohaha *et al. Nippon Kagaku Kaishi*; **1974**, 297.
[286] Krowicki, Krzysztof; Lown, J. William; *J. Org. Chem. 52*, 16, **1987**, 3493.
[287] Lee, Ki Sun; Adhikary, Keshab Kumar; Lee, Hai Whang; Lee, Bon-Su; Lee, Ikchoon. *Organic & Biomolecular Chemistry* **2003**, *1,* (11), 1989.
[288] Gaillot, Jean Marc; Gelas-Mialhe, Yvonne; Vessiere, Roger. *Canadian Journal of Chemistry,***1979**, *57*, (15), 1958.
[289] Gowda, S.; Gowda, D. C. *Tetrahedron*, **2002**, *58*, 2211.
[290] Ann Marie Fanning PhD Thesis Trinity College Dublin **2006**



Appendix

Appendices

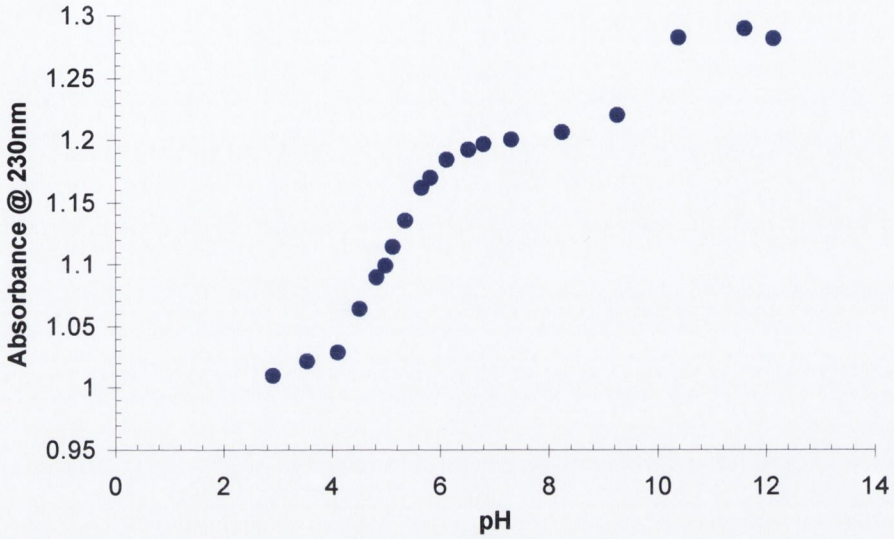

Figure 1. Changes in absorbance at 230 nm with respect to pH for 106, showing hypochromic shift upon deprotonation the amide

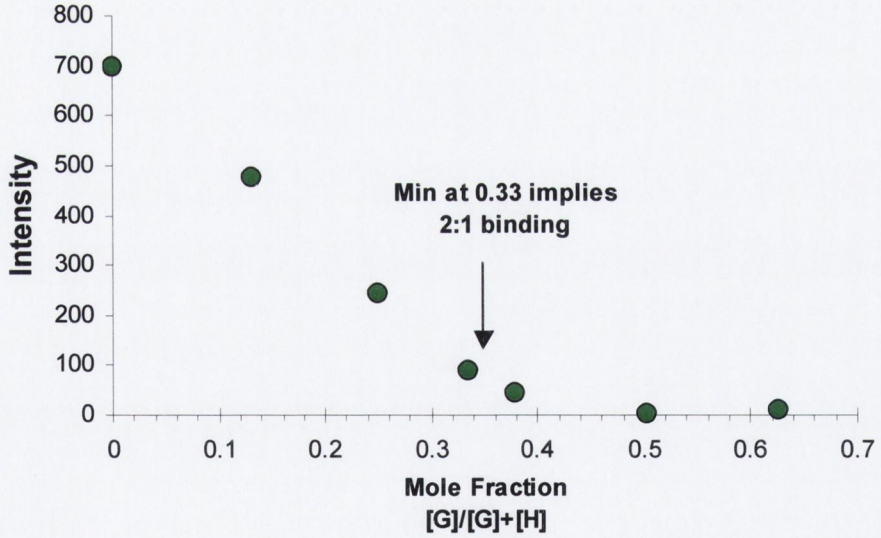

Figure 2. Eu(III) Luminescence JOB Plot where [G] is the concentration of guest *i.e.* Cu(II) and [H] the concentration of host *i.e.* Eu.104

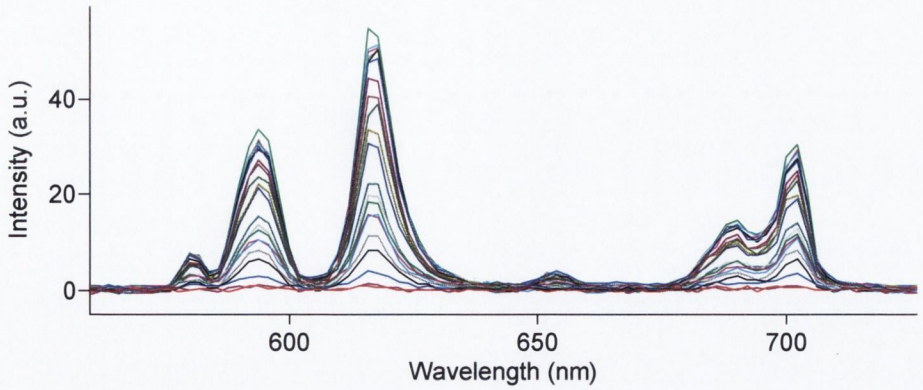

Figure 3. Luminescence spectra of Eu.104 in pH 7.4 buffered solution is quenched upon addition of Fe(II). Excited at 266 nm

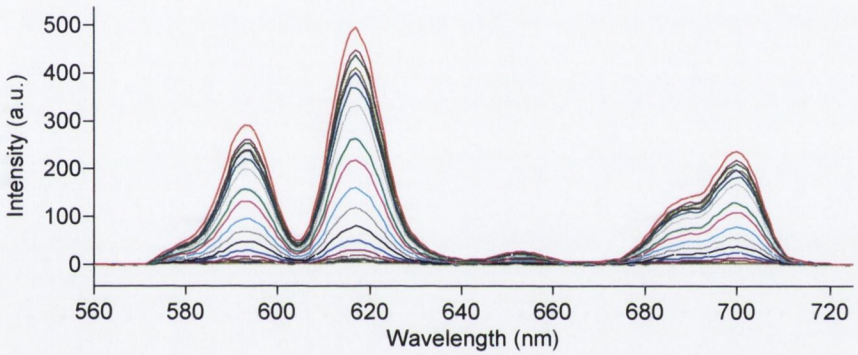

Figure 4. Luminescence spectra of Eu.104 in pH 7.4 buffered solution is quenched upon addition of Co(II). Excited at 266 nm. Slit widths at 10 nm resulted in broader peaks

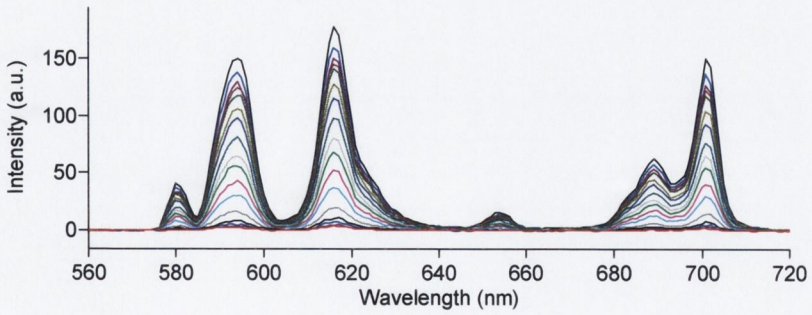

Figure 5. Luminescence spectra of Eu.104 in pH 7.4 buffered solution (0.1M TMACl) is quenched upon addition of Co(II). Excited at 266 nm. Note J2/J1 ratio

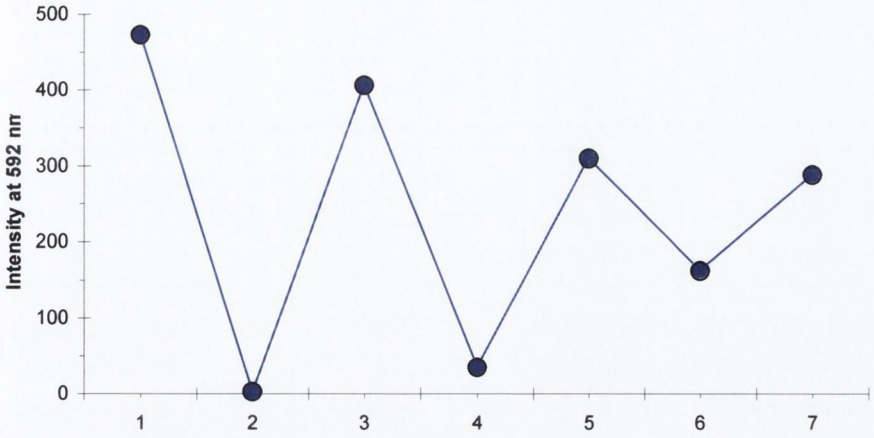

Figure 6. Effect upon luminescence intensity of Eu.104 after additions 1 equivalent of Cu(II) followed by 1 equivalent of EDTA, pH7.4

Empirical formula	'C56 H100 Cl24 I2 N14 Na2 O8'	
M chemical formula weight	2248.08	
Crystal size /mm	0.45 x 0.22 x 0.05	
Crystal system	Monoclinic	
Space group Z	P2(1)/c	
Cell length a	14.7350(5)	
Cell length b	14.8471(5)	
Cell length c	21.8612(8)	
Cell angle alpha	90.00	
Cell angle beta	96.1240(10)	
Cell angle gamma	90.00	
Cell volume U/Å^3	4755.3(3)	
Crystal density diffrn	1.570	
Crystal F(000)	2268	
μ(Mo-Kα)/mm^{-1}	exptl absorpt coefficient mu	1.397
ω scans; 2θ range/°	diffrn_reflns_theta_max	25.01 50.02
Reflections number total	8370	
Reflections number gt	7433	
wR2 (R1)	0.0935(0.0428)	
refine_ls_wR2_factor_gt	0.0935	
refine_ls_R1_factor_gt	0.0428	

Table 1. Crystal data sheet for 117.$Na_2.I_2.(H_2O)_2(CHCl_3)_8$

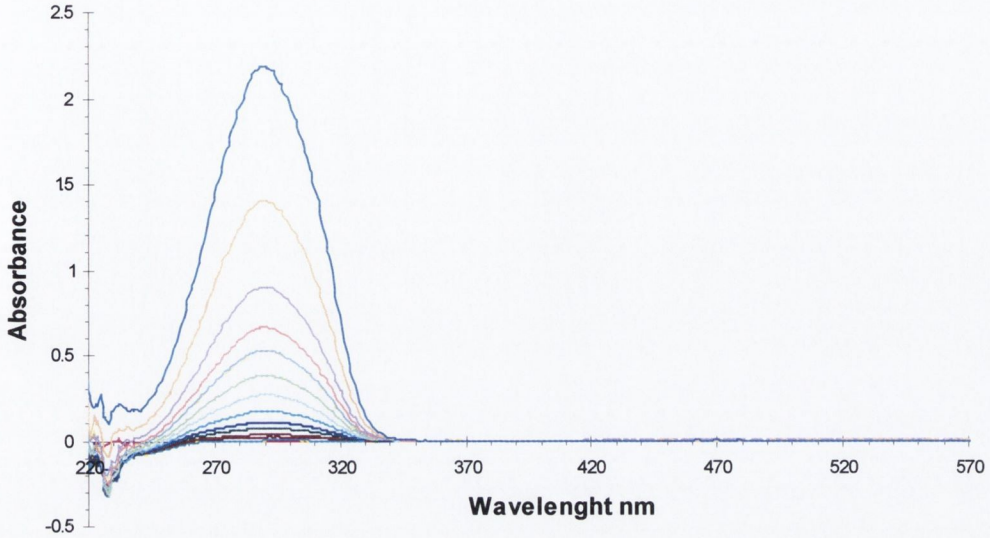

Figure 7. Absorption spectra for DMABA, Tb.117 titration, pH 7.4, 0.1 M TMACl

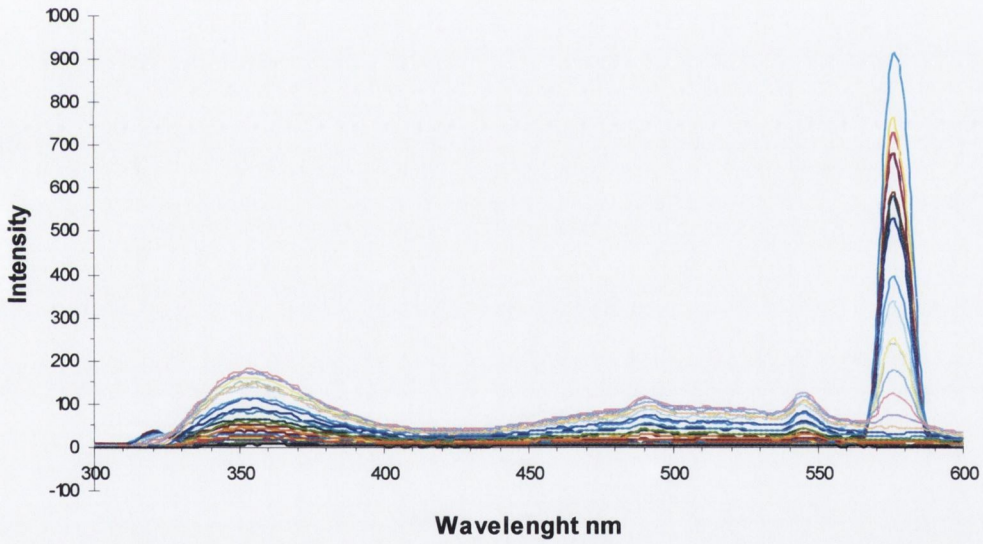

Figure 8. Changes in fluorescence spectra for DMABA Tb.117 titration pH 7.4, 0.1 M TMACl, excite at 288 nm. Note band at 320 nm due to Tb.117

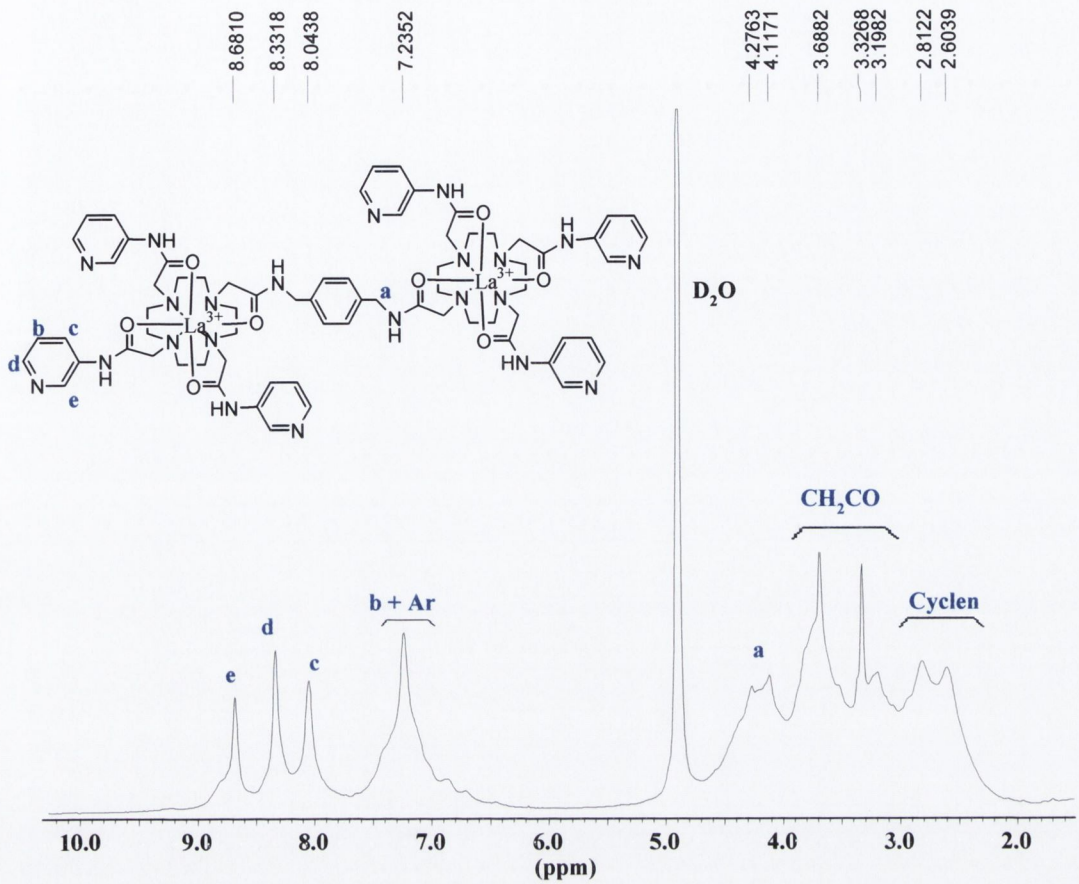

Figure 9. 400 MHz ^{1}H NMR of La.165 in D_2O

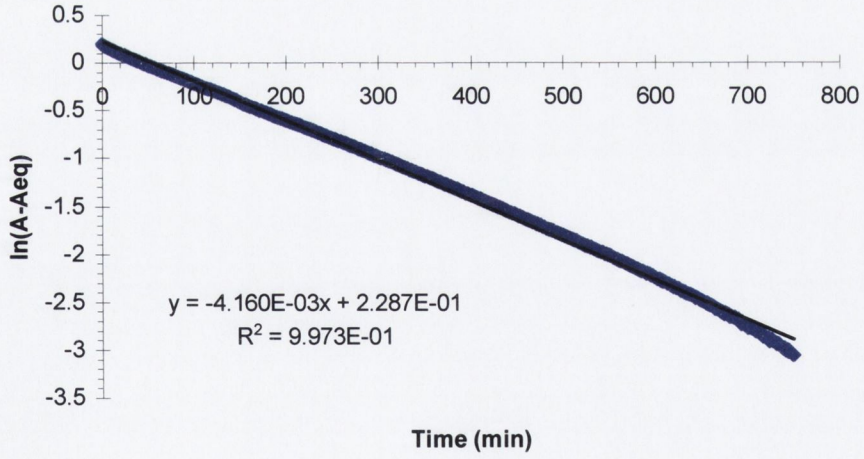

Figure 10. Manual plot of ln(Abs_{400}) Vs time for La.157 gave a rate constant of 4.16 x 10^{-3} min^{-1} or 0.249 hr^{-1}

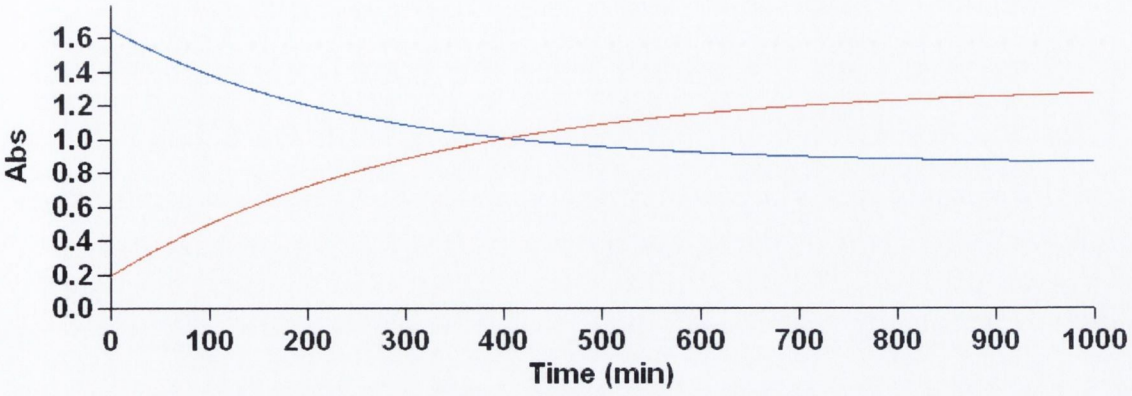

Figure 11. Kinetics profile for the hydrolysis of HPNP (0.18 mM) by La.163 at pH 7.4, 37°C

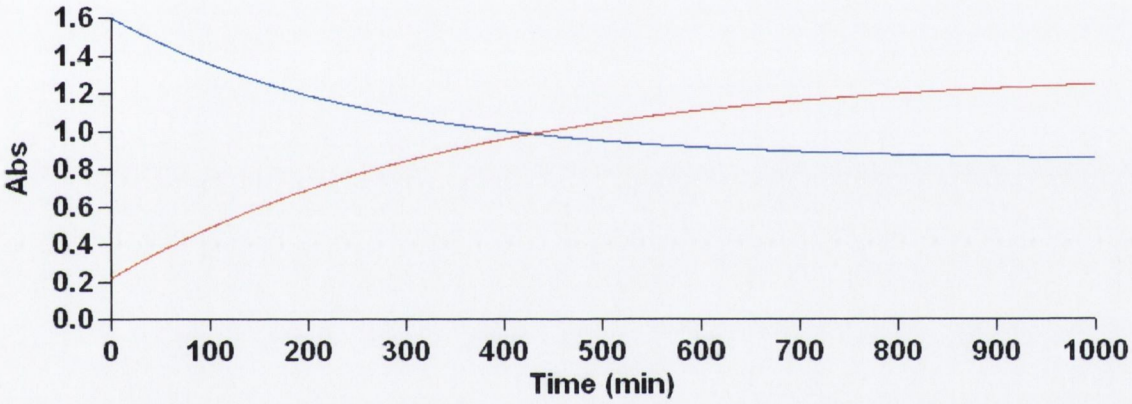

Figure 12. Kinetics profile for the hydrolysis of HPNP (0.18 mM) by La.164 at pH 7.4, 37°C

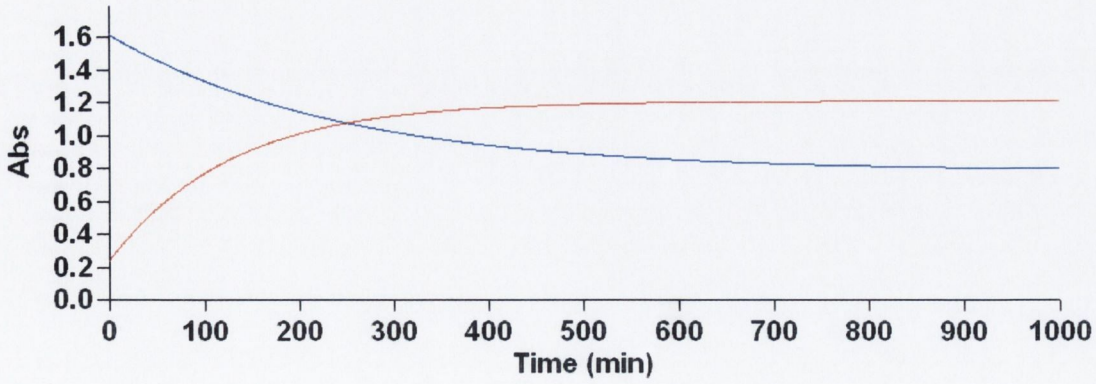

Figure 13. Kinetics profile for the hydrolysis of HPNP (0.18 mM) by Eu.164 at pH 7.4, 37°C

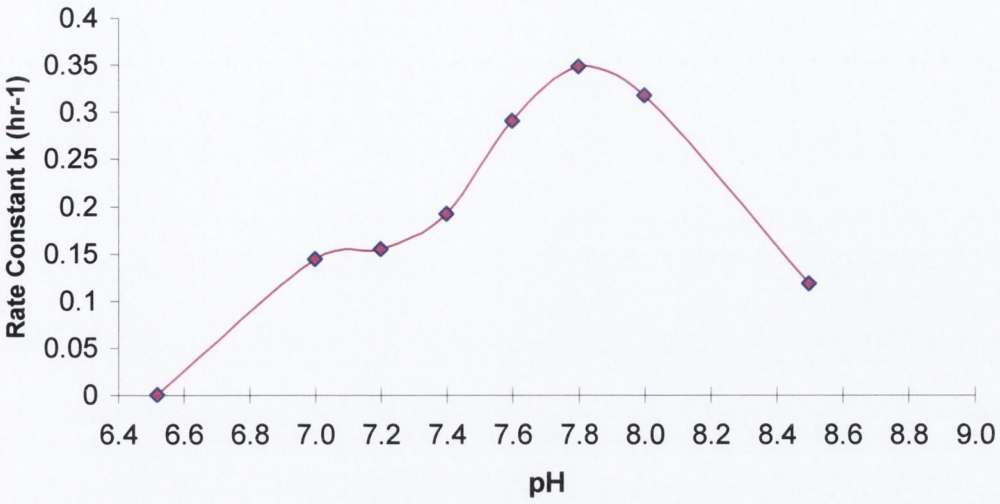

Figure 14. pH profile for the hydrolysis of 0.18 mM HPNP by La.163



Publications

ChemComm
www.rsc.org/chemcomm

Delayed lanthanide luminescence sensing of aromatic carboxylates using heptadentate triamide Tb(III) cyclen complexes: the recognition of salicylic acid in water†

Thorfinnur Gunnlaugsson,*[a] Andrew J. Harte,[a] Joseph P. Leonard[a] and Mark Nieuwenhuyzen[b]

[a] *Department of Chemistry, Trinity College Dublin, Dublin 2, Ireland. E-mail: gunnlaut@tcd.ie; Fax: 00 353 1 671 2826; Tel: 00 353 1 608 3459*

[b] *School of Chemistry, Queen's University of Belfast, Belfast, Northern Ireland, UK BT9 5AG*

Received (in Cambridge, UK) 22nd May 2002, Accepted 5th August 2002
First published as an Advance Article on the web 22nd August 2002

The coordinately unsaturated terbium complexes Tb.1 and Tb.2 possess two labile metal-bound water molecules that can be displaced upon metal chelation to aromatic carboxylic anions such as salicylic acid in water, which gives rise to large enhancements in the Tb(III) luminescence.

The use of fluorescence detection[1] for the sensing and physiological monitoring of cations,[2] anions[3] and neutral molecules has been extensively investigated.[4] For *in vivo* sensing, it has been shown to be essential to use fluorophores that absorb and emit at long wavelengths, or have long lived excited states. This is to prevent poor signal-to-noise ratio caused by short-lived (~ns) background emission or autofluorescence and light scattering from the active biological environment.[5] One way of overcoming these drawbacks is the use of delayed lanthanide luminescence.[6] The attractiveness of such metal ion emission is the occurrence of long-lived excited states (in the ms range), long emission wavelengths (500–700 nm), and line-like emission bands (10–30 nm bandwidth) under ambient conditions.[6] Using Eu(III) and Tb(III) based cyclen (1,4,7,10-tetraazacyclododecane) complexes we have made both luminescent sensors and switches for several cations and neutral molecules.[7] Since lanthanide ions are generally considered to be photophysically inert ($\varepsilon \sim 10\ M^{-1}\ cm^{-1}$), we have covalently incorporated into these complexes antennae, or chromophores whose function is to populate the exited states of the lanthanide ions indirectly ($^5D_0$ and $^5D_4$ for Eu(III) and Tb(III), respectively) *via* energy transfer.[5–7] Recognition at these receptor sites consequently modulates the energy transfer process causing the Eu(III) or Tb(III) emission to be *'switched on'*.[6,7] Concurrently, Parker *et al.* have developed lanthanide luminescent sensors for anions such as bicarbonate using coordinated unsaturated complexes with covalently bonded chiral antennae.[8] In these, the oxy-anions displayed quenching of metal bound water molecules, which caused the lanthanide ion emission to be 'switched on'. Inspired by this work, we were interested in developing new types of luminescent chemosensors for aromatic carboxylic acids, such as *N,N*-dimethylaminobenzoic acid (**3**) and salicylic acid (**6**), with biological concentration of *ca.* 0.4 mM. Here, the sensing action would be due to enhanced sensitisation of the lanthanide ion excited state by *the aromatic acid itself* upon displacement of the labile metal-bound water molecules. The attractiveness of such complexes is that they do not have covalently attached antennae, and as such are photophysically silent prior to the anion recognition. Hence, only upon coordination of the chromophore, *e.g.* the aromatic anion, and the formation of a ternary complex, would give rise to an effective population of the excited state.[9]

The heptadentate tri-arm ligands **1** and **2** were made in a one-pot synthesis from cyclen and the corresponding α-chloroacetamide (1 : 3.1) in CH_3CN and purified by tituration or flash column chromatography for **1** and **2**, respectively. The corresponding cationic complexes **Tb.1**, **Tb.2**, **Eu.1** and **Eu.2** were made upon complexation to triflate salts of Tb(III) and Eu(III), respectively, in refluxing dry CH_3CN (ESI†). Due to the high coordination requirements of the lanthanide ions (usually 9–10), the heptadentate lanthanide ion complexes have vacant coordination sites that are occupied by solvent molecules such as water.[10] The presence of two water molecules was confirmed by X-ray crystallography for both **Eu.1** and **Eu.2**, the latter being shown in Fig. 1.‡ As far as we know, these are the first crystal structures of heptadentate tri-arm amide cyclen complexes showing two metal bonded water molecules.[10] The structure shows that the ion is coordinating to the four nitrogens of the cyclen structure and the three oxygens of the amides, with N···Eu distances of 2.610(7), 2.625(6), 2.655(6) and 2.647(6) Å and O···Eu distances of 2.341(5), 2.364(5) and 2.378(5) Å. The Eu···O1W and Eu···O2W distances were measured to be 2.418(5) and 2.421(5) Å with a O1W–Eu–O2W bite angle of 72.20(18)°.

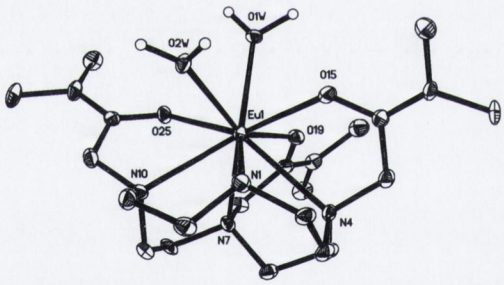

Fig. 1 Diagram of **Eu.2** showing the two coordinated water molecules with atomic displacement parameters at the 30% level. Hydrogen atoms have been omitted from the ligand for clarity.

The ability of **Tb.1**, **Tb.2**, **Eu.1** and **Eu.2** to bind and recognise the aromatic carboxylic acids **3**, **6** and **7**, the ester **4** and the ketone **5**, was investigated in water, in both pH 7.4 TRIS and pH 7.4 HEPES buffers, and in the presence of 0.1 M of tetramethylammonium chloride to maintain constant ionic strength. In a typical experiment, 17 μM solutions of the complexes were titrated with several potential sensitisers (chromophores) **3**–**7** and the changes in the lanthanide emission spectra and in lanthanide excited state lifetimes monitored. All of these sensitisers have triplet state energies[11] of *ca.* 22000–26000 cm^{-1} which is close to that found for Eu(III) $^5D_0$ (E = 17200 cm^{-1}) and Tb(III) $^5D_4$ (E = 20500 cm^{-1}),[7] suggesting that energy transfer from their excited states to the

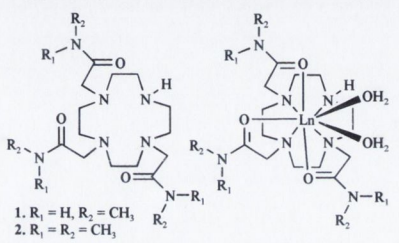

† Electronic supplementary information (ESI) available: experimental section, Fig. S1, Table S1. See http://www.rsc.org/suppdata/cc/b2/b204888d/

DOI: 10.1039/b204888d

This journal is © The Royal Society of Chemistry 2002

excited state of the lanthanide ions is feasible.[7b] As expected none of the above complexes were emissive in the absence of these chromophores indicating that the complexes were *photophysically silent* at low concentration (when excited at 300 nm). However, it was possible to determine the hydration number q,[6,7] for all the complexes by measuring their excited state lifetimes in H_2O and D_2O at high concentration. All of these gave a q value of *ca.* 2, indicating that two water molecules were coordinating to the metal centres in solution.

Initially the ability of the complexes to recognise **3** was evaluated in water. Of the above four complexes, only **Tb.1** and **Tb.2** became emissive upon titrating with **3**, when excited at 300 nm. For **Tb.2** the emission at 491, 548, 587 and 622 nm was *'switched on'* with luminescent enhancement factors of *ca.* 680, the largest changes being in the 548 nm band for the $^5D_4 \rightarrow {}^7F_5$ transition. For **Tb.1** the changes were somewhat smaller, *ca.* 220. When these measurements were carried out in buffered solutions and high ionic strength, large emission enhancements were also observed as shown in Fig. 2 for **Tb.2**, but the $^5D_4 \rightarrow {}^7F_3$ transition was not observed at 622 nm. For **Tb.2** the lifetimes of the excited state of **Tb.2** in the presence of 0.40 mM of **3** was measured to be 1.79 and 1.59 ms in D_2O and H_2O, respectively, which gives $q \approx 0$ (using $q = 5[(1/\tau)_{H_2O} - (1/\tau_{D_2O}) - 0.06]$[6] See ESI†), *i.e.* both water molecules had been displaced upon coordination of the carboxylic acid to Tb(III). By plotting the changes in the Tb(III) emission at 548 nm as a function of the concentration of **3** (as $-\log[\mathbf{3}]$) a bell-shaped curve[7a] was observed (see insert in Fig. 2). Examination of this curve showed that the emission was 'switched on' from $-\log[\mathbf{3}]$ *ca.* 5.8 to 4 (*ca.* 2 log units), which is an indication of 1:1 binding and simple equilibrium [an estimated $\log \beta = 5 (\pm 0.1)$ can be deduced from these changes between $-\log[\mathbf{3}] = 5.8$–4]. However, between $-\log[\mathbf{3}] = 4$–3.4 the emission was 'switched off'. No pH changes were observed upon titrating **Tb.2** with **3** (in buffered solution) indicating that that this was not due to protonation of **3** and concomitant dissociation of the ternary complex. We believe that this 'switching off' is rather due to self-quenching but we are currently investigating these features more closely. Upon titrating **Tb.2** using **4** or **5**, no Tb(III) emission was observed. However, the addition of 0.4 mM of **3** to a solution of **Tb.2** and **4** (3 mM) gave rise to large enhancements in the Tb(III) emission, indicating the selective recognition and binding of **3** to the Tb(III) ion and the formation of a ternary complex structure. These results suggest that efficient binding and population of the Tb(III) $^5D_4$ excited state is only possible if the metal bounded water molecules are removed upon binding.[8]

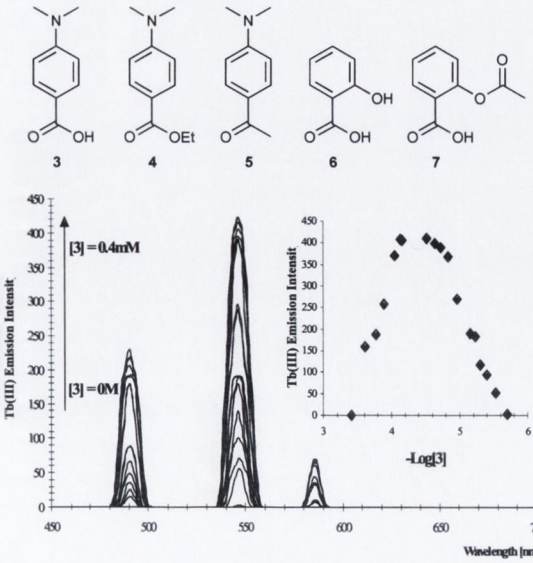

Fig. 2 The change in the Tb(III) emission in **Tb.2** upon addition of **3** in water when excited at 300 nm under physiological conditions. *Insert*: The changes in the Tb(III) emission at 548 nm as a function of $-\log[\mathbf{3}]$.

The effect on the Tb(III) emission upon binding of salicylic acid **6** ($\lambda_{ex.} = 296$) and its acetate ester **7** (Aspirin®) under physiological conditions was also investigated. As described above, the emission from **Tb.2** was highly dependent on the concentration of **6**, with a larger order of magnitude enhancement in the Tb(III) emission (see ESI†). The enhancement factor for **Tb.1** was somewhat smaller. However, unlike that seen for **3**, only two emission bands at 491 and 548 nm were observed. As for **3**, the binding of **6** ($-\log[\mathbf{6}]$) to **Tb.2** gave a bell-shaped dependence from $-\log[\mathbf{6}] = 2.6$–4.5 when measured at 548 nm ($\log \beta \sim 4.5$ in the range of 3.5–4.9, see ESI†). In contrast, the binding of **7** to **Tb.2** was *not* observed, *i.e.* no Tb(III) luminescence was observed. We propose that this lack of binding and hence sensitisation, is due to steric effects since **7** might be too large to approach the metal ion centre efficiently. Therefore **Tb.2** is an excellent chemosensor for **6**, the biologically active form of **7** under physiological conditions. We predict that upon recognition of **3** and **6**, the oxygen atoms of the aromatic carboxylates bind to the Tb(III) ion, forming a four-membered ring chelate, but a similar (five-membered) binding mode has been reported by Dickins *et al.* for lactate[12] (see also ref. 8) However, it is also possible that **6** binds to **Tb.2** *via* a one of the coarboxylate oxygens and the phenolic oxygen in a six-membered chelate. This is currently under investigation.

We thank National Pharmaceutical Biotechnology Centre, BioResearch Ireland, Enterprise Ireland, Kinerton Ltd, and TCD for financial support, Dr Hazel M. Moncrieff, Dr Angelo Taglietti and Dr Stephen Faulkner for helpful discussion and Dr John E. O'Brien for assisting with NMR.

Notes and references

‡ Data were collected on a Bruker SMART diffractometer using the SAINT-NT[13] software with phi/omega scans. A crystal was mounted on to the diffractometer at low temperature (*ca.* 120 K). The structure was solved using direct methods and refined with the SHELXTL program package.[13] *Crystal data* for **1**: $C_{23}H_{49}EuF_9N_7O_{16}S_3$, $M = 1098.83$, triclinic, space group $P1$, $a = 8.7196(19)$, $b = 13.147(3)$, $c = 18.427(4)$ Å, $\alpha = 95.805(3)$, $\beta = 97.220(3)$, $\gamma = 104.013(3)°$, $U = 2014.3(7)$ Å^3, $Z = 2$, $\mu = 1.828$ mm^{-1}, $R_{int} = 0.0788$. A total of 23924 reflections were measured for the angle range $2 < 2\theta < 58°$ and 9229 independent reflections were used in the refinement. The final parameters were $wR2 = 0.1659$ and $R1 = 0.0546$ [$I > 2\sigma I$]. CCDC reference number 186595. See http://www.rsc.org/suppdata/cc/b2/b204888d/ for crystallographic data in CIF or other electronic format.

1 *Chemosensors of Ion and Molecule Recognition.*, ed. J.-P. Desvergne and A. W. Czarnik, NATO ASI Series, Kluwer Academic Publishers, Netherlands, 1996.
2 T. Gunnlaugsson, M. Nieuwenhuyzen, L. Richard and V. Thoss, *J. Chem. Soc., Perkin Trans. 2*, 2002, 141 and references therein.
3 T. Gunnlaugsson, A. P. Davis and M. Glynn, *Chem. Commun.*, 2001, 2556 and references therein.
4 K. Rurack and U. Resch-Genger, *Chem. Soc. Rev.*, 2002, 116; A. P. de Silva, D. B. Fox, A. J. M. Huxley and T. S. Moody, *Coord. Chem. Rev.*, 2000, **205**, 41.
5 D. Parker and J. A. G. Williams, *J. Chem. Soc., Dalton Trans.*, 1996, 3613.
6 D. Parker, *Coord. Chem. Rev.*, 2000, **205**, 109.
7 (*a*) T. Gunnlaugsson, *Tetrahedron Lett.*, 2001, **42**, 8901; (*b*) T. Gunnlaugsson, D. A. MacDónaill and D. Parker, *J. Am. Chem. Soc.*, 2001, **123**, 12866; (*c*) T. Gunnlaugsson, D. A. MacDónaill and D. Parker, *Chem. Commun.*, 2000, 93.
8 J. I. Bruce, R. S. Dickins, L. J. Govenlock, T. Gunnlaugsson, S. Lopinski, M. P. Lowe, D. Parker, R. D. Peacock, J. J. B. Perry, S. Aime and M. Botta, *J. Am. Chem. Soc.*, 2000, **122**, 9674.
9 J. Georges, *Analyst*, 1993, **118**, 1481; N. Arnaud and J. Georges, *Analyst*, 1999, **124**, 105; M. A. Mortellaro and D. G. Nocera, *J. Am. Chem. Soc.*, 1996, **118**, 7414.
10 P. Caravan, J. J. Ellison, T. J. McMurry and R. B. Lauffer, *Chem. Rev.*, 1999, **99**, 2293.
11 *Handbook of Photochemsitry 2nd Edition*, ed. S. L. Murov, I. Carmichael and G. L. Hug, Marcel Dekker, New York, 1993.
12 R. S. Dickins, C. S. Love and H. Puschmann, *Chem. Commun.*, 2001, 2308.
13 SAINT-NT, Brüker AXS Madison, Wisconsin, 1998; G. M. Sheldrick, University of Göttingen, Göttingen,Germany, 1998.

Supramolecular Chemistry, 2003 Vol. 15 (7–8), pp. 505–519

Taylor & Francis
Taylor & Francis Group

The Formation of Luminescent Supramolecular Ternary Complexes in Water: Delayed Luminescence Sensing of Aromatic Carboxylates Using Coordinated Unsaturated Cationic Heptadentate Lanthanide Ion Complexes

THORFINNUR GUNNLAUGSSON[a,*], ANDREW J. HARTE[a], JOSEPH P. LEONARD[a] and MARK NIEUWENHUYZEN[b]

[a]*Department of Chemistry, Trinity College Dublin, Dublin 2, Ireland;* [b]*School of Chemistry, Queen's University of Belfast, Belfast BT9 5AG, UK*

Received 8 November 2002; Accepted 13 January 2003

The synthesis of four lanthanide ion complexes Eu·1, Eu·2, Tb·1 and Tb·2, from the heptadentate tri-arm cyclen (1,4,7,10-tetraazacyclododecane) ligands 1 and 2 that were made in one-pot syntheses is described. These coordinatively unsaturated complexes have two labile metal-bound water molecules, as demonstrated by X-ray crystallography. This was also confirmed by evaluating their hydration state ($q \sim 2$) by measuring their lifetimes in D_2O and H_2O, respectively. The above complexes were all designed as being "photophysically silent" prior to the recognition of the anion, since they do not possess antenna that can participate in sensitisation of the Eu(III) or the Tb(III) excited state. However, the two water molecules can be displaced upon anion binding by the appropriate aromatic carboxylates to give ternary complexes in water, through either four- or six-member ring chelates ($q \sim 0$), or possibly via a monodentate binding. In the case of Tb·1 and Tb·2, large luminescence enhancements were observed upon the formation of such ternary complexes with *N,N*-dimethylaminobenzoic acid at ambient pH. Such binding and luminescent enhancements were also observed for Tb·1 in

The Future of Supramolecular Chemistry

There is no doubt that Supramolecular Chemistry is a fast growing field of research. As the field grows, and more complex targets and applications are addressed, we must ensure that we do not neglect the fundamental science needed to achieve many of our principle aims. Recognition and signalling using chemosensors have become an ever more important part of supramolecular chemistry, particularly from a medical diagnostic point of view, since it enables the use of non-invasive, real-time monitoring of physiological species *in vivo*, something that we all will benefit from. In this paper, we try to address some of these fundamental aims such as recognition and signalling by developing "simple" self-assembly lanthanide-based sensors.

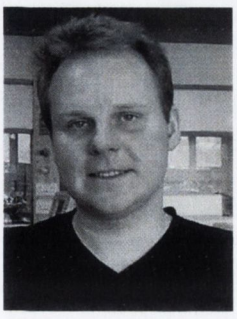

Thorfinnur (Thorri) Gunnlaugsson was born in Iceland in 1967. He obtained his PhD with Professor A. P. de Silva at Queen's University Belfast, working on luminescent switches and sensors. He then moved to Durham University, England, as a postdoctoral fellow with Professor David Parker, working on developing luminescent lanthanide sensors, an area which still features strongly in his work. In 1998. he was appointed as the Kinerton Lecture in Medicinal Chemistry at Trinity College Dublin, and in 2000 as a lecturer in Organic Chemistry. In 2002 he was elected as Fellow of Trinity College Dublin. His main research interests are in the areas of Supramolecular and Medicinal Chemistry, and particularly in the fields of recognition and targeting.

*Corresponding author. Tel.: +353-1-608-3459. Fax: +353-1-671-2826. E-mail: gunnlaut@tcd.ie

ISSN 1061-0278 print/ISSN 1029-0478 online © 2003 Taylor & Francis Ltd
DOI: 10.1080/1061027031000160510

the presence of salicylic acid. On all occasions, the anion recognition "switched" the emission "on" over two logarithmic units. At higher concentrations, the emission is reduced possibly due to quenching. In the case of aspirin, the binding was too weak to be measured, indicating that Tb·1 selectively detects salicylic acid, the active form of aspirin in water. In the case of Eu·1 and Eu·2, the affinity of these complexes towards such aromatic carboxylates was too weak for efficient ternary complex formation.

Keywords: Lanthanide luminescence; Lanthanide complexes; Sensing; Aspirin; Salicylic acid

INTRODUCTION

The use of luminescence detection for the sensing and monitoring of ions and molecules is of great current interest [1–13]. Whereas earlier work was mainly focused on the use of fluorescence as the mode of detection, which has excited state lifetimes in the nanosecond time range, the need for the development of luminescent chemical sensors that can be employed for online detection *in vivo* has led to the need to develop chemosensors that possess long-lived excited states [14–18]. The use of such delayed emission has great advantages over fluorescence, since it overcomes the poor signal-to-noise ratio that is caused by short-lived background emission (autofluorescence) and light scattering of the surrounding biological environment [19,20]. As in the case of fluorescence detection, the recognition event can be monitored by observing the changes in the various photophysical properties of the emitting moiety such as wavelength, intensity (or quantum yield of luminescence: Φ_L) or lifetime [21–25].

We have been interested in the sensing of cations and anions by employing fluorescence and/or colorimetric detection [26–32]. Recently, we have developed both luminescence switches [33,34] and chemosensors [35–37] which utilise lanthanide luminescence, by preparing well-defined and stable octadentate Eu(III) and Tb(III) cyclen (1,4,7,10-tetraazacyclododecane) macrocyclic complexes [38–40]. Such complexes possess long-lived excited states (approximately in the millisecond range) and emit at long wavelengths (500–750 nm) with large Stokes shifts and characteristic line-like emission bands (10–30 nm bandwidth) under ambient conditions [41–44]. These are all qualities necessary for online *in vivo* monitoring. However, normally the lanthanide ions are photophysically inert due to low molar absorptivities, which is related to Laporte forbidden f–f transitions making direct excitation difficult [33–46]. Nevertheless, this drawback can be overcome by incorporating one or more antennae covalently into the lanthanide complexes, ensuring that the lanthanide-excited states [which are $^5D_0$ and $^5D_4$ for Eu(III) and Tb(III), respectively] are efficiently populated through sensitisation [33–47]. This is a well-established process that occurs via an energy-transfer mechanism from the singlet-excited states of the antenna to the lanthanide excited states via the antenna triplet state [33–48]. Such lanthanide sensitisation has also been demonstrated by using non-covalently linked antennae by employing β-diketones [45–51] and other related organic ligands [52–63], and also by using β-cyclodextrins (CD)-based lanthanide complexes, as recently demonstrated by several researchers [64–69].

In designing our lanthanide chemosensors, we took advantage of the use of the sensitising antennae by simply incorporating the recognition site into the antennae themselves [33–37]. Hence, any perturbation at this site, i.e. recognition, subsequently led to the modulation in the sensitisation process with concomitant changes in the lanthanide luminescence. However, the drawback to such chemosensors is the elaborate synthetic pathways required for the desired sensors, which is both time-consuming and often results in a low overall yield. Because of this, we have recently turned our attention to the development of kinetically stable heptadentate coordinative unsaturated cyclen complexes that do not have the receptor-antenna moieties as an integrated part of their structures [70]. Examples are the triarm amide complexes **Eu·1**, **Eu·2**, **Tb·1** and **Tb·2** [70]. It has recently been reported by Parker *et al.* [71,72] that in water at pH 7.4, such related coordinatively unsaturated complexes have two water molecules associated with their structures, since the lanthanide ions fulfil their high coordination requirements (typically 9–10) by binding two solvent molecules. Furthermore, it has also been shown that these are labile water molecules, which can be removed upon binding of anions such as bicarbonates, acetate, phosphates and halides [71,72].

Inspired by this work, our aim was to develop novel chemosensors where the two labile metal-bonded water molecules could be displaced upon metal chelation yielding self-assembly ternary complexes between **Eu·1**, **Eu·2**, **Tb·1** and **Tb·2** and several aromatic carboxylates [70]. Here, the idea was that instead of having the antenna covalently bound to

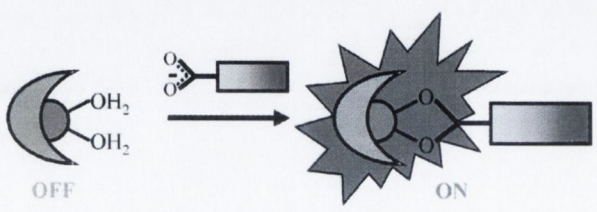

FIGURE 1 Schematic diagram of the self-assembly process that leads to the formation of the luminescent ternary complex between the lanthanide complex and the carboxylate antenna.

the ligand, the aromatic carboxylate themselves would act as antennae. Hence, only upon coordination of the aromatic anion, through self-assembly, would the lanthanide ion emission be "switched on" (via excitation of the antennae). Such a recognition event is depicted in Fig. 1. Furthermore, because of the population of the lanthanide excited state by the coordinated anions, the above complexes could all be considered to be "photophysically silent" prior to the anion recognition. Moreover, as the binding of these antennae would be directly to the metal centre, the population of the lanthanide ions would be greatly improved due to the small distance between the antenna and the metal ion (assuming a Förster mechanism where efficiency is dependent on $\sim 1/r^6$) [73,74]. Furthermore, such binding would be expected to be in a 1:1 ratio. However, it would be expected that this binding would be highly dependent on the nature and the structure of the antenna, and their ability to chelate to the metal centre. Furthermore, the choise of aromatic carboxylates as sensitisers is somewhat limited by their triplet excited state energy, which needs to be greater than that of the excited states of Eu(III) and Tb(III) (20,400 and 17,200 cm^{-1} for $^5D_0$ and $^5D_4$, respectively). With this in mind, we decided to use neutral pendent amide arms, as they would ensure that the complexes were cationic, and as such would maximise the binding interactions.

In this paper, we give a full account of the synthesis of **Eu·1**, **Eu·2**, **Tb·1** and **Tb·2** from the heptadentate tri-arm functionalised cyclen ligands **1** and **2**, and the photophysical evaluations of these compounds in the presence of several aromatic carboxylic acid derivatives.

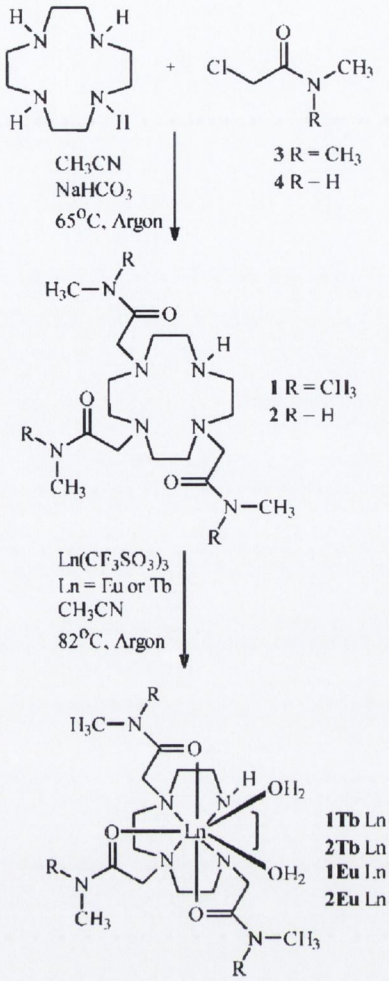

SCHEME 1 Synthesis of ligands **1** and **2** and their corresponding Eu(III) and Tb(III) complexes **Eu·1**, **Eu·2**, **Tb·1** and **Tb·2**.

DESIGN AND SYNTHESIS OF 1 AND 2 AND THEIR Eu(III) AND Tb(III) COMPLEXES

We set out to develop simple lanthanide ion complexes that would allow for the monitoring of important aromatic carboxylic acids such as salicylic acid, the active form of the prodrug aspirin, at the same time of requiring only minimal synthetic efforts [75]. With this in mind, we set out to make the two ligands **1** and **2** in one-pot syntheses.

The synthesis of **1** and **2** was achieved by reacting the α-chloroamides of *N*-methylacetamide (**3**) and *N*,*N*-dimethylacetamide (**4**), respectively, with cyclen in dry CH_3CN (in 3:1 ratio of acetamide: cyclen) at 65°C for 3 days in the presence of $NaHCO_3$ (Scheme 1). For **1**, the macrocycle was purified by alumina column chromatography using CH_2Cl_2, followed by gradient elution using NH_3-saturated MeOH ($0 \rightarrow 3\%$). For **2**, the macrocycle was purified by tituration with diethyl ether. Both **1** and **2** were obtained in over 50% yield after purification. The ligands were characterised using standard methods. However, both were found to be hydroscopic, and elemental analyses were therefore not obtained. High-resolution accurate masses were obtained for both **1** and **2**. The ^1H NMR spectrum of both ligands showed the presence of C_2 symmetry that runs along an axis through the unalkylated amine in *position 1* and the tertiary amine in *position 7* of the cyclen ring. The ^1H NMR spectrum of **2** is shown in Fig. 2 and shows the presence of two N–H resonances at 7.60 and 7.30 ppm, in a ratio of 1:2, for the two amide protons. The two α-protons for the pendent arms appear as singlets at 3.06 and 2.97 ppm (in a ratio of 4:2), respectively, whereas the N–CH_3 protons appeared as two doublets in a ratio of 6:3 at 2.75 and 2.67 ppm, respectively. The cyclen methyl protons appear as four broad resonances in the region of 2.7–2.4 ppm. The ^1H NMR spectrum for **1** showed similar characteristics.

The Eu(III) and Tb(III) complexes of **1** and **2** were made by refluxing together an equivalent amount of **1** or **2** with either Eu(III) or Tb(III) triflate $(SO_3CF_3)_3$ in dry CH_3CN under an inert atmosphere for 24 h.

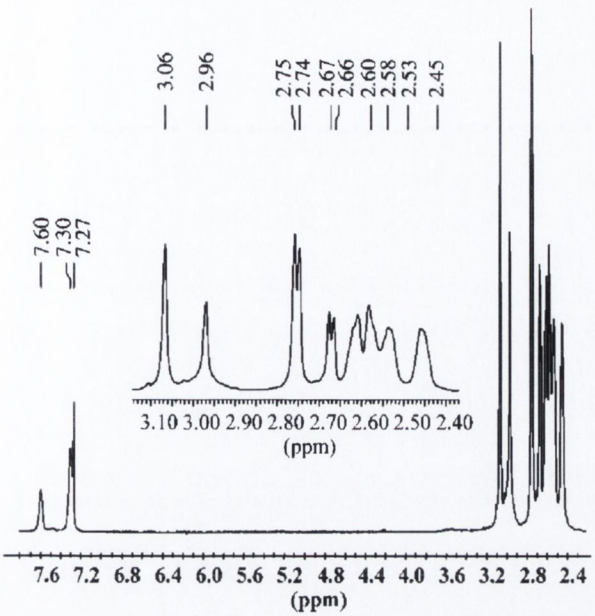

FIGURE 2 ^{1}H NMR spectrum of the ligand **2** in $CDCl_3$ (400 MHz) showing the presence of the C_2 symmetry in **2**.

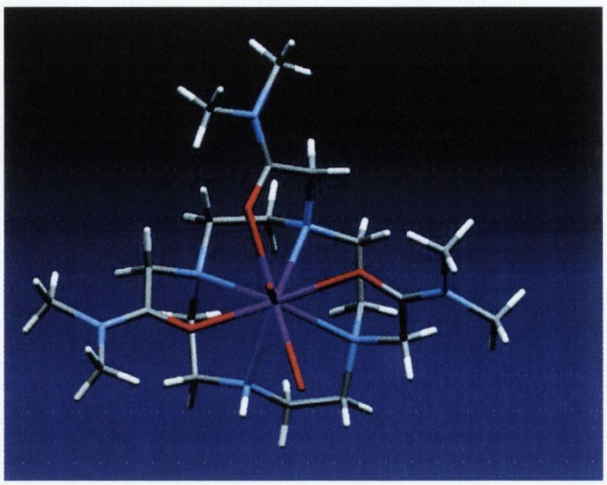

FIGURE 3 View from the top of **1·Tb** showing the binding of Tb(III) to **1** and the two water molecules. Anions and solvent molecules have been removed for clarity. (See colour plate 1 at the end of this issue.)

Upon cooling to room temperature the solution was poured into a stirring solution of dry diethyl ether, which resulted in oily residues that were collected by decanting the organic layers and rinsing the resulting residues with either CH_2Cl_2 or $CHCl_3$. These complexes were characterised by elemental analysis, electrospray MS (ESMS), IR and by NMR. The ^{1}H NMR spectrum of all the complexes showed the presence of the paramagnetic metal centres, as indicated by several broad resonances appearing over a large ppm range [76]. The ESMS for the four complexes showed the presence of two triflate counterions as the major peak with several other combinations of multiple charges, which had an identical isotopic pattern to the corresponding calculated spectrum. In the ESMS, the presence of the two expected metal-bonded water molecules was not observed. We were, however, able to obtain X-ray crystal structures of three of the four complexes, namely **Eu·1**, **Eu·2** and **Tb·1**.

X-RAY CRYSTALLOGRAPHIC INVESTIGATION OF Eu·1 AND Tb·1

We were able to grow crystals of **Eu·1**, **Eu·2** (not shown) and **Tb·1** that were suitable for X-ray crystallographic determination [77,78]. The Eu(III) crystals were obtained by slow evaporation from CH_3CN, whereas for **Tb·1**, this was achieved by slow evaporation from a mixture of CH_3CN and CH_2Cl_2 (in the ratio of 1:1). All the crystal structures showed the presence of the two metal-bonded water molecules. The structure of **Tb·1** is shown in Fig. 3, but we have previously published the structure of the Eu(III) analogue [70]. To the best of our knowledge, these are the first examples of such tri-amide lanthanide ion-based cyclen complexes [70,76,79]. From Fig. 3, it is evident that the Tb(III) centre is coordinating to the four nitrogen of the macrocyclic ring and to the three oxygens of the carboxylic amides on the pendent arms, with average Tb···N and Tb···O distances of 2.634(4) Å and 2.347(3) Å, respectively. In general, the lanthanide ions prefer a high-coordination environment, which is usually in the order of 9–10 [77,78]. For **Tb·1**, seven of these are provided by the ligand, with two further coordination sites being occupied by two metal-bound water molecules. The Tb···O1W and Tb···O2W distances are almost identical, being 2.429(3) Å and 2.441(3) Å, respectively. For the isostructural **Eu·1** complex, these distances were measured to be 2.418(5) and 2.421(5), respectively. Table I lists selected bond angles and distances for the two complexes. From these, it can be seen that there are only minimal differences observed for the two complexes. Similar results were observed for **Eu·2** (not shown here). From the crystal structure data of the complexes, it is apparent that they all adapt a general square antiprism geometry in the solid state. Such geometry is well known for the tetra-substituted octadentate lanthanide-based cyclen complexes.[†]

[†]For such square antiprism geometry, two elements of chirality can be observed, which are associated with the sign of the torsion angles of the NCCO chelate (Δ or Λ) and the NCCN chelate rings (δ or λ) helicity of the *N*-alkylated pendent arms [80,81]. For **Tb·1** (as shown in Fig. 3), these were determined to be an average of 19.2° and −58.5°, respectively. However, for **Tb·1**, the complex crystallised in a centrosymmetric space group containing both Δ and Λ conformations. Similar results were observed for **Eu·1**.

TABLE I Selected bond lengths and angles for **Eu·1** [70] and **Tb·1**

	Eu·1	**Tb·1**
Ln–O (Å)	2.342(5), 2.364(5), 2.378(5)	2.326(3), 2.348(3), 2.368(3)
Ln–O (water) (Å)	2.418(5), 2.421(5)	2.429(3), 2441(3)
Ln–N (Å)	2.605(6), 2.624(6), 2.625(6), 2.647(6)	2.600(4), 2.637(4), 2.642(4), 2.656(3)
N–C–C–N (°)	58.9(9), 59.4(9), 62.2(9), 57.0(9)	−57.7(6), −61.7(6), −58.0(6), −58.4(6)
N–C–C–O (°)	−2.5(11), −27.6(10), −25.4(10)	5.6(7), 25.6(6), 26.5(6)
OW1–Ln–OW2 (°)	72.20(18)	71.80(11)

For our design, it is essential that all the complexes possess two water-bonded molecules, as seen for **Tb·1** in Fig. 3. There are two main reasons for this. First, even though both ligands lack the covalently functionalised antennae, it is possible to generate an excited state in both Eu(III) and Tb(III) by direct excitation of the metal centres (see later). However, the water molecules can efficiently quench the excited state through OH vibrations (or by any other energy-matched oscillators), which further diminishes any lanthanide luminescence prior to the recognition event (the formation of the ternary complex). Secondly, the need for two "vacant" coordination sites at the metal centre would ensure that the binding of the carboxylate would be possible through a bidentate manner (for instance by both of the oxygens of the carboxylate). Subsequently, the water molecules would be expelled and no longer able to quench the lanthanide excited state. From the above crystal structures, it can be seen that this criterion is fulfilled. However, the angle at which these two water molecules bind to the ions is also of importance, since the nature of the binding mode would depend on the bite angle between the two water molecules. For **Tb·1**, the O1W–Tb–O2W bite angle was measured to be 71.80(11)° whereas for **Eu·1**, the O1W–Eu–O2W bite angle was measured to be 72.20(18)°, indicating that both complexes would be able to interact with the carboxylates via such a bidentate manner.

Recently, Parker *et al.* [71] and Dickins *et al.* [82] have shown that related three-arm cyclen complexes can form bidentate adducts with organic anions such as acetate, citrate, glycinate, and lactate through four- and five-member chelates. The bite angles for all of these complexes were between 54° and 69°. In the case of acetate, this binding occurred through both of the carboxylate oxygens. We thus proposed that the aromatic carboxylates would bind to **Eu·1**, **Eu·2**, **Tb·1** and **Tb·2** in a similar manner. However, to date, we have not been able to crystallise these complexes in the presence of any of the aromatic carboxylates to prove this theory.

LUMINESCENCE STUDIES

Determining the Hydration Numbers of Eu·1, Eu·2, Tb·1 and Tb·2 in the Absence and Presence of *N,N*-Dimethylaminobenzoic Acid (7) Antenna

As stated above, both the Eu(III) and the Tb(III) complexes were expected to possess two labile metal-bound water molecules. This was verified for three of these complexes by determining their solid-state structures. The number of metal-bound water molecules can also be evaluated by estimating the hydration state or number of the complexes using a luminescent method, where the rate constant for the radiative decay (k) of the $^5D_0$ excited state of Eu and the $^5D_4$ excited state of Tb are measured in H_2O (k_{H_2O}) and D_2O (k_{D_2O}), respectively [83]. These values can be obtained by direct excitation of the lanthanide ion complexes at high concentrations. The hydration number (q) can then be determined from Eqs. (1) and (2) for the Eu and Tb complexes, respectively.

$$q^{Eu(III)} = 1.2[(1/\tau_{H_2O} - 1/\tau_{D_2O}) - 0.25 - 0.075x] \quad (1)$$

$$q^{Tb(III)} = 5[(1/\tau_{H_2O} - 1/\tau_{D_2O}) - 0.06] \quad (2)$$

Here, the prefixes 1.2 and 5 in Eqs. (1) and (2), respectively, are proportionality constants that mirror the sensitivity of the corresponding ions to quenching by metal-bound water molecules. The correction terms −0.25 and −0.66 represent quenching by second sphere water molecules, whereas $-0.075x$ in Eq. (1) represents the quenching by N–H oscillators, where x is the number of such oscillators within a given complex [83–85].

Table II summarises the observed lifetimes (τ_{Ln}), the corresponding k_{H_2O} and k_{D_2O} values and

TABLE II Measured lifetimes and rate constants for **Eu·1**, **Eu·2**, **Tb·1** and **Tb·2** and the corresponding hydration number ($q \pm 0.5$) in the *absence* of any carboxylate antennae

Complex	τ_{H_2O} (ms)	k_{H_2O} (1/ms)	τ_{D_2O} (ms)	k_{D_2O} (1/ms)	q
Eu·1	0.281	3.55	0.855	1.17	2.55
Eu·2	0.315	3.17	0.936	1.07	1.95
Tb·1	0.720	1.38	1.080	0.92	2.01
Tb·2	0.869	1.15	1.386	0.72	1.85

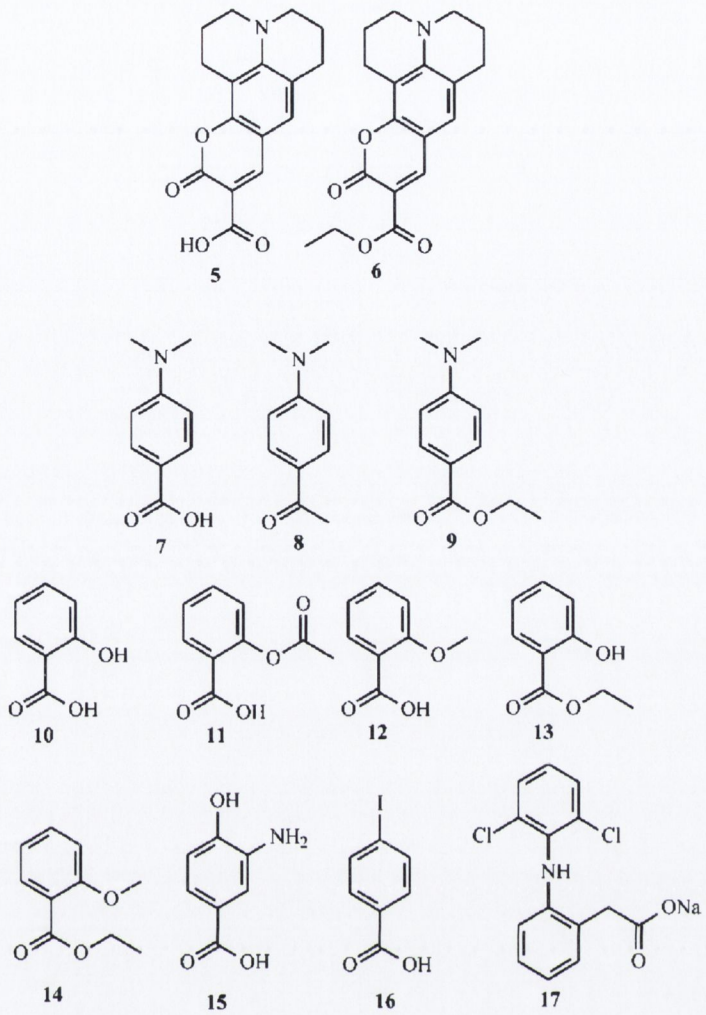

SCHEME 2 Various carboxylic-acid-based antennae tested.

the $q(\pm 0.5)$ values for the above complexes in the absence of any carboxylate antennae [hence, by direct excitation of the Ln(III) ions] [84,85]. From these data, it can be seen that all the complexes have two water molecules associated with their structure in solution. The above measurements were repeated by exciting the lanthanide ions at 300 nm, the same wavelength that most of the carboxylate antennae (Scheme 2) absorb at. However, in all cases, the emission was too weak for evaluating q accurately.

As stated above, it was hoped that the formation of a ternary complex between the lanthanide complexes and the antenna would lead to large enhancements in the lanthanide luminescence of these complexes. Such ternary complexes can be formed only if both or one of the water molecules are displaced. To evaluate this, the q values were measured in the presence of several antennae (Scheme 2). Here, the proof for the formation of such ternary complexes would be achieved if $q \approx 0$, with concomitant enhancements in the lanthanide luminescence.

Initially, the ability of the coumarin antennae **5** and **6** was investigated in water. However, neither of these gave rise to any enhancements in the Eu(III) or Tb(III) luminescence. This suggests that these antennae were unable to bind to the metal centre, because, according to their triplet state energies (T_1), the sensitisation by the Tb(III) excited state should be energetically favourable. Because of this, a series of structurally more simple carboxylates were tested, namely the benzoic acids and derivatives **7–16**. All of these have triplet state energies of ca. 22,000–26,000 cm^{-1}, which is close to that found for $^5D_0$ and $^5D_4$ for Eu(III) and Tb(III), respectively [86]. This suggested that an effective energy transfer form these antennae to the excited state of the lanthanide ions would be feasible, provided that the antennae were able to form stable ternary complexes with **Ln·1** and **Ln·2**. The first of these antennae to be investigated was the *N*,*N*-dimethylaminobenzoic acid **7**. Upon addition of **7** to either **Eu·1** or **Eu·2** (ca. 17 mM) in water, no Eu(III) emission was observed when excited at 300 nm, indicting that **7** was either not

TABLE III Measured lifetimes and rate constants for **Eu·1**, **Eu·2**, **Tb·1** and **Tb·2** and the corresponding hydration number ($q \pm 0.5$) in the presence of *N,N*-dimethylaminobenzoic acid

Complex	τ_{H_2O} (ms)	k_{H_2O} (1/ms)	τ_{D_2O} (ms)	k_{D_2O} (1/ms)	q
Eu·1	0.235	4.25	0.438	2.28	1.79
Eu·2	0.276	3.62	0.733	1.35	2.15
Tb·1	1.593	0.62	1.795	0.55	0.06
Tb·2	1.626	0.61	1.895	0.52	0.14

binding to the Eu(III) centre or not able to populate the Eu(III) excited state efficiently. Furthermore, it is also known that the Eu(III) excited state can be quenched by an electron-transfer mechanism using similar antennae [72].

When these measurements were repeated using **Tb·1** and **Tb·2**, a positive sensitisation occurred, with the Tb(III) emission being clearly visible. For instance, upon addition of 4 equivalents of **7**, the emission of **Tb·1** at 491, 548, 687 and 622 nm was "switched on" with luminescence enhancement factors of ca. 700 (the quantum yield was not determined). Here, the largest changes were seen in the $^5D_4 \rightarrow {}^7F_5$ transition at 548 nm, which is magnetic-dipole allowed. For **Tb·1**, these enhancements factors were somewhat smaller or ca. 220. These results indicate that for both **Tb·1** and **Tb·2**, the carboxylate was binding to the Tb(III) centres and successfully populating their excited states (upon excitation of the antenna at 300 nm).

Having established that **7** was able to sensitise the Tb(III) excited states, we measured the lifetimes of the excited states of **Eu·1**, **Eu·2**, **Tb·1** and **Tb·2**, in the presence of **7** (0.68 mM, 4 equivalents) with the aim of determining the hydration numbers of the four complexes. These results are summarised in Table III. From these measurements it can be seen that for either **Eu·1** or **Eu·2** q was evaluated to be ca. 2, indicating that both have two water molecules associated with their structures and that neither are binding to **7**. However, for **Tb·1** and **Tb·2**, both give rise to similar excited state lifetimes in either H_2O or in D_2O, which indicates that no inner-sphere solvent molecules were present, so q was evaluated to be ca. 0 for both of these complexes. This signifies that for both **Tb·1** and **Tb·2**, a self-assembly process occurs between **7** and these complexes, giving rise to the formation of luminescent ternary complexes in solution. Furthermore, since both of the water molecules have been displaced upon coordination of the carboxylates to Tb(III), we conclude that such binding occurs through both of the oxygens of the carboxylate in a bidentate manner via a four-member ring chelates. This is depicted in Fig. 4, where the Tb(III) emission of **Tb·2** is only "switched on" upon sensitisation by **7** after the formation of the ternary complex.

Luminescent Sensing of Aromatic Amino Carboxylates and Related Derivatives

Having observed the self-assembly process between the Tb(III) complexes and **7**, which gives rise the formation of luminescent ternary complexes, we carried out a titration of all the complexes (typically in 17 μM solution) in the presence of **7**–**15** in H_2O and at pH 7.4 using either Tris or Hepes buffers containing 0.1 M of tetramethylammonium chloride to maintain a constant ionic strength. All measurements were carried out in aerated solutions. At such low concentrations, none of the complexes were particularly luminescent, and as such, the emission from these complexes is "switched off".

When **Tb·1** was titrated in water using **7**, the Tb(III) emission was switched on as previously described. When these measurements were repeated in buffered solution at pH 7.4, the emission was also "switched on". However, the enhancement factors

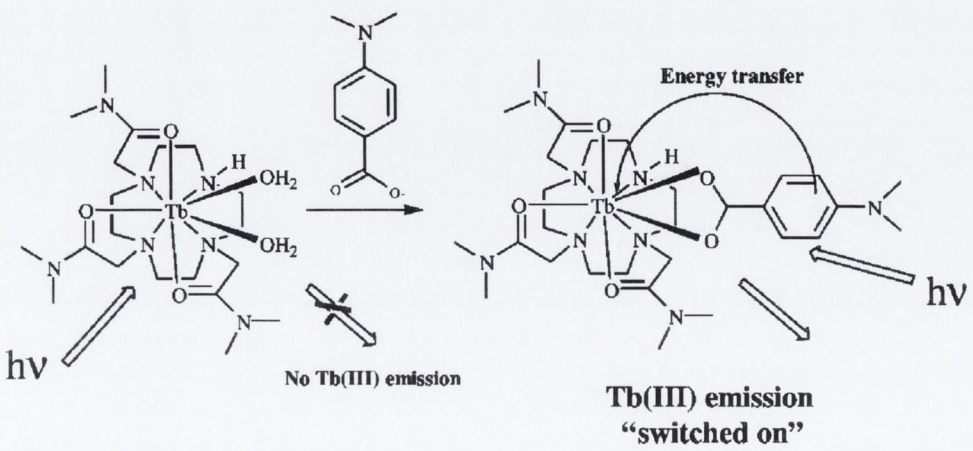

FIGURE 4 Formation of the ternary complex between **7** and **Tb·1** giving rise to large enhancements in the Tb(III) emission. The emission from **Tb·1** is said to be "switched on" upon excitation at 300 nm.

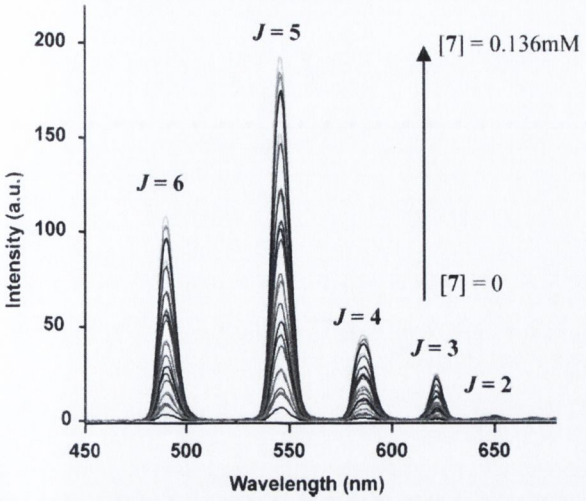

FIGURE 5 Changes in the Tb(III) emission of **Tb·1** upon addition of **7**. $J = 6$, 5, 4, 3 and 2 represent the bands corresponding to the deactivation of the $^5D_4 \rightarrow {}^7F_J$ transitions.

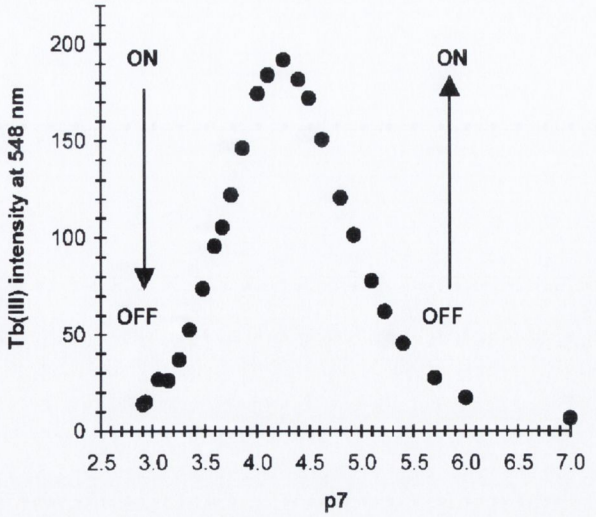

FIGURE 6 Changes in the $J = 5$ transition of **Tb·1** as a function of p7.

were somewhat smaller or 480 for **Tb·1**. The changes in the Tb(III) emission as a function of increased concentration of **7**, between pN 0–4.2 (where pN = −log[N], and N is the number of the compound in Scheme 2), can be seen in Fig. 5, where J represents the emission bands corresponding to the deactivation of the $^5D_4 \rightarrow {}^7F_J$ transitions. Here, the largest changes occurred in the $J = 5$ and 6. However, to our surprise, upon increasing the concentration of the antenna, the emission was "switched off" again. This became apparent when plotting the changes in the intensity of the 548 nm transition as a function of p7 (Fig. 6). From these changes, a sigmoidal curve was observed between p7 = ca. 6.5 and 4.5, where the emission was "switched on". Since this occurs over ca. two pN units, it can be concluded that this represents a 1:1 binding and a simple equilibrium between the Tb(III) centre of **Tb·1** and **7** [26–32,48]. From these changes, a binding constant, log β, of 4.9 (±0.2) was determined [48]. However, between p7 = 4.2–2.9, the emission was "switched off", giving rise to the formation of a sigmoidal "Off–On–Off" switch.

To investigate this, we looked at the changes in the 548-nm transition as a function of (equivalents of) **7**. These changes can be seen in Fig. 7, where the emission is highly dependent on the concentration of **7**. From 0 to ca. 3 equivalents of **7**, the Tb(III) is dramatically "switched on", with large order of magnitude enhancements (with ca. 80% of the emission being switched on after 1 equivalent). However, beyond these equivalents, the emission is quenched (see insert in Fig. 7 for 0 → 80 equivalents). Furthermore, the pH of the solution upon addition of **7** did not change during these measurements (in buffered solution), indicating that this quenching was not due to the protonation of **7** with concomitant dissociation of the ternary complex, but rather was directly due to the increased concentration of the antenna. Consequently, we investigated the effect of increasing the concentration of the complexes in the presence of high concentration of the carboxylate (in ca. 20-fold excess prior to increasing the concentration of **Tb·1**). As expected, this gave rise to large enhancements in the Tb(III) emission, suggesting that the luminescent ternary complex was formed.‡ Degassing the solution only led to minor additional increase in the luminescence, indicating that quenching of T_1 by oxygen was only minor.

Similar results were observed when **Tb·2** was titrated using **7**, but the enhancement factors were somewhat smaller. This is possibly due to additional quenching of the Tb(III) excited state by N–H oscillators in **Tb·2** which are absent in **Tb·1**. As before, the emission was highly dependent on the concentration of the antenna. Between p7 = 6.2 and 4.4, the emission was "switched on", with log β = 5.0 (±0.2), whereas between 3.5 and 4.5, the emission was "switched off".

The above measurements were repeated using other related derivatives of *N,N*-dimethylaminobenzoic acid, namely the ketone **8** and the ester **9**. No changes were seen in the emission spectra of **Eu·1**, **Eu·2**, **Tb·1** and **Tb·2** upon titration with either **8** or **9**, suggesting that it was necessary to have

‡There is also a possibility that at a very high concentration of **7** (OD ~ 0.6 at its max.), some inner filter effects are observed. However, **8** and **9** (see below), which absorb at similar wavelengths, did not give rise to any sensitisation when interacting with **Tb·1**. Furthermore, using **10**, this quenching was much less pronounced (see Fig. 11) for the same concentration range (see later).

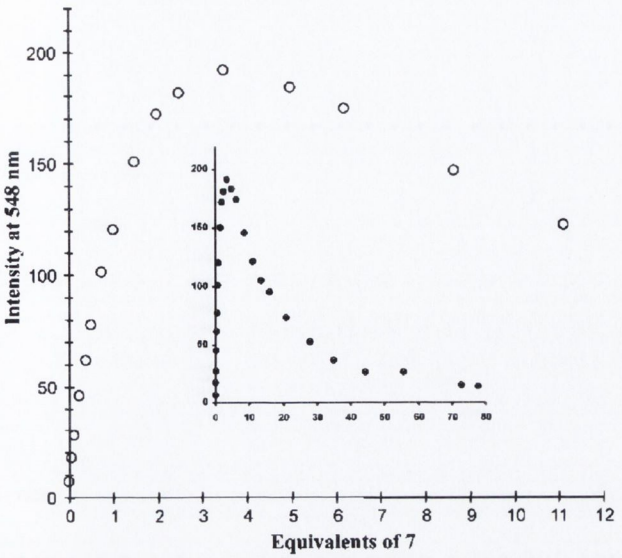

FIGURE 7 Changes in the intensity of the $J = 5$ transition of **Tb·1** as a function of added equivalents of **7**. Inserted are the changes up to 80 equivalents of **7**.

the carboxylate present as the part of the antenna for efficient binding to the metal ion and for sensitisation to occur. Hence, such binding would have to take place through the formation of at least a four-member ring chelate, involving the two oxygens of the carboxylate binding to the metal centre in a bidented manner. This is depicted in Fig. 8A. Furthermore, addition of **7** to a solution of **Tb·1** and **8** or **9** gave rise to large enhancements in the Tb(III) emission, indicating that these potential antennae were not able to bind to the metal ion centre. We thus conclude that **7** can be selectively recognised in the presence of these potential antennae.

Over the last few months, two other research groups have reported the use of similar complexes to bind aromatic carboxylates. Faulkner *et al.* [87] have shown that using tetrathiafulvalene carboxylic acid, the sensitisation of neutral Yb(III)-based triarm carboxylate derived cyclen complexes is possible in the near IR, whereas Li and Wong [88] have shown that Tb(III)-based cyclam complexes functionalised with pendent crown ethers can be used to determining Na^+ and K^+ in the presence of *p*-chlorobenzoate. On both occasions, the q values were found to be reduced from ca. 2 to ~0 after binding to these carboxylates antennae to the metal centre for these complexes.

Luminescent Sensing of Salicylic Acid and Related Derivatives

The above luminescence studies were also repeated using salicylic acid (which has a biological concentration of ca. 0.4 mM), and several of its derivatives. Salicylic acid is the active form of aspirin, a well-known non-steroidal anti-inflammatory drug. Salicylic acid is also a good painkiller but causes gastric bleeding due to the free phenolic group [89]. Because of this, it is necessary to mask the phenolic group as an ester (aspirin), which is hydrolysed by esterases to yield the free active drug in circulating blood. Furthermore, aspirin has many other pharmacological actions, some of which have the salicylic acid as the active form. For instance, it has anti-thrombotic action *via* the suppression of plated COX-1 (cyclooxygenase) activity and is thought to have potential anti-tumour actions [90]. However, the cause of gastric bleeding is of major concern, since it can lead to fatal conditions, but currently it is estimated that up to 17,000 people die from this condition every year in USA. The fatal dose of salicylic acid is estimated to be 0.2–0.5 g/kg [91]. Toxic effects appear at varying plasma levels, depending on the duration of poisoning, but are uncommon below 30 mg/dL [91]. However, ingestion of 4 g of salicylic acid has been fatal to infants. It is thus valuable to be able to monitor salicylic acid levels in blood or in serum. With this in mind, we investigated the effect on the Eu(III) and Tb(III) emission of our complexes upon binding to **10** and **11**.

As in the case of **7**, no enhancements were observed in the Eu(III) emission using **Eu·1** and **Eu·2** in the presence of **10** or **11** when measured in either H_2O or in buffer solution at pH 7.4. However, for both **Tb·1** and **Tb·2**, significant enhancements were seen in the Tb(III) emission upon addition of **10**. For instance, upon addition of 10 equivalents of **10**, the Tb(III) emission of **Tb·1** was enhanced by a factor of ca. 40 and 30 in H_2O and in buffer at pH 7.4, respectively. The changes in the Tb(III) emission of

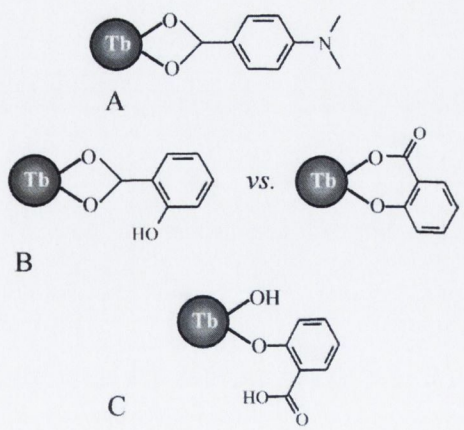

FIGURE 8 (A) Binding of **7** via four-member ring chelate to the Tb(III) centre. (B) Two possible binding modes for salicylic acid: (i) through the four member bidentated carboxylate (left) and (ii) through the six-member chelate involving one of the carboxylate oxygen and the phenolic oxygen. (C) Monocoordinating.

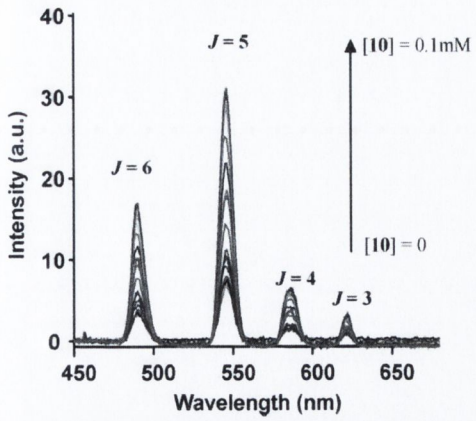

FIGURE 9 Changes in the Tb(III) emission of **Tb·1** upon addition of **10**.

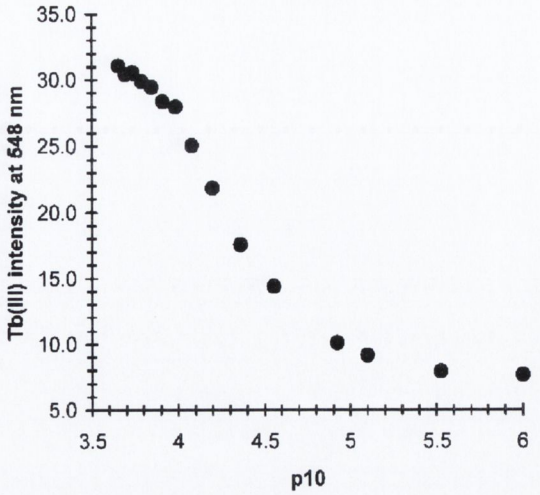

FIGURE 10 Changes in the Tb(III) emission of **Tb·1** at 548 nm as a function of p10.

Tb·1 can be seen in Fig. 9 when recorded in 0.1 M Tris buffer and in the presence of 0.1 M TMACl. However, these are substantially smaller changes than that seen previously for **7**, with the $J = 5$ transition showing the largest changes. For **Tb·2**, the relative enhancement was large, but the relative intensities were much smaller than that seen for **Tb·1**, and it was thus not investigated any further.

As before, the changes in the Tb(III) emission were highly concentration-dependent, though not to the same extent as that seen for **7**. This is clear from Fig. 10, where the intensity at 548 nm is plotted vs. p10. Here, the luminescence is switched on over ca. 2 log units from 5.5 to 3.5, an indication of 1:1 binding and simple equilibrium. From these changes, a binding constant $\log \beta = 4.5 (\pm 0.2)$ was determined. The self-quenching by the anion was also less pronounced, as can be seen in Fig. 11. Here, the Tb(III) emission gradually increases until ca. 6 equivalents have been added. However, between 6 and ca. 15 equivalents of **10**, the emission was not dependent on the concentration of **10**. At higher concentrations, ca. 17 equivalents and above, the emission was however "switched off" (not shown).[§]

When these titrations were repeated using **11**, no luminescent enhancements were observed in the Tb(III) emission for either **Tb·1** or **Tb·2**. This indicates that aspirin was not able to bind to the metal centre strongly enough. It is possible that this is due to the size of the compounds (the presence of the ester), which hinders the access to the metal centre. This was confirmed by measuring the $q \sim 2$ for **Tb·1** in the presence of **11**. Hence, even though **11** has a free carboxylate, no binding was observed.

To investigate the discrimination of **10** over **11** by **Tb·1**, we carried out a series of tritrations using other derivatives of salicylic acid, namely **12**–**14**. As expected, no luminescence enhancements were observed when the mixed ether–ester derivative **14** was used, since both of its possible binding sites are protected. However, when either **12** or **13** was used, large enhancements were seen in the Tb(III) emission. For **12**, these enhancements were in the order of ca. 80, whereas for **13**, a factor of several hundred was observed. These are very interesting results, since they suggest that two possible binding modes can exist for the binding of these salicylic acid derivatives, as depicted in Fig. 8B and C, respectively. In the former, the binding to the Tb(III) centre occurs through a bidentate manner, where the binding occurs via either a four-member ring chelate which involves both of the oxygens of the carboxylates, whereas in the latter, or only one of these oxygens can participate in the binding, and the second coordination site is occupied by the phenolic oxygen, giving rise to a six-member chelate. Nevertheless, since **13** was also found to be a good sensitiser, this suggests that the binding can occur through the phenolic oxygen alone as depicted in Fig. 8 C.

With the aim of shedding some light on this puzzle, we evaluated the q values for **Tb·1** in the presence of **10**, **12** and **13** (0.68 mM). The results of this investigation indicated that $q \sim 0$–1, so it is obvious that the removal of the two metal-bound water molecules is not as pronounced as in the case

[§]In our earlier communication [70], we reported that we were unable to observe more than two emission bands (at 491 and 548 nm corresponding to $J = 6$ and 5, respectively) when measuring these antennae. Though we did not conclude why this was the case, we have since then recorded all the above measurements on a new fluorimeter. As can be seen from Fig. 9, only the $J = 2$ transition is not observed. Hence, our original measurements were carried out on a machine that was not sensitive to these long-wavelength emission bands.

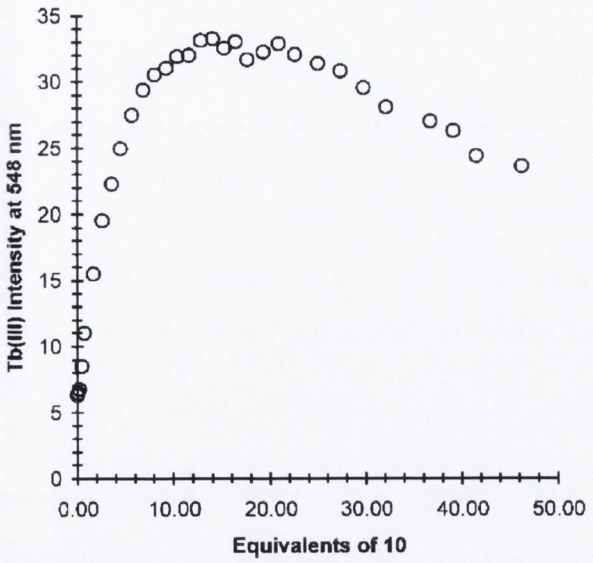

FIGURE 11 Changes in the Tb(III) emission of **Tb·1** at 548 nm as a function of equivalents of **10**.

of **7**. An estimated error of ± 0.5 is generally acceptable for determining q by this method. It is thus quite likely that only one of the metal-bound water molecules is replaced upon the binding of these compounds. This is most likely the case for **13**, which also might explain the relatively smaller luminescent enhancement factors observed for **13** in comparison with **12**. However, we have not been able to fully determine to date whether one or both of these metal-bound water molecules are removed either concurrently or in a stepwise manner. It is also possible that a mixture of these binding modes is operating in the case of **10**, **12** and **13**. Nevertheless, from the above results, we can conclude that **Tb·1** can selectively bind salicylic acid **10** over aspirin **11**. We are currently studying these interactions in greater detail. The above measurements were also carried out in the presence of several other carboxylates, namely **15**, **16** and **17**. Of these, **17** (Diclofenac®) is another well-known non-steroidal anti-inflammatory drug like aspirin. However, for all of these compounds, no enhancements were observed in the Tb(III) emission of either **Tb·1** or **Tb·2**.

We are also interested in the potential application of these complexes in highly competitive environments. For instant, using the sodium salts of AMP, ADP or ATP, which can potentially bind to the Tb(III) complexes via their phosphate ester terminus, no luminescence enhancements were observed when measured at neutral pH. Concurrently, Parker *et al.* have shown that coordinately unsaturated Eu(III) and Tb(III) complexes with covalently bonded chiral antennae can be employed as lanthanide luminescent sensors for simple aliphatic carboxylates such as bicarbonate, carbonate and amino acids [71]. In these complexes, the acetate and carbonates were found to have a stronger affinity for Tb(III) complexes over that of Eu(III). Because of this, we were interested in investigating the effect of competitive binding of carbonate and other biologically active acids to our complexes in the presence of **7** or **10**. We thus monitored the changes in the Tb(III) emission upon addition of a solution containing 30 mM of $NaHCO_3$, 2.3 mM lactate (Na^+ salt), 0.13 mM citric acid and 0.9 mM of $Na_2H_2PO_4$. However, these additions led to a reduction in the Tb(III) emission, most likely indicting that HCO_3^- or the acids were binding to the Tb(III) centre in a competitive manner and causing the dissociation of the ternary luminescent complex within their physiological concentration ranges. We thus conclude that for the monitoring of **10** in serum, it would be necessary to at least degas the sample prior to its use, but we are currently developing new systems for overcoming these drawbacks.

CONCLUSION

We have shown that it is possible to develop simple sensory systems for aromatic carboxylates by employing self-assembly ternary complexes, where the analyte can function as an antenna, and give rise to the population of the lanthanide excited state in water or in buffered aqueous solution at pH 7.4. We have shown using X-ray crystallography that these complexes have two metal-bound water molecules that can be displaced upon binding to aromatic carboxylates such as **7** and **10**. The presence of these water molecules was also confirmed by measuring the luminescent lifetimes of the lanthanide-excited states of these commplexes in H_2O and D_2O. Of the four complexes **Eu·1**, **Eu·2**, **Tb·1** and **Tb·2**, the Eu(III) complexes did not give rise to the formation of such self-assembly complexes. We conclude that this is due to a lower affinity of these complexes towards the carboxylates antennas. Similar observations have been made by other researchers [71,72]. We propose that the binding of **7** to either **Tb·1** or **Tb·2** is *via* the formation of four-member bidented ring chelate, whereas for the binding of **10** to **Tb·1**, this can be through either a mono- or bidentate manner. Such binding was confirmed using **12** and **13**. In retrospect, salicylic acid **10**, the active form of **11**, was found to bind to **Tb·1** (and **Tb·2**) with concomitant enhancements in the Tb(III) luminescence. Related structures such as **17**, another well-known non-steroidal anti-inflammatory drug like aspirin, was not detected. These complexes all gave bell-shaped dependent p*N* profiles, which were determined to be due to self-quenching of the anions. Proof for such quenching was obtained by gradually increasing the amount of the Tb(III) complexes in the presence

of excess amount of **7** or **10**. On both occasions, large enhancements were seen in the Tb(III) emission, indicating the formation of luminescent ternary complexes.

In summary, we have developed new types of chemosensors for anions such as aromatic carboxylates. We are currently working towards enhancing the selectivity and sensitivity of these complexes towards important drugs such as salicylic acid the active form of aspirin for use in blood or serum analysis.

EXPERIMENTAL

General Procedures

Infrared spectra were recorded on a Mattson Genesis II FTIR spectrophotometer equipped with a Gateway 2000 4DX2-66 workstation. Oils were analysed using NaCl plates, and solid samples were dispersed in KBr and recorded as clear pressed discs. ^{1}H NMR spectra were recorded at 400 MHz using a Bruker Spectrospin DPX-400 instrument. Tetramethylsilane (TMS) was used as an internal reference standard, with chemical shifts expressed in parts per million (ppm or δ) downfield from the standard. ^{13}C NMR spectra were recorded at 100 MHz, and ^{19}F NMR spectra were recorded at 376 MHz using a Bruker Spectrospin DPX-400 instrument. Mass spectroscopy was carried out using HPLC-grade solvents. Mass spectra were determined by detection using Electrospray on a Micromass LCT spectrometer, Waters 9360 to pump solvent. The whole system was controlled by MassLynx 3.5 on a Compaq Deskpro workstation. Starting materials were obtained from Sigma Aldrich, Strem Chemicals and Fluka. Columns were run using aluminium oxide (activated, Neutral, Brockmann I STD grade 150 mesh). Solvents were used at GPR grade unless otherwise stated.

X-ray Crystallography

Crystal data for $C_{23}H_{49}F_9N_7O_{16}S_3Tb$ (**Tb·1**): $M = 1105.79$, triclinic, space group $P\bar{1}$, $a = 8.930$ (2) Å, $b = 13.321$ (3) Å, $c = 18.691$ (4) Å, $\alpha = 95.615$ (4), $\beta = 97.542$ (4), $\gamma = 104.149$ (4), $U = 2117.6$ (9) Å^{-3}, $Z = 2$, $\mu = 1.928\,\text{mm}^{-1}$, $R_{\text{int}} = 0.0275$, transmission ratio(max, min) = 0.738. A total of 18,996 reflections were measured for the angle range $2 < 2\theta < 57$, and 9140 independent reflections were used in the refinement. The final parameters were $wR2 = 0.1069$ and $R1 = 0.0406$ [$I > 2\sigma$I].

Diffraction data were collected on a Bruker SMART diffractometer using the SAINT-NT [77,78] software with graphite monochromated Mo-K_α radiation. A crystal was mounted on the diffractometer at room temperature (ca. 298 K) for **Tb·1**. Lorentz and polarisation corrections were applied. Empirical absorption correction was applied using SADABS. The structure was solved using direct methods and refined with the program package [77,78], and the non-hydrogen atoms were refined with anisotropic thermal parameters. Hydrogen-atom positions were added at idealised positions, and a riding model with fixed thermal parameters [$U_{ij} = 1.2U_{eq}$ for the atom to which they are bonded (1.5 for CH_3)] was used for subsequent refinements. Hydrogen atoms could not be located for the water molecules. The function minimised was $\Sigma[w(|F_o|^2 - |F_c|^2)]$ with reflection weights $w^{-1} = [\sigma^2|F_o|^2 + (g_1P)^2 + (g_2P)]$ where $P = [\max|F_o|^2 + 2|F_c|^2]/3$. Additional material available from the Cambridge Crystallographic Data Centre comprises relevant tables of atomic coordinates, bond lengths and angles, and thermal parameters (CCDC number 198706).

Luminescence Studies

All luminescence studies were carried out in aqueous solution or in aqueous solution with a buffer and high ionic strength at pH 7.4. Buffered solutions were made up in aqueous phase with 0.1 M TMACl, 0.1 M HEPES and or 0.1 M Tris buffer, at pH 7.4. Solution concentrations were ~16.7 μM. Test solutions were 5 mL or 10 mL Sensitising chromophore solutions were made up in water 2.0×10^{-3} M and 5.0×10^{-4} M. Luminescence measurements were made on a Perkin Elmer LS 50B and repeated on a Varian Cary Eclipse.

2-(4,10-Bis-dimethylcarbamoylmethyl-1,4,7,10-tetraaza-cyclododec-1-yl)-*N*,*N*-dimethyl-acetamide (1)

1,4,7,10-Tetraazacyclododecane (98%), (0.375 g, 2.13 mmol) was placed in a 50-mL single-necked RBF. To this were added $NaHCO_3$ (0.537 g, 6.39 mmol) and 15 mL of dried acetonitrile. 2-Chloro-*N*,*N*-dimethylacetamide (0.804 g, 6.6 mmol) was added, and the mixture was stirred at 65°C for a further 72 h. The resulting solution was then cooled and passed through a celite filter. The pale yellow solution was reduced to a yellow residue and dried under vacuum for 1 h to produce (0.829 g, 90.89% yield) a mixture of products, as shown by TLC, that were purified by alumina column using 100% DCM, with a gradient elution to 97:3 DCM:MeOH(NH_3) mobile phase. 0.470 g (1.1 mmol), 52% yield, of 2-(4,10-bis-dimethylcarbamoylmethyl-1,4,7,10-tetraaza-cyclododec-1-yl)-*N*,*N*-dimethylacetamide was collected as a white foam after drying under vacuum, which returned to a residue state over time. Calculated for $C_{20}H_{42}N_7O_3$: [M + H peak] $m/z = 428.3344$, found: 428.3349; δ_H ($CDCl_3$, 400 MHz) 10.00 (broad s, 1H, N–H), 3.61(s, 2H, CH_2– acetamide), 3.58(s, 4H, CH_2– acetamide),

3.09(s, 8H), 3.04(s, 3H), 2.96(s, 6H), 2.90(s, 10H), 2.84 (s, 7H); δ_C($CDCl_3$, 100 MHz) 170.25, 170.15, 55.51, 53.80, 51.70, 50.57, 49.72, 46.70, 36.39, 35.27; Mass Spec (MeOH, ES +) m/z. Expected: 427.59. Found: 428.33 (M + H), 450.30 (M + Na), 472.30 (M + K); IR ν_{max} (cm^{-1}) 3434, 2927, 2852, 1637, 1508, 1475, 1402, 1338, 1261, 1103, 1064, 1022, 881, 806, 769, 667, 649, 574, 484.

2-(4,7-Bis-methylcarbamoylmethyl-1,4,7,10-tetraaza-cyclododec-1-yl)-*N*-methylacetamide (2)

1,4,7,10-Tetraazacyclododecane (98%) (0.375 g, 2.13 mmol) was placed in a 50-mL single-necked RBF. To this were added $NaHCO_3$ (0.537 g, 6.39 mmol) and 15 mL of dried acetonitrile. 2-Chloro-*N*-methylacetamide, (0.706 g, 6.6 mmol) was added, and the mixture was stirred at 65°C for a further 72 h. The resulting inorganic precipitate was filtered and the filtrate reduced to dryness and triturated from a solution of ethanol by dropping on to ether, giving the desired compound in 59% yield. Calculated for $C_{17}H_{36}N_7O_3$: [M + H peak] $m/z = 386.2880$. Found: 386.2874; δ_H($CDCl_3$, 400 MHz) 7.60 (s, 1H, N–H), 7.30 (s,2H, N–H), 3.06 (s, 4H, CH_2 acetamide), 2.96 (s, 2H, CH_2 acetamide), 2.75 (d, 6H, $J = 4.52$ N–CH_3), 2.67 (d, 3H, $J = 4.52$ N–CH_3), 2.60 (s, 4H, CH_2), 2.58 (s, 4H, CH_2), 2.53 (s, 4H, CH_2), 2.49 (s, 4H, CH_2); δ_C($CDCl_3$, 100 MHz) 171.51, 171.41, 59.54, 57.53, 53.31, 52.63, 51.18, 46.15, 25.89, 25.72. Mass Spec. (MeOH, ES+) m/z. Expected: 385.51. Found: 386.3(M + H), 408.4 (M + Na), 424.4 (M + K); IR ν_{max}(cm − 1) 3430, 2846, 2103, 1643, 1567, 1456, 1415, 1367, 1311, 1257, 1164, 1110, 989, 482.

General Synthesis of 2-(4,10-Bis-methylcarbamoylmethyl-1,4,7,10-tetraaza-cyclododec-1-yl)-*N*-methylacetamide Ln(III) (1Ln), and 2-(4,10-Bis-dimethylcarbamoylmethyl-1,4,7,10-tetraaza-cyclododec-1-yl)-*N*,*N*-dimethylacetamide Ln(III) (2Ln)

88.2 mg (0.23 mmol) of **1** or 94.7 mg (0.22 mmol) of **2** and 0.26 mmol of Ln (III) Trifluoromethane sulphonate [$Ln(SO_3CF_3)_3$] was added to a 25-mL single-necked RBF which contained 10 mL of freshly dried acetonitrile. The solution was freeze–thawed three times, placed under an argon atmosphere and left stirring at 82°C for 24 h. The resulting solution was cooled to room temperature and then dropped slowly on to 100 mL of dry diethyl ether. The diethyl ether was poured off to leave **1Ln or 2Ln** as oil that was washed with CH_2Cl_2 or $CHCl_3$ and dried under high vacuum. Yields were ca. 95% in all cases.

2-(4,10-Bis-dimethylcarbamoylmethyl-1,4,7,10-tetraaza-cyclododec-1-yl)-*N*,*N*-dimethylacetamide Tb(III) (Tb·1)

Calculated for $C_{23}H_{41}N_7O_{12}F_9S_3Tb\cdot(H_2O)_2(CHCl_3)_2$: C, 22.95; H, 3.62; N, 7.49. Found: C, 22.23; H, 3.71; N, 7.36. Calculated for $C_{22}H_{42}N_7O_6F_3STb$: [M + H peak] $m/z = 736.2123$. Found: 736.2148; δ_H(CD_3OCD_3, 400 MHz); 39.92, 32.70, 9.00, 3.95, 3.02, 1.02 δ_F (CD_3OCD_3, 376 MHz) − 78.74. Mass spec. (MeCN, ES +) m/z. Expected: 586.5. Found: 884.15 (M[Triflate]$_2$ + H), 736.21 (M[Triflate] + H); IR ν_{max} (cm^{-1}) 3434, 2957, 2927, 2856, 1625, 1508, 1465, 1438, 1412, 1279, 1256, 1171, 1084, 1171, 1084, 1030, 960, 824, 761, 640, 574, 518.

2-(4,10-Bis-dimethylcarbamoylmethyl-1,4,7,10-tetraaza-cyclododec-1-yl)-*N*,*N*-dimethylacetamide Eu(III) (Eu·1)

Calculated for $C_{23}H_{41}N_7O_{12}F_9S_3Eu\cdot(H_2O)_2(CHCl_3)_2$: C, 23.07; H, 3.64; N, 7.53. Found: C, 22.67; H, 3.74; N, 7.55. Calculated for $C_{21}H_{42}N_7O_6F_3SEu$: [M + H peak] $m/z = 730.2082$. Found: 730.2045; δ_H (CD_3OCD_3, 400 MHz) 13.91, 3.24, 2.60, 2.06, 1.30, 0.89, 0.01, −1.32, −4.95, −8.95, −12.87, −17.65; δ_F (CD_3OCD_3, 376 MHz) − 78.74. Mass spec. (MeCN, ES +) m/z. Expected: 579.56. Found: 878.15 (M[Triflate]$_2$ + H), 730.20 (M[Triflate] + H); IR ν_{max} (cm^{-1}) 3434, 2982, 2927, 2884, 1625, 1508, 1459, 1438, 1413, 1280, 1258, 1173, 1084, 1031, 960, 824, 762, 641, 573, 518.

2-(4,10-Bis-methylcarbamoylmethyl-1,4,7,10-tetraaza-cyclododec-1-yl)-*N*-methylacetamide Tb (III) (Tb·2)

Calculated for $C_{20}H_{35}N_7O_{12}F_9S_3Tb\cdot(H_2O)_2(CH_2Cl_2)_2$: C, 22.07; H, 3.62; N, 8.19, Found: C, 21.61; H, 3.59; N, 7.85. Calculated for $C_{19}H_{36}N_7O_9F_6S_2Tb$: [M + H peak] $m/z = 843.1174$. Found: 843.1171. Calculated for $C_{18}H_{36}N_7O_6F_3STb$: [M + H peak] $m/z = 694.1653$. Found: 694.1674; δ_H(MeOD, 400 MHz) 121.87, 107.11, 78.35, 71.89, 68.58, 39.94, 14.52, 7.75, 6.28, 4.26, 1.96, 1.78, 1.49, 1.07, − 7.21; δ_F (MeOD, 376 MHz) − 85.54. Mass spec. (MeCN, ES+) m/z. Expected: 544.4. Found: 272.3 (M + H/2), 843.1(M[Triflate]$_2$ + H), 694.16 (M[Triflate] + H); IR ν_{max}(cm^{-1}) 3435, 3137, 2960, 2924, 1637, 1420, 1259, 1169, 1087, 1030, 994, 974, 798, 639, 574, 519.

2-(4,10-Bis-methylcarbamoylmethyl-1,4,7,10-tetraaza-cyclododec-1-yl)-*N*-methylacetamide Eu (III) (Eu·2)

Calculated for $C_{20}H_{35}N_7O_{12}F_9S_3Eu\cdot(H_2O)_2(CH_2Cl_2)_2$: C, 22.19; H, 3.64; N, 8.24, Found: C, 22.29; H, 3.74; N, 8.38. Calculated for $C_{17}H_{36}N_7O_3Eu$: [M+H peak]

$m/z = 539.2092$, found: 539.2087. Calculated for $C_{18}H_{36}N_7O_6F_3SEu$: [M + H peak] $m/z = 688.1612$, found: 688.1548. Calculated for $C_{19}H_{36}N_7O_9F_6S_2Eu$: [$MH^+$ peak] $m/z = 837.1133$, found: 837.1181; δ_H(MeOD, 400 MHz) 27.04, 14.96, 11.44, 5.20, 3.68, 2.76, 2.41, 1.55, −0.09, −1.84, −4.93, −7.35, −10.77, −12.31, −16.66; δ_F(MeOD, 376 MHz) − 80.45. Mass spec. (MeCN, ES+) m/z. Expected: 538.2. Found: 539.2(M+H), 668.1 (M[Triflate] + H), 837.1 (M[Triflate]$_2$ + H); IR ν_{max} (cm^{-1}) 3455, 3386, 3297, 3143, 3000, 2933, 2885, 1639, 1587, 1465, 1419, 1288, 1245, 1160, 1091, 1027, 725, 638, 576, 516.

Acknowledgements

We thank Kinerton Ltd, Enterprise Ireland (Postgraduate Scholarships to A.J.H. and J.P.L.), National Pharmaceutical Biotechnology Center, Bio Research Ireland and Trinity College Dublin for financial support. We thank Dr Steven Faulkner, Dr Hazel M. Moncrieff and Dr Julie Tierney for their helpful discussions, and Dr John E. O'Brien for assisting with running NMR.

References

[1] Rurack, K.; Resch-Genger, U. *Chem. Soc. Rev.* **2002**, 116.
[2] Lavigne, J. J.; Anslyn, E. V. *Angew. Chem., Int. Ed.* **2001**, *40*, 3119.
[3] Fabbrizzi, L.; Licchelli, M.; Rabaioli, G.; Taglietti, A. F. *Coord. Chem. Rev.* **2000**, *205*, 85.
[4] Czarnik, A. W. *Acc. Chem. Res.* **1994**, *27*, 302.
[5] Fabbrizzi, L.; Licchelli, M.; Pallavicini, P. *Acc. Chem. Res.* **1999**, *32*, 846.
[6] Desvergne, J. P., Czarnik, A. W., Eds. *Chemosensors of Ion and Molecular Recognition*; Kluwer Academic: Dordrecht, 1997.
[7] Czarnik, A. W. *Fluorescent Chemosensors for Ion and Molecular Recognition*; ACS Books: Washington, DC, 1993.
[8] Czarnik, A. W. *Acc. Chem. Res.* **1994**, *27*, 302.
[9] Bissell, R. A.; de Silva, A. P.; Gunaratne, H. Q. N.; Lynch, P. L. M.; Maguire, G. E. M.; McCoy, C. P.; Sandanayake, K. R. A. S. *Top. Curr. Chem.* **1993**, *168*, 223.
[10] Gale, P. A. *Coord. Chem. Rev.* **2001**, *213*, 79.
[11] Gale, P. A. *Coord. Chem. Rev.* **2000**, *199*, 181.
[12] Beer, P. D.; Gale, P. A. *Angew. Chem., Int. Ed.* **2001**, *40*, 486.
[13] Beer, P. D. *Chem. Commun.* **1996**, 689.
[14] Gudgin-Dickson, E. F.; Pollak, A.; Diamandis, E. P. *J. Photochem. Photobiol. B: Biol.* **1995**, *27*, 3.
[15] deSilva, A. P.; Fox, D. B.; Huxley, A. J. M.; Moody, T. S. *Coord. Chem. Rev.* **2000**, *205*, 41.
[16] de Silva, A. P.; Fox, D. B.; Huxley, A. J. M.; McClenaghan, N. D.; Roiron, J. *Coord. Chem. Rev.* **1999**, *186*, 297.
[17] de Silva, A. P.; Gunaratne, H. Q. N.; Rice, T. E. *Angew. Chem., Int. Ed. Engl.* **1996**, *35*, 2116.
[18] Licini, M.; Williams, J. A. G. *Chem. Commun.* **1999**, 1943.
[19] Beeby, A.; Bushby, L. M.; Maffeo, D.; Williams, J. A. G. *J. Chem. Soc., Perkin Trans. 2* **2000**, 1281.
[20] Parker, D.; Williams, J. A. G. *J. Chem. Soc., Dalton Trans.* **1996**, 3613, and references therein.
[21] Rurack, K. *Spectrochem. Acta A* **2001**, *57*, 2161.
[22] Amendola, V.; Fabbrizzi, L.; Mangano, C.; Pallavicini, P. *Acc. Chem. Res.* **2001**, *34*, 488.
[23] de Silva, A. P.; Gunaratne, H. Q. N.; Gunnlaugsson, T.; Huxley, A. J. M.; McCoy, C. P.; Rademacher, J. T.; Rice, T. E. *Chem. Rev.* **1997**, *97*, 1515.
[24] Lowe, M. P.; Parker, D. *Chem. Commun.* **2000**, 707.
[25] de Silva, A. P.; Dixon, I. M.; Gunaratne, H. Q. N.; Gunnlaugsson, T.; Maxwell, P. R. S.; Rice, T. E. *J. Am. Chem. Soc.* **1999**, *121*, 1393.
[26] Gunnlaugsson, T.; Davis, A. P.; O'Brien, J. E.; Glynn, M. *Organic Lett.* **2002**, *4*, 2449.
[27] Nieuwenhuyzen, M.; Richard, L.; Thoss, V. *J. Chem. Soc., Perkin Trans. 2* **2002**, 141.
[28] Gunnlaugsson, T.; Bichell, B.; Nolan, C. *Tetrahedron Lett.* **2002**, *43*, 4989.
[29] Gunnlaugsson, T.; Gunaratne, H. Q. N.; Nieuwenhuyzen, M.; Leonard, J. P. *J. Chem. Soc., Perkin Trans. 1* **2002**, 1954.
[30] Gunnlaugsson, T.; Leonard, J. P. *J. Chem. Soc., Perkin Trans. 2* **2002**, 1980.
[31] Gunnlaugsson, T.; Davis, A. P.; Glynn, M. *Chem. Commun.* **2001**, 2556.
[32] Gunnlaugsson, T.; Nieuwenhuyzen, M.; Richard, L.; Thoss, V. *Tetrahedron Lett.* **2001**, *42*, 4725.
[33] Gunnlaugsson, T. *Tetrahedron Lett.* **2001**, *42*, 8901.
[34] Gunnlaugsson, T.; Mac Dónaill, D. A.; Parker, D. *Chem. Commun.* **2000**, 93.
[35] Reany, O.; Gunnlaugsson, T.; Parker, D. *Chem. Commun.* **2000**, 473.
[36] Reany, O.; Gunnlaugsson, T.; Parker, D. *J. Chem. Soc., Perkin Trans. 2* **2000**, 1819.
[37] Gunnlaugsson, T.; Parker, D. *Chem. Commun.* **1998**, 511.
[38] Gunnlaugsson, T.; Davies, R. J. H.; Nieuwenhuyzen, M.; O'Brien, J. E.; Stevenson, C. S.; Viguier, R.; Mulready, S. *Polyhedron* **2003**, *22*, 711.
[39] Gunnlaugsson, T.; Davies, R. J. H.; Nieuwenhuyzen, M.; Stevenson, C. S.; Viguier, R.; Mulready, S. *Chem. Commun.* **2002**, 2136.
[40] Gunnlaugsson, T.; O'Brien, J. E.; Mulready, S. *Tetrahedron Lett.* **2002**, *43*, 8493.
[41] Parker, D. *Coord. Chem. Rev.* **2000**, *205*, 109.
[42] Parker, D.; Williams, J. A. G. *Chem. Commun.* **1998**, 245.
[43] de Silva, A. P.; Gunaratne, H. Q. N.; Rice, T. E.; Stewards, S. *Chem. Commun.* **1997**, 1891.
[44] Sabbatini, N.; Guardigli, M.; Lehn, J.-M. *Coord. Chem. Rev.* **1993**, *123*, 201.
[45] Lis, S.; Elbanowski, M.; Makowska, B.; Hnatejko, Z. *J. Photchem. Photobiol., A. Chem.* **2002**, *150*, 233.
[46] Bunzli, J.-C. G. In *Lanthanide Probes in Life, Chemical and Earth Sciences, Theory and Practice*; Bunzli, J.-C. G., Choppin, G. R., Eds.; Elsevier: New York, 1989; p 219.
[47] Bruce, J. I.; Lowe, M. P.; Parker, D. In *The Chemistry of Contrast Agents in Medical Magnetic Resonance Imaging*; Merbacl, A. E., Tóthe, É., Eds.; Chichester, 2001.
[48] Gunnlaugsson, T.; Mac Dónaill, D. A.; Parker, D. *J. Am. Chem. Soc.* **2001**, *123*, 12866.
[49] Yu, J.-A.; Lessard, R. B.; Bowman, L. E.; Nocera, D. G. *Chem. Phys. Lett.* **1991**, *187*, 263.
[50] Bhaumik, M. L.; El-Sayed, M. A. *J. Chem. Phys.* **1965**, *34*, 743.
[51] Crosby, G. A.; Whan, R. E.; Alire, R. M. *J. Chem. Phys.* **1961**, *34*, 743.
[52] Arnaud, N.; Georges, J. *Analyst* **1999**, *124*, 1075.
[53] Aguilar-Caballos, M. P.; Gómez-Hens, A.; Pérez-Bendito, D. *Analyst* **1999**, *124*, 1079.
[54] Panadero, S.; Gómez-Hens, A.; Pérez-Bendito, D. *Anal. Chem. Acta* **1996**, *329*, 135.
[55] Lianidou, E. S.; Ioannou, P. C.; Polydorou, C. K.; Efstathiou, C. E. *Anal. Chem. Acta* **1996**, *320*, 107.
[56] Ioannou, P. C.; Lianidou, E. S.; Konstantianos, D. G. *Anal. Chem. Acta* **1995**, *300*, 237.
[57] Georges, J. *Analyst* **1993**, *118*, 1481.
[58] Linger, G.; Mohan, R.; Knittel, S.; Duportail, G. *Spectrochem. Acta* **1990**, *46A*, 797.
[59] Bailey, M. P.; Rocks, F.; Riley, C. *Anal. Chem. Acta* **1987**, *201*, 335.
[60] Zhu, G.; Yang, J. *Anal. Lett.* **1984**, *17*, 1827.
[61] Richardson, F. S. *Chem. Rev.* **1982**, *82*, 541.
[62] Kleinerman, M. *Anal. Lett.* **1977**, *10*, 205.
[63] Weissman, S. I. *J. Chem. Phys.* **1942**, *10*, 214.
[64] Michels, J. J.; Huskens, J.; Reinhoudt, D. N. *J. Am. Chem. Soc.* **2002**, *124*, 2056.
[65] Skinner, P. J.; Beeby, A.; Dickins, R. S.; Parker, D.; Aime, S.; Botta, M. *J. Chem. Soc., Perkin Trans. 2* **2000**, 1329.
[66] Rudzinski, C. M.; Engebretson, D. S.; Hartmann, W. K.; Nocera, D. G. *J. Phys. Chem. A.* **1998**, *102*, 7442.

[67] Mortellaro, M. A.; Nocera, D. G. *J. Am. Chem. Soc.* **1996**, *118*, 7414.
[68] Pikramenou, Z.; Yu, J.; Lassard, R. B.; Ponce, A.; Wong, P. A.; Nocera, D. G. *Coord. Chem. Rev.* **1994**, *132*, 181.
[69] Pikramenou, Z.; Nocera, D. G. *Inorg. Chem.* **1992**, *31*, 532.
[70] Gunnlaugsson, T.; Harte, A. J.; Leonard, J. P.; Nieuwenhuyzen, M. *Chem. Commun.* **2002**, 2134.
[71] Dickins, R. S.; Gunnlaugsson, T.; Parker, D.; Peacock, R. D. *Chem. Commun.* **1998**, 1643.
[72] Dickins, R. S.; Aime, S.; Batsanov, A. S.; Beeby, A.; Botta, M.; Bruce, J. I.; Howard, J. A. K.; Love, C. S.; Parker, D.; Peacock, R. D.; Puschmann, H. *J. Am. Chem. Soc.* **2002**, *124*, 12697.
[73] Beeby, A.; Faulkner, S.; Williams, J. A. G. *J. Chem. Soc., Dalton Trans.* **2002**, 1918.
[74] Werts, M. H. V.; Verhoeven, J. W.; Hofstraat *J. Chem. Soc., Perkin Trans. 2* **2000**, 433.
[75] Bruce, J. I.; Dickins, R. S.; Govenlock, L. J.; Gunnlaugsson, T.; Lopinski, S.; Lowe, M. P.; Parker, D.; Peacock, R. D.; Perry, J. J. B.; Aime, S.; Botta, M. *J. Am. Chem. Soc.* **2000**, *122*, 9674.
[76] Parker, D.; Dickins, R. S.; Puschmann, H.; Cossland, C.; Howard, J. A. K. *Chem. Rev.* **2002**, *102*, 1977.
[77] *SAINT-NT*; Brüker AXS, Madison, WI, 1998.
[78] Sheldrick, G. M. University of Göttingen, Göttingen, Germany, 1998.
[79] Caravan, P.; Ellison, J. J.; McMurray, T. J.; Lauffer, R. B. *Chem. Rev.* **1999**, *99*, 283.
[80] Howard, J. A. K.; Kenwright, A. M.; Moloney, J. M.; Parker, D.; Port, M.; Navet, M.; Rousseau, O.; Woods, M. *Chem. Commun.* **1998**, 1381.
[81] Dickens, R. S.; Howard, J. A. K.; Maupin, C. L.; Moloney, J. M.; Parker, D.; Peacock, R. D.; Riehl, J. P.; Siligardi, G. *New J. Chem.* **1998**, 891.
[82] Dickins, R. S.; Love, C. S.; Puschmann, H. *Chem. Commun.* **2001**, 2308.
[83] Beeby, A.; Clarkson, I. M.; Dickins, R. S.; Faulkner, S.; Parker, D.; Royle, L.; de Sousa, A. S.; Williams, J. A. G.; Woods, M. *J. Chem. Soc., Perkin Trans. 2* **1999**, 493.
[84] Beeby, A.; Dickins, R. S.; Faulkner, S.; Parker, D.; Williams, J. A. G. *Chem. Commun.* **1997**, 1401.
[85] Dickins, R. S.; Parker, D.; de Sausa, A. S.; Williams, J. A. G. *Chem. Commun.* **1996**, 697.
[86] Murov, S. L.; Carmichael, I.; Hug, G. L. *Handbook of Photochemistry*; Marcel Dekker: New York, 1993.
[87] Faulkner, S.; Burton-Pye, B. P.; Khan, T.; Martin, L. R.; Wray, S. D.; Sakabara, P. *J. Chem. Commun.* **2002**, 1668.
[88] Li, C.; Wong, W.-T. *Chem. Commun.* **2002**, 2034.
[89] Patrick, G. L. *An Introduction to Medicinal Chemistry*; Oxford University Press: Oxford, 1997.
[90] Saunders, M.A. *International Aspirin® Award*, March 2, 2002, Madrid.
[91] In *Handbook of Poisoning*, 12th ed. Chapter 21, Dreisbach, R. H., Robertson, Eds.; *Lange Medical Book*; 1987, USA.

J|A|C|S
COMMUNICATIONS

Published on Web 09/12/2003

pH Responsive Eu(III)−Phenanthroline Supramolecular Conjugate: Novel "*Off*−*On*−*Off*" Luminescent Signaling in the Physiological pH Range

Thorfinnur Gunnlaugsson,*,† Joseph P. Leonard,† Katell Sénéchal,†,‡ and Andrew J. Harte†

Department of Chemistry, Trinity College Dublin, Dublin 2, Ireland

Received April 2, 2003; E-mail: gunnlaut@tcd.ie

The development of luminescent signaling devices is an active area of supramolecular chemistry.[1] Those where the emission is modulated by single or several external sources (*inputs*) such as light, ions, and molecules are of particular interest.[2] In this regard luminescent switches, sensors, and logic gate mimics have recently been reported.[2,3] Many life processes, such as enzymes, operate within a very narrow pH window, where their function or activity can be described as being "*switched on*" or "*switched off*" as a function of pH.[4] Attempts to mimic such "*off*−*on*−*off*" or "*on*−*off*−*on*" behavior by constructing luminescence devices that are modulated by a single *input*, e.g., pH, have recently been achieved by employing organic fluorophores.[5] Lately, Pallavicini et. al. have extended this kind of work and reported "*on*−*off*−*on*" fluorescent indicators for H^+ using a tetraaza ligand, Cu(II) and Coumarin 343 as a fluorescent "chemosensing ensemble".[6]

We have been particularly interested in designing robust multifunctional lanthanide complexes from cyclen (1,4,7,10-tetraazacyclododecane) as kinetically and thermodynamically stable luminescent chemosensors, switches, and logic gate mimics, as well as ribonuclease mimics.[7−9] Herein we present the synthesis and the photophysical evaluation of the cationic tetraamide 1,10-phenanthroline (*phen*)-based Eu(III) complex **1.Eu**, which is the first example of a fully reversible pH controlled "*off*−*on*−*off*" signaling system that employs lanthanide luminescence rather than fluorescence, where the "*off*−*on*−*off*" process is due to pH modulation of the *phen* ligand.[10] In addition to being purely metal-based emission, the Eu(III) emission changes occur in the physiological pH range, in a pH window between ca. 4−8. Moreover, the emission of **1.Eu** is long-lived (ms range), emitting at long wavelengths (between 500 and 750 nm) with line-like emission bands under ambient conditions. As such, **1.Eu** holds greater advantages over fluorescence systems that can be seriously affected by autofluorescence and light scattering, for instance from the physiological environment.

The synthesis of **1.Eu** (ESI) was achieved as shown in Scheme 1. **1.Eu** was purified by multiple precipitation; first from ether and then from CH_2Cl_2, giving the desired complex in 80% yield from **1**. **1.Eu** was characterized by conventional methods (calculated for **1.Eu**: $C_{35}H_{51}N_{10}O_7F_3SEu$: 965.2876. Found: 965.2827). The ESMS showed peaks at 406.9 and 481.9 (*m*/*z*) for the M^{+2} and (M + triflate)/2 respectively, whereas the ^1H NMR (400 MHz, D_2O) indicated a typical mono-capped square antiprism geometry[11] as a major isomer (ca. 95%) in solution, with resonances at 28.4, 0.28, −3.3, −8.8, −12.1, and −15.7 ppm for the equatorial and axial ring, and the methylene protons of the pendent arms.

The pH dependence of the Eu(III) emission was evaluated in H_2O in the presence of 0.1 M tetramethylammonium perchlorate to maintain constant ionic strength (*I*).[8] Due to the low molar absorptivities of Eu(III) the population of the Eu(III) excited state ($^5D_0$) is achieved indirectly by the *phen* antenna via sensitization.[8,9,11] We predicted that the ability of the *phen* ligand to engage in such sensitization would be pH dependent since both the amide and the nitrogens of the *phen* ligand are sensitive to protonation. Indeed, this was found to be the case. In alkaline solution between pH 12−8.5 only a weak Eu(III) emission was observed at 581, 593, 615, 624, 654, 686, and 702 nm for the deactivation of the $^5D_0$ to the ground states ^7F_J (J = 0, 1, 2, 3, and 4) after excitation at 266 nm. This signifies the rather inefficient population of the $^5D_0$ by the *phen* ligand in this pH range. The hydration number (q) for **1.Eu** was determined by measuring the Eu(III) luminescent lifetimes [$\tau_{Eu(III)}$] in H_2O and D_2O. This gave $\tau_{Eu(III)}$ = 0.271 ms and 0.371 ms for H_2O and D_2O, respectively (at pH 11), giving $q \approx 1$, and as such an overall nine-coordinated complex.[11] Upon further acidification, this sensitization process was greatly enhanced, and the Eu(III) emission was "*switched on*" between pH 8.5−5.5, with sharp luminescence enhancements as demonstrated in Figure 1; e.g. LE ≈ 20 for $^5D_0 \rightarrow {}^7F_1$, with $\tau_{Eu(III)}$ = 0.395 and 0.952 ms in H_2O and D_2O respectively, which gives $q \approx 1.3$, again indicating that the complex was monohydrated. Further acidification gave rise to two effects; notably between pH 5−6.5 the Eu(III) emission was almost constant, whereas between pH 5−3 the emission was gradually "*switched off*", being ca. 70% quenched at pH 2.5 vs that at pH 6 (Supporting Information). Similarly, using I = 0.1 M

Scheme 1. Synthesis of the Eu(III)-Based Cyclen Derivative **1**[a]

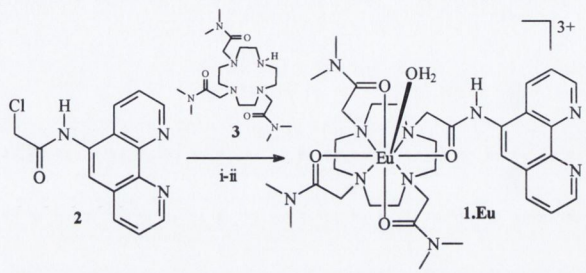

[a] Reaction conditions: (i) Cs_2CO_3, **2** and **3**,[7] DMF reflux; (ii) $Eu(SO_3CF_3)_3$, CH_3CN, reflux.

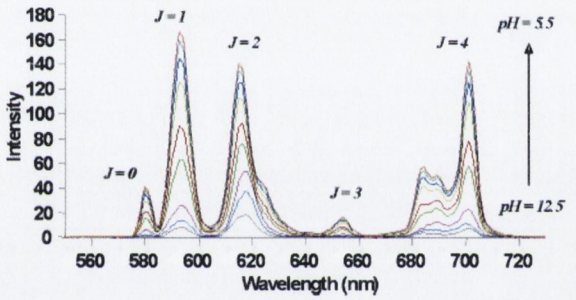

Figure 1. Changes in the Eu(III) emission as a function of pH between 12.5 (bottom spectrum) and 5.5 (top spectrum) upon excitation at 266 nm.

† Department of Chemistry, Trinity College Dublin.
‡ Laboratorie de Chimie de Coordination et Catalyse, UMR 6509 CNRS Université Rennes I, Institut de Chimie, Campus de Beaulieu.

10.1021/ja035425a CCC: $25.00 © 2003 American Chemical Society

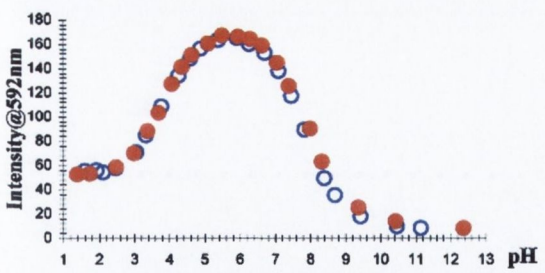

Figure 2. pH-dependence in the luminescent profile for **1.Eu**, showing the "*off*–*on*–*off*" pH-dependent changes in the Eu(III) emission at 592 nm. This pH dependence was fully reversible: in blue the changes from pH 12 → 1.5, and in red the back-titration of the same sample.

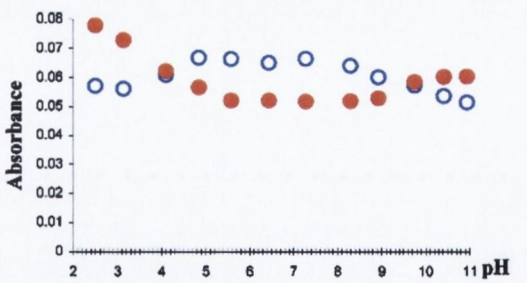

Figure 3. pH dependence in the absorption spectra of **1.Eu**, at 266 nm blue circles, and at 278 nm in red.

of tetramethylammonium chloride showed identical luminescence behavior, i.e. these changes were not anion dependent.[7]

By plotting the changes in the intensity of the $^5D_0 \rightarrow {}^7F_J$ transitions as a function of pH gave, for all of these emission bands, a bell shaped curve, consisting of two sigmoidal slopes, between pH ca. 3–5 and 6.5–8.5, with maximum intensity being reached at pH 5.8–6.0. Figure 2 shows these changes for the $^5D_0 \rightarrow {}^7F_1$ in blue for the titration of the alkaline solution with HCl, and the back-titration of this same solution in red, indicating that this pH dependence is fully reversible. It also clearly shows that the changes of these "*off*–*on*–*off*" pH-dependent emissions clearly transpire over the physiological pH range, and, as such, mimic the pH dependences of many enzymatic processes.[4,9] From these luminescence changes two pK_as were determined as 3.8 (±0.1) and 8.1 (±0.1), the latter being assigned to the deprotonation of the aryl amide proton in alkaline solution, whereas the former was assigned to the protonation of one of the *phen* nitrogen moieties. In comparison, potentiometric titrations of **1.Eu** gave pK_as of 3.6 (±0.1) and 7.6 (±0.1), respectively, which is similar to those observed spectroscopically. Furthermore, **1.Eu** was found to be stable to Eu(III) dissociation in this solution over a period of months, without any loss of its luminescence properties. To the best of our knowledge **1.Eu** is the first example of a lanthanide luminescent system capable of successfully mimicking such pH dependence by modulating the sensitization process from the antenna. Furthermore, these changes cannot be attributed to changes in q as it was pH independent, with $q = 1$.[7]

The concomitant changes in the fluorescence emission spectra between 300 and 550 nm (λ_{ex} = 266 nm) were less drastic, being ca. 40% quenched upon acidification from pH 11 to 1.5 with an associated shift in λ_{em} max from ca. 420 nm to 440 nm (Supporting Information). In tandem, the absorption spectrum of **1.Eu** showed hypochromic effects and evidence of some bell-shaped pH dependence, but these were much less drastic in comparison to the Eu(III) emission, as is evident from Figure 3.

From these combined spectroscopic changes, it is obvious that only the lanthanide luminescence is substantially affected by pH. However, what determines the large observed bell-shaped pH dependence for the Eu(III) emission? We predict that in an established manner, the excitation of the antenna sensitizes the Eu(III) $^5D_0$ excited state via an energy-transfer mechanism,[7,8,10] and that, in relatively alkaline solution, the Eu(III) ion can be reduced by an electron transfer[11] to Eu(II) which is not emissive. Secondly, the deprotonation of the amide proton increases the reduction potential of the antenna which is reflected in its reduced ability to populate the excited state of the Eu(III) ion.[8] Within a narrow pH window of ca. pH 5–6.5 and within experimental error, the emission is fully pH independent. In acidic solution upon protonation of the *phen* nitrogen moiety, the oxidation potential is increased in conjunction with modification of the ICT excited state of the *phen*–amide ligand,[9] which reduces the ability of the ligand to populate the $^5D_0$ state efficiently. We are currently investigating these features in greater detail.

In summary we have developed a novel lanthanide luminescence device that displays a clear and complete bell-shaped luminescent "*off*–*on*–*off*" switching as a function of pH in water. This dual switching takes place over 4–5 pH units, being centered at pH ≈ 6, as well as being fully reversible.

Acknowledgment. We thank Enterprise Ireland and TCD for financial support, and Drs. Hazel M. Moncrieff and Dr. John E. O'Brien for valuable discussion.

Supporting Information Available: Synthesis and experimental details for **1.Eu**, UV–vis, fluorescence, lanthanide luminescence spectra and q as a function of pH. Potentimetic titration of **1.Eu** (PDF). This material is available free of charge via the Internet at http://pubs.acs.org.

References

(1) Rurack, K.; Resch-Genger, U. *Chem. Soc. Rev.* **2002**, 116; Lavigne, J. J.; Anslyn, E. V. *Angew. Chem., Int. Ed.* **2001**, *40*, 3119; Amendola, V.; Fabbrizzi, L.; Mangano, C.; Pallavicini, P. *Acc. Chem. Res.* **2001**, *34*, 488; deSilva, A. P.; Fox, D. B.; Huxley, A. J. M.; Moody, T. S. *Coord. Chem. Rev.* **2000**, *205*, 41.

(2) Fabbrizzi, L.; Licchelli, M.; Pallavicini, P. *Acc. Chem. Res.* **1999**, *32*, 846; Czarnik, A. W. *Acc. Chem. Res.* **1994**, *27*, 302.

(3) Raymo, F. M. *Adv. Mater.* **2002**, *14*, 401; Raymo, F. M.; Giordani, S. *J. Am. Chem. Soc.* **2002**, *124*, 2004; de Silva, A. P.; Gunaratne, H. Q. N.; Gunnlaugsson, T.; Huxley, A. J. M.; McCoy, C. P.; Rademacher J. T.; Rice, T. E. *Chem. Rev.* **1997**, *97*, 1515.

(4) Stryer, L. *Biochemistry*, 3rd ed.; Freeman: New York, 1988.

(5) Fabbrizzi, L.; Gatti, F.; Pallavicini, P.; Parodi, L. *New J. Chem.* **1998**, 1403; de Silva, A. P.; Gunaratne, H. Q. N.; McCoy, C. P. *Chem. Commun.* **1996**, 2399.

(6) Pallavicini, P.; Amendola, V.; Massera, C.; Mundum, E.; Taglietti, A. *Chem. Commun.* **2002**, 2452.

(7) Gunnlaugsson, T.; Harte, A. J.; Leonard, J. P.; Nieuwenhuyzen, M. *Supramol. Chem.* **2003**, *13*, in press; Gunnlaugsson, T.; Harte, A. J.; Leonard, J. P.; Nieuwenhuyzen, M. *Chem. Commun.* **2002**, 2134.

(8) Gunnlaugsson, T.; Mac Dónaill, D. A.; Parker, D. *J. Am. Chem. Soc.* **2001**, *123*, 12866; Gunnlaugsson, T.; Mac Dónaill, D. A.; Parker, D. *Chem. Commun.* **2000**, 93.

(9) Gunnlaugsson, T.; Davies, R. J. H.; Nieuwenhuyzen, M.; Stevenson, C. S.; O'Brien, J. E.; Mulready, S. *Polyhedron* **2003**, *22*, 711; Gunnlaugsson, T.; Davies, R. J. H.; Nieuwenhuyzen, M.; Stevenson, C. S.; Viguier, R.; Mulready, S. *Chem. Commun.* **2002**, 2136; Gunnlaugsson, T.; O'Brien, J. E.; Mulready, S. *Tetrahedron Lett.* **2002**, *43*, 8493.

(10) Gunnlaugsson, T. *Tetrahedron Lett.* **2001**, *42*, 8901; Lowe, M. P.; Parker, D. *Chem. Commun.* **2000**, 707; Bazziclupi, C.; Bencini A.; Bianchi, A.; Giorgi, C.; Fusi, V.; Masotti, A.; Valtancoli, B.; Roque, A.; Pina, F. *Chem. Commun.* **2000**, 561; Parker, D.; Senanayake, K.; Williams, J. A. G. *Chem. Commun.* **1997**, 1777; de Silva, A. P.; Gunaratne H. Q. N.; Rice, T. E. *Angew. Chem., Int. Ed. Engl.* **1996**, *35*, 2116; Parker, D. *Coord. Chem. Rev.* **2000**, *205*, 109; Parker D.; Senanayake, P. K.; Williams, J. A. G. *J. Chem. Soc., Perkin Trans. 2* **1998**, 2129.

(11) Parker, D.; Dickins, R. S.; Puschmann, H.; Cossland, C.; Howard, J. A. K. *Chem. Rev.* **2002**, *102*, 1977; Caravan, P.; Ellison J. J.; McMurray, T. J.; Lauffer, R. B. *Chem. Rev.* **1999**, *99*, 283.

JA035425A

ChemComm
www.rsc.org/chemcomm

Eu(III)–cyclen–*phen* conjugate as a luminescent copper sensor: the formation of mixed polymetallic macrocyclic complexes in water†

Thorfinnur Gunnlaugsson,* Joseph P. Leonard, Katell Sénéchal and Andrew J. Harte
Department of Chemistry, Trinity College Dublin, Dublin 2, Ireland. E-mail: gunnlaut@tcd.ie; Fax: +353 1 671 2826; Tel: +353 1 608 3459

Received (in Cambridge, UK) 10th December 2003, Accepted 13th February 2004
First published as an Advance Article on the web 3rd March 2004

The cationic cyclen based Eu(III)–*phen* conjugated 1·Eu was synthesised as a chemosensor for Cu(II), where the recognition in water at pH 7.4 gave rise to quenching of the Eu(III) luminescence and the formation of tetranuclear polymetallic Cu(II)–Eu(III) macrocyclic complexes in solution where Cu(II) was bound by three 1·Eu conjugates.

The development of photochemically based supramolecular devices is a dynamic area of research, where many excellent examples of luminescent sensors, switches, logic gates and wires have been reported.[1–5] To this end we have developed and studied several lanthanide luminescence Tb(III) and Eu(III) complexes as sensors, switches and logic gate mimics by employing ionic and molecular *inputs*.[6] The benefits of such lanthanide devices lie in their long lived excited states (~ ms) and their emission at long wavelengths (500–750 nm) with line-like emission bands which confer an advantage over most fluorescent systems.[6,7] Herein, we discuss the development of **1·Eu**, a kinetically stable cationic tri-amide cyclen (1,4,7,10-tetraazacyclododecane) based Eu(III) macrocycle conjugated to a 1,10-phenanthroline (*phen*) ligand. The role of the *phen* ligand is dual as it serves both as an antenna sensitizing chromophore[4,6,7] for the indirect population (*via* $S_1 \rightarrow T_1$) of the Eu(III) excited state ($^5D_0$), as well as a receptor for either H^+ or Cu(II). Both of these ionic *inputs* are expected to modulate the photophysical properties of the *phen* ligand upon ion recognition, and consequently the Eu(III) sensitisation process.[4,6,7] Furthermore, the interaction of the Cu(II) with **1·Eu** leads potentially to the formation of a mixed supramolecular macrocyclic complex in solution, containing three **1·Eu** complexes coordinating to the Cu(II) ion. Such mixed polymetallic transition–lanthanide ion arrays, using coordination macrocyclic systems, are rare.[8] **1·Eu** is also the first example of a kinetically stable lanthanide luminescent sensor that shows good selectivity and sensitivity for Cu(II) over other competitive cations in pH 7.4 water .

The synthesis of **1·Eu** was achieved in good yield by first reacting the α-chloroamide **2** with one equivalent of tri-substituted *N,N*-dimethylacetamide cyclen macrocycle[9] at 80 °C in DMF and Cs_2CO_3 giving the ligand **1**, followed by reaction with Eu$(CF_3SO_3)_3$ in CH_3CN and precipitation from diethyl ether. ^1H NMR (400 MHz, D_2O) studies showed that **1·Eu** has a typical mono-capped square antiprism geometry in solution.

The pH dependence of the Eu(III) emission of **1·Eu** was investigated in water in the presence of 0.1 M tetramethylammonium chloride (I = 0.1 M TMACl) to maintain constant ionic strength. At neutral pH, **1·Eu** gave rise to typical Eu(III) emission bands[6] (λ_{ex} = 266 nm), at 581, 593, 615, 654, 686 and 702 nm due to the deactivation of the $^5D_0$ excited state to the ground states ^7F_J (J = 0, 1, 2, 3 and 4). A pH titration of **1·Eu** indeed showed that in the physiological pH range the Eu(III) emission was 'switched on' whereas at more acidic or alkaline pH the emission was 'switched off', giving rise to a bell-shaped emission-pH profile with pK_as of 3.8 (±0.1) and 8.1 (±0.1) respectively (ESI†). This process was fully reversible. Most importantly, the concomitant changes in the absorption and the fluorescence were only minor. The hydration state (q) of the sensor was found to be ~ 1 over the entire pH range, hence **1·Eu** has a single metal bound water molecule.

The ability of **1·Eu** to detect several group I, II and transition metal ions such as Fe(II), Fe(III), Co(II), Cu(II) and Zn(II) was investigated under three different sets of conditions: at pH 7.4 using 0.1M HEPES buffer; at pH 7.4 and with I = 0.1 M TMACl and finally at pH 7.4 in the presence of 'mimicked' biological ionic strength. For all of these conditions, Zn(II) and group I and II ions did not modulate the excited state properties of the *phen* ligand or the Eu(III) emission. However, the rest of the transition metal ions did. The absorption spectra of the free *phen* ligand of **1·Eu** was centred at 266 nm. Upon Cu(II) titration, it was slightly red shifted with the formation of an isosbestic point at 280 nm (ESI), signifying the coordination of Cu(II) by the *phen* moiety. Similar results were seen for the other transition metal ions. The concurrent changes in the fluorescence emission spectra of **1·Eu**, which had a $\lambda_{Fmax} \approx 430$ nm, showed *ca.* 80% quenching with a shift to the red, due to complexation, and consequent electron transfer quenching of the *phen* S_1 excited state by Cu(II). From these results it is clear that the delayed lanthanide luminescence of **1·Eu** would also be expected to be strongly effected by Cu(II) recognition, as the population of the $^5D_0$ excited state would be substantially reduced or removed. Indeed this was found to be the case, as seen in Fig. 1, where the well defined and line-like emission bands of the Eu(III) emission were gradually 'switched off' (~ 100%) upon recognition of Cu(II) by the *phen* ligand at pH 7.4.‡ By plotting the changes of any of these transitions, as a function of Cu(II) concentration it was possible to evaluate the binding affinity of **1·Eu** for Cu(II). These changes are shown in Fig. 2 for the J = 2 transition, as a function of −log [M], where M = Cu(II). From these changes it is evident that the binding of Cu(II) occurs over a narrow concentration range (−log [Cu] ≈ 6–5, which overlaps with that of the physiological concentration of Cu(II)). This is not surprising, given the high coordination requirement of the Cu(II) and its affinity for *phen* type ligands.[10] Importantly, the addition of EDTA (using the same concentration that gave rise to fully 'switched off' state by Cu(II)) to this fully quenched solution, switched the emission back 'on'. This signifies that the Cu(II) detection by **1·Eu** is reversible. Similar titrations were carried out using other transition metal ions. From Fig. 2, it is evident that in water at pH 7.4 the Cu(II) is selectively detected over both Co(II) and Fe(II) (M = Co(II) and Fe(II)). For both the Eu(III) emission is quenched upon recognition but at significantly higher concentration than for Cu(II). We also evaluated the recognition of Cu(II) at high ionic strength, I = 0.1

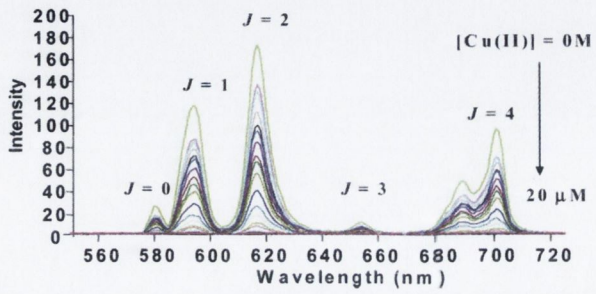

Fig. 1 The quenching of the Eu(III) emission of **1·Eu** upon titration with Cu(II) at pH 7.4. Excitation 266 nm.

† Electronic supplementary information (ESI) available: experimental and spectroscopic data. See http://www.rsc.org/suppdata/cc/b3/b316176e/

DOI: 10.1039/b316176e

 This journal is © The Royal Society of Chemistry 2004

TMAACl as well as in a simulated biological cationic background of 150 mM NaCl, 10 mM KCl, 5 mM $MgCl_2$, and 5 mM $CaCl_2$ at pH 7.4 (Fig. 2). As previously demonstrated the Eu(III) emission was always 'switched off' upon titration with Cu(II) in both media, and upon addition of EDTA it was switched back on. However, under these conditions the Cu(II) sensitivity was marginally increased. Similar results were observed for Co(II), but in high ionic strength the Co(II) sensitivity was substantially modulated and become similar to that of Cu(II) (ESI†).

The stoichiometry of the above interactions between Cu(II) and **1·Eu** was investigated using various methods. By plotting the emission changes as a function of equivalents of Cu(II), it became apparent that the emission was fully quenched after *ca.* 0.35 equivalents of Cu(II) (ESI) suggesting that Cu(II) was indeed coordinating to three **1·Eu** complexes. Cu(II) is known to be able to coordinate to *phen* in either 1 : 2 or 1 : 3 ratio, the latter being achieved by distorted octahedral geometry.[10] However, the most reliable proof for the stoichiometric ratio between Cu(II) and **1·Eu** was obtained from Job method analysis.[11] By plotting the changes in the Eu(III) emission (Fig. 3) against mole fraction, and analysing these changes using the equation: Ratio = $f_{extr}/(1 - f_{extr})$ (where f_{extr} is ([Cu]/[Cu]+[**1·Eu**]) when the Eu(III) emission is fully quenched (extreme)) we determined that the Ratio = 3. This suggests the formation of mixed 1 : 3 Cu(II) : Eu(III) supramolecular complexes in solution, as many isomeric 1 : 3 complexes are possible due to the asymmetry of **1·Eu** ligand. To the best of our knowledge, such mixed multinuclear macrocyclic transition–lanthanide ion complexes are not common, and have not previously been shown for cyclen based Cu(II)–Eu(III) macrocyclic *phen* ligands.[8] Furthermore, this supramolecular complex is reversibly formed as the addition of EDTA switches the Eu(III) emission back on, signifying its dissociation. In comparison, when the fluorescence emission spectra of *Acm-phen*[12] was monitored upon addition of Cu(II), the emission was *ca.* 90% quenched after *ca.* 0.5 equivalents of Cu(II), suggesting 1 : 2 complex formation.

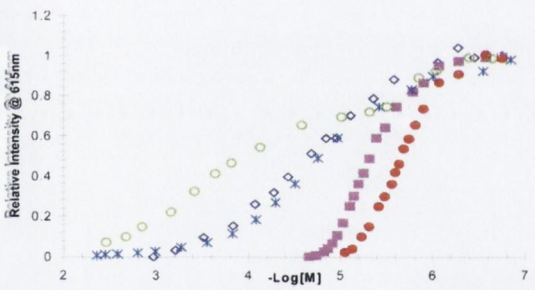

Fig. 2 The relative changes in the Eu(III) emission of **1·Eu** as function of various transition metal ions at $J = 2$ at 615 nm. All measured at pH 7.4 : pink ■ = Cu(II); blue * = Co(II); black ◇ = Fe(II); green ○ = Fe(III); red ● = Cu(II) in the presence of 150 mM NaCl, 10 mM KCl, 5 mM $MgCl_2$, and 5 mM $CaCl_2$.

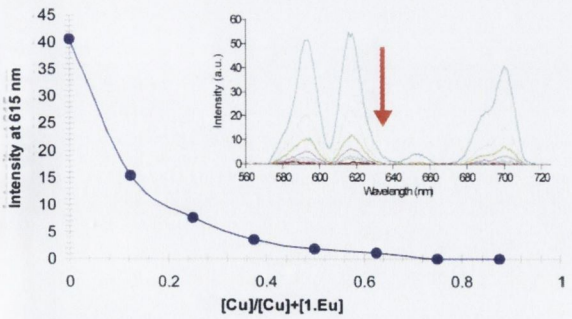

Fig. 3 Job plot analysis (intensity changes *vs.* molar fraction) for the changes in the Eu(III) emission at 700 nm at pH 7.4. $[\mathbf{1\cdot Eu}]_{initial} = 7.16\ \mu M$; $[\mathbf{1\cdot Eu}]_{final}$ 0.89 μM; $[Cu(II)]_{initial} = 0$ M, $[Cu(II)]_{final} = 6.26\ \mu M$. Insert are the changes in the Eu(III) emission when recorded at this low concentration..

In summary we have developed a delayed lanthanide luminescent sensor for Cu(II), which shows good selectivity for Cu(II) over other ions such as Co(II), Fe(II) and Fe(III) at pH 7.4. Job method analysis of the Cu(II) recognition indicated the formation of a cationic (11+) tetranuclear mixed polymetallic macrocyclic supramolecular complexes in solution where the Cu(II) ion is coordinating to three **1·Eu** complexes. For all the cases, these supramolecular complexes were reversibly formed as the Eu(III) emission was reversibly 'switched on' upon addition of EDTA. We are currently investigating these systems in greater detail, as well as using other lanthanide ions.

We thank Enterprise Ireland, TCD and BMRI for financial support, Dr Hazel M. Moncrieff for helpful discussion and Dr John E. O'Brien for assisting with NMR.

Notes and references

‡ The Eu(III) emission quenching can also been envisaged in the form of a truth-table where the Eu(III) emission change is the *output* and the *input* (A or B) are either H^+ (or OH^-) and Cu(II). This gives rise to the two ionic based logic-gate mimics A·B′ or A′·B (depending on the *input* order). This is the *inhibit* logic gate function, which is an extension of our mixed Tb(III) based *molecular-ionic* logic gate mimic described in reference 6 (*e*) and (*f*).

1 A. P. de Silva, B. McCaughan, B. O. F. McKinney and M. Querol, *Dalton Trans.*, 2003, 1902; V. Balzani, *Photochem. Photobiol. Sci.*, 2003, **2**, 459; V. Balzani, A. Credi and M. Venturi, *Pure Appl. Chem.*, 2003, **75**, 541; K. Rurack, *Spectrochem. Acta A*, 2001, **57**, 2161.

2 K. Rurack and U. Resch-Genger, *Chem. Soc. Rev.*, 2002, **31**, 116; P. A. Gale, *Coord. Chem. Rev.*, 2001, **213**, 79; A. P. de Silva, H. Q. N. Gunaratne, T. Gunnlaugsson, A. J. M. Huxley, C. P. McCoy, J. T. Rademacher and T. E. Rice, *Chem. Rev.*, 1997, **97**, 1515.

3 F. M. Raymo, *Adv. Mater.*, 2002, **14**, 401; A. P. de Silva, D. B. Fox, A. J. Huxley and T. S. Moody, *Coord. Chem. Rev.*, 2000, **205**, 41.

4 D. Parker and J. A. G. Williams, *J. Chem. Soc., Dalton Trans.*, 1996, 3613; D. Parker, *Coord. Chem. Rev.*, 2000, **205**, 109.

5 T. Gunnlaugsson and J. P. Leonard, *J. Chem. Soc., Perkin Trans. 2*, 2002, 1980; T. Gunnlaugsson, A. P. Davis, J. E. O'Brien and M. Glynn, *Org. Lett.*, 2002, **4**, 2449; T. Gunnlaugsson, A. P. Davis and M. Glynn, *Chem. Commun.*, 2001, 2556; T. Gunnlaugsson, M. Nieuwenhuyzen, L. Richard and V. Thoss, *J. Chem. Soc., Perkin Trans. 2*, 2002, 141.

6 (*a*) T. Gunnlaugsson and J. P. Leonard, *Chem. Commun.*, 2003, 2424; (*b*) T. Gunnlaugsson, J. P. Leonard, K. Sénéchal and A. J. Harte, *J. Am. Chem. Soc.*, 2003, **125**, 12062; (*c*) T. Gunnlaugsson, A. Harte, J. P. Leonard and M. Nieuwenhuyzen, *Supramol. Chem.*, 2003, **15**, 505; (*d*) T. Gunnlaugsson, A. Harte, J. P. Leonard and M. Nieuwenhuyzen, *Chem. Commun.*, 2002, 2134; (*e*) T. Gunnlaugsson, D. A. Mac Dónaill and D. Parker, *J. Am. Chem. Soc.*, 2001, **123**, 12866; (*f*) T. Gunnlaugsson, D. A. Mac Dónaill and D. Parker, *Chem. Commun.*, 2000, 93; (*g*) T. Gunnlaugsson, *Tetrahedron Lett.*, 2001, **42**, 8901.

7 D. Parker, R. S. Dickins, H. Puschmann, C. Cossland and J. A. K. Howard, *Chem. Rev.*, 2002, **102**, 1977.

8 S. J. A. Pope and S. Faulkner, *J. Am. Chem. Soc.*, 2003, **125**, 10526; N. M. Shavaleev, L. P. Moorcraft, S. J. A. Pope, Z. R. Bell, s. Faulkner and M. D. Ward, *Chem. Commun.*, 2003, 1134; S. J. A. Pope, A. M. Kenwright, V. A. Boote and S. Faulkner, *Dalton Trans.*, 2003, 3780; V. Comblin, D. Gilsoul, M. Hermann, V. Humblet, V. Jacques, M. Mesbahi, C. Sauvage and J. F. Desreux, *Coord. Chem. Rev.*, 1999, **185–6**, 451; S. Aime, M. Botta, F. Fasano and E. Terreno, *Spectrochim. Acta*, 1993, **49A**, 1315.

9 T. Gunnlaugsson, J. P. Leonard, S. Mulready and M. Nieuwenhuyzen, *Tetrahedron*, 2004, **60**, 105.

10 F. A. Cotton and G. Wilkinson, in *Advanced Inorganic Chemistry*, fifth edn., John Wiley & Sons, New York, 1988.

11 H-J. Schneider and A. Yatsimirsky, in *Principles and Methods in Supramolecular Chemistry*, Wiley, England, 2000.

12 D. García-Fesnadillo and G. Orellana, *Helv. Chm. Acta*, 2001, **84**, 2708.